

**MODEL-BASED DEVELOPMENT OF A FUZZY LOGIC
ADVISOR FOR ARTIFICIALLY VENTILATED PATIENTS**

by

Kevin Michael Goode

December 2000

Thesis submitted for the Degree of Doctor of Philosophy
Department of Automated Control and Systems Engineering
The University of Sheffield

FOR
RUTH AND DANIEL

Summary

This thesis describes the model-based development and validation of an advisor for the maintenance of artificially ventilated patients in the intensive care unit (ICU). The advisor employs fuzzy logic to represent an anaesthetist's decision making process when adjusting ventilator settings to safely maintain a patient's blood-gases and airway pressures within desired limits. Fuzzy logic was chosen for its ability to process both quantitative and qualitative data.

The advisor estimates the changes in inspired O₂ fraction (FIO₂), peak inspiratory pressure (PEEP), respiratory rate (RR), tidal volume (VT) and inspiratory time (TIN), based upon observations of the patient state and the current ventilator settings. The advisor rules only considered the ventilation of patients on volume control (VC) and pressure regulated volume control (PRVC) modes.

The fuzzy rules were handcrafted using known physiological relationships and from tacit knowledge elicited during dialogue with anaesthetists. The resulting rules were validated using a computer-based model of human respiration during artificial ventilation. This model was able to simulate a wide range of patho-physiology, and using data collected from ICU it was shown that it could be matched to real clinical data to predict the patient's response to ventilator changes.

Using the model, five simulated patient scenarios were constructed via discussion with an anaesthetist. These were used to test the closed-loop performance of the prototype advisor and successfully highlighted divergent behaviour in the rules. By comparing the closed-loop responses against those produced by an anaesthetist (using the patient-model), rapid rule-refinement was possible. The modified advisor demonstrated better decision matching than the prototype rules, when compared against the decisions made by the anaesthetist.

The modified advisor was also tested using data collected from ICU. Direct comparisons were made between the decisions given by an anaesthetist and those produced by the advisor. Good decision matching was observed in patients with well behaved physiology but soon ran into difficulties if a patients state was changing rapidly or if the patient observations contained large measurement errors.

Acknowledgements

This project was a joint venture between The University of Sheffield and the Royal Hull Hospitals Trust. Funding for the project was provided by the East Yorkshire Health Authority.

- Prof. Derek A. Linkens:** My Ph.D. supervisor and source of inspiration when the words just wouldn't come. I really am truly grateful for his continued support and encouragement over the years.
- Dr. Peter Bourne** My Hull-based supervisor and major point of contact until his untimely death in 1997. He was instrumental in the project's initial conception.
- Dr. Graham Cundill** The consultant anaesthetist assigned to the project to provide clinical input. His willingness to continue working on the project even after moving away to York was pivotal to the completion of the simulated closed-loop validation of the advisor. Originally assigned to cover data collection from Castle Hill Hospital, Hull.
- Dr. Chris Langton** For stepping into the shoes of Peter Bourne and providing me with office space to continue my write-up, and for the loan of the laser-jet printer at the final hour.
- Dr. John Waterland** Another consultant anaesthetist originally assigned to cover data collection from Hull Royal Infirmary, Hull, however this role fell predominantly to Dr. Phil Gray.
- Dr. Phil Gray** Facilitated all data collection made at Hull Royal Infirmary to test both the patient-model and the advisor.
- Dr. Ruth Hunter** For providing my financial and emotional support, without which I am certain this would never have been completed. All my love, now and always.

To all my friends and family who have willed me silently from sidelines to complete my thesis.

Contents

SUMMARY	iii
AKNOWLEDGEMENTS.....	iv
CHAPTER 1: INTRODUCTION.....	1
CHAPTER 2: FUZZY LOGIC & ITS APPLICATION IN BIOMEDICINE	6
2.1 INTRODUCTION	6
2.2 BASICS PRINCIPLES AND CONCEPTS OF FUZZY LOGIC.....	6
2.2.1 <i>Set Membership and Geometry</i>	6
2.2.2 <i>Fuzzy Inference</i>	8
2.2.3 <i>Defuzzification</i>	10
2.3 BIOMEDICAL APPLICATIONS OF FUZZY LOGIC.....	11
2.3.1 <i>Post-surgical Control of Mean Arterial Pressure</i>	11
2.3.2 <i>Depth of Anaesthesia</i>	11
2.3.3 <i>Ventilator Control</i>	13
2.3.4 <i>Miscellaneous Applications</i>	14
2.4 SUMMARY & CONCLUSIONS.....	15
CHAPTER 3: REVIEW OF RESPIRATORY MODELS.....	16
3.1 INTRODUCTION	16
3.2 GREY-BOX MODELS	17
3.2.1 <i>Respiratory Mechanics Models</i>	17
3.2.2 <i>Gas Exchange Models</i>	18
3.2.3 <i>Gas Dissociation Models</i>	19
3.2.4 <i>Respiratory Control Models</i>	19
3.2.5 <i>Integrated Models</i>	21
3.2.6 <i>Models of Respiration During Artificial Ventilation</i>	22
3.2.7 <i>Model-based Nomograms</i>	23
3.3 BLACK-BOX MODELS	26
3.4 SUMMARY & CONCLUSIONS.....	26
CHAPTER 4: SOPAVENT - PATIENT MODEL DEVELOPMENT	27
4.1 INTRODUCTION	27
4.2 PATIENT MODEL ARCHITECTURE.....	27
4.2.1 <i>Overview</i>	27
4.2.2 <i>Oxygen Transport Equations</i>	30

4.2.3 Oxygen Dissociation Function	34
4.2.4 Inverse O ₂ Dissociation Function.....	37
4.2.5 Carbon Dioxide Transport Equations.....	38
4.2.6 Carbon Dioxide Dissociation Function.....	39
4.2.7 Ventilator Model.....	40
4.2.8 Unit Conversion.....	41
4.3 O ₂ DISSOCIATION FUNCTION DEVELOPMENT.....	44
4.3.1 Functional Validity.....	44
4.3.2 Clinical Validity.....	44
4.3.3 Inverse O ₂ GDF Validity.....	47
4.4 O ₂ TRANSPORT DYNAMICS DEVELOPMENT	50
4.4.1 Model Implementation	50
4.4.2 Derivation & Source of System Parameters.....	51
4.4.3 Ball Park Validation	57
4.4.4 Results & Analysis.....	57
4.5 CO ₂ DISSOCIATION FUNCTION DEVELOPMENT	59
4.5.1 Functional Validity.....	59
4.5.2 Inverse CO ₂ Dissociation Function (IGDF).....	61
4.6 CO ₂ TRANSPORT DYNAMICS DEVELOPMENT	61
4.6.1 Ball Park Validity.....	63
4.7 O ₂ AND CO ₂ MODEL INTEGRATION.....	63
4.8 SUMMARY & CONCLUSIONS.....	64
CHAPTER 5: CLINICAL VALIDATION OF PATIENT MODEL.....	67
5.1 INTRODUCTION.....	67
5.2 MODEL SENSITIVITY ANALYSIS.....	67
5.2.1 Theory.....	68
5.2.2 Sensitivity Analysis Method.....	70
5.2.3 Analysis.....	72
5.2.4 Conclusions of Sensitivity Analysis.....	75
5.3 DATA COLLECTION	76
5.3.1 Data Collection Protocol	78
5.3.2 Summary of Collected Data.....	80
5.4 DATA PROCESSING & MODEL TUNING.....	81
5.4.1 Metabolic Computer Results	81
5.4.2 Calculation of Cardiac Output.....	81
5.4.3 Generation of PRIOR and POST Data.....	83

5.4.4 Model Tuning	85
5.5 CLINICAL VALIDITY	88
5.5.1 Qualitative Trend Analysis	88
5.5.2 Statistical Analysis	96
5.5.3 Causes of Response Errors	97
5.6 SUMMARY & CONCLUSIONS	100
CHAPTER 6: FAVEM – ADVISOR DEVELOPMENT	103
6.1 INTRODUCTION	103
6.2 ADVISOR ARCHITECTURE	103
6.2.1 Overview	103
6.2.2 Observation Processing Module (OPM)	105
6.2.3 Subsystems Architecture	106
6.2.4 Output Quantisation	107
6.3 INFERENCE METHODOLOGY	107
6.3.1 Choice of Membership Function	108
6.3.2 Membership Function Geometry	108
6.3.3 Choice of Inference Algorithm & Implication Operator	110
6.3.4 Choice of Liaison Operator	112
6.3.5 Choice of Defuzzification Method	112
6.3.6 Analysis of Inference Methods	113
6.3.7 Choice of Output Quantisation	115
6.4 RULE DEVELOPMENT METHODOLOGY	116
6.4.1 Rule Prototyping and Completeness	116
6.4.2 Fuzzy Consequent Construction	117
6.4.3 Rule Reduction Algorithm	117
6.5 FiO ₂ RULE DEVELOPMENT	120
6.5.1 Elicitation of PaO ₂ Membership Functions	120
6.5.2 Rule Prototyping Using Iso-Shunt Diagram	121
6.5.3 Evaluation of Iso-Shunt Rules	123
6.6 PEEP RULE DEVELOPMENT	125
6.6.1 Clinical Benefits of PEEP	125
6.6.2 Disadvantages of PEEP	126
6.7 MV RULE DEVELOPMENT	128
6.7.1 Ventilation-PaCO ₂ Relationship	128
6.7.2 Acid-Base Balance	129
6.7.3 Calculation of pH Fuzzy Sets	131

6.7.4 <i>Volume Constraints</i>	135
6.8 VT-RR RULE DEVELOPMENT	137
6.8.1 <i>Normalised Vt</i>	138
6.8.2 <i>Normalised Iso-Mv Lines</i>	138
6.8.3 <i>Ideal Vt-RR Relationship</i>	139
6.8.4 <i>Rule Estimation</i>	142
6.8.5 <i>Handling Mv Changes</i>	143
6.8.6 <i>Volume Constraints</i>	145
6.9 SUMMARY & CONCLUSIONS.....	145
CHAPTER 7: CLOSED LOOP ADVISOR VALIDATION.....	147
7.1 INTRODUCTION	147
7.2 RATIONALE & OVERVIEW	147
7.3 MODEL IMPROVEMENTS.....	150
7.3.1 <i>pH Modelling</i>	150
7.3.2 <i>Airway Modelling</i>	152
7.3.3 <i>Modelling Benefits and Disadvantages of PEEP</i>	156
7.3.4 <i>Cardiac Output & Metabolic Function</i>	158
7.3.5 <i>Event Profiling</i>	160
7.3.6 <i>Graphical User Interface</i>	162
7.4 PATIENT SCENARIO DEVELOPMENT	162
7.4.1 <i>Anaesthetist Decision Histories</i>	163
7.5 CLOSED-LOOP VALIDATION & RULE REFINEMENT.....	164
7.5.1 <i>FiO₂ Advisor Performance Analysis</i>	168
7.5.2 <i>PEEP Advisor Performance Analysis</i>	171
7.5.3 <i>MV Advisor Performance Analysis</i>	174
7.5.4 <i>RR-Vt Advisor Performance Analysis</i>	178
7.5.5 <i>TIN Advisor Performance Analysis</i>	183
7.6 SUMMARY & CONCLUSIONS.....	185
CHAPTER 8: CLINICAL VALIDATION OF ADVISOR.....	202
8.1 INTRODUCTION	202
8.2 PROCEDURE.....	202
8.3 SYNOPSIS OF COLLECTED DATA	203
8.4 STATISTICAL PERFORMANCE ANALYSIS.....	205
8.5 QUALITATIVE PERFORMANCE ANALYSIS.....	207
8.6 DISCUSSION.....	208

8.7 SUMMARY & CONCLUSIONS.....	211
CHAPTER 9: CONCLUSIONS & FUTURE WORK.....	212
APPENDIX A: SIMULINK BLOCK DIAGRAMS OF THE PATIENT MODEL.....	217
APPENDIX B: DATA COLLECTED FOR PATIENT-MODEL VALIDATION AND ETHICAL COMMITTEE GUIDLINES.....	223
APPENDIX C: SIMULATED PATIENT DEFINITIONS	243
APPENDIX D: CLOSED LOOP DECISION HISTORY DATA.....	250
APPENDIX E: ADVISOR CONTROL RULES AND CONTROL SPACE MAPS.....	266
APPENDIX F: ADVISOR RESPONSES TO CLINICAL DATA AND DECISION SCORING ...	287
NOMENCLATURE	296
BIBLIOGRAPHY	300

Chapter 1: Introduction

Hypothesis: Using fuzzy-logic it is possible to construct an advisory system that emulates the changes made by an anaesthetist to the ventilator settings, on patients in intensive care (ICU). Knowledge elicitation and rule-refinement can be improved through the use of a computer-based model of a ventilated patient. The model can be used to simulate closed-loop control and provide stability analysis of the control rules. This can have advantages over validation made using only clinical data, and highlights a design methodology that facilitates future advisor design.

Artificial ventilation is defined as the provision of minute volume (MV) of respiration by external forces. It is usually required when there is either severe dysfunction of the mechanics of breathing, impairment to the patient's respiratory muscles or a need to improve the oxygenation of the arterial blood. The main situations in which it is employed are;

- 1). Resuscitation following acute apnoea (cessation of breathing).
- 2). Anaesthesia with paralysis.
- 3). Intensive care with failure of one or more vital functions.
- 4). Prolonged treatment of chronic ventilatory failure.

Patients are usually connected to a ventilator using an endotracheal tube via a humidifier, see Figure 1.1. The vital functions of the patient (i.e. heart rate, oxygen saturation, cardiac output, blood pressure, etc) are recorded using a bedside monitoring system, and accurate measurement of arterial and venous blood O_2 and CO_2 are made using a blood-gas analyser.

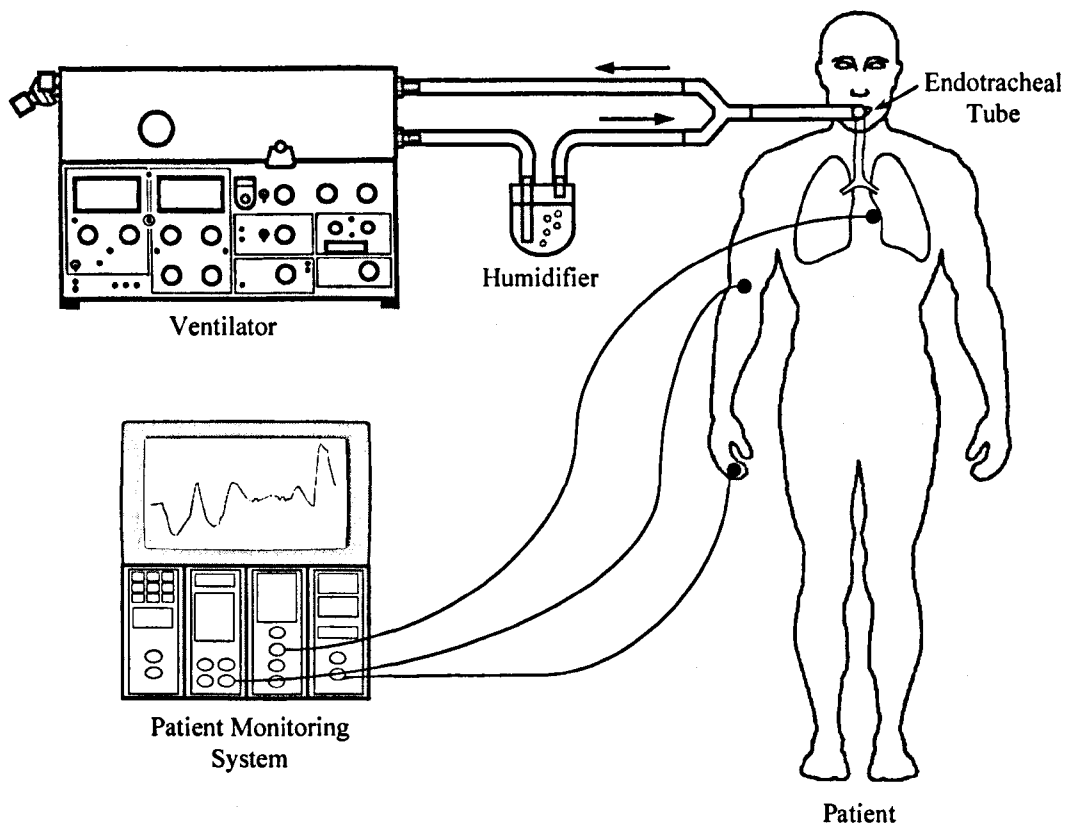


Figure 1.1: Overview of patient on artificial ventilation.

Ventilatory support is continued, until the underlying causes of respiratory failure have been resolved. From the start of intubation, the anaesthetist has to maintain the patient's blood-gases and airway pressures within safe limits with a view to eventually weaning them from the ventilator. This involves adjustment of the ventilator settings in response to the gradual improvement or degradation of the patient's condition. It is this decision process that we wish to emulate using a fuzzy-logic based advisor.

The potential benefits of an advisory system for the ventilatory care of patients in ICU have been expressed for many years, and previous studies have highlighted advantages in terms of improved patient care and anaesthetist training. Many attempts to represent anaesthetists' knowledge in ventilatory care have been made, for example Fagan, 1980; Miller, 1985; Summers *et al*, 1987 and 1988; Singh & Roth, 1988; Sittig, 1988; Farr & Fagan, 1989; Hernándezsande, *et al*, 1989; Rudowski *et al*, 1989; Shabsavar *et al*, 1989 and 1991; Arkad *et al*, 1991; Summers *et al*, 1991 and 1992; Miksch *et al*, 1993; Fernando *et al*, 1995; Dojat *et al*, 1996 and 1997; Snowden *et al*, 1997; to name but a few.

However, increased understanding of the ventilation care problem has led to changes in the ventilation strategies employed, causing advisory systems to become outmoded, and no longer applicable to new clinical practices. Consequently, new advisor rules need to be constructed and re-tested against clinical data to ensure that the advice generated is safe. This is an extremely time consuming process since it has to be repeated each time the rules are modified. To make matters worse, the data used for validation may contain significant measurement errors, complicating any decision comparisons made. Whilst a truly useful system must be able to deal with such errors, developing an advisor in this way for complex processes can prove extremely labour intensive. Such investment will be wasted when conceptually very different care strategies are introduced into ICU. Furthermore, unless the control-loop can be closed between the advisor and the process then no guarantee of rule stability can be assured. The rules may contain divergent or limit-cycle behaviour that is not detectable using one-off comparisons of decision differences. Since clinicians are unlikely to close the control loop until safe control has been demonstrated we are left with somewhat of a design dilemma.

There is a better way – model-based advisor development! If control system design is to keep abreast of current care developments then a more rapid method for rule validation is required. By constructing a computer-based model of the process, closed-loop control can be simulated and the performance of the rules assessed. Because this is closed-loop control (albeit simulated) the incidence of rule instability, divergence and limit-cycle behaviour can be rapidly identified and resolved.

With careful selection of the model, virtual patient scenarios can be constructed to represent a wide range of respiratory pathology and trauma. These have the advantage of being repeatable and free from measurement errors, a quality not possible using clinical data. This allows quantitative comparisons to be made between anaesthetists' decisions and those produced by the advisor, thus enabling rapid identification of rule errors and the elicitation of tacit knowledge that may have been missed during the prototype advisor design. Better still, the efficacy of alternative advisor designs can be quantitatively measured.

Fuzzy-logic was chosen as the method for rule representation since it is able to process the uncertainties of the problem. Its applicability to process control has been widely demonstrated and recent work has shown its use in the maintenance of end-tidal PCO₂ during mechanical ventilation in anaesthesia [Schaublin *et al*, 1996] and during high-frequency jet ventilation [Noshiro *et al*, 1994]. Interacting and conflicting rules can be processed with the same degree of ease, due to the simple computational mechanics of fuzzy logic. Also its use of linguistic classifiers (e.g. inspired O₂ is *high*) makes the system readily interpretable by an expert (i.e. an anaesthetist). The simplicity of rule representation makes for rapid modification and methods exist for self-organisation of control rules. This makes it well suited for future design.

Whilst developing an advisor capable of handling all aspects of ventilatory care is the long term objective, this research was restricted to a sub-set of the care-problem in order to prove the capabilities and benefits of fuzzy-logic and model-based controller design. The advisor was therefore restricted to the maintenance of arterial O₂ partial pressure (PaO₂), arterial CO₂ partial pressure (PaCO₂), pH and peak inspiratory pressure (PIP) via the adjustment of inspired O₂ fraction (FIO₂), positive end-expiratory pressure (PEEP), respiratory rate (RR), tidal volume (VT) and inspiratory-expiratory ratio (I:E), in patients ventilated using continuous mandatory ventilation (CMV) and in particular those on volume control (VC) or pressure regulated volume control (PRVC) modes. These patients are expected to be well sedated and therefore performing no breathing for themselves or indeed triggering any breaths. The patient model was selected to meet the requirements of this sub-problem.

A summary of the thesis chapters is given below;

Ch 2: Fuzzy Logic and its Application to Control in Biomedicine

This provides a brief overview of fuzzy logic concepts and principles, followed by a review of the previous applications of fuzzy logic to biomedical control with particular reference to advisory systems and ventilator management.

Ch 3: Respiratory Models

This provides a review of respiratory models with particular reference to their classification and suitability for advisor development. Models are grouped according to the process they are describing and whether they are theoretically (white-box) or empirically (black-box) based. Also described are model-based nomograms that are useful descriptors of physiological behaviour.

Ch 4: SOPAVent – Patient Model Development

The architecture of the patient model is presented together with a detailed description of the equations behind it and their sources. This includes explanations of the O₂ and CO₂ mass transport equations and the O₂ and CO₂ gas dissociation function (GDF) together with the computation of their inverse (IGDF). A simple ventilator model is also described, and equations for the conversion of gas-volume, gas-fraction and gas flow-rate from observed units and conditions to the units and conditions required by the model are presented (e.g. STPD – standard temperature pressure dry converted to BTPS – body temperature pressure saturated).

The functional implementation of the O_2 GDF and its validation using clinical data available in the literature is discussed, followed by the implementation of its inverse. Methods employed to optimise the inverse function, are described. The implementation of the O_2 transport equations using SIMULINK is presented and its ability to match expected normal blood-gas values is demonstrated using patient parameters representative of a healthy male subject. This is repeated for the CO_2 GDF and CO_2 transport equations, and then the behaviour of the integrated O_2 and CO_2 model is examined. This does not constitute the final model and further improvements are discussed in the beginning of Chapter 7.

Ch 5: Clinical Validation of Patient Model

This chapter describes the attempts to validate the patient-model using data collected from ICU. The primary objective was to ascertain whether the model could predict blood-gas responses to changes in ventilator settings. Whether this can be achieved depends very much on the quality of the data collected and the parametric sensitivity of the model. The first section therefore provides a brief review of sensitivity analysis methodology including descriptions of the problems that can be encountered and their implications when interpreting sensitivity results. The classical sensitivity analysis of the patient-model is then described and the implication of the results to clinical measurement and model tuning are discussed.

Next, the data collection protocols and data processing required to produce all of the inputs of the model are described. The method used for tuning the model to match the observed blood-gases is described and the ability of the model to match blood-gas responses to ventilator changes is assessed using qualitative and quantitative techniques. Finally, the possible causes of response errors are discussed.

Ch 6: FAVeM – Advisor Development

The advisor architecture is presented together with a detailed examination of the choice of inference methodology. This is followed by a discussion of techniques used to implement the rules, including the need for completeness, the method of fuzzy consequent construction and the description of a rule reduction algorithm to reduce computational overheads.

The development of the FIO_2 , PEEP, MV and VT -RR advisor subsystems is presented in turn, highlighting the sources of knowledge and methods employed to elicit them. The FIO_2 rule development describes the elicitation of fuzzy classifications for PaO_2 from an anaesthetist and the use of iso-shunt nomograms to deduce prototype control rules. The evaluation of these rules by an anaesthetist is described, and the suitability of the advice generated assessed. The modifications made to the control rules based on this assessment are described. PEEP rule development is described next with an explanation of the benefits and disadvantages of PEEP and how these might be expressed using fuzzy control rules. The FIO_2 and PEEP rules work together to provide maintenance of PaO_2 .

$PaCO_2$ maintenance via the adjustment of MV is explored and simple control rules proposed. The importance of goal-orientated $PaCO_2$ maintenance to encapsulate particular ventilation requirements such as patients with head injury is discussed. These control rules are then extended to include acid-base imbalance. The causes of imbalance are described in detail and

the elicitation of pH fuzzy classes using the Henderson-Hasselbalch equation presented. The rules are further extended to include consideration of PIP and thus prevent possible barotrauma.

Finally, the development of rules to correctly convert changes in MV to changes in RR and/or VT is described. The concept of an ideal RR-VT relationship is presented together with its use to estimate the control rules. The rules are extended to include restrictions due to elevated PIP.

Ch 7: Closed-loop Advisor Validation

The prototype rules are then evaluated using simulated closed-loop control. This chapter highlights the advantages that such an approach has over other validation methods and describes its implementation. Before closed-loop validation could be performed, improvements were made to the model so that it would respond realistically to changes in ventilator settings. These include modelling of pH changes, airway pressures, effects of PEEP and the inclusion of relationships governing nominal cardiac output (\dot{Q}_t), O₂ consumption ($\dot{V}O_2$) and CO₂ production ($\dot{V}CO_2$). The equations describing these improvements are presented.

The use of this improved model to construct virtual patient scenarios with input from an anaesthetist is described. These are then used to provide simulated closed-loop evaluation of the prototype advisor's performance. Behavioural discrepancies are highlighted and modifications made to the rules described. The advisor is then re-evaluated and the level of performance improvement assessed. Any remaining decision differences are examined and potential solutions discussed.

Ch 8: Clinical Validation of Advisor

In the final chapter the modified advisor is validated against real clinical decisions. The causes of decision mismatch are explored in detail and possible solutions outlined. Analysis is made using both qualitative scoring techniques and statistical measures.

Chapter 2: Fuzzy Logic & its Application in Biomedicine

2.1 Introduction

Fuzzy logic theory was first developed by Zadeh in 1965, and combines elements of multi-valued logic, probability theory and artificial intelligence. It provides the concept of fuzzy linguistic variables and uses fuzzy sets to express linguistic rules that can produce a realistic control strategy. It is therefore well suited to problems that require human judgement or loose linguistic descriptors of the control process, and for controlled systems that have non-linear characteristics that are difficult to model mathematically.

This chapter provides a brief overview of the principles and concepts of fuzzy set representation, rule inference and defuzzification. For more detailed explanations of these and other related concepts the reader is directed towards the work of Driankov *et al* (1993) and Yan *et al* (1994).

This is followed by a review of fuzzy logic control applications, and is restricted to examples occurring in biomedicine. Tong (1977) gives a survey of early FLC applications, and Sugeno (1988) describes the use of FLC in industrial processes such as heat exchangers, blast furnaces, waste water treatment and train operation.

2.2 Basics Principles and Concepts of Fuzzy Logic

Fuzzy logic is a branch of logic that represents membership within a set as a continuous function rather than having strict true/false membership. The degree of membership is the certainty (expressed as a number from 0 to 1) of a particular observation value belonging to a fuzzy set. This enables complex computing tasks with imprecise or fuzzy answers to be processed easily. It enables linguistic concepts such as *hot* and *cold* to be described mathematically and thus used to represent statements such as 'The room temperature is *hot*'.

2.2.1 Set Membership and Geometry

Several different shapes can be used to model linguistic uncertainty, see Figure 2.1. The most popular fuzzy set shapes are the triangular and trapezoidal ones, because of their simplicity of representation, and ease of computer implementation. The fuzzy singleton is a special class of crisp set, with full membership only occurring for a unique observation value.

The way in which linguistic terms of a fuzzy variable are mapped onto its domain (or universe of discourse, UoD) can affect the performance of the controller in a number of ways, see Section 6.3.2. In order to discuss these influences it is necessary to introduce some definitions of parameters which characterise a membership function.

Peak Value

This is the point at which the degree of membership for a given linguistic value (μ) is 1, i.e. $\mu(x_{\text{peak}}) = 1$, see Figure 2.2. In the case of trapezoidal membership functions the peak value is an interval.

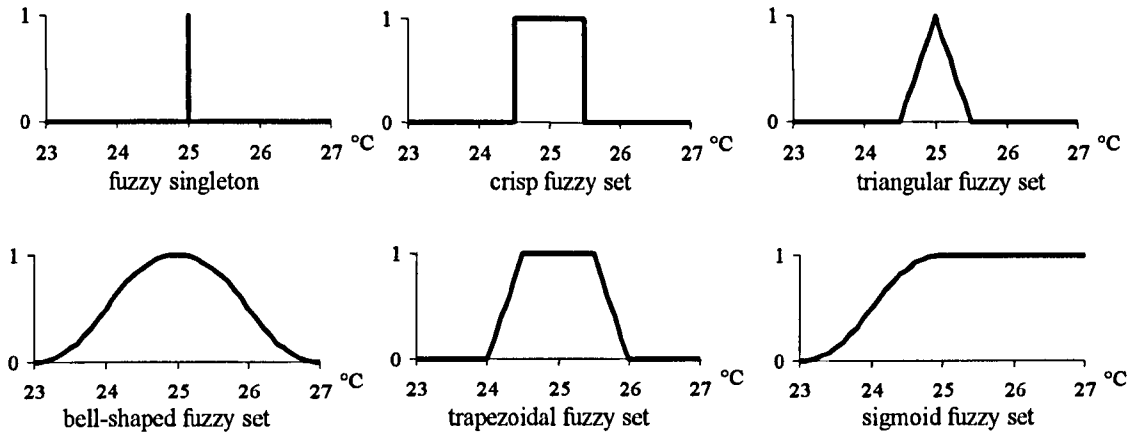


Figure 2.1: Different fuzzy set membership functions

Left and Right Width

The left width of a membership function μ is the length of the interval from the peak value to the point when the degree of membership equals zero. Similarly the right width is the interval from the peak value to the point to the right of the peak value when $\mu(x) = 0$. The sum of the left and right widths defines the support of μ , see Figure 2.2. If the left and right intervals are equal the membership function is said to be symmetrical.

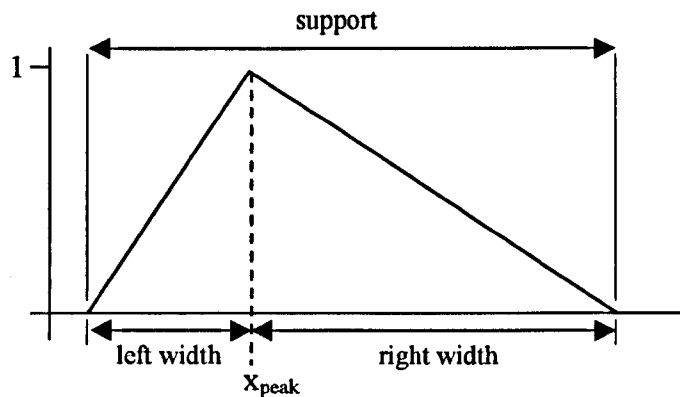


Figure 2.2: The peak-value, left width, right width and support of a triangular membership function.

Cross-point

Usually, neighbouring membership functions on a given UoD intersect, allowing an observation to exist in more than one set simultaneously. Let μ_1 and μ_2 be two membership functions representing two linguistic values upon the same universe of discourse. A cross-point between μ_1 and μ_2 is that value x_{cross} within the universe of discourse such that;

$$\mu_1(x_{\text{cross}}) = \mu_2(x_{\text{cross}}) > 0 \quad (2.1)$$

The cross-point level is defined by the degree of membership at $\mu_1(x_{\text{cross}})$ which by definition of the cross-point is the same as $\mu_2(x_{\text{cross}})$. The cross point ratio is the number of cross-points between two neighbouring membership functions. In triangular sets this can only ever be 1 or 0.

Figure 2.3 illustrates the above definitions in the case of triangular functions. It is important to remember that all of the above notions are relevant for any type of membership function.

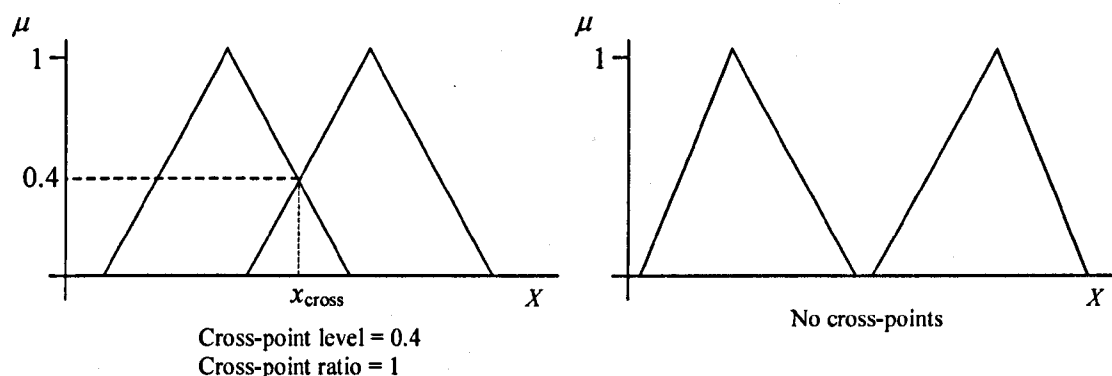


Figure 2.3: Cross-points and cross-point levels of triangular membership functions.

2.2.2 Fuzzy Inference

In a fuzzy logic controller (FLC) the possible output actions are defined using a number of IF-THEN rules. A collection of these rules forms the rule-base or knowledge-base of the FLC. Most FLCs use rules that have two inputs (or antecedents) and one output (or consequent). The inputs usually considered are the error from a desired set-point and the change in error. The output is either the actual control level or the change in control level (increment or decrement). Typically the fuzzy inputs and fuzzy outputs are described by seven linguistic sets, ranging from *positive big* to *negative big*. An example of a simple rule-base might be;

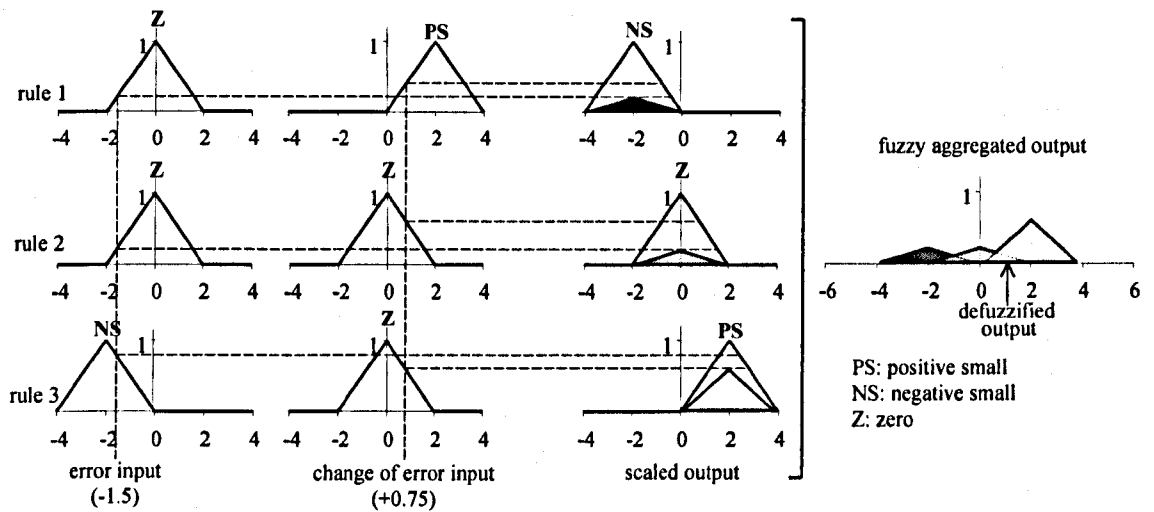
- 1). IF (*error is zero*) AND (*change in error is positive small*)
THEN (*output is negative small*).
- 2). IF (*error is zero*) AND (*change in error is zero*)
THEN (*output is zero*).
- 3). IF (*error is negative small*) AND (*change in error is zero*)
THEN (*output is positive small*).

The controller inputs are used to obtain the contribution of each rule to the final output. This is a process known as fuzzy inference. Using what is known as individual-rule based inference, one first ‘fires’ each rule with a fuzzy singleton and obtains n scaled or clipped consequent fuzzy sets that are aggregated to form the fuzzy output. Scaled sets are produced using Larsen’s implication operation (also known as MAX-DOT inference) [Kaufman, 1975] and clipped sets are produced using Mamdani’s implication operation (also known as MAX-MIN inference) [Mamdani *et al*, 1981]. This process is best clarified graphically using the above rule-base example, see Figure 2.4.

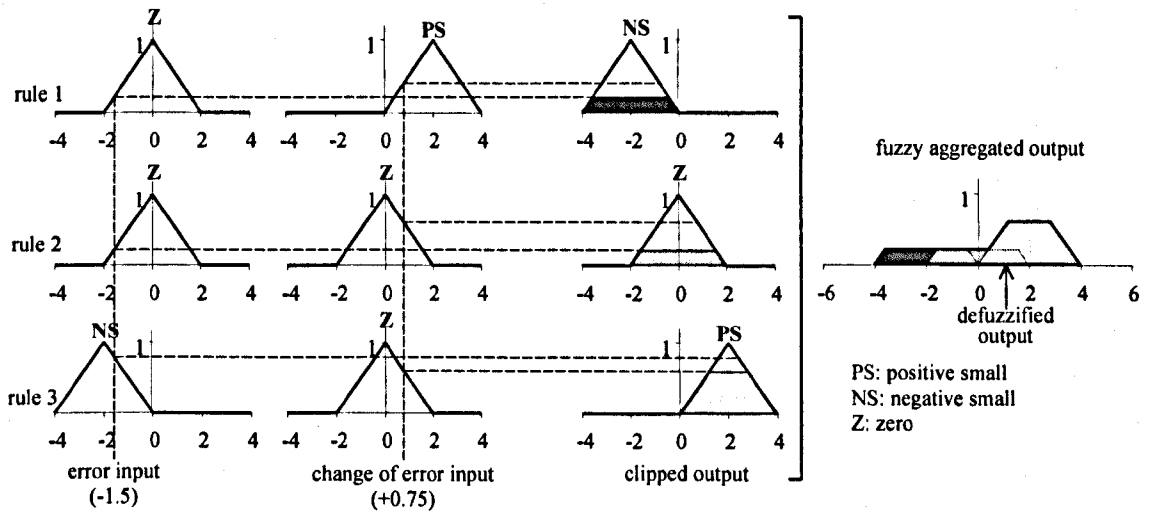
The firing weight of a rule (as defined by the height of the clipped or scaled fuzzy set) is normally obtained using the minimum height of the antecedent memberships. This is known as the liaison operator, and other operators include algebraic product, bounded sum, bounded product and drastic product. The minimum and algebraic products are the most commonly used liaison operators and have different advantages depending upon their application.

Algebraic product will produce smaller firing weights than the minimum operator if the input memberships are less than 1, see Figure 2.5.

The final stage of the inference process is to derive a scalar output from the fuzzy aggregated output. This is known as defuzzification and is discussed in the next section.



(a)



(b)

Figure 2.4: Diagram of the fuzzy inference mechanism using (a) scaled fuzzy sets (Larsen's implication) and (b) clipped fuzzy sets (Mamdani's implication).

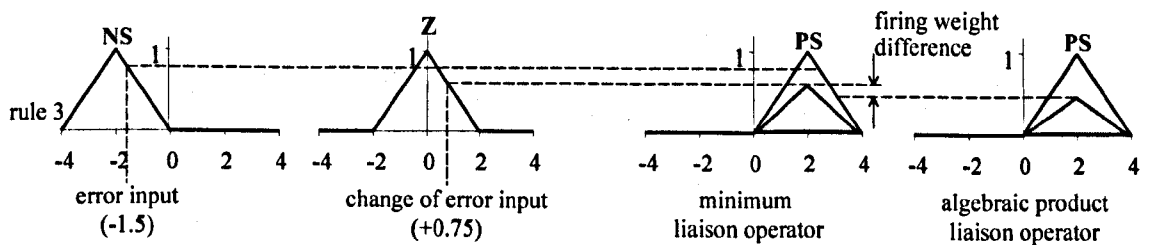


Figure 2.5: Difference in rule-firing outputs using the minimum and algebraic liaison operators.

2.2.3 Defuzzification

Many methods exist for output defuzzification, but perhaps the most widely used are centre-of-gravity (CoG) and centre-of sums (CoS). The main function of the defuzzification process is to take the distributed fuzzy output derived using the inference process (as described above) and produce a single output value that can be used to drive the controlled process.

The CoG method finds the balance point of the aggregated fuzzy output. In this case the aggregated fuzzy output is the union of the scaled (or clipped) rule consequents. The CoS method is identical to CoG except the aggregated fuzzy output is the sum of the rule consequents, see Figure 2.6.

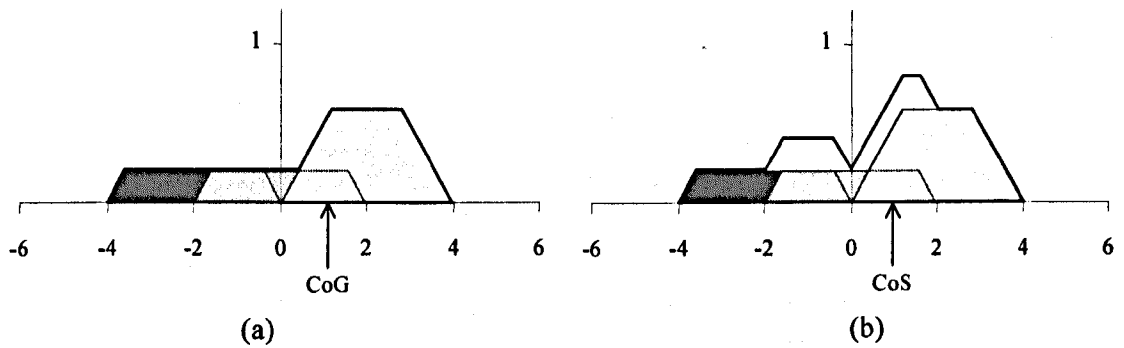


Figure 2.6: Comparison between (a) centre-of-gravity defuzzification method where the aggregate is formed by taking the union of the consequent sets and (b) centre-of-sums defuzzification method where the aggregate is formed by taking the sum of consequent sets. The bold line indicates the aggregated fuzzy output.

2.3 Biomedical Applications of Fuzzy Logic

The following biomedical applications of FLC have been found and are discussed in more detail below;

- 1). Post-surgical control of mean arterial pressure (MAP).
- 2). Control of depth of anaesthesia (DOA).
- 3). Ventilator control.
- 4). Control of FiO_2 and isoflurane delivery in minimal flow anaesthesia.
- 5). Pace-maker regulation.
- 6). Treatment of renal anaemia.
- 7). Post-operative pain control.

2.3.1 Post-surgical Control of Mean Arterial Pressure

The fast-acting vasodilator drug sodium nitroprusside (SNP) is used to treat patients who demonstrate elevated systemic arterial blood pressure after open-heart surgery. The rapid and powerful action of SNP requires the frequent monitoring of mean arterial pressure (MAP), followed by adjustment of SNP infusion rate. Ying *et al* (1992) proposed a closed-loop controller that would relieve nurses of this task, leaving them free to perform other duties. A simple 4 rule FLC [Ying, 1988] that derived changes in SNP infusion rates based upon error from MAP set-point (e) and rate of change in error (\dot{e}), was converted into a set of 10 non-fuzzy control algorithms. This gave a precise analytical representation of the fuzzy controller, a feature not usually possible since most FLC structures are very complex. These non-fuzzy algorithms describe the control relationship in terms of the input and output scaling factors and the turning point of the fuzzy sets. These were optimised using a Laplace model of the SNP/MAP relationship, to give the best generalised control of patients with a wide range of sensitivities to SNP.

Ruiz *et al* (1993) produced a much simpler FLC that used 3 trend measures of MAP over 160, 80 and 20 second observation windows, to determine whether the SNP infusion rate should be increased, decreased or maintained. These trends gave an indication of the long-term and short-term MAP behaviour. Having established the action required, the SNP infusion rate was then adjusted using quantitative relationships. This approach was shown to give adequate performance with small over and undershooting outside of predefined limits, and produced significantly better performance than manual control. The control algorithm separates the problem into qualitative "What to do?" using FLC and quantitative "How much?" using clinically proven relationships.

2.3.2 Depth of Anaesthesia

Two areas of anaesthesia control have been explored using FLCs; unconsciousness using inhaled anaesthetics, and muscle relaxation using infused neuromuscular block. Unconsciousness is considered to be the depth of anaesthesia (DOA) necessary to counteract physiological response to surgical stimuli (i.e. the incision of a scalpel). Muscle relaxation on the other hand is necessary to prevent potentially fatal involuntary movements in a patient.

Unconsciousness Anaesthesia

Traditionally DOA has been controlled by maintaining systolic blood pressure (SBP) at pre-anaesthetic levels. Tsutsui & Arifa (1994) described an FLC for the closed-loop control of SBP via enflurane anaesthesia. The SBP was sampled every 30 seconds and the current value and previous value were used as the inputs to the FLC, with the output being the enflurane percentage concentration. Rules were constructed to establish an initial SBP value of MAC-BAR (minimum alveolar concentration to block adrenergic response in 50 % of patients [Roizen *et al*, 1981]), and maintain it at AD_{95} (the known value of anaesthetic effective dose for 95 % of patients [Dejong & Eger, 1975]). In clinical trials the FLC maintained SBP to within ± 20 % of the pre-anaesthetic SBP in 82 % of cases, compared to 83 % using manual control.

Meier *et al* (1992) developed a similar FLC for the control of DOA using proportional-integral (PI) control. Instead of SBP, the inputs to the FLC were the error from mean arterial pressure (MAP) set-point and the integral of the error. The output was the % concentration of isoflurane and the integral of the inspired isoflurane fraction. In clinical trials [Zbinden *et al*, 1995], the FLC outperformed human control at skin incision (maintaining 48.2 % of all MAP values within ± 10 % of the desired level, compared to 40.4 % using human control), but performed slightly worse during the rest of the operation (78.3 % using FLC and 82.3 % using human control).

It is questionable whether arterial blood pressure alone provides an accurate measure of the DOA and therefore a guarantee of unconsciousness in the patient. This problem was addressed by Shieh *et al* (1998) using a hierarchical control structure based on SAP, heart rate (HR) and end-tidal gas concentrations (Et) to adjust desflurane concentration. The first hierarchical level used an FLC to control SAP at set-point. The second level used a rule-base to control HR in the stable condition. A third level used anaesthetists' experience to tune the SAP set point level when Et reaches upper and lower limits. To prevent awareness during anaesthesia a fourth level used the low limit of Et to determine the dose of inhaled anaesthetics, and finally an alarm level to warn when SAP and Et are going out of safe limits. In clinical trials automatic control was maintained for 89.15 % of the time, with manual control being necessary when the patient's condition fell outside the abilities of the controller or the controller was failing to maintain the patient as required.

Another multi-factorial approach to DOA control was employed by Abbod & Linkens (1998). They used fuzzy logic fusion to combine two measures of DOA; auditory evoked response (AER) depth of anaesthesia (AER_DOA) and cardio-vascular based DOA (CV_DOA); into a final measure of DOA (F_DOA) that was used to control the infusion rate of propofol given to a patient. The AER_DOA was based on wavelet analysis of the AER signal and was classified using an Adaptive Network Based Fuzzy Inference System (ANFIS) [Jang, 1993]. Using a hybrid learning procedure, ANFIS can learn input-output mapping based on human knowledge (in the form of IF-THEN fuzzy rules). The AER_DOA was classified as *awake*, *light*, *ok_light*, *ok_deep* and *deep*. The CV_DOA used the same classifications of DOA and was based upon observations of HR and SAP, with the rule-base derived from anaesthetist's experience [Linkens *et al*, 1996]. The final DOA produced from the fuzzy logic fusion module was fed to the propofol plasma concentration controller. This fuzzy logic rule-based controller, used the current target concentration and the measured DOA to calculate a new target plasma concentration. From this

the drug infusion rate was derived using a 3-compartment patient model with an additional effect compartment. The overall DOA control system was validated using a computer simulated patient model, describing the pharmacokinetics and pharmacodynamics of propofol in the plasma. The outputs of the model were SBP, HR and AER. The results obtained from closed-loop simulations showed that the system effectively maintained the patient at clinically acceptable DOA. Clinical trials were being undertaken at the time of publishing.

Muscle Relaxant Anaesthesia

In 1988, Linkens & Mahfouf described a simple FLC for automated drug infusion of atracrium for muscle relaxant anaesthesia, where the problem of knowledge elicitation was tackled using self-organising fuzzy logic techniques. The efficacy of the controller was investigated via extensive simulation studies using a non-linear model of the drug response. Linkens & Abbod (1993) discussed the importance of such anaesthesia simulators for the design of supervisory rule-based control in the operating theatre.

Mason *et al* (1994) described a similar fuzzy controller using a PD + I (proportional, differential plus integral) configuration. The rules of the FLC were handcrafted based on simulations involving the non-linear atracrium dose-response characteristics. This was assessed clinically [Mason *et al*, 1996] and gave good control performance although the infusion rate appeared erratic. An alternative schema, using a self-learning fuzzy logic controller (SLFLC) was proposed in 1997 [Mason *et al*, 1997]. This started with a blank PD (proportional-differential) rule-base and adapted the outputs of the fuzzy control rules in real time to match the needs of each individual patient. In clinical trials the atracrium infusion rate was observed to be much less erratic than when using the earlier simple FLC with a fixed rule-base, and the overall control performance was very good. A hierarchical approach to muscle relaxant anaesthesia, similar to that applied to desflurane anaesthesia, was considered by Shieh *et al* (1996 and 1997).

2.3.3 Ventilator Control

The use of fuzzy-logic for ventilator control (and this includes advisory systems) has not been that widely explored. One of the earliest examples is that of Vasil'eva *et al* (1989). They used an FLC to adjust the inspiratory gas flow (\dot{V}_I) produced by a ventilator in response to changes in alveolar pressure ($PA(t)$). A simple model of the lung mechanics during inspiration and expiration was used to test the FLC.

Sun *et al* (1994) described an FLC for the adjustment of FIO_2 in ventilated new-born infants. The controller utilised rules elicited from neonatologists and was implemented in real-time. Clinical trials were being conducted at the time of publication.

In the 1980s, high-frequency jet ventilation (HFJV) came into vogue. This uses much smaller tidal volumes (typically 2.2 to 5.0 ml/kg) and higher respiratory frequencies (60 to 300 rpm) than conventional mechanical ventilation. Its ability to provide ventilation at much lower inspiratory pressures promised much, unfortunately the complex and non-linear relationship between RR, VT and $PaCO_2$ made routine application difficult. Noshiro *et al* (1994) used a fuzzy PI control system to successfully regulate end-tidal PCO_2 ($P_{ET}CO_2$) in a new HFJV ventilator. They compared the

closed-loop response of the FLC and a conventional PI compensator on 11 anaesthetised and intubated mongrel dogs. The performance of the two systems was almost identical, however the FLC was found to give better generalised control.

Shäublin *et al* (1996) described the closed-loop control of end-tidal CO₂ content fraction (F_{ETCO_2}) via the adjustment of VT and RR, in artificial ventilation during anaesthesia. This was done whilst minimising the deviation of VT and RR from normal values of 10 ml/kg and 10 rpm respectively, and attempting to maintain the plateau airway pressure (P_{plat}) within suitable limits (<3 – 4 kPa). Compared with human controllers, the FLC maintained desired F_{ETCO_2} with similar precision and stability and gave good dynamic response to set-point changes. The breathing pattern, selected by the FLC was within clinically acceptable ranges. However, apart from maintaining P_{plat} within acceptable limits, the controller did not adapt the ventilator settings to the lung function or lung mechanics of an individual patient, a feature offered by the adaptive ventilator controllers of Labscher *et al* (1994) and Weiler *et al* (1994).

Most recently, Nemoto *et al* (1999) developed a fuzzy-logic based advisory system (FLBAS) for the control of pressure support (PS) ventilation in patients with chronic obstructive pulmonary disease (COPD). Pressure support is prescribed for spontaneously breathing patients that are triggering breaths for themselves but require additional pressure to aid inflation of the lung because of muscle insufficiency or increased work of breathing. It enables the patient to be gradually weaned from artificial ventilation by gradually reducing the amount of pressure support (in cmH₂O) required.

Nemoto *et al* used observations of heart rate, arterial O₂ saturation (SaO_2) and current RR and VT settings to determine the percent change in PS required. These observations defined a measure of the patient's status and were assigned to a quantity called CONDITION, having four possible categories: POOR, QUESTIONABLE, MODERATE and GOOD. A second quantity called TREND used observations of RR, change of RR, and change of SaO_2 to derive a measure of whether the patient's condition is STABLE, IMPROVING, DETERIORATING or CRASHING. These were then combined using fuzzy-logic fusion to produce the controller output % PS-change, labelled as INCREASE A LOT, INCREASE, MAINTAIN and DECREASE. Validation of the control rules was only made using retrospective comparison against actual clinical decisions made on 13 ICU patients. Consequently, whilst the advisor was found to have generally good agreement, there is no evidence of the controller's stability in closed-loop control.

2.3.4 Miscellaneous Applications

These have been included to illustrate the breadth of biomedical fuzzy-logic applications, and represent applications not falling into the above larger categories.

Sugiura *et al* (1991) applied fuzzy-logic to the control of cardiac-pacemaker rate based upon observations of RR and body temperature (T_{BODY}). The fuzzy relationship between RR and T_{BODY} on intrinsic heart rates were derived using 3 mongrel dogs. The pace-rates calculated using the derived fuzzy rules were then compared against the intrinsic heart rates of 2 different dogs.

Carolla *et al* (1993) reported the use of FLC for the control of alfentanil infusion for post-operative pain relief. This was achieved using a simulated patient model of drug pharmacodynamic relationships.

Bellazzi *et al* (1994) described the use of FLC in the delivery of recombinant human erythropoietin (r-HuEPO) for the treatment of renal anaemia. Validation was achieved by performing a case-simulation study using a multi-compartmental model of the erythropoietic response to r-HuEPO. The FLC was able to adapt to patient drug sensitivity.

Curatola *et al* (1996) used fuzzy logic to control inspired isoflurane and O₂ concentrations during minimal flow anaesthesia (MFA). The FLC enabled isoflurane and FIO₂ to be maintained at set levels during MFA performed by anaesthetists not trained in minimal flow technique. When using MFA the inspired gas concentrations do not correspond with those in the fresh gas because of mixing with exhaled alveolar gas, making human control difficult. The FLC was able to demonstrate reliable isoflurane and FIO₂ control and reduced anaesthetic gas delivery and costs over the human operator.

Becker *et al* (1997) described the design and validation of a fuzzy logic based intelligent patient monitoring and alarm system to ease the cognitive load of anaesthetists during high invasive surgery.

2.4 Summary & Conclusions

The basic principles of fuzzy set representation and an overview of the mechanics of individual rule-based inference and defuzzification have been described.

The review of FLC applications highlighted an increased interest in the use of FLCs in biomedical applications, and this has led to their clinical acceptance in certain areas. Some simple controllers have been developed for the maintenance of artificially ventilated patients, but these have been restricted to subsets of the overall care problem. Model-based validation has been demonstrated to be of particular benefit for stability analysis and controller optimisation, although it has not yet been applied to ventilatory care.

The next chapter reviews the models suitable for the development of a patient simulator for the validation of a fuzzy-logic-based advisor for the ventilation of patients on artificial ventilation.

Chapter 3: Review of Respiratory Models

3.1 Introduction

This chapter presents a critical review of mathematical models of the human respiratory system, placing them within historical context and according to various classification criteria. Particular attention is given to those models, or model elements suited to the development of a patient simulator for the purpose of advisor validation. The correct choice of model is a trade-off between complexity and clinical usefulness. A model with too much complexity becomes difficult to implement, whereas over simplification limits the range of physiological behaviour that can be represented. Consideration also needs to be given to the estimation of the model parameters to match its behaviour to that observed clinically. Again if the model is too complex then this becomes increasingly difficult to achieve as the number of unknown parameters increases.

Classification According to Process

Historically, models of the human respiratory system have been developed to explain various aspects of the process and can be categorised accordingly;

- 1). **Lung Mechanics:** models of the mechanics of breathing being concerned with volume, flow and pressure characteristics of the lung system.
- 2). **Ventilators:** models describing artificial mechanical ventilators, often developed in conjunction with models of lung mechanics.
- 3). **Gas Exchange:** models concerned with gas exchange in the lungs. Usually only O₂ and CO₂ but may also include the transport of N₂ (nitrogen) and CO (carbon monoxide).
- 4). **Gas Dissociation:** models of the relationship between blood-gas partial pressures and contents.
- 5). **Respiratory Control:** models concerned with the self-regulating mechanisms of breathing to maintain O₂, CO₂ and pH homeostasis.
- 6). **Integrated:** a combination of any number of the above model elements, describing their interaction to form a cohesive description of the entire respiratory process.

The lung mechanics, ventilator, gas transport, gas dissociation and respiratory control models are known as *local models* and only deal with part of the respiratory system, whereas the integrated models are *global*. This is not a measure of their complexity, since integrated models may contain many simplifications resulting in poor specificity, whilst local models can contain deep physiological knowledge that make them comprehensive within their domain of operation.

Classification According to Method of Implementation

A number of approaches to model implementation are available and these fall into one of three broad categories;

- 1). **White-Box Models:** also known as theoretical models, these are based soundly and explicitly upon the underlying physical and chemical processes.
- 2). **Black-box Models:** also known as empirical models, these are concerned with the interaction and interdependence of system variables, being mathematically representative of the process but imparting little in the way of physical meaning. Such models include regression models, neural models and parametric identification models.
- 3). **Grey-box Models:** also known as empirico-theoretical models, these cover the majority of models, being based where possible upon the underlying physical and chemical processes but also dependent upon empirical relationships.

Usually, model development aims to be as theoretical as possible (white-box modelling) enabling interpretation by the widest possible audience. It also helps to identify possible model inadequacies and assumptions made in the model, a process often difficult using black-box models.

3.2 Grey-Box Models

It is difficult to draw a distinction between gas exchange/transport models and respiratory control models, since their development is often dependent and interrelated. However, the research has often focused more on either physiological process modelling or ventilatory control modelling. More complex models also began to introduce many integrated physiological components including lung mechanics and empirical physiological relationships describing disease states. The following reviews have therefore been grouped according to the process types, however there will inevitably be some overlap between them.

3.2.1 Respiratory Mechanics Models

Respiratory mechanics models describe the relationship between inspiratory and expiratory flow rates and the pressures generated across the airway and alveolar space. Typically they describe the lung mechanics in terms of total flow resistance (R) and total compliance (C), but may also include terms describing the properties of the ventilator (if artificial ventilation is being considered). Compliance (in l/cmH₂O) is an indicator of lung and chest-wall elasticity and flow resistance (cmH₂O/l/sec) reflects resistive properties of both the tissue and peripheral airways.

Several studies characterising the main aspects of breathing have been published. These have used different lumped-parameter models, ranging from a simple two-element resistance-compliance linear model to more sophisticated physiological models which include tissue viscoelasticity, the inertial effects of the airways and branching networks [Lutchen & Costa, 1990], to non-linear models [Ben-Haim *et al*, 1988].

Barbini *et al* (1994) compared the Bode diagrams of four lumped-parameter resistance-compliance models against those clinically observed on mechanically ventilated patients. They found that the simple two-element series R-C model (see Figure 3.1a) produced Bode diagrams basically different from the clinical responses. This was resolved by the inclusion of an additional parallel compliance (C_p), see Figure 3.1b, although no physical meaning was attributed to this new element.

More complex models have been suggested; a 4-element R-C model [Mead, 1969]; 6-element R-C-I model (where I is an inductance component) [Dorkins *et al*, 1988] and a 9-element R-C-I model [Jackson & Lutchen, 1987]. However, this level of complexity may be useful in describing the frequency behaviour of the lungs across the range 0-200 Hz, but does not provide any real benefits in terms of clinical understanding.

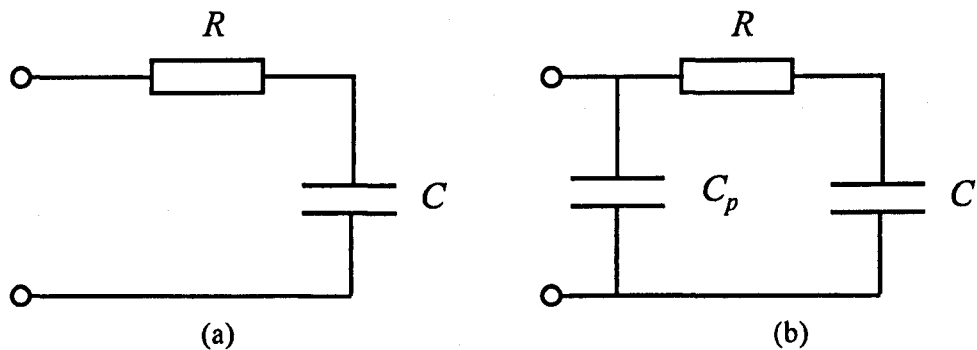


Figure 3.1: Electrical analogues of (a) the simple 2-element R-C airway model and (b) with an additional parallel compliance as proposed by Barbini *et al* (1994).

3.2.2 Gas Exchange Models

These models are concerned with descriptions of the gas diffusion between the alveolar space and the pulmonary capillaries. They form a key component in integrated model development and represent a significant part of the “controlled” process in models of respiratory control.

The diffusion boundary is usually described in terms of a linear homogenous blood-gas barrier offering resistance to diffusion of the gases [Piiper & Scheid, 1981]. This assumes diffusion occurs only perpendicular to the barrier and is governed by Fick’s law of diffusion.

Early gas exchange models represented the lung as a single ideal alveolus compartment with a ventilation-perfusion ratio of unity ($\dot{V}/\dot{Q}=1$) [Grodins *et al*, 1954]. This was extended to include dead space and shunt compartments with $\dot{V}/\dot{Q} = \infty$ and $\dot{V}/\dot{Q} = 0$ respectively [Riley & Cournard, 1949]. Using this classical gas exchange model it was possible to represent a wide range of patho-physiology. However, \dot{V}/\dot{Q} varies across the lung in an approximately log-normal manner [Farhi & Rahn, 1955] and this gives rise to differences in O_2 uptake from those obtainable using the 3-compartment model. West (1969) examined lung models with 3-1000 respiratory segments and found that 10-compartments was sufficient to describe this log-normal \dot{V}/\dot{Q} distribution. Kelman (1970) used a 25-compartment approximation to the log-normal \dot{V}/\dot{Q} distribution. Recently, 4-compartment models of gas exchange have been employed [Petros *et al*, 1993; Rutledge (1994 & 1995), providing a trade-off between representative O_2 uptake (and CO_2 elimination) and clinical usefulness.

3.2.3 Gas Dissociation Models

Models of the relationship between blood-gas tensions (partial pressures) and blood-gas contents have been used to bridge the gap between the mass transport blood circulation models (concerned with gas contents) and the lung diffusion models that are driven by differences in partial pressure between the alveoli and pulmonary capillaries. Similarly, gas partial pressures and not contents drive the chemoreceptors for ventilatory control. The relationship between pressure and content of each gas was determined early this century by driving off the gases from blood in successive steps – hence the term “dissociation curve”.

Oxygen Dissociation Curves

In 1966 Kelman published an empirical description of the O₂ dissociation curve (ODC), suitable for computer implementation. It extended the previous work of Adair (1925) and accounted for shifts in the position of the curve due to pH, PCO₂, temperature and haemoglobin concentration, and has widely been accepted to be accurate for the majority of applications.

However, at lower PO₂ the curve was found to diverge from experimentally determined values and Kelman (1968) corrected for this by switching to a different expression for O₂ saturation when PO₂ was below 10 mmHg.

Ingram & Bloch [1986] developed a very similar algorithm to that of Kelman, using the same equation to derive O₂ saturation. However shifts in the position of the curve were based upon organic phosphate 2,3-diphosphoglycerate (2,3-DPG) concentration in haemoglobin, temperature, pH and base excess (BE). Corrections to the pH and BE effects were made according to the 2-3-DPG levels. Additional shifts in the ODC position were accommodated by the inclusion of the ratio $26.833/P_{50}$ in the expression for virtual O₂ pressure, where P₅₀ reflects the 50% saturation point of the ODC and 26.833 mmHg is the normal operating point.

Earlier ODC formulations are reviewed by Roughton (1964).

Carbon Dioxide Dissociation Curves

Kelman (1967) also formulated an algorithm for the conversion of PCO₂ into CO₂ content, taking into account the effects of haematocrit, pH, temperature and PO₂. This was based upon the earlier nomogram of Singer & Hastings (1948).

Inverse Dissociation Curves

Unfortunately the gas exchange and respiratory control models require the calculation of the inverse of the dissociation functions. This is normally achieved using an iterative solution-searching algorithm. Severinghaus (1979) did attempt to derive an explicit inverse function but it did not handle corrections required for shifts in pH and temperature.

3.2.4 Respiratory Control Models

These models attempt to describe the regulation of respiration via physiological feedback mechanisms, which indirectly monitor the amount of O₂ and CO₂ in the blood and adjust the level of alveolar ventilation to maintain homeostasis. This element of the respiratory system describes

the respiratory “controller” (respiratory centre) and has usually been developed alongside models of the controlled process, i.e. respiratory plant (lung apparatus and body tissues).

In 1954 Grodins *et al* presented one of the earliest chemo-stat models of respiratory control. It described changes in ventilation in response to partial pressures of CO₂ (PCO₂). The process model was based upon the laws of mass transfer and the respiratory centre was described by an empirical “black-box” model, that of a simple proportional controller;

$$\dot{V} = K_1 \cdot P\bar{v}CO_2 + K_2 \quad (3.1)$$

where K₁ and K₂ are constants and P \bar{v} CO₂ is the mixed venous PCO₂. However, basing feedback on P \bar{v} CO₂ was incorrect and later studies used arterial PCO₂. The alveolar PCO₂ was provided as a model output, enabling experimental confirmation of responses to the input stimulus of inspired gas PCO₂.

Significant improvements in descriptions of the gas transport models were made and in 1960 Defares *et al* added a brain tissue compartment with cerebral blood flow varying with PCO₂. Further details of earlier models relating to the control of breathing in general and the relation of chemical and non-chemical factors are reviewed by Defares (1964) and Yamamoto and Raub (1967).

In 1965, Milhorn *et al* published a model that included elements of the chemical control of respiration previously ignored. These included the role of O₂ and circulatory time delays in the feedback loop. They considered the regulation of respiration to be a function of brain tissue PCO₂ (PbCO₂, central component), aortic-carotid body PO₂ (PaCO₂, peripheral component) and hydrogen ion concentration ([H⁺]). Making use of the relationship between [H⁺] and PCO₂ the alveolar ventilation was reduced to a function of two variables;

$$\dot{V}_A = f(PbCO_2, PaO_2) \quad (3.2)$$

The mechanical status of the lung was also included in the controller. The controlled process was represented using lung, brain and tissue compartments with gas storage and transport equations derived from mass balance relationships. Cerebral blood flow depended upon arterial PCO₂ and PO₂. The ventilation was continuous with no breath-by-breath modelling.

Grodins *et al* (1967) extended the process model further and the controller described the ventilation as a function of brain PCO₂, the fractional concentration of alveolar O₂ and the H⁺ concentration in the cerebral spinal fluid. This model represented a major advance towards a comprehensive model that could be used to test a wide variety of forcing inputs.

Milhorn and Brown (1971) published a comparison of two older models of the controller subsystem connected to an updated process model. They compared the classical controller equation of Gray (1950) against the more recent work of Lloyd and Cunningham (1963). Both equations were developed using curve-fitting methods, the former incorporating an additive combination of CO₂ and O₂ whereas the Lloyd model contained multiplicative as well as additive CO₂ terms. Milhorn and Brown concluded that the Lloyd-Cunningham version was more accurate over the range for which it was intended, although the equation would need to be extended if the entire control range was to be covered, i.e. the low O₂ and CO₂ range.

The next significant advance was the inclusion of the response to perfusion of the medulla resulting in high cerebrospinal fluid PCO_2 [Millhorn and Reynolds, 1973]. This increased the range of stimulus to which the model could successfully be subjected and therefore significantly increased its validity.

In 1980 Saunders *et al* produced a comprehensive model of the human respiratory system, incorporating effects within the respiratory cycle. This extended what had previously only been a continuous ventilation model into one that described control on a breath-by-breath basis. This model was based upon that developed by Grodins *et al* (1967) and was adapted to include cyclic ventilation, dead space, blood shunt and a separate muscle compartment. Sarhan (1983) in his Ph.D. thesis modified this cyclical model to explore the relationships between the elements of the breathing pattern.

More recent work has modified earlier respiratory control models to examine apnea response and unstable breathing [Longobardo *et al*, 1989] and more dynamically the maturation of chemo-reflex loops in new-born infants [Revow *et al*, 1989].

3.2.5 Integrated Models

Early attempts at integrated models were often only theoretical since the relationships between system elements required numerical methods only possible using a computer. These were either not invented or were inadequate for the complexities of the task. Perhaps one of the most significant breakthroughs occurred in 1973 with the model proposed by Farrel and Siegel. At the time it represented one of the most complete descriptions of a respiratory system and contained 10-compartment alveolar-pulmonary gas exchange [West, 1969], lung mechanics [Wald *et al*, 1969; Mead, 1961], lumped arterial, venous and tissue pools, non-linear gas dissociation relationships for O_2 and CO_2 [Kelman, 1966 and 1967], the interaction of cardiac function and tissue metabolism, and respiratory control in response to pH, PaCO_2 and PaO_2 [Lloyd and Cunningham, 1963]. More importantly, it attempted to address the problem of matching model inputs and outputs to quantifiable physiological parameters that could be measured in man or animals to facilitate thorough testing of the simulations.

The benefits of such a system for self-instruction were highlighted by Modell *et al* (1974) who created a collection of 15 programs written in BASIC for teaching the principles of lung mechanics, general gas exchange, ventilation-perfusion relationships and acid-base balance. Their approach was to split the system into separate modules, providing assumptions about the boundary conditions.

Dickinson (1979) took the next logical step and integrated all of these aspects of respiration into a comprehensive computer model called MacPuf, specifically for the purposes of teaching and self-instruction. It was a difficult model to interpret, due to its constant use of computational approximations and the explanation of the physiology in FORTRAN statements rather than using mathematical conventions. It was based strongly on the work of Farrel and Siegel, although the alveolar-pulmonary gas exchange was described using a much simpler 3-compartment model [Riley and Cournard, 1949], with ideal alveolus, dead space and shunt compartments. No attempt

was made to model the respiratory dynamics, and although ventilation was divided into inspiratory, gas exchange and expiratory phases, the net result approximated to a continuous ventilation model with average gas tensions in the ideal alveolus. Whilst it did contain a respiratory control model, this could be bi-passed to allow the simulation of assisted ventilation. This appears to be the first attempt to provide modelling of both spontaneously ventilated and mechanically ventilated subjects. It allowed respiratory rate, tidal volume and inspired O₂ fraction to be specified with allowances for the addition of positive end-expiratory pressure (PEEP) and its effect on both venous admixture and cardiac output were modelled. The usefulness of the model for the purposes of teaching was evaluated by Hinds *et al* (1982) at in-service training courses for anaesthetists and specialists in intensive care, and for the undergraduate teaching of anaesthesia [Skinner *et al*, 1983].

The ultimate extension of a teaching model is one that encompasses all aspects of human physiology [Coleman and Randall, 1983] and these have been developed to aid anaesthesiology training [Schwid 1987; Schwid and O'Donnell, 1992]. However models of this complexity and depth are not required for the testing of the advisor developed in this thesis. Of particular interest are models developed specifically to simulate patients on artificial ventilation in ICU. Dickinson's MacPuf model has been used by other researchers as a basis for such development.

Whilst comprehensive, integrated models can exhibit a high level of realism, matching the number of system parameters to available data becomes more difficult with increased complexity. So although physiological model development will continue to increase in complexity as further understanding is gained, the true usefulness of a model is its applicability to the problem in hand. Selecting the right level of complexity is often a matter of trial and error. One might start with simple models, moving on to more complex ones if inadequacies are identified, or a complex model can be reduced in a principled manner to arrive at a model that can be matched to the data available.

3.2.6 Models of Respiration During Artificial Ventilation

Using Dickinson's model with the respiratory control stimulus disengaged, attempts were made to match the parameters of the model to clinically available data [Hinds *et al*, 1980]. This was done in an attempt to predict the steady-state arterial and venous blood-gases and hence check the physiological meaning of the model. Twelve patients ventilated after uncomplicated cardiac surgery were studied. The basic information required to simulate an individual patient was measured or derived and then the model unknowns adjusted iteratively to match the model predictions to the clinical measurements. The variables computed were then compared with those measured or derived clinically. Correlation between predicted and measured variables was generally good ($r > 0.9$) although PvO₂ correlated less well ($r = 0.85$).

This study was extended [Hinds *et al*, 1984] by tuning the steady-state model to individual patient data (as above) and then assessing its ability to predict changes caused by adjustments to the ventilator settings. The predictions were deemed acceptable given clinical variability and routine measurement inaccuracies.

A much simpler model, describing the mass transport of O₂ and CO₂ through a 3-compartment alveolus [Riley & Cournard, 1949] and lumped arterial, tissue, venous and pulmonary pools was used as an integral part of a system combining qualitative and quantitative data for mechanical-ventilator management, known as VentPlan [Thomsen & Sheiner, 1989]. The paper only described the O₂ transport equations fully, inferring that the CO₂ transport equations were analogous. Two alternative O₂ gas dissociation functions (GDF) were used depending upon the complexity of the problem. If corrections for temperature and pH were required then Kelman's (1966) function was used, and its inverse derived using a solution-searching algorithm. When these corrections were not needed an explicit inverse function was employed [Severinghaus, 1979], greatly reducing computational overheads.

More recently this model was extended to include better ventilator modelling, airway mechanics, and representation of ventilation-perfusion (\dot{V}/\dot{Q}) mismatch [Rutledge, 1994, 1995]. The ventilator model explicitly simulates volume-cycled, constant-flow ventilation. During inspiration the default setting represents a plunger moving at constant velocity to deliver the desired tidal volume. The simulator then leaves a short inspiratory hold time after the plunger stops, to allow remaining pressure to equilibrate with the airway. Then during expiration the pressure drops to the value of PEEP, and the outflow of air from the patient is limited by a variable outflow resistor (retard setting). The default configuration is for constant mandatory volume (CMV) mode of ventilation, but adjustable parameters allow it to simulate many volume-cycled constant-flow ventilators.

Instead of the Riley 3-compartment alveolar-pulmonary diffusion model there are 5-compartments: a series anatomical dead space, a parallel physiological dead space, a shunt and two alveolar compartments. The alveolar compartments can have different \dot{V}/\dot{Q} ratios to represent asymmetric ventilation perfusion distributions. Each alveolar compartment can also have different resistance and compliance values meaning that the distribution of ventilation will vary as a function of frequency of ventilation. Kelman's O₂ gas dissociation function was replaced by that of Hill *et al* (1973).

All of these models have used continuous rather than breath-by-breath models of the ventilation process, since the time scale of interest is in the order of 10 seconds rather than milliseconds. What matters is the change in average blood-gases, and not fluctuations during the breath-cycle.

3.2.7 Model-based Nomograms

These are really a sub-category of the models described previously, developed with the specific purpose of producing curves of practical use to clinical staff. We have already come across one example in the CO₂ dissociation models, that of the Singer-Hastings nomogram (1948). Severinghaus (1966) developed a similar tool for O₂ dissociation in the form of the "blood gas calculator".

Many other such nomograms have been developed to aid the understanding of respiratory physiology and assist clinical decision making. However, the iso-shunt diagrams of Benetar *et al* (1983) is of particular interest, since it enables the prescription of changes to inspired O₂ fraction (FIO₂) to achieve a desired PaO₂ (see Figure 3.2). This can be thought of as a crude therapy advisor tool. In Chapter 6 the relationships behind the iso-shunt lines are used to construct simple

rules pertaining to the maintenance of PaO₂ via adjustment of FiO₂. Because of this a detailed description of the equations behind the nomogram is given below.

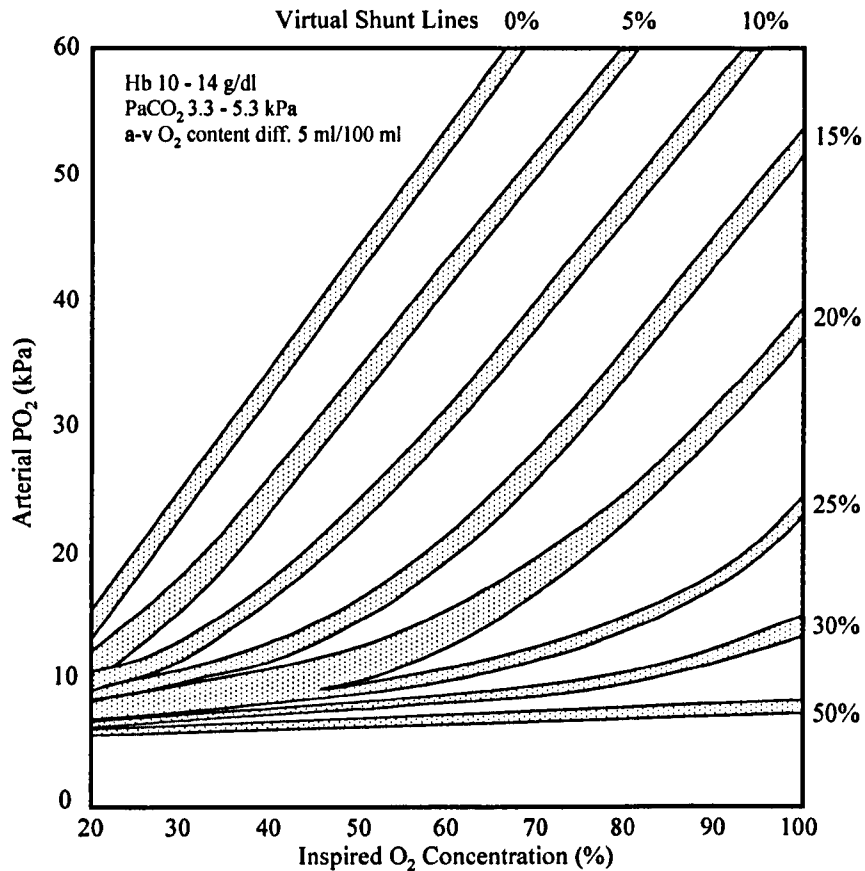


Figure 3.2: Iso-shunt diagram (redrawn from Benatar, Hewlett and Nunn (1973)). Iso-shunt bands have been drawn to include all values of Hb, PaCO₂ and arterial-venous oxygen content difference shown above.

Iso-Shunt Lines

The calculations used to construct the iso-shunt lines are as follows;

Calculate PAO₂ (alveolar oxygen tension)

$$PAO_2 = (P_{B_{dry}} \times F_{IO_2}) - \frac{PaCO_2}{R} \times (1 - F_{IO_2} \times (1 - R)) \quad (\text{kPa}) \quad (3.3)$$

where P_{B_{dry}} is the dry barometric pressure (assumed to be P_B - P_{H₂O}, where P_B is standard barometric pressure (101.325 kPa) and P_{H₂O} is the saturated water vapour pressure at body temperature (6.27 kPa)), R is the respiratory exchange ratio (assumed 0.8) and PaCO₂ is assumed to be 5.33 kPa.

Calculate $Sc'O_2$ (pulmonary end-capillary saturation)

$$Sc'O_2 = \frac{PAO_2^3 + 2.667 \times PAO_2}{PAO_2^3 + 2.667 \times PAO_2 + 55.47} \quad (3.4)$$

This assumes there is negligible alveolar/pulmonary end-capillary PO_2 gradient. It is the Severinghaus *et al* (1978) equation, a modified and more convenient alternative to the Kelman (1966) ODC.

Calculate $Cc'O_2$ (pulmonary end-capillary oxygen content)

$$Cc'O_2 = \alpha_b \cdot PAO_2 + Hb \cdot \beta_h \cdot Sc'O_2 \quad (\text{ml/dl}) \quad (3.5)$$

where Hb is the haemoglobin concentration, β_h is the Hb O_2 carrying capacity (assumed 1.31 ml/g) and α_b is the solubility of O_2 in blood (assumed 0.024 ml/dl/kPa).

Calculate CaO_2 (arterial oxygen content) for a given shunt

$$CaO_2 = Cc'O_2 - C(a-v)O_2 \times \frac{\dot{Q}_s/\dot{Q}_t}{1 - \dot{Q}_s/\dot{Q}_t} \quad (\text{ml/dl}) \quad (3.6)$$

where \dot{Q}_s/\dot{Q}_t is the shunt and $C(a-v)O_2$ is the arterial-mixed venous O_2 content difference (assume 5 ml/dl).

Calculate PaO_2 (arterial oxygen tension)

$$CaO_2 = \alpha_b \cdot PaO_2 + Hb \cdot \beta_h \cdot SaO_2 \quad (\text{ml/dl}) \quad (3.7)$$

where SaO_2 is the arterial O_2 saturation as given by the Severinghaus equation;

$$SaO_2 = \frac{PaO_2^3 + 2.667 \times PaO_2}{PaO_2^3 + 2.667 \times PaO_2 + 55.47} \quad (3.8)$$

PaO_2 is calculated by substituting equation 3.8 for SaO_2 into equation 3.7 and obtaining the positive, real root of the following quadratic equation;

$$\alpha_b \cdot PaO_2^4 + (Hb \cdot \beta_h - CaO_2) \cdot PaO_2^3 + (2.667 \cdot \alpha_b) \cdot PaO_2^2 + (55.47 \cdot \alpha_b + 2.667 \cdot Hb \cdot \beta_h - 2.667 \cdot CaO_2) \cdot PaO_2 - 55.47 \cdot CaO_2 = 0 \quad (3.9)$$

using an iterative programme capable of solving such equations.

The iso-shunt lines produced by these equations were found to give satisfactory prediction of PaO_2 for FiO_2 in the range 35 to 100 %. Petros *et al* (1993) extended the model behind the iso-shunt lines so that it would behave correctly for FiO_2 below 35 %, as found during O_2 delivery via a ventimask. This required the inclusion of a 2-compartment representation of mismatch of ventilation-perfusion ratios in addition to shunt.

3.3 Black-Box Models

An altogether different approach to the prediction of alveolar oxygen and carbon dioxide tensions from those previously mentioned has been proposed by Rudowski *et al* [1991]. They have used linear multiple regression techniques with PaO_2 and $PaCO_2$ as the dependent variables to construct statistical models for individual patients, specific diagnostic groups and general patients. The usefulness of the approach is that such analysis may bring about a better understanding of the factors influencing arterial gas tensions in ventilated patients with acute respiratory failure. This can be thought of as clinically-based sensitivity analysis.

Twenty patients were assessed falling into three patients groups; those with pneumonia, chronic obstructive pulmonary disease (COPD) and left ventricular failure (LVF). The equations used for regression analysis were of the form;

$$\begin{aligned} PaO_2 &= \hat{y}_1 = a_{11}x_1 + \dots + a_{1n}x_n + a_{10} \\ PaCO_2 &= \hat{y}_2 = a_{21}x_1 + \dots + a_{2n}x_n + a_{20} \end{aligned} \quad (3.10)$$

where \hat{y} are the predicted values, x_i are the independent variables (i.e. the settings and measured variables) and a_{ij} are the regression coefficients, determining the significance of each variable. The variables initially included in the regression for $PaCO_2$ models were as follows; VT (tidal volume), RR (respiratory rate), slope- CO_2 (phase III capnogram slope), $CetCO_2$ (end-tidal CO_2 concentration), VCO_2 (CO_2 production), HR (heart rate), BPSYS (systolic blood pressure), and BPDIAS (diastolic blood pressure). For the PaO_2 models; VT, RR, HR, BPSYS, BPDIAS, slope- CO_2 , VD (dead space volume) and PEEP (end expiratory pressure) were considered.

The pertinent variables were selected after regression using the full variable set, using the F-statistic set at a certain threshold. The regression coefficients were then re-calculated.

Correlation coefficients for the models obtained were highly variable, ranging from 0.22 to 0.98. This variability is unacceptable and highlights the major problem with linear regression analysis applied to what is after all a non-linear system. Also, any models arrived at do not readily imply information about the various physiological states, since parameters such as dead space are not always included in the final equation.

3.4 Summary & Conclusions

This chapter has described the classification of respiratory models according to process and implementation. Models of lung mechanics, gas exchange, gas dissociation and respiratory control have been described, as well as integrated models combining aspects of the aforementioned elements. Particular attention has been drawn to integrated models describing respiration during mechanical ventilation of patients performing no breathing for themselves, since such a model is required to test the ventilator advisor developed in this thesis. The next chapter describes the development of just such a patient model, followed in Chapter 5 by its clinical validation.

Chapter 4: SOPAVent - Patient Model Development

4.1 Introduction

This chapter describes the development of SOPAVent (Simulation Of Patient under Artificial Ventilation), a patient model suitable for the validation of the ventilator therapy advisor. The model equations are presented first. However these do not constitute the final model, since improvements were required in order to provide patient observations not initially fore seen. These modifications are discussed in Chapter 7. The prototype model equations fall into five broad categories;

- 1). Oxygen transport equations.
- 2). Oxygen dissociation function and the calculation of its inverse.
- 3). Carbon dioxide transport equations.
- 4). Carbon dioxide dissociation function, again with the calculation of its inverse.
- 5). Airway mechanics and ventilator equations.

The model elements were implemented using MATLAB and SIMULINK, with the O₂ and CO₂ systems developed independently since cross coupling only occurs within the gas dissociation functions. In this way each model subsystem could be tested for functional validity before finally integrating them. The O₂ gas dissociation function was developed first and tested against available data. Since the transport equations require the inverse of this function a suitable solution-searching algorithm is discussed. This was then incorporated into the O₂ transport equations. In order to derive confidence in the O₂ subsystem, a normal healthy patient scenario was constructed using available empirical formulae to set the parameters of the system. This was found to give reasonable arterial PO₂ figures and using known physical relationships the functional validity of the system is shown.

This was then repeated for the CO₂ subsystem, starting first with the development of the CO₂ dissociation function and its inverse. Again this was tested against published data. The CO₂ transport dynamics were tested using the normal patient scenario and gave realistic values for arterial PCO₂. The two subsystems were then integrated and tested to see if normal patient values were maintained.

4.2 Patient Model Architecture

4.2.1 Overview

Model complexity can soon escalate, as deeper physiological concepts are included, consequently a balance needs to be made between model complexity and functionality. A model with over simplifications will become unrealistic, providing little in the way of patient specificity. Conversely a complex model incorporating all known physiology becomes unusable, since model parameters cannot be matched to real patient data for the simple reason that they cannot be easily measured. Statistical models could be used but these cannot be physically interpreted.

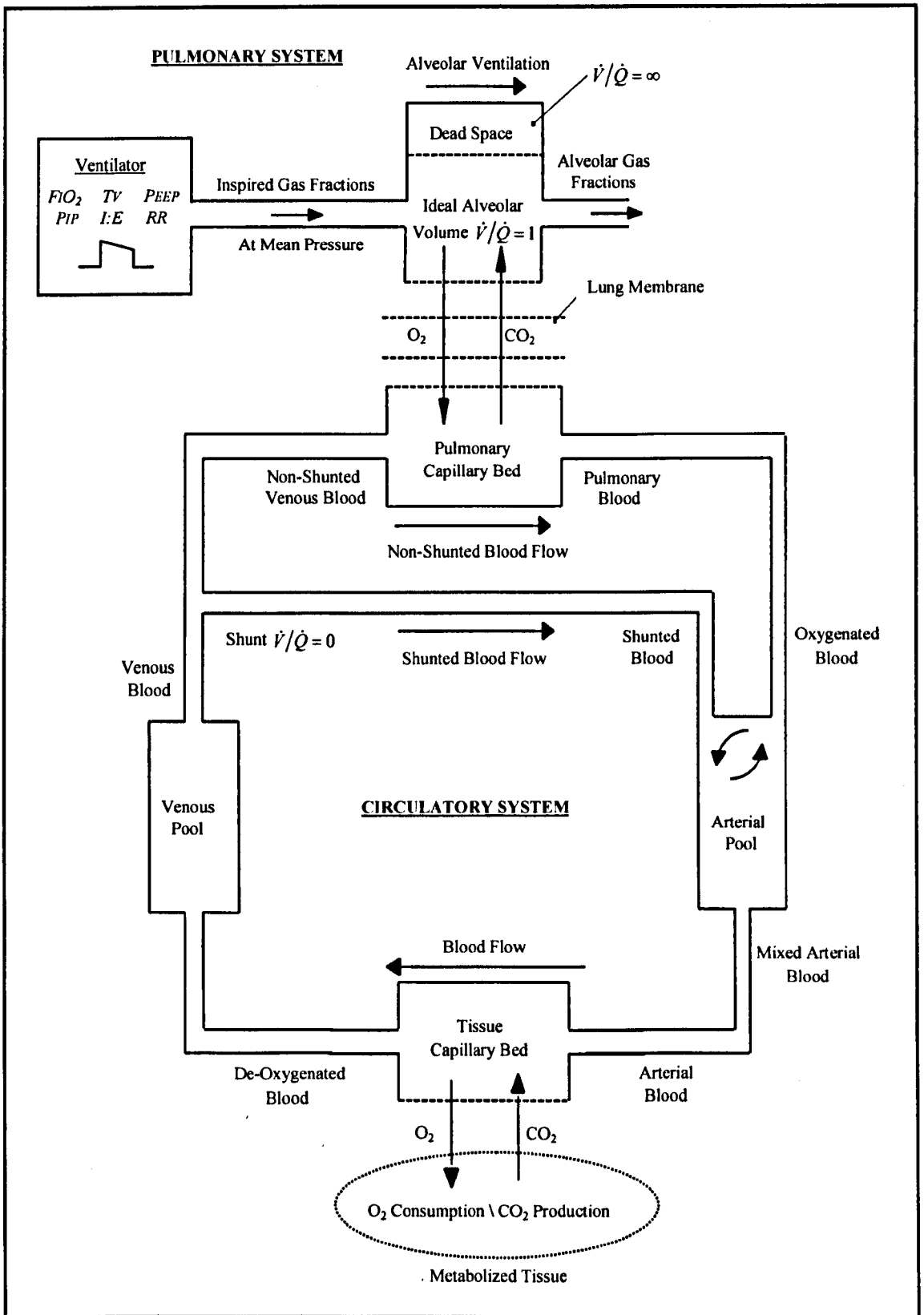


Figure 4.1: Schematic overview of patient model.

Consequently the chosen model needed to be physiologically based but simple enough so that the majority of its parameters could be routinely measured within ICU. In this way the model could be matched to real patient data and would therefore be clinically meaningful.

Based on these trade-offs, models describing the respiratory process on a breath-by-breath basis were rejected in preference for a continuous ventilation model describing the transport of gas volumes around the body using compartmental models. Also the modelling of the neurogenic drive was abandoned since the patients were assumed to be fully sedated and therefore unable to perform normal respiratory drive. The model constructed needed to respond to changes in the following ventilator settings; RR, V_T , FIO_2 , PEEP and I:E. It then needed to provide output of arterial and venous PO_2 and PCO_2 . Later this would be extended to include arterial and venous pH and PIP since they were required by the advisor (information that was not available during initial model development).

The transport of O_2 within the patient is described by a set of five linked differential equations and the CO_2 transport by a set of five similar equations [Thomsen *et al* , 1989]. These represent a seven-compartment model that can be divided into two main groups, the lung system and the circulatory system, see Figure 4.1.

The lung system is sub-divided into three functional areas (or compartments); the ideal alveolus where all gas exchange takes place (ideal perfusion-diffusion, $\dot{V}/\dot{Q}=1$), dead space representing lungs that are ventilated but not perfused ($\dot{V}/\dot{Q} = \infty$) and shunt representing those area that are perfused but not diffused as well as the anatomical shunts ($\dot{V}/\dot{Q} = 0$). This three-compartment model of the lung was devised by Riley (1949) and is now well accepted, although it does not enable the modelling of \dot{V}/\dot{Q} mismatch.

The circulatory system is made up of four compartments representing the arterial pool, venous pool, pulmonary capillary bed and systemic tissue capillary bed. The venous pool behaves as a first order exponential time lag, emulating venous return. The arterial pool provides mixing of the shunted venous blood with the oxygenated blood from the lungs. The tissue capillary bed allows for the consumption of O_2 and the production of CO_2 as a result of the metabolic processes. The pulmonary capillary bed provides diffusion of the respiratory gases to and from the alveolar space.

Embedded in the model are two inverse gas dissociation functions (GDFs) that convert O_2 and CO_2 contents to partial pressures. This facilitates the calculation of diffusion rates across the alveolar membrane since diffusion is driven by pressure gradient, whereas gas transport in the blood is described in terms of concentrations. These functions turn what is apparently a linear model into a non-linear one.

4.2.2 Oxygen Transport Equations

The O₂ transport dynamics are described by the following set of five linked differential equations, each describing the transport process of one circulatory compartment.

$$\frac{\partial C_{aO_2}}{\partial t} \cdot V_a = \dot{Q}_t \cdot [X \cdot C_{vO_2} + (1-X) \cdot C_{pO_2} - C_{aO_2}] \quad (4.1)$$

$$\frac{\partial C_{tO_2}}{\partial t} \cdot V_t = \dot{Q}_t \cdot [C_{aO_2} - C_{tO_2}] - \dot{V}_{O_2} \quad (4.2)$$

$$\frac{\partial C_{vO_2}}{\partial t} \cdot V_v = \dot{Q}_t \cdot [C_{tO_2} - C_{vO_2}] \quad (4.3)$$

$$\frac{\partial C_{pO_2}}{\partial t} \cdot V_p = \dot{Q}_t \cdot (1-X) \cdot [(C_{vO_2} - C_{pO_2}) + O_2 Diff] \quad (4.4)$$

$$\frac{\partial C_{AO_2}}{\partial t} \cdot V_A = RR \cdot (V_T - V_D) \cdot (F_I O_2 - C_{AO_2} / 1000) - \dot{Q}_t \cdot (1-X) \cdot O_2 Diff \quad (4.5)$$

$$O_2 Diff = B_{O_2} \cdot (P_B \cdot (C_{AO_2} / 1000) - P_p O_2) \quad [ml O_2/l blood] \quad (4.6)$$

$$P_p O_2 = f_{inv}(C_{pO_2}) \quad (4.7)$$

where

V_x	Where x = A, a, t, v, p - Volumes of alveolar, arterial, tissue, venous, and pulmonary compartments, respectively (litres)
\dot{Q}_t	Cardiac output (ml blood/min)
X	Fraction of blood shunted past lungs
\dot{V}_{O_2}	Oxygen consumption by tissues (ml O ₂ /min, BTPS)
V_D	Alveolar dead-space volume (ml, BTPS)
V_T	Tidal volume (ml, BTPS)
RR	Respiratory rate (breath / min)
C_{AO_2}	Alveolar O ₂ content (ml O ₂ /l alveolar gas)
C_{xO_2}	Where x = a, t, v, p - Arterial, tissue, venous and pulmonary O ₂ content, respectively (ml O ₂ /l blood)
$P_p O_2$	Pulmonary partial pressure of O ₂ (kPa)
t	Time (min)
$F_I O_2$	Inspired O ₂ gas fraction
P_B	Barometric pressure (kPa)
B_{O_2}	Diffusion constant (ml O ₂ /kPa/l blood)

Equation 4.1 describes the rate of change of arterial O_2 content (CaO_2) and can be thought of as a fixed volume compartment (V_a), with two inputs and a single output, see Figure 4.2. Oxygenated blood from the pulmonary capillaries mixes with shunted blood from the venous pool to form the arterial blood. Blood flow rate through the arterial pool is determined by the cardiac output.

The size of the arterial volume affects the transient response of the compartment, with larger V_a giving a slower response. Dickinson [1977] used a pool volume of 1 litre, but this is a purely notional volume, since systemic blood volumes are well distributed and not easily separable. Estimates of compartment blood volumes taking into account a patient's mass are discussed in Section 4.4.2

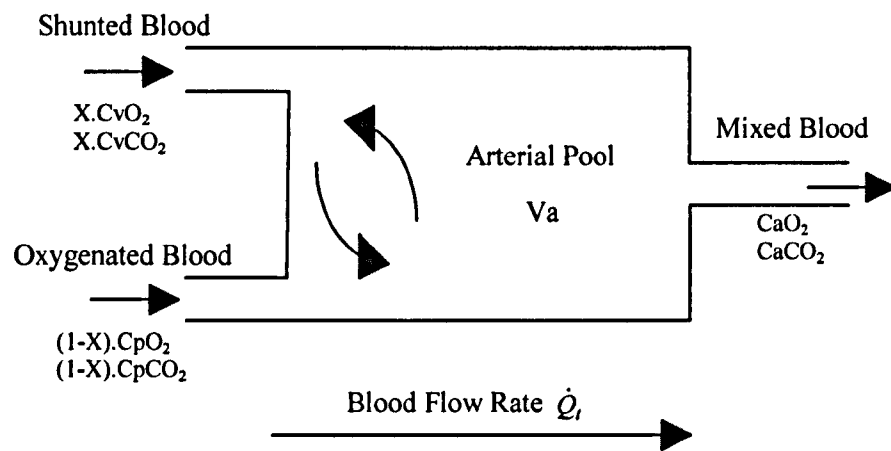


Figure 4.2: Schematic of gas transport in the arterial compartment

The rate of change of O_2 content within the tissue capillary bed is described by equation 4.2. It represents a single input, dual output compartment with a fixed volume V_t . Mixed arterial blood (CaO_2) enters the compartment and loses O_2 as it diffuses into the neighbouring tissue, resulting in de-oxygenated blood flowing out of the tissue capillary bed, see Figure 4.3. The diffusion occurs because of a positive pressure gradient across the capillary membrane, and the rate of transfer is determined by $\dot{V}O_2$.

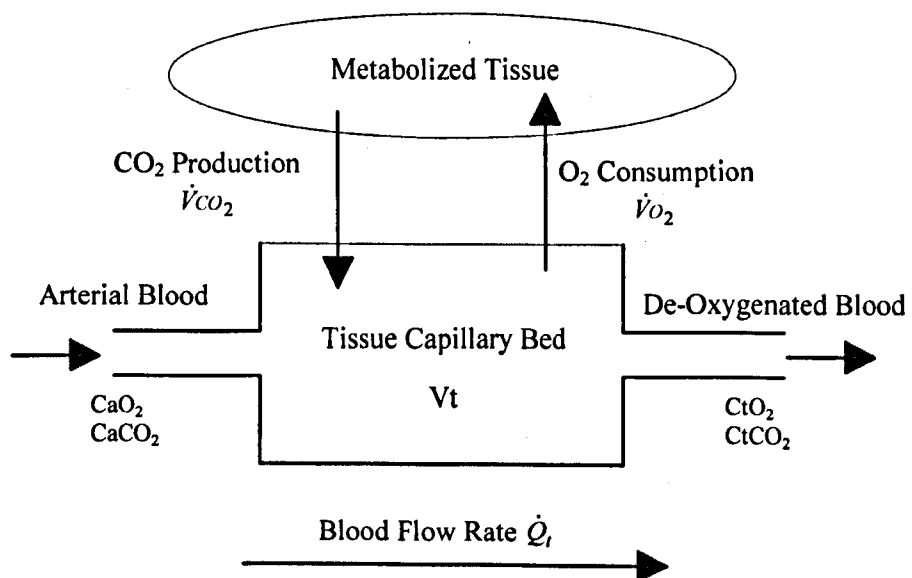


Figure 4.3: Schematic of gas transport in the tissue compartment

Equation 4.3 describes the rate of change of venous O_2 content (CvO_2) within the venous pool. It represents a simple compartment of volume V_v , with tissue O_2 content (CtO_2) as the input and venous O_2 content (CvO_2) as the output, see Figure 4.4. This simply behaves as an exponential time lag.

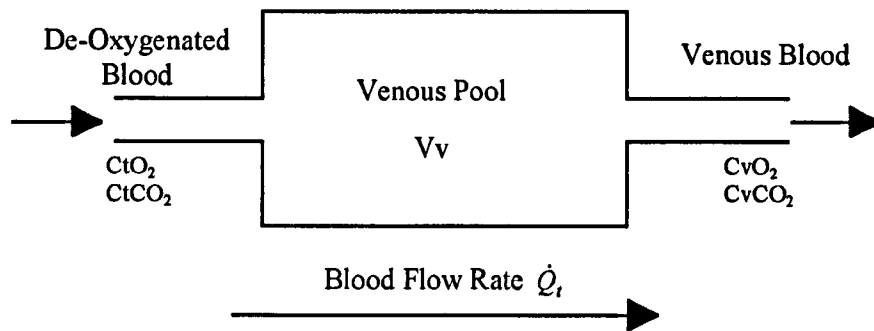


Figure 4.4: Schematic of gas transport in the venous compartment

Equation 4.4 corresponds to the pulmonary capillary bed and describes a compartment of volume V_p , with two inputs and a single output. The inputs are; (1) non-shunted venous O_2 content (CvO_2), and (2) the O_2 diffusing across the lung membrane (O_2Diff). The compartment output is the mixed and oxygenated pulmonary O_2 content (CpO_2). The blood flow rate through the compartment is $(1 - X) \cdot \dot{Q}_t$ (l/min), i.e. only non-shunted blood, see Figure 4.5.

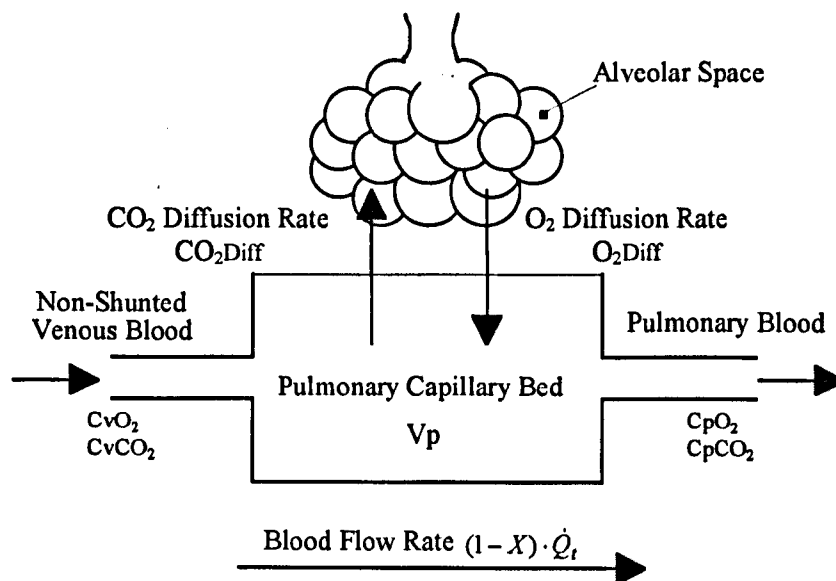


Figure 4.5: Schematic of gas transport in the pulmonary compartment

Equation 4.5 represents the change of alveolar O_2 content (CAO_2) within the alveolar space, where the input is the inspired O_2 fraction (FI_{O_2}) and two outputs are; (1) the alveolar O_2 content and (2) the O_2 diffusing across the lung membrane (O_2Diff). It is apparent from Figure 4.6 that this does not represent the bi-directional nature of the lung (i.e. the same input and output path), but describes the lung in terms of a fixed volume compartment (V_A) with continuous input and output. Consequently the lung ventilation rate does not vary for each breath but remains constant so long as the tidal volume (VT) and the respiratory rate (RR) remain constant.

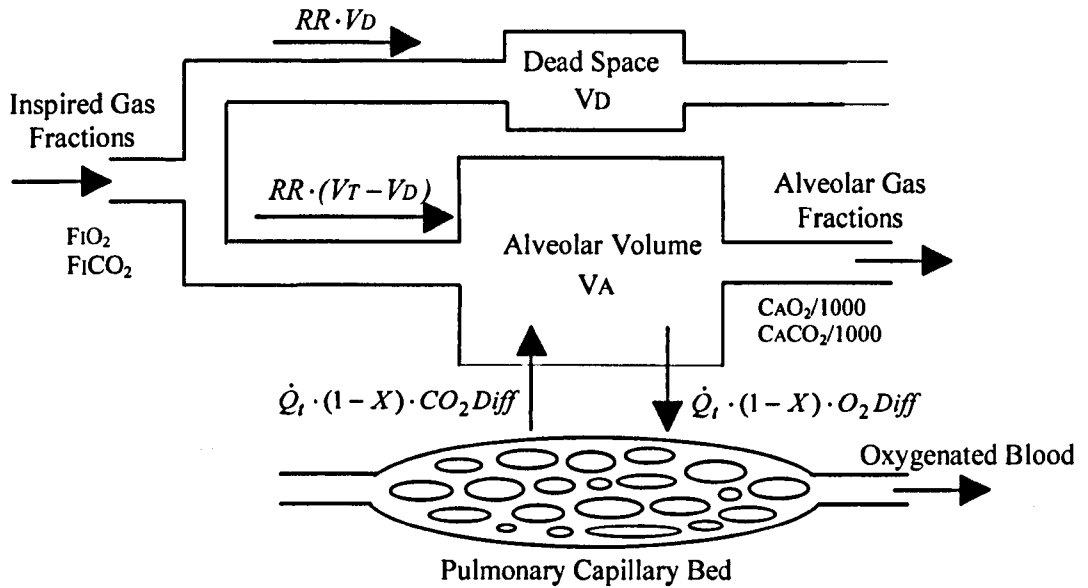


Figure 4.6: Schematic of gas transport in alveolar compartment

The alveolar ventilation (\dot{V}_A) depends upon the size of the dead space (V_D), corresponding to the anatomical dead space lumped together with other physiological dead space components, and is given in the first part of the equation 4.5 as;

$$\dot{V}_A = RR \cdot (V_T - V_D) \quad (\text{ml/min}) \quad (4.8)$$

Equation 4.6 calculates the rate of O_2 diffusing into the capillary bed per litre of blood flowing through it and is derived from Fick's first law of diffusion. This law states that the volume of gas that diffuses per unit time (\dot{V}) across a membrane, is directly proportional to the surface area of the membrane (A), the partial pressure difference of gas on either side of the membrane ($P_1 - P_2$) and the diffusion coefficient for a particular gas (D), and is inversely proportional to the thickness of the membrane (ΔX);

$$\dot{V} = \frac{D \cdot A \cdot (P_1 - P_2)}{\Delta X} \quad (\text{ml/min}) \quad (4.9)$$

However, A and ΔX remain unknown since the thickness and surface area of the alveolar-capillary membrane cannot be measured in a living subject. By rearranging equation 4.9 we arrive at an expression for the diffusion capacity as uptake of gas per minute (\dot{V}) per kPa pressure difference ($P_A - P_p$) with units of conductance (ml/min/kPa);

$$D_L = \frac{D \cdot A}{\Delta X} = \frac{\dot{V}}{(P_A - P_p)} \quad [\text{ml/min/kPa}] \quad (4.10)$$

where

P_A Alveolar partial pressure of gas (kPa)

P_p Pulmonary capillary partial pressure of gas (kPa)

Dividing the diffusion coefficient for O₂ (D_{O₂}) by the pulmonary blood flow gives the rate of O₂ diffusion per kPa difference per litre of blood;

$$BO_2 = \frac{DO_2}{\dot{Q}_l(1-X)} \quad [\text{ml O}_2/\text{kPa/l blood}] \quad (4.11)$$

Since de-oxygenated blood that flows into the pulmonary capillaries is at a lower partial pressure of O₂ than in the alveolar space, the resulting negative pressure differential causes O₂ to diffuse into the pulmonary capillaries. Conversely the pulmonary blood contains lower PCO₂ than the alveolar space, causing a positive differential with the consequent diffusion of CO₂ from the blood into the alveolar space.

The pressure gradient across the lung membrane is the difference between the alveolar O₂ partial pressure (PAO₂) and the pulmonary compartment O₂ partial pressure (PpO₂). The alveolar PO₂ is simply the alveolar O₂ fraction multiplied by the airway pressure, which is assumed to be atmospheric pressure (PB);

$$PAO_2 = P_B \cdot \frac{CAO_2}{1000} \quad [\text{kPa}] \quad (4.12)$$

However, calculation of the PpO₂ is not a straightforward matter. It is derived by calculating the inverse of the O₂ gas dissociation function (O₂ GDF), adding non-linearity into a system, which has so far only been described in terms of linear first order differential equations. The O₂ GDF derives O₂ content from O₂ partial pressure. However no explicit solution exists for the calculation of partial pressures from contents. Consequently an iterative procedure is required to calculate the inverse function. The next section describes the explicit O₂ dissociation function and the method used to compute it's inverse.

4.2.3 Oxygen Dissociation Function

The O₂ content of blood consists predominantly of oxygen in combination with haemoglobin plus a smaller component dissolved in the blood plasma;

$$C(o_2) = \beta_h \cdot Hb \cdot SO_2 + \alpha_b \cdot PO_2 \quad [\text{ml/l blood}] \quad (4.13)$$

The O₂ combined with the haemoglobin is the product of the haemoglobin concentration (Hb), the O₂ saturation fraction (SO₂) and the haemoglobin O₂ combining capacity (β_h). The O₂ dissolved in the plasma is the product of the O₂ carrying capacity of blood plasma (α_b) and the partial pressure of O₂ (PO₂).

Values for α_b are normally quoted as 0.225 ml/l/kPa [Nunn, 1993; Taylor *et al*, 1989 and others] and its effect is small, accounting for approximately 2% of the total O₂ content. Typically haemoglobin content is 148 g/l for men and 135 g/l for women [Dickinson, 1977, p.123]. Values for β_h vary considerably and the following levels have been quoted; 1.34 [Dickinson, 1977; Severinghaus, 1979; Nunn, 1993], 1.38 [Taylor, 1989], 1.39 [Alwan, 1992; Nunn, 1993] and 1.306 ml/g [Nunn, 1993; Gregory, 1974]. Of these 1.34 ml/g is the most widely accepted and has been used within the patient model developed here; where as 1.39 ml/g is the theoretical maximum.

The saturation fraction is a function of O₂ partial pressure. Several attempts to formulate this curve have been made [Severinghaus, 1979; Sharan, 1989; Alwan, 1992] but the most widely accepted formulation is the empirical set of equations derived by Kelman (1966) as used in the works of Dickinson (1977); Thomsen *et al* (1989) and Hinds *et al* (1984). His equation generates a curve indistinguishable from the true curve above a PO₂ of about 1 kPa (7.5 mmHg), and is given as;

$$SO_2 = \frac{(a_1x + a_2x^2 + a_3x^3 + x^4)}{(a_4 + a_5x + a_6x^2 + a_7x^3 + x^4)} \quad x \geq 10 \text{ mmHg} \quad [\text{fraction}] \quad (4.14)$$

where	$a_4 = 9.3596087 \times 10^5$
$a_1 = -8.5322289 \times 10^3$	$a_5 = -3.1346258 \times 10^4$
$a_2 = 2.1214010 \times 10^3$	$a_6 = 2.3961674 \times 10^3$
$a_3 = -6.7073989$	$a_7 = -6.7104406$

and x is the virtual PO₂ as given by;

$$\text{Virtual } PO_2 = \left[\frac{3.5774}{P_{50}} \cdot PO_2 \times 10^{(A+B+C)} \right] \times \left[\frac{760}{101.325} \right] \quad [\text{mmHg}] \quad (4.15)$$

$$A = 0.024(37 - T) \quad (4.16)$$

$$B = 0.40(\text{pH} - 7.4) \quad (4.17)$$

$$C = 0.06 \cdot \log(5.3329/P_{CO_2}) \quad (4.18)$$

Shifts in the dissociation curve due to abnormal pH, PCO₂ and temperature (known as the Bohr effect) are accounted for by the modifiers A, B and C. A normal curve is produced when the temperature is 37 °C, pH is 7.4, and PCO₂ is 5.3329 kPa (40 mmHg). An increase in temperature or PCO₂ right shifts the curve where as a reduction shifts the curve to the left. Conversely an increase in pH shifts the curve to the left and a reduction in pH shifts it to the right, see Figure 4.7 (b) to (c).

Also included within the virtual PO₂ equation, and not originally included by Kelman is an effect due to shifts in the P_{50} point [Ingram & Bloch, 1986]. This is the 50% saturation normal operating point of the curve and can be offset by various pathological conditions. It is normally 3.5774 kPa but can have higher values in haemoglobin abnormalities such as San Diego and Chesapeake, or lower values in sickle and Kansas. The presence of the organic phosphate 2,3-diphosphoglycerate in the erythrocyte can also have a pronounced effect on P_{50} , with higher levels increasing the P_{50} point.

Finally, the ratio 760/101.325 converts the virtual PO₂ from kPa to mmHg since equation 4.14 expects the partial pressures in mmHg.

However, Kelman's original polynomial expression produces negative values for virtual PO_2 below 1 kPa (see Figure 4.7a). He suggested an improved formulation of saturation for virtual PO_2 below 1.33 kPa (10 mmHg), [Sharan *et al*, 1989];

$$S_{O_2} = 0.003683x + 0.000584x^2 \quad x < 10 \text{ mmHg} \quad [\text{fraction}] \quad (4.19)$$

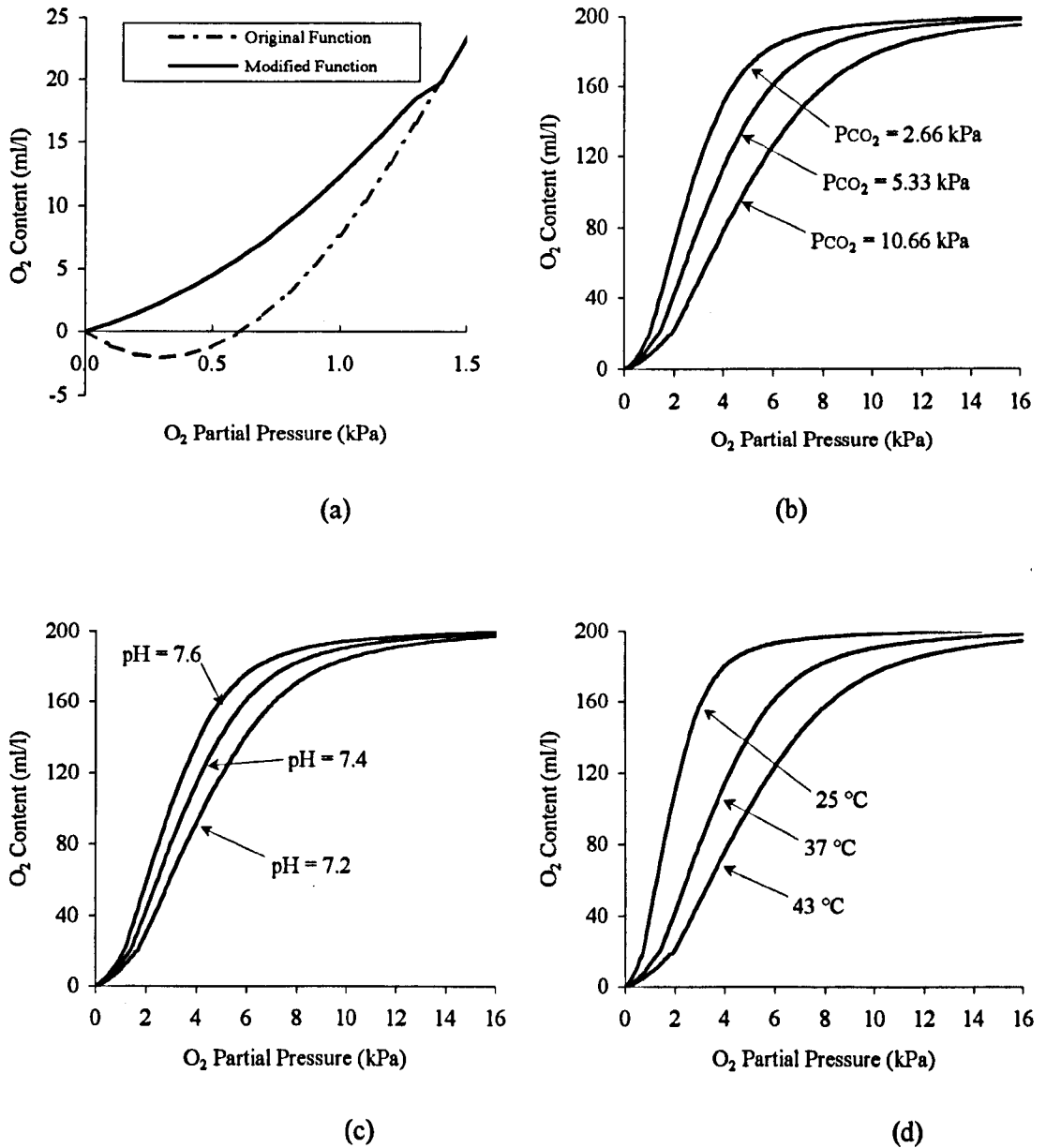


Figure 4.7: (a) Errors associated with Kelman's GDF and their correction using the improved formulae below 10 mmHg; (b) Shifts in the GDF curve associated with changes in PCO_2 from the normal of 5.333 kPa; (c) Shifts in the GDF curve associated with changes in pH from 7.4; (d) Shifts in the GDF curve associated with changes in temperature from 37 °C.

4.2.4 Inverse O₂ Dissociation Function.

However, the inverse of the O₂ GDF is required, since diffusion across the pulmonary-alveolar membrane is driven by the pressure gradient across it and O₂ in the pulmonary compartment is modelled as content (ml O₂/ l blood). Explicit solutions do not exist and therefore an iterative approximation method must be employed. For the sake of simplicity a simple secant gradient approach method was used [Atkinson *et al*, 1989]. This uses an estimate of the curve's gradient to derive a new approximation of PO₂ (P_{est}), given a target value of O₂ content (C_f), see Figure 4.8.

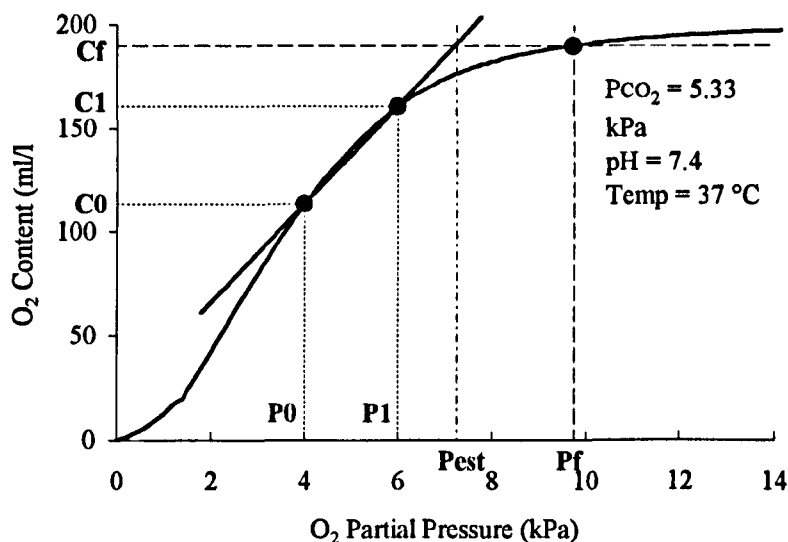


Figure 4.8: Secant approximation of PO₂ from C(O₂).

The gradient estimate is established from starting values of PO₂ (P_0 and P_1) and their corresponding O₂ contents (C_0 and C_1), calculated using the O₂ GDF. A new estimate of PO₂ is then given by;

$$P_{est} = \left[(C_f - C_0) \cdot \frac{(P_1 - P_0)}{(C_1 - C_0)} \right] + P_0 \quad (4.20)$$

The initial estimates of P_0 and P_1 are then updated;

$$P_0 = P_1; \quad P_1 = P_{est} \quad (4.21)$$

This procedure is then repeated until;

$$|P_{est} - P_0| \leq err \quad (4.22)$$

where *err* is the convergence error tolerance (kPa). For each calculation of O₂ content the other blood parameters must be specified; i.e. temperature, pH, PCO₂ and Hb.

4.2.5 Carbon Dioxide Transport Equations

The CO₂ transport equations are analogous to those of the O₂ system and are given as;

$$\frac{\partial C_aCO_2}{\partial t} \cdot V_a = \dot{Q}_t \cdot [X \cdot C_vCO_2 + (1 - X) \cdot C_pCO_2 - C_aCO_2] \quad (4.23)$$

$$\frac{\partial C_tCO_2}{\partial t} \cdot V_t = \dot{Q}_t \cdot [C_aCO_2 - C_tCO_2] + \dot{V}CO_2 \quad (4.24)$$

$$\frac{\partial C_vCO_2}{\partial t} \cdot V_v = \dot{Q}_t \cdot [C_tCO_2 - C_vCO_2] \quad (4.25)$$

$$\frac{\partial C_pCO_2}{\partial t} \cdot V_p = \dot{Q}_t \cdot (1 - X) \cdot [(C_vCO_2 - C_pCO_2) - CO_2Diff] \quad (4.26)$$

$$\frac{\partial C_aCO_2}{\partial t} \cdot V_A = RR \cdot (V_T - V_D) \cdot (F_I CO_2 - C_aCO_2 / 1000) + \dot{Q}_t \cdot (1 - X) \cdot CO_2Diff \quad (4.27)$$

$$CO_2Diff = B_{CO_2} \cdot (P_B \cdot (C_aCO_2 / 1000) - P_pCO_2) \quad [\text{ml CO}_2/\text{l blood}] \quad (4.28)$$

$$P_pCO_2 = f_{inv}(C_pCO_2) \quad (4.29)$$

where all parameters are as before except for;

$\dot{V}CO_2$ Carbon dioxide production by tissues (ml CO₂/min, BTPS)

C_aCO_2 Alveolar CO₂ content (ml CO₂/l alveolar gas)

C_xCO_2 Where x = a, t, v, p - Arterial, tissue, venous and pulmonary CO₂ content, respectively (ml CO₂/l blood)

P_pCO_2 Pulmonary partial pressure of CO₂ (kPa)

$F_I CO_2$ Inspired CO₂ gas fraction (BTPS)

B_{CO_2} Diffusion constant (ml CO₂/kPa/l blood)

Within the pulmonary compartment the pressure gradient is reversed with PCO₂ higher in the pulmonary capillaries than in the alveolar space, since inspired air contains effectively zero CO₂ (F_ICO₂ = 0.04% [Martini, 1992]). As a consequence, CO₂ diffuses out of the blood into the lungs, see Figure 4.5. This is expressed via the sign changes in the CO₂Diff components of Equations 4.26 and 4.27.

Similarly within the tissue compartment (equation 4.24) the pressure gradient is reversed since CO₂ is produced by the metabolised tissue at a rate of $\dot{V}CO_2$ (ml/min) and diffuses into the tissue capillaries, see Figure 4.3.

As with O₂Diff, the calculation of CO₂Diff requires the inverse calculation of the CO₂ gas dissociation function. The explicit dissociation function for computation of C(CO₂) from PCO₂ is described in the next section.

4.2.6 Carbon Dioxide Dissociation Function

The CO₂ gas dissociation function was based upon Kelman's algorithm [1967]. This first derives the total CO₂ content of the plasma (square brackets indicate total CO₂ concentration, i.e. dissolved plus combined CO₂ within this algorithm description) from its pH and PCO₂, using the Henderson-Hasselbalch equation;

$$[\text{CO}_2]_{\text{PLASMA}} = \alpha \cdot \text{PCO}_2 \cdot \left\{ 1 + 10^{(\text{pH} - \text{pK})} \right\} \quad [\text{ml/litre}] \quad (4.30)$$

where α is the solubility of CO₂ in plasma. Both α and pK are temperature dependent, and in addition pK varies with pH. The temperature dependence of α is expressed as;

$$\alpha = \left(0.0307 + 0.00057 \cdot (37 - T) + 0.00002 \cdot (37 - T)^2 \right) \cdot \left(\frac{760}{101.325} \right) \quad [\text{mM/litre/kPa}] \quad (4.31)$$

where T is blood temperature and the fraction (760/101.325) converts the units from mM/L/mmHg to mM/L/kPa. The expression for pK is given by;

$$\text{pK} = 6.086 + 0.042 \cdot (7.4 - \text{pH}) + (38 - T) \cdot (0.0047 + 0.0014 \cdot (7.4 - \text{pH})) \quad (4.32)$$

The ratio of [CO₂] in the cells to [CO₂] in plasma is then computed by linearly interpolating between experimentally derived quadratic expressions of the ratio for fully oxygenated and reduced blood;

$$\text{Reduced Ratio} = 0.664 + 0.2275(7.4 - \text{pH}) - 0.0938(7.4 - \text{pH})^2 \quad (4.33)$$

$$\text{Oxygenated Ratio} = 0.590 + 0.2913(7.4 - \text{pH}) - 0.0844(7.4 - \text{pH})^2 \quad (4.34)$$

The ratio is then determined using the observed oxyhaemoglobin saturation fraction (SO₂), as calculated within the O₂ GDF;

$$d = \{ (\text{Oxygenated} - \text{Reduced}) \times \text{SO}_2 \} + \text{Reduced} \quad (4.35)$$

Finally the whole blood CO₂ content is then calculated from the expression;

$$[\text{CO}_2]_{\text{BLOOD}} = 22.2 \cdot \{ [\text{CO}_2]_{\text{CELLS}} \cdot \text{pcv} + [\text{CO}_2]_{\text{PLASMA}} \cdot (1 - \text{pcv}) \} \quad (4.36)$$

Substituting d and re-arranging, gives;

$$[\text{CO}_2]_{\text{BLOOD}} = 22.2 \cdot [\text{CO}_2]_{\text{PLASMA}} \cdot \{ d \cdot \text{pcv} + (1 - \text{pcv}) \} \quad [\text{ml/L}] \quad (4.37)$$

where pcv is the packed cell volume fraction (or haematocrit), and the factor 22.2 converts final units from mM/litre to ml/L.

A typical dissociation curve produced using these formulae is given in Figure 4.9. The blood temperature was assumed to be 37 °C, the O₂ saturation 90 % and the haematocrit 40%.

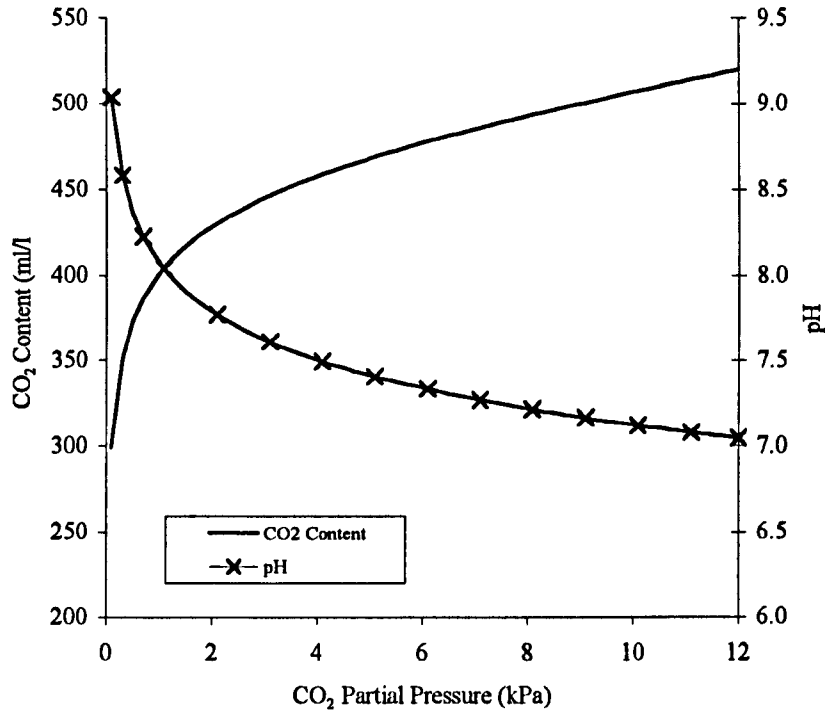


Figure 4.9: The CO₂ dissociation curve with pH derived using the modified Henderson-Hasselbalch equation [Taylor *et al*, 1989, p244] (see Section 6.7.3); since increased PCO₂ will reduce the effective pH.

4.2.7 Ventilator Model

In the gas transport equations 4.6 and 4.28, the partial pressures of O₂ and CO₂ within the alveolar space are calculated using barometric pressure (P_B) as given by;

$$P_{A_x} = P_B \cdot (C_{A_x} / 1000) \quad (\text{kPa}) \quad (4.38)$$

where P_{A_x} and C_{A_x} are the partial pressures and contents of gas x respectively. This is used to determine the pressure gradient across the lung membrane. A better solution is to use the mean airway pressure (P_{MEAN}) instead of P_B, since during inspiration and expiration the pressure in the alveoli will vary, but the transport dynamics model does not operate on a breath-by-breath basis.

Since the patient model will only represent ventilated patients (and of these only the subset under volume controlled ventilation) the pressure waveform can be described by a square wave. This represents intermittent positive pressure ventilation (IPPV) and will deliver a fixed volume (V_T) within time t_i , see Figure 4.10.

P_{MEAN} is therefore given by;

$$P_{MEAN} = \left\{ (P_{IP} - P_{EEP}) \times \frac{t_i}{t_i + t_E} \right\} + P_{EEP} + P_B \quad (\text{kPa}) \quad (4.39)$$

$$\text{and } \frac{t_i}{t_i + t_E} = \frac{I:E}{I:E + 1}$$

where;

PEEP is positive end-expiratory pressure (kPa)

PIP is peak-inspiratory pressure (kPa)

I:E is inspiratory-expiratory ratio

t_i is inspiratory time (sec)

t_E is expiratory time (sec)

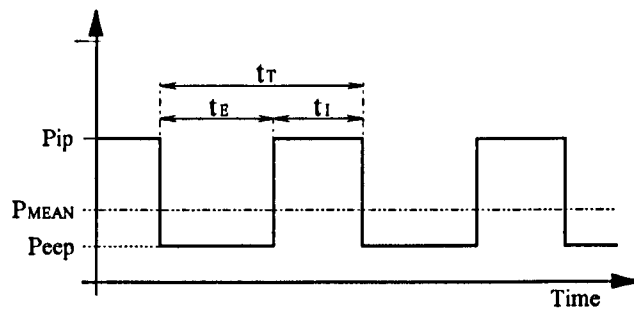


Figure 4.10: Pressure waveform of mechanical ventilator

In a fixed volume delivery system PIP will depend upon the resistance of the airway (R_{AW}) and the compliance of the lung (C_{AW}). This influences ventilator strategy since high ventilation pressures can lead to clinical complications. In spontaneously breathing patients this would lead to reduced tidal volumes and increased respiratory frequency due to the increased work of breathing.

This ventilator model assumes that PIP can be measured. However, if the model is to be useful for advisor validation then it must be able to model changes in PIP due to changes in ventilator strategy. This and other model improvements are dealt with in Section 7.3.

4.2.8 Unit Conversion

Many of the observations made in ICU are recorded using units and observation conditions that do not match those assumed within the patient model equations. The patient model assumes that all measures of gas volume, fraction and flow-rate are expressed at BTPS (body temperature pressure saturated) in standard international (S.I.) units, and that all other model parameters are in S.I. units. For example inspired O_2 fraction is routinely expressed as percentage of inspired gas at STPD (standard temperature pressure dry), but the model assumes it to be fraction of inspired gas at BTPS. Therefore conversion is required from one unit to another and from one set of observation conditions to another.

In order to keep track of what units and conditions an observation is expressed in, a three-valued representation for each patient parameter was employed, thus $[value, unit, conditions]$. The first term represents the value of the parameter, the second term an index corresponding to the units of the value (e.g. CMH₂O=1, MMHG=2, KPA=3, etc) and the third term an index referring to the observation conditions (STPD=1, BTPS=2, etc).

Gas Volumes & Flow Rates

Three factors affect the actual volume of a gas (1) the temperature of the sample, (2) the water vapour pressure of the sample and (3) the atmospheric pressure at which the sample was made. If a volume of gas is measured at STPD then the temperature is 0 °C, the water vapour pressure is 0 kPa and the atmospheric pressure is 101.325 kPa.

At increased temperature the volume of the gas increases. If the gas sample is saturated with water vapour (i.e. 100 % relative humidity) then any increase in temperature, will increase the water vapour pressure, which will reduce the gas volume. The level of water vapour pressure (P_{H_2O}) is dependent upon temperature, because the warmer the air the more water it can retain. This is the reason why it rains when a cold air front meets warm air since the cooling air is less able to retain the water vapour.

Using these relationships it is possible to derive an expression that converts a volume of gas from one set of observation conditions to another;

$$volume_{(NEW)} = volume_{(OLD)} \left(\frac{273.15 + T_{(NEW)}}{273.15 + T_{(OLD)}} \right) \left(\frac{P_{B(OLD)} - P_{H_2O(OLD)}}{P_{B(NEW)} - P_{H_2O(NEW)}} \right) \quad (4.40)$$

where $volume_{(OLD)}$, $T_{(OLD)}$ and $P_{B(OLD)}$ are the observed volume and conditions under which it was measured, and $P_{H_2O(OLD)}$ is the water vapour pressure at the observation temperature and relative humidity (RH). Similarly, $T_{(NEW)}$, $P_{B(NEW)}$ and $P_{H_2O(NEW)}$ are the new conditions under which the volume needs to be expressed. Temperature is given in units of °C and PB and P_{H_2O} are given in kPa.

P_{H_2O} is calculated using the polynomial expression of equation 4.41, derived from the empirical relationship between temperature (T) and P_{H_2O} (see Figure 4.11). The additional term $RH/100$ accounts for the relative humidity of the sample.

$$P_{H_2O} = (683.67 \times 10^{-3} T^3 - 12.985 \times 10^{-3} T^2 + 673.55T + 49.269) \times \left(\frac{RH}{100} \right) \quad (\text{kPa}) \quad (4.41)$$

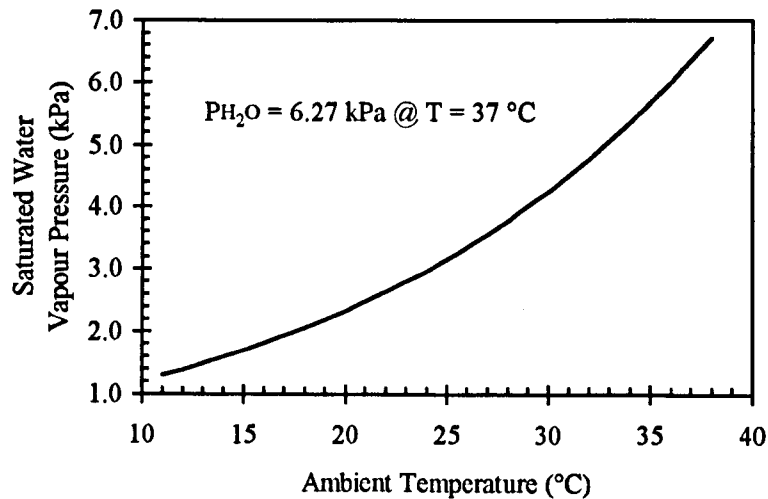


Figure 4.11: Relationship between air temperature and saturated water vapour pressure.

(i) STPD to BTPS Conversion

If a volume is to be converted from STPD to BTPS equation 4.40 reduces to;

$$volume_{(BTPS)} = volume_{(STPD)} \left(\frac{273.15 + T_{(BODY)}}{273.15} \right) \left(\frac{P_B}{P_B - PH_2O_{(BODY)}} \right) \quad (4.42)$$

where $T_{(BODY)}$ is the patient's temperature and $PH_2O_{(BODY)}$ is the saturated water vapour pressure at body temperature (approximately 6.27 kPa). O_2 consumption and CO_2 production are normally given in STPD and therefore require this conversion before being used by the model equations.

(ii) ATPS to BTPS Conversion

If a volume is converted from ATPS (atmospheric temperature pressure dry) to BTPS then equation 4.40 becomes;

$$volume_{(BTPS)} = volume_{(STPD)} \left(\frac{273.15 + T_{(BODY)}}{273.15 + T_{(AIR)}} \right) \left(\frac{P_B - PH_2O_{(AIR)}}{P_B - PH_2O_{(BODY)}} \right) \quad (4.43)$$

where $T_{(AIR)}$ is the ambient temperature ($^{\circ}C$) and $PH_2O_{(AIR)}$ is the PH_2O at $T_{(AIR)}$.

Parameter	Typical Observation Units & Conditions	Model Units & Conditions
FIO_2	percent, STPD	fraction, BTPS
$FICO_2$	percent, STPD	fraction, BTPS
PEEP	cmH ₂ O	kPa
VT	ml, ATPS	ml, BTPS
BPSYS	mmHg	kPa
\dot{V}_{O_2}	ml/min, STPD	ml/min, BTPS
\dot{V}_{CO_2}	ml/min, STPD	ml/min, BTPS
\dot{Q}_s/\dot{Q}_t	percent	fraction
R_{AW}	cmH ₂ O/litre/s	kPa/litre/s
C_{AW}	litre/cmH ₂ O	litre/kPa
PIP	cmH ₂ O	kPa
PB	mmHg	kPa
PCV	percent	fraction

Table 4.1: Summary of observation units and conditions of various parameters used within the patient model, together with the units and conditions required by the model equations.

Gas Fractions

With gas volumes expressed as percentages (or fractions) of total volume then assuming that all the atmospheric gases obey an ideal gas law, the fraction of gas will remain constant with increase in temperature. However, increased water vapour pressure will reduce the effective gas fraction as given by;

$$fraction_{(NEW)} = fraction_{(OLD)} \left(\frac{P_B - PH_2O_{(OLD)}}{P_B - PH_2O_{(NEW)}} \right) \quad (4.44)$$

Table 4.1 summarises those parameters used within the patient model that are routinely measured using different units and/or conditions.

That concludes the descriptions of the equations behind the original model architecture and the next sections 4.3 through 4.7 describe the implementation of the equations and there functional validation.

4.3 O₂ Dissociation Function Development

4.3.1 Functional Validity

The O₂ gas dissociation equations described in Section 4.2.3 were implemented as a MATLAB function with the input-output structure as shown in Figure 4.12 and tested for functional validity. The results obtained using the MATLAB function matched published results of the Kelman algorithm [Sharan *et al*, 1989], indicating correct functional implementation.

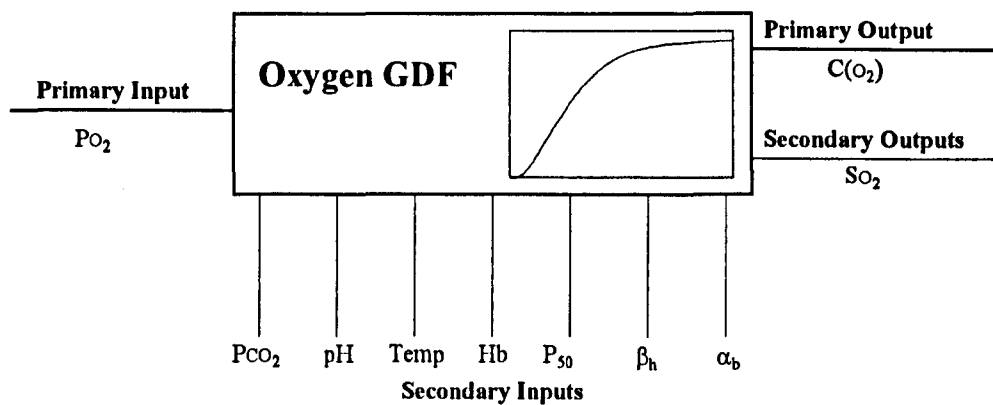


Figure 4.12: Schematic representation of the O₂ GDF showing inputs and output parameters.

4.3.2 Clinical Validity

No papers could be located in which the O₂ dissociation function was validated against clinical data. Instead those that were found continued to compare new curves against a series of older and assumed GDFs. The one source of clinical data that was found (Sharan *et al*, 1989) used assumed or calculated values of pH rather than directly measured values, neither of which was wholly satisfactory. However, in order to gain a 'feel' of the GDF's validity, two tests were made.

Validation against Severinghaus Data

The first of these used the data of Roughton & Severinghaus (1973) which they termed the Standard Human Blood O₂ Dissociation Curve (SHBODC), see Table 4.2. The difference between the computed saturation using the MATLAB GDF and that of the SHBODC were calculated, see Figure 4.13. PCO₂ was assumed to be 5.333 kPa (the normal position of the dissociation curve), pH to be 7.4 and blood temperature to be 37 °C, as per the SHBODC. Also compared against the SHBODC were saturations estimated using the modified Hill equation described by Severinghaus, as expressed by the following equation;

$$Sat = \frac{1}{\left(\frac{1}{(P_{O_2})^3 + 150P_{O_2}} \times 23,400 \right) + 1} \quad (4.45)$$

PO ₂ (mmHg)	Saturation (%)	PO ₂ (mmHg)	Saturation (%)	PO ₂ (mmHg)	Saturation (%)
1	0.60	34	65.16	80	95.84
2	1.19	36	68.63	85	96.42
4	2.56	38	71.94	90	96.88
6	4.37	40	74.69	95	97.25
8	6.68	42	77.29	100	97.49
10	9.58	44	79.55	110	97.91
12	12.96	46	81.71	120	98.21
14	16.89	48	83.52	130	98.44
16	21.40	50	85.08	140	98.62
18	26.50	52	86.59	150	98.77
20	32.12	54	87.70	175	99.03
22	37.60	56	88.93	200	99.20
24	43.14	58	89.95	225	99.32
26	48.27	60	90.85	250	99.41
28	53.16	65	92.73	300	99.53
30	57.54	70	94.06	400	99.65
32	61.69	75	95.10	500	99.72

Table 4.2: Values for the Standard Blood O₂ Dissociation Curve @ 37 °C, pH = 7.4 [Severinghaus, 1979]

Errors in Calculated Saturation Compared with
Severinghaus' Standard Human Blood GDF

pH=7.4; T=37 °C; P(CO₂)=5.333 kP

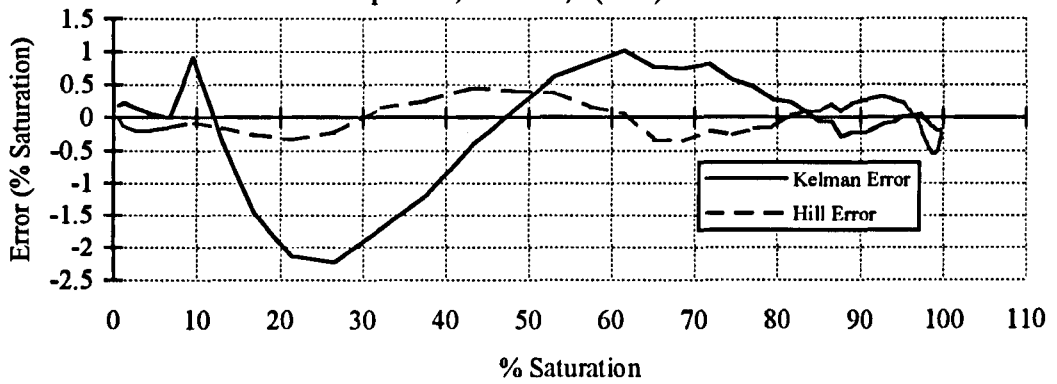


Figure 4.13: Errors between Standard Human Blood O₂ Dissociation Curve and computed values using Kelman equations (1966) and Hill equations [Severinghaus, 1979]

No .	P(O ₂) (mmHg)	P(CO ₂) (mmHg)	pH	% Saturation			
				Measured (Sharan <i>et al</i>)	Calculated (Kelman)	Error	% Error
1	96.0	43.0	7.40	98.00	97.23	0.77	0.78
2	66.0	36.5	7.40	91.00	93.22	-2.22	-2.43
3	52.0	34.8	7.40	84.90	86.97	-2.07	-2.43
4	41.0	33.8	7.40	76.20	76.07	0.13	0.17
5	36.0	31.8	7.40	71.20	68.73	2.47	3.46
6	35.0	29.4	7.40	70.80	67.30	3.50	4.94
7	74.0	40.6	7.40	94.00	94.90	-0.90	-0.95
8	57.0	39.4	7.40	88.70	89.70	-1.00	-1.13
9	55.0	35.0	7.40	88.10	88.84	-0.74	-0.84
10	49.0	40.0	7.40	83.00	84.31	-1.31	-1.58
11	36.0	33.2	7.40	72.20	68.57	3.63	5.03
12	94.0	41.0	7.39	98.00	97.05	0.95	0.97
13	60.0	33.9	7.44	91.00	92.14	-1.14	-1.25
14	51.7	28.8	7.49	86.70	89.82	-3.12	-3.60
15	47.6	29.5	7.48	84.50	86.79	-2.29	-2.93
16	44.6	27.1	7.51	78.00	85.56	-7.56	-9.69

Table 4.3: Comparison of experimental and calculated saturation using data of Sharan (1989)

It would appear from these graphs that the Modified Hill equation performed better than the Kelman algorithm, having a maximum error of 0.546 % saturation, compared to 2.229 % saturation using the Kelman algorithm. However, this merely indicates that the Modified Hill equation fits the Standard Human Blood data more accurately. Since the SHBODC was of unknown source and validity, it does not tell us much. Also the Hill equation does not provide correction for pH, temperature and PCO₂ and therefore the Kelman algorithm provides a more comprehensive interpretation of the dissociation curve.

Validation against Sharan Data

The second pseudo-clinical validation was performed against the data of Sharan *et al* (1989). These data were taken from Environmental Biology (1966, Ed. Altman P.L. & Dittmer D.S., *Pub. Federation of American Societies for Experimental Biology, Bethesda, Maryland*, pp.362-364). The first eleven values correspond to simulated altitude, where they have assumed pH is equal to 7.4. The remaining values correspond to incomplete acclimation, where pH was calculated from the PCO₂, using the procedure described by Kelman (1968), see Table 4.3.

Excluding entry 16, which appears to indicate experimental error, the largest observed saturation error was 3.63 % saturation (entry 11), compared to 2.32 % using the Sharan data. The mean absolute error was 1.75 % ± 0.84 (confidence interval 99 %), compared to 1.03 % ± 0.56 (confidence interval 99 %) using the Sharan O₂ GDF equation. Given possible inaccuracies in the experimental data, the Kelman function has performed with a similar degree of accuracy.

Whilst these assessments do not provide a complete picture of the dissociation function's clinical validity, they do show that its behaviour matches expected dissociation curve characteristics.

4.3.3 Inverse O₂ GDF Validity

The inverse of the explicit dissociation function was implemented as a MATLAB function with the input-output structure as shown in Figure 4.14.

In order to assess the validity, accuracy and performance of its implementation, a range of O₂ contents were calculated from known O₂ partial pressures using the previously validated O₂ GDF. These were then applied to the IGDF. Any differences between the known and estimated PO₂ were recorded, along with the number of iterations taken to reach the solution and the final pressure error. The original PO₂ values used for this test were 1 to 50 kPa in 1 kPa steps.

As expected the resulting PO₂ errors fell below the iteration error tolerance (*err*), see Figure 4.15, which in this case was 0.01 kPa. This was repeated for convergence error tolerances of 0.001, 0.1 and 0.5 kPa. The function call times and number of iterations required to converge were recorded for each PO₂ step. These were then averaged to give a measure of function performance. In this way the effect of increasing *err* could be assessed, see Table 4.4 (test 1 to 4). Improvements in iteration performance were not large, even with an *err* of 0.5 kPa.

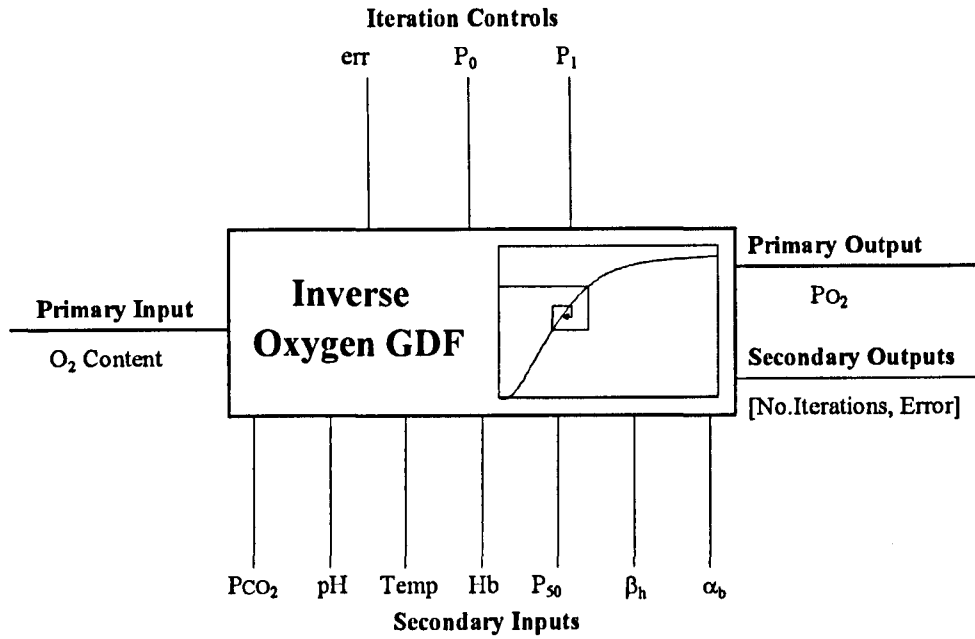


Figure 4.14: Schematic representation of the inverse O₂ GDF showing inputs and outputs.

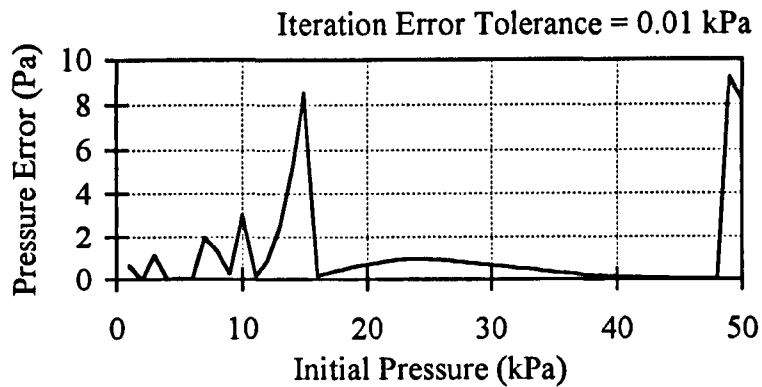


Figure 4.15: Observed errors in PO₂ across the PO₂ space generated using the IGDF.

Test	<i>err</i> (ml/l)	P ₀ (kPa)	P ₁ (kPa)	Run Time (sec)	Ave. No. Iteration
1	0.001	4	6	12.69	8.28
2	0.01	4	6	12.57	8.10
3	0.1	4	6	11.26	7.20
4	0.5	4	6	9.72	6.38
5	0.01	± 10 % †		5.28	3.22
6	0.1	± 10 % †		3.95	2.34

† P₀ and P₁ updated using bounded tracking

Table 4.4: Comparison of average computation times and number of iterations for various convergence error tolerances. Performed using normal (1 to 4) and bounded PO₂ tracking (5-6). [Hb = 140 g/l, pH = 7.4, T = 37 °C, PCO₂ = 5.333 kPa, P₅₀ = 3.577 kPa]. Run times are based upon a 486DX 33 MHz computer.

Improved Algorithm: (Bounded PO₂ Tracking)

During simulation C(O₂) values are unlikely to make rapid changes as they are restricted by a first order differential law. Consequently the last PO₂ estimate may be utilised to give improved convergence times.

New values for P₀ and P₁ are obtained by subtracting and adding respectively, a fraction of the last PO₂ estimate, thus encapsulating the last PO₂ estimate and providing a good initial estimate of the function gradient near to the expected solution, see Figure 4.16;

$$\begin{aligned} P_0 &= (1 - \text{fraction}) \times \text{last } PO_2 \\ P_1 &= (1 + \text{fraction}) \times \text{last } PO_2 \end{aligned} \quad (4.46)$$

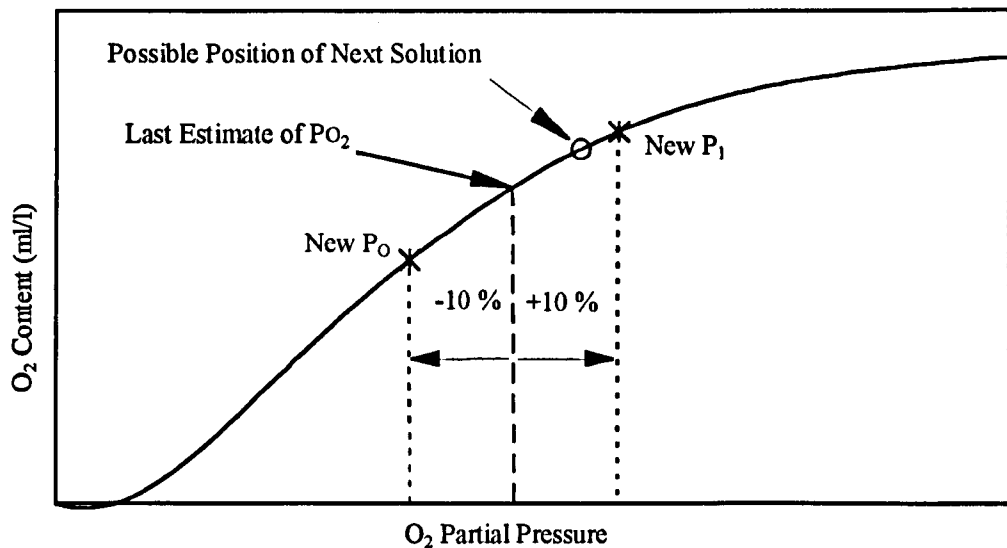


Figure 4.16: Diagram showing how bounded PO₂ tracking improves solution targeting by bracketing the next theoretical PO₂ estimate.

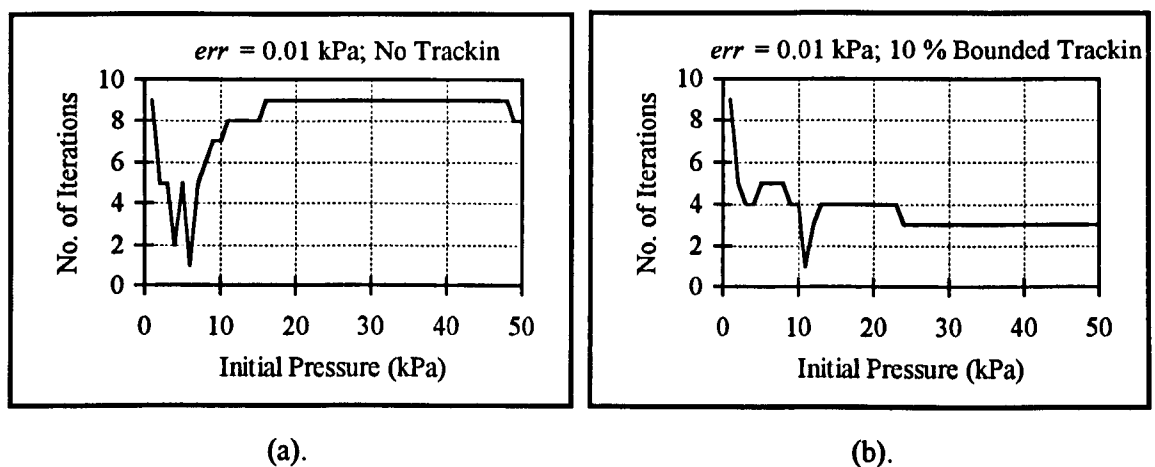


Figure 4.17: Graphs comparing the number of iterations required to arrive at PO₂ solution across the PO₂ space with an iteration error tolerance of 0.01 kPa; (a). with normal iteration and (b). with 10 % bounded PO₂ tracking.

With a bracketing fraction of $\pm 10\%$ the average number of iterations reduced from 8.10 to 3.22 for an error tolerances of 0.01 kPa and from 7.20 to 2.34 for an error tolerance of 0.1 kPa.

Examination of the iteration performance across the PO_2 space for normal and bounded iteration (see Figure 4.17) indicated a broad band improvement in performance by utilising bounded PO_2 tracking. Normal iteration provides optimal performance between 2 and 8 kPa. However, typical PO_2 values in ventilated patients tend to be higher, between 8 and 20 kPa. This would lead to poor function performance. A more uniform iteration distribution was achieved with bounded PO_2 tracking, giving less than 5 iterations in the range 2 to 50 kPa, hence a greater likelihood of reduced call times.

4.4 O_2 Transport Dynamics Development

4.4.1 Model Implementation

The equations describing the O_2 transport were implemented using the MATLAB and SIMULINK environment described in Appendix A. Each transport equation was converted into a state space form where the compartment output is expressed in terms of the integral of the partial derivative. This is best explained by way of an example. Consider the equation for O_2 transport in the venous compartment (see equation 4.3); this can be rearranged to give;

$$CvO_2 = \int \frac{\dot{Q}_t \cdot (CtO_2 - CvO_2)}{V_v} dt \quad (\text{ml/litre}) \quad (4.47)$$

Using this equation an analogue computer of the compartment can be constructed, see Figure 4.18. It is then a simple matter to build such a model using SIMULINK (see Figure 4.19) which can be solved using numerical integration techniques.

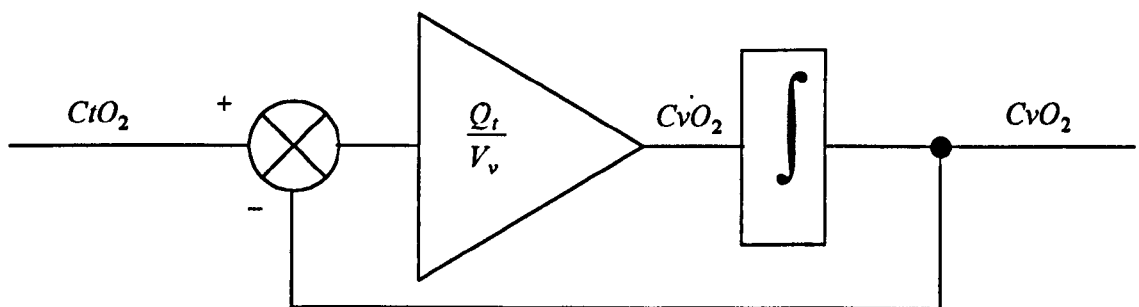


Figure 4.18: Analogue computer representation of venous compartment equation.

Of the methods provided by SIMULINK the Adams/Gear [The Math Works Inc, 1991] approach was used, being well suited to systems with both fast and slow dynamics. It is a variable step-length method switching between Adams and Gear algorithms depending upon the rate of change of the state variables. This gives good accuracy during periods of rapid change (e.g. after a step change in input) and fast simulation times once the transients of a system have settled. Using the block diagram approach it was possible to rapidly construct state space models for

each of the model equations, see Appendix A (note these are the final model diagrams and not the prototype model). Since SIMULINK enables the construction of sub-systems the compartmental models can be linked to form a complete patient model.

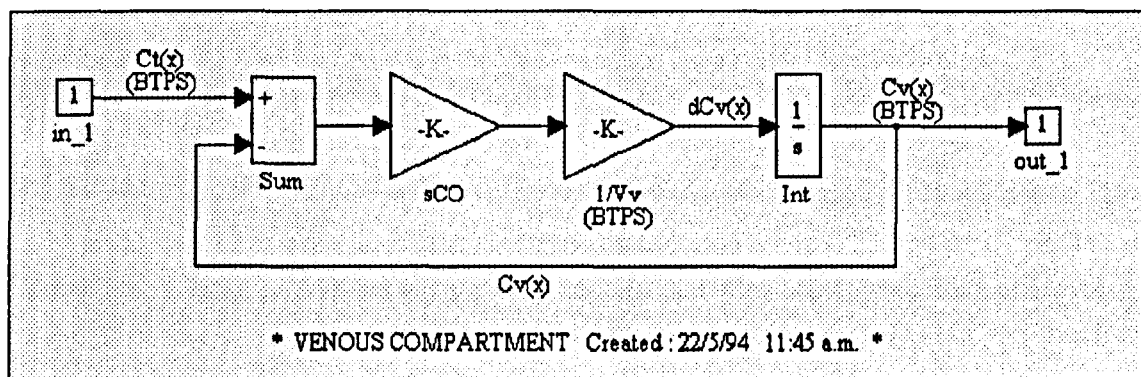


Figure 4.19: Venous compartment modelled using SIMULINK (see Appendix A) for explanation of model components.

The SIMULINK model (BROPUS – Block Representation of Patient Under Simulation) is controlled from the MATLAB workspace via program scripts. These scripts declare the patient parameters appertaining to a given patient scenario and are passed into the SIMULINK environment via variable declarations within the SIMULINK blocks. For example in the venous compartment there is a block that defines the cardiac output (labelled sCO). This is a gain block and by double clicking on the block a dialogue box appears enabling the value of the gain block to be defined. Instead of it containing a value, it contains a pointer (sCO) to a value in a globally declared patient scenario array. In this way a value for cardiac output can be declared within MATLAB and passed into BROPUS before simulation commences.

4.4.2 Derivation & Source of System Parameters

There were a lot of parameters to be defined within the O₂ dynamics model. Some of these would be provided by patient measurements and some would be derived from other parameters. In order to clarify this the following section describes each system parameter according to its classification (e.g. Blood, Patient, Ventilator parameter) and to what clinical sources it can be attributed. This was done so that a 'normal' patient could be constructed in order to assess the 'ball park' accuracy of the model. Some of the parameters are based on quoted values, whilst others are obtained using empirical formulae.

Blood Parameters

(i) Temperature & pH

Normal values for these parameters are widely accepted to be 37 °C and 7.4 respectively. These are the values that cause no left or right shifting of the gas dissociation curves [Kelman, 1967].

(ii) Haemoglobin

Values for the standard average haemoglobin (Hb) contents are given as 148 g/L for males and 135 g/L for females [Dickinson, 1977, p.123].

(iii) p50: 50 % Saturation Point

This is simply the 50 % saturation operating point of the O₂ GDF curve. It is calculated empirically from the normal blood GDF curve, produced using the Kelman equations [Kelman, 1967]. The normal curve is produced when pH = 7.4, temperature = 37 °C and P(CO₂) = 5.333 kPa. The default value for P50 is 3.5774 kPa, and this is the value assumed for a normal healthy patient.

Patient Parameters

(i) Oxygen Consumption

Early tendencies have been to assume that patients consume approx. 250 ml of O₂ per minute (\dot{V}_{O_2}) [Nunn, 1993, p.259], but many factors co-exist that often lift it above this basal level in a patient supposedly at rest. It is not possible to deal with these here, but the empirical relationship between \dot{V}_{O_2} and weight is dealt with by Dickinson (1977, p.122), and is given by;

$$\dot{V}_{O_2 REST} = 10.33 \times WT^{0.75} \quad (\text{ml/min, STPD}) \quad (4.48)$$

where $\dot{V}_{O_2 REST}$ is the O₂ consumption at rest and WT is the patient's weight in kg.

(ii) Cardiac Output

Typical values for cardiac output, \dot{Q}_t , are quoted at 5 l/min [Selvakumar *et al*, 1992], but a more useful formula exists [Dickinson, 1977, p.122] using the previously described term, $\dot{V}_{O_2 REST}$;

$$\dot{Q}_{t(nom)} = 0.0195 \times \dot{V}_{O_2 REST} \quad (\text{l/min}) \quad (4.49)$$

where $\dot{Q}_{t(nom)}$ is the nominal resting cardiac output.

(iii) Dead Space

Typical values for dead space (V_D) are quoted as between 150 and 170 ml [Dickinson, 1977]. A more useful empirical solution is provided by Taylor *et al* [1989, p.33];

$$V_D = 2.205 \times WT \quad (\text{ml}) \quad (4.50)$$

where WT is body weight in kilograms.

(iv) Shunt or Venous Admixture

Estimates of normal shunt (\dot{Q}_s/\dot{Q}_t) vary from source to source; Dickinson (1977, p.51) gives < 3 %; Taylor *et al* (1989, p.130) gives < 2-3 %; and Nunn (1993, p.180) gives ≈ 1-2 %. A \dot{Q}_s/\dot{Q}_t of 3 % of cardiac output has been assumed for the purposes of 'ball park' validation.

(v) O₂ Diffusion Rate

A formula to estimate O₂ diffusion capacity (DO₂) using estimates of the functional residual capacity (FRC) and age (AGE), is given by Dickinson (1977, p.123);

$$DO_2 = (7.6 \times FRC + 5) \times \left(\frac{100 - \Delta AGE}{100} \right) \quad (\text{ml/min/mmHg}) \quad (4.51)$$
$$\Delta AGE = |20 - AGE|$$

where ΔAGE is the difference in age from 20 years old and FRC is calculated using equation 4.56. A 6' 0" tall (183-cm), 20-year-old male will have an FRC of 3.81 litres, giving a DO_2 of 34 ml/min/mmHg (or 255 ml/min/kPa). This is lower than the normal DO_2 values quoted by Selvakumar *et al* (1992) of 60 ml/min/mmHg (450 ml/min/kPa) and Piiper & Scheid (1981, p.204) of 54 ml/min/mmHg (405 ml/min/kPa).

(vi) Age, Height, Weight & Sex

These are self-explanatory and for the purposes of 'ball park' validation a 20 year old male, weighing 75 kg and of height 183 cm (6' 0") was assumed.

(vii) Compartmental Volumes

Venous Blood Volume: is typically quoted as 3 litres, which is given as approximately 60 % of the whole blood volume (V_{WB}) [Dickinson, 1977, p.44]. V_{WB} (in litres) can be estimated by taking 7 % of body weight (WT) in kilograms [Martini, 1992, p.607];

$$V_{\text{WB}} = 0.07 \times \text{WT} \quad (\text{litre}) \quad (4.52)$$

Alternatively, V_{WB} can be considered equal to the resting nominal cardiac output, $\dot{Q}_{\text{t(nom)}}$, in normal healthy patients [Dickinson, 1977, p.122] as given by equation (4.49).

Then if we know V_{WB} , the venous blood volume (V_{v}) is simply;

$$V_{\text{v}} = 0.6 \times V_{\text{WB}} \quad (\text{litre}) \quad (4.53)$$

Given a patient of weight 75-kg, V_{WB} is 5.25 litres using equation (4.52), which gives a V_{v} of 3.15 litres. This compares to a V_{WB} of 5.13 litres using $\dot{Q}_{\text{t(nom)}}$, which gives a V_{v} of 3.08 litres; a difference of 2.2 %. This indicates that the equations are comparable and can be substituted in place of one another. Both results agree well with the V_{v} rule of thumb value of 3 litres.

Figure 4.20 shows the relative distribution of blood in the circulatory system [Martini, 1992]. The venous blood volume includes the venous reservoirs (21 %), the large veins (18 %) and the venules (25 %), giving a total systemic venous volume of 64 %. This agrees closely with Dickinson's approximation of 60 %.

Arterial Blood Volume: By referring again to Figure 4.20, we can consider the heart, aorta, elastic arteries, muscular arteries and arterioles to constitute the arterial blood volume (V_{a}), giving a percentage of whole blood of 20 %. Again by taking 20 % of 5.25 litres we arrive at a V_{a} of 1.08 litres, which correlates well with Dickinson's [1977, p.22] approximation of 1 litre. The heart was included as part of the systemic arterial system since its volume is not modelled anywhere else in the O_2 dynamics model.

Tissue Blood Volume: This includes all the blood in the capillaries, excluding those of the pulmonary circuit and approximates to about 7 % of the total blood volume. Based on a V_{WB} of 5.25 litres this gives a tissue blood volume (V_{t}) of 0.368 litres.

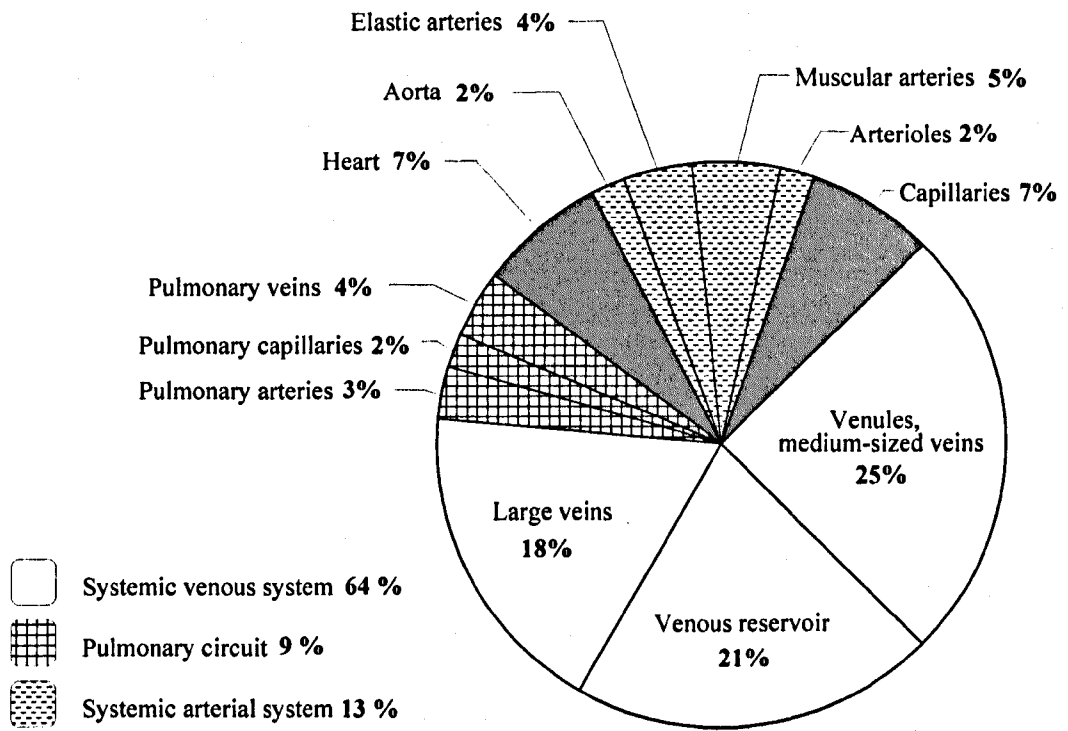


Figure 4.20: Distribution of blood in the circulatory system [Martini, 1992, p.672]

Pulmonary Blood Volume: Approximately 9 % of the total blood volume is contained within the pulmonary circuit (or 10 % according to Nunn *et al*, 1993), giving a pulmonary blood volume (V_p) of 0.473 litres, based on a V_{WB} of 5.25 litres. Table 4.5 summarises the percentages of total blood volume for each compartment and gives expected volumes based on a V_{WB} of 5.25 litres.

Alveolar Volume: can be derived from functional residual capacity (FRC), which can be predicted using one of the following pairs of empirical formulae. The first of these calculates total lung capacity (TLC) [Taylor *et al*, 1989, p.162]. The equations below are divided by a factor of two since FRC is widely considered to be 50 % of the TLC;

$$\begin{aligned} \text{Male FRC} &= (0.076H - 6.69)/2 && \text{(litres, BTPS)} && (4.54) \\ \text{Female FRC} &= (0.0646H - 5.44)/2 \end{aligned}$$

where H is height in centimetres. The second formula calculates the functional residual capacity (FRC) or resting lung volume directly [Dickinson, 1977, p.122 and p.204];

$$\begin{aligned} \text{Male FRC} &= 0.047H - 0.0075A - 4.583 && \text{(litres, BTPS)} && (4.55) \\ \text{Female FRC} &= 0.026H - 0.0090A - 2.180 \end{aligned}$$

where A is age in years.

Figure 4.21 shows the resultant TLCs (results multiplied by 2) computed using these equations for a 40 year-old over a range of heights. Curves are shown for both males and females. It can be seen that there were some disparities between the curves for each equation. In males, equation 4.55 produced a higher gradient, leading to larger TLC values for taller subjects (a difference of -12.8 % at H = 200 cm). In females there was a negative bias using equation 4.55 of 24.7 % at H = 200 cm).

Compartment	% of V_{WB}	Effective Volume (l) $V_{WB} = 5.25$ l
VENOUS	64	3.360
ARTERIAL	20	1.050
TISSUE	7	0.368
PULMONARY	9	0.473

Table 4.5: Summary of estimated compartment blood volumes based on percentage of V_{WB} .

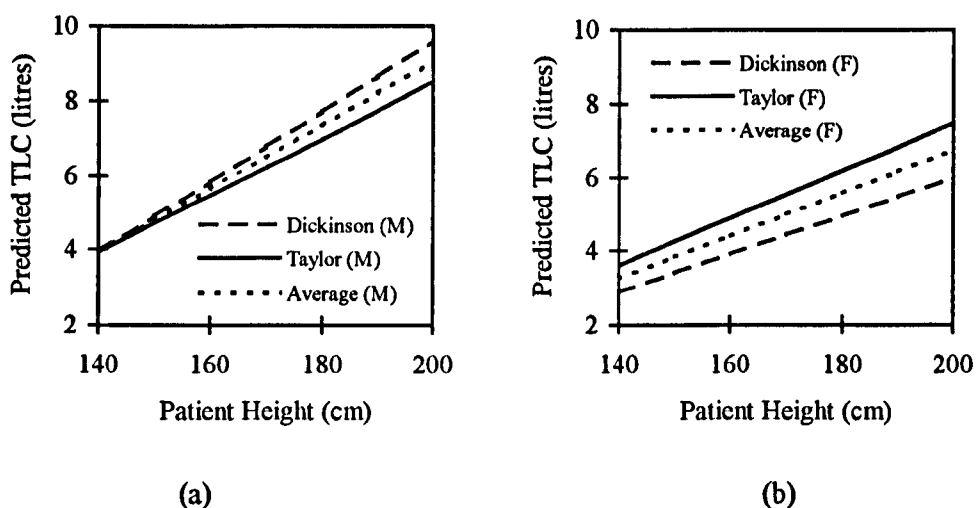


Figure 4.21: Computed total lung capacity for a 40 year-old (a) male and (b) female at various heights, using Dickinson's, Taylor's and average empirical formulae.

Since no clinical validity was provided for either of these equations, it was decided to average the two functions for each sex. The effect of age on predicted TLC using Dickinson's equation, is approximately 2.6 % from 20 to 100 years. When one considers the differences between the Dickinson and Taylor curves, this age effect is small and can be ignored. It was therefore possible to think of both sets of equations as simply functions of height. The average functions were calculated by taking the mean results from each function over a range of heights, and applying simple first order least squares polynomial fitting, resulting in;

$$\begin{aligned} \text{Male FRC} &= 0.0425H - 3.968 && \text{(litres, BTPS)} && (4.56) \\ \text{Female FRC} &= 0.0292H - 2.455 && && \end{aligned}$$

The TLC curves produced using these equations are also shown in Figure 4.21. In order to derive the alveolar volume (V_A), dead space (V_D) has to be subtracted from TLC;

$$\text{Alveolar Volume (} V_A \text{)} = \text{FRC} - V_D \quad \text{(litres)} \quad (4.57)$$

Ventilator Parameters

(i) Inspired O_2 Fraction

Table 4.6 shows the composition of the earth's atmosphere. Only the primary gases are shown and are quoted in percentage by volume in dry gas (STPD – standard temperature pressure dry).

Since under normal conditions (i.e. not half way up a mountain) a person will breath this composition of air, the inspired O₂ fraction (F_IO₂) is assumed to be 0.20946 (or 20.946 %). For this to be of use in the blood-gas dynamics model it needs to be converted to BTPS (body temperature pressure saturated). This is because inspired air is warmed as it travels through the nasal cavities and humidified by the mucus linings. The equations for this conversion are given in Section 4.2.8. Expressed at BTPS the atmospheric inspired O₂ fraction is 0.1964.

GAS NAME	PERCENTAGE (%)
Nitrogen	78.084
Oxygen	20.946
Argon	0.934
Carbon Dioxide	0.035

Table 4.6: Composition of the atmosphere of earth (by volume in dry gas) [Nunn, 1993, p.4]

(ii) Respiratory Rate

Typically the respiratory rate (RR) is assumed to be 15 breaths/min [West, 1979, p.13; Nunn, 1993, p.127]. Variations from this value depend upon many factors, such as CO₂ neurogenic drive, patient size, etc., which is too complicated to model for these purposes, and since the patients will be artificially ventilated can be ignored.

(iii) Tidal Volume

Normal values for tidal volume (V_T) are quoted at 500 ml [West, 1979, p.13, etc.] or 1/6th of the functional residual capacity (FRC). By implementing tidal volume as;

$$V_T = \frac{FRC}{6} \times 1000 \quad (\text{ml}) \quad (4.58)$$

where the 1000 multiplier converts FRC in litres to ml, the expected increase in alveolar ventilation (ml/min) with height is modelled.

(iv) PEEP, PIP & I:E

These are not normally used for a spontaneously breathing subject, but are available during artificial ventilation and are set by the ventilator. However, a peak inspiratory pressure (PIP) is generated by the lifting action of the rib cage and there is also a normal inspiratory/expiratory ratio (I:E) of approx. 0.66 (i.e. the inspiratory time is two thirds of the expiratory time) [Dickinson, 1977, p.61]. During inspiration PIP is approximately equal to the transmural¹ pressure gradient; normally between 6 and 7 cmH₂O (or 0.6 to 0.7 kPa).

¹ transmural - between the intrapleural space and the upper airway tract.

4.4.3 Ball Park Validation

A typical healthy 20-year-old male subject, 183 cm tall and weighing 75-kg was constructed using the empirical formulae and normal values outlined in the previous section, see Table 4.7. Since the CO₂ transport was not yet modelled PaCO₂ was assumed to be 5.333 kPa when using the O₂ GDF to calculate CpO₂ from PpO₂. This represents the normal CO₂ position of the dissociation curve.

The PaO₂ was calculated by using the inverse O₂ dissociation function with CaO₂ as the input. The other blood parameters required by this calculation were assumed to be the same as for the pulmonary compartment. This is not entirely valid since the mixing of shunted blood will reduce the pH slightly from the pulmonary end-capillary value.

<u>BREATHING PARAMETERS (VENTILATOR SETTINGS)</u>	
FiO ₂ = 0.2095 STPD	Tv (ml) = 634.9
RR (rpm) = 15	PEEP (cmH ₂ O) = 0
PIP (cmH ₂ O) = 6	I:E ratio = 0.6667
<u>BLOOD PARAMETERS</u>	
Temp. (°C) = 37	pH = 7.4
Hb (g/dl) = 148	P ₅₀ (kPa) = 3.577
PaCO ₂ (kPa) = 5.333	α _b (ml/l/kPa) = 0.225
β _h (g/l) = 1.34	
<u>PATIENT PARAMETERS</u>	
Height (cm) = 183	Weight (kg) = 75
Age (years) = 20	Sex = male
dVo ₂ (ml/min) = 263.3	C.O. (l/min) = 5.134
V _D (ml) = 165.4	Shunt (%) = 3
DO ₂ (ml/min/kPa) = 254.7	Bo ₂ (ml/l/kPa) = 51.14
<u>ATMOSPHERIC CONSTANTS</u>	
Air Temp (°C) = 20	P _B (kPa) = 101.325
P _{MEAN} (kPa) = 101.56	
<u>COMPARTMENT VOLUMES</u>	
FRC (l) = 3.81	V _{wB} (l) = 5.25
V _A (l) = 3.644	V _p (l) = 0.4725
V _a (l) = 1.05	V _t (l) = 0.3675
V _v (l) = 3.36	

Table 4.7: Patient parameters used in the ballpark assessment of the O₂ transport dynamics model

4.4.4 Results & Analysis

Using the patient described above, the simulated steady state PaO₂ was 13.318 kPa. This falls nicely into the expected range of PaO₂ values for a 20 year old subject derived using the relationship suggested by Marshall and Wyche (1972) [Nunn 1993, p.269];

$$\text{Mean PaO}_2 = 13.6 - 0.044 \times \text{AGE} \quad (\text{kPa}) \quad (4.59)$$

where AGE is in years. About this line there are 95 % confidence limits (2 S.D.) of ±1.33 kPa. Using this equation the expected range of PaO₂ values for a 20-year-old is 11.39 to 14.05 kPa (12.72 ± 1.33 kPa).

The steady state compartment O₂ contents for the 'normal' subject were; CpO₂ = 197.31 ml/L, CaO₂ = 196.33 ml/L, CtO₂ = 145.05 ml/L, CvO₂ = 145.05 ml/L and CAO₂ = 159.09 ml/L.

By using well accepted simple physiological relationships some of the parameters defined using the empirical formulae can be derived, thus confirming the functional validity of the O₂ model.

Oxygen Consumption

Oxygen consumption can be derived from the classic Fick equation [Taylor *et al*, 1989, p.55]. This is simply the product of the arterial-venous content difference, (CaO₂-CvO₂) and the cardiac output, \dot{Q}_t ;

$$\dot{V}_{O_2} = (CaO_2 - CvO_2) \times \dot{Q}_t \quad (\text{ml/min}) \quad (4.60)$$

Using the steady-state values for arterial and venous O₂ content;

$$\begin{aligned} \dot{V}_{O_2} &= (CaO_2 - CvO_2) \times \dot{Q}_t \\ &= (196.33 - 145.05) \times 5.134 = 263.3 \text{ ml/min} \end{aligned}$$

which matches the calculated value.

O₂ Diffusion Constant

The rate of O₂ uptake from the lungs can be calculated from the pulmonary-venous content difference, (CpO₂-CvO₂) and the pulmonary blood flow, $\dot{Q}_t \cdot (1 - \dot{Q}_s/\dot{Q}_t)$;

$$\dot{V}_{O_2 \text{ lung}} = (CpO_2 - CvO_2) \times \dot{Q}_t \cdot (1 - \dot{Q}_s/\dot{Q}_t) \quad (\text{ml/min}) \quad (4.61)$$

Where $(1 - \dot{Q}_s/\dot{Q}_t)$ is the non-shunted blood fraction, i.e. that which flows through the pulmonary circuit. Again using the steady state values for CpO₂ and CvO₂;

$$\begin{aligned} \dot{V}_{O_2 \text{ lung}} &= (CpO_2 - CvO_2) \times \dot{Q}_t \cdot (1 - \dot{Q}_s/\dot{Q}_t) \\ &= (197.91 - 145.05) \times 5.134 (1 - 0.03) = 263.24 \text{ ml/min} \end{aligned}$$

Dividing $\dot{V}_{O_2 \text{ lung}}$ by the alveolar-pulmonary pressure difference, (PAO₂-PpO₂) will give us the O₂ diffusion constant. The pulmonary O₂ tension, PpO₂ was measured from the model using the inverse O₂ GDF module and gave a value of 15.123 kPa. The alveolar O₂ tension, PAO₂ can be calculated from the alveolar O₂ content, CAO₂ and the mean inspiratory pressure, P_{MEAN};

$$PAO_2 = \frac{CAO_2}{1000} \times P_{MEAN} = \frac{159.09}{1000} \times 101.56 = 16.157 \quad (\text{kPa}) \quad (4.62)$$

Therefore the alveolar-pulmonary pressure difference is;

$$PAO_2 - PpO_2 = 16.157 - 15.123 = 1.034 \quad (\text{kPa}) \quad (4.63)$$

from which DO₂ can be calculated;

$$DO_2 = \frac{\dot{V}_{O_2 \text{ lung}}}{(PAO_2 - PpO_2)} = \frac{263.24}{1.034} = 254.6 \quad (\text{ml/min/kPa}) \quad (4.64)$$

The predicted DO₂ was 254.7 ml/min/kPa, indicating correct functioning of the diffusion mechanics.

Shunt Fraction

The arterial O₂ content, CaO₂ can be calculated from the sum of the non-shunted pulmonary blood content, CpO₂ and the shunted venous blood content, CvO₂ as follows;

$$CaO_2 = (1 - \dot{Q}_s/\dot{Q}_t) \cdot CpO_2 + \dot{Q}_s/\dot{Q}_t \cdot CvO_2 \quad (\text{ml/L}) \quad (4.65)$$

By expanding the CpO₂ term, collecting together the \dot{Q}_s/\dot{Q}_t terms and rearranging we arrive at the following expression for shunt;

$$\dot{Q}_s/\dot{Q}_t = \frac{CaO_2 - CpO_2}{CvO_2 - CpO_2} = \frac{196.33 - 197.91}{145.05 - 197.91} = 0.0299 \quad (4.66)$$

This correlates with the set value of 0.3, indicating that the shunt modelling is performing correctly.

4.5 CO₂ Dissociation Function Development

4.5.1 Functional Validity

The CO₂ gas dissociation algorithm (see Section 4.2.6), as with the O₂ gas dissociation was implemented as a MATLAB function with the input-output structure as shown in Figure 4.22 and was tested for functional validity.

Kelman's paper (1967) included a comparison of C(CO₂) results obtained using this algorithm with the nomograms of Singer & Hastings (1948). For comparison purposes the dissociation constant, pK was fixed at 6.11; rather than making use of the algebraic expression given in equation 4.32, since this was the value used in the construction of the original Singer-Hastings nomogram. Table 4.8 shows the results of Kelman's comparison together with results obtained using the MATLAB GDF. It can be seen that the MATLAB implementation matched Kelman's data exactly (allowing for rounding errors) and gave good correlation with the Singer-Hastings nomogram (R=0.999), see Figure 4.23. As expected this correlation fell slightly when using algebraically derived pK (R=0.998), although its inclusion is likely to produce more accurate results in real patients since there is an inter-dependence between pK and pH (Dickinson, 1977; Kelman, 1967; Nunn, 1993).

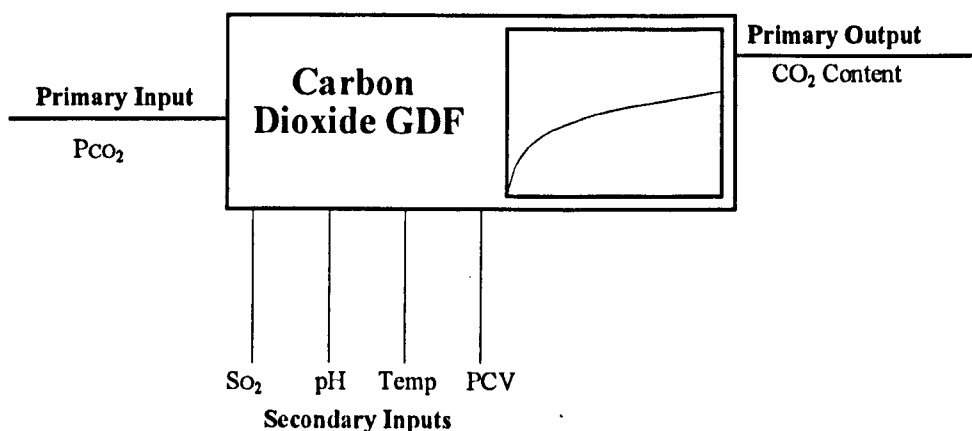


Figure 4.22: Schematic representation of the carbon dioxide GDF showing inputs and output.

PCO ₂ (mmHg)	pH	SO ₂ (%)	PCV (%)	Singer-Hastings (ml/dl)	Kelman (ml/dl)	MATLAB pK=6.11 (ml/dl)	MATLAB Algebraic pK (ml/dl)
14.5	7.01	60	40	67.0	78.0	78.1	78.5
11.8	7.59	80	59	188.0	184.0	184.1	195.8
26.0	7.43	66	55	320.0	304.0	304.1	318.2
44.2	7.25	97	42	384.0	377.0	377.3	387.9
28.5	7.53	60	40	460.0	442.0	442.0	467.2
27.7	7.64	95	51	508.0	497.0	497.2	531.4
132.0	6.89	99	50	546.0	543.0	542.6	539.6
66.0	7.25	97	48	564.0	559.0	548.8	564.1
48.0	7.48	97	48	643.0	634.0	634.0	666.7
55.8	7.41	60	40	696.0	675.0	674.7	704.6
62.3	7.41	89	59	700.0	677.0	677.2	707.2
45.5	7.54	60	40	718.0	720.0	720.5	762.3

Table 4.8: Comparison between whole blood [CO₂] derived using the Singer-Hastings nomogram, the Kelman algorithm and the MATLAB implemented GDF (with both fixed and algebraic pK).

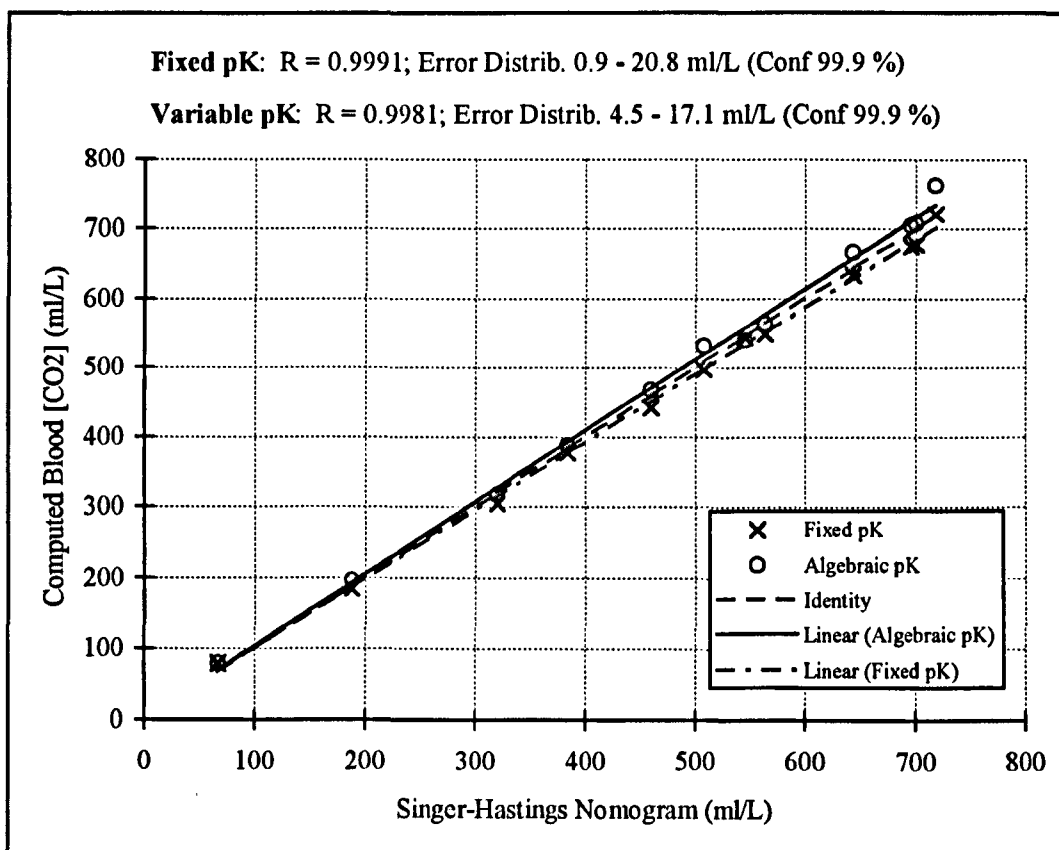


Figure 4.23: Graph showing the correlation between CO₂ contents calculated using the Singer-Hastings nomogram and the Kelman algorithm implemented using a fixed pK of 6.11 (as used by Singer) and an algebraic pK.

4.5.2 Inverse CO₂ Dissociation Function (IGDF)

The CO₂ IGDF was implemented in much the same way as its O₂ counterpart (see Section 4.3.3). The shell of the secant iteration function was maintained, with the differences being internal calls to the CO₂ GDF and fewer parameters passed into the iteration shell (7 instead of 10), as shown in Figure 4.24. The function was shown to perform correctly and gave convergence to solution in only 2 iterations, due to the almost linear nature of the CO₂ GDF curve.

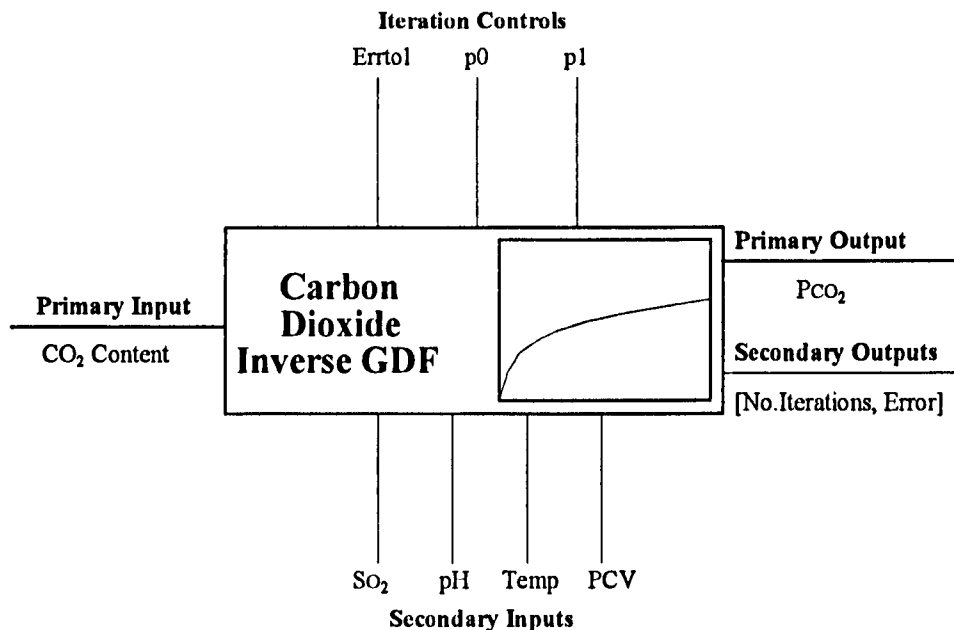


Figure 4.24: Schematic representation of the inverse carbon dioxide GDF showing its inputs and outputs.

4.6 CO₂ Transport Dynamics Development

The general structure of the CO₂ equations is identical to that of the O₂ equations and was duplicated to form the CO₂ transport model. Some of the O₂ system specific parameters were replaced with their CO₂ counterparts as follows;

CO ₂ production, \dot{V}_{CO_2}	<i>replaces</i>	O ₂ consumption, \dot{V}_{O_2}
CO ₂ diffusion constant, D_{CO_2}	<i>replaces</i>	O ₂ diffusion constant, D_{O_2}
Inspired CO ₂ fraction, F_{ICO_2}	<i>replaces</i>	inspired O ₂ fraction, F_{IO_2}

This made the SIMULINK implementation simply a matter of duplicating the basic model structure and inserting the relevant parameter or module differences. Again the subsystem was validated using a normal patient scenario. This required the derivation of additional parameters, which are given below.

(i) Packed Cell Volume

Packed cell volume (PCV) or haematocrit is related to haemoglobin by the following simple formula [NOVA SP2 mobile blood analyser, User's handbook];

$$\text{PCV} = \text{Hb} \times 0.3 \quad (\%) \quad (4.67)$$

where Hb is in g/L. This is required by the CO₂ dissociation function.

(ii) Inspired Co₂ Fraction

The inspired CO₂ is negligible and can be assumed to be zero. It is actually 0.035 % [Nunn 1993, p.4], which is the value used for the purposes of the model validation.

(iii) CO₂ Production

The respiratory quotient (RQ) describes the ratio of CO₂ production to O₂ consumption and has a normal value of 0.8 [West 1979, p.164; Petros *et al* 1993; Taylor *et al* 1989, p.133, etc.]. Therefore having established \dot{V}_{O_2} from Dickinson's empirical formula (see equation 4.48), we can derive \dot{V}_{CO_2} at rest;

$$\begin{aligned} \dot{V}_{CO_2} &= \text{RQ} \times \dot{V}_{O_2 \text{ rest}} \\ &= \text{RQ} \times 10.33 \cdot \text{WT}^{0.75} \end{aligned} \quad (\text{ml/min}) \quad (4.68)$$

RQ has been shown to correlate to the type of substrate that is being oxidised by the metabolic process. An RQ of 0.8 corresponds to the oxidation of protein. A slightly higher value than this might be expected, to reflect the addition of carbohydrate oxidation in the metabolic process (an RQ of 1.0 indicates that only carbohydrates are being burnt). A value of 0.9 would reflect a mixed substrate oxidation.

Typical values for \dot{V}_{CO_2} are given as approximately 200 ml/min [Taylor *et al*, 1989, p.60]. This is based on a \dot{V}_{O_2} of 250 ml/min and an RQ of 0.8

(iv) CO₂ Diffusion Constant

Quoted values for the CO₂ diffusion constant vary. In McPuf [Dickinson 1977] DCO₂ is assumed equal to DO₂, which when calculated for a typical male (183 cm, 75 kg, 20 yr.) is 254.7 ml/min/kPa. Selvakumar *et al* (1992) gives a much larger value of 1500 ml/min/kPa. The theoretical diffusion constant of CO₂ across an aqueous membrane is approximately 20.5 times greater than that for O₂, giving a DCO₂ of approx. 5220 ml/min/kPa (based on a DO₂ of 254.7 ml/min/kPa). There is not a lot of agreement between these estimates, so for the ballpark validation DCO₂ was assumed equal to DO₂. However, it will be seen that the final choice of DO₂ and DCO₂ had to be altered due to model sensitivity issues during tuning to clinical data (see Section 5.4.4).

(v) O₂ Saturation

A typical O₂ saturation, SO₂ was hard to come by, as it is dependent upon many factors. Since at a later stage the O₂ and CO₂ sub-systems would be integrated some relationship with the former would be necessary. As a consequence it was decided to use the SO₂ derived from the standard patient scenario used in the assessment of the O₂ sub-system. This was calculated to be 98.08 %.

4.6.1 Ball Park Validity

The patient simulation was set up as in Table 4.7 with the inclusion of the parameters mentioned above and run until steady state was reached. Since the $S_{(O_2)}$ value was derived from a fixed $P_{a(CO_2)}$ value of 5.333 kPa this becomes the target arterial pressure for the sub-system. In the first test DCO_2 was assumed equal to DO_2 .

The resulting steady state arterial PCO_2 was 4.396 kPa. This was 0.953 kPa (17.9 %) below the target pressure. This was deemed unacceptable. Now, since only four parameter changes had been made in the CO_2 sub-system equations; SO_2 , DCO_2 , $FICO_2$ and \dot{V}_{CO_2} ; this error could only be due to one of these parameters or the CO_2 dissociation function.

Under normal blood conditions (which is true for this test) a change of SO_2 from 100 % to 90 % only causes a change in PCO_2 of 0.021 kPa (approx. 0.4 % error). This does not account for the large observed error of 17.9 %

The sensitivity of the model to changes in $FICO_2$ was also small. A doubling of $FICO_2$ from its atmospheric value gave rise to an increase in $PaCO_2$ of only 0.034 kPa (approx. 0.8 % error). Again this error is small and does not account for the large error observed.

The level of CO_2 production may give rise to this error since this was dependent upon the respiratory quotient (RQ). An increase of RQ from 0.9 to 1.0, giving an effective increase in \dot{V}_{CO_2} from 237 to 263 ml/min (an 11% increase), gave an increase of 0.485 kPa in $PaCO_2$ (an 11% increase). This would account for more than half of the observed error but since RQ cannot be increased beyond 1.0 in normal patient scenarios, this leaves approx. 8 % unaccounted for. It could equally be argued that an RQ of more than 0.9 is unrealistic in an intensive care setting.

This leaves one of two possible hypotheses;

- 1). DCO_2 is too high, giving rise to increased CO_2 elimination.
- 2). Alveolar ventilation is too high, leading to the same effect.

The first of these seems improbable since other sources have quoted larger DCO_2 than used here. The latter is plausible when one considers that a reduction in alveolar ventilation can be achieved by reducing the respiratory rate (RR).

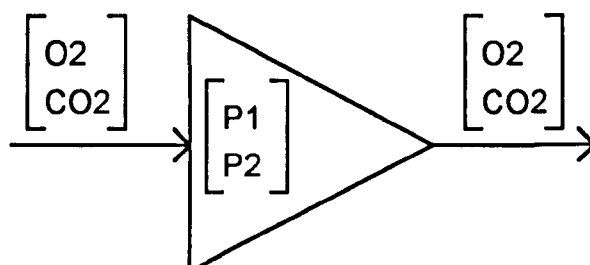
By reducing RR to 11 b.p.m., the $PaCO_2$ is increased to 5.64 kPa and PaO_2 is reduced to 12.32 kPa. The $PaCO_2$ error is now acceptable at 5.8 %, and PaO_2 has not fallen outside of its normal range.

4.7 O_2 and CO_2 Model Integration

Having constructed and assessed the gas sub-systems the next obvious step was to integrate them. Rather than have two large block diagrams strapped together to form the model, it was decided to exploit the symmetry of the problem. Both gases travel through the same physiological structures of the model and therefore a vector can represent the state of the gases at any point in the model;

$$\begin{bmatrix} O_2 \\ CO_2 \end{bmatrix} \quad \text{or in MATLAB format } [O_2; CO_2] \quad (4.69)$$

Any subsequent computations within the SIMULINK block diagram are applied to each vector element. If there are different parameters associated with each gas, as in the case of diffusion at the lung membrane, then these are implemented within the given block as vectors, see Figure 4.25



Block with parameters implemented vectorally

Figure 4.25: SIMULINK gain block showing implementation of parameters as vectors

In this way the gas models function independently whilst making use of the same process structure. Cross coupling between the two gas systems occurs within the dissociation functions, where PO_2 is affected by PCO_2 , which is in turn affected by SO_2 (being a function of PO_2). pH is also affected by PCO_2 which will modify PO_2 , however this was not represented in the prototype model.

The parameters of the two sub-systems were combined and a *standard* 20-year-old male subject generated as before. This was then run to steady state resulting in a PaO_2 of 12.33 kPa and $PaCO_2$ of 5.33 kPa. These results are promising with PaO_2 within its normal range and $PaCO_2$ matching the target of 5.33 kPa.

4.8 Summary & Conclusions

O₂ Dissociation Function

The O₂ GDF based on Kelman's algorithm (1966) was found to be functionally valid, matching published function results exactly.

It performed moderately well against the SHBODC of Severinghaus (1979), with an observed maximum saturation error of 2.23 % compared to 0.55 % for the Hill equation. The larger errors occurred below 40 % saturation which is well below the normal operating point for either arterial or venous blood, except in cases of critical blood loss. Both of these equations were tested against Severinghaus' data, however, no indication of how the Hill equation should be modified to account for shifts in pH, temperature and PCO_2 were given.

The GDF performed well against the experimental data of Sharan *et al* with a mean absolute saturation error of 1.75 % \pm 0.84 (confidence interval 99 %) compared to 1.03 % \pm 0.56 (confidence interval 99 %) using the Sharan O₂ GDF equation. The maximum observed saturation error was 3.63 % compared to 2.32 % using the Sharan equation.

The Kelman algorithm was deemed suitable for incorporation into the O₂ transport model.

Inverse O₂ GDF

The inverse O₂ GDF was resolved using an iterative secant based method and proved functionally valid. It arrived at a target solution in an average of 8.1 iterations, when tested across a PO₂ test space of between 1 and 50 kPa. This was with an iteration error tolerance of 0.01 kPa and initial pressure estimates of 4 and 6 kPa for p₀ and p₁ respectively.

An improved secant algorithm using bounded PO₂ tracking was proposed and gave improved iteration performance. The average number of iterations reduced to 3.22 with little change in PO₂ accuracy.

O₂ Transport Dynamics

Normal patient-values and appropriate formulae to calculate them were elicited from the available literature, for each parameter used within the O₂ transport model.

The O₂ transport model was successfully implemented using SIMULINK and gave an arterial PO₂ of 13.32 kPa for a pre-defined 20-year-old male subject, weighing 75 kg and of height 183 cm. This fell within the range of typical values for a 20 to 29 year old age group, quoted by Nunn (1993).

It would appear from this assessment that the O₂ transport model has been constructed correctly and was functioning in a reasonably predictive manner. The assessment was of course mainly qualitative and the CO₂ transport was not included, but the indications of a useful working patient model were promising.

CO₂ Dissociation Function

The implemented CO₂ GDF, based on Kelman's algorithm (1967) was found to be functionally correct matching the published results exactly. Comparison with the results obtained using the Singer-Hastings nomogram showed excellent correlation with both fixed pK (R=0.999) and algebraically derived pK (R=0.998).

Inverse CO₂ GDF

The inverse function was implemented using the same shell as the O₂ IGDF and was proven to be functionally correct, giving convergence to solution in 2 iterations, due to the near-linear properties of the function.

CO₂ Transport Dynamics

All parameter values were identical to those for the O₂ sub-system with the exception of FICO₂, DCO₂, and SO₂. Suitable values or derivation formulae were located for all of these, although there was some uncertainty regarding DCO₂.

With DCO₂ equal to DO₂ (255 ml/min/kPa) and an RQ of 0.9 the model gave a PaCO₂ of 4.396 kPa, 17.9 % below the target value of 5.333 kPa. This was with a pre-defined 20-year-old male subject as used for the O₂ sub-system ballpark assessment.

Reasons for this were considered and the main source pinpointed to a high RR. This was reduced from 15 b.p.m. to 11 b.p.m. and gave a PaCO₂ of 5.64 kPa, reducing the error to 5.8 %. In normal patients such compensation is performed via neurogenic drive, with the alveolar

ventilation changing in response to the level of PCO_2 in the brain. Therefore the discrepancies observed could be ignored and the CO_2 sub-system deemed to be functioning correctly.

System Integration

The O_2 and CO_2 sub-systems were combined into the same model shell by representing the gases through out the system in a vector form. This negated the need for replicated model block diagrams and greatly simplified interaction with the model inputs and outputs.

Using the *standard* healthy patient scenario the resultant PaO_2 was 12.32 kPa and the PaCO_2 was 5.33 kPa, both being within normal ranges.

SOPAVent was now ready for validation using real clinical data and this is discussed in the next chapter, together with an investigation of the parameter sensitivity of the model.

Chapter 5: Clinical Validation of Patient Model

5.1 Introduction

So far it has been shown that the patient model produces normal blood-gases when simulated using parameters representing a healthy male patient breathing atmospheric air. However, if it is to be useful for advisor development and validation, it must be able to correctly predict blood-gases when changes are made to the ventilator settings. This must be possible for the types of patient routinely found in ICU. This chapter presents the clinical validation of the model's predictive performance using data collected from patients in ICU at the Hull Royal Infirmary.

Before attempting any clinical validation the parameter sensitivity of the model was investigated (see Section 5.2), in order to identify those parameters within the model that required accurate measurement, or indeed parameters that because of measurement inaccuracies might contribute to poor predictive performance.

In Section 5.3, the data collection methods and protocol are presented, and the problems encountered in trying to meet them discussed. This is followed by a brief summary of the patient data collected (full details are given in Appendix B). These data were processed to generate the parameters required by the patient model, see Section 5.4. This involved the calculation of prior and post patient parameters to facilitate tuning of the model unknowns, i.e. \dot{Q}_s/\dot{Q}_t , V_D and P_{50} . The model-tuning algorithm is described and the estimated unknowns for each patient presented.

The model-predicted and actual blood-gases produced in response to ventilator changes are compared, see Section 5.5. These comparisons are made using qualitative trend analysis and conventional statistical analysis. Finally the possible causes of response mismatch are explored.

5.2 Model Sensitivity Analysis

Before commencing clinical validation of the model, attention was given to the behaviour of the patient model in response to control and parameter disturbances. This is known as sensitivity analysis and is used to identify those parameters that have greatest influence over the model outputs. If a model is to reflect a patient's state realistically, parameters identified as sensitive will need to be measured accurately for good patient-model matching. However, this may not always be possible, and the combination of measurement errors coupled with parameter sensitivity may lead to poor blood gas prediction. This reflects problems with the data quality rather than the inability of the model to represent true physiology.

Sensitivity analysis can be complex and therefore a simple methodology was employed. Even so, it was still able to provide useful information about the model. The following section describes the analysis used and presents the limitations associated with it, when applied to larger models.

5.2.1 Theory

There are many approaches to sensitivity analysis. The simplest is known as classical sensitivity analysis and looks at the changes in the state variable X_i with respect to a parameter P_j [Tomovic, 1963], and can be expressed thus;

$$S_{ij}(t) = \frac{\partial X_i}{\partial P_j} \quad (5.1)$$

Where $S_{ij}(t)$ is the sensitivity of the state variable i to parameter j , and is time dependant. Since at this stage of model development we are only concerned with steady state sensitivity (i.e. the influence of a parameter when there is no change in model inputs), the sensitivity can be rewritten as;

$$S_{ij} = \left. \frac{\partial X_i}{\partial P_j} \right|_{t=\infty} \quad (5.2)$$

The simplest implementation of this approach is to vary each parameter by a fixed percentage, say 10 % and compare the effects on a given state output. However, it will be seen that this leads to problems when interpreting the results.

Within the blood-gas model the state variables (X_i) are the arterial and venous blood-gas tensions, PaO_2 , $PaCO_2$, PvO_2 and $PvCO_2$; and the disturbance parameters are (listed by category);

- 1). *Patient Parameters*: cardiac output, haemoglobin content, body temperature, pH, O_2 consumption, CO_2 production, peak inspiratory pressure, O_2 diffusion constant, CO_2 diffusion constant.
- 2). *Atmospheric Constants*: barometric pressure, air temperature.
- 3). *Ventilator Parameters*: inspired O_2 and CO_2 fraction, respiratory rate, tidal volume, inspiratory-expiratory ratio, and positive end-expiratory pressure.
- 4). *Unknown (tuned) Parameters*: shunt and dead-space.

Not included in this list are the patient's age, weight, height, sex, O_2 haemoglobin binding capacity (β_h), plasma O_2 absorption constant (α_b) and 50 % saturation point (P_{50}); since these were assumed constant for a given patient during data collection. In retrospect there may be a good argument to have included β_h , and P_{50} since inaccurate values may skew the patients physiology. However, these are not routinely measured and their values are often theoretical. Also not included in this analysis were the compartment volumes since these are concerned with the time constants of the compartments and do not affect steady-state gases. However, short time intervals between blood-gas samples could lead to insufficient settling of the CO_2 dynamics (since they are slower than the O_2 dynamics) leading to model-patient mismatch.

In total, 19 parameters were considered. The model was therefore large and the following problems can arise when sensitivity analysis is attempted on such a model [Rose, 1987].

Excessive computation requirements

The computational cost of repeated simulation runs of a large model can become excessive, due to the large number of possible permutations required.

Strong parameter interaction effects

In some models there is a strong interaction between parameter influences, such that the sensitivity of a given state to parameter change, depends upon the value of some other parameter. Let us consider a simple two-parameter example (see Figure 5.1). The output of a model state X is observed under two conditions for a fixed parameter $P1$. One with $P2 = K$, and the other with $P2 = K'$. When observed under the condition $P2 = K$ the sensitivity of X to parameter $P1$ is low and therefore "unimportant", but when $P2 = K'$ then its sensitivity becomes "significant".

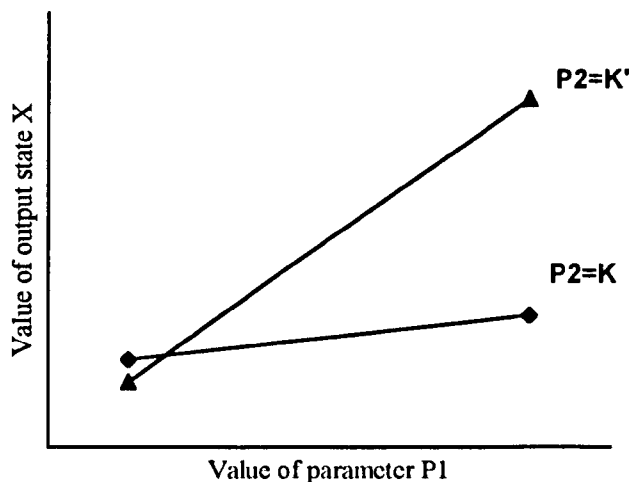


Figure 5.1: Hypothetical responses depicting an interactive effect between parameters $P1$ and $P2$, upon the output X .

Size and shape of the parameter space for valid sensitivity conclusions

The size and shape of the parameter space will dramatically affect the results of a sensitivity analysis. For example a 10 % change in all parameters, irrespective of their nominal values and standard deviation estimates will give very different results to changes based on the average amount each parameter is normally varied. Figure 5.2, illustrates this point by considering the variability distributions PDF1 and PDF2 for two parameters $P1$ and $P2$, with nominal values $N1$ and $N2$. If each parameter is changed by $\pm 10\%$ of their nominal values then $P1$ is being searched across considerably more of its probable values than $P2$, since its nominal (average) value is positively offset. This will result in a lower sensitivity score for $P1$ than if a similar proportion of the PDF was tested.

It might seem reasonable, on the basis of these problems to employ a more rigorous sensitivity technique than provided by the classical sensitivity analysis, and this may well be the case for a truly quantitative analysis. However, the time and effort required for this would be prohibitive and we were forced to settle for a qualitative picture of the respective parameter sensitivities.

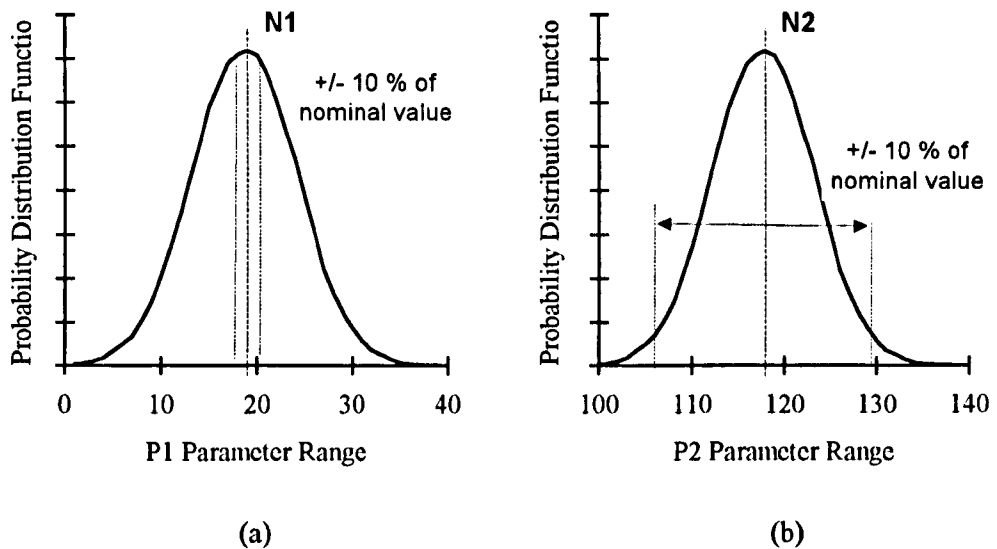


Figure 5.2: Hypothetical parameter space variability showing how this can lead to inaccurate sensitivity conclusions, when the parameter disturbance is much smaller than the normal parameter distribution.

5.2.2 Sensitivity Analysis Method

The model sensitivity analysis (SA) was performed as follows;

- 1). A single real patient data set was used for the test, in this case Patient 1 Record 1 (obtained during the clinical data collection). This provided the initial parameter values and blood gas levels before any parameters were disturbed.
- 2). Only one parameter was varied at a time with all other parameters remaining at their initial value. Each parameter was varied by $\pm 10\%$ of its original value, irrespective of its normal range and initial value.
- 3). The effect of each parameter disturbance on the blood gases PaO_2 , PaCO_2 , PvO_2 and PvCO_2 was recorded, giving a positive and negative response for each.
- 4). The magnitudes of the output responses were then averaged to give a sensitivity measure for each parameter on each output. This was expressed in terms of percentage change from original blood gas levels.

Figure 5.3 compares the output sensitivities for each blood gas to each parameter disturbance. The responses are grouped according to the parameter type (i.e. patient, atmospheric, input and unknown). Blood pH was expressed in terms of hydrogen ion concentration $[\text{H}^+]$, since pH is logarithmic and would otherwise result in non-linear disturbance behaviour.

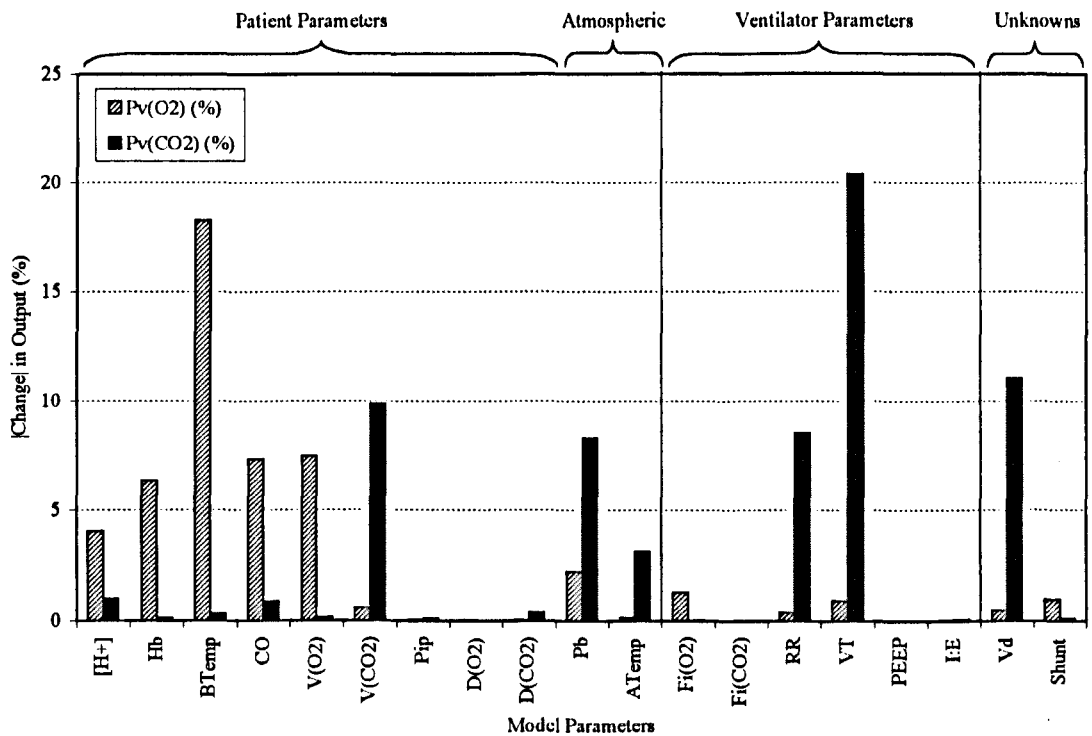
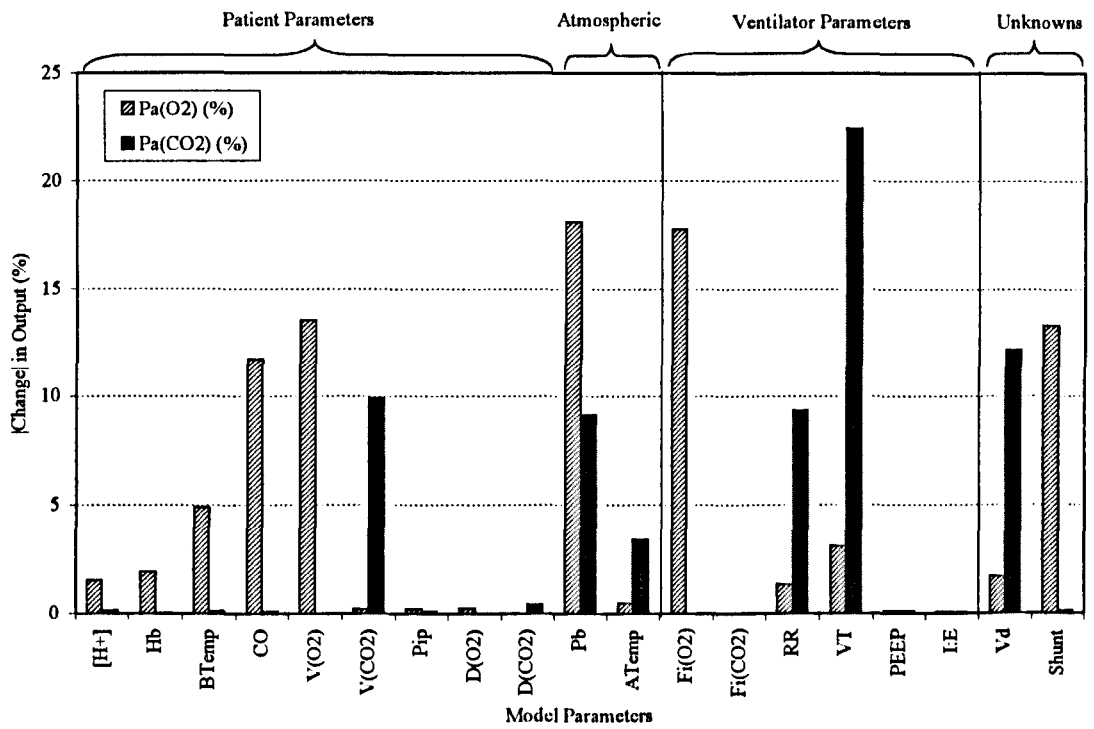


Figure 5.3: Comparison of PaO₂ and PaCO₂ (top chart) and PvO₂ and PvCO₂ (lower chart) output sensitivities to 10 % changes in model parameters. Parameters are grouped by type and sensitivities are expressed as a percentage change from initial blood gases. Initial parameter and gases are based upon patient 1 record 1 (see Appendix B).

5.2.3 Analysis

Over Sensitivity to Barometric Pressure

Initial inspection of the results indicated a larger than expected sensitivity to changes in PB. However the applied change of ± 10.26 kPa is equivalent to changes in altitude of approximately ± 3000 feet (914 m). An individual breathing atmospheric air at sea level would experience a drop in PaO₂ of approximately 2 kPa when elevated to 3000 feet (interpolated from the data of West *et al* (1938) [Nunn, 1993, p340]), a reduction of about 15 %. This is in line with the observed change of 18.11%. Since the sensitivity scores for PB are exaggerated they have been ignored for all of the subsequent comparisons.

Under Sensitivity to PEEP

Conversely PEEP exhibited a very low score, which does not support expected therapeutic effects. This may simply be due to its small disturbance size. However, PEEP also increases PaO₂ by increasing the resting volume of the lung. Reduced lung volumes are often due to the closure of small airways, which are then not ventilated and thus leads to arterial hypoxaemia (Nunn, 1993, p.451). PEEP can hold the airways open throughout the entire respiratory cycle and may therefore restore ventilation to previously perfused but unventilated regions, improving oxygenation. Since the model at this stage does not account for this behaviour, PEEP has no net effect. This effect needs to be included in the model before it can be used for advisor development (see Model Improvements – Section 7.3). Consequently PEEP has been omitted from any subsequent analysis.

Comparison of Parameter Sensitivity Scores

In order to compare the relative sensitivity of the O₂ and CO₂ systems the parameter sensitivity scores (PSS) for the arterial and venous blood gases were averaged;

$$\begin{aligned} PSS_{i(O_2)} &= \frac{S_{i(PaO_2)} + S_{i(PvO_2)}}{2} \\ PSS_{i(CO_2)} &= \frac{S_{i(PaCO_2)} + S_{i(PvCO_2)}}{2} \end{aligned} \tag{5.3}$$

where i is the parameter under consideration and $S_{i(x)}$ is the sensitivity of output x to parameter i .

Having calculated the PSS for each parameter, they were then ranked according to size and grouped using semantic classifiers (e.g. 'very sensitive', 'sensitive', etc.). By doing this it was then possible to construct a visual representation of the sensitivity groupings, see Table 5.1.

The boundaries for the classification were as follows;

- Very Sensitive $PSS_{i(x)} > 10$
- Sensitive $5 < PSS_{i(x)} \leq 10$
- Slightly Sensitive $0.5 < PSS_{i(x)} \leq 5$
- Insensitive $PSS_{i(x)} \leq 0.5$

OXYGEN SYSTEM	CARBON DIOXIDE SYSTEM
INSENSITIVE	
F_{iCO_2} (0.000) D_{CO_2} (0.015) PIP (0.120) DO_2 (0.140) TA_{IR} (0.320) \dot{V}_{CO_2} (0.410)	DO_2 (0.000) F_{iCO_2} (0.000) F_{iO_2} (0.020) Hb (0.085) \dot{V}_{O_2} (0.090) PIP (0.100) Shunt (0.120) T_{BODY} (0.225) D_{CO_2} (0.415) \dot{Q}_t (0.490)
SLIGHTLY SENSITIVE	
RR (0.860) V_D (1.110) V_T (2.010) $[H^+]$ (2.770) Hb (4.120)	$[H^+]$ (0.575) TA_{IR} (3.270)
SENSITIVE	
Shunt (7.140) \dot{Q}_t (9.500) F_{iO_2} (9.550)	RR (8.960) \dot{V}_{CO_2} (9.890)
VERY SENSITIVE	
\dot{V}_{O_2} (10.510) T_{BODY} (11.580)	V_D (11.605) V_T (21.420)

Table 5.1: Comparison of the parameter sensitivity ranking for the O₂ and CO₂ systems.

As expected gas specific parameters were more sensitive in their native system than in the opposite system. For example \dot{V}_{CO_2} was *sensitive* in the CO₂ system but *insensitive* in the O₂ system. Similarly, \dot{V}_{O_2} was *very sensitive* in the O₂ system but *insensitive* in the CO₂ system. This pattern was repeated for the diffusion constants DO_2 , DCO_2 and F_{iO_2} . However F_{iCO_2} was also *insensitive* in the CO₂ system. This can be attributed to poor parameter disturbance, since F_{iCO_2} was effectively zero to begin with.

Alveolar Ventilation

Respiratory rate, tidal volume and dead space changes influenced O₂ tensions less than CO₂ tensions by about a factor of 10. All of these parameters affect alveolar ventilation, which will increase the rate of O₂ flowing into the lung and CO₂ flowing out of it. This has the effect of raising the alveolar O₂ content and reducing the alveolar CO₂ content. The diffusion gradient

across the lung membrane is higher for CO₂ than for O₂ and therefore the effect is greatest in the CO₂ system. This is in keeping with the therapeutic benefits of changing the ventilation rate to bring CO₂ tensions to normal.

Shunt

The O₂ system was *sensitive* to shunt changes, where as the CO₂ system was *insensitive*. Qualitatively, venous shunt reduces the overall efficiency of gas exchange and results in arterial blood gases closer to venous levels, depending on the level of shunt involved. Considering the gases in terms of content the mixing is easily explained by the mass transport equations;

$$\begin{aligned} C_{aO_2} &= \dot{Q}_s / \dot{Q}_t \cdot C_{vO_2} + (1 - \dot{Q}_s / \dot{Q}_t) \cdot C_{pO_2} \\ C_{aCO_2} &= \dot{Q}_s / \dot{Q}_t \cdot C_{vCO_2} + (1 - \dot{Q}_s / \dot{Q}_t) \cdot C_{pCO_2} \end{aligned} \quad (\text{ml/l}) \quad (5.4)$$

As \dot{Q}_s / \dot{Q}_t increases, the arterial O₂ content will be reduced by mixing with the lower venous O₂ content level. Conversely the arterial CO₂ content will be increased slightly by the higher venous level. This effect is linear, so does not explain the difference in sensitivities. However, due to the steep gradient of the CO₂ dissociation curve near the arterial point, the effect on the CO₂ tension is small. The O₂ dissociation curve is almost flat at the arterial point (assuming good saturations) and therefore small changes in content produce large differences in O₂ tension. If the blood is poorly oxygenated then the effects of changes in shunt are reduced and PaO₂ remains relatively unaffected since the arterial point now lies on a steeper part of the O₂ dissociation curve.

Air Temperature

Changes in air temperature had little effect on the O₂ system but a more marked effect on the CO₂ system. This is because tidal volumes are expressed at ATPS and require conversion to BTPS. Since tidal volume exerts a greater influence on the CO₂ system then the increased CO₂ sensitivity was expected.

Acid / Base System

Changes in pH (reflected here as changes in hydrogen ion concentration) exert their effect through the gas dissociation functions. The effect on each system depends very much on the position of the content-pressure point on the curves. Again because the CO₂ GDF tends to be steeper than the O₂ GDF the shifting of the curves produces a larger effect in the O₂ system than the CO₂ system

Body Temperature

This affects both of the gas dissociation functions, but was more marked in the O₂ system. Again the relative position of the content-pressure point on the gas dissociation curves explains this difference.

Haemoglobin Concentration

Haemoglobin concentration determines the carriage of O_2 in the blood as given by equation 4.13 and therefore its greater sensitivity in the O_2 system would be expected. The small effect it does exert on the CO_2 system, is through the CO_2 dissociation function, since changes to O_2 saturation affect the CO_2 cell to plasma content ratio (see equation 4.35).

Cardiac Output

O_2 system sensitivity to \dot{Q}_t makes problems for patient-model matching since \dot{Q}_t is very difficult to measure reliably. It is probably this single factor alone that will negate the possibility of patient matching. The reason being that an erroneous \dot{Q}_t measurement, say 10 % below true \dot{Q}_t , would give rise to a reduced shunt estimate when the model was tuned. This would increase the model's sensitivity to step changes in FIO_2 and impair its predictive performance.

Cardiac output measurements are normally made using thermo dilution and at the time of data collection, was only made on a need to know basis. Almost continuous \dot{Q}_t measurement is now possible enabling sample precision to be improved. However, measurement accuracy is still uncertain and anaesthetists tend to use changes in \dot{Q}_t as an indication of changing cardiac performance rather than rely on the values themselves.

This does not however mean the model is unsuitable, just that validation against patient data is difficult using current measurement technologies.

Peak Airway Pressure

Neither system is very sensitive to changes in PIP. In truth this parameter should not be viewed as a model-input, since it is really a product of the airway dynamics and the ventilator driving waveform. Later improvements to the model derive PIP as a model output (see Section 7.3.2).

5.2.4 Conclusions of Sensitivity Analysis

So what can be concluded from all of this? Firstly, the greater sensitivity of the O_2 system to shunt and the CO_2 system to dead space meant that shunt could be adjusted to match PaO_2 with little disturbance of $PaCO_2$, and VD could be adjusted to match $PaCO_2$, with only a slight disturbance of PaO_2 . This made model tuning a lot simpler to implement.

Secondly, the high PO_2 sensitivity to cardiac output changes posed the biggest obstacle to patient matching, since this measurement suffers from the largest measurement errors. Similarly the high sensitivity of the model to O_2 consumption and CO_2 production meant they required accurate measurement. Unfortunately at the time of the data collection, metabolic performance was not routinely monitored at the target ICUs and therefore a metabolic computer needed to be borrowed. This provided accurate measurement abilities, but unfortunately could only be loaned for a limited period. Forearmed with this knowledge of the model's sensitivity, the patient data were collected.

5.3 Data Collection

The primary objective of the data collection period (and consequently its major restricting factor) was to collect enough patient measurements such that the number of unknowns in the patient model was kept to a minimum. Most of the patient parameters could be obtained from routine measurements made within the ICU. However cardiac output (\dot{Q}_t), O_2 consumption ($\dot{V}O_2$) and CO_2 production ($\dot{V}CO_2$) were also required by the model and these were not as readily available.

Arterial blood samples were taken via a radial artery catheter (RAC) which is routinely inserted into most patients. However, patients with circulatory problems such as those suffering from shock may require a femoral artery catheter (FAC) instead. The use of radial catheters is preferable to femoral ones both in terms of accessibility and associated risks, since the femoral artery has an increased risk of catastrophic bleeding, being more central to the heart. All patients in this study were catheterised at the radial artery.

Venous blood samples were taken from either a central venous catheter (CVC) inserted into the right atrium or from a pulmonary artery catheter (PAC). Samples taken via a PAC will give true mixed venous blood readings, whereas CVC samples may not, since there is no guarantee that they have mixed fully. Both pulmonary artery and central venous catheters carry a degree of risk with their use, but this level is not unacceptable. Figure 5.4 indicates the positions of the radial artery, central venous and pulmonary artery catheters within the patient when viewed from a model-based perspective.

Blood samples taken were analysed using an IL System 1302 pH/Blood Gas Analyser, which gives direct measurement of pH, PO_2 and PCO_2 . This system also measures haemoglobin content and calculates standard bicarbonate, base excess and O_2 saturation amongst other variables.

The radial artery catheter was also used to carry a pressure transducer from the M1006A Pressure Module (part of the HP Component Monitoring System) to measure systolic, diastolic and mean arterial blood pressure as well as pulse rate. A similar module was used to measure mean pulmonary blood pressure and wedge pressure via a transducer inserted down the pulmonary artery catheter. Wedge pressure measurement required the CO1 module option with an intra-aortic balloon pump. If a central venous catheter was connected then a third similar module was used to measure the central venous blood pressure.

Cardiac output was measured using the M1012A C.O. Module (HP Component Monitoring System - HPCMS). This measures \dot{Q}_t using the thermal dilution method and requires the use of a Swan-Ganz catheter inserted down the PAC. However, this measurement technique is usually only reserved for unstable patients.

This posed a dilemma since the patients needed to be stable but catheterised. This was overcome by opting for patients in the period prior to removal of the PAC when they had stabilised; a window of between 1-3 days. In reality this was not always practicable and all catheterised patients were recorded. Also on occasions during the data collection period there were no suitable patients available. In order to maximise the available time with the metabolic computer, patients without a PAC were recorded and \dot{Q}_t was estimated using O_2 consumption and the arterial-venous O_2 content difference.

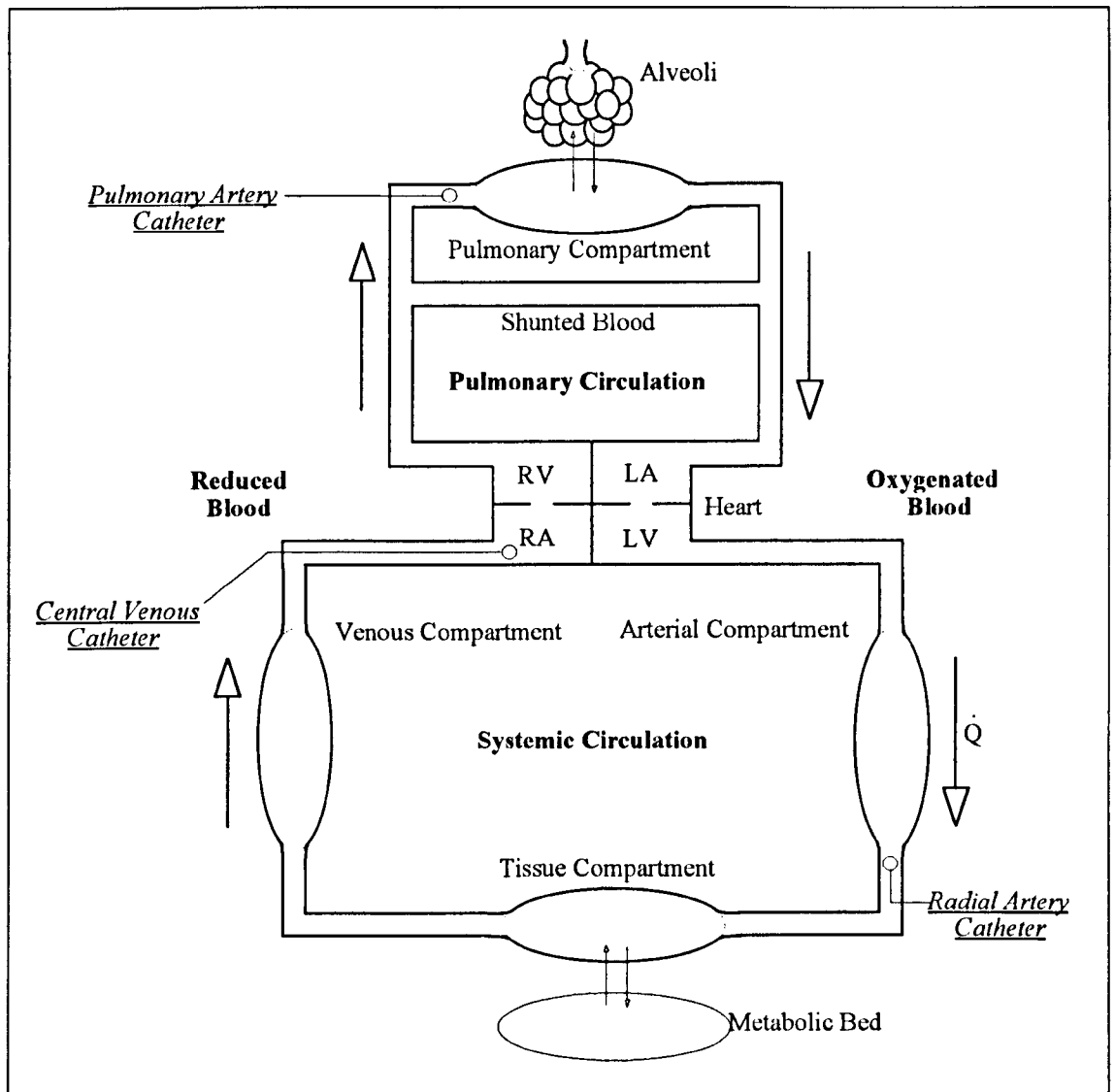


Figure 5.4: Schematic of Model Circulation Showing Patient Measurement Points.

Blood temperature was measured using the temperature probe that forms part of a Swan-Ganz catheter. In the absence of a Swan-Ganz catheter, rectal or skin temperature was recorded. These provide good estimates of actual blood temperature in stable patients. However, collapse of periphery circulation in a post-operative patient may cause a blood-rectal temperature differential of as much as 6 °C.

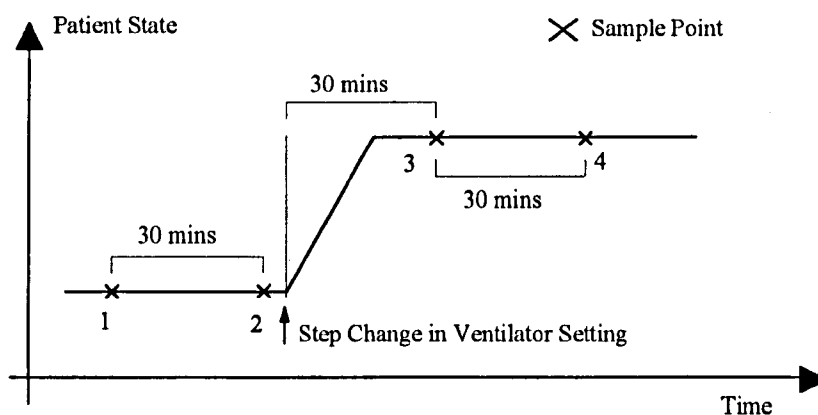
O₂ consumption and CO₂ production were measured using a metabolic computer (MC). Since neither of the ICU's involved in the study possessed one, a Deltatrac-II had to be loaned from Datex for a limited period of 3 weeks. This was the largest restricting factor on the data collection study and explains why the data set was so small. $\dot{V}O_2$ and $\dot{V}CO_2$ can be calculated indirectly from the arterial-venous blood-gas difference and \dot{Q}_t , but this can lead to large errors due to the inaccuracies associated with \dot{Q}_t measurement.

The M1020A SaO₂/Plethysmography Module (HPCMS) was used to give a continuous non-invasive measurement of SaO₂, using pulseoximetry techniques. It actually measures end capillary O₂ saturation and gives poor accuracy if there is peripheral shut down.

As mentioned previously there still remained a number of unknowns of which some had to be assumed, namely haemoglobin O_2 binding capacity, O_2 dissolved in plasma coefficient and haematocrit, since their measurement would be impractical in such a study. This left \dot{Q}_s/\dot{Q}_t , VD and P_{50} , which were estimated using an iterative solution searching method.

5.3.1 Data Collection Protocol

- 1) Identify *suitable patients* for data collection purposes and record where possible two *sets of measurements* prior to and after a *ventilator change*, see Figure 5.5. The prior measurements should be approximately 30 minutes apart in order to establish the steady state of the patient. The second measurement should directly precede the ventilator change. The first post measurement should occur 30 minutes after the ventilator change and be followed 30 minutes later by a second measurement.



SAMPLING PROTOCOL : FOUR SAMPLE POINTS

- [1] 30 min before ventilator change.
- [2] Just before ventilator change.
- [3] 30 min after ventilator change
- [4] 60 min after ventilator change.

Figure 5.5: Steady state sampling protocol.

- 2) A *suitable patient* should ideally have a PAC inserted and be beyond any period of instability, but prior to removal of the PAC. This constitutes a window of approximately 1-3 days when the patient should be stable and cardiac output can be measured, see Figure 5.6.

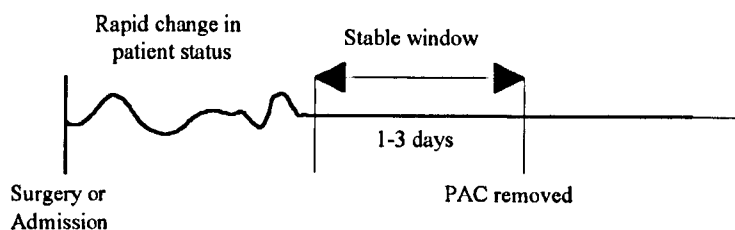


Figure 5.6: Stable period during which measurements can be made.

- 3) A *set of measurements* comprises the following (those measurements required by the patient model are indicated by *, all others to be recorded for completeness);

General Patient Details

Height*, Weight*, Age*

Patient diagnosis, supporting therapies (drugs, dialysis, etc.)*

From Radial Artery Catheter

PaO₂*, PaCO₂*, arterial pH*, Hb*, SaO₂, standard bicarbonate (SBC), base excess (BE)

Systolic, diastolic and mean arterial pressure.

From Central Venous Catheter

PvO₂, PvCO₂*, venous pH, SBC, BE and SvO₂

From Pulmonary Artery Catheter

P \bar{v} O₂*, P \bar{v} CO₂*, mixed-venous pH*, SBC, BE, S \bar{v} O₂, T_{BLOOD}*, \dot{Q}_t *

Mean pulmonary blood pressure and wedge pressure.

Using Metabolic Computer

O₂ consumption*, CO₂ production*, respiratory quotient (RQ) and metabolic rate (MR).

Air temperature*, ambient pressure* and ambient CO₂*

Basal metabolic rate, non-protein RQ, energy substrate utilisation, body surface area

Ventilator Settings / Measurements

FIO₂*, RR*, VT*, PEEP*, PIP*, P_{MEAN}, I:E ratio*

Driving waveform characteristics, ventilator type, ventilation mode.

Tubing and filter arrangement.

Miscellaneous

Pulseoximeter O₂ saturation, heart rate, rectal temperature, skin temperature

- 4) A *ventilator change* comprises a step changes in one of the 5 primary ventilator settings; FIO₂, RR, VT, PEEP and I:E ratio. These changes are to be made within the ethical committee guidelines, see Appendix B. An optimal test regime will be to make at least two changes in a ventilator setting, ideally in opposite directions and not returning to its original value. Figure 5.7 gives an optimal regime, with FIO₂ increased to 45 % but then reduced to 30 % rather than its original value.

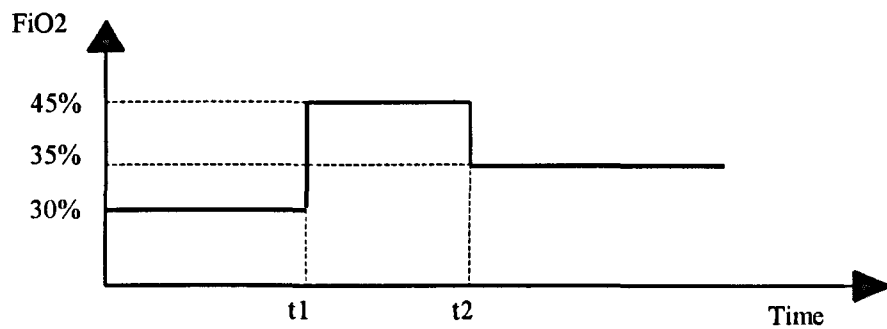


Figure 5.7: Optimal control change regime.

It was found through interaction with ICU staff and observation of the patient management methodologies that trying to restrict the collection of the data to this protocol would be very limiting. Consequently;

- Sometimes only one PRIOR and POST measurement were made, where the protocol stipulated two, in order to establish the steady state condition of the patient before and after therapy change.
- Sometimes not all of the measurements required were recorded due to the time constraints on the anaesthetists making the measurements.
- Sometimes the patients were very unstable and not really suitable for validation purposes, but were recorded anyway.
- Sometimes the patients were not connected to a PAC, thus negating the possibility of cardiac output measurements.
- Sometimes drug maintenance or physiotherapy interfered with a study, introducing a further unknown artefact into the data.

5.3.2 Summary of Collected Data

Four patients were identified as suitable for study during the 3-week data collection window, and from these 9 ventilator changes were recorded. These are detailed in full in Appendix B, with a synopsis of each patient, a description of the ventilator arrangement used, atmospheric conditions derived from the metabolic computer and full records of the patient measurements and ventilator settings.

5.4 Data Processing & Model Tuning

In order to produce parameter values usable by the patient model, the measurements prior to the ventilator change needed to be averaged to give a single snapshot of the patient, which could be entered into the model. Similarly the post measurements needed to be averaged to give a snapshot of what happened after the ventilator change. However before this could be done the metabolic computer results for O₂ consumption and CO₂ production rates needed to be processed to produce a single value at each measurement time. In addition to this certain patients did not have a Swan-Ganz catheter inserted. This prevented the measurement of cardiac output and it therefore had to be derived using other patient measurements.

Once the data sets were complete and had been averaged to produce the prior and post patient snapshots, it was then possible to tune the prior data to match the measured gases. This was done by iteratively adjusting shunt, dead space and P₅₀. It was only after this that the performance of the model could be assessed.

5.4.1 Metabolic Computer Results

The O₂ consumption rate (\dot{V}_{O_2}) and CO₂ production rate (\dot{V}_{CO_2}) of the patient at the sample time (i.e. when the venous and arterial blood gas samples were taken) were obtained by taking a 10-point average of the metabolic computer (MC) data centred on the sample time. Since the metabolic computer takes measurements once every minute, this gave an average based upon 5 minutes prior to and 5 minutes after the sample point. During the measurement period the MC would sometimes generate artefact flags indicating that \dot{V}_{O_2} and \dot{V}_{CO_2} measurements were unstable and therefore to be treated with caution, see Figure 5.8. If these caused deviations of greater than 5 % from mean when calculating the sample average, then the next nearest non-artefact data were used.

5.4.2 Calculation of Cardiac Output

In records P1-3, P1-4 and P2-1 the patients were not fitted with a pulmonary artery catheter (PAC) and therefore it was not possible to measure cardiac output using thermo-dilution techniques. However, \dot{Q}_t can be estimated using O₂ consumption (\dot{V}_{O_2}) and the arterial-venous O₂ content difference (CaO₂ – CvO₂) via the following equation;

$$\dot{Q}_t = \frac{\dot{V}_{O_2}}{CaO_2 - CvO_2} \quad (5.5)$$

This is only possible because of the use of the metabolic computer to measure \dot{V}_{O_2} . The arterial-venous content difference was calculated from the blood gas tensions using the O₂ gas dissociation function together with the other blood measurements (haemoglobin, blood temperature, etc). The haemoglobin binding capacity was assumed to be 1.34 g/l, the plasma O₂ carrying coefficient to be 0.225 ml/l/kPa and the P₅₀ point to be 3.5774 kPa. Table 5.2 shows the results of these calculations.

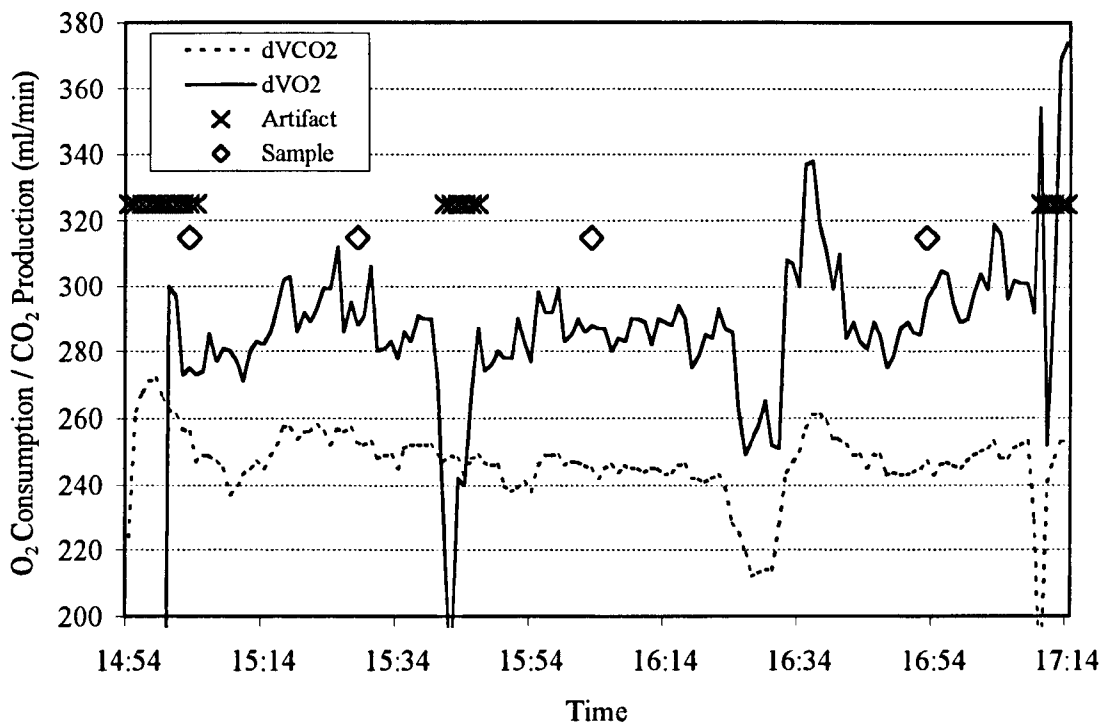


Figure 5.8: Example of output generated by Deltatrac II Metabolic Computer for O_2 consumption and CO_2 production in Patient 1-2. The computer indicates regions of artefact (x) when the measurements cannot be relied upon since they vary well beyond expected ranges. Averages taken around the sample points (◊) need to avoid these artefacts.

Reference	CaO_2 (ml/l)	CvO_2 (ml/l)	$C(a-v)O_2$ (ml/l)	$\dot{V}O_2$ (ml/min)	\dot{Q}_t (l/min)
P1-1 / 1	123.21	101.55	21.66	289.4	13.36
2	123.04	101.64	21.40	282.1	13.18
3	127.36	106.51	20.85	279.1	13.38
4	131.25	109.64	21.61	284.4	13.16
P1-2 / 1	127.36	106.51	20.85	279.1	13.38
2	131.25	109.64	21.61	284.4	13.16
3	132.30	111.99	20.31	266.2	13.11
P2-1 / 1	148.06	100.18	47.88	368.5	7.70
2	148.07	94.98	53.09	314.2	5.91
3	151.69	106.46	45.23	309.7	6.85
4	143.18	104.98	38.20	308.4	8.07

Table 5.2: Estimated cardiac output for patients without pulmonary artery catheters. Arterial-venous content difference calculated using O_2 gas dissociation function and arterial/venous measurements. O_2 consumption measured using metabolic computer.

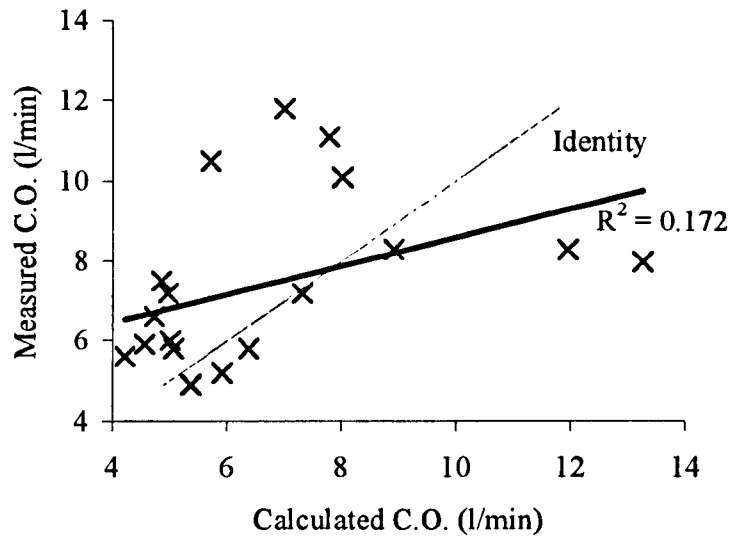


Figure 5.9: Correlation between measured cardiac output (using thermo-dilution) and calculated cardiac output using O_2 consumption and arterial-venous O_2 content difference.

However, deriving \dot{Q}_t in this manner is very approximate as illustrated when measured \dot{Q}_t (using thermo-dilution) was compared with that calculated using equation 5.5, for those patient records where \dot{Q}_t was measured, see Figure 5.9.

Indeed, the values derived for P1-3 and P1-4 appear to be a lot higher than previous measurements would suggest. However, the absence of any other measure for \dot{Q}_t meant that these values had to be used. By implication this will lead to larger estimates of shunt than might be expected, reducing the sensitivity of the model and therefore perhaps the accuracy of the model.

5.4.3 Generation of PRIOR and POST Data

In order to apply the data to the patient model, measurements made prior to a ventilator change were averaged to give a starting patient scenario. This was repeated for measurements made after the ventilator change. Two prior and two post measurements were not always available and in these instances a single measurement had to suffice. No consideration was taken of the data quality and all points were considered. The data resulting from this averaging is given in Table 5.3 and Table 5.4.

This generated most of the parameters required to run a patient simulation with the exception of those which were not easily measured (because they are not routinely monitored or because of the physical difficulties in measuring them). This includes shunt, dead space and P_{50} , which were adjusted to match the simulated blood gases to the measured values. The parameters obtained from the data collection, were as follows;

- FIO_2 , RR, VT, PEEP, I:E and PIP
- pH(art), pH(ven), Hb, blood temperature, \dot{Q}_t , $\dot{V}O_2$ and $\dot{V}CO_2$
- PB, air temperature and $FICO_2$ (ambient CO_2)
- Height, weight, age and sex.

	P1-1	P1-2	P1-3	P1-4	P2-1	P3-1	P3-2	P3-3	P4-1
VENTILATOR SETTINGS									
FIO2 (%)	55	50	55	60	40	65	70	75	50
Respiratory Rate (rpm)	24	20	18	18	17	16	16	16	14
Tidal Volume (ml)	680	670	870	870	700	618	615	590	693
PEEP (cmH2O)	10	5	7.5	7.5	2	10	10	10.3	5
I:E Ratio (I/E)	0.8	1.1	1	1	0.333	2	2	1.43	1.56
PIP (cmH2O)	30.2*	22.6*	24*	24*	36*	35*	33.8*	39.6*	31
ARTERIAL									
PaO2 (kPa)	17.55	12.35	8.65	9.25	20.9	8.1*	7.8*	11.7	11.5
PaCO2 (kPa)	4.3	5.48	4.795	4.735	5.255	5.12*	5.31*	5.245	3.79
pH	7.535	7.4725	7.4635	7.487	7.376	7.349*	7.356*	7.3655	7.3535
Hb (g/100ml)	11.6*	10.6*	9.6*	9.95	10.8*	10.4*	10.1*	10.4*	13.6
VENOUS									
PvO2 (kPa)	4.5	4.9	5.3	5.5	4.85	4.5*	4.6*	4.6	5.95
PvCO2 (kPa)	4.95	5.905	5.465	5.315	6.405	5.61*	5.48*	5.67	4.125
pH	7.49	7.4595	7.468	7.467	7.3225	7.359*	7.351*	7.3565	7.3515
OTHER MEASUREMENTS									
Blood Temperature (°C)	36.45	36.45	36.7	36.6*	36.25	38.8*	38.8*	37.2	37.95
Cardiac Output (l/min)	5.35	7.75	13.27	13.27	6.805	7.5*	7.2*	5.8	11.15
O2 Consumption (ml/min)	276	286.35	285.75	281.75	341.35	218.6*	202.1*	214.7	237.9
CO2 Production (ml/min)	239	249	252.9	242.8	273.55	179.6*	162.1*	190.2	203.55
ATMOSPHERIC CONSTANTS									
Air Temperature (°C)	28.4*	28.4*	29.2*	29.2*	29.1*	29.6*	29.3*	29.3*	25.4
Ambient Pressure (kPa)	102.525*	100.391*	100.791*	100.791*	100.658*	100.658*	100.658*	100.658*	100.395
Ambient CO2 (%)	0.05*	0.06*	0.04*	0.04*	0.05*	0.05*	0.06*	0.06*	0.04

Table 5.3: Averaged PRIOR patient data (* indicates only a single measurement was available).

	P1-1	P1-2	P1-3	P1-4	P2-1	P3-1	P3-2	P3-3	P4-1
VENTILATOR SETTINGS									
FIO2 (%)	55	45	60	65	35	70	75	70	50
Respiratory Rate (rpm)	26	20	18	18	16	16	16	16	12
Tidal Volume (ml)	680	670	870	880	700	615	615	590	689
PEEP (cmH2O)	10	5	7.5	7.5	3	10	10	10.2	5
I:E Ratio (I/E)	0.6	1.1	1	1	0.333	2	2	1.43	1.85
PIP (cmH2O)	36.2*	22.7*	24*	24*	32*	33.8*	33.8*	38.8*	35
ARTERIAL									
PaO2 (kPa)	16.9	10.45	9.25	9.7*	17.8	7.8*	10*	11.5	11.7
PaCO2 (kPa)	3.95	4.9	4.735	4.79*	4.685	5.31*	5.28*	5.345	4.095
pH	7.56	7.501	7.487	7.503*	7.4175	7.356*	7.348*	7.3685	7.3735
Hb (g/100ml)	11.6*	10.6*	9.95	10.1*	10.85	10.1*	9.9*	10.6*	11.75
VENOUS									
PvO2 (kPa)	4.2	5.47	5.5	5.6*	5.35	4.6*	4.8*	4.7	5.9
PvCO2 (kPa)	4.65	4.7	5.315	5.29*	5.675	5.48*	5.15*	5.835	4.42
pH	7.52	7.482	7.467	7.476*	7.3695	7.351*	7.346*	7.3615	7.361
OTHER MEASUREMENTS									
Blood Temperature (°C)	36.55	36.5	36.6*	36.5*	37.05	38.8*	38.8*	37.2	37.9
Cardiac Output (l/min)	5.05	8.15	13.27	13.11*	7.46	7.2*	5.9*	6.2	10.6
O2 Consumption (ml/min)	281.65	289.7	281.75	266.2*	309.05	202.1*	210.5*	216.8	265.6
CO2 Production (ml/min)	240.5	245.25	242.8	235.6*	267.55	162.1*	173.3*	186.75	203.9
ATMOSPHERIC CONSTANTS									
Air Temperature (°C)	28.4*	28.4*	29.2*	29.2*	29.1*	29.6*	29.3*	29.3*	25.4
Ambient Pressure (kPa)	102.525*	100.391*	100.791*	100.791*	100.658*	100.658*	100.658*	100.658*	100.395
Ambient CO2 (%)	0.05*	0.06*	0.04*	0.04*	0.05*	0.05*	0.06*	0.06*	0.04

Table 5.4: Averaged POST patient data (* indicates only a single measurement was available).

From these the patient model calculated the following additional parameters;

- Haematocrit (or PCV) from Hb (see equation 4.67).
- Mean airway pressure from ventilator settings (see equation 4.39).
- Compartment volumes from weight (see equation 4.52).
- Functional residual capacity (FRC) from height (see equation 4.56).
- Gas diffusion coefficients from FRC and age (these were later replaced by fixed coefficients).

This left the model unknowns;

- P_{50} , \dot{Q}_s/\dot{Q}_t and VD to be derived during model tuning.
- Hb O₂ combining capacity, assume to be 1.34 ml/g (see Section 4.2.3).
- Plasma O₂ solubility coefficient, assumed to be 0.225 ml/l/kPa

Applying these measured, calculated and tuned parameters for each patient to the model, it can then be used to predict the effects of ventilator changes on the blood gases. However, before this can be done the PRIOR model snapshot needs to be tuned, such that the arterial and venous blood gases match with those measured.

5.4.4 Model Tuning

The tuning of the model's steady-state blood-gases to match those measured was performed in an iterative manner as shown in Figure 5.10. Shunt was adjusted to match PaO₂, dead space to match PaCO₂ and P₅₀ to match PvO₂. The parameter tuning was performed using a secant-searching algorithm similar to that used in Section 4.2.4. Due to parameter interaction the matching procedure had to be repeated until the error between the model and measured blood-gases was less than 0.01 kPa. Tuning of PvCO₂ was not possible and the value arrived at by tuning the other variables was accepted.

Convergence was possible because shunt primarily affects PaO₂ and dead space primarily affects PaCO₂. The tuning of P₅₀ to match PvO₂ accommodates errors in the position of the saturation curve. This is similar to the approach used by Hinds *et al* (1983).

Problems were encountered during the initial attempts to tune the model. In some cases VD estimates were unrealistically high, in others the search algorithm was unable to find a positive solution for shunt. Investigation of possible causes showed that the empirical formula used to calculate the gas diffusion constant (see equation 4.51) was giving very low values for some of the patients. This resulted in higher PaCO₂ levels requiring larger VD estimates and lower PaO₂ levels requiring lower or negative shunts. It was decided to remove this variable factor and use a fixed DO₂ of 450 ml/kPa/min and DCO₂ of 1500 ml/kPa/min as quoted by Selvakumar *et al* (1992).

Examination of the effects of changing DO₂ and DCO₂ supported this assumption and also showed that the new fixed values sat within an less sensitive region of the curves, see Figure 5.11. In some cases the model was arriving at DO₂ and DCO₂ values of less than

200 ml/min/kPa, which according to the graphs would give deviations in the predicted O₂ and CO₂ of greater than 5 %. The results of the model tuning, using fixed DO₂ and DCO₂ values, are shown in Table 5.5.

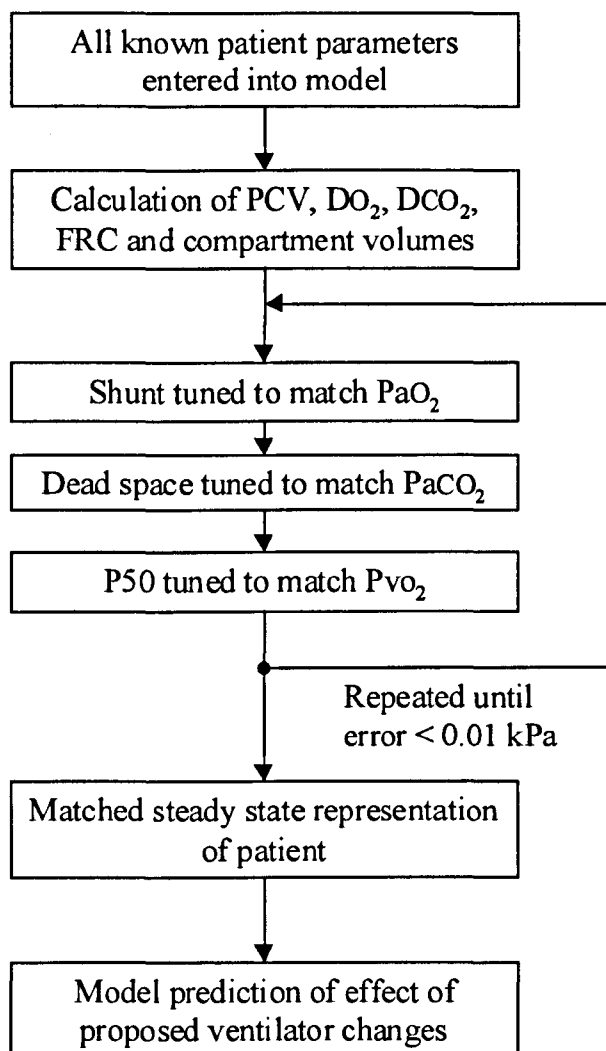
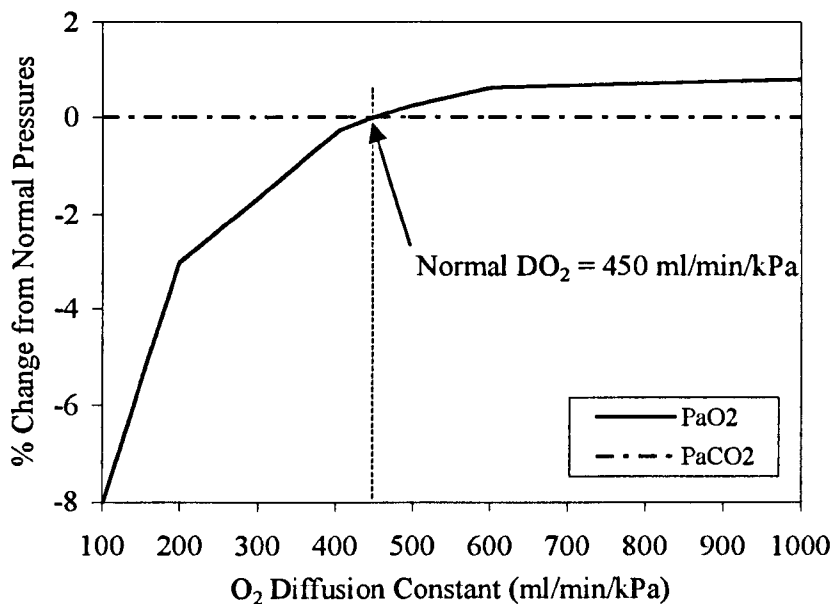


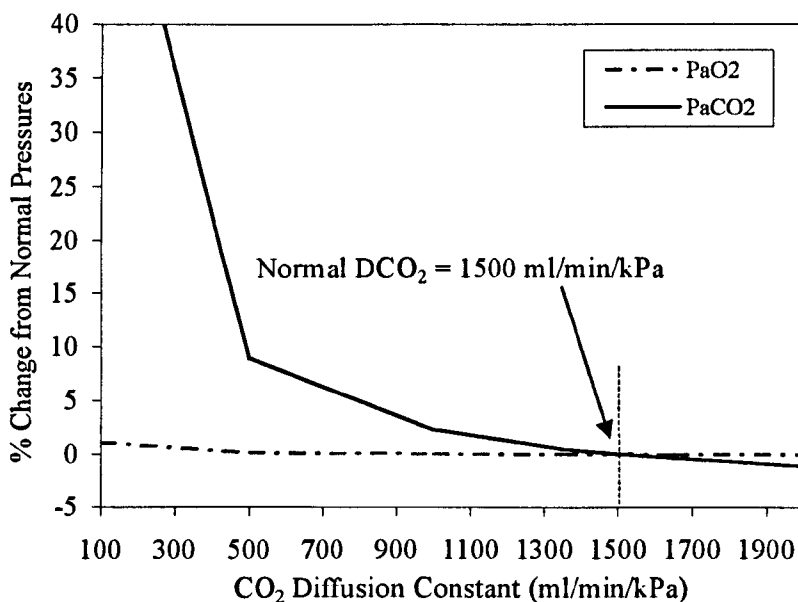
Figure 5.10: Flow diagram of the model tuning algorithm.

	P1-1	P1-2	P1-3	P1-4	P2-1	P3-1	P3-2	P3-3	P4-1
Iso shunt (%)	14.76	19.38	31.47	30.22	6.42	36.02	38.38	27.47	21.13
Shunt (%)	12.84	18.90	40.63	39.55	4.96	36.92	41.12	26.91	31.17
VD (ml)	405.22	404.16	516.40	528.45	331.31	352.35	389.73	311.77	219.37
P₅₀ (kPa)	4.2242	4.0577	3.9315	3.9066	3.9934	2.9473	3.0729	3.3773	3.2383

Table 5.5: Shunt, VD and P₅₀ estimates obtained by matching the model to the measured PRIOR blood-gases. Also shown for comparative purposes are the shunt estimates arrived at using the iso-shunt diagram of Benetar *et al* (1973).



(a)



(b)

Figure 5.11: (a) The effect of changes in DO_2 on the arterial gases. As DO_2 falls below 200 ml/min/kPa the PaO_2 is more affected. A low DO_2 would create lower model PaO_2 and therefore the possibility of negative venous shunt if the simulated and measured PaO_2 are to match. DCO_2 was fixed at 1500 ml/min/kPa; (b) the effect of changes in DCO_2 on the arterial blood gases. As DCO_2 falls below 1000 ml/min/kPa the $PaCO_2$ becomes more affected. A low DCO_2 would create higher model $PaCO_2$ and therefore the possibility of excessively large dead space estimates. DO_2 was fixed at 450 ml/min/kPa and all other parameters were taken from patient P1-1.

5.5 Clinical Validity

So far we have; (1) examined the model's sensitivity to parameter disturbances enabling the identification of those parameters that may contribute to poor predictive performance; (2) defined a data collection protocol and used this to collect 4 patient records (containing 9 ventilator changes); (3) processed the collected data to form snap-shots of the patient's state, prior to and after a ventilator change; and (4) tuned the model unknowns for each prior data set to match the measured blood gases.

It was now possible to assess the model's predictive performance by changing the ventilator settings of the model, as per the changes made on the real patients. The simulated patient responses can then be compared with those measured. The measured and model-predicted responses are shown in Figure 5.13, with the actual response values given in Table 5.7.

There are clearly some instances when the model-predicted responses match the measured responses, some when the direction is the same but the magnitudes are different and others when the changes are in opposite directions. There also appears to be a greater disturbance of the O₂ system than the CO₂ system as shown by the overall difference in magnitude of the PaO₂ and PaCO₂ changes.

Two methods of analysis were employed to assess the accuracy of these model predictions. The first of these, *qualitative trend analysis* looks at the direction of the responses rather than their magnitude [Leaning, 1980; Leaning *et al*, 1983]. This gives an indication of whether the patient and/or model are responding to ventilator changes as expected.

The second method uses statistical measures such as standard error and correlation coefficient to quantify the model's predictive performance. A similar (though not identical model) was assessed by Hinds *et al* (1983), and the results of their analysis are used as a yard stick against which to gauge the model's performance.

5.5.1 Qualitative Trend Analysis

Three qualitative trend comparisons were made. The first of these compared the measured trends with the expected trends. The expected trends (or *intuitive trends*) were derived from the simple rules used by an anaesthetist to achieve blood-gas management, see Table 5.6. By comparing these *intuitive trends* with the *measured trends* it was possible to assess the quality of the measured responses. This was not an indicator of measurement error, more a means of distinguishing between well behaved and poorly behaved patient responses.

Note that the effects of ventilator changes on PvO₂ and PvCO₂ were not considered. However, PvO₂ changes will normally match the PaO₂ changes in terms of direction but with much smaller magnitude (lower sensitivity) and PvCO₂ will change in a similar manner to PaCO₂.

This can be explained by the relative positions of the dissociation curves. Because the O₂ dissociation curve is non-linear, the arterial points lie on a flatter portion of the curve than the venous points. Therefore when the haemoglobin saturation changes by a small amount at the

arterial point, it results in large shift in PO_2 , whereas at the venous point, where the curve is much steeper the effect is greatly reduced (see Figure 5.12). The CO_2 dissociation curve on the other hand is fairly linear and therefore changes in CO_2 content cause similar changes in CO_2 tension at the arterial and venous points.

This behaviour is confirmed in Figure 5.13, where the model-predicted PvO_2 responses match the PaO_2 responses in terms of direction but are considerably smaller in magnitude. The $PvCO_2$ and $PaCO_2$ responses on the other hand are almost identical.

Direct Therapy Trends	Cross-coupled Therapy Trends
An increase in FiO_2 will increase PaO_2	An increase in RR will increase PaO_2
A decrease in FiO_2 will decrease PaO_2	A decrease in RR will decrease PaO_2
An increase in PEEP will increase PaO_2	An increase in VT will increase PaO_2
A decrease in PEEP will decrease PaO_2	A decrease in VT will decrease PaO_2
An increase in RR will decrease $PaCO_2$	An increase in FiO_2 gives no change in $PaCO_2$
A decrease in RR will increase $PaCO_2$	A decrease in FiO_2 gives no change in $PaCO_2$
An increase in VT will decrease $PaCO_2$	An increase in PEEP gives no change in $PaCO_2$
A decrease in VT will increase $PaCO_2$	A decrease in PEEP gives no change in $PaCO_2$

Table 5.6: Summary of intuitive responses to ventilator changes. Direct therapy trends correspond to the intended therapeutic effects of a ventilator change, and cross-coupled trends are the indirect consequences of a ventilator change.

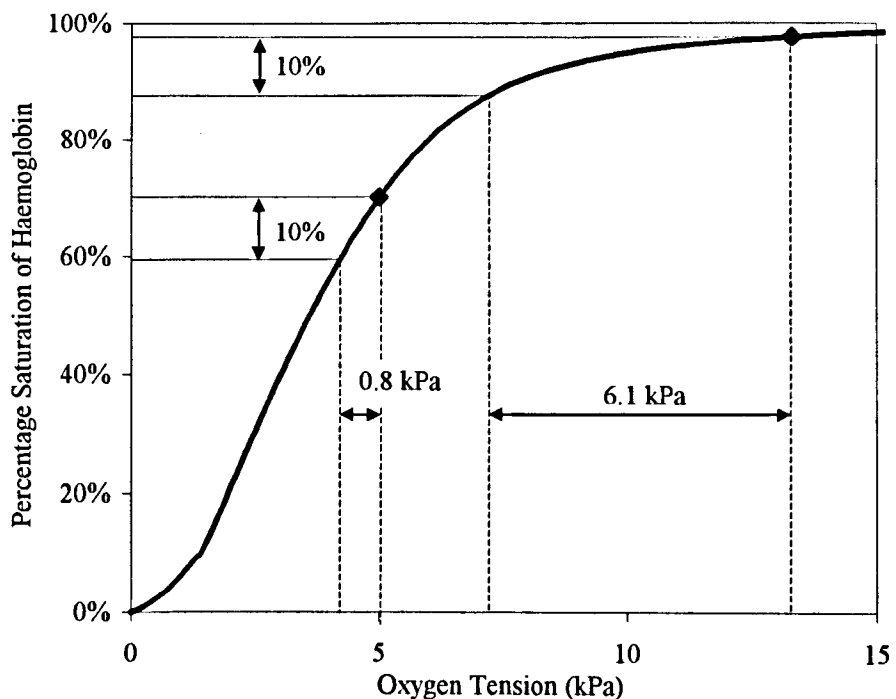


Figure 5.12: Sensitivity of the oxygen dissociation curve at typical arterial and venous points, illustrating how shifts in the haemoglobin saturation cause larger shifts in O_2 tension at the arterial point (13.3 kPa) than at the venous point (5 kPa).

The second comparison was made between the *intuitive trends* and the model predictions (or *predicted trends*). Since the patient model should reflect a well-behaved patient, it was anticipated that the model predicted trends would match the intuitive trends in all cases.

By implication therefore patients deemed well behaved from the first trend comparison should match the *predicted trends*. This constitutes the third and final comparison between the *measured trends* and the *predicted trends*.

Scoring of Intuitive Trends

Using the following symbolic notation the expected patient trends were scored for each patient record based upon the ventilator changes, see Table 5.8;

- ↑ Increase in gas tension expected.
- ↑ Small increase in gas tension expected.
- ↔ No change in gas tension expected.
- ↓ Small decrease in gas tension expected.
- ↓ Decrease in gas tension expected.

Scoring of Measured and Model-Predicted Trends

The measured and predicted responses were scored using the following classification boundaries to give the *measured trends* and *predicted trends*;

- ↑ Increase in gas tension: response ≥ 0.1 kPa
- ↔ No change: $-0.1 < \text{response} < 0.1$ kPa
- ↓ Decrease in gas tension: response ≤ -0.1 kPa

The choice of classification threshold was somewhat arbitrary but was made such that very small changes would be classes as no change whilst retaining information about the direction of smaller but not insignificant responses. Setting the threshold too high would lead to a broad classification of ↔ (no change). The measured and predicted trend classification is also given in Table 5.8.

Comparison of Measured and Intuitive Trends

The *measured trends* were found to match the *intuitive trends* in;

6 cases for PaO₂ (P1-2, P1-3, P1-4, P2-1, P3-2, P3-3)

4 cases for PaCO₂ (P1-1, P1-3, P3-2, P4-1)

The venous gases were not considered.

The reasons for mismatch were not always obvious, but each measurement that failed to match was assessed and possible reasons identified.

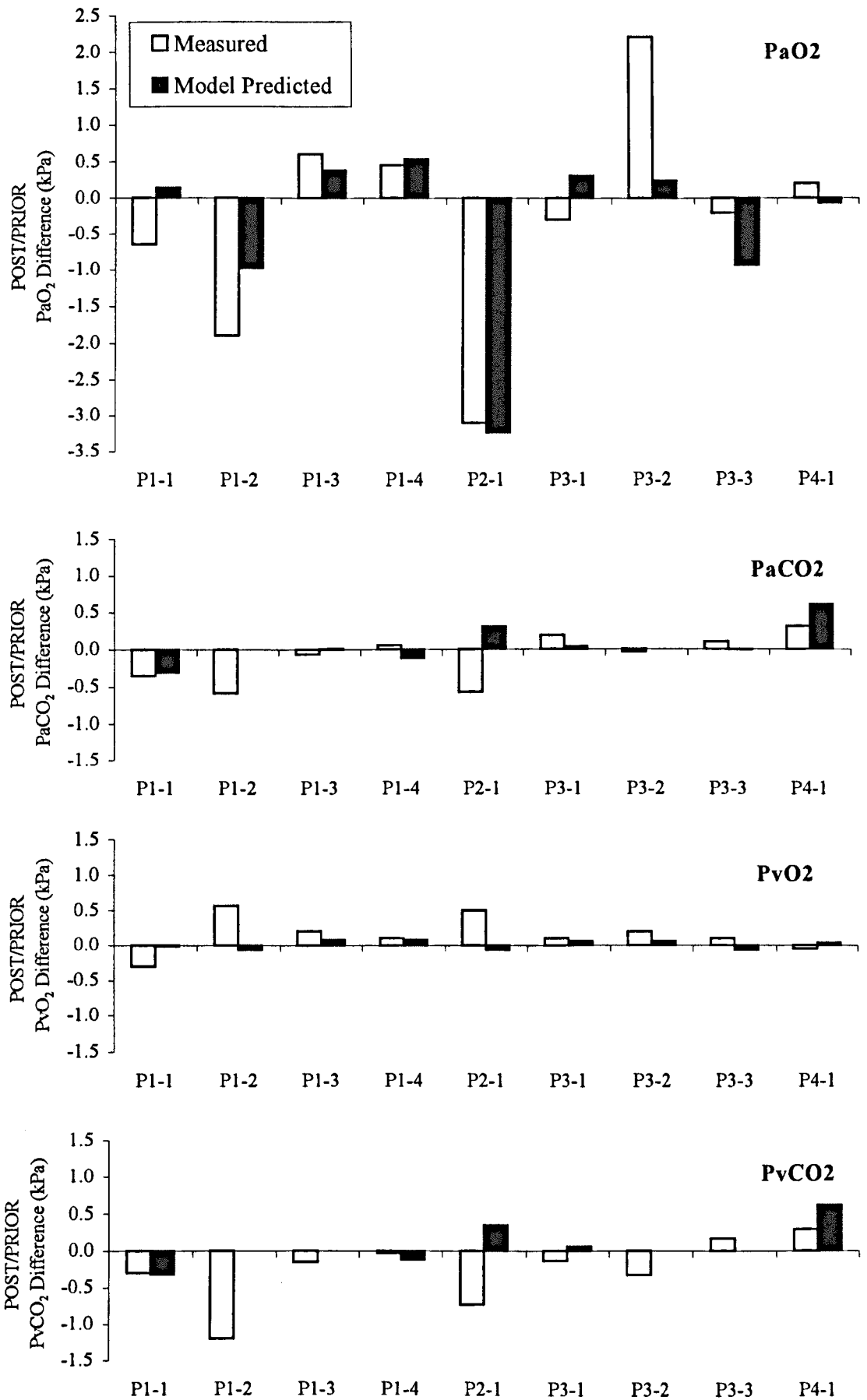


Figure 5.13: Comparison of the POST-PRIOR difference between measured and model predicted responses to ventilator changes for PaO₂, PaCO₂, PvO₂ and PvCO₂. See Table 5.7 for actual values.

	P1-1	P1-2	P1-3	P1-4	P2-1	P3-1	P3-2	P3-3	P4-1
PRIOR Measured Gases									
PaO2 (kPa)	17.55	12.35	8.65	9.25	20.90	8.10	7.80	11.70	11.50
PaCO2 (kPa)	4.30	5.48	4.80	4.74	5.26	5.12	5.31	5.25	3.79
PvO2 (kPa)	4.50	4.90	5.30	5.50	4.85	4.50	4.60	4.60	5.95
PvCO2 (kPa)	4.95	5.91	5.47	5.32	6.41	5.61	5.48	5.67	4.13
POST Measured Gases									
PaO2 (kPa)	16.90	10.45	9.25	9.70	17.80	7.80	10.00	11.50	11.70
PaCO2 (kPa)	3.95	4.90	4.74	4.79	4.69	5.31	5.28	5.35	4.10
PvO2 (kPa)	4.20	5.47	5.50	5.60	5.35	4.60	4.80	4.70	5.90
PvCO2 (kPa)	4.65	4.70	5.32	5.29	5.68	5.48	5.15	5.84	4.42
POST Model-Predicted Gases									
PaO2 (kPa)	17.69	11.38	9.03	9.79	17.66	8.41	8.04	10.77	11.44
PaCO2 (kPa)	4.00	5.48	4.80	4.62	5.56	5.16	5.31	5.24	4.40
PvO2 (kPa)	4.49	4.83	5.38	5.58	4.79	4.56	4.66	4.54	5.98
PvCO2 (kPa)	4.63	5.90	5.47	5.19	6.75	5.66	5.48	5.67	4.74
POST Model-Predicted (+pH changes) Gases									
PaO2 (kPa)	17.50	11.15	8.86	9.66	17.45	8.36	8.10	10.74	11.27
PaCO2 (kPa)	3.99	5.48	4.79	4.62	5.56	5.16	5.31	5.24	4.39
PvO2 (kPa)	4.36	4.74	5.40	5.54	4.59	4.60	4.68	4.52	5.94
PvCO2 (kPa)	4.54	5.95	5.75	5.26	6.62	5.84	5.46	5.64	4.83
PRIOR-POST Measured Difference									
PaO2 (kPa)	-0.65	-1.90	0.60	0.45	-3.10	-0.30	2.20	-0.20	0.20
PaCO2 (kPa)	-0.35	-0.58	-0.06	0.05	-0.57	0.19	-0.03	0.10	0.31
PvO2 (kPa)	-0.30	0.57	0.20	0.10	0.50	0.10	0.20	0.10	-0.05
PvCO2 (kPa)	-0.30	-1.21	-0.15	-0.02	-0.73	-0.13	-0.33	0.17	0.30
PRIOR-POST Model-Predicted Difference									
PaO2 (kPa)	0.14	-0.97	0.38	0.54	-3.24	0.31	0.24	-0.93	-0.06
PaCO2 (kPa)	-0.30	0.00	0.00	-0.12	0.31	0.04	0.00	0.00	0.61
PvO2 (kPa)	-0.01	-0.07	0.08	0.08	-0.06	0.06	0.06	-0.06	0.03
PvCO2 (kPa)	-0.32	0.00	0.00	-0.12	0.35	0.05	0.00	0.00	0.62
PRIOR-POST Model-Predicted (+pH changes) Difference									
PaO2 (kPa)	0.60	0.70	-0.40	-0.04	-0.35	0.56	-1.90	-0.76	-0.43
PaCO2 (kPa)	0.04	0.57	0.05	-0.18	0.88	-0.15	0.03	-0.11	0.29
PvO2 (kPa)	0.16	-0.73	-0.10	-0.06	-0.77	0.00	-0.12	-0.18	0.04
PvCO2 (kPa)	-0.11	1.25	0.43	-0.03	0.94	0.36	0.31	-0.19	0.41

Table 5.7: Measured and model-predicted responses resulting from the ventilator changes (see Table 5.8 for the ventilator changes made)

Ventilator Change	P1-1	P1-2	P1-3	P1-4	P2-1	P3-1	P3-2	P3-3	P4-1
	inc. RR sm. red. I:E	red. FiO2	inc. FiO2	inc. FiO2 sm. inc. Vt	red. FiO2 sm. red. RR sm. inc. Peep	inc. FiO2	inc. FiO2	red. FiO2	red. RR sm. red. Vt sm. inc. I:E
PaO₂									
Intuitive	↑	↓	↑	↑	↓	↑	↑	↓	↓
Measured	↓	↓	↑	↑	↓	↓	↑	↓	↑
Model Predicted	↑	↓	↑	↑	↓	↑	↑	↓	↔
PaCO₂									
Intuitive	↓	↔	↔	↓	↑	↔	↔	↔	↑
Measured	↓	↓	↔	↔	↓	↑	↔	↑	↑
Model Predicted	↓	↔	↔	↓	↑	↔	↔	↔	↑
PvO₂									
Intuitive	↑	↓	↑	↑	↓	↑	↑	↓	↓
Measured	↓	↑	↑	↔	↑	↔	↑	↑	↔
Model Predicted	↔	↔	↔	↔	↔	↔	↔	↔	↔
PvCO₂									
Intuitive	↓	↔	↔	↓	↑	↔	↔	↔	↑
Measured	↓	↓	↓	↔	↓	↓	↓	↑	↑
Model Predicted	↓	↔	↔	↓	↑	↔	↔	↔	↑

Key: ↑ increase ↓ reduction ↔ no change ↑ sm. increase ↓ sm. reduction

Table 5.8: Comparison of measured and model predicted response trends to therapy changes.

PaO₂ mismatch in P1-1: the post measurements for PaO₂ varied by 2.2 kPa indicating either a measurement error in one of the measurements or patient instability. Ignoring point 3 (the most likely candidate for measurement error) the measured response would be ↑, matching the intuitive trend. Additionally \dot{V}_{O_2} increased from 276 ml/min to 281.6 ml/min, contributing further to the negative trend in PaO₂.

PaO₂ mismatch in P3-1: only a single sample was available for this measurement and therefore may be subject to patient instability. The dip in O₂ saturation (recorded using a pulse-oxymeter) from 96% to 94% seems to support this hypothesis. Since the FiO₂ was increased it follows that the O₂ saturation should increase, but it does not.

PaO₂ mismatch in P4-1: the increase in PaO₂ was very small (0.2 kPa) and since the intuitive trend was ↓ (a small reduction). Such a discrepancy is well within possible measurement errors, especially when it is observed that there was a 12.5% variation in prior \dot{Q}_t measurements and a 9.9% in post \dot{Q}_t measurements.

PaCO₂ mismatch in P1-2: the main cause of this mismatch seems to be a general instability in the acid-base balance as indicated by the spread of pH and standard HCO₃⁻ values. Since only FiO₂ was adjusted these should remain constant across the whole test. The pH range was 7.452 to 7.507 (a difference of 0.055) and the standard HCO₃⁻ range was 28.4 to 30.7 mmol/l (a difference of 2.3 mmol/l). Since this patient was known to be clinically unstable and did eventually die (after withdrawal of treatment) the instability observed and resulting trend mismatch were expected.

PaCO₂ mismatch in P1-4: the measured response was zero (actually +0.055 kPa), and was based upon a single post measurement. The intuitive trend was a small PaCO₂ reduction, which given possible measurement errors, means that the trends are similar.

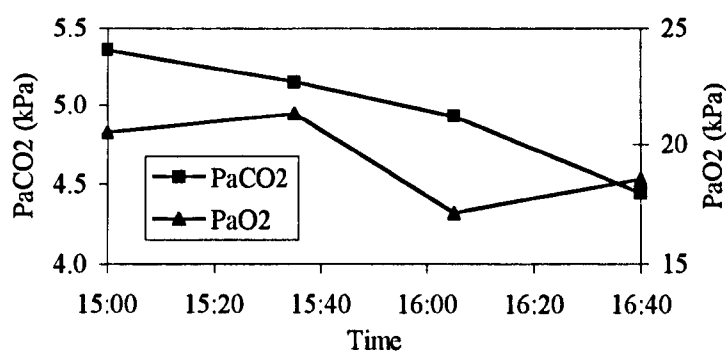


Figure 5.14: Improvement in patient P2-1, caused by re-inflation of collapsed alveoli through the application of PEEP. The increased alveolar ventilation gives rise to increased PaO₂ and reduced PaCO₂. The drop in PaO₂ occurring after 15:40 is due to a reduction in FiO₂.

PaCO₂ mismatch in P2-1: this patient was improving after an emergency operation and therefore it seems likely that airways will have collapsed during anaesthesia. This explains the application of a small amount of PEEP. Since the collapsed alveoli will begin to re-inflate, alveolar ventilation will improve and consequently CO₂ elimination will improve. This is

confirmed if we plot the PaCO₂ data, see Figure 5.14. Supporting this theory is the general increase in O₂ tension, which would be expected as the physiological shunt reduces. The intuitive trend should be modified to ↓, to reflect this more complex and dynamic physiology.

PaCO₂ mismatch in P3-1: the intuitive trend was ↔, but the measured trend was ↑. However the increase in PaCO₂ was only 0.19 kPa. Given possible measurement errors and only one prior/post data point this can be considered reasonable trend matching.

PaCO₂ mismatch in P3-3: the measured increase was small (0.305 kPa) and appears to be an artefact of gradually rising PaCO₂ levels, see Figure 5.15. Reasons for this are unclear.

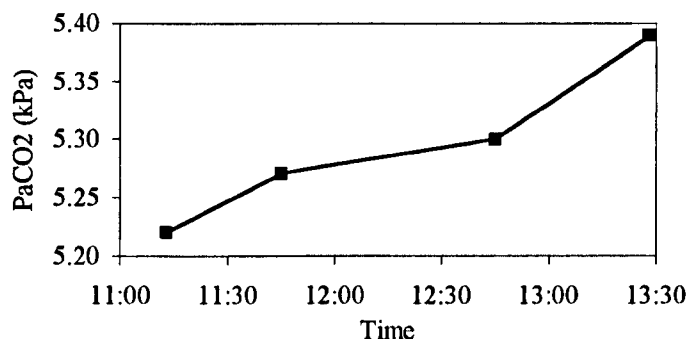


Figure 5.15: Arterial PaCO₂ measurements for patient P3-3 showing gradually increasing trend.

Comparison of Model Predicted and Intuitive Trends

The *predicted trends* were found to match the *intuitive trends* in all cases with the exception of the PaO₂ trend in patient P4-1, where because of the classification boundary used, the model trend was classed as ↔, instead of ↓.

Comparison of Model Predicted and Measured Trends

As anticipated, it was found that those measured trends, which matched the intuitive trends, also matched the model-predicted trends.

To summarise then; the model was able to match the intuitive rules in all cases, although some of the responses were small, due to low model stimulation. The model matched the measured trends in all cases when the measured trends behaved intuitively. This is encouraging as a first indicator of model performance. However, a measured response may be in the same direction as a model response yet of such varying sizes to consider the match poor.

5.5.2 Statistical Analysis

Before attempting any statistical analysis of the model's performance it has to be noted that the data set was very small and therefore likely to be statistically unrepresentative. The accumulated effect of measurement errors on the model means that large numbers of patient observations would be required to make the analysis meaningful. This proviso aside it was important to obtain a quantitative indication of the model's performance using the limited data collected.

The accuracy of the model predictions was assessed using correlation analysis. Figure 5.16 shows the comparison between the model predicted and measured blood gas tensions for the arterial and venous gases. Predictions for PaO₂ showed a good correlation ($r = 0.97$), which was slightly better than the correlation obtained by Hinds *et al* (1983), see Table 5.9. However PaCO₂ predictions gave much poorer correlation ($r = 0.76$) than PaO₂ and was worse than Hinds *et al*.

Two possible explanations for this reduced performance in PaCO₂ correlation are;

- 1) At this point in the model development the pH was assumed constant and was set at the prior value, even after changes in the ventilator settings. This does not reflect what actually happens, especially after changes to minute volume which directly affect the pH.
- 2) Changes made to minute volume were small and therefore the CO₂ system was under stimulated. This is evident when we compare the size of changes observed in the PaO₂ and PaCO₂ systems (see Figure 5.13) This coupled with possible patient instability masks any underlying changes.

The first of these was simple enough to confirm by including the post pH values with the ventilator changes before simulating. However this gave no improvement in PaO₂ correlation ($r = 0.97$) or PaCO₂ correlation ($r = 0.76$), see Table 5.9. Therefore, it can be concluded that patient instability coupled with under stimulation was the major contributing factor to response mismatch.

The situation was much the same for the venous gases. The predicted PvO₂ correlation ($r = 0.86$) whilst not as good as the arterial case was much better than that observed by Hinds *et al*. The PvCO₂ correlation ($r = 0.65$) was the worst of all four gases, comparing unfavourably with Hinds *et al*. Inclusion of post pH values slightly degraded the PvO₂ correlation ($r = 0.83$) and made no difference to PvCO₂ correlation ($r = 0.65$).

	PaO ₂		PaCO ₂		PvO ₂		PvCO ₂	
	r	σ _E	r	σ _E	r	σ _E	r	σ _E
Hinds <i>et al</i>	0.94	2.31	0.89	0.27	0.61	0.51	0.88	0.29
Model Predicted	0.97	0.89	0.76	0.36	0.86	0.29	0.65	0.39
Model Predicted (with updated pH)	0.97	2.10	0.76	0.63	0.83	0.58	0.65	0.89

Table 5.9: Comparison between correlation coefficients (r) and standard deviation of the mean response error (σ_E) for the predicted model responses.

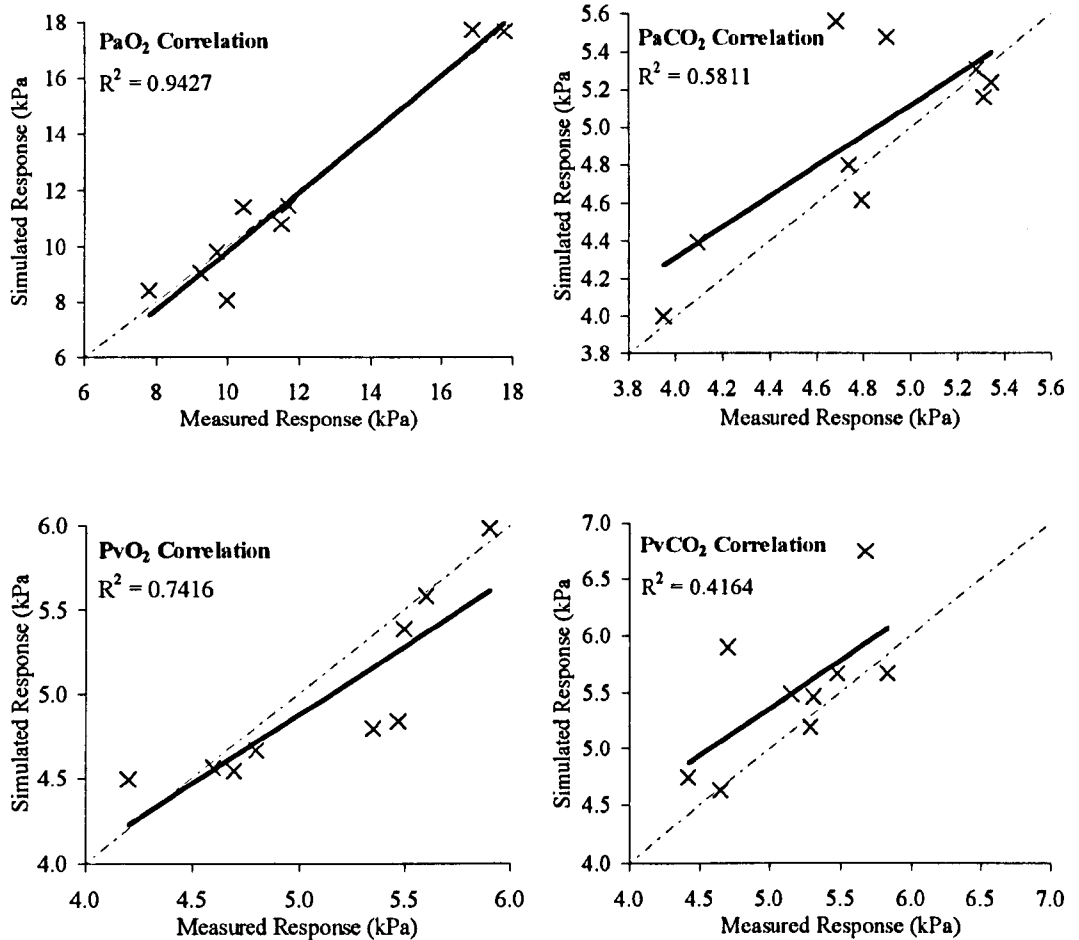


Figure 5.16: Regression analysis of predicted model responses against measured responses for arterial and venous O₂ and CO₂. The dashed line indicates the ideal correlation and the dark line the calculated regression line.

5.5.3 Causes of Response Errors

There are many reasons why the measured and predicted responses do not match and obviously poor representation of patient physiology within the model may be one of those reasons. However, other sources of error exist and need to be considered. The purpose of this section is not to quantify such errors but simply to identify them. Four possible sources of response errors have been identified;

1). Patient instability:

The patient state may be changing erratically over relatively short time periods. In such cases the measured data may be accurate but the patient is pathologically unsuited to this type of validation. The model will be unable to predict such behaviour, even if its complexity is increased.

2). Physiological glitches at measurement time:

The overall trend of the patient response may be in the correct direction or of the correct magnitude but momentary fluctuations in the patients physiological states (such as a cardiac

surge) give the appearance of incorrect response. Problems such as these are removed with rapid data sampling and response filtering.

3). Drift in underlying patient state:

Patient parameters such as \dot{Q}_t or $\dot{V}O_2$ may have changed over the period of the patient test. However, these changes are not caused by patient instability, but by slow trends in one or more of the patient parameters. Maybe \dot{Q}_t was stabilising after the infusion of a stimulant, or there was lessening of internal bleeding in response to a drug. PCO_2 has a much slower time constant than PO_2 and may not have stabilised by the time POST blood-gases are taken.

4). Measurement errors:

Differences caused by human error, clinical error or instrumental error may all conspire to obscure the underlying patient response and therefore cause poor response behaviour.

Of these hypotheses the first three can be classified as physiological, since they are due to changes in the patient state. A clearer separation of these effects would be established with an increased measurement rate and longer test length. However, close involvement with the data collection process has indicated that there would be many problems in trying to establish a more rigorous collection regime.

The measurement errors can be classified as one of three primary types;

1). *Clinical measurement errors:*

Even if the patient state was assumed to be stable throughout the period of the test, there will always be errors due to the nature of the physiological processes and how they can be measured. For example, blood sample lines cannot be inserted at any location, and consequently their position may cause errors associated with blood mixing. This is certainly true with samples taken using a central venous line where venous return will not always have mixed properly. Other examples of this error include breath-by-breath fluctuations observed in the arterial $PaCO_2$. The contribution of these effects is unknown.

2). *Experimental measurement errors.*

This probably accounts for the largest contribution to the overall error since they are caused by the human factor. Intensive care patient management is such that many people will be involved in the patient blood sampling and measurement acquisition. Therefore problems are likely to occur due to poor or inconsistent blood sampling techniques, inconstant thermo-dilution injections, incorrect instrument calibration, etc.

For example Gosling (1995) described the following errors associated with blood-gas sampling;

- The incomplete withdrawal of heparinised saline solution (anticoagulant) from line before sampling of the blood may cause dilution errors. However about 0.05 ml will always remain in the syringe dead space, which for a 1 ml blood sample will give an overall dilution of 5%. Plasma constituents that can easily pass into the red blood cells such as CO_2 will be reduced by about 5%. Blood pH is less effected

since it is dependent upon the ratio between dissolved CO₂ and plasma bicarbonate, which dilution does not greatly disturb.

- Bubbles introduced into the syringe during sampling, which is usually unavoidable, will if allowed to equilibrate with the blood increase PaO₂. For example, 1 % of introduced air (0.01 ml in a 1 ml sample) can increase PaO₂ by up to 15 % if allowed to equilibrate.
- The delay between sample and analysis time, should be less than 10 min's. For example, a measured PaO₂ of 13.3 kPa after 10 min's, will be approx. 0.7 kPa lower than at sample time, the PCO₂ approx. 0.08 kPa higher and pH 0.006 lower (0.98 increase in [H⁺]), [Nunn 1993, p.570].
- Red cells settle out of the plasma rapidly, especially in critically ill patients. If the sample is not shaken thoroughly before introduction into the analyser, measurements will be made on a red cell rich or red cell deficient sample, leading to inaccurate Hb, pH, PCO₂ and PO₂ results.
- Violent injection into the analyser can cause haemolysis increasing potassium and in some instruments PO₂ results.

Similar analysis could be applied to the other measurement procedures and potential errors identified. However, their likelihood and degree of influence of each error source for each measurement are a matter of speculation. We can merely identify their potential and hope that reasonable precautions are taken by clinical staff to minimise their effects.

3). Instrumental measurement errors.

Assuming correct calibration these will tend to be the smaller of the error contributions. Typical machine accuracy is given below;

IL System 1302 pH/Blood Gas Analyser

pH

Accuracy	-0.007 ± 0.007	([H ⁺] -0.984 ± 0.984)
Precision	0.0046 ± 0.0026	([H ⁺] -0.989 ± 0.994)

PCO₂

@ 4.666 kPa (35 mmHg)	Accuracy	+0.067 ± 0.047
	Precision	0.093 ± 0.027
@ 6.666 kPa (50 mmHg)	Accuracy	-0.067 ± 0.053
	Precision	0.080 ± 0.040
@ 12.666 kPa (95 mmHg)	Accuracy	0 ± 0.240
	Precision	0.107 ± 0.040

PO₂

@ 6.666 kPa (50 mmHg)	Accuracy	-0.133 ± 0.067
	Precision	0.093 ± 0.067
@ 12.666 kPa (95 mmHg)	Accuracy	+0.160 ± 0.133
	Precision	0.080 ± 0.040
@ 18.665 kPa (140 mmHg)	Accuracy	-0.133 ± 0.040
	Precision	0.080 ± 0.053

C.O. Module: HP Component Monitoring System

Cardiac Output Accuracy

2 % standard deviation @ blood / injectate temp. diff. > 10 °C

Temperature Accuracy

±0.1 °C (0.2 °F)

The interaction of the above physiological and measurement errors (and others not considered) is complex. It would be a large undertaking to establish the approximate effects of most of them and then to arrive at an estimate of their combined effect. However, as a crude rule of thumb, a physiological measurement is deemed to have changed if it increases or decreases by at least 10%. Turning the argument around, we can say that physiological measurements might have combined errors of up to 10 %. With careful measurement procedures, errors should be much less than this, but they do remain the overriding factor in being able to accurately assess the performance of the model.

5.6 Summary & Conclusions

Sensitivity Analysis of the Model

A simple sensitivity analysis methodology was used in preference to more involved methods. This provided a preliminary indication of the relative parameter sensitivities of the model. The method used is known as 'Classical Sensitivity Analysis' and ignores parameter interaction and variability in the size of the parameter's disturbance space.

Direct comparison between sensitivities of the state outputs was possible since they were expressed in the same units (i.e. all measures of partial pressure and in kPa), and it was observed that PaO₂ was more sensitive than the other state outputs by a factor of 5:1. Since this is one of the primary therapy decision variables, it has important considerations in terms of model-patient matching.

The O₂ system was found to be most sensitive to FiO₂, with much smaller sensitivities to VT and RR. Conversely, the CO₂ system was most sensitive to VT and RR, with little response to FiO₂ changes. This matched the changes in blood-gases predicted by the intuitive therapy rules.

The O₂ system was found to be very sensitive to \dot{Q}_s/\dot{Q}_t , but insensitive to VD, whilst the CO₂ system was sensitive to VD and insensitive to \dot{Q}_s/\dot{Q}_t . The tuning of the patient model used this difference to arrive at unique solutions of \dot{Q}_s/\dot{Q}_t and VD that produced blood-gases to match those observed clinically.

Sensitivity to PEEP and I:E was extremely low which does not correlate with their known therapeutic effects. This was because the model did not simulate the effect of PEEP and I:E on the physiology of the lung. The inclusion of PEEP, opens up more airways and has the result of reducing the dead space to alveolar volume ratio (an effective increase in ventilation rate), and reduces the effective physiological shunt.

Cardiac output was found to be very sensitive in the O₂ system, and since this parameter is subject to large measurement uncertainties, poses the likeliest cause of model-patient mismatch.

Quality of Measured Data

Not all of the patients responded in an intuitive manner to changes in ventilator therapy; only 69 % of cases for the PaO₂ and PaCO₂ trends. This indicates either underlying measurement problems or instability in the patient.

The amount of data collected was very small and highlights the problems associated with clinical data collection. The following restrictions to successful data collection were identified;

- 1). The lack of suitable patients.
- 2). The need to use a PAC to measure \dot{Q}_t in the absence of non-invasive methods. This set up a contradiction between the need to measure many parameters, which are only routinely monitored in highly critical patients, and the need for 'stable' patients. Consequently many of the records obtained were unsuitable due to their unstable nature.
- 3). Lack of equipment to measure metabolic function (namely O₂ consumption and CO₂ production), hence the need to hire a metabolic computer.
- 4). Restrictions imposed by ethical considerations;
- 5). Number of measurements on any given patient restricted, especially with reference to \dot{Q}_t measurements.
- 6). Limitation on size of ventilator therapy change causing under stimulation of both the patient and the model.
- 7). Interference during a patient record by priority treatments such as physiotherapy and drug changes, which could dramatically alter patient state.
- 8). The difficulty of asking clinical staff to perform extra work, albeit small.
- 9). The time consuming nature of the data collection itself, waiting for the therapy changes to be made and for suitable patients to become available. Since overseeing the collection itself is not always practicable, there is a need to stimulate enough interest and understanding of the data collection objectives to maintain collection over long periods.

The problem of \dot{Q}_t measurement should improve as alternatives to thermal dilution begin to emerge, such as partial CO₂ re breathing [Mahutte *et al*, 1991; Vidal Melo *et al*, 1992; Gedeon *et al*, 1980; Capek *et al*, 1988]; thoracic electrical bioimpedance [Young & McQuillan, 1993]; and doppler ultrasound. Such methods would increase the pool of available patients, and might be considered in a more extended study.

Clinical Validity

Given the limitations of the patient data and the unsuitability of the available patients the model was shown to predict the therapy responses well. The model responded intuitively to all therapy changes, although some responses were small due to the small therapy step sizes, or large \dot{Q}_s/\dot{Q}_t and VD estimates. Consequently the model trends matched the measured trends in all cases when the measured trends behaved intuitively (69 % of cases).

The overall impression of this analysis is that the model behaves well to therapy changes, with the exception of PEEP and I:E which require the inclusion of additional model elements. However, its ability to match real patient data is limited, primarily because of the errors attributable to physiological measurement. To validate the model more rigorously would require either accurate data from a lung function lab on healthy patients that are known to be stable; or observation of ICU patients using continuous and where possible non-invasive measurement techniques. This is especially necessary with respect to cardiac output. By having continuous data, local instabilities in the data can be rejected or averaged out. The use of non-invasive techniques eliminates the problem associated with say PACs, which are usually only used on very unstable patients. Since unstable patients are not likely to behave predictably, they can hardly be used for model validation purposes.

The introduction of automated data collection techniques within the ICU and the non-invasive measurement of certain critical parameters will facilitate a more rigorous statistical analysis of the model in the future.

The model still needs some improvement for it to be truly useful for advisor validation, and these modifications are presented in Chapter 7. The next chapter presents the prototype development of the ventilator advisor itself.

Chapter 6: FAVeM – Advisor Development

6.1 Introduction

Thus far development and testing of a patient model suitable for the simulation of patients on volume control (VC) and pressure regulated volume control (PRVC) modes of ventilation has been presented. This model has been shown to provide a reasonable level of patient realism, and together with the improvements discussed in Section 7.3, can be used to validate and improve the fuzzy advisor via simulated closed-loop control.

This chapter provides a comprehensive account of the fuzzy advisor's prototype development. It includes an overview of the advisor architecture (see Section 6.2) followed by a discussion of the reasons behind the choice of membership functions, inference algorithm and defuzzification method employed (see Section 6.3).

In Section 6.4 the methods used to implement the advisor rules are presented. This includes reasons for the avoidance of rule-holes and approaches taken to avoid them, the method of representation of the rule-consequents and a description of a rule-reduction algorithm.

Sections 6.5 to 6.8 present the initial attempts to encapsulate the anaesthetist's decision process for the FiO_2 , PEEP, VT and RR controls when ventilating patients using VC and PRVC. FiO_2 and PEEP are described first, representing the controls used for PaO_2 maintenance. The FiO_2 rule development shows how the iso-shunt diagrams were used to produce the first rule-map, and then how this was modified according to feedback from an anaesthetist. Next the PEEP rule development is presented, introducing the benefits and disadvantages of PEEP and how these might be encapsulated.

The MV and RR-Vt control rules provided PaCO_2 and PIP maintenance. The elicitation of the MV control rules with particular reference to PaCO_2 and pH imbalance is described, followed by their improvement via the introduction of rules pertaining to high levels of PIP. Finally the balancing of RR and VT settings through the use of rules derived from normalised iso-MV lines is described.

6.2 Advisor Architecture

6.2.1 Overview

The advisor comprises four primary maintenance pathways;

- 1). Safe control of PaO_2 .
- 2). Normalisation of PaCO_2 and to a lesser degree arterial pH.
- 3). Prevention of harmful PIP levels.
- 4). Establishing of ideal VT and RR settings.

These maintenance objectives are accomplished via the manipulation of five ventilator controls FiO_2 , PEEP, RR, VT and TIN, and are associated with volume-cycled modes of ventilation, such as

volume control (VC) and pressure-regulated volume control (PRVC). The fuzzy knowledge-based controller (FKBC) advises changes to these settings based upon the following information;

- 1). Current Ventilator Settings; FiO_2 , PEEP, RR, VT and TIN .
- 2). Patient Observations; PaO_2 , $PaCO_2$, pH, PIP and weight.
- 3). Patient Goals; $PaCO_2$ and pH set points.
- 4). Patient Alarms; high PIP.

These inputs are processed by the observation processing module (OPM) to produce the crisp values used in the rule-antecedents of the advisor sub-systems, see Figure 6.1. In the prototype version of FAVeM, there were four advisor sub-systems, each with its own set of control rules. The FiO_2 and PEEP sub-systems combine to provide PaO_2 maintenance. The MV and VT-RR sub-systems combine to provide $PaCO_2$, pH and PIP maintenance with consideration to normalisation of VT and RR settings. These sub-systems operate independently of one another, with the exception of the VT-RR sub-system, which relies upon the output of the MV sub-system to calculate the new observed RR (one of the VT-RR sub-system antecedents). The reasoning being that changes in MV affects how changes to VT and RR are distributed.

After analysing the close-loop performance of the FAVeM (see Section 7.5) it was deemed necessary to introduce a fifth advisor subsystem for the control of TIN .

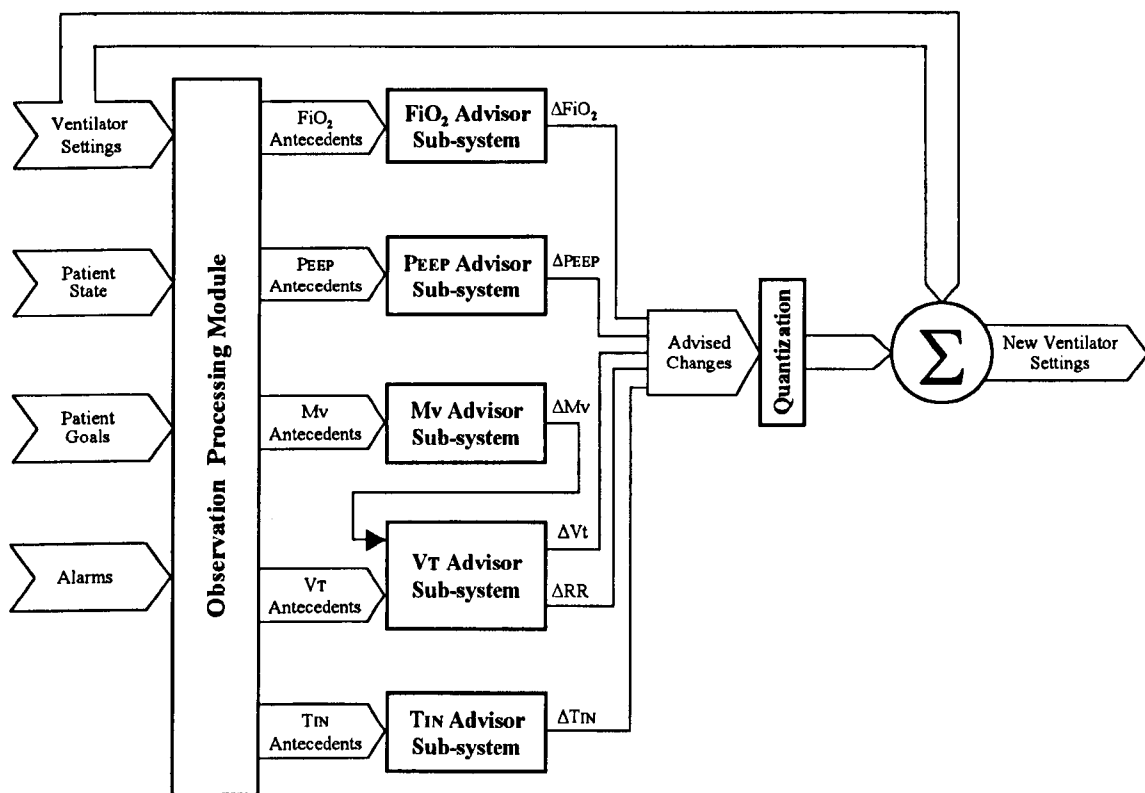


Figure 6.1: Overview of FAVeM's architecture. Note that the TIN subsystem was not present in the prototype version of FAVeM.

Each sub-system generates the required change in ventilator setting (i.e. ΔFIO_2 , $\Delta PEEP$, ΔRR , ΔVT and ΔTIN). This is quantised and added to the current ventilator settings to give the new settings. The quantisation or rounding of the advice enables the changes to be expressed in steps that match the ventilator resolution or the smallest changes likely to be made by a clinician.

6.2.2 Observation Processing Module (OPM)

This uses the patient observations, ventilator settings and patient goals/alarms to derive the inputs required by the advisor subsystems. This process was abstracted from the subsystem modules themselves, since some antecedents are used by more than one module (see Table 6.1). It also meant that the modules themselves could be based upon the same code structure, simplifying and speeding up system development.

Two processes are performed by the OPM; (i) the calculation of normal ventilator settings and (ii) the calculation of observation errors.

Advisor Sub-system	Inputs required by Prototype Advisor	Inputs required by Modified Advisor
FIO ₂	PaO ₂ , FIO ₂	PaO ₂ , FIO ₂
PEEP	PaO ₂ , FIO ₂ , PEEP	PaO ₂ , FIO ₂ , PEEP
MV	ePaCO ₂ [§] , epH [§] , ePIP [§]	ePaCO ₂ [§] , PIP, eVT _{NORM} [§]
VT-RR	eVT _{NORM} [§] , RR, ePIP [§]	eVT _{NORM} [§] , RR, PIP
TIN	N/A	PIP, TIN

[§] Calculated by Observation Processing Module

Table 6.1: Rule-antecedents required by each sub-system, for the prototype and modified advisor

Calculation of Normal Ventilation Settings

For the majority of patients (approx. 80%) their prescribed normal tidal volume (VT_{NORM}) is proportional to their weight, being about 10 – 15 ml/kg body weight [Anderson, 1988, p12]. FAVeM assumes VT_{NORM} to be 10 ml/kg. The use of VT_{NORM} enables an optimal VT to be defined for any given patient irrespective of their weight.

Calculation of Observation Errors

Of the 9 fuzzy variables used by the advisor sub-systems (see Table 6.1); 2 represent errors from set point level (ePaCO₂ and epH); 1 represents error from alarm level (ePIP); and 1 represents distance from normal ventilation levels (eVT_{NORM}).

These are all measures of distance from some pre-defined norm and are calculated as follows;

pH Error (epH): this represents how far the observed pH is from the normal pH of 7.4;

$$epH = \text{Observed } pH - 7.4 \quad (6.1)$$

PIP Error (ePIP): this represents the distance from the maximum PIP threshold or alarm;

$$ePIP = \text{Observed } PIP - PIP \text{ Alarm} \quad (\text{cmH}_2\text{O}) \quad (6.2)$$

PaCO₂ Error (ePaCO₂): this represents the distance from the target PaCO₂ and is expressed as a percentage error, rather than an absolute error since there is a roughly inverse proportional relationship between PaCO₂ and MV (see Section 6.7.1);

$$ePaCO_2 = \frac{\text{Observed } PaCO_2 - PaCO_2 \text{ Set Point}}{\text{Set Point}} \times 100 \quad (\%) \quad (6.3)$$

For example if the PaCO₂ set point is 5 kPa and the observed PaCO₂ is 6 kPa this gives an ePaCO₂ of 20 %. If the MV is raised by 20 %, the new PaCO₂ should be approximately 5 kPa, i.e. a 20 % increase in MV produces a 20 % reduction in PaCO₂. If PaCO₂ error were expressed in kPa the change required in MV for different PaCO₂ set points would vary for the same PaCO₂ error.

VT Error (eVT_{NORM}): represents distance of observed VT from normal VT. This is expressed as a percentage error, since a 100 ml discrepancy in a large patient with a high VT_{NORM} would be of less significance than in a smaller patient with low VT_{NORM}. By using a percentage error the relative significance of such a volume difference can be inferred;

$$eVT_{NORM} = \frac{\text{Observed } V_T - V_{T_{NORM}}}{V_{T_{NORM}}} \times 100 \quad (\%) \quad (6.4)$$

6.2.3 Subsystems Architecture

Each advisor sub-system follows the same basic structure, see Figure 6.2. The crisp inputs required by each module are passed to the inference module, which uses individual rule-based inference with Larsen's implication and the arithmetic product liaison operator. The fuzzy consequent generated by this inference is then defuzzified using the Centre-of-Sums method to produce the crisp controller output. The choice of inference method, liaison operator and defuzzification strategy is discussed in detail in Section 6.3.

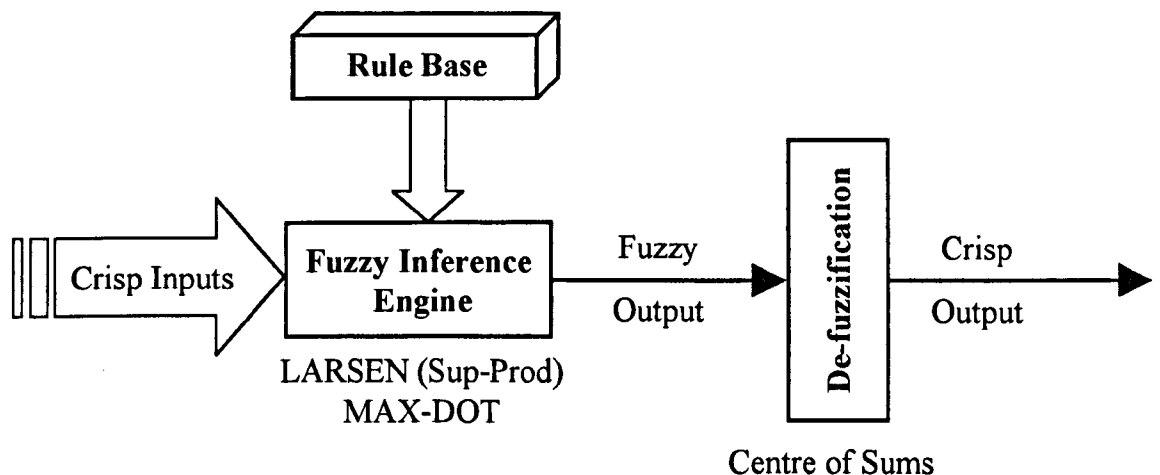


Figure 6.2: Ventilator control sub-system architecture.

6.2.4 Output Quantisation

Once the advice has been de-fuzzified it is then quantised. Three quantisation options were defined; *raw*, *ventilator* and *clinician*, see Table 6.2. The first of these *raw*, returns the unprocessed output of the inference engine, although a small amount of quantisation is applied to prevent very small changes that result from the defuzzification process. The second option *ventilator*, sets the quantisation to the expected resolution of the ventilator, thus preventing advice that cannot be implemented because the step change is too small. The final option *clinician* sets the quantisation to the minimum step change routinely made by an anaesthetist.

Advisor Output	<i>raw</i>	<i>ventilator</i>	<i>clinician</i>
FiO ₂ (%)	0.1	1	5
PEEP (cmH ₂ O)	0.01	0.5	1
RR (r.p.m.)	0.01	0.5	1
VT (ml)	0.1	10	50
TIN (%)	10	10	10

Table 6.2: Advice quantisation levels provided by FAVeM. The fixed quantisation level for TIN reflects the winner-takes-all strategy employed when computing the generated advice (see Section 7.5.5).

6.3 Inference Methodology

Early advisor development was more concerned with rule construction and little focus was given to the choice of inference method. It was felt that this oversight needed to be addressed, and the influence of differing methodology on advisor behaviour investigated. In this way subsequent rule construction would correctly reflect the implementation chosen. Seven elements of the inference process were identified that might impact controller behaviour;

- 1). Choice of membership function.
- 2). Membership function geometry.
- 3). Choice of inference algorithm.
- 4). Choice of implication operator.
- 5). Choice of liaison operator.
- 6). Choice of defuzzification method.
- 7). Choice of output quantisation level.

A more detailed description of membership function geometry and the mechanics of fuzzy inference are given in Chapter 2. This section will only give a brief outline of the options available to each process element, together with justification of the selection made.

6.3.1 Choice of Membership Function

Six main types of fuzzy membership function are referred to throughout the literature;

- 1). sigmoid or S-functions
- 2). bell-shaped or π -functions
- 3). triangular form or T-functions / Λ -functions
- 4). trapezoid form or Π -functions
- 5). exponential forms; includes variants of π -functions and S-functions
- 6). crisp sets and singletons

Crisp sets and singletons are used for binary logic, i.e. true or false; and with the exception of fuzzy singletons, which are used to represent crisp inputs upon a fuzzy domain, are not useful for fuzzy control. Sigmoid and bell-shaped sets (and their exponential variants) provide membership functions that gradually reduce to zero. These may have advantages in strongly linguistic operators such as *dilation* and *concentration* and are frequently used in fuzzy logic, but seldom in fuzzy control.

Triangular and trapezoid membership functions have become the norm in fuzzy control applications, since they are functionally simple to represent and are computationally efficient. Due to this convention in fuzzy control and in the absence of strong evidence for the use of alternative representations; Π -functions and T-functions were chosen as the method of set representation for the antecedent and consequent terms in FAVeM.

6.3.2 Membership Function Geometry

The way in which linguistic terms of a fuzzy variable are mapped onto its domain (or universe of discourse, UoD) can affect the performance of the controller in a number of ways. Three characteristics of membership function geometry were identified as having greatest impact upon the inference process. These were (1) cross point; (2) symmetry and (3) condition width.

Influence of Cross-Point Level and Ratio

The cross-point level (as defined in Section 2.2.1) for any two neighbouring membership functions must be greater than zero, such that a crisp observation upon that domain will belong to at least one membership function. If this condition is not met, input values will exist that do not match a rule-antecedent, leading to *incompleteness* in the control space. This can cause discontinuities in the controller output. Furthermore if the cross-point ratio (i.e. the number of cross-points between neighbouring membership functions) is zero then only one rule at a time will fire, since a crisp observation will only have membership in at most one set. In a rule-base with only a single antecedent, this behaves as though the observation universe is defined using crisp linguistic sets.

Boverie *et al* (1991) has shown that for linear systems up to 3rd order with symmetrical membership functions there exists “optimal” values for the cross-point level and ratio, although

this evidence was only empirical. A cross-point level of 0.5 and a ratio of 1 provide for significantly less overshoot, undershoot and faster rise times. The shape does not play an important role, although trapezoid functions are responsible for slower rise times. This choice of values matches those reported elsewhere in the literature.

The choice of cross-point parameters has greatest influence over system behaviour when applied to antecedent set definitions. Consequent sets are able to have a cross-point ratio of zero, so long as the sets have equal area and are symmetrical. However, this may affect the plausibility of the crisp control output (see Section 6.3.5).

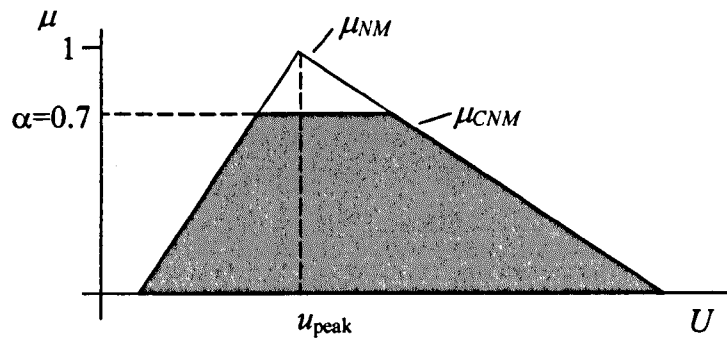


Figure 6.3: The membership function of *NM* and its clipped version caused by a firing weight of 0.7 (shaded area).

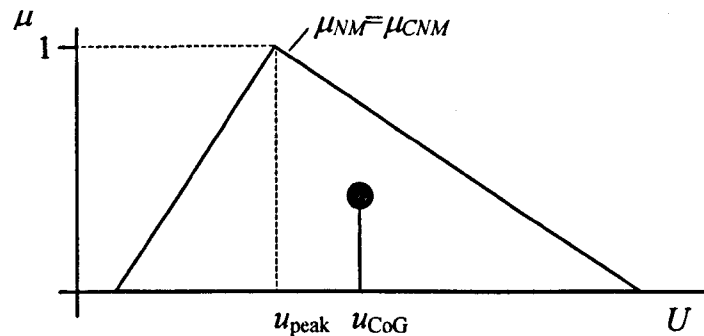


Figure 6.4: When the degree of membership is 1 the clipped consequent and the original consequent are the same. In the case of asymmetric membership functions the peak value is different from the Centre-of-Gravity.

Influence of Symmetry and Width

Inference performed using single rule firing, may produce as a result of some crisp observation x_0 , a “clipped” control output. Consider the rule “if x is Z then u is NM ”, and x_0 has a degree of membership α in μ_Z of 0.7. If the membership function describing the consequent NM is asymmetrical then the meaning represented by μ_{NM} is given in Figure 6.3 and the certainty of the rule (α) results in the clipped version of the consequent μ_{CNM} .

Calculation of the crisp control output u^* requires the application of a defuzzification method, for example the Centre-of Gravity (CoG) method. This obtains a single control output by

averaging across every element of the output domain U . If we consider the case when the degree of match in the rule antecedent is 1 (i.e. $\alpha = 1$) then the fuzzy consequent μ_{CNM} is a triangular shape. Only one element of U satisfies to a degree of 1, namely μ_{peak} . Thus it makes interpretative sense to take μ_{peak} to be the actual value of u^* . However, if we take the CoG of μ_{CNM} then $\mu_{\text{peak}} \neq \mu_{\text{CoG}}$ as shown in Figure 6.4.

Different defuzzification methods such as Centre-of-Maxima (CoM) are able to resolve this conflict but as discussed in Section 6.3.5, these can themselves have a disadvantageous effect on the control output. The simplest way to resolve this problem is by making the consequent μ_{NM} symmetrical about μ_{peak} . Symmetry is not important in the rule antecedent, however condition width *must* be satisfied.

Condition Width

Two neighbouring membership functions on the same universe of discourse must have left width equal to right width in the interval between the two peak values. Also, the widths must equal the interval between the peak values.

To illustrate how contravention of condition width can affect control behaviour, consider the following example. A proportional FKBC has two rules;

- 1). If e is PM then u is PB
- 2). If e is PS then u is PM

Let the meaning of the linguistic terms PM and PS in the rule-antecedent be denoted by μ_{PM} and μ_{PS} . These are mapped onto the observation universe E in two different manners, see antecedent universe in Figure 6.5 and Figure 6.6. In version 1, the condition width is met. In version 2 μ_{PS} has a left width less than the interval between e_{peak1} and e_{peak2} and the condition width is not met.

In version 1 when e changes smoothly from e_{peak1} to e_{peak2} , and after inference and CoG defuzzification, one observes that u^* also changes smoothly from u_{peak1} to u_{peak2} as illustrated in Figure 6.5. However in version 2, u^* changes step wise from u_{peak1} to u_{peak2} , see Figure 6.6. It is therefore preferable that condition width be met by two adjacent membership functions describing the meaning of the linguistic values in the rule-antecedent.

6.3.3 Choice of Inference Algorithm & Implication Operator

The inference-engine or rule-firing algorithm can be of two basic types;

- 1). Compositional Rule of Inference (CRI)
- 2). Individual-Rule based Inference (IRI)

IRI is preferred as the method of reasoning since it is computationally very efficient and saves on the memory required to express the fuzzy relation of a large rule-base using CRI. It can also be shown that compositional based inference is equivalent to individual rule-based inference for crisp observations [Driankov *et al*, 1993, p129] and therefore there is no loss of meaning using IRI. Although the FISMAT toolbox provides both compositional and individual rule-based inference, the latter was chosen for its simplicity and computational efficiency.

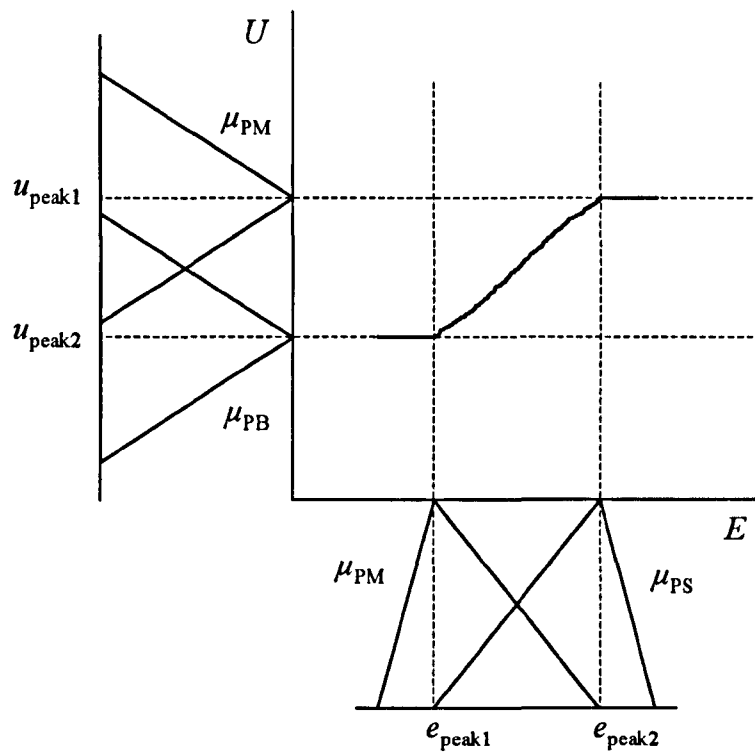


Figure 6.5: The smooth (continuous) change in control output when condition width is satisfied -version 1.

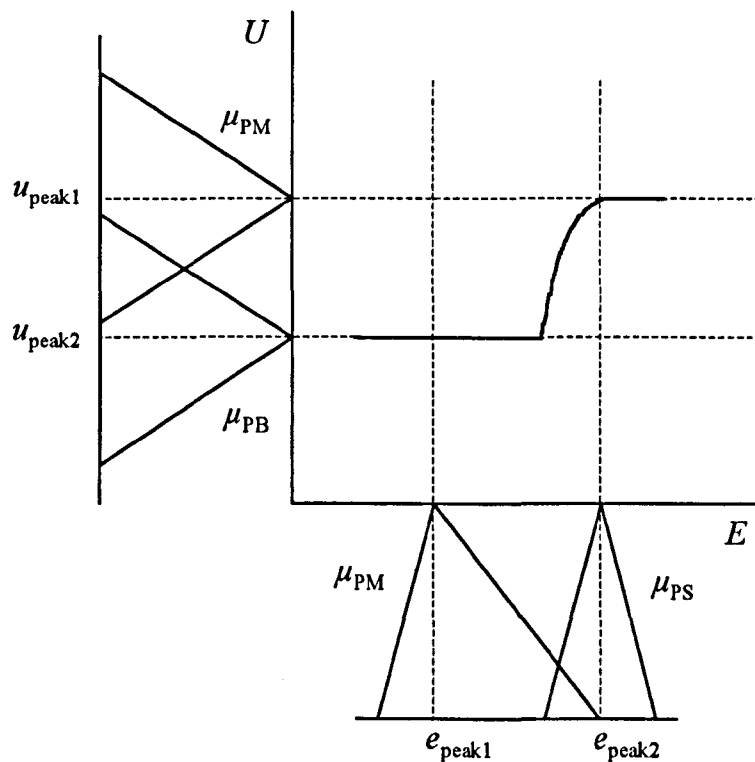


Figure 6.6: The step-wise (discontinuous) change in control output when condition width is not satisfied - version 2.

Of the various fuzzy-inference methods available, the most commonly used in today's industrial fuzzy logic controllers are;

- 1). *Mamdani's implication operation*: Also known as sup-min inference, 'clipped' inference and MAX-MIN inference.
- 2). *Larsen's implication operation*: Also known as sup-product inference, 'scaled' inference and MAX-DOT inference.

It will be shown in Section 6.3.6 that the choice of inference method has very little impact upon the resulting crisp consequent. A far greater impact on controller output is caused by the choice of defuzzification strategy and the antecedent liaison operator.

6.3.4 Choice of Liaison Operator

Conventionally the firing weight of a rule using individual rule inference is defined as;

$$\alpha = \min (\mu_A(x_0), \mu_B(y_0)) \quad \text{or}$$

$$\alpha = \mu_A(x_0) \wedge \mu_B(y_0) \quad (6.5)$$

However, any number of alternative liaison operators could be used, namely algebraic product, bounded sum, bounded product, and drastic-product. Of these only algebraic product is routinely used and is defined as;

$$\alpha = \mu_A(x_0) \bullet \mu_B(y_0) \quad (6.6)$$

Remember that x_0 and y_0 are crisp and therefore equations 6.5 and 6.6 resolve to scalar operations. The algebraic product liaison operator was chosen since it avoided the exaggeration of rule importance observed using the min operator.

6.3.5 Choice of Defuzzification Method

The six most often-used defuzzification methods are;

- 1). Centre of Area or Centre of Gravity (CoG)
- 2). Centre of Sums (CoS)
- 3). Centre of Largest Area (CoLA)
- 4). First of Maxima (FoM) / Last of Maxima (LoM)
- 5). Middle of Maxima (MIDoM)
- 6). Height or Mean of Maxima (MoM)

The choice of method depends on whether it meets certain 'ideal' criteria for the application it is intended. Driankov *et al* [1993] describes the most important of these criteria, and for fuzzy control in general and FAVeM in particular, these criteria should have the following properties;

Continuity:- a small change in the input should not result in a large change in output, since such behaviour may cause instability in the system being controlled (i.e. the patient).

Disambiguity:- defuzzification must be able to arrive at a single crisp value.

Plausibility:- the crisp defuzzified output should lie approximately in the middle of the support of the fuzzy output and have a high degree of membership within it. This is not always possible if the consequent sets are to remain symmetrical in a system with non-uniformly spaced control actions.

Computational Complexity:- the method must be suited to the time constraints of the problem. Advice will be required approximately every 30 minutes so this is not really of any significance.

Weight Counting:- all fired rules are reflected in the aggregated control output. This is thought to provide a more intuitive control profile.

The CoS method was chosen since it met all of the above criteria. Although this assumes the use of symmetrical and uniformly spaced consequent set declarations.

6.3.6 Analysis of Inference Methods

The effect of the various methods of reasoning upon the advisor output was investigated by examining a subset of the PEEP control space. The crisp output dPEEP was plotted for PaO₂ between 5 and 12 kPa, with values for the other observations as specified in Table 6.3. These values were chosen such that multiple rule firing occurred, thus enabling the comparison of weight and non-weight counting methods.

Decision plots (see Figure 6.7) were generated for the following combinations of inference method;

- 1). Mamdani's implication (sup-min).
- 2). Larsen's implication (sup-prod).

and with the following combinations of defuzzification method and liaison operator;

- 1). Centre of sums, product liaison (CoS-prod).
- 2). Centre of sums, min liaison (CoS-min).
- 3). Centre of gravity, product liaison (CoG-prod).
- 4). Centre of gravity, min liaison (CoG-min).

Observation	Value	Set Membership
PaO ₂	5 – 12 kPa	VLOW to NORM
eBPsys	-10 mmHg	LOW (0.5), OKAY (0.5)
FiO ₂	60 %	MEDIUM (1)
PEEP	6 cmH ₂ O	LOW (0,5), MEDIUM (0.5)

Table 6.3: Observation settings for a subset of the dPEEP control space, indicating grade of membership within the appropriate linguistic sets.

There was little observed difference between the sup-min and sup-prod inference methodologies. This would result in a negligible difference in any advice given. Consequently the remainder of this analysis only focuses on the plots generated using Larsen's implication.

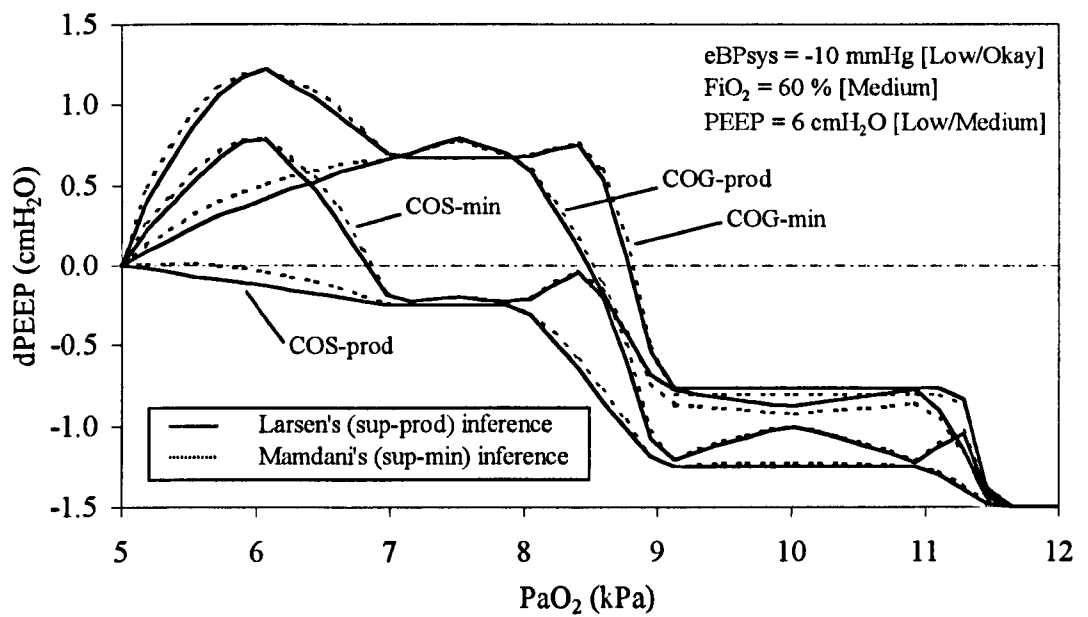


Figure 6.7: Comparison of control output for various combinations of inference method, defuzzification method and liaison operator.

Fire Weight for Each Rule					
Rule No.	COG-min	COS-min	COG-prod	COS-prod	Rule CSQ Label
27	0.5	0.5	0.125	0.125	PM ⁽²⁷⁾
29	0.5	0.5	0.125	0.125	PS ⁽²⁹⁾
32	0.5	0.5	0.25	0.25	NS ⁽³²⁾
42	0.5	0.5	0.125	0.125	Z ⁽⁴²⁾
44	0.5	0.5	0.125	0.125	PS ⁽⁴⁴⁾
48	0.5	0.5	0.25	0.25	NS ⁽⁴⁸⁾
Total Consequent Weight					
PM	0.5	0.5	0.125	0.125	
PS	0.5	1	0.125	0.25	
Z	0.5	0.5	0.125	0.125	
NS	0.5	1	0.25	0.5	
Crisp Output					
u*	1.25	0.833	0.4	-0.125	

Table 6.4: Comparison of rule-firing weight, aggregated consequent weight and crisp output using different combinations of defuzzification method and liaison operator. These are based upon observations made at PaCO₂ = 6 kPa.

In order to compare each method, the rule firing weights for each were generated for an observed PaO₂ of 6 kPa (membership VLOW = 0.5, LOW = 0.5). This point was chosen since it corresponds to the point of largest difference between the curves.

Min Liaison, Centre-of-Gravity

This method generates the most positive output relative to the other methods. It can be seen that in this example, the min-operator results in equal plausibility for all of the rules (Table 6.4, col. 2). It is felt that this does not meaningfully reflect the certainty of the rule, since more than one observation has a certainty less than one and therefore the evidence to support the rule is further diminished. Using the min-operator only the smallest evidence is considered, which means the observations could have values ranging from this minima up to one (certainty) without affecting the rules credibility.

Using CoG defuzzification, contributions made by rules PS⁽⁴⁴⁾ and NS⁽⁴⁸⁾ are lost, since this is a non-weight counting method. The loss of these rule-consequents coupled with exaggeration of PM⁽²⁷⁾ caused by the min liaison operator, lead to a crisp output (u^*) of 1.25 cmH₂O.

Min Liaison, Centre-of-Sums

The exaggeration of rule plausibility imparted by the min-operator leads to regions of increased control. However, this is offset against the fact that CoS defuzzification, being a weight counting method, re-introduces the effects of PS⁽⁴⁴⁾ and NS⁽⁴⁸⁾. Now since these consequents are themselves exaggerated by the min-operator, it leads to oscillations in the control space not consistent with changes to the input.

Product Liaison, Centre-of-Gravity

The measure of rule certainty is now reflected through the product of the antecedent memberships. However, using CoG the influences of PS⁽⁴⁴⁾ and NS⁽⁴⁸⁾ are again no longer felt. This accounts for the rise in dPEEP as PaO₂ increases towards 8 kPa, since PM⁽²⁷⁾ is provided proportionally greater significance.

Product Liaison, Centre-of-Sums

This approach appears to have the balance between scaling of the rule significance and inclusion of lesser rule-consequents. The result is a smooth fuzzy control space, consistent with input changes and without apparent bias. This combination of liaison operator and defuzzification method matches those finally chosen for use in the advisor.

6.3.7 Choice of Output Quantisation

Once the advice has been generated and the proposed changes to the ventilator settings computed from it, they then need to be quantised. It was found that changes derived using the *raw* quantisation levels would occasionally produce decision creep. This was caused by very small firing weights in rules with non-zero consequents. The advised change was not enough to prevent the rule from firing at the next decision point but large enough to cause gradual increase or decrease in the controller output. This behaviour is symptomatic of systems using only proportional control. Creep does eventually stop, once the rule-antecedents fall wholly within a region of zero consequent. However, the anaesthetist's decision process is discrete and therefore a method of preventing unnecessarily small changes from being made is required.

The solution was to use larger quantisation levels, which only allow changes to the controller output when the advised change is at least as large as the quantisation level. However, make the quantisation interval too large and the control can become crude, with the possibility of limit-cycle behaviour. The *ventilator* quantisation levels were felt to be the best compromise between decision creep and crude control that also allowed the true behaviour of the rules to be observed.

6.4 Rule Development Methodology

6.4.1 Rule Prototyping and Completeness

In safety critical systems there should never exist a combination of input values that result in no rule being fired. This is especially true with patients in the intensive care environment, when acute events can occur that give unexpected controller inputs. Incomplete rule definition in such circumstances may prove fatal.

Linguistic rule statements of the form 'If *A* is *x* and *B* is *y* then *C* is *z*' provide a rapid method for rule-base construction, especially when elicited from a knowledge expert (i.e. an anaesthetist), and are simple to interpret. However, construction of a rule-base using only rule-statements can be susceptible to rule holes or *incompleteness*, see Figure 6.8.

Rules

If (X_1 is N) and (X_2 is Z) then (Y is PS)

If (X_1 is N) and (X_2 is P) then (Y is Z)

If (X_1 is Z) and (X_2 is Z) then (Y is Z)

If (X_1 is Z) and (X_2 is P) then (Y is NS)

If (X_1 is P) and (X_2 is N) then (Y is PB)

If (X_1 is P) and (X_2 is Z) then (Y is PS)

If (X_1 is P) and (X_2 is P) then (Y is NS)

Rule Map

		X_2		
		P	Z	N
X_1	P	NS	PS	PB
	Z	NS	Z	
	N	Z	PS	

Figure 6.8: Using the above rule-statements the resulting rule-map is incomplete. Whilst it would be a simple matter to spot such occurrences in a small knowledge-base like this, in a large *n*-dimensional system it is easy to see how rule-holes might be missed.

These rule-holes were avoided by declaring the rule-base using a matrix rather than via rule-statements. In this way every possible observation event will have a consequent action defined for it. For example, consider the subset of the minute volume control rules, see Figure 6.22, this is declared in the MATLAB environment using a 5-by-5 matrix;

$$R = \begin{bmatrix} -60 & -30 & -15 & 0 & 0 \\ -45 & -30 & -5 & 0 & 0 \\ -30 & -15 & 0 & +25 & +50 \\ 0 & 0 & 0 & +50 & +75 \\ 0 & 0 & +15 & +50 & +100 \end{bmatrix} \quad (6.7)$$

This does not mean that elicitation of rule-statements from an expert was negated. Merely that these statements were mapped onto the rule-matrix and then all empty elements given a consequent action, in order to complete it. The choice of consequent action at these hole-regions was estimated from the values in neighbouring cells by either (1) averaging the values at neighbouring regions or (2) by making intuitive guesses. This prevented decision space discontinuity.

Rule prototyping was also made using known physiological relationships and nomograms regularly referred to in the literature. This resulted in fewer if any holes, but did require modification of the consequents at the observation extremes. This was done via discussion with an anaesthetist.

6.4.2 Fuzzy Consequent Construction

The values defined for the consequent actions in equation 6.7, represent the peak value of the fuzzy consequent sets. The sets themselves were defined with a support twice the smallest interval between neighbouring peaks and were made to be symmetrical about the peak value. So in the above example the fuzzy sets will have a support of 10 (twice the distance between N1 and Z). The result is narrow fuzzy sets, distributed across the output domain with only N1 and Z having intersection, see Figure 6.9b.

This approach could be criticised in that the defuzzified output may be implausible, falling at a point in the output domain with no set membership. However, if the cross-points are fixed at 0.5 and the peak values are non-uniformly distributed, then the resulting membership functions become asymmetrical, see Figure 6.9a. Using the centre-of-gravity or centre-of-sums defuzzification methods, this approach skews the crisp output in favour of the heavier side of the set's support. This gives rise to biased controller output and is best avoided rather than adhering strictly to the notion of plausibility.

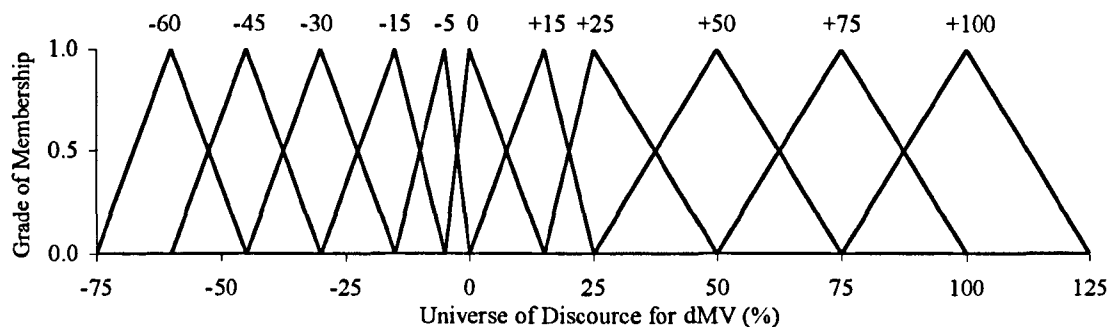
In the worst case scenario, that of very narrow consequent support with a cross-point ratio of zero, the defuzzification behaves as though it were a mean-of-maxima (or height) method. When the cross-point is 0.5 the defuzzification behaves as a centre-of-sums method. Both of these methods provide a smooth control space and therefore the approach taken was considered appropriate.

6.4.3 Rule Reduction Algorithm

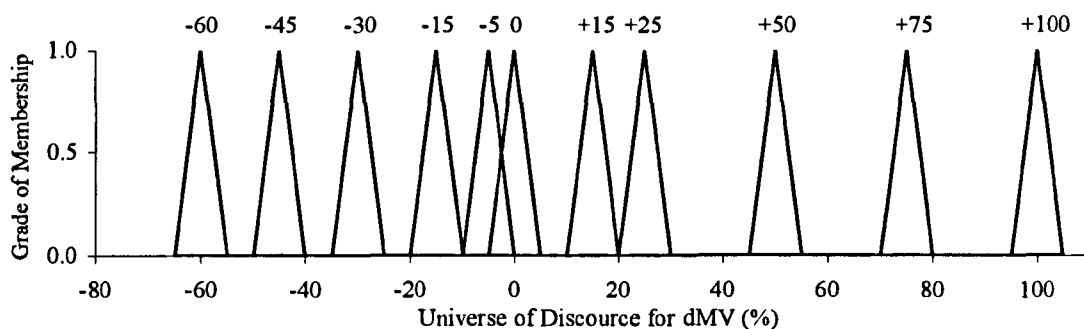
In order for the rule-matrices to be used by the inference engine they have to be converted back into rule statements of the form;

If [x_1 is A] and [x_2 is B] and [x_3 is C] then [y is D]

This appears to be reverting back to the original expert rule-statements. However, it is more a symptom of the FISMAT toolbox than part of the rule design process. The design of the rule-map using the matrix definition is by far the most practical method of declaring the rules, but the rules are more easily processed by the fuzzy toolbox when declared as rule-statements.



(a)



(b)

Figure 6.9: Comparison of consequent set declaration methods using (a) asymmetrical sets with a cross-point of 0.5 and (b) symmetrical sets with a support of twice the smallest distance between consequent neighbours.

It would be possible to generate a rule-statement for every observation co-ordinate. However, in large rule-maps this would result in $n_1 \times n_2 \times \dots \times n_i$ rule-statements, where i is the number of fuzzy input variables and n is the number of fuzzy sets for each input i . Whilst theoretically not a problem, computationally it would be excessive, since every rule must be checked to determine its firing weight. Therefore a rule reduction algorithm was written enabling regions of neighbouring and identical consequent action to be described via a single rule-statement.

The algorithm works by taking a 2-dimensional slice (or hyper-plane) of the n -dimensional decision space (see Figure 6.10) and searches for blocks of identical neighbours within it. So returning again to the example of equation 6.7. This represents a hyper-plane obtained from the 3-dimensional rule-map for the condition when ePIP is OKAY. The reduction algorithm will identify 16 regions, of which 5 contain more than one identical neighbour, see Figure 6.11.

These regions are then coded using a co-ordinate system. So for example region 'c' will be coded as [2, 2, 4, 5, 1, 1, -30]. The first two elements are the start and stop co-ordinates in the X direction (ePaCO₂) and correspond to the observation class NS. The second value pair is the start and stop co-ordinates in the Y direction (epH) and corresponds to the observation classes ALK to VALK. The third pair is the start and stop co-ordinates in the Z direction (ePIP) which corresponds to the hyper-plane axis and an observation class of OKAY. The last value is the consequent action attributed to this region.

The codes resulting from the rule-reduction were then used to generate the rule statements. So considering *region c* again, this is described by the rule “If [ePaCO₂ is NS] and [epH is ALK to VALK] and [ePIP is OKAY] then [dMV is N3 (-30 %)]”

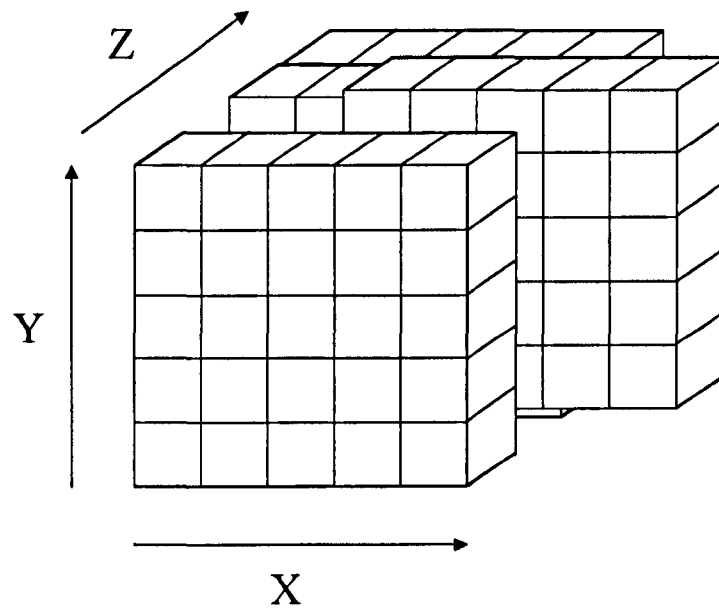


Figure 6.10: A 2-dimensional hyper-plane taken from the 3-dimensional rule-map along the Z-axis. Hyper-plane slices can be taken along any of the observation axes.

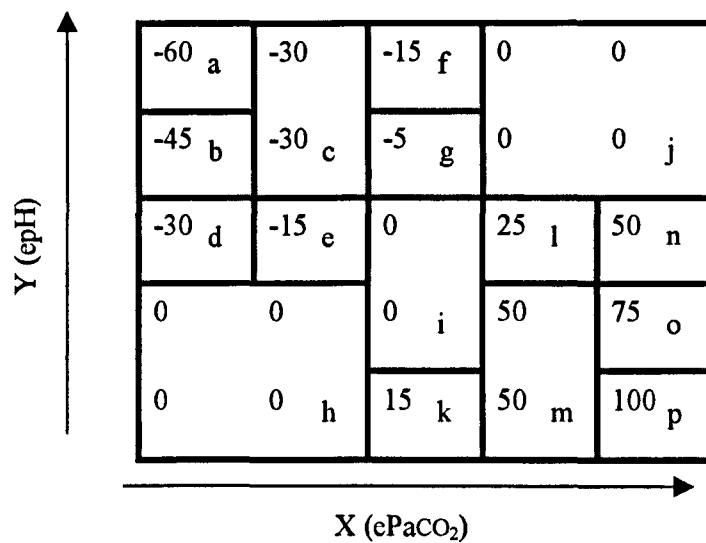


Figure 6.11: Regions of identical and neighbouring consequent action identified by the rule-reduction algorithm.

Phrase Construction

The phrase [epH is ALK to VALK] is expressed as a bounded sum of the fuzzy sets ALK and VALK;

$$\mu_{ALK-VALK} = \mu_{ALK} \oplus \mu_{VALK} \quad (6.8)$$

This gives an augmented membership functions (see Figure 6.12) that will return a membership weight of 1 for all epH observation in the range *alkaline to very alkaline*.

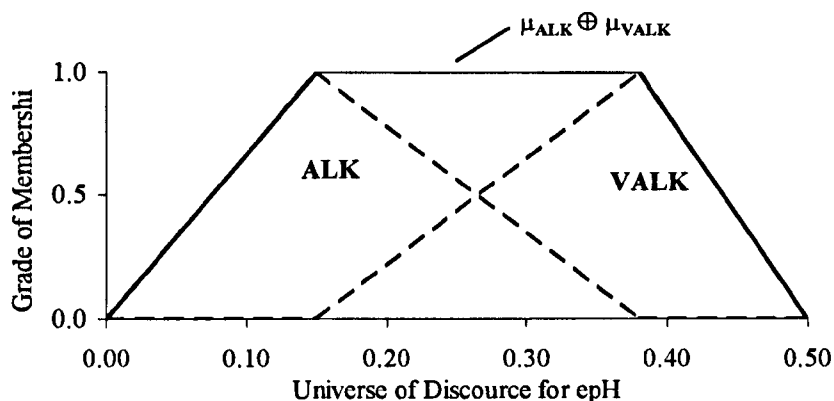


Figure 6.12: Representation of the phrase “epH is ALK to VALK” using bounded sum.

Algorithm Improvements

This rule-reduction algorithm was optimised by the inclusion of hyper-cube searching. This enabled large regions with identical consequents spanning n-dimensions to be described by a single rule. This greatly reduces the number of rules required to describe more complex rule-maps and therefore improves computation times. Typically a 60 % reduction in the number of rules required to describe the rule-map was achieved.

6.5 FIO₂ Rule Development

6.5.1 Elicitation of PaO₂ Membership Functions

Inspired O₂ fraction is the main mechanism for the maintenance of blood gas oxygenation and the normal indicator of this is arterial O₂ tension (PaO₂). In order to construct rules for the control of PaO₂ it was first necessary to identify and elicit the fuzzy set membership functions for it. This was achieved via discussion with a consultant anaesthetist.

They were asked to assign values to the linguistic classes very low (VL), low (L), slightly low (SL), normal (N), slightly high (SH), high (H) and very high (VH). This was performed with reference to the iso-shunt diagrams since they were to be used to prototype the control rules.

The fuzzy sets arrived at are shown in Figure 6.13. The cross-points were fixed at 0.5 and the cross-point ratio at 1. It can be seen that VH lies at some distance from the other sets and reflects the level of PaO₂ that might be observed when a patient has little or no effective shunt and a FiO₂ of between 50 and 70 %. The remaining sets are very similar to those derived in a later study [Kwok *et al*, 2000].

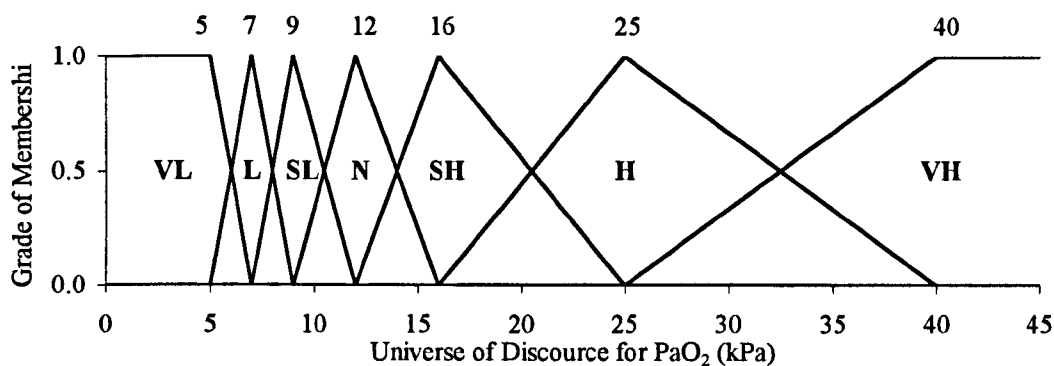


Figure 6.13: Fuzzy set definition for PaO₂.

6.5.2 Rule Prototyping Using Iso-Shunt Diagram

The iso-shunt diagram (see Figure 3.2) of Benetar *et al* (1973) and Pedros *et al* (1993) is used by some anaesthetists to adjust inspired O₂ concentration to obtain a required level of PaO₂ that prevents hypoxia while avoiding the administration of unnecessarily high O₂ concentrations. This follows a goal-orientated approach similar to that required by FAVeM.

Using the equations behind the iso-shunt curves, it was possible to estimate the changes required in FiO₂ needed to bring PaO₂ towards the set point for a range of initial PaO₂ and FiO₂ levels. The set point was assumed to be 12 kPa, corresponding to expected normal values defined previously.

If we take the iso-shunt equation for arterial O₂ content (CaO₂), see Section 3.2.7;

$$CaO_2 = Cc'O_2 - C(a-v)O_2 \times \left(\frac{\dot{Q}_s/\dot{Q}_t}{1 - \dot{Q}_s/\dot{Q}_t} \right) \quad (\text{ml/l}) \quad (6.9)$$

where $Cc'O_2$ is the end pulmonary capillary O₂ content (ml/dl)

$C(a-v)O_2$ is the arterial-venous O₂ difference (ml/dl)

\dot{Q}_s/\dot{Q}_t is the shunt fraction

This can be re-arranged to calculate the shunt fraction;

$$\dot{Q}_s/\dot{Q}_t = \frac{R}{R-1} \times 100 \quad \text{where } R = \frac{CaO_2 - Cc'O_2}{C(a-v)O_2} \quad (\%) \quad (6.10)$$

Assuming $C(a-v)O_2$ to be 50 ml/l and using the equations given by Pedros *et al* for CaO₂ and Cc'O₂ (see equations 3.7 and 3.5), it is possible to estimate a patient's shunt, based upon observations of PaO₂ and FiO₂. For example, given an observed PaO₂ of 19 kPa and a FiO₂ of 0.9, the calculated shunt would be 24.3 %. The PaO₂-FiO₂ relationship for this shunt can then be computed using the original iso-shunt equations and interpolated to estimate the new FiO₂ required to achieve a given PaO₂ set point, see Figure 6.14. Subtracting this from the observed FiO₂ gives the change required in FiO₂.

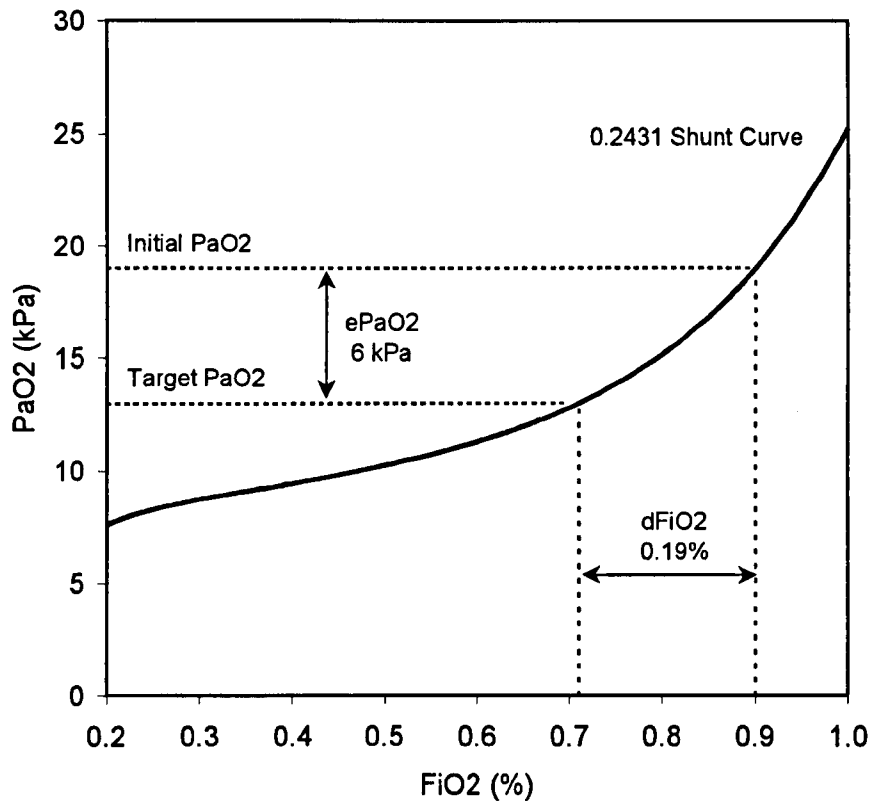


Figure 6.14: Iso-shunt curve calculated for an observed PaO₂ of 19 kPa and FiO₂ of 0.9, showing how the FiO₂ change can be estimated for a given PaO₂ target.

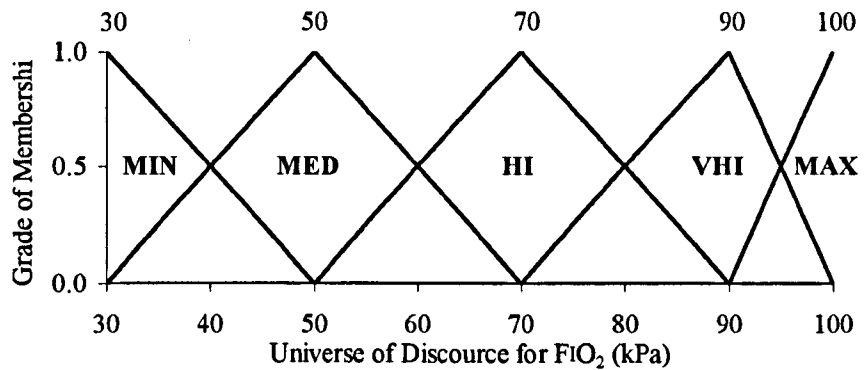


Figure 6.15: Fuzzy set definition for FiO₂.

By repeating this process for every peak value of the PaO₂ and FiO₂ fuzzy variables, an array of consequent actions was produced. The choice of fuzzy membership functions for FiO₂ are shown in Figure 6.15. The classes MIN and MAX reflect the lower and upper limits of deliverable FiO₂, since an FiO₂ below 30 % will be almost atmospheric air and an FiO₂ of 100 % is a pure oxygen. The class MED reflects the default level of O₂ support for healthy post-operative patients and the remaining classes HI and VHI were chosen to have increments of 20 % above MED.

The calculated consequent actions were rounded to the nearest 5 % in order to reduce the number of consequent classes required to specify the rule-map. Any derived $d\text{FiO}_2$ estimates that would cause the new FiO_2 level to exceed the upper or lower limits (100 % and 30 % respectively) were reduced accordingly. The resulting 7-by-5, prototype rule map is shown in Figure 6.16.

		FiO_2				
		MIN	MED	HI	VHI	MAX
PaO_2	VH	0	-20	-40	-50	-50
	H	0	-20	-35	-35	-35
	SH	0	-15	-20	-20	-20
	N	0	0	0	0	0
	SL	+30	+35	+30	+10	0
	L	+70	+50	+30	+10	0
	VL	+70	+50	+30	+10	0

Figure 6.16: Prototype FiO_2 rule map derived from iso-shunt diagram.

6.5.3 Evaluation of Iso-Shunt Rules

The main criticism of the rule-map derived using the iso-shunt equations, was that it attempted to drive PaO_2 towards the target regardless of other therapeutic considerations, such as the need to balance PaO_2 against undesirable levels of FiO_2 . In an attempt to identify these weaknesses in the rule-map, an anaesthetist was presented with random observations of PaO_2 and FiO_2 together with the changes proposed by the advisor, and asked the following;

- 1). Whether they agreed with the advice?
- 2). What action they would take?
- 3). What additional therapy might they consider?

However, in order to cover as much of the observation space as possible without resorting to large numbers of observations, the random selection of observation data was regionalised, by defining three target regions for FiO_2 ; 30–50 %, 55–75 % and 80–100 %. Each peak value of PaO_2 (see Figure 6.13) was then given an observed FiO_2 falling randomly within each of these three ranges, resulting in 21 observations. The observation data, iso-shunt responses and the clinician's comments are shown in Table 6.5.

Since the primary objective of the advisor was to mimic clinical decision making, the differences outlined by the anaesthetist were incorporated into a modified set of rules, see Figure 6.17.

Observed PaO ₂ (kPa)	Observed FiO ₂ (%)	Proposed FiO ₂ (%)	Anaesthetist's Comments
12	30	30	No action – adequate oxygenation
9	35	65	Increase FiO ₂ to 50%. 65% appears rather excessive
7	40	100	Increase FiO ₂ to 70% and increase PEEP unless contraindicated. FiO ₂ greater than 70% are used cautiously and only if absolutely required to maintain oxygenation because of the risk of oxygen toxicity
16	45	30	Decrease O ₂ to 35% The proposed step seems a bit large as the PaO ₂ is only slightly above normal
25	50	30	Agree
5	50	100	Agree and increase PEEP if not contraindicated
40	50	30	Agree
9	55	90	Increase to 70% The proposed increase seems large considering that the PaO ₂ is not too far below normal
40	55	30	Agree
12	65	65	Agree
16	65	45	Decrease to 50% The proposed reduction seems a little generous. It is better when reducing FiO ₂ to err on the side of caution to avoid inadvertent hypoxia
25	75	40	Reduce to 50% for the same reason as above
5	75	100	Agree and increase PEEP if not contraindicated
7	75	100	Agree and increase PEEP if not contraindicated
40	80	30	Reduce to 40% to be cautious
9	85	100	Agree and increase PEEP if possible
25	90	55	Agree
12	95	95	Agree. Increase PEEP if not contraindicated
5	95	100	Agree. Increase PEEP if not contraindicated
16	95	75	Agree
7	95	100	Agree. Increase PEEP if not contraindicated

Table 6.5: Comments made by anaesthetist to prescribed FiO₂ changes derived from iso-shunt diagram using randomly generated PaO₂-FiO₂ observations (see text).

		FiO ₂				
		MIN	MED	HI	VHI	MAX
PaO ₂	VH	0	-20	-30	-50	-50
	H	0	-20	-20	-35	-35
	SH	0	-10	-15	-20	-20
	N	0	0	0	0	0
	SL	+20	+20	+20	+10	0
	L	+40	+30	+30	+10	0
	VL	+70	+50	+30	+10	0

Figure 6.17: Modified FiO₂ rule map based upon knowledge derived from anaesthetist. The shaded regions indicate those regions that have been modified from the original rule-map of Figure 6.16.

6.6 PEEP Rule Development

Whilst FiO₂ provides the principal mechanism for O₂ maintenance, PEEP also plays an important role in certain patient conditions. In order to construct sensible control rules it was necessary to understand the clinical benefits and disadvantages of PEEP.

6.6.1 Clinical Benefits of PEEP

The clinical benefits of PEEP can be summarised as follows;

- 1). Opens up closed alveoli improving arterial oxygenation. This allows lower levels of FiO₂ to be used, reducing the risks of O₂ toxicity.
- 2). Increases functional residual capacity (FRC), preventing air trapping and lowering airway resistance caused by alveolar collapse. This has the overall effect of reducing peak inspiratory pressure (PIP).
- 3). Increases lung compliance as collapsed alveoli are recruited, again lowering PIP

From these benefits it is possible to identify three potential observation variables; PaO₂, PIP and FiO₂. PEEP can be increased in response to low PaO₂ levels to prevent excessively high FiO₂ or reduced as PaO₂ levels improve. However the degree to which PEEP is modified will also depend upon the current level of PEEP applied. As PEEP approaches 15 – 20 cmH₂O the suitability of PEEP reduces as the risks associated with PEEP increase.

The possible reduction in PIP associated with PEEP (see benefits 2 and 3) will depend upon the nature of the patient condition. However a single observation of PIP imparts no knowledge about the effect that additional PEEP will have on subsequent airway pressures. This makes construction of rules pertaining to PIP optimisation via PEEP adjustment difficult to realise, since the calculation of 'mechanical-best PEEP' requires the step-wise increase of PEEP without adjusting other ventilator

settings. Such a manoeuvre whilst occasionally necessary does not fit within the initial objectives of FAVeM and would require a hierarchical decision process, see Chapter 9: Future Work.

Using PaO_2 , FiO_2 and PEEP as the observation variables, it was possible to construct a simple set of guidelines for PEEP change.

- 1). If PaO_2 is low then increase level of Peep.
- 2). If PaO_2 is high then reduce level of Peep.
- 3). If FiO_2 is high then increase level of Peep.
- 4). If FiO_2 is low then reduce level of Peep.
- 5). If Peep is high then limit any Peep increases.
- 6). If Peep is high then increase any Peep reductions.
- 7). If Peep is low then limit any Peep reductions.
- 8). If Peep is low then increase any Peep increases.

The membership functions for PaO_2 and FiO_2 observations were kept as for the FiO_2 control rules (see Figure 6.13 and Figure 6.15 respectively) and the membership functions for PEEP was defined as in Figure 6.18.

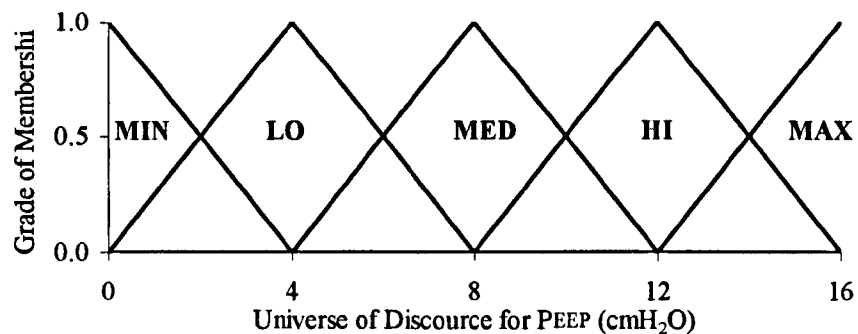


Figure 6.18: Fuzzy set definition for PEEP

Using these fuzzy set definitions and the simple guidelines outlined above, a draught set of rule-consequents was constructed, see Figure 6.19. This includes modifications made to the consequents based upon discussions with an anaesthetist. However, most of these were limited to the regions PEEP is OFF and LOW.

6.6.2 Disadvantages of PEEP

The benefits of PEEP are often contraindicated by other patient observations or it does not impart any benefit to the patient at all. Such instances can be summarised as follows;

- 1). Alveolar recruitment does not occur in healthy lungs, therefore little improvement to PaO_2 will be seen.
- 2). PEEP is additive to airway pressure and at high levels can increase risk of barotrauma.

- 3). Hyperinflation of open alveoli can lead to impaired perfusion, increasing the effective dead space. However, this only usually occurs in lungs with regions of differing compliance.
- 4). Increases intrathoracic pressure, which impedes venous return, increasing pulmonary vascular resistance and thus reducing cardiac output. This effect is least when the lungs are stiff, and therefore more of a problem in healthy lungs. Consequently low systolic blood pressure (BP_{SYS}) contraindicates the use of PEEP.

		FiO ₂				
		MIN	MED	HI	VHI	MAX
PaO ₂	VHI	0	0	0	0	0
	HI	0	0	0	0	0
	SHI	0	0	0	0	0
	N	0	0	0	4	4
	SLO	0	4	4	4	4
	LO	4	4	4	4	8
	VLO	4	4	4	8	8

(a) PEEP = OFF

		FiO ₂				
		MIN	MED	HI	VHI	MAX
PaO ₂	VHI	-8	-8	-8	-8	-8
	HI	-6	-6	-6	-4	-4
	SHI	-6	-4	-4	-4	-2
	N	-4	-4	-4	-2	0
	SLO	-2	-2	0	0	2
	LO	-2	-2	0	0	2
	VLO	0	0	2	2	4

(d) PEEP = HIGH

		FiO ₂				
		MIN	MED	HI	VHI	MAX
PaO ₂	VHI	-4	-3	-3	-2	-2
	HI	-3	-2	-1	0	0
	SHI	-3	0	0	0	0
	N	-2	0	0	0	0
	SLO	0	0	0	2	4
	LO	0	2	2	4	4
	VLO	2	2	4	4	4

(b) PEEP = LOW

		FiO ₂				
		MIN	MED	HI	VHI	MAX
PaO ₂	VHI	-16	-12	-12	-12	-12
	HI	-12	-8	-8	-8	-8
	SHI	-12	-8	-8	-8	-8
	N	-8	-6	-4	-4	-4
	SLO	-4	-4	0	0	0
	LO	-4	-4	0	0	0
	VLO	-2	0	0	0	0

(e) PEEP = MAX

		FiO ₂				
		MIN	MED	HI	VHI	MAX
PaO ₂	VHI	-6	-6	-6	-6	-6
	HI	-4	-4	-4	-4	-2
	SHI	-4	-4	-2	-2	2
	N	-4	-4	-2	0	2
	SLO	-2	0	0	2	4
	LO	-2	0	0	2	4
	VLO	0	2	2	4	4

(c) PEEP = MED

Figure 6.19: Prototype rule-map for PEEP changes based upon observations of PaO₂, FiO₂ and current PEEP.

The disadvantages of PEEP are less easily converted into a set of rules. The first statement is not so much a disadvantage, more a reason for not increasing PEEP, since patients with no collapsed alveoli will not benefit from it. Therefore increasing PEEP will only serve to raise PIP, although some reduction in airway pressure may result due to dilation of the bronchioles. The risk of barotrauma is more likely with high PIP (statement 2) and there is some argument for limiting PEEP in such circumstances.

At this stage in the advisor development it was felt best to forgo the inclusion of PEEP rules pertaining to BPSYS and/or PIP, since the rule set was already quite large and hand-crafting of larger sets is very time consuming. It was considered best to optimised the current rules adding the new observation variables afterwards, time permitting.

6.7 MV Rule Development

6.7.1 Ventilation-PaCO₂ Relationship

It is known that PaCO₂ follows an approximately inverse-proportional relationship with alveolar ventilation (\dot{V}_A) [Mushin *et al*, 1980, p39]. Hence if \dot{V}_A is doubled then PaCO₂ will be halved. Alveolar ventilation can be expressed as the total ventilation or minute volume (MV) minus the dead space ventilation (\dot{V}_D);

$$\begin{aligned} \dot{V}_A &= MV - \dot{V}_D \\ \text{or } \dot{V}_A &= (RR \cdot V_T) - (RR \cdot V_D) \end{aligned} \quad (\text{ml/min}) \quad (6.11)$$

where RR is the respiratory rate (r.p.m.), V_T is the tidal volume (ml) and V_D is the dead space volume (ml). Consequently a doubling of V_T will not result in a doubling of \dot{V}_A (unless V_D is very small), but a doubling of RR will. If we assume that MV is adjusted using RR only, then we can say that \dot{V}_A is proportional to MV. For example, a 50% increase in MV will result in a 50% reduction in PaCO₂.

Clinical practice requires that PaCO₂ maintenance be goal driven, since conditions exist when it needs to held artificially above or below its normal level (e.g. during the care of head injury patients). Consequently FAVeM expresses the observed PaCO₂ as error from the PaCO₂ set point (ePaCO₂). However, expressing ePaCO₂ in kPa will not allow the implementation of the above inverse relationship since the size of MV depends upon the PaCO₂ set point. Therefore ePaCO₂ is expressed as a percentage error from set point (see equation 6.3).

During mechanical ventilation the primary objective is to normalise PaCO₂ levels. Consideration can then be given to acid-base imbalances indicated by abnormal pH values. It is therefore possible to construct a simple set of rules using the above inverse PaCO₂-MV relationship, which will normalise PaCO₂ (see Table 6.6).

The choice of fuzzy classes was made to reflect the range of normally observed PaCO₂ values. Based upon a target of 5.3 kPa, the minimum observed PaCO₂ error (NB) corresponds to an observed PaCO₂ of approximately 2 kPa. Levels below this are rarely seen. The maximum PaCO₂

error (PB) was set to +100% corresponding to an observed PaCO₂ of approximately 10 kPa. Whilst PaCO₂ levels greater than this are common in ventilatory failure, it was felt appropriate to restrict MV changes to +100% (effectively a doubling of the lung ventilation) so as to prevent possible problems with high inspiratory pressures. The intermediate classes PS and NS were set to lie halfway between PB and zero (Z) and NB and Z respectively (see Figure 6.20).

However, it is unlikely that these simple rules would give good control behaviour since a trade-off often has to be made between ideal PaCO₂ levels and the type of acid-base imbalance present. In the next section the various types of imbalance are discussed and how they were used to extend the simple PaCO₂ correction rules.

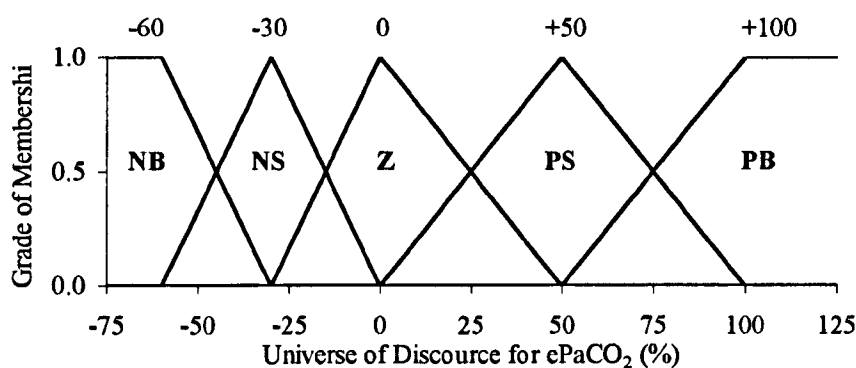


Figure 6.20: Fuzzy set definition for ePaCO₂.

ePaCO ₂				
NB	NS	Z	PS	PB
-60%	-30%	0%	+50%	+100%

Table 6.6: Simple rule map for PaCO₂ correction using inverse MV-PaCO₂ relationship

6.7.2 Acid-Base Balance

Several causes of acid-base imbalance can occur and are categorised as either respiratory or metabolic in nature. Respiratory acid-base disturbances are related to CO₂ elimination, where elevated PaCO₂ causes reduced pH (acidaemia) and low PaCO₂ causes high pH (alkalaemia). These are known respectively as *respiratory acidosis* and *respiratory alkalosis*. Metabolic acid-base disturbances involve either gain or loss of fixed acid H⁺ or buffer (predominantly HCO₃⁻) in the extra-cellular fluid. The causes are varied but the net result is either acidaemia or alkalaemia, known as *metabolic acidosis* and *metabolic alkalosis* respectively. A single type of acid-base disturbance is rarely seen, being normally of mixed origin.

Usually changes in pH are compensated for by either metabolic or respiratory mechanisms depending upon the type and duration of the disturbance. Respiratory mechanisms involve the increase or decrease of alveolar ventilation via the influence of plasma pH on the central chemoreceptors. Metabolic mechanisms involve HCO₃⁻ salvage and excretion of excess acid or

base into the urine. Patients under mandatory mechanical ventilation will not perform any respiratory compensation, since this is controlled by the ventilator and is at the discretion of the attending anaesthetist.

Figure 6.21 attempts to summarise the physiological compensation mechanisms and therapeutic correction methods of acid-base and PaCO₂ disturbances. A more detailed explanation of each of these regions is given below.

1). Normal pH / PaCO₂ (Region E)

Both respiratory and metabolic components are in balance, resulting in normal pH and normal PaCO₂. Under normal circumstances such a patient would require no intervention. However, preservation of the airway in obstructive airway disease may require permissive hypocapnia in order to prevent excessive inflation pressures. Also, patients coming off of sedation post-operatively sometimes require their ventilatory drive kick started by increasing the brain PCO₂. This is often the case in patients that have suffered from chronic hypoventilation.

2). Respiratory Acidosis (Region I)

This is indicated by high PaCO₂ (hypercapnia) and plasma pH below 7.4 caused by hypoventilation. In mechanically ventilated patients this may simply be the result of under ventilation and is corrected very easily by increasing the minute volume (patient moves from region I to E).

Prolonged under ventilation, perhaps as a consequence of obstructive lung disease, will be compensated for by the kidneys. Bicarbonate is conserved and H⁺ secretion into the urine is increased. These renal effects cause the pH to approach normal (patient moves from region I to F) resulting in *respiratory acidosis with renal compensation*. Chronic respiratory disorders such as chronic bronchitis will exhibit hypercapnia with normal pH. It might also arise from prolonged prescriptive under ventilation. In this case the patient can be returned to normal by gradually increasing the ventilation. This has to be done in small steps since the metabolic compensation changes slowly compared to the respiratory effects and rapid respiratory correction would give rise to sudden temporary alkalosis.

3). Respiratory Alkalosis (Region A)

This is indicated by low PaCO₂ (hypocapnia) and plasma pH above 7.4 caused by hyperventilation. In mandatory ventilation, correction is made by reduction of MV (patient moves from region A to E). Chronic hyperventilation produces reduced HCO₃⁻ absorption and less H⁺ secretion into the urine by the kidneys, both of which cause the pH to become more acidic (patient moves from region A to D). This condition is defined as *respiratory alkalosis with renal compensation*.

4). Metabolic Acidosis (Region H)

This is indicated by normal PaCO₂ together with acidaemia caused by abnormal accumulation of fixed acids in the plasma. The central chemoreceptors are activated and the alveolar ventilation increases (patient moves from region H to D). This increases CO₂ elimination and raises plasma pH, known as *metabolic acidosis with respiratory compensation*.

Obviously in mechanically ventilated patients the respiratory compensation will remain at the discretion of the anaesthetist. Mild acidosis will be tolerated and may be preferable to elevated airway pressures associated with increased ventilation.

5). Metabolic Alkalosis (Region B)

This is indicated by normal PaCO₂ with alkalaemia and results from the loss of H⁺ due to nasogastric suction. The high pH depresses the central chemoreceptors and alveolar ventilation decreases, causing pH to fall as PaCO₂ builds up in the plasma (patient moves from region B to F). This defines *metabolic alkalosis with respiratory compensation*.

6). Acute Metabolic Acidosis + Hyperventilation (Region G)

This occurs when acute metabolic acidosis produces a compensatory hyperventilation (air hunger), as described for normal levels of metabolic acidosis (region H), but is not sufficient to normalise pH. Treatment requires correction of the underlying metabolic acidosis first, since respiratory correction of PaCO₂ would only further antagonise the acidaemia.

7). Acute Metabolic Alkalosis + Hypoventilation (Region C)

This time the patient is chronically under ventilating with metabolic alkalosis. Again normal compensatory mechanisms are insufficient and the underlying metabolic alkalosis must be treated first before normalising PaCO₂.

When the normal compensatory mechanisms fail, clinical intervention is necessary. However not all pH / PaCO₂ abnormalities can be controlled via changes to the ventilator regime. Others require intervention at a metabolic level with the introduction of buffers or acids. Table 6.7 summarises the clinical actions required for the conditions detailed above in terms of ventilator and/or intravenous correction. This forms a framework around which pH aspects of the Mv rule construction were made.

6.7.3 Calculation of pH Fuzzy Sets

In order to implement the MV rules sensible values for the pH fuzzy classes had to be chosen. These were expressed as error from normal pH (epH). As with the FIO₂ rule development there are physiological relationships that can be utilised to provide meaningful fuzzy sets and rule constructs.

It is possible to derive approximations of pH using the logarithmic form of the modified Henderson-Hasselbalch equation [Nunn, 1993, p222];

$$pH = pK + \log \frac{[HCO_3^-]}{\alpha \cdot P_{CO_2}} \quad (6.12)$$

where PCO₂ is in kPa, [HCO₃⁻] is in mmol/l and pK is the logarithm of the inverse of the *apparent* first dissociation constant of carbonic acid, and has an experimentally derived value of approximately 6.1. However, it is variable with both pH and blood-temperature (T) and can be derived using equation 4.32 (see Section 4.2.6).

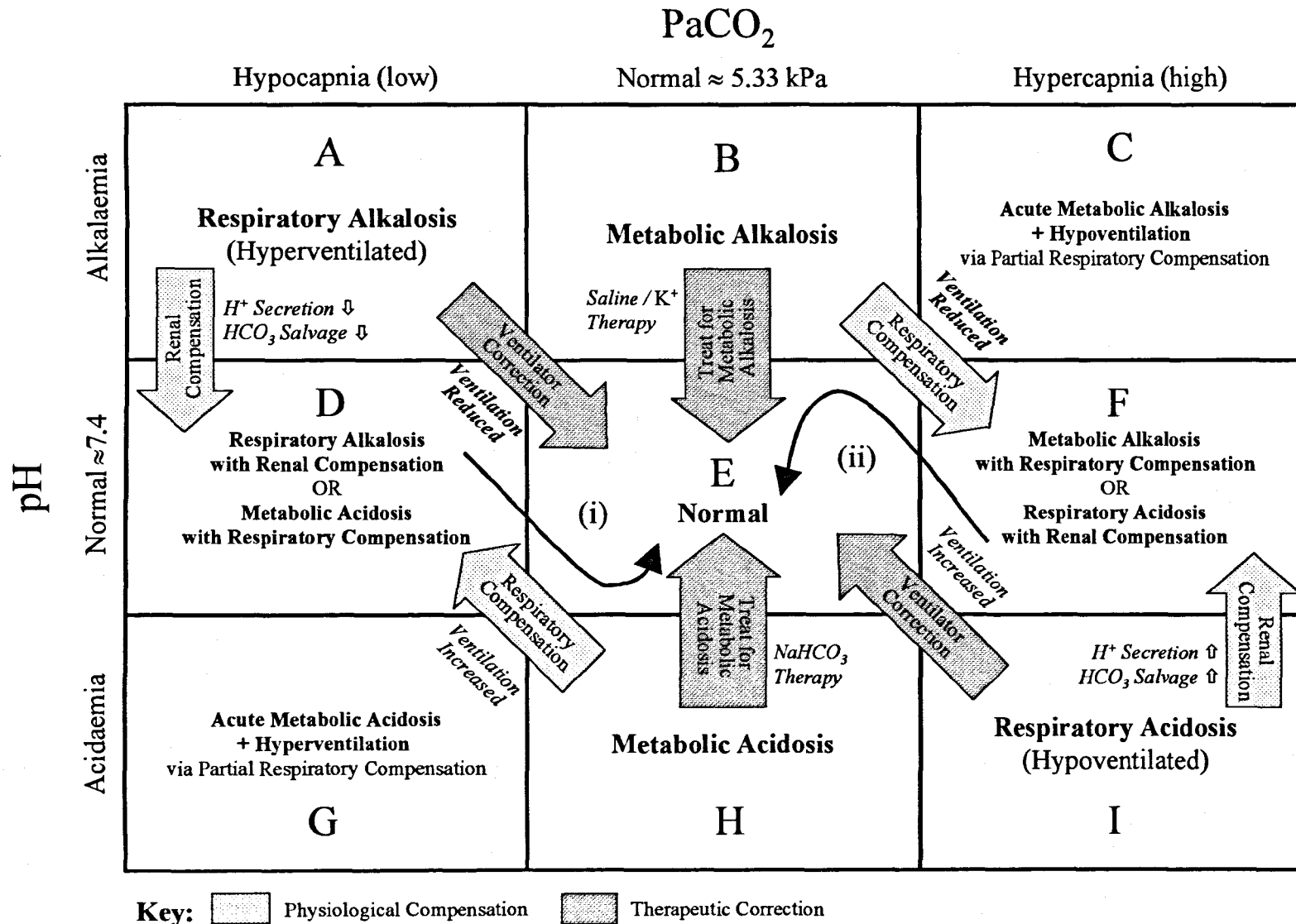


Figure 6.21: Physiological compensation and therapeutic correction of acid-base and PaCO₂ disturbances

Region	Imbalance & Clinical Action
A	Respiratory Alkalosis Reduce MV to increase PaCO ₂ and normalise pH
B	Metabolic Alkalosis Reduce MV slightly in short term and treat alkalosis with intravenous saline and potassium or as appropriate for pathology.
C	Acute Metabolic Alkalosis + Hypoventilation Treat underlying metabolic alkalosis first with intravenous saline/potassium, which will reduce pH and move patient into region F where small increases in ventilation can be made whilst continuing to treat the alkalosis.
D	Respiratory Alkalosis with Renal Compensation or Metabolic Acidosis with Respiratory Compensation Difficult to identify cause of condition and compensatory mechanism in operation. Consequently a cautious reduction of MV is required. In compensated respiratory alkalosis a temporary acidosis will occur until renal compensation normalises pH (see curve (i), Figure 6.21). In metabolic acidosis with respiratory compensation the pH will not normalise and may require bicarbonate therapy or other therapy of the underlying cause of the metabolic acidosis.
E	Normal pH / PaCO₂ No changes normally required
F	Respiratory Acidosis with Renal Compensation or Metabolic Alkalosis with Respiratory Compensation As with region D it is difficult to identify the cause, therefore tentative increases in MV will be required, only treating the resultant alkalaemia if renal compensation not evident. Respiratory acidosis with renal compensation will return pH to normal via counter renal compensation (see curve (ii), Figure 6.21).
G	Acute Metabolic Acidosis + Hyperventilation Treat the underlying acidosis first by treating the cause and administering bicarbonate if appropriate, so increasing pH and moving the patient into region D.
H	Metabolic Acidosis Increase MV slightly and treat the acidaemia by treating the cause of the metabolic acidosis and administering bicarbonate if appropriate.
I	Respiratory Acidosis Increase MV to reduce PaCO ₂ and normalise pH

Table 6.7: Summary of ventilator therapy decisions associated with pH / PaCO₂ observations.

The solubility of CO₂ in plasma (α) has an experimentally derived value of 0.231 mmol/l/kPa but is variable with blood temperature as given by equation 4.31. Since pK is itself dependent upon pH we have to substitute equation 4.32 into equation 6.12 and solve for pH;

$$pH = \frac{6.3968 + 0.01506 \cdot (38 - T) + \log \frac{[\text{HCO}_3^-]}{\alpha \cdot P_{\text{CO}_2}}}{1.042 + 0.0014 \cdot (38 - T)} \quad (6.13)$$

This equation enables the calculation of pH for observed PaCO₂ and [HCO₃⁻]. This makes it possible to estimate a patient's pH at the observed ePaCO₂ points defined earlier (see Table 6.6). However before this can be done, the [HCO₃⁻] at the normal pH-PaCO₂ point must be calculated by using the rearranged form of equation 6.12;

$$[\text{HCO}_3^-] = \alpha \cdot P_{\text{CO}_2} \cdot 10^{(pH - pK)} \quad (\text{mmol/l}) \quad (6.14)$$

At a normal pH of 7.4 and PaCO₂ of 5.3 kPa, the bicarbonate concentration will be 24.878 mmol/l. We can now use this value to estimate the pH at the ePaCO₂ point. For example let us assume the observed PaCO₂ is 60% below the nominal target of 5.3 kPa (i.e. ePaCO₂ = -60 %). Therefore the actual observed PaCO₂ is calculated as;

$$P_{\text{aCO}_2} = 5.3 \cdot \left(1 + \frac{\text{ePaCO}_2}{100}\right) = 5.3 \cdot \left(1 + \frac{(-60)}{100}\right) = 2.12 \text{ kPa} \quad (\text{kPa}) \quad (6.15)$$

Using equation 6.13 with an assumed blood temperature of 37 °C, the pH will be 7.781. Subtracting this from the normal pH of 7.4, we arrive at a value of 0.381 for epH.

This process was repeated for each peak value of the ePaCO₂ fuzzy sets. The epH values obtained were assigned to the linguistic classes V.ALK, ALK, NORM, ACID, and V.ACID (see Figure 6.23), and were found not to be symmetrical about zero due to the logarithmic nature of pH.

The ePaCO₂-epH observation points [NB, V.ALK], [NS, ALK], [Z, NORM], [PS, ACID] and [PB, V.ACID] describe the line of normal pH-PaCO₂ relationship and have consequents as per the initial PaCO₂ correction rules. These form the diagonal of the ePaCO₂-epH rule map (see Figure 6.22 shaded area). The remaining rules were inferred from the principles outlined in Table 6.7.

ePaCO ₂ (%)	-60	-30	0	50	100
PaCO ₂ (kPa)	2.12	3.71	5.30	7.95	10.60
pH	7.781	7.549	7.400	7.231	7.112
epH	0.38	0.15	0.00	-0.17	-0.29

Table 6.8: Estimated epH values at the ePaCO₂ points using equation 6.13. Assumes a nominal PaCO₂ of 5.3 kPa, nominal pH of 7.4, [HCO₃⁻] of 24.878 mmol/l and blood temp. of 37 °C.

		ePaco2				
		NB	NS	Z	PS	PB
epH	V.ALK	-60	-30	-15	0	0
	ALK	-45	-30	-5	0	0
	NORM	-30	-15	0	25	50
	ACID	0	0	0	50	75
	V.ACID	0	0	15	50	100

Figure 6.22: MV rule map for observed epH and ePaCO₂. Shaded region indicates normal respiratory correction as per inverse MV-PaCO₂ relationship. The ePaCO₂ fuzzy sets are as per Figure 6.20 and the epH fuzzy sets as per

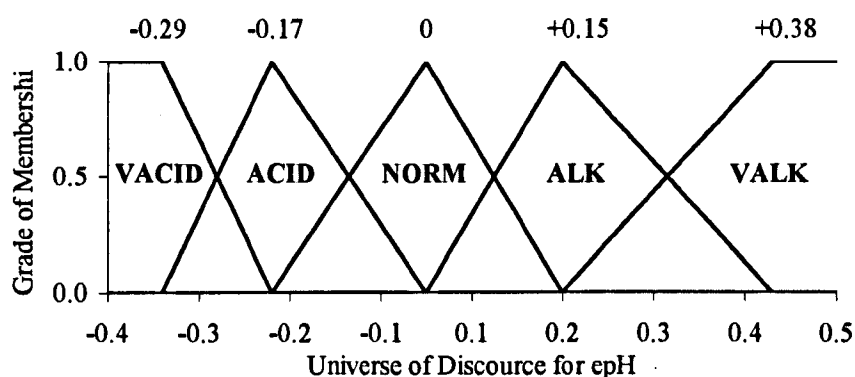


Figure 6.23: Fuzzy set definition for epH.

6.7.4 Volume Constraints

The acid-base / PaCO₂ rules thus far do not account for limitations that might be imposed on upper and lower ventilation volumes. It is important not to under ventilate a patient as this may cause hypoxia, especially in patients with high shunt and/or dead space volumes. Conversely over ventilation can lead to high inspiratory pressures with the possibility of airway damage.

PIP Alarm

There are times when a need to increase MV (normally due to high PaCO₂) is precluded by high peak inspiratory pressures (PIP). In such cases anaesthetists allow *permissive hypercapnia* in order to reduce the risks of barotrauma. The level of PIP that can be tolerated very much depends upon the pathology or trauma present. It was therefore necessary to introduce a PIP alarm. If this PIP threshold is approached or exceeded then the original MV rules can be modified to prevent further increases in MV. The proximity to the alarm threshold was expressed as an error (ePIP) such that PIP values below the alarm are negative and above it they are positive.

Five decision regions were identified, corresponding to five fuzzy classes of observed PIP error;

- 1). Pip is well below the given alarm threshold and therefore the Mv rules can remain unchanged. Typically the alarm threshold will be 35-40 cmH₂O.
- 2). Pip is below but approaching the alarm threshold and any increases in Mv must be moderated.
- 3). Pip is at the alarm threshold and all Mv increases must be drastically reduced. Some increase may still be necessary, especially in cases of acute hypercapnia.
- 4). Pip is just above the alarm threshold and Mv should be reduced in all but extreme cases of hypercapnia.
- 5). Pip is well above the alarm threshold and Mv must be reduced regardless of the current Paco₂ to reduce the chance of barotrauma.

Using the original epH-ePaco₂ rule map as a template the regions 2 to 5 were created by modifying the appropriate rules (see shaded areas Figure 6.24). This resulted in a 5-by-5-by-5 set of rules for MV control. The choice of peak values for the membership functions of ePIP (see Figure 6.25) were estimated from observations made during clinical data collection for the validation of the patient model.

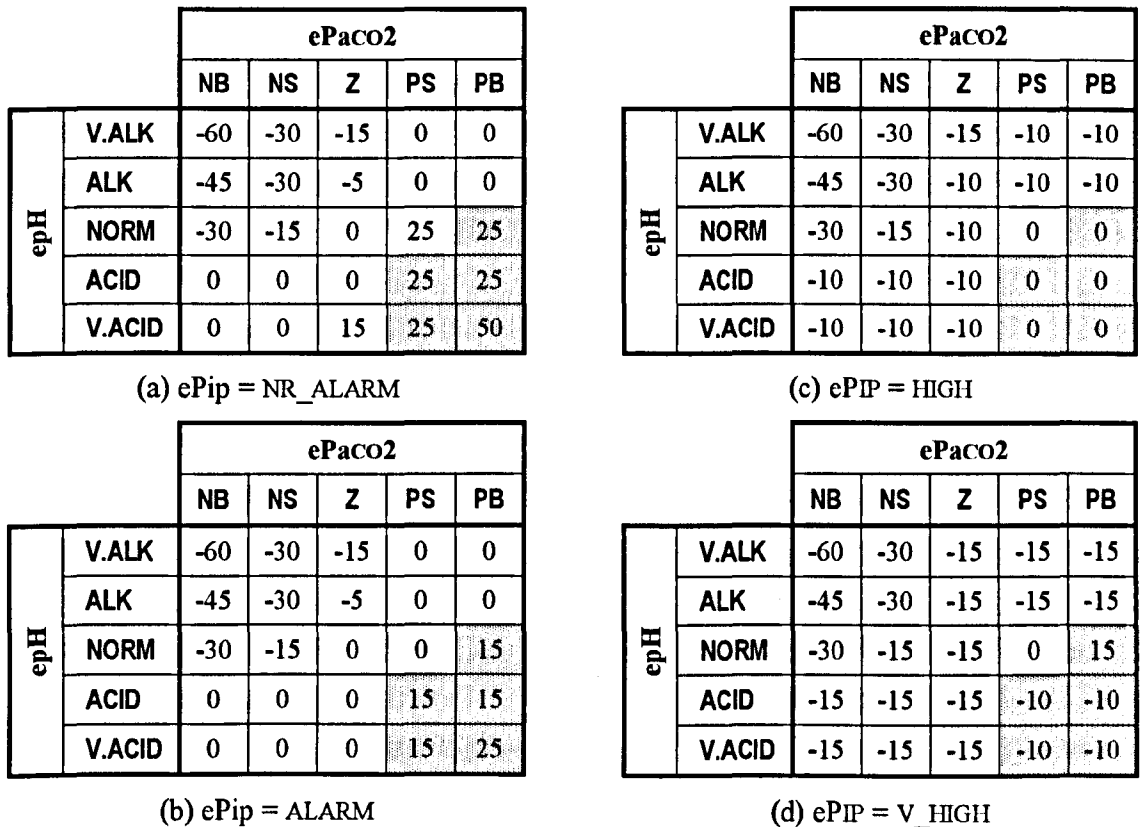


Figure 6.24: Extensions to the Mv rule map to include proximity to PIP alarm. Shaded regions indicate areas of rule map that have been altered from the original map of Figure 6.22.

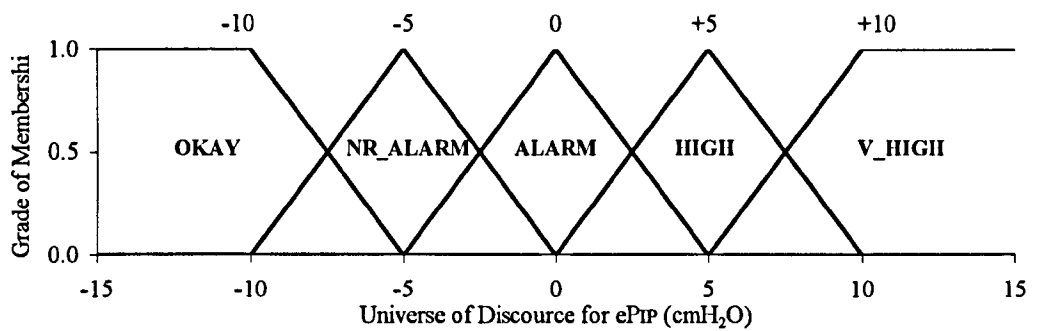


Figure 6.25: Fuzzy set definition for ePIP.

MV Constraints

As mentioned in Section 6.2.2 the majority of patients (approx. 80%) have a prescribed normal tidal volume (VT_{NORM}) that is proportional to their weight, being about 10 – 15 ml/kg body weight [Anderson, 1988, p12]. Similarly approximately 80% of all patients will have a prescribed RR of 12 to 16 r.p.m. Since MV is the product of VT and RR, this corresponds to a prescribed normal MV range of 120 – 240 ml/min/kg body weight.

Situations will require ventilation outside of this range and therefore the safe upper and lower limits of MV were set to +/- 50 % of normal MV. This gives a minimum of 60 ml/min/kg and a maximum of 360 ml/min/kg. By expressing these limits in units per kilo of body weight the upper and lower limits will reflect differences in patient size such that a minimum MV for a heavy male patient will be appropriate for a smaller female patient. This limit was not incorporated as a rule-antecedent, since it was a simple matter to limit any advice generated by the MV rules so that these limits were not exceeded. The advisor reports the limiting of Mv advice, so that rule behaviour can be properly understood.

As explained previously the product of RR and Vt determines Mv, and therefore any changes to MV must be met by changes to one or both of these ventilator controls. Choosing in which way they are adjusted is a complex matter and required careful rule construction. This is discussed in the next section.

6.8 VT-RR Rule Development

Having established a new minute volume using the MV advisor rules, this has to be translated into changes in one or both of the ventilator settings RR and VT. It has already been seen that RR is the best parameter for adjusting MV since it ignores any losses in ventilation attributable to dead space volumes (be they physiological or apparatus based). However, adjustments to patient ventilation based solely on RR changes do not reflect the actions made in practice. At small MV it is also necessary to reduce VT in order to prevent periods of prolonged expiration and at higher MV the increased volume load is better met by increases in both RR and VT.

For any given MV there exist a large number of possible RR-VT combinations that will generate the same ventilation, as illustrated in Figure 6.26. However certain combinations are unsuitable. For example very small VT should be avoided, due to dead space effects, and very high VT may generate

excessive inflation pressures. Therefore for any given MV there will exist preferred RR and VT values. By establishing this ideal VT-RR relationship the best settings can be calculated for any observed MV.

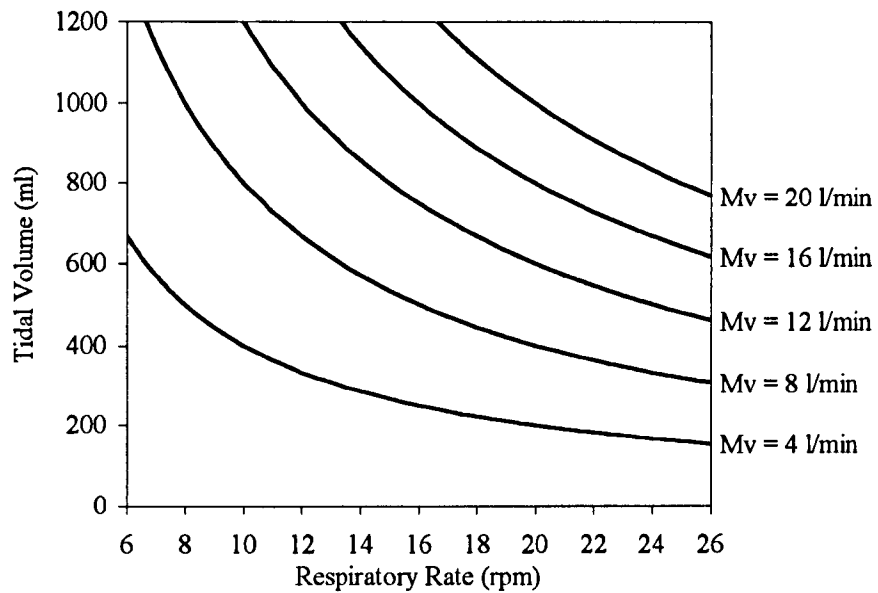


Figure 6.26: Iso-MV lines showing how for any given MV there exist a wide range of theoretical respiratory rate and tidal volume combinations.

6.8.1 Normalised VT

In normal clinical practise tidal volume is maintained at approximately 10 ml/kg body weight and therefore varies from patient to patient. Unfortunately this would affect any VT-RR relationship since what might be prescriptively normal for one patient will not be appropriate for another. Similarly classification of the observed VT will differ. For example, a VT of 600 ml for a 60 kg patient would be classed as *normal*, but for an 80 kg patient this would best be classed as *small*. This was resolved by representing observed VT as percentage error from normal prescriptive VT ($eV_{T_{NORM}}$);

$$eV_{T_{NORM}} = \frac{V_T - V_{T_{NORM}}}{V_{T_{NORM}}} \times 100 \quad (\%) \quad (6.16)$$

$$\text{where } V_{T_{NORM}} = 10 \times \text{Weight} \quad (\text{ml}) \quad (6.17)$$

A similar approach to normalisation of VT was implemented by Schaublin *et al* (1996), see Section 2.3.3.

6.8.2 Normalised Iso-MV Lines

The iso-MV lines of Figure 6.26 assume an explicit value for VT and RR. However, by using $eV_{T_{NORM}}$ to represent any VT, it is possible to generate normalised iso-MV lines (iso-MV_{NORM}) that hold true for all patients independent of weight. Normalised MV is given by;

$$MV_{NORM} = RR \times \left(\frac{eVT_{NORM}}{100} + 1 \right) \quad (6.18)$$

The eVT_{NORM} is normalised about 1 to avoid zero iso- MV_{NORM} points. By rearranging this equation it is possible to calculate eVT_{NORM} for any RR on a given iso- MV_{NORM} line;

$$eVT_{NORM} = \frac{100 \times MV_{NORM}}{RR} - 1 \quad (\%) \quad (6.19)$$

Using these normalised iso-MV lines and the normalised VT error it was possible to construct an ideal VT-RR relationship curve applicable to any patient.

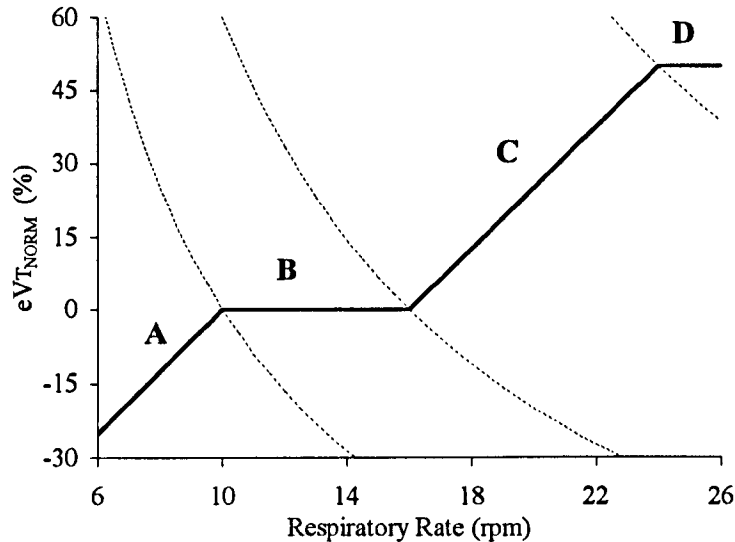


Figure 6.27: Anticipated normal RR-VT relationship as MV increases.

6.8.3 Ideal VT-RR Relationship

Based upon dialogue with a consultant anaesthetist, through preliminary observations made in ICU and some personal assumptions, the ideal VT-RR relationship was constructed (see Figure 6.27). It comprises four regions as detailed below

- 1). Approximately 80 % of all patients have a prescribed RR of 12 to 16 r.p.m. Under normal circumstances this would be accompanied by a normal tidal volume. Clinical observations confirmed that this relationship often extended to RR as low as 10 r.p.m. This defines region B of the ideal Vt-RR curve and implies that changes in MV falling between 100 – 160 ml/min/kg will be met by increases or decreases in RR only.
- 2). At MV above 160 ml/min/kg, increases are met by proportional increases in RR and VT up to a maximum VT of 1.5 times VT_{NORM} (or 15 ml/kg). It was assumed that the ratio between VT and RR should remain constant as MV increases. At the beginning of region B the ratio is;

$$r = \frac{V_T}{RR} = \frac{10 \cdot W}{16} = 0.625 \cdot W \quad (6.20)$$

where W is weight (kg). Therefore at the upper V_T limit RR can be calculated as;

$$RR = \frac{1.5 \cdot V_{T_{NORM}}}{r} = \frac{15 \cdot W}{0.625 \cdot W} = 24 \quad (\text{r.p.m.}) \quad (6.21)$$

- 3). Beyond this further MV increase is met by increases in RR only, to avoid excessive tidal volumes (see region C).
- 4). Below 100 ml/min/kg (the lower extent of region B), further reductions in MV again require a proportional reduction in RR and V_T (see region A)

The $eV_{T_{NORM}}$ obtained using the ideal V_T - RR relationship is a function of observed RR , and can be described mathematically as;

$$\begin{aligned} eV_{T_{NORM}} &= 6.25 \cdot RR - 62.5 & RR < 10 \\ &= 0 & 10 \leq RR \leq 16 \\ &= 6.25 \cdot RR - 100 & 16 < RR \leq 24 \\ &= 50 & RR > 24 \end{aligned} \quad (\%) \quad (6.22)$$

Let us call this functional relationship $f(RR)$. Now by substituting it into equation 6.18 the normalised MV for any observed RR can be calculated;

$$MV_{NORM} = RR \times \left(\frac{f(RR)}{100} + 1 \right) \quad (6.23)$$

However, the original problem was to derive the ideal V_T and RR settings given an observed MV . It was therefore necessary to calculate the inverse relationship between MV_{NORM} and RR . This was done by calculating the cubic spline polynomial of this inverse relationship;

$$pp = \text{spline}(MV_{NORM}, RR)^\dagger \quad (6.24)$$

It is then possible to calculate the ideal RR for any observed MV_{NORM} using the function;

$$RR = f(MV_{NORM}) = \text{ppval}(pp, MV_{NORM})^{\dagger\dagger} \quad (\text{r.p.m.}) \quad (6.25)$$

[†] $pp = \text{spline}(x,y)$ – MATLAB function that calculates a piece-wise cubic polynomial expression of the relationship between x and y , where x must be monotonically increasing and x and y are equal size vectors.

^{††} $y = \text{ppval}(pp,x)$ – MATLAB function that uses the polynomial expression pp derived using $\text{spline}()$ to derive an estimate of y based upon observation x .

		RR					
		MIN	LO	MED	HI	VHI	MAX
eVT _{NORM}	PVB	-38	-38	-26	-16	-7	-6
	PB	-35	-31	-22	-12	-3	3
	PM	-30	-23	-18	-7	3	12
	PS	-24	-13	-13	-1	9	19
	Z	-17	0	0	6	17	27
	NS	-8	11	18	18	27	38
	NM	5	25	42	43	43	52

Figure 6.28: Rule map describing percentage change required in VT to normalise RR-VT relationship. Consequent values were derived using the rule estimation algorithm given in section 0, and based upon observations of respiratory rate (RR) and percentage error, from normal tidal volume (eVT_{NORM}).

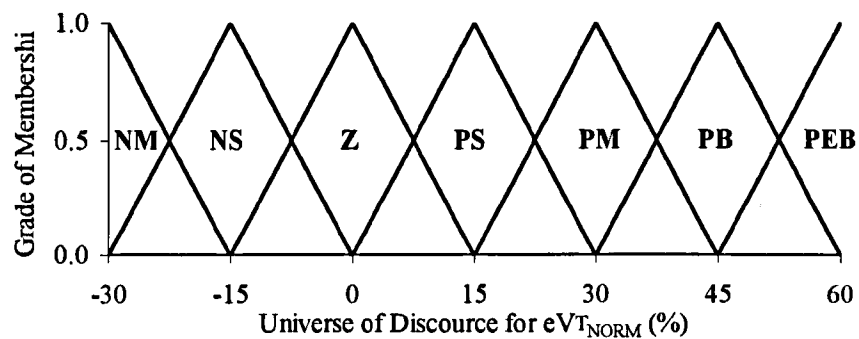


Figure 6.29: Fuzzy set definition for eVT_{NORM}.

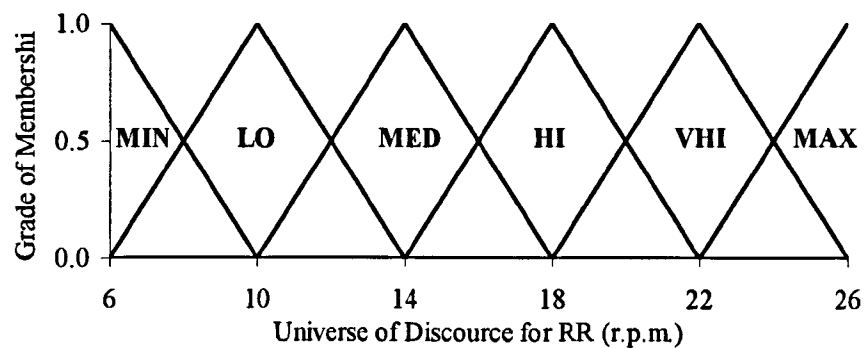


Figure 6.30: Fuzzy set definition for RR.

6.8.4 Rule Estimation

Using the above polynomial expression of $f(MV_{NORM})$ it was possible to calculate for any observed RR and VT the change required in VT to bring the VT-RR relationship in line with the VT-RR curve. The estimation algorithm is as follows;

- 1). Calculate VT_{NORM} from patient's weight using equation 6.17.
- 2). Calculate eVT_{NORM} from VT_{NORM} using equation 6.16.
- 3). Calculate MV_{NORM} from observed RR and eVT_{NORM} using equation 6.18.
- 4). Estimate ideal RR (RR_i) from MV_{NORM} using $f(MV_{NORM})$, see equation 6.25.
- 5). Calculate VT change required from RR_i , original MV (MV_0) and original VT (VT_0);

$$\Delta VT = \frac{MV_0}{RR_i} - VT_0 \quad (\text{ml}) \quad (6.26)$$

- 6). Expressing this as a percentage change from VT_0 , means that the consequent action holds true for all VT irrespective of patient weight;

$$\Delta VT = \left(\frac{\frac{MV_0}{RR_i} - VT_0}{VT_0} \right) \times 100 \quad (\%) \quad (6.27)$$

- 7). The result is then rounded to the nearest percent.

By applying this algorithm to every combination of peak values for the RR and eVT_{NORM} fuzzy sets, a rule map of changes required in VT to achieve optimal VT-RR settings was produced (see Figure 6.28). Initially, seven equal-spaced fuzzy classes were defined for eVT_{NORM} , ranging from -30% to +60% in 15% steps (see Figure 6.29). These were the expected limits of VT settings. Therefore a 60 kg-patient will have a VT range of 420 – 960 ml. Similarly the initial RR fuzzy classes ranged from 6 to 26 r.p.m. in 4 r.p.m. steps (see Figure 6.30), giving six sets.

From this preliminary rule map, attempts were made to reduce the number of sets without adversely affecting the advisor performance. It was found that;

- 1). The number of eVT_{NORM} sets could be reduced from 7 to 5 with little perceptible difference in advisor subsystem outcomes. This involved the removal of the fuzzy sets PS and PB.
- 2). The number of RR sets could not be reduced. In fact the addition of $RR = 8$ (VLO) was required to give better curve matching, see Figure 6.31.
- 3). The number of consequent sets could be reduced from 26 to 15 by rounding the advice to the nearest 5 % change where possible. This was performed judiciously in an attempt to prevent estimate overshoot. Consequently if the original advise was to increase VT, the consequent was rounded down. Conversely reductions were rounded up, to give smaller VT changes.

The revised rule-map is shown in Figure 6.32.

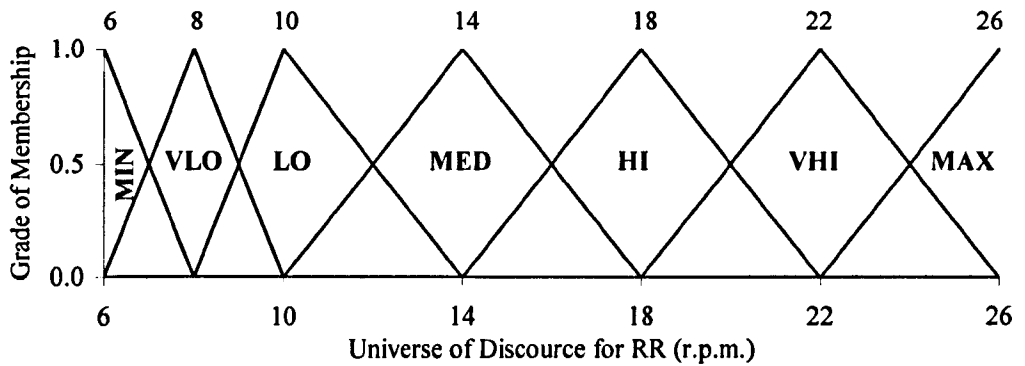


Figure 6.31: Modified fuzzy set definition for RR.

		RR						
		MIN	VLO	LO	MED	HI	VHI	MAX
eVT _{NORM}	PVB	-35	-35	-35	-25	-15	-5	-5
	PM	-30	-20	-20	-15	-5	2	10
	Z	-15	-5	0	0	5	15	25
	NS	-5	2	10	15	15	25	35
	NM	5	15	25	40	40	40	50

Figure 6.32: Modified VT rule map after set reduction and consequent rounding.

6.8.5 Handling Mv Changes

The rule-map described thus far has assumed fixed observations of initial RR-VT. However, a prescribed change in MV (as derived using the Mv advisor sub-system) will result in a different set of observation conditions. However, we only have knowledge of the original RR-VT observations. In order to provide the VT advisor with sufficient information, it was assumed that any changes in MV are implemented as changes in RR. This new RR estimate (RR_{new}) and the original VT observation (VT_0) are used to stimulate the VT-RR rules.

The advantages of this approach are;

- 1). The rules are applicable for initial patient observations as well as for when MV changes.
- 2). Unnecessary refinements to VT are avoided by first changing RR and then using the rules to ascertain if the new observations require VT to be modified.

		RR						
		MIN	VLO	LO	MED	HI	VHI	MAX
eVT _{NORM}	PVB	-35	-35	-35	-25	-15	-5	-5
	PM	-30	-20	-20	-15	-5	0	5
	Z	-15	-5	0	0	0	10	10
	NS	-5	0	5	10	10	10	10
	NM	5	10	10	10	10	10	10

(a). ePIP = NR_ALARM

		RR						
		MIN	VLO	LO	MED	HI	VHI	MAX
eVT _{NORM}	PVB	-35	-35	-35	-25	-15	-5	-5
	PM	-30	-20	-20	-15	-5	-5	0
	Z	-15	-10	-5	-5	-5	0	0
	NS	-5	-5	-5	0	0	0	0
	NM	0	0	0	0	0	0	0

(b). ePIP = ALARM

		RR						
		MIN	VLO	LO	MED	HI	VHI	MAX
eVT _{NORM}	PVB	-35	-35	-35	-25	-15	-5	-5
	PM	-30	-20	-20	-15	-5	-5	-5
	Z	-15	-10	-10	-10	-5	-5	0
	NS	-5	-5	-5	-5	-5	-5	0
	NM	0	0	0	0	0	0	0

(c). ePIP = HIGH

		RR						
		MIN	VLO	LO	MED	HI	VHI	MAX
eVT _{NORM}	PVB	-35	-35	-35	-25	-15	-10	-10
	PM	-30	-20	-20	-15	-10	-10	-10
	Z	-15	-15	-15	-15	-15	-15	0
	NS	-10	-10	-10	-10	-10	-10	0
	NM	0	0	0	0	0	0	0

(d). ePIP = V_HIGH

Figure 6.33: Extensions made to the VT rule-map of Figure 6.32. The shaded regions indicate areas of the rule-map that have been altered.

6.8.6 Volume Constraints

As identified during the MV rule construction, there are occasions when prescribed increases in delivered volume cannot be realised due to the risks associated with high airway pressures. When the observed PIP was high, increases to MV were moderated or restricted. A similar restriction has to be applied to any proposed increases in VT. Whilst the MV rules will prevent inappropriate increases in MV, there will exist situations when a lower VT with higher RR will produce a reduced airway pressure (assumes a fixed volume cycle ventilation regime).

It was therefore possible to modify the original rules of Figure 6.32 to account for observations of PIP. Observed PIP was expressed as error from a prescribed alarm threshold (ePIP), as per the Mv rules and the same fuzzy classes were used (see Figure 6.25), describing ePIP as OKAY, NR_ALARM, ALARM, HIGH and V_HIGH.

When observed PIP is well below the alarm threshold (ePIP is OKAY) the normal VT rule-map of Figure 6.32 applies. However, as observed PIP approaches and then exceeds the alarm threshold the rules pertaining to VT increases are moderated and eventually stopped. The extended rule-maps (see Figure 6.33) were derived using intuitive guess work, since rapid rule refinement would be made during the closed loop simulation of the advisor.

6.9 Summary & Conclusions

This chapter has described the development of the prototype advisor.

Inference Methodology

By comparing the pros and cons of different methods it was proposed to use *individual rule-based inference* with *Larsen's implication*. Rule significance will be imparted using the *product antecedent liaison operator* and the crisp control output will be derived using the *Centre of Sums* defuzzification method, a weight counting approach. Membership functions in the rule-antecedent are to be constructed using *triangular* and *trapezoid functions*. They must meet condition width criteria, have cross-point levels of 0.5 and a cross-point ratio of 1. Membership functions in the rule-consequent must be symmetrical, have equal area but do not necessarily require a cross-point ratio of 1. With non-uniformly spaced control actions (as observed within elements of FAVeM) plausibility is negated. However this approach will still produce smooth decision surfaces.

Rule Development Methodology

The importance of rule completeness was highlighted, and rule-holes were avoided by declaring the rule-base using a matrix rather than rule-statements. This rule-matrix was converted into rule-statements using a rule-reduction algorithm in order to minimise the number of rules required. This greatly reduced the amount of memory required to code the rule-matrix and also minimised the computational overheads of calculating the advice.

FIO₂ Rule Development

Suitable membership functions for the PaO₂ observations were elicited from an anaesthetist, and these were found to be similar to those reported by Kwok *et al* (2000). These classifications

were then used in a modified form of the iso-shunt diagram to derive an initial prototype version of the FIO_2 control rules. When assessed by an anaesthetist these preliminary rules were found to advise excessive FIO_2 changes, and were modified accordingly.

PEEP Rule Development

The clinical benefits and disadvantages of PEEP were identified and from these a preliminary set of rules drafted. Areas of improvement were proposed but these required the addition of new antecedents. It was considered best to establish some validity in the prototype rules before attempting any rule-base modifications.

MV Rule Development

MV was used to adjust PaCO_2 since there is an inverse proportional relationship between them. PaCO_2 was represented in the rule-antecedent as error from PaCO_2 set point (ePaCO_2) enabling goal-orientated control. This allowed different therapeutic needs to be met; for example in head injury patients when PaCO_2 must be kept low to help reduce brain swelling.

The causes of respiratory and metabolic pH imbalance were discussed and possible therapeutic actions identified. Suitable peak values for the pH membership function were derived using the Henderson-Hasselbalch equation and represented in the rule-antecedent as error from normal pH. An initial rule-map was generated using the ePaCO_2 and epH fuzzy classes, coupled with the inverse MV- PaCO_2 relationship and the therapeutic actions previously identified.

This preliminary rule-base was extended to include consideration of PIP, preventing increases in MV as the risk of barotrauma increases. Volume constraints were also applied to the maximum and minimum allowable MV that can be suggested.

VT-RR Rule Development

Having established a new level of MV, this was converted by the VT-RR rules into the best combination of RR and VT setting. However any given MV can be generated using a wide range of possible RR and VT combinations as explained by the concept of iso-MV lines. This idea was extended using the representation of VT as error from normal (eVT_{NORM}) to produce normal iso-MV lines, applicable to any patient irrespective of weight. Normal VT was derived as 10 ml/kg.

Using the normal iso-MV lines an ideal eVT_{NORM} -RR relationship was proposed. This was used to calculate the changes required in VT based upon observations of eVT_{NORM} and RR. Fuzzy classes for eVT_{NORM} and RR were chosen to give a good approximation of the ideal eVT_{NORM} -RR curve. Changes in MV were handled by expressing all of the change via RR only and then using this new RR together with the old VT to drive the VT-RR rules.

The VT-RR rule-base was extended to include consideration of PIP, with VT reduced and RR increased preferentially when PIP was high.

The prototype advisor now required validating and refining. This was best achieved using the patient model to facilitate simulated closed-loop control, and is the subject of the next chapter.

Chapter 7: Closed Loop Advisor Validation

7.1 Introduction

Having established a prototype set of rules for the advisor, their validity needed to be tested. It has already been demonstrated in the FiO_2 control rules that what might appear a good control strategy (in this case based upon the iso-shunt models), falls short of what is actually practised. Predominantly this is exhibited as greater caution on the part of the anaesthetist. It is likely therefore that rule refinement will be required as a consequence of advisor testing. Identifying the reasons for any rule modifications requires a clear understanding of the context within which the observations were made. After all, a given set of observations may lead to ventilator changes in one class of patient that would be inappropriate for another, based upon the same observations. Isolating these differences helps to identify insufficiency in the rule-base and may highlight new observations required to better separate the decision space.

This chapter describes the closed-loop validation of the prototype advisor using the patient model described earlier (see Chapter 4). The next section discusses the rationale behind the choice of validation methodology, together with an overview of the validation process itself. However, before model-based validation could be performed, improvements needed to be made to the patient model (see Section 7.3). Using this improved patient model, virtual scenarios were constructed via dialogue with an anaesthetist (see Section 7.4), and employed to test the closed-loop performance of the prototype advisor. Decision histories generated by the advisor were compared with those produced by an anaesthetist (see Section 7.5) and modifications made to the rules where necessary. The new rule-base was then re-evaluated using the same patient scenarios in simulated closed-loop.

7.2 Rationale & Overview

The simplest method to test rule validity would be to generate random observations, apply these to the advisor and then test the response generated against that of an anaesthetist. However, this method has two major disadvantages. Firstly, and perhaps most importantly, all therapeutic decisions are based not only upon the key observations, but also upon the context within which they occur. This includes factors such as patient pathology or trauma, their treatment history and recent response characteristics, all of which may contribute to an anaesthetist's prescribed course of action. This information would be absent using randomly generated observations and therefore the clinician's response would be ill informed. Secondly, the number of possible permutations required to exhaustively test the rule-base is large and not all combinations would be meaningful.

A preferable approach would be to use real clinical data that can be carefully recorded so as to preserve as much contextual information as possible. This provides not only observation context but also information regarding the actual course of action taken. Records thus obtained can be used not only to compare actual and advised responses, but also provide a means for third party appraisal. An independent anaesthetist can be recruited to give the decisions they would have

made, based upon the observations recorded. This would not be intended to assess the credibility of the observed anaesthetist (highly unethical without prior consent), but rather to highlight that differing approaches are equally valid. One anaesthetist's decision may better match the computed advice. This would say more about the variability of anaesthetist practice within ICU, than of weaknesses in the advisor.

Whilst clinical validation is an important stage in the assessment of the advisor, it does have distinct disadvantages. Most significantly are the difficulties associated with data collection. These problems have been highlighted previously during the clinical validation of SOPAVent and focused principally on the time involved to accurately record all relevant information. The type of patient available for study is very much luck of the draw, although there will be different potential groups depending on the ICU site. Of the two ICUs used in this research, one focused predominantly on post-operative cardio-thoracic care and the other dealt with all possible scenarios including post-operative care, accident and emergency and acute pathology. Approximately 90% of the data were collected from the latter.

Even if the data collection issues could be overcome and a large sample set was available, it still would not provide a flexible framework for advisor testing and validation. This arises because differences between actual and advised decisions cannot be explored beyond the fact that they differ. Ideally we would want to apply the computer-advised changes as well as the actual changes to the patient, in order to compare patient outcomes. Ethically this would not be possible and it would still not enable comparison of patient outcomes beyond a single decision, since we cannot repeat the patient's history. More importantly, small differences between actual and computed advice (which might be considered as a good decision match) may mask any divergent instability or limit cycle behaviour within the rules. This has very real safety implications and can only be investigated using a simulated closed loop methodology.

By using a computer-based patient model, scenarios can be constructed that are both repeatable and unaffected by measurement errors. An anaesthetist can then attempt to ventilate these virtual patients to produce benchmark decision profiles that can then be compared against computer-generated advice. If the advisor and patient model are connected together to simulate closed-loop control then patient outcomes can be compared in a manner not possible using real patients.

The patient model also provides the flexibility to incorporate measurement errors and process disturbances that would aid the understanding of the clinician's response to poor observations as well as the robustness of the advisor. Also, because every element of the patient's behaviour is repeatable, any rule modifications can be tested to see if the expected improvements have occurred.

However, in order to provide simulated closed loop behaviour the patient model must generate all of the observations required by the advisor, and they must respond to ventilator changes in a manner appropriate to the pathology or trauma being considered. Throughout the rule prototyping certain inadequacies and omissions in the patient model became apparent. These can be summarised as follows;

pH Modelling: The prototype minute volume (MV) control rules required observation of pH. In the early SOPAVent model, pH was assumed fixed which clearly does not model changes in pH caused by respiratory acidosis and alkalosis, as well as changes due to metabolic dysfunction.

PIP Modelling: PIP was required by both the MV and RR-VT control rules as a measure of the possible risk of barotrauma. As the ventilation is adjusted the airway pressures changes according to the mechanics of the lung. No mechanical modelling had been included in the original patient model.

PEEP Effects: PEEP is applied to open up previously closed airways, but can also have disadvantageous effects on cardiac output and arterial blood pressure. These require the inclusion of modifiers to shunt and cardiac output respectively.

BPSYS Index: Low systolic blood pressure contraindicates the use of PEEP and therefore any relationships governing its behaviour needed to be considered.

Miscellaneous Improvements: Empirical relationships governing O₂ consumption, CO₂ production and cardiac output may improve model behaviour. These include the effects of body temperature, metabolic activity, weight and hypoxia.

These improvements together with the introduction of a graphical user interface (GUI) to improve the usability of the model and event profiling to facilitate time variations in certain model parameters are discussed in detail in the next section.

The updated SOPAVent model was then used to construct patients with a variety of trauma and pathology (e.g. head injury, lobar pneumonia, etc). This was done with direct input from an anaesthetist in order to generate as much clinical realism in the scenarios as possible. They were then asked to ventilate these virtual patients to produce '*ideal*' decision histories. At each decision point they were asked to state when they would next take a blood-gas sample. The patient would then be simulated to this point and the process repeated until weaning from the ventilator was proposed or the patient was stable and no further action was possible, e.g. waiting for a patient to regain consciousness. For each patient simulated, the anaesthetist was also asked to identify their therapeutic objectives and define set-point goals.

The prototype advisor was then connected to these patient scenarios and allowed to run in simulated closed-loop control, see Figure 7.1. New advice was generated at the blood-gas sample times established by the anaesthetist when they ventilated the virtual patients. At each advice cycle a report was generated, stating the antecedent set membership and rules fired, with their respective weightings to help identify the causes of any decision mismatch.

The performance of the prototype advisor in simulated closed-loop control was analysed and refinements made to the rules accordingly. In some instances this only required changes to be made to the rule-consequent, in others new fuzzy classes were required and occasionally a new observation variable was identified. The modification process was performed in an iterative manner with each change or group of changes being evaluated by re-running the closed-loop simulation and comparing the patient outcomes. In most cases the rules were modified so that

they matched the anaesthetists, but sometimes advised decisions were deemed preferable to those of the clinician and no further rule-modification was made.

Modifications made in response to a scenario sometimes caused errors in other scenarios that were previously giving good decision matching. In such circumstances either a compromise was made in the consequent action or a new fuzzy class or variable was introduced to better separate the decision space. The modified rule-base was then re-evaluated using closed-loop simulation and the performance of the advice analysed.

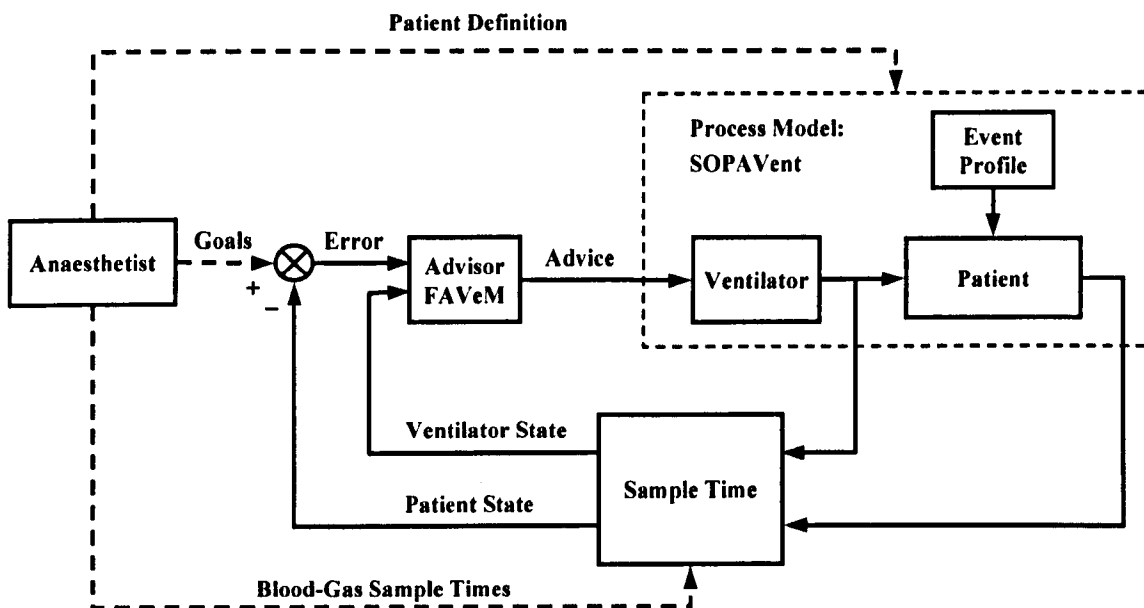


Figure 7.1: Closed loop simulation of advisor performance using a process model of a ventilated patient (SOPAvent). The dashed connections from the anaesthetist indicate input prior to the closed-loop simulation (i.e. definition of the patient scenario, blood-gas sample times and set-point goals).

7.3 Model Improvements

7.3.1 pH Modelling

Perhaps the single most significant omission from SOPAvent was the ability to model changes in pH. This shortfall affected not only its ability to match real patient behaviour, but also its usefulness for advisor rule testing. The prototype Mv advisor rules (see Section 6.7) use the observed error from normal pH as one of the controller's antecedents. Without pH modelling there is no feedback from the process model in response to advised ventilator changes. Consequently, the controller will continue to generate advice based upon the initial pH observation. It is not difficult to see how this will lead to erroneous and possibly dangerous ventilator changes (albeit simulated).

Modelling of pH behaviour was achieved using the modified Henderson-Hasselbalch equation;

$$pH = \frac{6.3968 + 0.01506 \cdot (38 - T) + \log \frac{[\text{HCO}_3^-]}{\alpha \cdot P_{\text{CO}_2}}}{1.042 + 0.0014 \cdot (38 - T)} \quad (7.1)$$

where P_{CO_2} is partial pressure of CO_2 (kPa), α is the solubility of CO_2 in plasma (mmol/l/kPa), T is blood temperature ($^{\circ}\text{C}$) and $[\text{HCO}_3^-]$ is bicarbonate concentration (mmol/l). This equation is identical to that used in the MV rule prototyping, see Section 6.7.3 for details.

The pH calculation was performed within the gas dissociation function (GDF) prior to the calculation of O_2 and CO_2 contents, since both algorithms have a pH dependent component. In the O_2 GDF this is in the equation for virtual PO_2 (see Section 4.2.3) and in the CO_2 GDF this is in the Henderson-Hasselbalch equation, the pK formula and the equations deriving the reduced and oxygenated cell to plasma $[\text{CO}_2]$ ratio (see Section 4.2.6).

A similar approach has been taken by Dickinson (1977) in his McPuf patient model, although in this case he used a much simpler form of the Henderson-Hasselbalch equation with no adjustments made to pK and α based upon pH and temperature.

SOPAVent requires the inverse of the GDF (i.e. calculation of gas tensions from contents) which was implemented using a simple secant-searching algorithm (see Section 4.7). Unfortunately the inclusion of the pH modification meant that it was possible for the inverse GDF to get stuck within an iterative loop. This occurred when changes in PCO_2 estimate generated changes in pH that itself produced changes in the PO_2 and PCO_2 estimates that would not converge.

This was overcome by adopting the 2-dimensional secant-searching algorithm as employed in the tuning of shunt and dead space. In this case the PCO_2 was estimated first (being the more sensitive variable to pH) and then PO_2 . This was repeated until the estimation error fell below a predetermined level in both PO_2 and PCO_2 .

Clinical Validation

The predictive performance of equation 7.1 was tested by using 151 observations of PaCO_2 , pH, bicarbonate and temperature taken as part of a second data collection phase (see Chapter 8). Allowing for measurement and recording errors, the equation performed well with a correlation coefficient of $r = 0.967$ (standard error of estimate 0.0281), see Figure 7.2.

Pulmonary Bicarbonate Approximation

The inverse GDFs are used not only to calculate arterial and venous PO_2 and PCO_2 , but also to derive the pulmonary gas tensions that drive diffusion across the lung membrane. However, the calculation of pH requires knowledge of $[\text{HCO}_3^-]$ which is easily measured in the arterial and venous circulation but is not available in the pulmonary compartment. It was therefore necessary to assume pulmonary $[\text{HCO}_3^-]$ to be equal to arterial $[\text{HCO}_3^-]$.

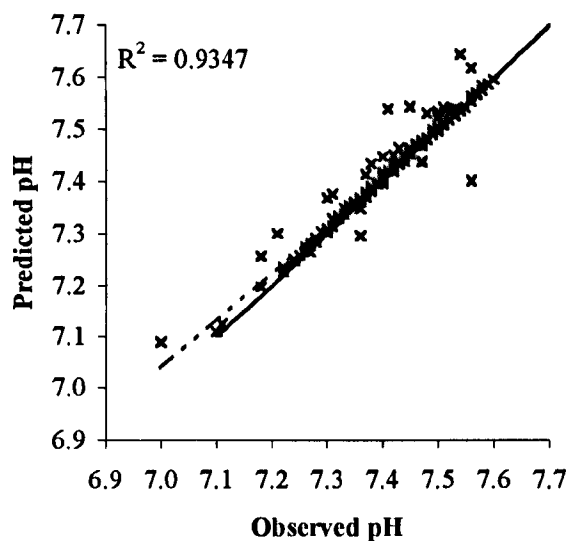


Figure 7.2: Correlation between observed pH and predicted pH, using data collected during the clinical validation of the advisor (see Appendix H).

7.3.2 Airway Modelling

Prescriptive changes in mechanical ventilation (e.g. VT, RR, driving waveform, etc) impact on the pressure at the mouth and the pressure in the alveoli. The relationship between these ventilator settings and observed pressures is determined by the respiratory mechanics of the patient and ventilator. The two main properties that characterise breathing mechanics are total compliance (C) being a measure of lung and chest-wall elasticity, and total flow resistance (R), which reflects properties of both the tissue and the peripheral airways. Compliance is measured in litres/cmH₂O or litres/kPa and flow resistance in cmH₂O/litre/sec or kPa/litre/sec.

This can be represented using a simple two-element resistance-compliance linear model. However, in such a model it has to be remembered that the lumped parameters R and C include any resistance and compliance between the ventilator and the patient as well as between the mouth and the alveoli. A first order approximation of this nature is sufficient for pseudo-realistic simulation of various mechanical abnormalities (e.g. stiff lungs associated with ARDS and high flow resistance associated with chronic obstructive airway disease). However there is good evidence that a three-element model with additional parallel compliance will give better matching to observed pressure and flow data in routine post-operative ICU [Barbini *et al*, 1994]. Making physical sense of a three-element model in physiological or mechanical terms is difficult even if it does give better frequency and time domain response characteristics, whereas the two-element model is readily understood by clinicians.

PIP Modelling

The prototype MV and VT-RR rules require that consideration be made of PIP. In theory this should be measured at the mouth, but in practice the manometer is almost invariably situated on the ventilator. However, resistance between the ventilator and the patient's mouth, and hence the pressure difference between the two is usually negligible. Therefore for all practical

purposes, the pressure at the ventilator can usually be taken to be the same as the mouth. In order to determine the simulated PIP we have to derive the equations describing the pressure at the mouth (P_m) during the inspiratory phase of the respiratory cycle.

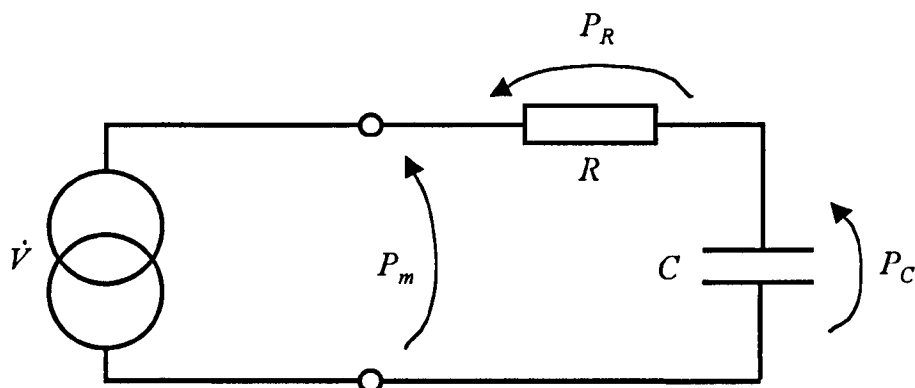


Figure 7.3: Electrical analogue of the respiratory mechanics during the inspiratory phase of the respiratory cycle.

The ventilator is assumed to be in volume control mode and delivers a certain pre-set volume during a pre-set time with a constant flow. This is analogous to a constant current generator in electrical terms. Similarly the flow resistance is analogous to electrical resistance and lung compliance to capacitance, see Figure 7.3.

The pressure at the mouth will be the sum of pressure drop across the flow resistance and the lung compliance;

$$P_m(t) = P_R(t) + P_C(t) = \dot{V}R + \frac{1}{C} \int \dot{V} \cdot dt \quad (\text{cmH}_2\text{O}) \quad (7.2)$$

where the flow \dot{V} is given by;

$$\dot{V} = \frac{V_T}{t_I} \quad (\text{l/sec}) \quad (7.3)$$

Substituting equation 7.3 in equation 7.2 and integrating we arrive at;

$$P_m(t) = \frac{V_T}{t_I} \cdot R + \frac{V_T}{C \cdot t_I} \cdot t + P_{EEP} \quad (\text{cmH}_2\text{O}) \quad (7.4)$$

The additional term PEEP represents the initial conditions of the system due to applied positive end-expiratory pressure.

The peak inspiratory pressure is simply this equation calculated at the end of inspiration ($t = t_I$);

$$PIP = \frac{V_T}{t_I} \cdot R + \frac{V_T}{C} + P_{EEP} \quad (\text{cmH}_2\text{O}) \quad (7.5)$$

Using this equation it is then possible to model the effect of changes in ventilator setting and patient lung mechanics on the observed PIP.

Mean Alveolar Pressure

Originally, mean alveolar pressure was approximated using equation 4.39 (see section 4.2.7). However, this equation is incorrect in three respects. Firstly, it does not actually represent the alveolar pressure but the pressure at the mouth; secondly the ventilator is a constant flow source, which does not result in a square pressure waveform; and finally it takes no account whatsoever of the respiratory mechanics.

The mean alveolar pressure is calculated by integrating the alveolar pressure across the whole ventilation cycle. However, this requires definitions of the equations describing the alveolar pressure wave. This ventilation cycle can be divided into three distinct regions; the inspiratory phase, the pause phase and the expiratory phase.

1). Inspiratory Phase

During the inspiratory phase the respiratory mechanics behave as in Figure 7.3 with a constant flow source connected to a lumped compliance and flow resistance network. The alveolar pressure (P_A) is equal to the pressure drop across the lung compliance;

$$P_A(t) = P_C(t) = \frac{1}{C} \int \dot{V} \cdot dt = \frac{V_T}{C \cdot t_I} \cdot t + PEEP \quad (\text{cmH}_2\text{O}) \quad (7.6)$$

The mouth pressure during inspiration is as described previously in equation 7.4.

2). Pause phase

During the pause phase (which is optional) the constant flow generator stops, but a non-return valve prevents gas from leaving the system. This is provided to allow the alveolar pressure to equilibrate with the mouth pressure and gives better gas mixing in the alveolar space. The model now behaves as though the mouth is effectively a fixed volume at pressure $P_m(t_i)$ discharging via the R-C network into the alveolar space which is already at pressure $P_A(t_i)$.

The relationship between P_m and P_A is described by a pair of simultaneous differential equations, since the pressure difference driving the equilibration decays as the pressures equalise.;

$$\begin{aligned} \dot{P}_m(t) + \frac{P_m(t)}{R \cdot C} - \frac{P_A(t)}{R \cdot C} &= 0 \\ \dot{P}_A(t) + \frac{P_A(t)}{R \cdot C} - \frac{P_m(t)}{R \cdot C} &= 0 \end{aligned} \quad (7.7)$$

Using Laplace transforms these equations resolve to;

$$\begin{aligned} P_m(t) &= \frac{1}{2} \left[P_{A0} \left(1 - e^{-\frac{2(t-t_I)}{RC}} \right) + P_{m0} \left(1 + e^{-\frac{2(t-t_I)}{RC}} \right) \right] \\ P_A(t) &= \frac{1}{2} \left[P_{A0} \left(1 + e^{-\frac{2(t-t_I)}{RC}} \right) + P_{m0} \left(1 - e^{-\frac{2(t-t_I)}{RC}} \right) \right] \end{aligned} \quad (\text{cmH}_2\text{O}) \quad (7.8)$$

where t_p is the length of the pause phase in seconds and P_{A0} and P_{m0} are the alveolar and mouth pressures at the end of inspiration as given by;

$$P_{A0} = \frac{V_T}{C} + P_{EEP} \quad (\text{cmH}_2\text{O}) \quad (7.9)$$

$$P_{m0} = \frac{V_T}{t_I} \cdot R + \frac{V_T}{C} + P_{EEP} \quad (\text{cmH}_2\text{O}) \quad (7.10)$$

3). Expiratory phase

Assuming that the internal resistance of the ventilator (r) during expiration is low (typically 2 cmH₂O) the alveolar pressure during the expiratory phase is given by;

$$P_A(t) = (P_{A1} - P_{EEP}) \cdot e^{\frac{-(t-(t_I+t_p))}{(R+r)C}} + P_{EEP} \quad (\text{cmH}_2\text{O}) \quad (7.11)$$

where P_{A1} is the alveolar pressure at the end of the pause phase as given by;

$$P_{A1} = \frac{1}{2} \left[P_{A0} \left(1 + e^{\frac{-2t_p}{RC}} \right) + P_{m0} \left(1 - e^{\frac{-2t_p}{RC}} \right) \right] \quad (\text{cmH}_2\text{O}) \quad (7.12)$$

The pressure at the mouth is only restricted by the internal resistance of the ventilator and therefore falls much more rapidly;

$$P_m(t) = (P_{m1} - P_{EEP}) \cdot e^{\frac{-(t-(t_I+t_p))}{rC}} + P_{EEP} \quad (\text{cmH}_2\text{O}) \quad (7.13)$$

where P_{m1} is the pressure at the mouth at the end of the pause phase. A typical pressure waveform generated by these equations is shown in Figure 7.4.

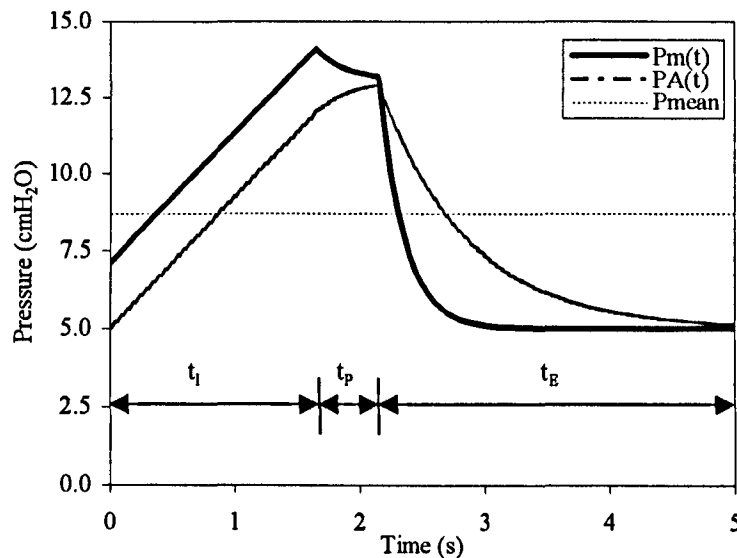


Figure 7.4: Typical pressure waveforms generated at the mouth and in the alveolar space using the airway mechanics model. The ventilator settings used were $V_T = 0.7$ litres, $RR = 12$ r.p.m., $PEEP = 5$ cmH₂O (0.49 kPa), $t_I = 33\%$, $t_p = 10\%$, and the ventilator-airway mechanics were defined by $R = 5$ cmH₂O/l/sec (0.49 kPa/l/sec), $C = 0.1$ l/cmH₂O (1.02 l/kPa), $r = 2$ cmH₂O/l/sec (0.2 kPa/l/sec).

Calculation of the mean alveolar pressure $\bar{P}_A(t)$ (or P_{MEAN}) requires integrating the equations for $P_A(t)$ in the three respiratory phases and averaging over a single respiratory cycle;

$$P_{MEAN} = \frac{1}{t_T} \int_0^{t_T} P_A(t) dt + P_B \quad (7.14)$$

$$= \frac{1}{t_T} \left\{ \int_0^{t_I} P_A(\text{insp}) dt + \int_{t_I}^{t_I+t_P} P_A(\text{pause}) dt + \int_{t_I+t_P}^{t_T} P_A(\text{exp}) dt \right\} + P_B$$

It should be noted that the units of P_{MEAN} are in kPa and therefore the average $P_A(t)$ value must first be converted from cmH₂O to kPa to be meaningful in this expression. The difference between the original and new estimates of mean alveolar pressure depends upon what the ventilator and airway mechanical parameters are set to. When the airway resistance is high (e.g. 120 cmH₂O/l/sec as seen in patients with acute asthma) the difference in estimates can be as much as 50 %.

7.3.3 Modelling Benefits and Disadvantages of PEEP

Since FAVeM will be advising changes to PEEP, some attempt needs to be made to model the advantages and disadvantages that it can impart upon the patient. The two most significant effects of PEEP are known to be: (1) the improvement in arterial oxygenation probably attributable to the opening up of collapsed alveoli – this can be modelled by a reduction in the effective shunt; and (2) a reduction in cardiac output known as cardiac tamponade. The latter is brought about by a reduction in venous return because of an increase in mean right atrial pressure.

Reduction in Shunt

The physiological shunt fraction is reduced from its nominal value (X_{phys}) as PEEP is applied. The amount of PEEP required to reduce X_{phys} to zero is determined by a notional threshold term (TH_{PEEP}), see equation 7.15. So for example with TH_{PEEP} set to 40 cmH₂O (3.92 kPa) the application of 15 cmH₂O (1.47 kPa) of PEEP has the effect of reducing the physiological shunt to 25/40 of its nominal value. Any fixed or anatomical shunt (X_{fixed}) remains unaffected by PEEP.

$$X_{eff} = X_{nom} \cdot \left(\frac{TH_{PEEP} - PEEP}{TH_{PEEP}} \right) + X_{fixed} \quad (7.15)$$

Cardiac Tamponade

The reduction of cardiac output due to PEEP depends upon the compliance of the lungs. If the compliance is low (i.e. stiff lungs) then there is little effect. If they are compliant then cardiac pumping is brought virtually to zero at maximum PEEP. Dickinson used the following equation to modify the resting cardiac output estimate (this forms part of a more involved formula to estimate changes in cardiac output, see equation 7.23);

$$PEEP\ CO\ Modifier = \frac{30 - (PEEP \times 5 \times C)}{30} \quad (7.16)$$

where C is the lumped compliance of the airway and lungs (l/cmH₂O). In the conscious subject compliance is approximately 0.2 litre/cmH₂O, which with 15 cmH₂O of PEEP would reduce the resting cardiac output by almost half.

This effect will underestimate the disadvantage of PEEP on cardiac output if filling of the right atrium is already inadequate and overestimate it if cardiac filling is adequate. Dickinson made no attempt to model this influence merely stating;

“The user of the artificial ventilation option has a choice: either he accepts the empirical formulation of the effects of PEEP as a reasonably realistic package correct for average conditions; or he fixes PEEP at zero, and uses the manually-changeable controls to make his own more appropriate changes in dead space, venous admixture, and cardiac output.”

As mentioned in Section 6.6.2, systolic blood pressure (BPSYS) is used as an indicator of cardiovascular suppression (i.e. inadequate right atrium filling), and when it is low contra-indicates the use of PEEP. Since the model wants to be used for simulated closed-loop control, the application of PEEP should produce an increased cardiac tamponade effect when BPSYS is low. Conversely, adequate filling (as indicated by a good level of BPSYS) should reduce the tamponade effect.

The problem is further complicated by the fact that arterial blood pressure also declines with increasing PEEP in a manner which closely follows the change in cardiac output [Jardin *et al*, 1981]. This further compromises filling, increasing the sensitivity of the tamponade effect to further increases in PEEP. The relationship between PEEP and BPSYS and their effect on cardiac output is the parameter feedback required by FAVeM to stimulate and test the PEEP advisor rules. Unfortunately, equations tying together PEEP, cardiac tamponade and arterial blood pressure could not be found.

The solution therefore was to include a sensitivity term (S_{tamp}) within the PEEP modifier expression;

$$PEEP\ CO\ Modifier = \frac{30 - (PEEP \times 5 \times C \times S_{tamp})}{30} \quad (7.17)$$

The user then has the option of modifying the tamponade effect as required. Similarly any further reduction in arterial pressure as a consequence of increased PEEP will have to be adjusted manually. This wasn't a satisfactory solution but will have to be accepted until a better tamponade model can be found. By setting S_{tamp} to 0, the tamponade model is turned off.

Miscellaneous Effects of PEEP

Whilst the above effects constitute the primary influences of PEEP, other effects should perhaps be mentioned, although they are not modelled here. These include amongst others;

- 1). *Lung Volume*. PEEP increases functional residual capacity (FRC), which in turn reduces the airway resistance (R) according to the inverse relationship between lung volume and airway resistance as reported by Mead and Agostoni (1964) and Zamel *et al* (1974). This will reduce the calculated PIP although little net increase will be observed since PEEP itself raises the inspiratory pressure.
- 2). *Dead Space*. There is indirect evidence that prolonged application of PEEP may cause a very large increase in the dead space, probably because of bronchiolar dilation [Slavin, 1982].

7.3.4 Cardiac Output & Metabolic Function

Oxygen Consumption

In the earlier SOPAVent model cardiac output, O₂ consumption and CO₂ production were defined explicitly by the user. Dickinson used a different approach whereby nominal values were derived using simple empirical formulae, which could then be adjusted using modifiers that related to other physiological aspects of the patient. So for example the nominal O₂ consumption at rest is dependent upon patient weight in kg (WT), and is given by [Dickinson, 1977, p122];

$$\dot{V}_{O_2 REST} = 10.33 \times WT^{0.75} \quad (\text{ml/min, STPD}) \quad (7.18)$$

This is the same formula as used to create a standard-normal patient for ballpark testing of the model (see Section 4.4.2). However, patient measurements may indicate a wholly different level of O₂ consumption. Dickinson dealt with this by adding two modifiers to account for increases in patient temperature (leading to increased metabolic activity), and a manual control for adjusting metabolic rate (MR). The modified O₂ consumption is then represented by the following expression [Dickinson, 1977, p110];

$$\dot{V}_{O_2} = \dot{V}_{O_2 REST} \times \left(\frac{T - 26}{37 - 26} \right)^{1.05} \times \frac{MR}{100} \quad (\text{ml/min, STPD}) \quad (7.19)$$

where T is temperature (°C) and MR is the percentage from normal metabolic activity. Using the above two equations the user can specify the patient weight and temperature to derive an estimate of O₂ consumption. If this value does not match the desired rate of O₂ consumption, or if the model is being tuned to some observed clinical data, then MR can be reduced or increased as required. If the user specifies a target \dot{V}_{O_2} then MR is calculated automatically.

Carbon Dioxide Production

The modified O₂ consumption can then be used to calculate the CO₂ production using the tissue respiratory quotient (normally 0.8);

$$\dot{V}_{CO_2} = \dot{V}_{O_2} \times RQ \quad (\text{ml/min, STPD}) \quad (7.20)$$

Again if a certain CO₂ production is required then RQ can be adjusted accordingly.

Cardiac Output

As with the estimation of O₂ consumption, Dickinson gives an expression for the resting cardiac output. However this is itself dependent upon the resting O₂ consumption;

$$\dot{Q}_t REST = 0.0195 \times \dot{V}_{O_2 REST} \quad (\text{l/min}) \quad (7.21)$$

If the patient is female then this estimate is reduced by a factor of 0.9.

The effective cardiac output is influenced by various factors and Dickinson included the effects of exercise, temperature, cardiac tamponade and hypoxia in his McPuf model [Dickinson, 1997, p100-103]. Cardiac tamponade has been dealt with previously (see above).

His equation for effective cardiac output was given as;

$$\dot{Q}_t = \left(\frac{A}{Y} + \frac{B}{Y^2} \right) \times \frac{CP}{100} \quad (\text{litres/min}) \quad (7.22)$$

This comprises two primary components; one pertaining to resting cardiac output - modified according to temperature and tamponade (A/Y), and the other to the effects of exercise as represented by the difference between the O_2 consumption at rest and during exercise (B/Y^2). These are additive and can be tuned to give the desired cardiac output using the percentage modifier CP . This can be taken to represent 'percentage normal cardiac function' and setting it to 200 % will give twice the normal average value for those conditions.

Tamponade and Temperature Effects

The modified cardiac output component is given by equation 7.23;

$$A = \left(\frac{30 - PEEP \times 5 \times C}{30} \right) \times \left(\frac{T - 12.2}{37 - 12.2} \right) \times 1.1904 \cdot \dot{Q}_{t,REST} \quad (7.23)$$

where the first bracketed element is the tamponade model as presented in equation 7.16; the second element is the effect of body temperature on resting cardiac output; and the additional coefficient 1.1904 was not clearly identified in Dickinson's work.

Exercise Effect

The exercise component of equation 7.22 is given by;

$$B = \frac{\dot{V}O_2 - \dot{V}O_{2,REST}}{100} \quad (7.24)$$

Whilst it may seem unnecessary to include a factor that accounts for exercise, the increase in metabolic function and body temperature associated with infection exhibit an increase in O_2 consumption and cardiac output. This can be thought of as increased work and therefore in nature very similar to exercise. Relating changes in cardiac output to increased O_2 consumption in this way enables the changes to apply not only to normal subjects but also to those of different age, sex and size.

Hypoxia Effect

Both the cardiac component (A) and the O_2 consumption component (B) are modified by the divisor Y ;

$$Y = \max\{0.35, CaO_2 \times 0.0056\} \quad (7.25)$$

This models the increase in cardiac output when arterial oxygen content falls, up to a realistic limit. The effect on the exercise component is smaller as indicated by squaring of the divisor. Figure 7.5 shows the effective cardiac output with changing arterial O_2 content at various body temperatures.

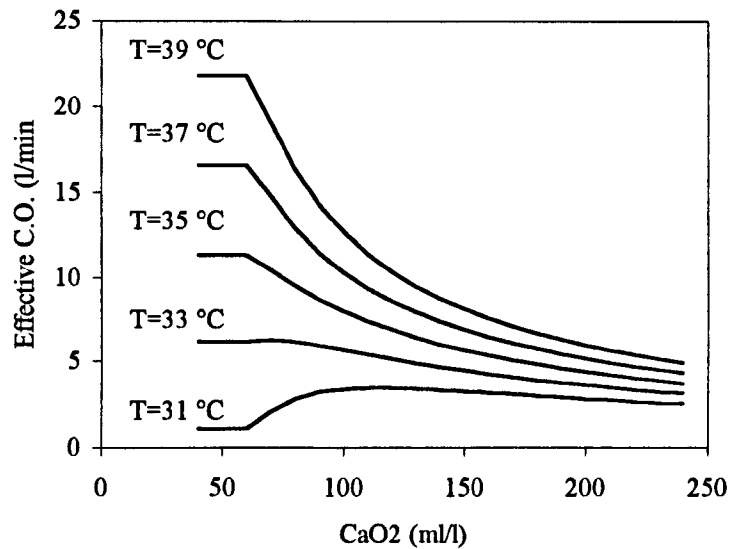


Figure 7.5: Effective cardiac output for varying arterial O₂ content and body temperature based on a resting cardiac output of 5 l/min.

It was decided to omit modelling of the hypoxia effect since its implementation would be problematic. Arterial O₂ content is constantly changing in response to ventilator adjustments and therefore cardiac output would constantly need recalculating. The model structure would not easily accommodate dynamic cardiac output without large scale redesign, although such an improvement may well need to be considered in the future. This feature was switched off by setting Y equal to 1.

7.3.5 Event Profiling

When constructing patient scenarios there are physiological parameters, which will vary over time. For example a patient suffering from pneumonia will initially begin with a high level of physiological shunt. Over a period of 24 hours this would reduce as the infection subsides. In addition there will be episodes of sudden shunt improvement, as plugs of consolidated sputum are removed during physiotherapy.

These changes are modelled in SOPAVent using a table of parameter events. The initial condition of the patient represents the first event, with each subsequent event being described by the following five term structure;

[Value, Unit, Condition, Time, Function]

where;

Value is the new setting that the parameter will have at the event time.

Unit is the observation unit for the parameter value (e.g. kPa, cmH₂O, %, etc) and enables event values to be declared in units other than those required by the patient model. A conversion program ensures that these event values are in the correct units before commencing simulation.

Condition is the observation conditions for the parameter value (e.g. STPD, BTPS, etc). Again this is because the model requires all parameters to be in BTPS, but events may be declared otherwise.

Time is the point in the simulation in minutes at which the event value takes effect.

Function is the manner in which the new event value is arrived at from the previous one. This can be either *step* or *ramp*. *Step* provides discrete level changes and *ramp* gives a linear increase or decrease in the parameter value.

So considering the pneumonia example given above, the changes in physiological shunt could be described by the event profile of Table 7.1, producing the parameter history of Figure 7.6. This is converted into a lookup matrix with time values in the first column and parameter values in the second column. In our example this would look like;

$$P.PhysShunt = \begin{bmatrix} 0 & 40 \\ 120 & 30 \\ 120 & 25 \\ 360 & 21 \end{bmatrix} \quad (7.26)$$

This matrix is then placed in a SIMULINK block called 'From Workspace' which interpolates between rows to derive the physiological shunt value at any given simulation time. Whilst only *ramp* and *step* functions have been implemented here, it would obviously be possible to extend this to include any number of alternative functions, e.g. exponential, random, etc.

Value	Unit	Condition	Time	Function
40	%	n/a	0	initial value
30	%	n/a	120	ramp
25	%	n/a	120	step
21	%	n/a	360	ramp
Continued as necessary...				

Table 7.1: Example of an event profile to describe changes in physiological shunt for a patient with pneumonia undergoing physiotherapy.

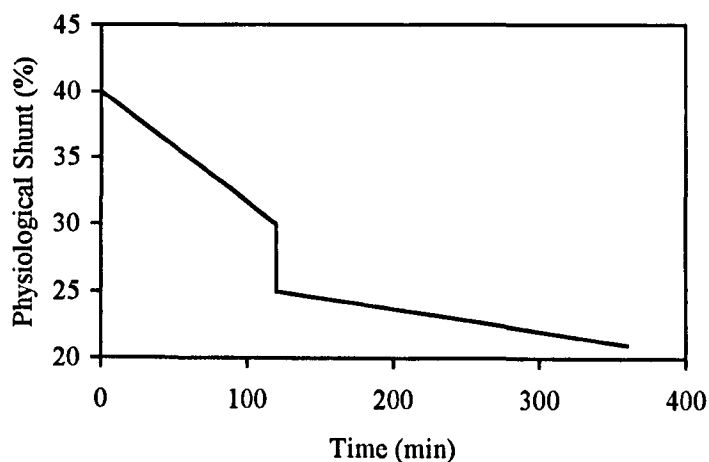


Figure 7.6: Time history of physiological shunt produced using the event profile of Table 7.1.

7.3.6 Graphical User Interface

In order to aid the usability of the patient model a graphical user interface (GUI) was designed using the GUI construction modules provided by MATLAB. This front-end to the model enabled rapid definition and modification of patient scenarios, as well as access to graphical reports and text summaries of simulations performed, see Figure 7.7.

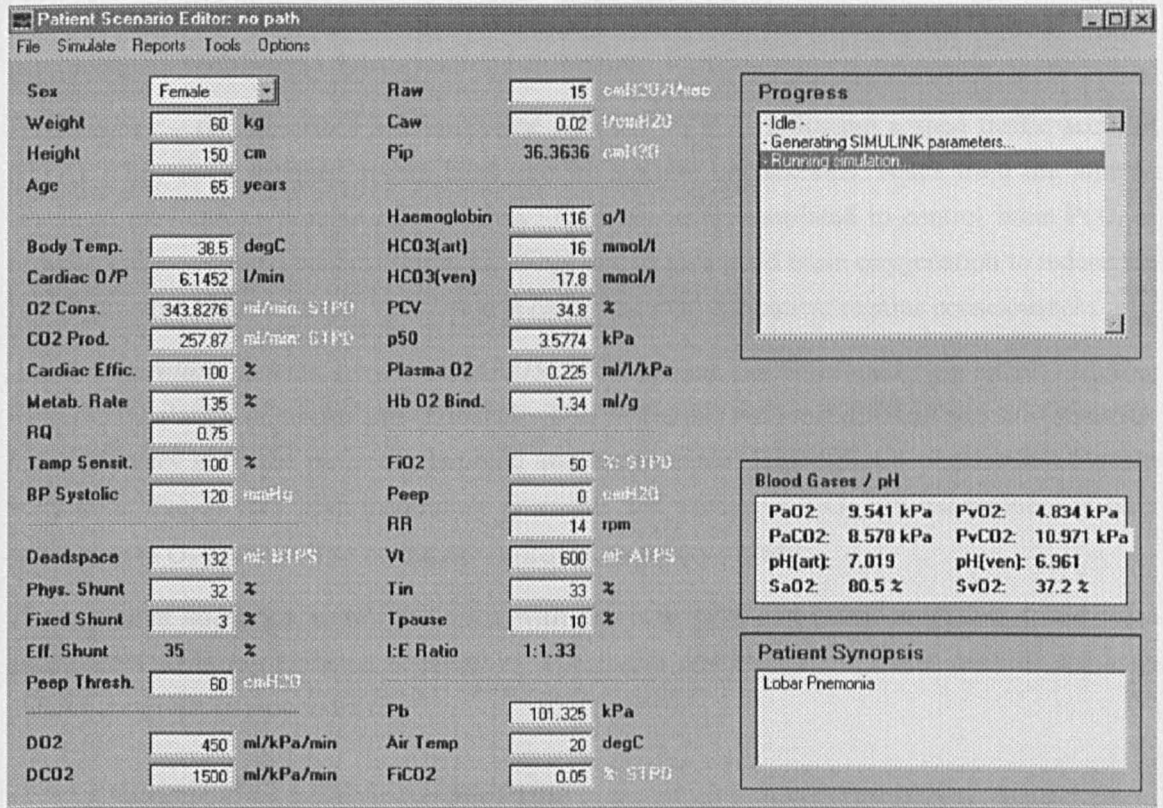


Figure 7.7: Patient definition screen used to create and modify patient scenarios. From here scenarios can be saved and loaded; simulations run; and reports generated. Links are available for closed loop simulation; patient tuning; airway calculator and simulation control options.

7.4 Patient Scenario Development

In order to test the simulated closed-loop performance of the advisor and hence facilitate rule refinement it was necessary to construct scenarios that would represent specific classes of patient. The range of possible pathologies, their severity and the nature of any complicating factors provide an almost endless number of potential scenarios. However, it was decided to limit this to five frequently encountered patient groups so that major rule-anomalies could be identified and corrected rapidly without the need for exhaustive scenario development.

The five patient classes modelled were;

Normal lungs – this describes a post-operative elective ventilation following abdominal surgery. The patient's lungs are healthy and there are no major complications to consider. This should be the simplest of the scenarios to control.

Lobar pneumonia – a long-term infection has weakened the patient and they require ventilatory support whilst antibiotics and physiotherapy can be administered. They are hypoxic due to large physiological shunts, resulting from the infection. The lungs are stiff with slightly elevated airway resistance, leading to raised PIP and a possible risk of barotrauma. Such patients provide a good balance of therapeutic needs but are normally fairly straightforward to ventilate.

Acute asthmatic – an acute episode induced by severe allergy. The predominant feature is high flow resistance culminating in dangerously high levels of PIP. The primary challenge here is to give adequate ventilation whilst avoiding barotrauma.

Head injury – this describes a motorcyclist admitted to ICU following a road traffic accident (RTA). They have received severe head injuries and are unconscious. Apart from the injuries sustained they can be thought of as healthy. They are being ventilated to control brain PCO₂ in order to reduce cerebral oedema (brain swelling) and to give good brain oxygenation to reduce the risk of possible brain damage. Ventilation is continued until the patient regains consciousness.

Adult respiratory distress syndrome (ARDS) – the patient has developed lung shock resulting from the inhalation of smoke and chemicals. This represents the most difficult scenario since the lungs are very stiff, the patient is hypoxic and hypercapnic. It is difficult to provide adequate ventilation due to very high inspiratory pressures and excessive FIO₂ can exacerbate the lung shock due to O₂ toxicity. The condition improves only very slowly.

These patient scenarios were developed with the help of a consultant anaesthetist and were constructed to be as realistic as possible. The initial conditions and event profiles for each patient are given in Appendix C.

7.4.1 Anaesthetist Decision Histories

Having developed the patient scenarios, an anaesthetist was then asked to ventilate them, basing their decisions upon the current simulated patient state and ventilator settings. The changes that they proposed were then entered into the patient model and the simulation continued until the next blood-gas sample time (for example 30 minutes or 3 hours) as agreed by the anaesthetist.

In this way a decision history for each patient was created against which any computer generated advice could be compared. Of course these decision histories do not represent a definitive solution to the patient ventilation problem and other clinicians may arrive at different but equally valid ventilation strategies. However, they do enable glaring errors in the advisor rules to be identified and provide a standard against which subsequent advisor versions can be judged.

Throughout this process, the anaesthetist involved felt that the patient model behaved in a convincing manner to the ventilator changes made. The simulated anaesthetist's decision histories are shown in Figure 7.29 to Figure 7.33 (see pages 187 to 201) and the actual response values are given in Appendix D.

7.5 Closed-Loop Validation & Rule Refinement

The virtual patient scenarios were then connected to the prototype rules and allowed to run in simulated closed-loop control, see Figure 7.8. New advice was generated at the predetermined blood-gas sample times that were established by the anaesthetist during their simulated ventilation of the virtual patients. At each decision point the advisor produced a report similar to that of Figure 7.10, enabling the rule-firing behaviour to be inspected and the causes of decision differences to be understood and if possible corrected.

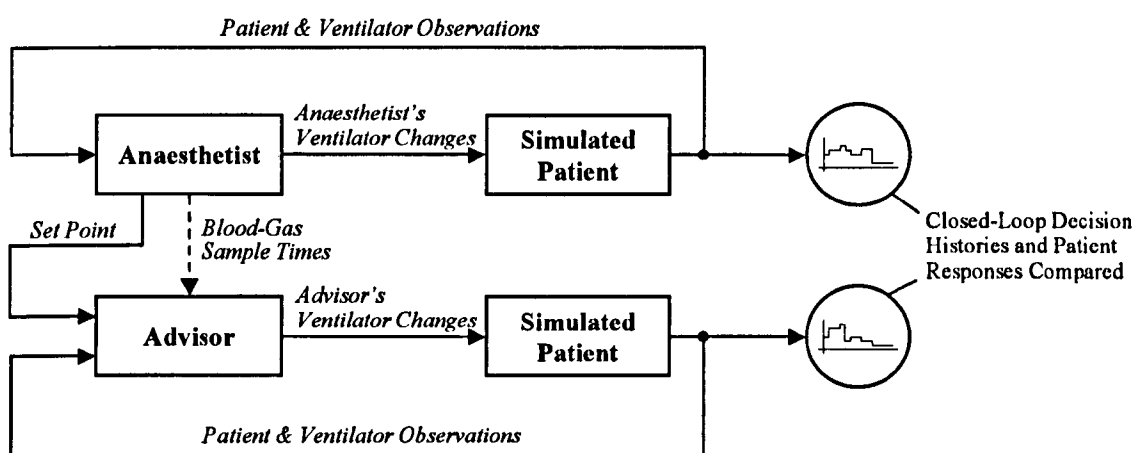


Figure 7.8: Block diagram showing how the simulated closed-loop behaviour of the advisor and that of the anaesthetist were compared.

The performance of the prototype rules was measured by calculating (i) the mean absolute error $|\bar{E}|$ between the ventilator settings made by the anaesthetist and those made by the advisor; (ii) the standard error of this mean $\sigma_{|\bar{E}|}$; and (iii) the maximum absolute error $|\hat{E}|$. The maximum error helps to highlight any extreme decision differences that may be dangerous to the patient. These three measures were made for each patient individually, as well as across the entire data set, enabling patient specific errors to be identified.

Careful inspection of the anaesthetist's decision histories identified occasions when they prescribed new ventilator settings outside of normally expected ranges. These were omitted from the statistical analysis, since they caused decision errors inconsistent with the advisor's performance. The following points were dropped from the MV, RR, VT and PaCO₂ error calculations;

- 1). *Normal lung* patient at 2.5 hours:- the anaesthetist made an MV change from 5.6 to 7 litres causing the PaCO₂ to drop to 4.73 kPa. This change was too large and was corrected by the anaesthetist at the next blood-gas sample time.
- 2). *Acute asthmatic* patient at 8.5 hours:- again the anaesthetist increased MV by too much, reducing PaCO₂ 0.62 kPa below the set-point goal.
- 3). *Head injury* patient at 2.5 hours:- again the MV was increased by too much reducing PaCO₂ 0.6 kPa below set-point goal. A decision that was corrected by the anaesthetist at the next blood-gas sample time.

- 4). *ARDS* patient at 26.5 and 34.5 hours:- the MV reduction caused an increase in the level of hypercapnia with only marginal improvement in PIP. Since PIP is already reducing and the patient is acidotic the decision appears inconsistent with previous behaviour.

Modifications were made to the advisor rules based upon the errors observed. The ventilator controls were considered in turn, starting with the FIO_2 subsystem. Each patient was dealt with separately and modifications were made to the rules in an attempt to reduce $|\bar{E}|$, $\sigma_{|\bar{E}|}$ and $|\hat{E}|$ where possible. The effect of each change on the remaining virtual patients was checked to ensure that the modification would not adversely affect their decision performance. Any changes that resulted in an overall improvement in decision matching were implemented. Those that didn't required either;

- 1). Better separation of the of the observation space via the inclusion of (i) new fuzzy classes or (ii) new observation variables.
- 2). OR a compromise in the final value of the rule-consequent to minimise the overall decision error.

The performance of the *modified* rule-base was then assessed and the causes of any remaining decision mismatch explored. The $|\bar{E}|$, $\sigma_{|\bar{E}|}$ and $|\hat{E}|$ of the prototype and modified advisor are given in Table 7.2.

The correlation between the anaesthetist and advisor's decisions was also assessed. This required the observation data produced by the anaesthetist during simulated closed-loop ventilation, to be applied to the advisor. By using the same observation data a direct comparison of decision difference could be made, see Figure 7.9. This was not possible using the data that resulted from the advisor's closed-loop ventilation, because the observations were different (resulting from slight variations in the decision histories).

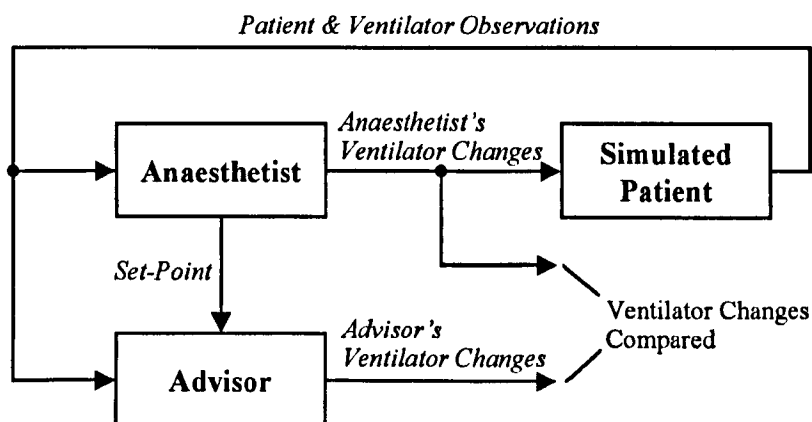


Figure 7.9: Block diagram showing how the data generated during the anaesthetist's closed-loop control was applied to the advisor in order to directly compare ventilator decisions.

Rule Versions: 1.2 1.1 2.1 3.1

Inference Methodology:

Larsen (Sup-Prod), Prod-Liaison

Centre of Sums Defuzzification, Ventilator-Quantisation

FiO₂ Rules Fired

- 13 [0.56] IF (PaO₂ = SLO) AND (FiO₂ = MIN-HI) THEN [dFiO₂ = P2 (20)]
- 12 [0.25] IF (PaO₂ = VLO-SLO) AND (FiO₂ = VHI) THEN [dFiO₂ = P1 (10)]
- 14 [0.19] IF (PaO₂ = LO) AND (FiO₂ = MED-HI) THEN [dFiO₂ = P3 (30)]

PEEP Rules Fired

- 38 [0.56] IF (PaO₂ = SLO) AND (FiO₂ = MED-HI) AND (PEEP = LOW-MED) THEN [dPEEP = Z (0)]
- 50 [0.19] IF (PaO₂ = LO) AND (FiO₂ = MED-HI) AND (PEEP = LOW) THEN [dPEEP = P1 (2)]
- 51 [0.19] IF (PaO₂ = SLO) AND (FiO₂ = VHI) AND (PEEP = LOW-MED) THEN [dPEEP = P1 (2)]
- 59 [0.06] IF (PaO₂ = LO) AND (FiO₂ = VHI) AND (PEEP = OFF-LOW) THEN [dPEEP = P2 (4)]

Mv Rules Fired

- 20 [0.64] IF (ePaco₂ = PS-PB) AND (epH = VACID-ACID) AND (ePIP = HIGH) THEN [dMv = Z (0)]
- 10 [0.19] IF (ePaco₂ = NB-Z) AND (epH = VACID-ACID) AND (ePIP = HIGH) THEN [dMv = N2 (-10)]
- 19 [0.09] IF (ePaco₂ = PS) AND (epH = NORM) AND (ePIP = ALARM-HIGH) THEN [dMv = Z (0)]
- 23 [0.04] IF (ePaco₂ = PS) AND (epH = VACID-ACID) AND (ePIP = ALARM) THEN [dMv = P1 (15)]
- 11 [0.03] IF (ePaco₂ = Z) AND (epH = NORM-ALK) AND (ePIP = HIGH) THEN [dMv = N2 (-10)]
- 16 [0.01] IF (ePaco₂ = Z) AND (epH = ACID-NORM) AND (ePIP = OKAY-ALARM) THEN [dMv = Z (0)]

Vt Rules Fired

- 21 [0.63] IF (RR = MED-VHIGH) AND (eVtnorm = NS) AND (ePIP = HIGH) THEN [dVt = N1 (-5)]
- 10 [0.28] IF (RR = LOW-MED) AND (eVtnorm = Z) AND (ePIP = HIGH) THEN [dVt = N2 (-10)]
- 29 [0.04] IF (RR = MED-MAX) AND (eVtnorm = NS) AND (ePIP = ALARM) THEN [dVt = Z (0)]
- 18 [0.03] IF (RR = VLOW-LOW) AND (eVtnorm = NS) AND (ePIP = ALARM-HIGH) THEN [dVt = N1 (-5)]
- 19 [0.02] IF (RR = LOW-HIGH) AND (eVtnorm = Z) AND (ePIP = ALARM) THEN [dVt = N1 (-5)]

<u>Advice</u>	<u>old</u>	<u>new</u>	<u>change</u>	<u>Goals</u>	
FiO ₂ (%)	75.0	94.0	19.0	Paco ₂ (kPa)	5.3
PEEP (cmH ₂ O)	4.00	5.00	1.00	pH	7.4
RR (rpm)	14.0	14.5	0.5		
Vt (ml)	670.0	640.0	-30.0		
Mv (ml)	9380	9235	-145		

<u>Antecedent Observations</u>		<u>Patient Observations</u>		<u>Ventilator Observations</u>	
PaO ₂	8.49 kPa	PaO ₂	8.49 kPa	FiO ₂	75.0 %
FiO ₂	75.0 %	Paco ₂	7.34 kPa	PEEP	4.0 cmH ₂ O
PEEP	4.0 cmH ₂ O	pH	7.252	RR	14.0 rpm
ePaco ₂	38.6 %	PIP	54.7 cmH ₂ O	Vt	670 ml
epH	-0.148	Weight	75.0 kg	Normal Vt	750 ml
ePIP	4.7 cmH ₂ O				
RR ₁	13.8 rpm				
eVtnorm	-10.7 %				

Membership for FiO₂ Observations

PaO₂ = 8.49 kPa: LO (0.25) SLO(0.75)
 FiO₂ = 75.0 %: HI (0.75) VHI(0.25)

Membership for PEEP Control Observations

PaO₂ = 8.49 kPa: LO (0.25) SLO(0.75)
 FiO₂ = 75.0 %: HI (0.75) VHI(0.25)
 PEEP = 4.0 cmH₂O: LOW (1)

Membership for Mv Control Observations

ePaco₂ = 38.56 %: Z (0.23) PS(0.77)
 epH = -0.148 : ACID (0.88) NORM (0.12)
 ePIP = 4.7 cmH₂O: ALARM (0.06) HIGH (0.94)

Membership for Vt Control Observations

RR = 13.8 rpm: LOW (0.05) MED (0.95)
 eVtnorm = -10.7 %: NS(0.7) Z (0.3)
 ePIP = 4.7 cmH₂O: ALARM (0.06) HIGH (0.94)

Figure 7.10: Typical report generated by the advisor at each blood-gas sample time during the closed-loop validation of the advisor rules. The report includes (i) the rule-base version numbers, (ii) the inference methodology and advice quantisation level used, (iii) the subsystem rules fired together with their weights (ordered according to significance), (iv) the crisp quantised advice, (v) the therapeutic goals, (vi) the patient observations, (vii) the antecedent observations and (viii) the antecedent set membership.

	Normal Lung			Lobar Pneumonia			Acute Asthmatic			Head Injury			ARDS			Total		
	$ \bar{E} $	$\sigma_{ \bar{E} }$	$ \hat{E} $	$ \bar{E} $	$\sigma_{ \bar{E} }$	$ \hat{E} $	$ \bar{E} $	$\sigma_{ \bar{E} }$	$ \hat{E} $	$ \bar{E} $	$\sigma_{ \bar{E} }$	$ \hat{E} $	$ \bar{E} $	$\sigma_{ \bar{E} }$	$ \hat{E} $	$ \bar{E} $	$\sigma_{ \bar{E} }$	$ \hat{E} $
Prototype Advisor																		
PaO ₂ (kPa)	3.68	2.22	5.98	1.94	1.56	4.56	5.30	1.25	6.51	5.66	2.43	8.67	1.57	1.03	3.93	2.88	2.21	8.67
PaCO ₂ (kPa)	0.16	0.19	0.44	0.28	0.18	0.50	0.36	0.07	0.43	0.23	0.09	0.31	1.05	0.88	2.98	0.55	0.66	2.98
pH	0.013	0.016	0.037	0.025	0.018	0.049	0.028	0.005	0.034	0.020	0.007	0.028	0.053	0.037	0.130	0.033	0.029	0.130
PIP (cmH ₂ O)	2.29	0.85	3.77	1.79	0.77	3.41	5.22	1.87	7.10	0.93	0.45	1.50	11.50	2.91	15.64	5.68	5.01	15.64
FIO ₂ (%)	3.80	2.17	5.00	6.10	3.18	10.00	8.75	2.50	10.00	7.80	2.59	10.00	19.00	9.67	30.00	11.05	8.76	30.00
PEEP (cmH ₂ O)	2.10	0.55	3.00	0.50	0.62	2.00	0.00	0.00	0.00	0.00	0.00	0.00	2.29	1.35	4.00	1.25	1.34	4.00
MV (litres)	0.165	0.173	0.400	0.388	0.365	1.125	0.128	0.063	0.185	0.620	0.068	0.705	1.643	1.217	3.740	0.822	0.983	3.740
VT (ml)	20.0	21.6	50.0	44.0	15.8	60.0	120.0	50.0	170.0	85.0	35.1	120.0	126.7	59.9	250.0	83.0	58.6	250.0
RR (rpm)	0.13	0.25	0.50	0.65	0.58	1.50	3.17	1.53	4.50	2.00	0.58	2.50	6.50	3.39	11.00	3.11	3.42	11.00
TIN (%)	n/a	n/a	n/a	n/a	n/a	n/a	n/a	n/a	n/a	n/a	n/a	n/a	n/a	n/a	n/a	n/a	n/a	n/a
Modified Advisor																		
PaO ₂ (kPa)	1.40	1.60	4.06	0.59	0.69	2.04	1.66	1.81	3.40	1.07	1.61	3.93	0.47	0.54	1.97	0.83	1.11	4.06
PaCO ₂ (kPa)	0.27	0.26	0.66	0.08	0.08	0.27	0.12	0.13	0.26	0.12	0.23	0.47	0.16	0.14	0.48	0.14	0.16	0.66
pH	0.022	0.022	0.055	0.007	0.008	0.026	0.009	0.010	0.020	0.011	0.020	0.042	0.009	0.008	0.025	0.010	0.012	0.055
PIP (cmH ₂ O)	2.00	0.48	2.74	1.40	0.45	2.00	1.13	0.88	2.11	0.35	0.22	0.50	1.67	0.97	3.85	1.41	0.84	3.85
FIO ₂ (%)	1.00	2.24	5.00	2.10	1.45	4.00	2.50	2.89	5.00	1.00	2.24	5.00	6.79	4.15	12.00	3.58	3.84	12.00
PEEP (cmH ₂ O)	1.70	0.27	2.00	0.15	0.34	1.00	0.38	0.25	0.50	0.20	0.27	0.50	0.89	0.86	3.00	0.66	0.76	3.00
MV (litres)	0.278	0.278	0.675	0.330	0.406	1.200	0.042	0.052	0.100	0.175	0.350	0.700	0.245	0.252	0.820	0.248	0.306	1.200
VT (ml)	17.5	15.0	40.0	15.0	24.2	50.0	30.0	26.5	50.0	0.0	0.0	0.0	26.7	22.2	70.0	19.1	22.0	70.0
RR (rpm)	0.25	0.29	0.50	0.85	0.67	2.00	1.00	0.87	1.50	0.25	0.50	1.00	1.13	0.96	2.50	0.82	0.80	2.50
TIN (%)	0.00	0.00	0.00	4.20	3.61	7.00	2.50	5.00	10.00	0.00	0.00	0.00	3.57	4.97	10.00	2.68	4.09	10.00

Table 7.2: Mean absolute error $|\bar{E}|$, standard error of estimate $\sigma_{|\bar{E}|}$ and maximum absolute error $|\hat{E}|$ for the prototype and modified advisors. Values have been calculated for each individual patient as well as across the complete data set. Numbers in italic indicate calculations made with anomalous anaesthetist decisions excluded – see text.

The next sections describe the prototype closed-loop performance of the advisor for each ventilator control. Possible causes of any decision mismatch are discussed and the modifications made to the rules presented. The modified advisor closed-loop performance is then re-evaluated and the causes of any remaining inaccuracies are discussed. Finally the correlation between the advisor and anaesthetist decisions is assessed.

The closed-loop behaviour of the prototype and modified advisor is shown in Figure 7.29 to Figure 7.33 (see pages 187 to 201). The PaO₂, PaCO₂, arterial pH, PIP, FIO₂, PEEP, RR, VT, MV and TIN responses are compared against those produced by the anaesthetist. Tables of the actual decision history values are given in Appendix D. Lists of the prototype and modified rules are given in Appendix E, together with plots showing how the shape of the decision space was modified by the changes made to the control rules.

7.5.1 FIO₂ Advisor Performance Analysis

Prototype Rule Closed-Loop Performance

It was found that the FIO₂ control rules repeatedly advised bigger changes than the anaesthetist, and accepted FIO₂ levels lower than and higher than those tolerated by the anaesthetist. This was evident in the *normal lung*, *acute asthmatic* and *head injury* patients where the anaesthetist executed more caution when reducing FIO₂, whereas the advisor rapidly reduced the FIO₂ to its minimum of 30 % (see Figure 7.29e, Figure 7.31e and Figure 7.32e). Also in the *lobar pneumonia* and *ARDS* patients the anaesthetist did not increase FIO₂ above 80 % despite low PaO₂ levels, whereas the advisor continued to make increases up to 90 % in the *pneumonia* patient and 100 % in the *ARDS* patient (see Figure 7.30e and Figure 7.33e). This explains the large overall decision errors observed ($|\bar{E}| = 11.05 \%$, $\sigma = 8.76 \%$, $|\hat{E}| = 30.0 \%$)¹. A difference in prescribed FIO₂ of 30 % as indicated by $|\hat{E}|$, would be unacceptable.

Rule Modifications

However, these errors do not indicate poor PaO₂ control. In fact, in every scenario the advisor maintained a PaO₂ closer to the normal level of 12 kPa than the clinician. The difference is that the clinician is not always attempting to maintain PaO₂ at this level. They will be constantly revising the PaO₂ goal based upon the current state of the patient. Three rules-of-thumb were observed;

- 1). A margin of safety should be maintained in the PaO₂ levels when reducing FIO₂. At O₂ levels of 40 % or lower a PaO₂ of approximately 20 kPa was desired. At 60 % FIO₂ the PaO₂ goal was lower at about 15 kPa, since higher FIO₂ levels should be avoided where possible. These safety margins can be lowered if the patient exhibits good stability over several hours, since the likelihood of sudden patient de-saturation is reduced.

¹ percentage refers to actual FIO₂ and not percentage error.

- 2). FiO_2 should not be increased above 80 % due to the toxic effects of high O_2 levels. Consequently a degree of hypoxia should be tolerated. In the *pneumonia* patient a PaO_2 of 10 kPa was tolerable and in the *ARDS* patient this was slightly lower at between 8 and 9 kPa. The lower value in the *ARDS* patient reflects the fact that the lungs are already shocked and further damage may result from the use of high O_2 levels.
- 3). FiO_2 is not normally reduced below 35 %, except when weaning is likely and the patient has produced good PaO_2 for several hours.

These new rules required the addition of 4 new FiO_2 fuzzy classes at 35, 40, 60 and 80 %, giving 9 fuzzy classes in all, see Figure 7.12. The linguistic classes very low (VLO), low (LO), medium-high (M_HI) and very high (VHI) are new, and the prototype class VHI was renamed as extremely high (EHI). The modified rule-map is shown in Figure 7.11.

		FiO_2								
		MIN	VLO	LO	MED	M_HI	HI	VHI	EHI	MAX
PaO_2	VH	0	-5	-5	-10	-20	-20	-30	-40	-50
	H	0	0	-5	-10	-15	-20	-25	-35	-35
	SH	0	0	-5	-10	0	-10	-10	-10	-20
	N	0	0	0	0	0	0	0	-5	-5
	SL	+20	+20	+20	+20	+15	+10	0	0	0
	L	+40	+35	+20	+20	+20	+10	+5	0	0
	VL	+70	+65	+50	+50	+40	+30	+10	+10	0

Key: New consequents Modified consequents

Figure 7.11: Refinements made to FiO_2 rule-map based upon closed-loop behaviour of the prototype rules.

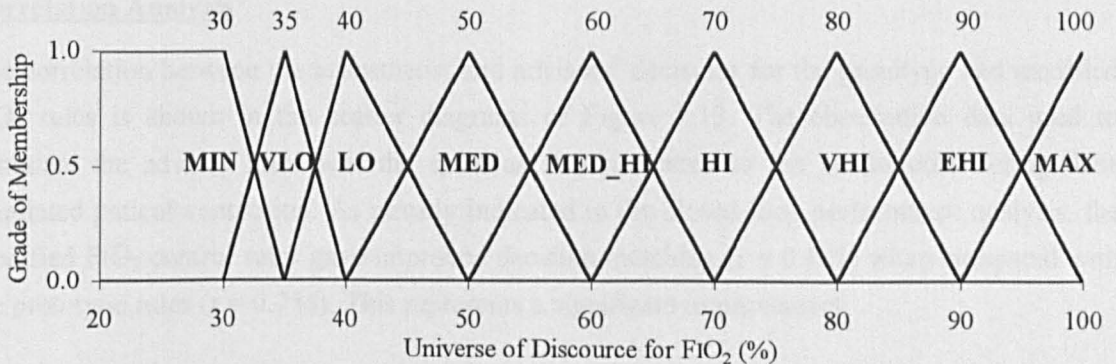


Figure 7.12: Modified fuzzy set definition for the FiO_2 antecedent in the FiO_2 advisor sub-system.

Modified Rule Closed-Loop Performance

The FiO_2 advice for the *normal lung* patient now matched the anaesthetist's decision history in all but the last change (at 5 ½ hours) when the clinician reduced the FiO_2 from 35 to 30 % (see Figure 7.29e). The anaesthetist did state that such a reduction was not entirely necessary and therefore this small difference can be ignored. The mean decision error was small ($|\bar{E}| = 1.00$ %, $\sigma = 2.24$ %), and the maximum decision error ($|\hat{E}| = 5.0$ %) was well within safe limits.

In the *lobar pneumonia* patient, the advisor performance improved and closely matched the anaesthetist's decisions ($|\bar{E}| = 2.10$ %, $\sigma = 1.45$ %, $|\hat{E}| = 4.00$ %). Unlike the prototype rules, the 80 % maximum FiO_2 prescribed by the anaesthetist was not exceeded (see Figure 7.30e). Good decision matching was also observed in the *acute asthmatic* patient ($|\bar{E}| = 2.50$ %, $\sigma = 2.89$ %, $|\hat{E}| = 5.00$ %) and the *head injury* patient ($|\bar{E}| = 1.00$ %, $\sigma = 2.24$ %, $|\hat{E}| = 5.00$ %), see Figure 7.31e and Figure 7.32e.

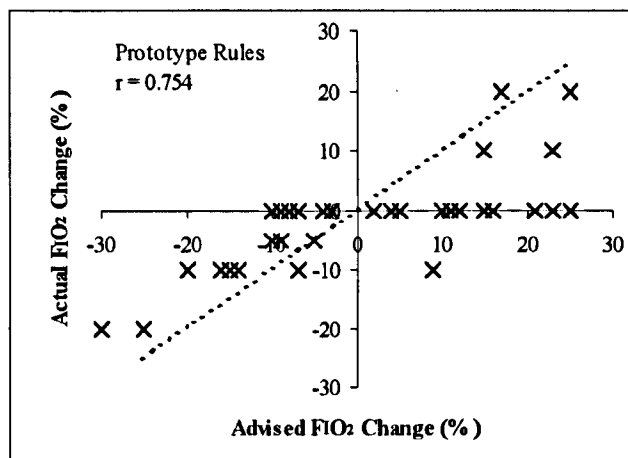
The *ARDS* patient produced the worst advisor performance ($|\bar{E}| = 6.78$ %, $\sigma = 4.15$ %, $|\hat{E}| = 12.00$ %), although it was considerably better than that produced by the prototype rules, with the advisor only marginally exceeded the 80 % FiO_2 limit. However, the anaesthetist was more reluctant to increase FiO_2 beyond 70 % and preferred to reduce it again sooner than the advisor. The anaesthetist appears to be waiting to see if the patient condition improves before increasing FiO_2 , and the reduction was made as soon as the PaO_2 had increased to approximately 10 kPa. This reduction in FiO_2 cannot be incorporated into the rules without conflicting with the *lobar pneumonia* patient decisions, since at 10 kPa the anaesthetist was still suggesting FiO_2 increases. These differences in FiO_2 decisions appear to be specific to the *ARDS* patient and would require unique rules to give the decision separation required.

The overall FiO_2 decision errors ($|\bar{E}| = 3.58$ %, $\sigma = 3.84$ %, $|\hat{E}| = 12.00$ %) showed an improvement of approximately 50 % over the prototype rules.

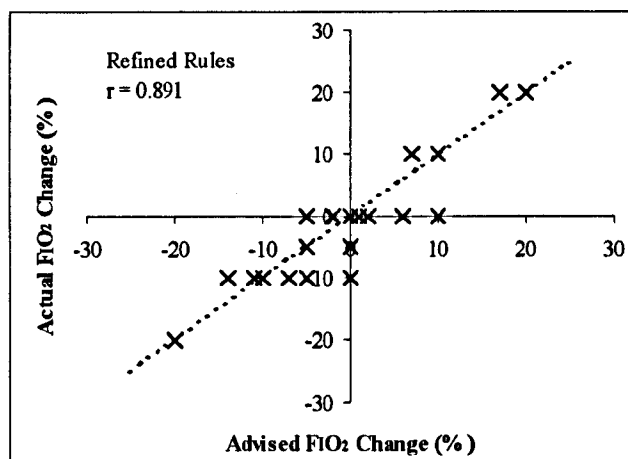
Comparison between the prototype and modified FiO_2 decision space plots (see Figure E.1 in Appendix E), clearly demonstrates that the rule modification process has altered the fuzzy control algorithm, adding small regions of non-linearity. It is also reflected in the increase in the number of rules required to describe the rule-map, from 18 to 34. Whether this is significant in therapeutic terms is unclear.

Correlation Analysis

The correlation between the anaesthetist and advisors' decisions for the prototype and modified FiO_2 rules is shown in the scatter diagrams of Figure 7.13. The observation data used to stimulate the advisor rules was the same as that presented to the anaesthetist during their simulated patient ventilation. As already indicated in the closed-loop performance analysis, the modified FiO_2 control rules gave improved decision matching ($r = 0.891$) when compared with the prototype rules ($r = 0.754$). This represents a significant improvement.



(a)



(b)

Figure 7.13: Scatter diagrams of the advisor's FiO_2 changes plotted against the anaesthetist's changes for (a) the prototype rules and (b) the modified prototype rules.

7.5.2 PEEP Advisor Performance Analysis

Prototype Rule Closed-Loop Performance

The prototype PEEP control rules correctly maintained zero PEEP in the *acute asthmatic* and *head injury* patients since its application was contraindicated. In the *acute asthmatic* this was because of high PIP and in the *head injury* patient it was to avoid raising the intra-cranial pressure. However, the advisor was avoiding increases in PEEP because the oxygenation was good and the FiO_2 low, and not for the reasons given above. This was why in the *normal lung* patient the PEEP was rapidly turned off and the advice matching was poor ($|\bar{E}| = 2.10 \text{ cmH}_2\text{O}$, $\sigma = 0.55 \text{ cmH}_2\text{O}$, $|\hat{E}| = 3.00 \text{ cmH}_2\text{O}$).

The *lobar pneumonia* patient gave good decision matching ($|\bar{E}| = 0.50 \text{ cmH}_2\text{O}$, $\sigma = 0.62 \text{ cmH}_2\text{O}$, $|\hat{E}| = 2.00 \text{ cmH}_2\text{O}$). However, the anaesthetist reduced the PEEP sooner than the advisor, basing their decision upon an observed FiO_2 of 60 % (moderately high) and a PaO_2 of 20 kPa (a good margin of safety above normal levels), see Figure 7.30a and Figure 7.30f. The *ARDS* patient gave the worst decision matching ($|\bar{E}| = 2.29 \text{ cmH}_2\text{O}$, $\sigma = 1.36 \text{ cmH}_2\text{O}$, $|\hat{E}| = 4.00 \text{ cmH}_2\text{O}$). This was caused predominantly by the poor FiO_2 advice and hence different observation data upon which PEEP decisions were based.

Rule Modifications

Only limited changes were made to the PEEP control rules, see Figure 7.14, since indications were that the advisor sub-system needed a complete re-think of its structure. The suitability of PEEP appears to be very patient specific as does the length of time it is maintained. As mentioned in Section 6.6.2, PEEP is also contraindicated by low BPSYS. This therefore needs to be included as an antecedent. None of these factors were implemented due to the lack of available time and are considerations for future work (see Chapter 9).

		FIO ₂				
		MIN	MED	HI	VHI	MAX
PaO ₂	VH	0	0	0	0	0
	H	0	0	0	0	0
	SH	0	+2	0	0	0
	N	0	+2	0	+4	+4
	SL	0	+4	+4	+4	+4
	L	+4	+4	+4	+4	+8
	VL	+4	+4	+4	+8	+8

(a) PEEP = OFF (0 cmH₂O)

		FIO ₂				
		MIN	MED	HI	VHI	MAX
PaO ₂	VH	-4	-2	-2	0	0
	H	-4	-2	-2	0	0
	SH	-2	0	0	0	0
	N	-2	0	0	0	0
	SL	0	0	0	0	+4
	L	0	+2	+4	+6	+6
	VL	+2	+2	+6	+6	+6

(b) PEEP = LOW (4 cmH₂O)

Figure 7.14: Refinements made to PEEP rule-maps based upon closed-loop behaviour of the prototype rules. Shaded regions indicate modified regions of the rule-map.

Modified Rule Closed-Loop Performance

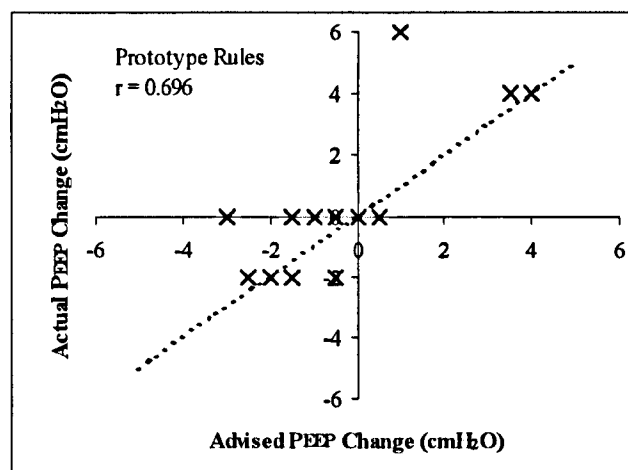
The *acute asthmatic* and *head injury* patients now incorrectly included a small increase in PEEP of 0.5 cmH₂O, see Figure 7.31f and Figure 7.32f. This is not significant, but does reflect a reduction in performance from that of the prototype rules. This was caused by the modifications made to the PEEP rules at PaO₂ = N/SH, FIO₂ = MED and PEEP = OFF (see Figure 7.14a), in an attempt to correct the excessive PEEP reductions observed in the *normal lung* patient. It is clear that the maintenance of PEEP for post-operative patients cannot be determined solely from observations of PaO₂, FIO₂ and PEEP. Therefore the modifications made will need to be reversed and a new observation variable defined determining whether PEEP is advantageous or not.

The *lobar pneumonia* patient now gave better matching than with the prototype rules ($|\bar{E}| = 0.15$ cmH₂O, $\sigma = 0.34$ cmH₂O, $|\hat{E}| = 1.00$ cmH₂O) as did the *ARDS* patient ($|\bar{E}| = 0.89$ cmH₂O, $\sigma = 0.86$ cmH₂O, $|\hat{E}| = 3.00$ cmH₂O), although this was still the worst of the five patients assessed, see Figure 7.30f and Figure 7.33f. These differences may well result from the errors generated in the FIO₂ control, since the advisor was being presented with slightly different observation data than the anaesthetist. Inspection of decision errors generated when using the same observation data as the anaesthetist showed that this was not the case, and the decision matching was worse in the *ARDS* patient ($|\bar{E}| = 1.03$ cmH₂O, $\sigma = 0.75$ cmH₂O, $|\hat{E}| = 4.00$ cmH₂O).

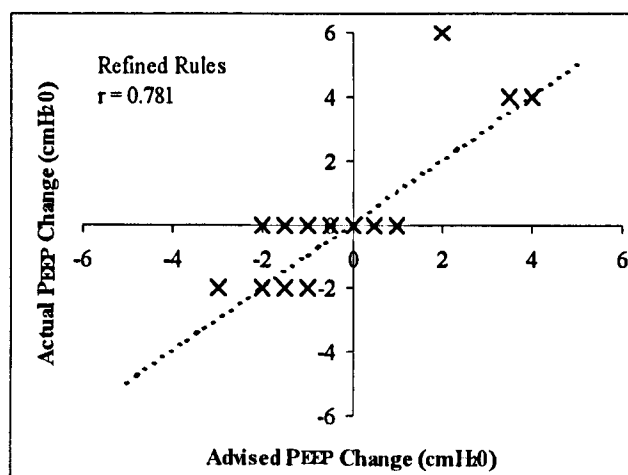
Overall the modified PEEP rules gave only slight improvement ($|\bar{E}| = 0.66$ cmH₂O, $\sigma = 0.76$ cmH₂O, $|\hat{E}| = 3.00$ cmH₂O) over the prototype rules.

Correlation Analysis

The correlation between the advised and anaesthetist's PEEP changes was only average, see Figure 7.15. There *was* some improvement from the prototype ($r = 0.696$) to the modified control rules ($r = 0.781$) but the modified rules still contained occasional large errors ($|\hat{E}| = 4.0$ cmH₂O). This was to be expected since as already stated the PEEP rules need significant re-structuring.



(a)



(b)

Figure 7.15: Scatter diagrams of the advisor's PEEP changes plotted against the anaesthetist's changes for (a) the prototype rules and (b) the modified prototype rules.

7.5.3 MV Advisor Performance Analysis

Prototype Rule Closed-Loop Performance

The *normal lung* and *acute asthmatic* patients exhibited good PaCO₂ maintenance (see Figure 7.29b and Figure 7.31b) via MV changes, and the decision matching was good ($|\bar{E}| = 0.165$ litres, $\sigma = 0.173$ litres, $|\hat{E}| = 0.400$ litres; and $|\bar{E}| = 0.128$ litres, $\sigma = 0.063$ litres, $|\hat{E}| = 0.185$ litres respectively).

The *head injury* patient regularly gave MV decisions lower than that of the anaesthetist (see Figure 7.32i), resulting in larger decision differences ($|\bar{E}| = 0.620$ litres, $\sigma = 0.068$ litres, $|\hat{E}| = 0.705$ litres). This was caused by smaller MV increases, triggered by the presence of mild alkalosis. The rules responsible for this behaviour were incorrect, since the normalisation of PaCO₂ is made via adjustments to the ventilation with the causes of any underlying acidosis or alkalosis treated separately. The correction of acute metabolic imbalance is sometimes necessary but is made through the administration of intravenous therapy and not through changes to the ventilation. This is contrary to the initial understanding outlined in Section 6.7.2

The moderation of MV changes observed above was repeated in the *lobar pneumonia* patient. In this case the underlying metabolic acidosis caused the MV reductions to be smaller than those made by the anaesthetist ($|\bar{E}| = 0.388$ litres, $\sigma = 0.365$ litres, $|\hat{E}| = 1.125$ litres). The rules were attempting to balance pH and PaCO₂ around normal values, resulting in normal pH with mild hypocapnia. This was clearly not the approach taken by the anaesthetist. They attempted to normalise PaCO₂ using changes in ventilation and letting the metabolic acidosis reduce as the infection subsided (treated via antibiotics).

MV decision matching in the *ARDS* patient was extremely poor ($|\bar{E}| = 1.643$ litres, $\sigma = 1.217$ litres, $|\hat{E}| = 3.740$ litres) and was triggered by a combination of factors. The advisor continued to reduce MV down to below 6 litres in response to the dangerously high levels of PIP being generated, see Figure 7.33i and Figure 7.33d. The anaesthetist was achieving much better PIP levels and therefore could tolerate higher MV settings.

The elevated PIP produced by the closed-loop behaviour of the advisor was caused by (i) the absence of TIN control rules and (ii) the reluctance of the VT-RR rules to reduce VT below 500 ml (or eVT_{NORM} of -30 %). The anaesthetist used a TIN of 60 % and VT of 425 ml to keep PIP as low as possible and then tolerated permissive hypercapnia.

Rule Modifications

There were four major changes made to the MV control rules;

- 1). The removal of epH as an observation variable since the normalisation of PaCO₂ appears to be the primary maintenance consideration when making changes to ventilation.
- 2). The replacement of ePIP, with direct observations of PIP, since the anaesthetist was shown to alter the PIP goal as the patient condition changed. The specification of a unique PIP alarm led to poor PaCO₂ and PIP maintenance. The new fuzzy set definition for PIP is shown in Figure 7.16.

- 3). The addition of eVT_{NORM} as an antecedent (Figure 7.17), allowing permissive hypercapnia in patients that have low VT caused by high PIP. This was needed because the VT-RR rules would not reduce VT below -45% of VT_{NORM} and therefore any prescribed increase to MV would cause an inappropriate increase in RR. Such behaviour was prevented by reducing the MV consequents (or setting them to zero) when the following observation criteria were met (i) PIP was greater than $40\text{ cmH}_2\text{O}$, (ii) the patient was hypercapnic and (iii) eVT_{NORM} was below -35% . By defining the peak of $eVT_{NORM} = \text{OKAY}$ to be -15% the use of permissive hypercapnia is restricted to those patients with poor respiratory mechanics (and consequently high PIP), since only these patients will normally have VT this low.
- 4). The inclusion of three new fuzzy sets at -15% , $+15\%$ and $+30\%$ in the $ePaCO_2$ universe, as well as redefining the peak values of the $+50\%$ and $+100\%$ to be $+60\%$ and $+90\%$ respectively, see Figure 7.18. The set names have been altered to accommodate these changes. The new sets NS and PS ($\pm 15\%$) were included to improve control near to the $PaCO_2$ set point. These changes were necessary to better describe the MV decisions made.

The MV modifications were made at the same time as the VT-RR rules and after the inclusion of the simple TIN controller (see Section 7.5.5). The consequents were then handcrafted to give the best apparent decision matching across the virtual patient scenarios, see Figure 7.19.

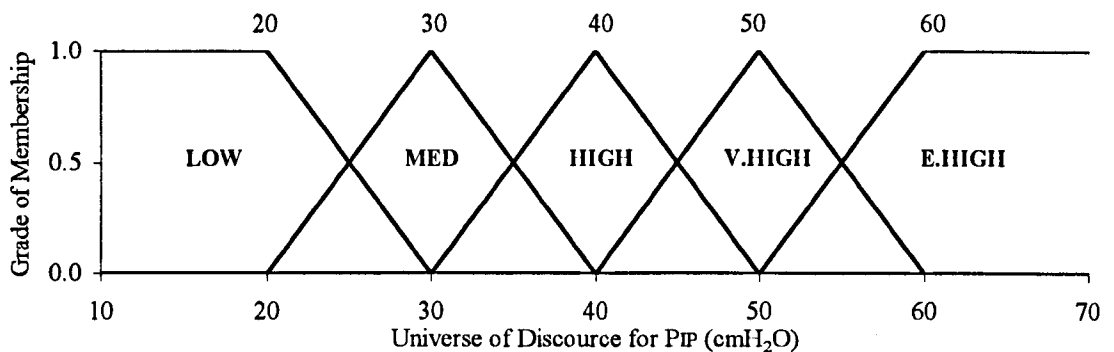


Figure 7.16: New fuzzy set definition for PIP, replacing ePIP.

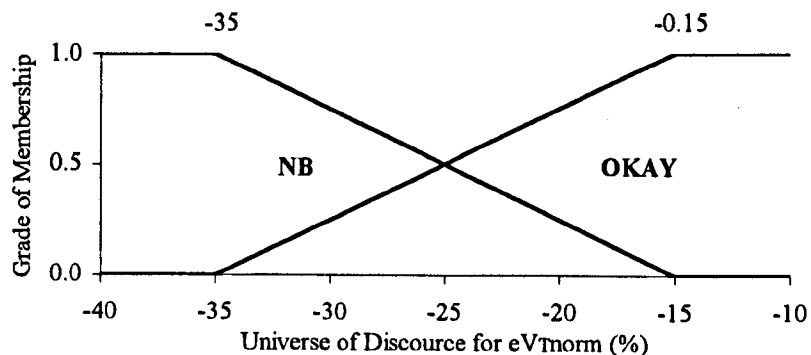


Figure 7.17: Fuzzy set definition for new antecedent eVT_{NORM} in MV advisor.

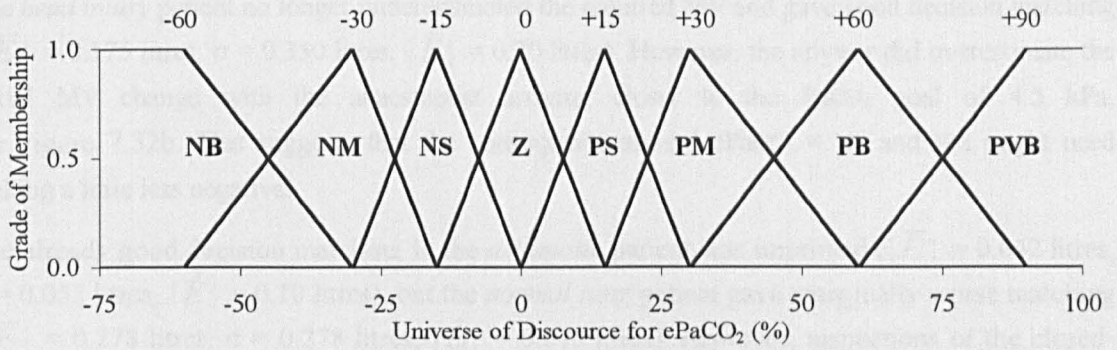


Figure 7.18: Modified fuzzy set definition for ePaCO₂.

		PIP				
		LOW	MED	HI	VHI	EHI
ePaCO ₂	PVB	+90	+30	+25	+10	+5
	PB	+60	+30	+25	+10	-10
	PM	+30	+15	+15	+5	-15
	PS	+15	+5	0	0	-15
	Z	0	0	0	-5	-15
	NS	-15	-15	-15	-15	-15
	NM	-30	-30	-30	-30	-30
	NB	-55	-55	-55	-60	-60

(a) eVT_{NORM} = OKAY (-15 %)

		PIP				
		LOW	MED	HI	VHI	EHI
ePaCO ₂	PVB	+90	+20	0	0	0
	PB	+60	+10	0	0	-10
	PM	+30	0	0	0	-15
	PS	+15	0	0	0	-15
	Z	0	0	0	-5	-15
	NS	-15	-15	-15	-15	-15
	NM	-30	-30	-30	-30	-30
	NB	-55	-55	-55	-60	-60

(b) eVT_{NORM} = NB (-35 %)

Figure 7.19: New rule maps for the modified MV advisor. Shade regions indicate the changes required, to facilitate permissive hypercapnia when VT is already low.

Modified Rule Closed-Loop Performance

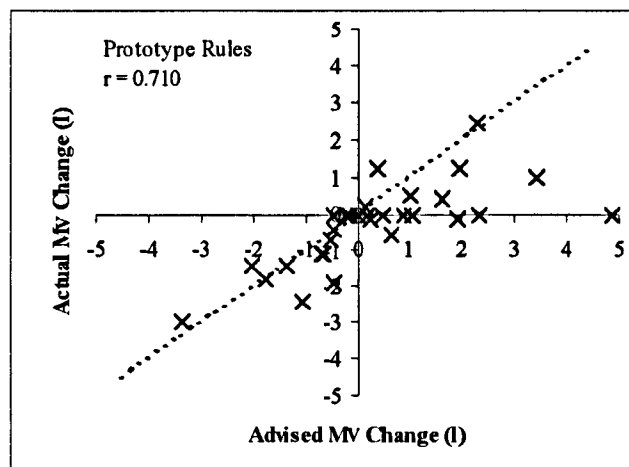
The greatest improvement was made in the *ARDS* patient ($|\bar{E}| = 0.245$ litres, $\sigma = 0.252$ litres, $|\hat{E}| = 0.820$ litres), with a performance now better than that observed in the *pneumonia* patient. The *pneumonia* patient showed a slight improvement in MV decision matching ($|\bar{E}| = 0.330$ litres, $\sigma = 0.406$ litres, $|\hat{E}| = 1.20$ litres) with excellent matching of PaCO₂ ($|\bar{E}| = 0.08$ kPa, $\sigma = 0.08$ kPa, $|\hat{E}| = 0.27$ kPa).

The *head injury* patient no longer underestimated the required MV and gave good decision matching ($|\bar{E}| = 0.175$ litres, $\sigma = 0.350$ litres, $|\hat{E}| = 0.70$ litres). However, the advisor did overestimate the initial MV change with the anaesthetist arriving closer to the PaCO₂ goal of 4.5 kPa, see Figure 7.32b. This suggests that the consequents around ePaCO₂ = NS and NM might need making a little less negative.

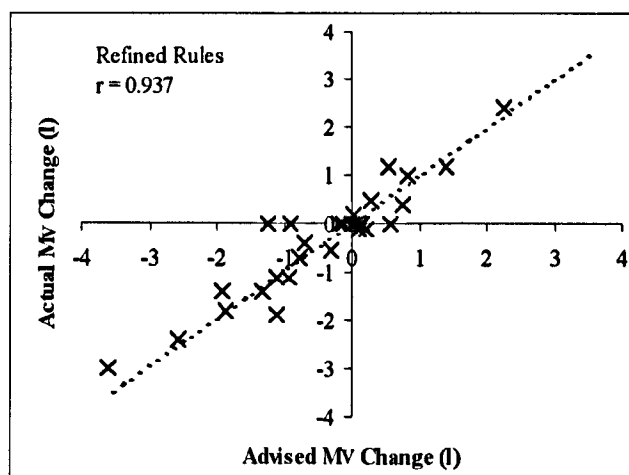
The already good decision matching in the *asthmatic* patient was improved ($|\bar{E}| = 0.042$ litres, $\sigma = 0.052$ litres, $|\hat{E}| = 0.10$ litres), but the *normal lung* patient gave marginally worse matching ($|\bar{E}| = 0.278$ litres, $\sigma = 0.278$ litres, $|\hat{E}| = 0.675$ litres). However, inspections of the closed-loop PaCO₂ behaviour (see Figure 7.29b) shows less overshoot and undershoot of the PaCO₂ goal than produced by the anaesthetist.

Correlation Analysis

The prototype rules only gave moderate MV decision correlation ($r = 0.710$). This was due mainly to the poor ARDS decision matching. The modified MV rules gave significantly better correlation ($r = 0.937$), with the best performance of all the ventilator controls, see Figure 7.20.



(a)



(b)

Figure 7.20: Scatter diagrams of the advisor's MV changes plotted against the anaesthetist's changes for (a) the prototype rules and (b) the modified prototype rules.

7.5.4 RR-VT Advisor Performance Analysis

Prototype Rule Closed-Loop Performance

The dependence of RR and VT upon the advised MV means that poor decision in the later will be reflected in the VT and/or RR decisions. Consequently in the *ARDS* patient the large decision errors (VT: $|\bar{E}| = 126.7$ ml, $\sigma = 59.9$ ml, $|\hat{E}| = 250.0$ ml; RR: $|\bar{E}| = 6.50$ rpm, $\sigma = 3.39$ rpm, $|\hat{E}| = 11.0$ rpm) are to be expected, since the MV errors were large (see Figure 7.33g and Figure 7.33h). The situation is made worse by the fact that the VT-RR rules only allow a maximum reduction in VT of -30% , whereas the anaesthetist reduces it by nearly 45% of VT_{NORM} .

In the *normal lung* patient the MV decision matching was good and this is reflected in the small VT and RR decision errors (VT: $|\bar{E}| = 20.0$ ml, $\sigma = 21.6$ ml, $|\hat{E}| = 50.0$ ml; RR: $|\bar{E}| = 0.13$ rpm, $\sigma = 0.25$ rpm, $|\hat{E}| = 0.50$ rpm). There was a tendency for the advisor to increase VT in preference to RR, even though RR was on the low side (8 to 8.5 rpm). This preferential increase in VT was repeated in the *asthmatic*, *head injury* and *pneumonia* patients. The anaesthetist was more inclined to adjust RR in the range 8-14 rpm than to make changes to VT.

Rule Modifications

The following changes were made to the VT-RR rules giving the VT-RR rule maps of Figure 7.22;

- 1). The fuzzy class PVB ($+60\%$) was dropped from the eVT_{NORM} universe, since tidal volumes this high are seldom required. An eVT_{NORM} of $+30\%$ gives a VT of 975 ml on a 75-kg patient, which should be more than adequate.
- 2). The inclusion of $eVT_{NORM} = NB$ (-45%), because a greater reduction in VT was required than provided by the prototype rules. Also, inclusion of $eVT_{NORM} = NS$ ($+15\%$) to give better control near to normal VT. These modifications are shown in Figure 7.21.
- 3). The calculation of VT_{NORM} was restricted to a maximum of 750 ml, since in the *head injury* patient VT was incorrectly increased towards a VT_{NORM} of 850 ml. What constitutes a normal VT appears to change from the 10 ml/kg rule of thumb as the patient size and weight increases.
- 4). The fuzzy variable ePIP was replaced by PIP as in the MV rules. The same membership functions were used as given in Figure 7.16.
- 5). A broadening of the region that represents normal VT and RR settings when no change is required. This is a region defined by RR = 8 to 14 rpm, $eVT_{NORM} = -15$ to 0 % and PIP is LOW (20 cmH₂O). This is better explained by comparing the decision behaviour of the prototype and modified VT-RR rules, see Figure 7.23. It can be seen that the decision behaviour is much more relaxed than the optimal VT-RR settings proposed by the prototype rules. However, they do still roughly follow the ideal VT-RR relationship.
- 6). A greater reduction in VT with increased PIP. This helps to improve the PIP maintenance by using smaller volumes to inflate the lungs.

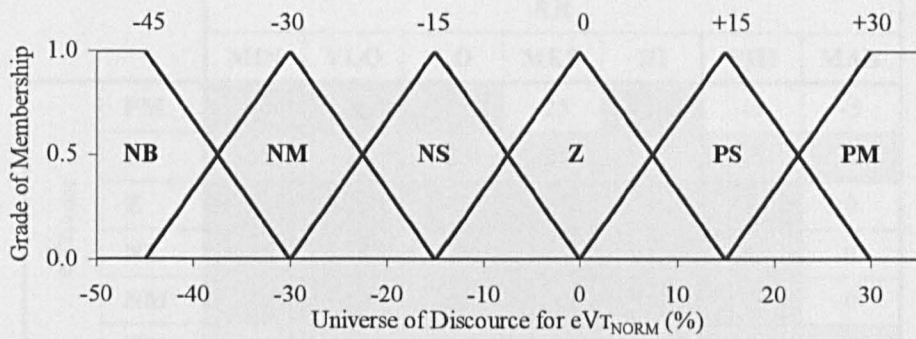


Figure 7.21: Modified fuzzy set definition for eVT_{NORM} in VT-RR advisor subsystem.

		RR						
		MIN	VLO	LO	MED	HI	VHI	MAX
eVT_{NORM}	PM	-30	-20	-20	-15	-5	2	10
	PS	-20	-10	-10	-5	0	0	15
	Z	-15	0	0	0	5	15	25
	NS	-5	0	0	0	15	25	35
	NM	0	0	5	20	40	40	50
	NB	0	15	25	40	50	60	60

(a) PIP = LOW (20 cmH₂O)

		RR						
		MIN	VLO	LO	MED	HI	VHI	MAX
eVT_{NORM}	PM	-30	-20	-20	-15	-5	0	5
	PS	-20	-10	-10	-10	0	0	5
	Z	-15	-5	-5	0	0	0	10
	NS	-5	-5	-5	-5	5	5	10
	NM	0	0	0	0	10	10	10
	NB	0	10	10	10	10	10	10

(b) PIP = MED (30 cmH₂O)

		RR						
		MIN	VLO	LO	MED	HI	VHI	MAX
eVT_{NORM}	PM	-30	-20	-20	-15	-5	-5	0
	PS	-20	-10	-10	-5	0	0	0
	Z	-15	-10	-10	0	0	0	0
	NS	-10	-10	-10	-10	0	0	0
	NM	-10	-10	-5	-5	0	0	0
	NB	0	0	0	0	0	0	0

(c) PIP = HIGH (40 cmH₂O)

Figure 7.22 continued overleaf...

		RR						
		MIN	VLO	LO	MED	HI	VHI	MAX
eVT _{NORM}	PM	-30	-25	-25	-25	-25	-5	-5
	PS	-25	-25	-25	-25	-25	-5	-5
	Z	-25	-25	-25	-25	0	0	0
	NS	-15	-15	-15	-15	-15	-5	0
	NM	-10	-10	-10	-10	-10	-5	0
	NB	0	0	0	0	0	0	0

(d) PIP = V.HIGH (50 cmH₂O)

		RR						
		MIN	VLO	LO	MED	HI	VHI	MAX
eVT _{NORM}	PM	-35	-35	-35	-25	-25	-10	-10
	PS	-25	-25	-25	-25	-25	-15	-10
	Z	-25	-25	-25	-25	-25	-15	0
	NS	-20	-20	-20	-20	-20	-10	0
	NM	-20	-20	-20	-20	-20	-10	0
	NB	0	0	0	0	0	0	0

(e) PIP = E.HIGH (60 cmH₂O)

Key: New consequents Modified consequents

Figure 7.22: Modified rule maps for the VT-RR advisor.

Modified Rule Closed-Loop Performance

The *normal lung* patient showed a small improvement in VT decision matching ($|\bar{E}| = 17.5$ ml, $\sigma = 15.0$ ml, $|\hat{E}| = 40.0$ ml), with the tendency to increase VT later in the simulation removed. The RR matching was slightly worse than with the prototype rules ($|\bar{E}| = 0.25$ rpm, $\sigma = 0.29$ rpm, $|\hat{E}| = 0.50$ rpm) but the error was still only small.

The *pneumonia* patient had improved VT matching ($|\bar{E}| = 15.0$ ml, $\sigma = 24.2$ ml, $|\hat{E}| = 50.0$ ml) although the advisor did not reduce VT at 12 ½ hours as the anaesthetist did, see Figure 7.30g. This decision by the anaesthetist appears unnecessary since the PIP had already reduced to 20 cmH₂O and the RR was almost normal (16 rpm). The advisor's decisions can therefore be considered safe. The RR matching was only slightly worse ($|\bar{E}| = 0.85$ rpm, $\sigma = 0.67$ rpm, $|\hat{E}| = 2.00$ rpm) and the differences were still small.

The *asthmatic* patient gave significantly improved decision matching in both VT and RR (VT: $|\bar{E}| = 30.0$ ml, $\sigma = 26.5$ ml, $|\hat{E}| = 50.0$ ml; RR: $|\bar{E}| = 1.00$ rpm, $\sigma = 0.87$ rpm, $|\hat{E}| = 1.50$ rpm) although the anaesthetist preferred to opt for slightly lower VT (by about 50 ml) and higher RR (by about 2 rpm). However, the PaCO₂ and PIP maintenance achieved was very good (see Figure 7.31b and Figure 7.31d).

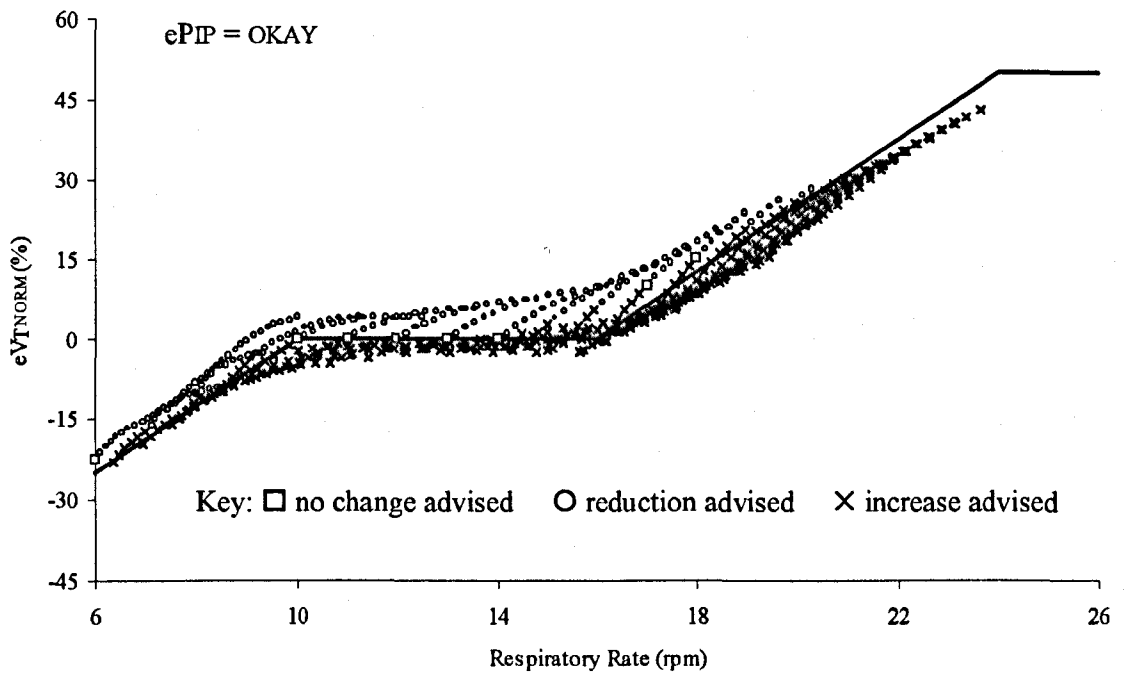
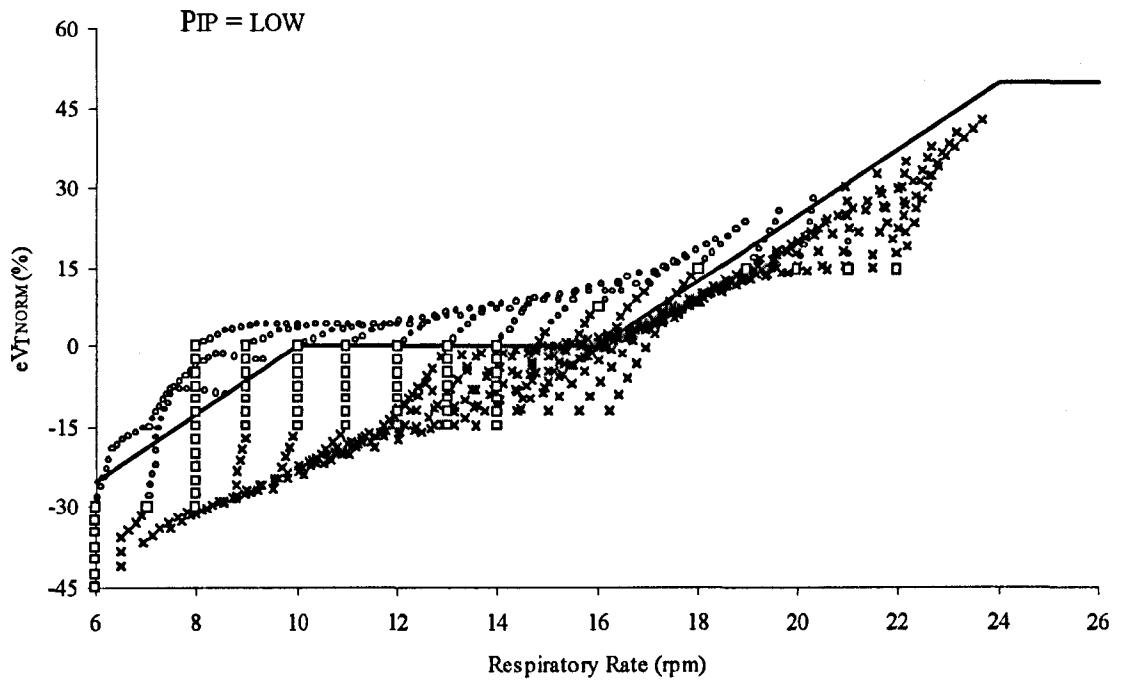
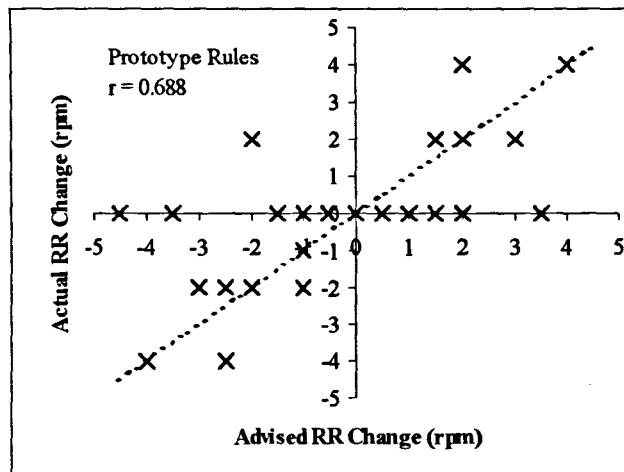
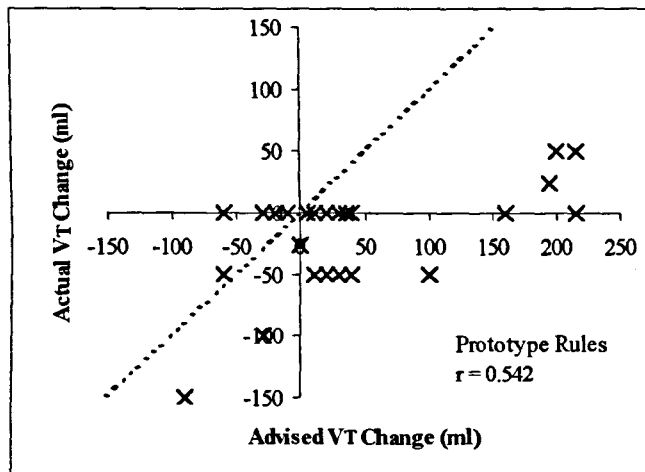
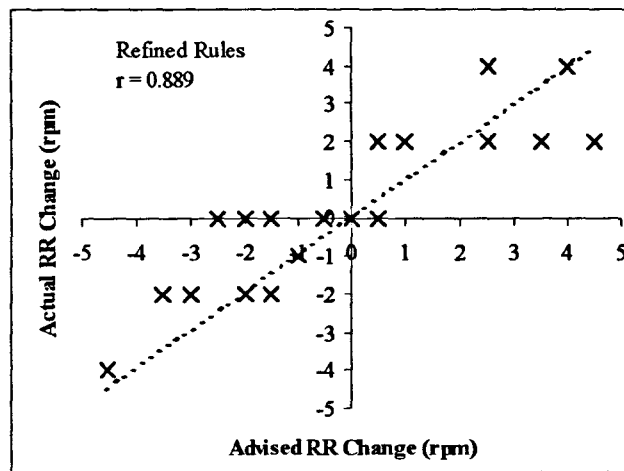
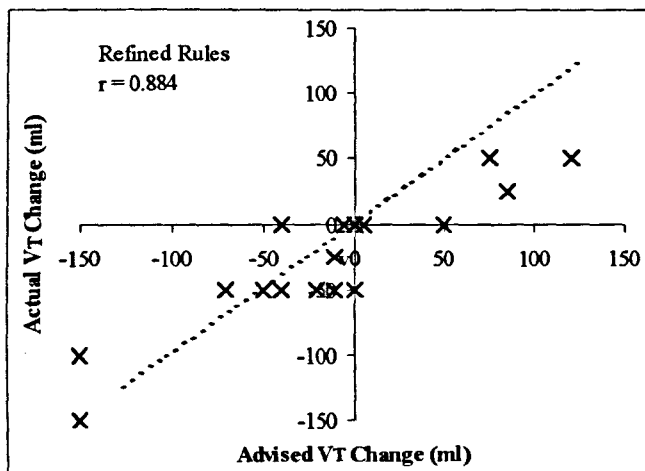


Figure 7.23: The decision behaviour of (a) the modified and (b) the prototype VT-RR rules when PIP is low (i.e. not affecting VT changes). The graphs were generated by applying every combination of eVT_{NORM} in the range -45 to $+45$ % (in 2.5 % steps) and RR observations in the range 6 to 24 rpm (in 1 rpm steps) to the VT-RR advisor subsystem. The advised VT change was then used to calculate the new RR and VT (expressed as eVT_{NORM}) values.



(a)



(b)

Figure 7.24: Scatter diagrams of the advisor's VT and RR changes plotted against the anaesthetist's changes for (a) the prototype rules and (b) the modified prototype rules.

The *head injury* patient exhibited exact VT matching and excellent RR matching ($|\bar{E}| = 0.25$ rpm, $\sigma = 0.50$ rpm, $|\hat{E}| = 1.00$ rpm). The *ARDS* patient exhibited greatly improved VT and RR matching (VT: $|\bar{E}| = 26.7$ ml, $\sigma = 22.2$ ml, $|\hat{E}| = 70.0$ ml; RR: $|\bar{E}| = 1.13$ rpm, $\sigma = 0.96$ rpm, $|\hat{E}| = 2.50$ rpm), although the anaesthetist was more cautious than the advisor when increasing VT and reducing RR in the later stages of the closed-loop simulation (see Figure 7.33g and Figure 7.33h).

Correlation Analysis

Both the VT and RR decisions showed significant improvements in correlation from the prototype to the modified rules. For VT this was an improvement from $r = 0.542$ to $r = 0.884$, and for RR, an improvement from $r = 0.688$ to $r = 0.889$, see Figure 7.24.

7.5.5 TIN Advisor Performance Analysis

As mentioned in the assessment of the MV advisor performance some of the differences in MV decisions were attributable to the lack of control rules for TIN. The anaesthetist would increase the I:E ratio (by increasing TIN) in patients with high PIP in an attempt to lower airway pressure and reduce the risk of barotrauma. A very simple set of rules was constructed to emulate this aspect of PIP maintenance, see Figure 7.27. The antecedents for this advisor were PIP (see Figure 7.26) and the current level of TIN (see Figure 7.25).

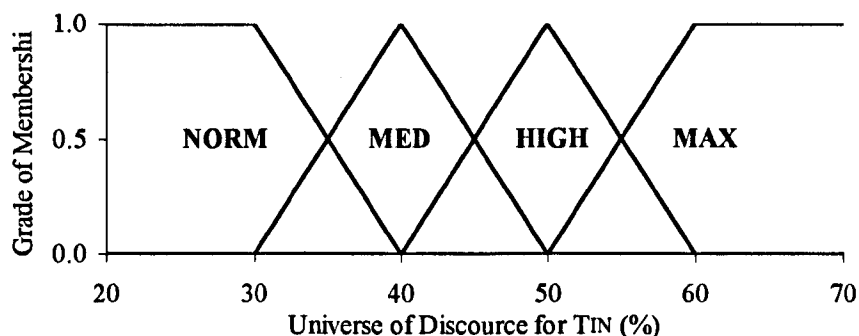


Figure 7.25: Prototype fuzzy set definition for TIN in the TIN controller.

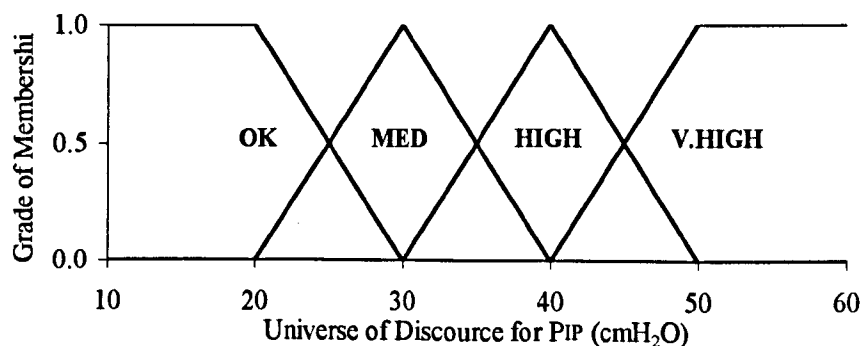


Figure 7.26: Prototype fuzzy set definition for PIP in the TIN controller.

		Tin			
		NRM	MED	HI	MAX
PIP	VHI	20	10	10	0
	HI	10	0	0	-10
	MED	0	0	0	-10
	OK	0	-10	-10	-20

Figure 7.27: Prototype rule map for the TIN advisor subsystem.

The advice generated was quantised at 10 % intervals, producing a winner-takes-all defuzzification strategy, avoiding intermediate settings.

Modified Rules Closed-Loop Performance

TIN was correctly maintained at 33 % in the *normal lung* and *head injury* patients, giving perfect decision matching. In the *lobar pneumonia* patient the advisor incorrectly prescribed an increase in TIN to 40 %, whereas the anaesthetist maintained a TIN of 33 %. This explains the large decision errors calculated ($|\bar{E}| = 4.20\%$, $\sigma = 3.61\%$, $|\hat{E}| = 7.00\%$)². It is a simple matter to resolve this by changing the consequent of the rule 'If PIP = HI and TIN = NRM' from PS (10 %) to Z (0 %).

The *asthmatic* patient saw a correct increase in TIN to 50 % at the start of the simulation, but reduced it back to 40 % at 8.5 hours, whereas the anaesthetist maintained it at 50%. This may be an oversight on the part of the anaesthetist since the PIP has reduced below 20 cmH₂O. Similarly with the *ARDS* patient the advisor matched the TIN increases but made reductions sooner than the anaesthetist. This can be corrected by increasing the consequent of the rule 'If PIP = HI and TIN = MAX' from NS (-10 %) to Z (0 %).

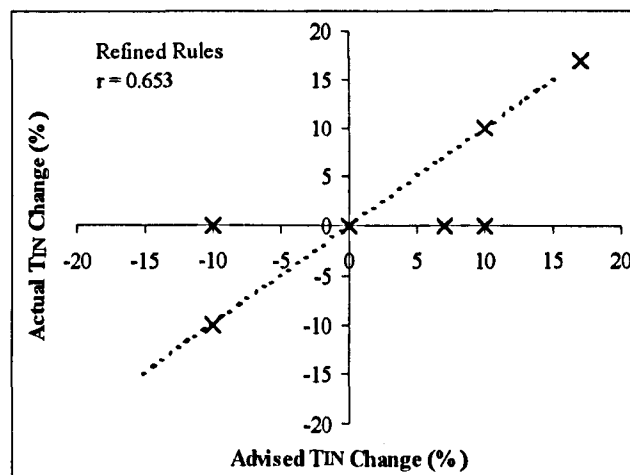


Figure 7.28: Scatter diagram of the advisor's TIN changes plotted against the anaesthetist's changes for the preliminary TIN control rules.

² percentage refers to actual TIN and not percentage error.

Correlation Analysis

The correlation between the advisor and anaesthetist's TIN changes was not striking ($r = 0.653$), see Figure 7.28. However, the correlation test is not entirely suitable, since a large proportion of the changes are zero which skews the results produced by the correlation coefficient formula.

7.6 Summary & Conclusions

Inadequacies in the patient model were identified and the improvements required were successfully implemented. The resulting model was then used to construct virtual patient scenarios that exhibited physiological behaviour similar to that observed in real patients. It was possible to model a wide range of physiological disturbances using *event profiling* to control model parameters such as shunt, airway resistance, etc.

Five patient scenarios were constructed (via discussion with an anaesthetist) representing patients with normal lungs, lobar pneumonia, acute asthma, head injury and ARDS. These facilitated simulated closed-loop validation of the advisor, and comparison with the anaesthetist's decision behaviour. This enabled rapid identification of possible rule errors and the subsequent assessment of the effectiveness of any modifications made. The virtual patient scenarios had the advantage over real clinical data of being repeatable and free from measurement errors. The true flexibility of using a model to test the advisor is that even measurement errors can be incorporated if so desired. The behaviour of the virtual patients to changes in the ventilation regime was deemed realistic by the anaesthetist.

Overall, the modified advisor exhibited significant improvement in decision matching and in closed-loop control, when compared with the prototype advisor. This was particularly evident for the FiO_2 , MV, VT and RR sub-systems.

The FiO_2 rules only required modification to the size of some of the rule-consequents, in order to match the more conservative approach to FiO_2 changes made by the anaesthetist. FiO_2 decision matching using the modified advisor was good ($r = 0.891$), with the only noticeable exception occurring in the ARDS patient. In this scenario the anaesthetist was reluctant to increase FiO_2 above 70 % due to the increased risk of O_2 toxicity. Such behaviour could not be incorporated into the rules without compromising the decisions required by the other scenarios. Therefore the controller's behaviour needs to be modified according to the type of pathology or trauma presented.

The MV rules were modified quite radically, with the removal of pH as an observation variable (although it will be seen in the next chapter that this needs to be reversed). In addition, PIP no longer required an upper alarm threshold and was instead handled by the advisor directly as PIP rather than ePIP (i.e. distance from alarm). This reflected the trade-off by the anaesthetist between acceptable PIP and desired PaCO_2 . The final MV modification was the addition of $e\text{VT}_{\text{NORM}}$ as a rule-antecedent. This was included to prevent MV increases, in patients requiring permissive hypercapnia due to high PIP, and consequently with low prescribed VT.

The MV rules were shown to give better PaCO_2 maintenance than the anaesthetist in the pneumonia and normal lung patients, and overall the level of decision matching was excellent

($r= 0.937$). The improvements in the MV performance were also influenced by changes made to the RR-VT rules and the inclusion of T_{IN} control rules.

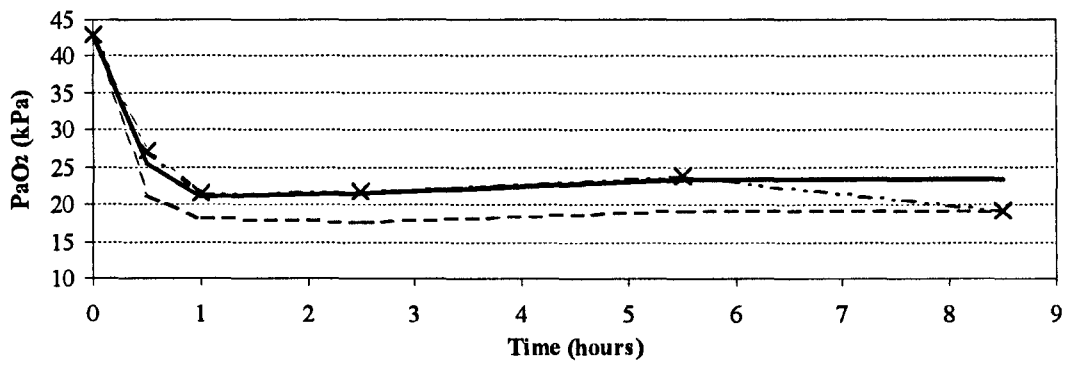
The T_{IN} advisor helped to reduce the problems associated with high PIP and its affect on the MV and RR-VT rules. However, this was only a crude first attempt to define the T_{IN} rules and gave only moderate decision matching ($r = 0.653$). This was due predominantly to the advisor's tendency to increase T_{IN} sooner than the anaesthetist, and keep it at an elevated level for longer.

Modifications required to the RR-VT rules included the limiting of $V_{T_{NORM}}$ to a maximum of 750 ml to prevent excessive VT and the addition of lower acceptable VT. The representation of PIP was also changed as per the MV rules. Overall the changes made to the rule-consequents and set membership produced a broadening in the range of RR and VT values that were deemed normal, and therefore not requiring adjustment. The decision matching was good for both RR and VT ($r= 0.889$ and $r = 0.884$ respectively).

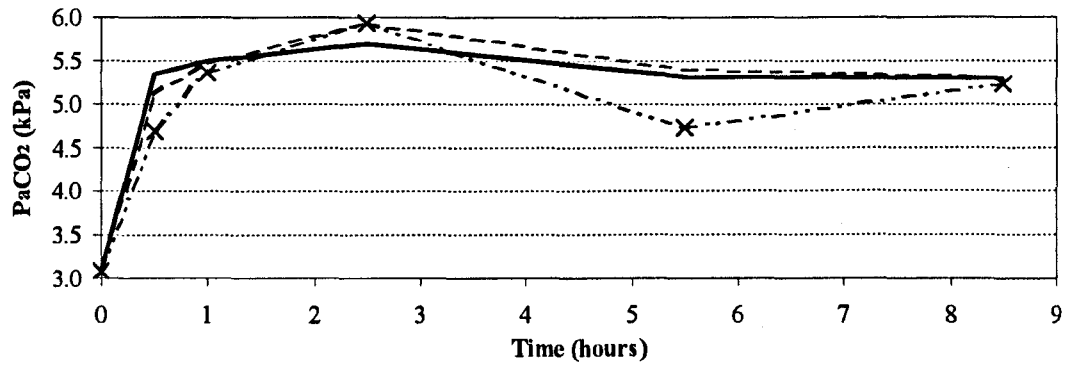
The PEEP control rules behaved less convincingly, with only a moderate level of decision matching ($r= 0.781$). The advisor did not contain knowledge pertaining to the prophylactic use of PEEP in post-operative patients with healthy lungs, and therefore when presented with low FIO_2 and normal PaO_2 did not prescribe PEEP (or reduced any currently applied). Attempts to modify the rule-consequents to prevent this only resulted in the inappropriate application of PEEP in the asthmatic and head injury patients. It will therefore be necessary to incorporate rules that determine the suitability of PEEP and modify any changes accordingly.

The closed-loop behaviour of the modified advisor is promising. However, the patients used to test it only represent a sub-set of the possible scenarios that can be encountered and consequently only a small percentage of the rules were tested. This has important safety implications and is best resolved by the construction of patient scenarios, which further explore the advisor's behaviour especially at the physiological extremes.

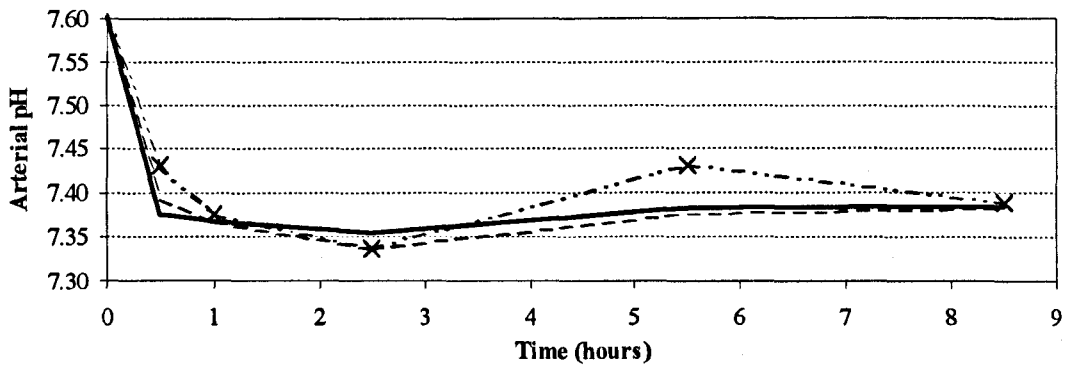
Whilst simulated closed-loop validation is a good methodology for rule testing, and provides rapid insights into patient-advisor interaction, the advisor must also demonstrate good decision matching using real patient data. The validation of the advisor using clinical data is presented in the next chapter.



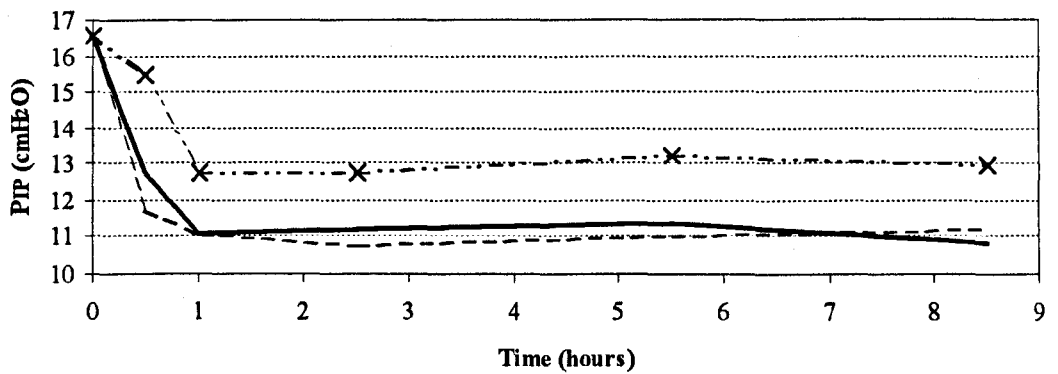
(a)



(b)



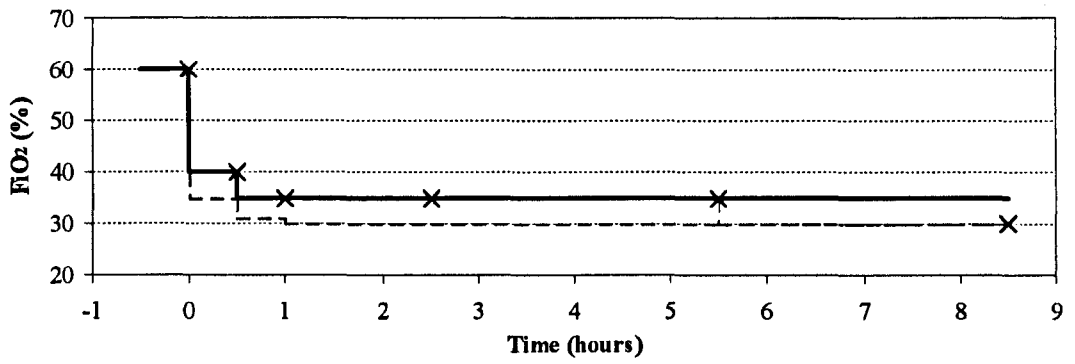
(c)



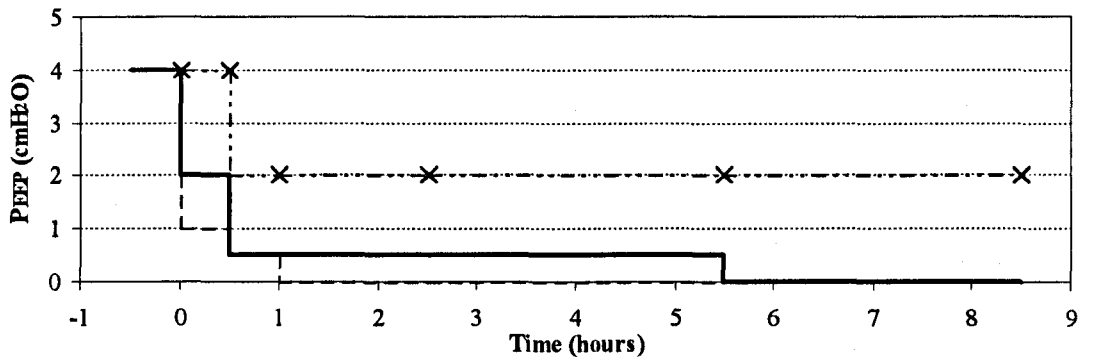
(d)

Key: — Refined Advisor --X-- Anaesthetist - - - - Prototype Advisor

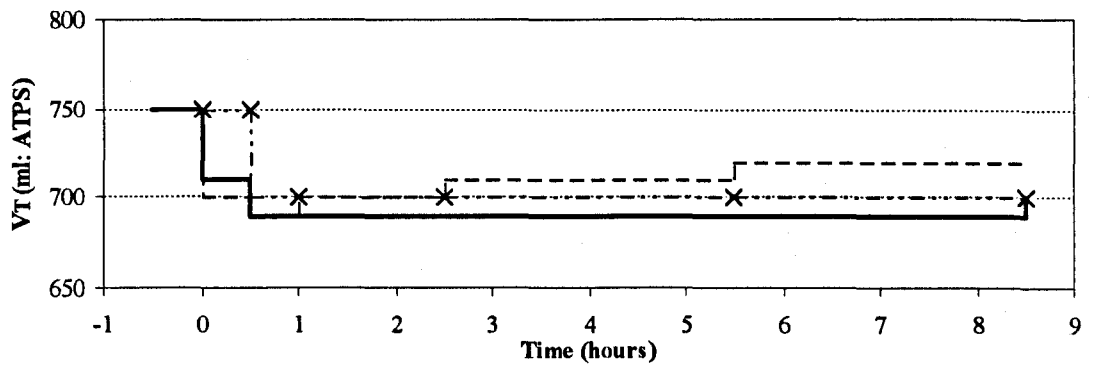
Figure 7.29 (normal lung) continues overleaf...



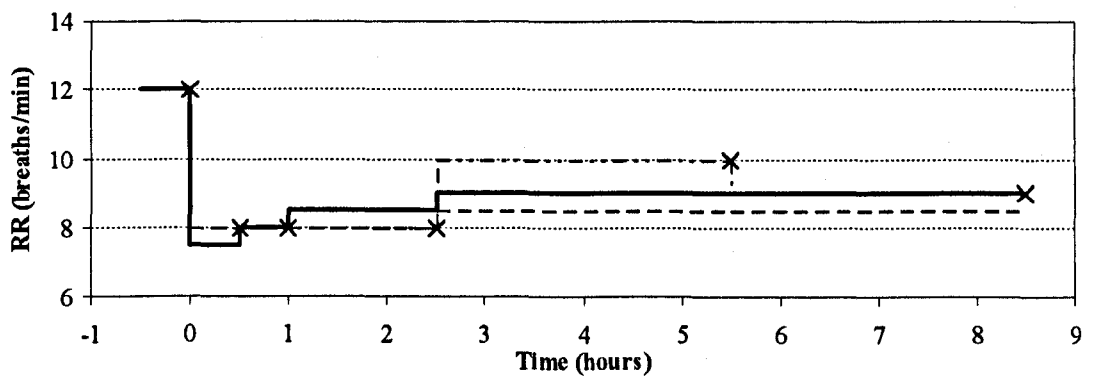
(e)



(f)



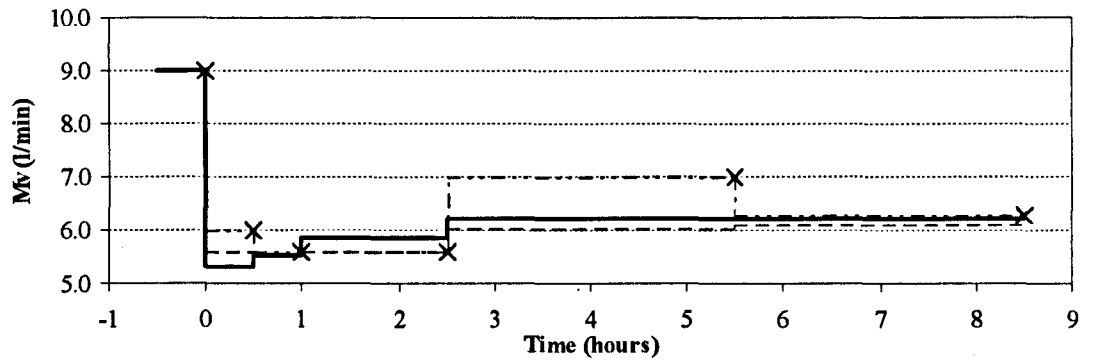
(g)



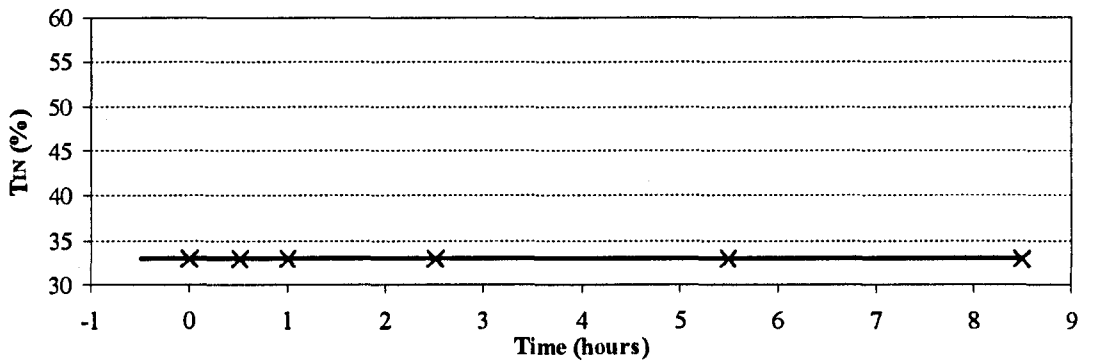
(h)

Key: — Refined Advisor - - x - - Anaesthetist - - - - Prototype Advisor

Figure 7.29 (normal lung) continues overleaf...



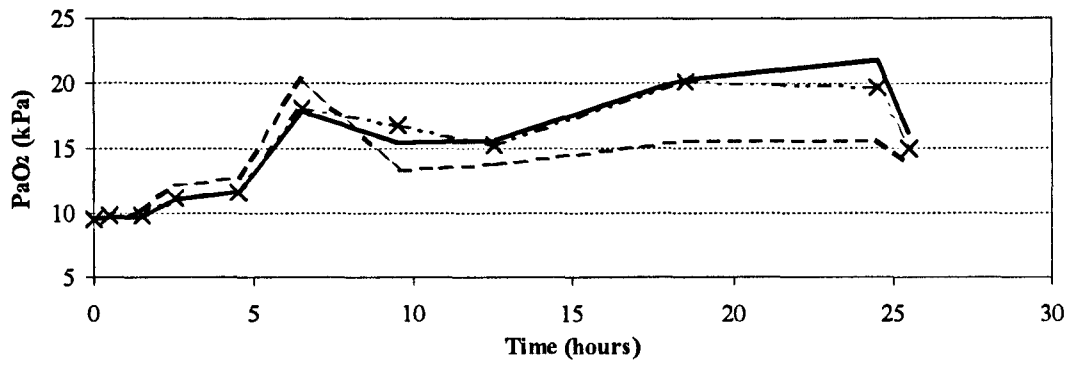
(i)



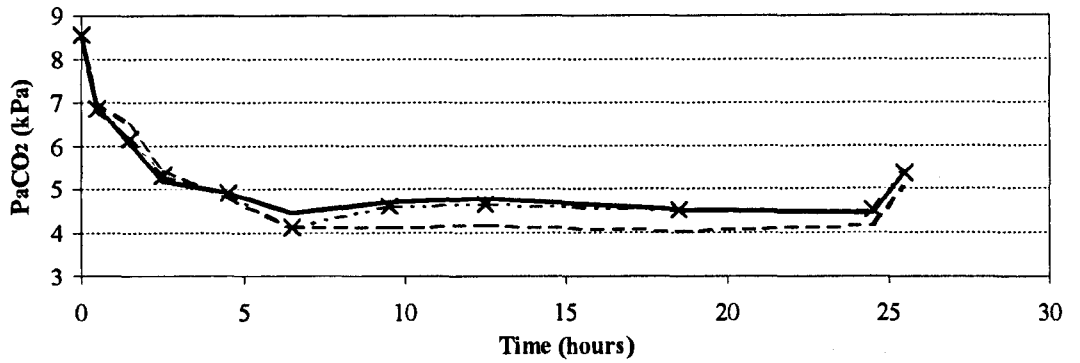
(j)

Key: — Refined Advisor - - x - - Anaesthetist - - - - Prototype Advisor

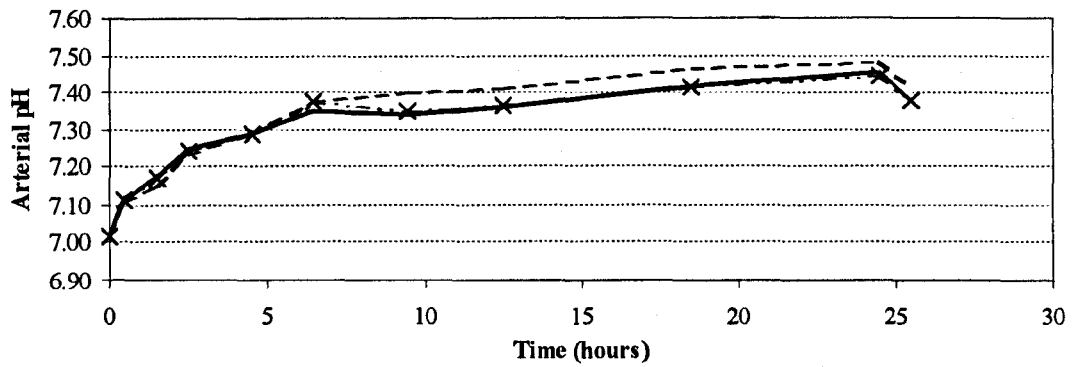
Figure 7.29: Comparison of anaesthetist, prototype advisor and refined advisor decision histories for the **Normal Lung** patient scenario. Patient responses are shown for (a) PaO₂, (b) PaCO₂, (c) arterial pH and (c) PIP. Ventilator changes are shown for (e) FIO₂, (f) PEEP, (g) VT, (h) RR, (i) Mv and (j) T1N.



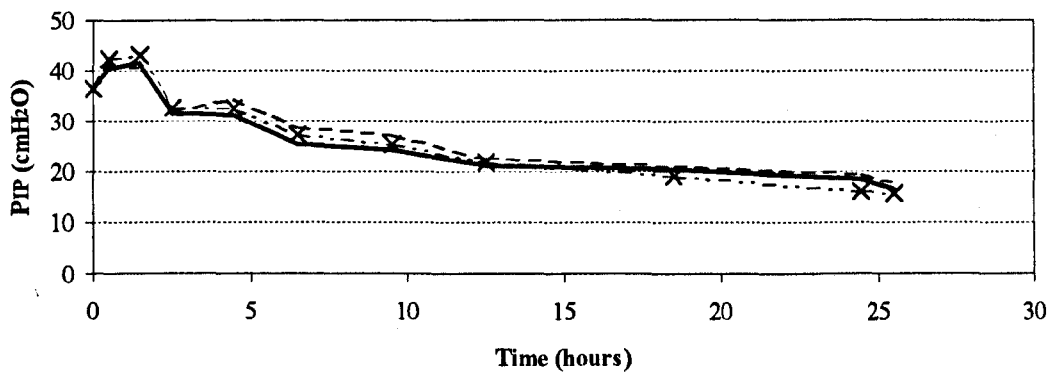
(a)



(b)



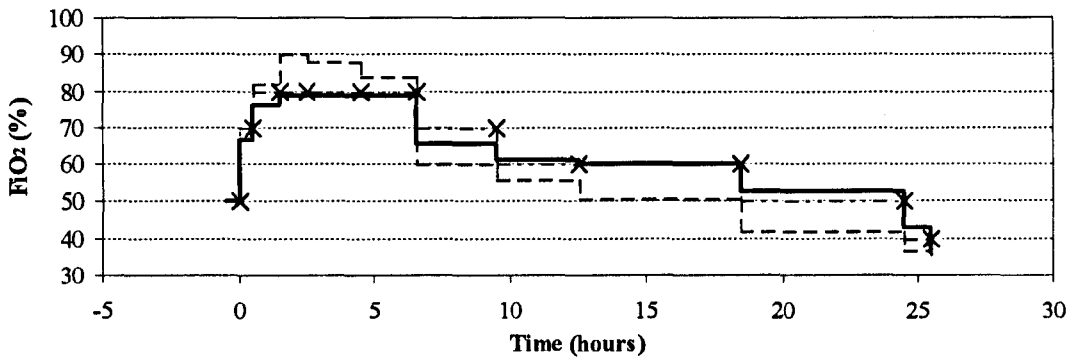
(c)



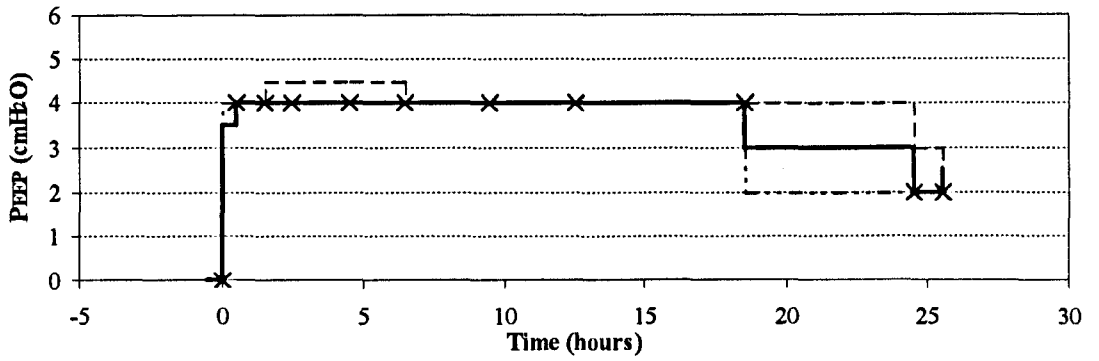
(d)

Key: — Refined Advisor -·- Anaesthetist - - - Prototype Advisor

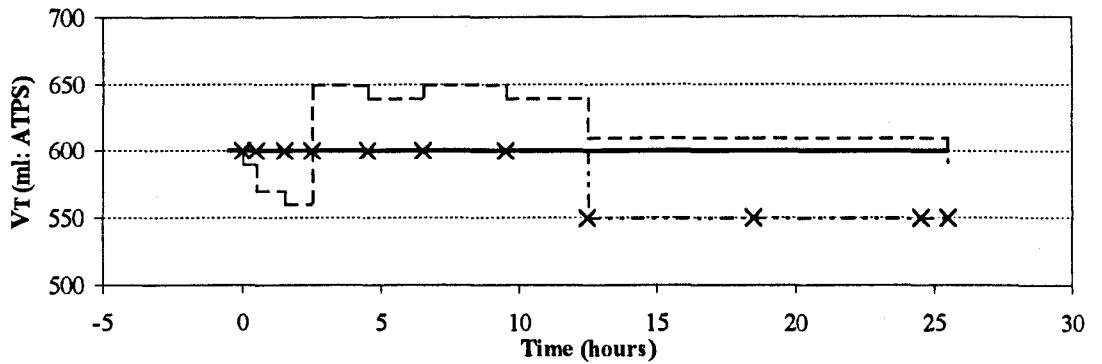
Figure 7.30 (lobar pneumonia) continues overleaf...



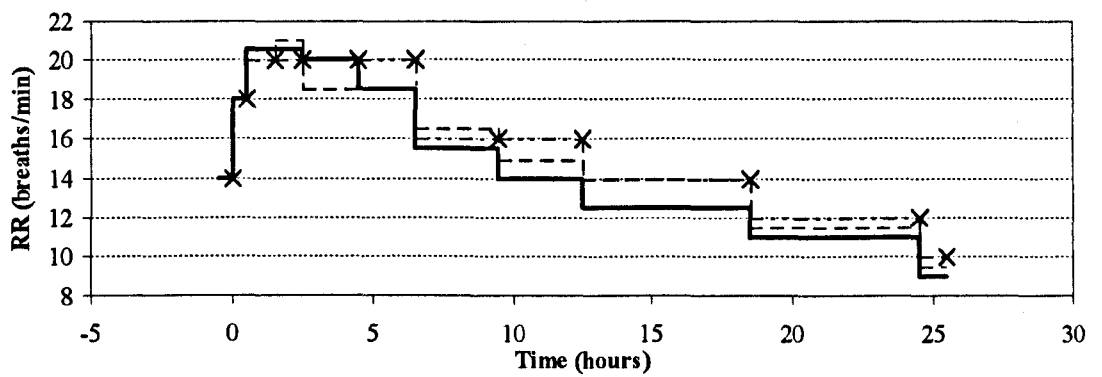
(e)



(f)



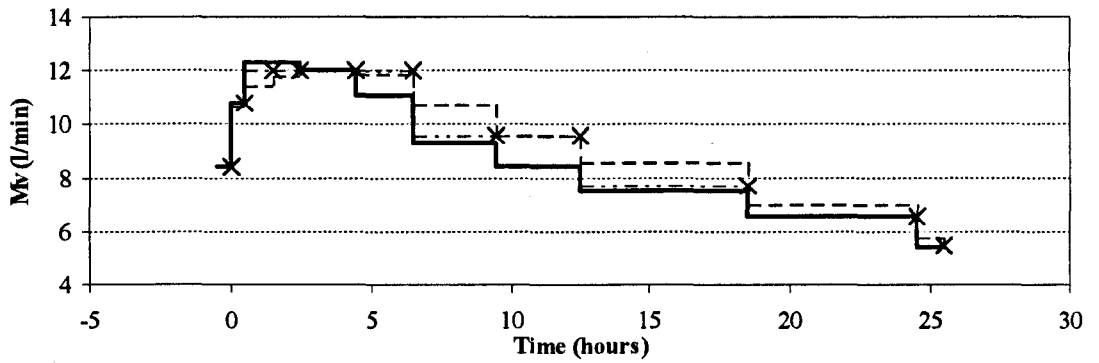
(g)



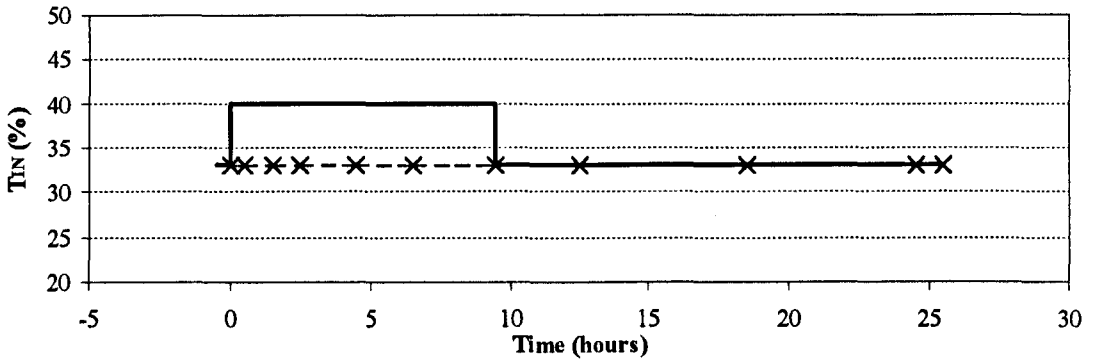
(h)

Key: — Refined Advisor - - x - - Anaesthetist - - - - Prototype Advisor

Figure 7.30 (lobar pneumonia) continues overleaf...



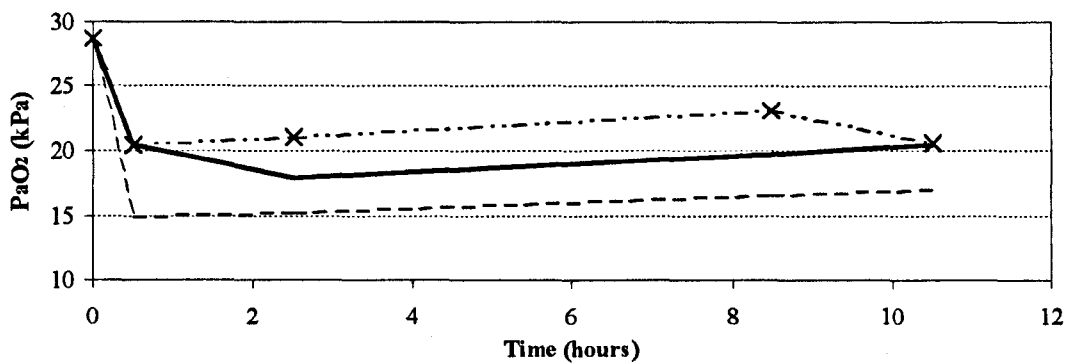
(i)



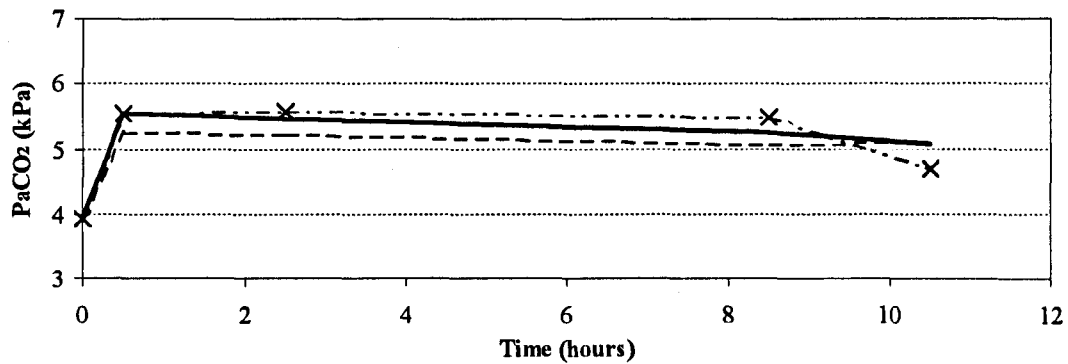
(j)

Key: — Refined Advisor - - x - - Anaesthetist - - - - Prototype Advisor

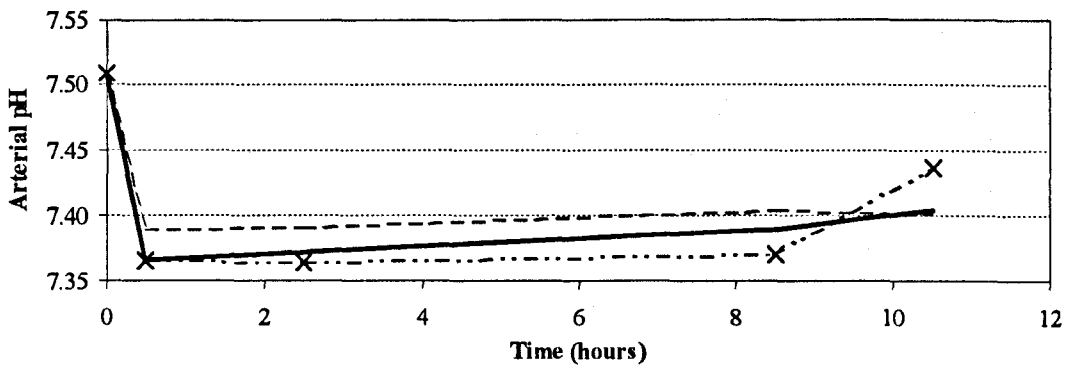
Figure 7.30: Comparison of anaesthetist, prototype advisor and refined advisor decision histories for the **Lobar Pneumonia** patient scenario. Patient responses are shown for (a) PaO_2 , (b) PaCO_2 , (c) arterial pH and (c) PIP. Ventilator changes are shown for (e) FIO_2 , (f) PEEP, (g) VT, (h) RR, (i) MV and (j) TlN.



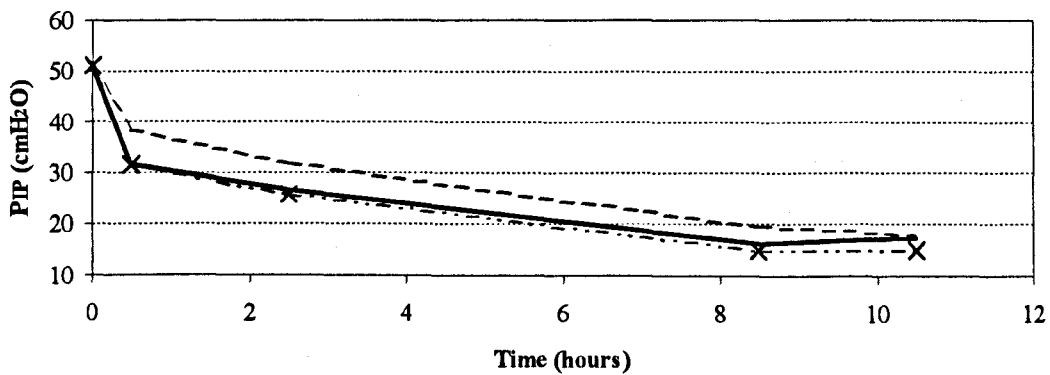
(a)



(b)



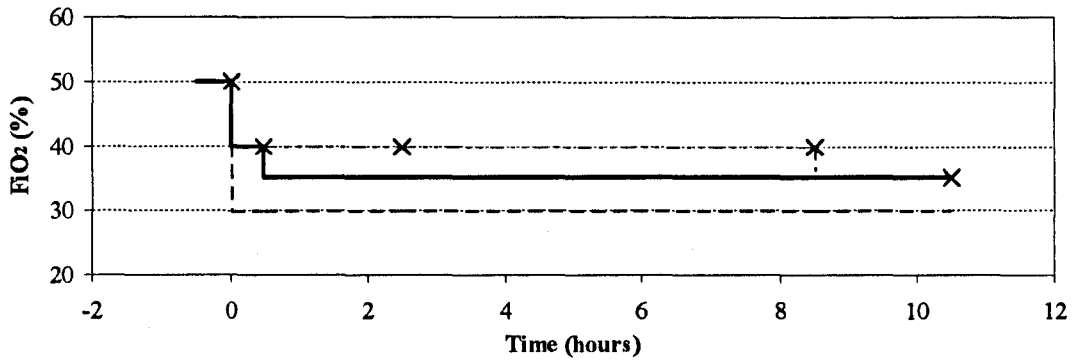
(c)



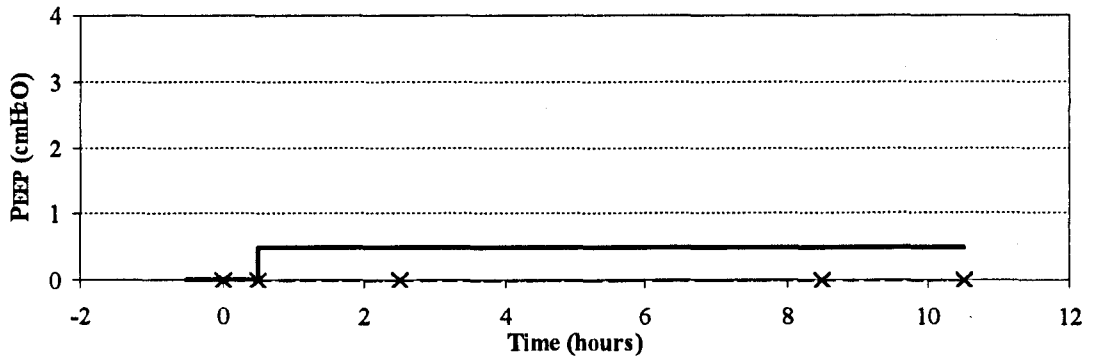
(d)

Key: — Refined Advisor - - x - - Anaesthetist - - - - Prototype Advisor

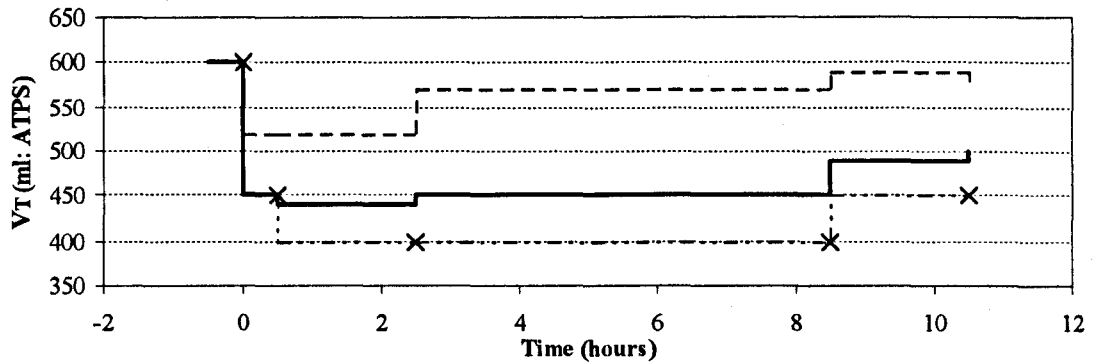
Figure 7.31 (acute asthmatic) continues overleaf...



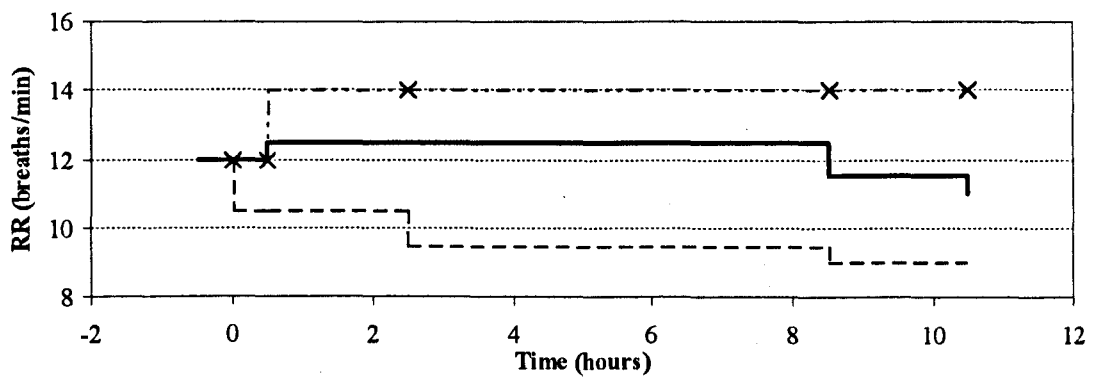
(e)



(f)



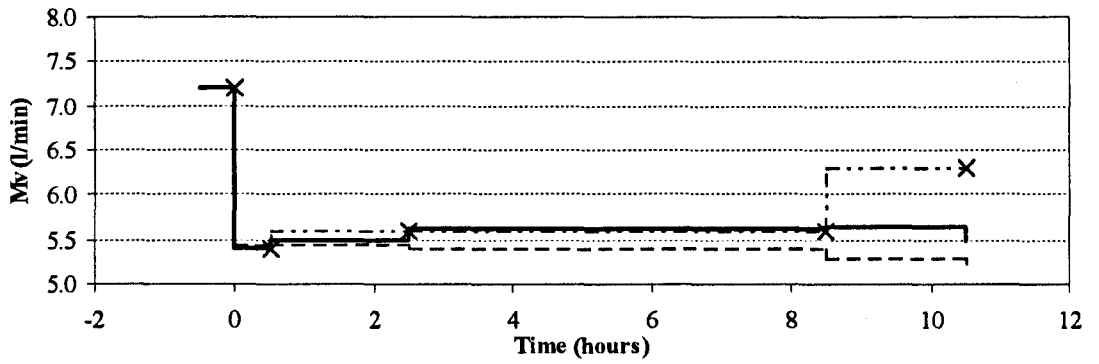
(g)



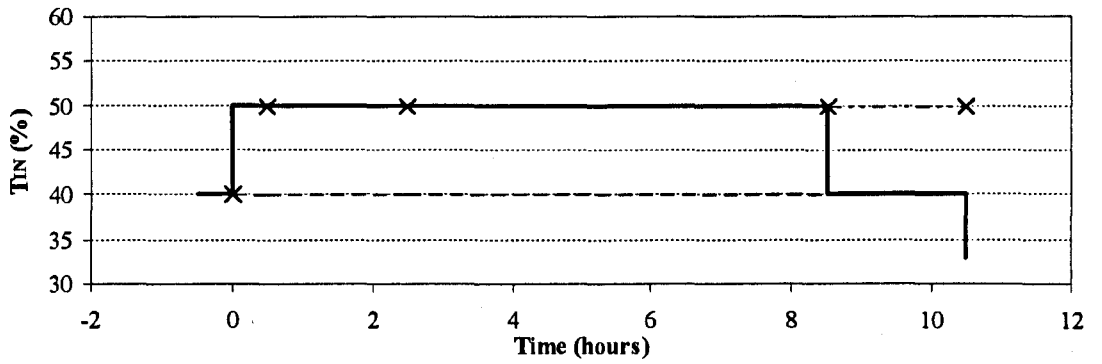
(h)

Key: — Refined Advisor - - X - - Anaesthetist - - - - Prototype Advisor

Figure 7.31 (acute asthmatic) continues overleaf...



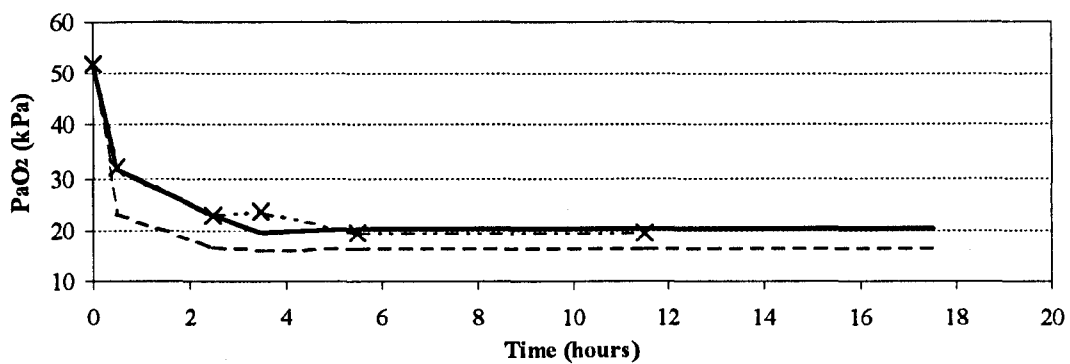
(i)



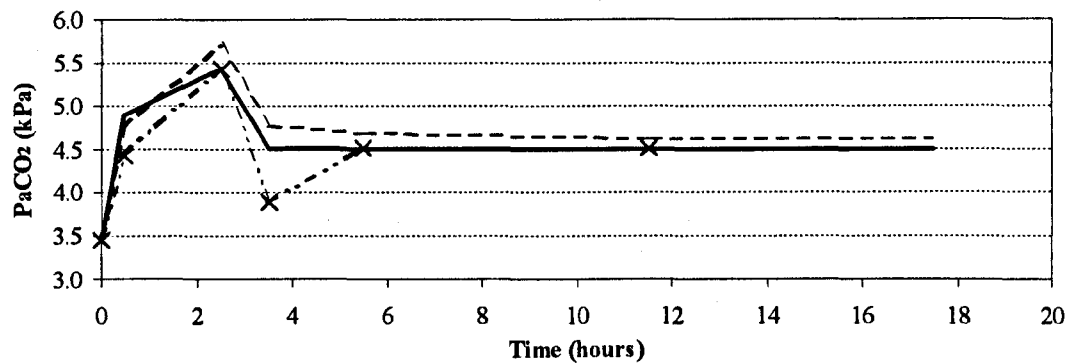
(j)

Key: — Refined Advisor -·-·- Anaesthetist - - - - Prototype Advisor

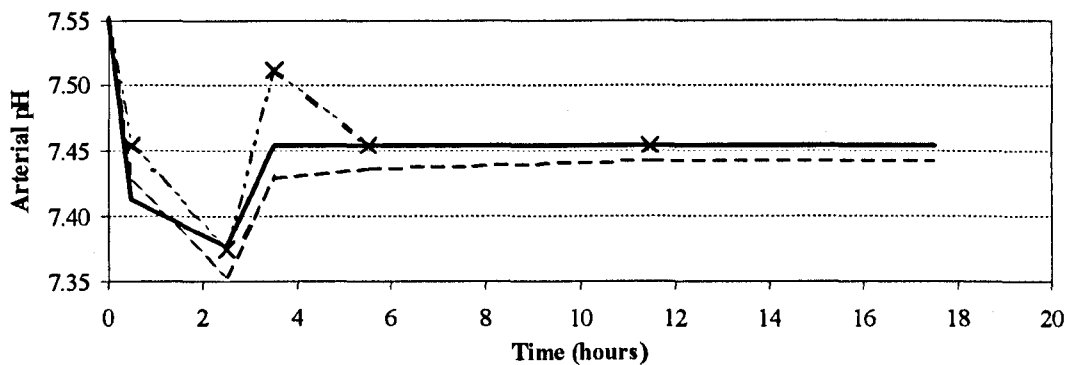
Figure 7.31: Comparison of anaesthetist, prototype advisor and refined advisor decision histories for the **Acute Asthmatic** patient scenario. Patient responses are shown for (a) PaO_2 , (b) PaCO_2 , (c) arterial pH and (c) PIP. Ventilator changes are shown for (e) FIO_2 , (f) PEEP, (g) VT, (h) RR, (i) MV and (j) TIN.



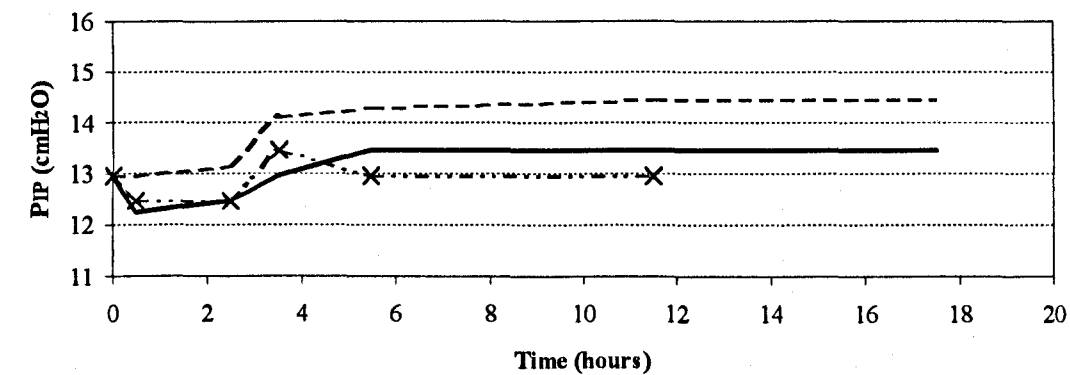
(a)



(b)



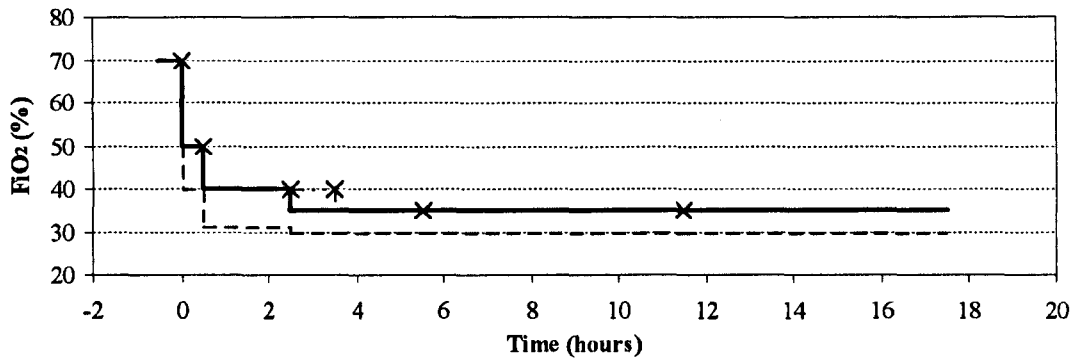
(c)



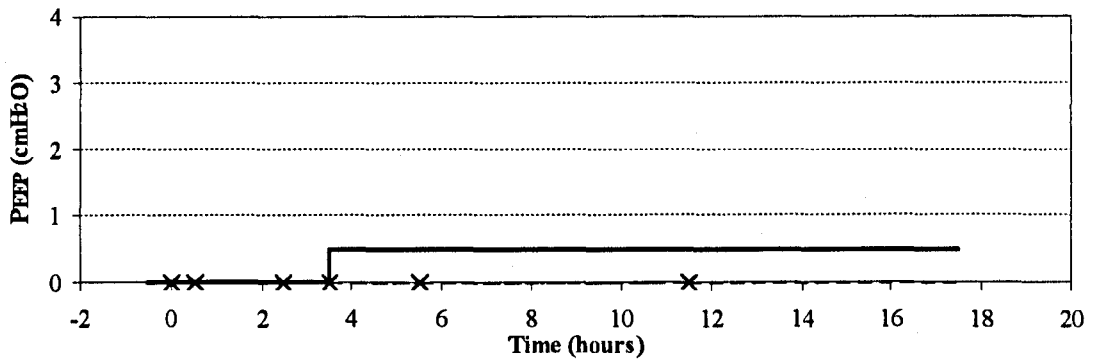
(d)

Key: — Refined Advisor -·-·- Anaesthetist - - - - Prototype Advisor

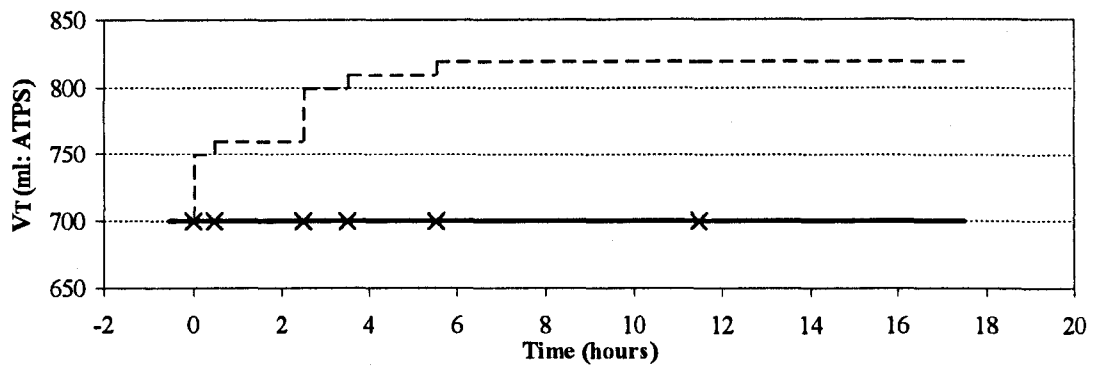
Figure 7.32 (head injury) continues overleaf...



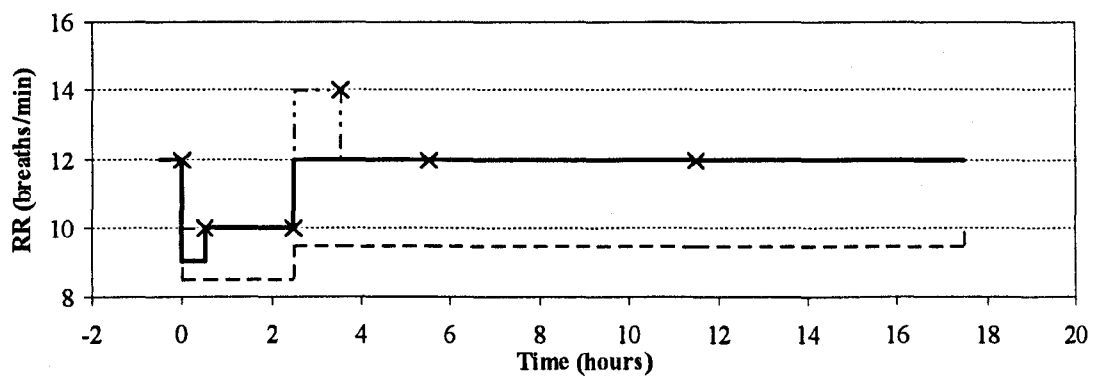
(e)



(f)



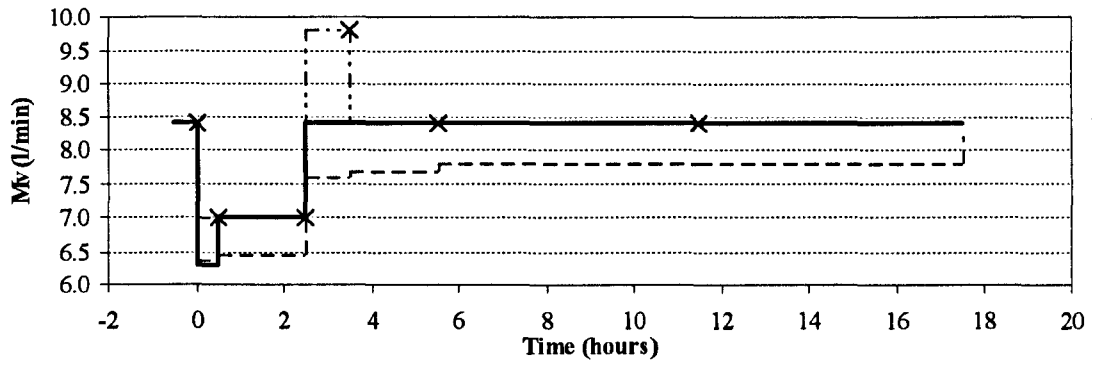
(g)



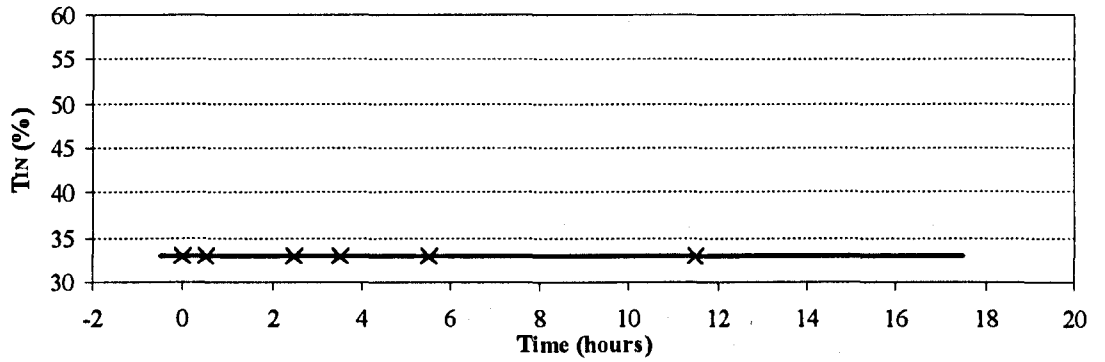
(h)

Key: — Refined Advisor - - x - - Anaesthetist - - - - Prototype Advisor

Figure 7.32 (head injury) continues overleaf...



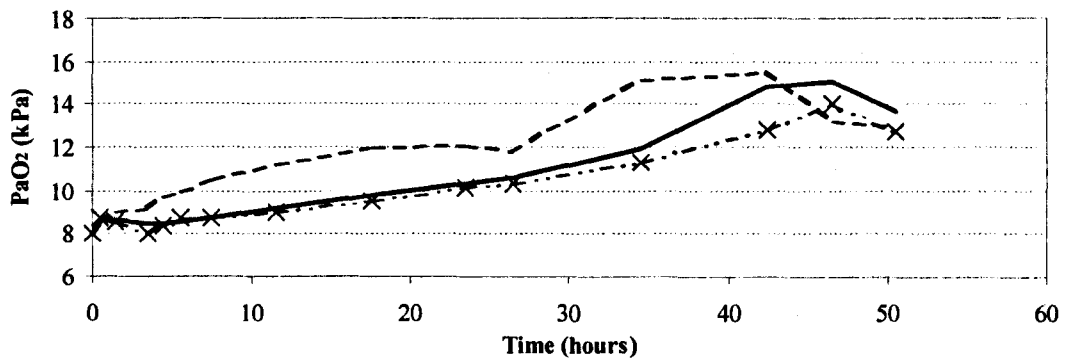
(i)



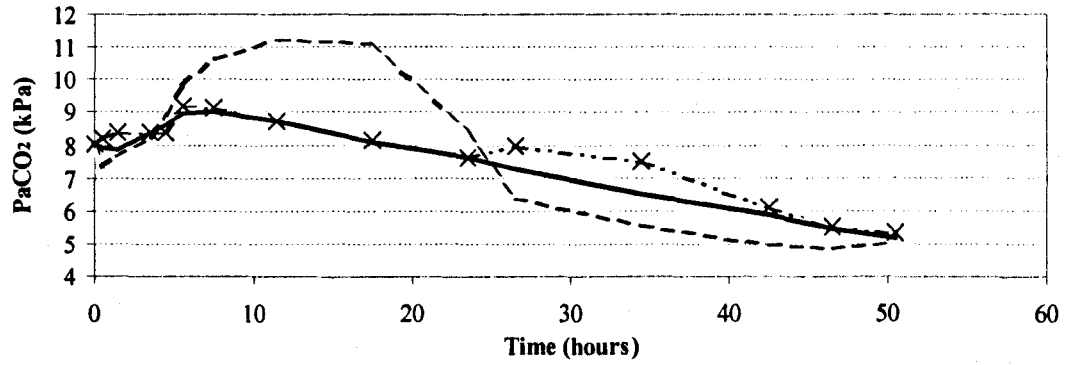
(j)

Key: — Refined Advisor -·x-· Anaesthetist - - - Prototype Advisor

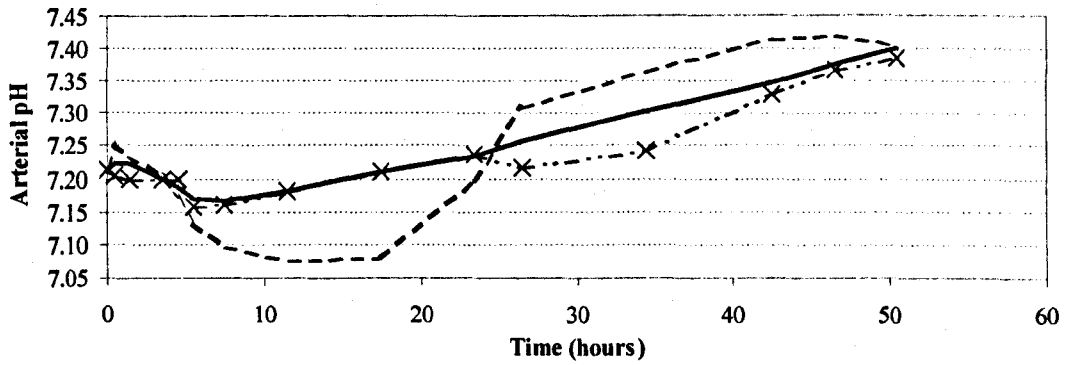
Figure 7.32: Comparison of anaesthetist, prototype advisor and refined advisor decision histories for the **Head Injury** patient scenario. Patient responses are shown for (a) PaO₂, (b) PaCO₂, (c) arterial pH and (c) PIP. Ventilator changes are shown for (e) FIO₂, (f) PEEP, (g) VT, (h) RR, (i) MV and (j) TIN.



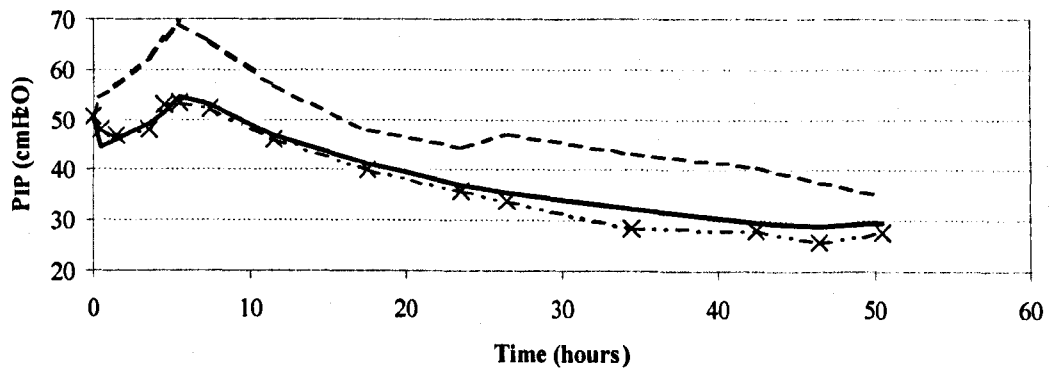
(a)



(b)



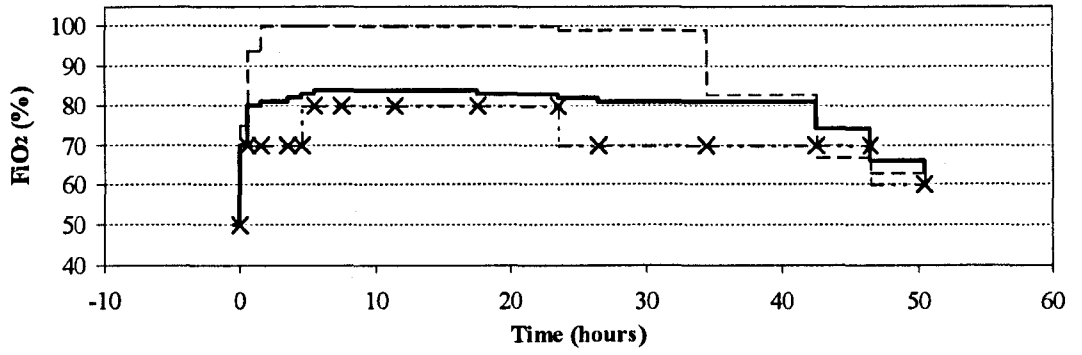
(c)



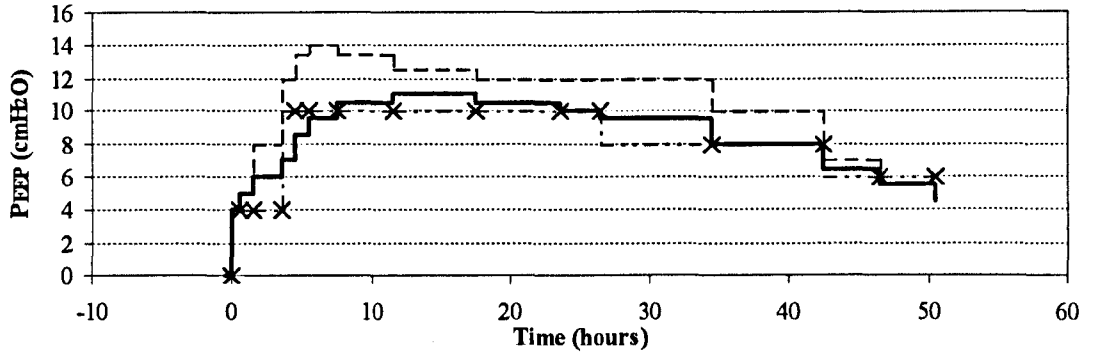
(d)

Key: — Refined Advisor -·-·- Anaesthetist - - - Prototype Advisor

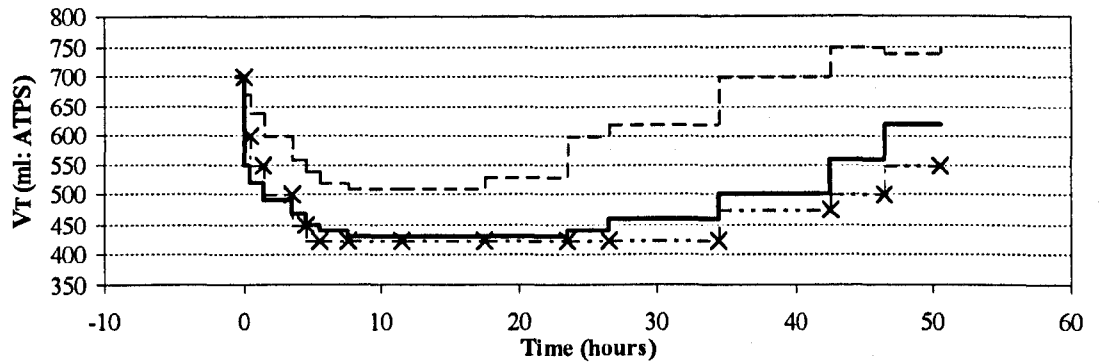
Figure 7.33 (ARDS) continues overleaf...



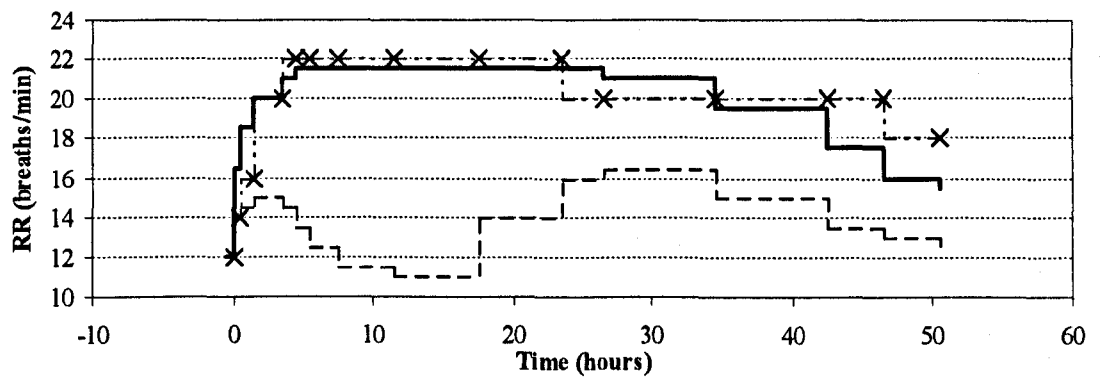
(e)



(f)



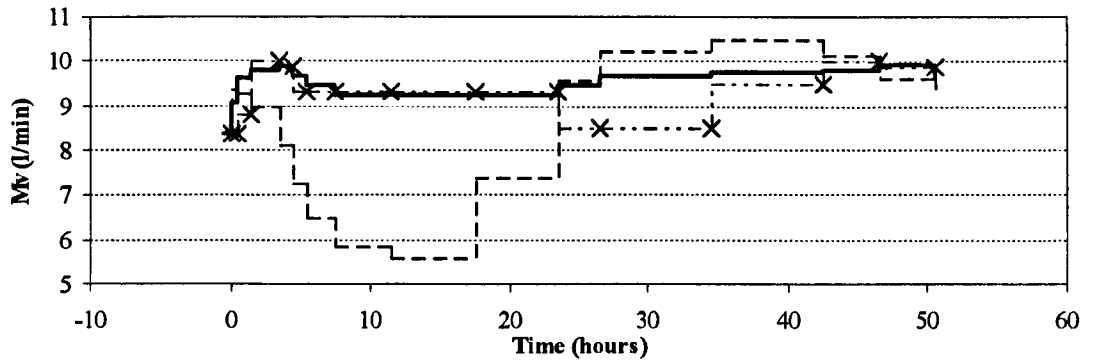
(g)



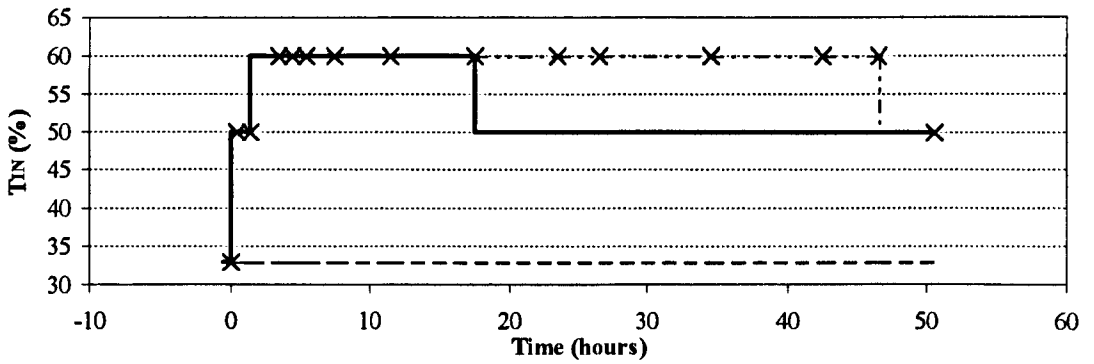
(h)

Key: — Refined Advisor -·-·- Anaesthetist - - - - Prototype Advisor

Figure 7.33 (ARDS) continues overleaf...



(i)



(j)

Key: — Refined Advisor -·x-· Anaesthetist - - - - Prototype Advisor

Figure 7.33: Comparison of anaesthetist, prototype advisor and refined advisor decision histories for the ARDS patient scenario. Patient responses are shown for (a) PaO₂, (b) PaCO₂, (c) arterial pH and (c) PIP. Ventilator changes are shown for (e) FIO₂, (f) PEEP, (g) VT, (h) RR, (i) MV and (j) TlN.

Chapter 8: Clinical Validation of Advisor

8.1 Introduction

The simulated closed-loop behaviour of the modified advisor was shown to give improved decision matching over the prototype rules, and in the majority of cases gave good patient maintenance. However, this was only based upon a sub-set of the possible patient scenarios. It remains to be seen whether the advisor can match decisions made by an anaesthetist using real patient data.

This chapter describes the clinical validation of the advisor using data collected during routine care in ICU. The validation procedure is presented first (see Section 8.2), followed by a synopsis of the data collected (see Section 8.3). This data was then applied to the advisor and the error between the anaesthetists' decisions and the advised decisions was analysed quantitatively using statistical techniques (see Section 8.4) and qualitatively using linguistic scoring (see Section 8.5). The reasons for any decision mismatch observed are then discussed (see Section 8.6).

8.2 Procedure

Ideally clinical validation would be done in an alongside advisory capacity, with the anaesthetist explaining the reasons for each and every change they make, and then commenting on the advice given by FAVeM. However such an exercise would be very time consuming and perhaps not justifiable with the advisor still in its infancy.

Instead data were collected over a 3-week period at the Hull Royal Infirmary ICU, with only patients on volume control (VC) or pressure regulated volume control (PRVC) being recorded. The attending anaesthetists were asked to explain their reasons for the care given and specify patient goals. All available details were recorded for the suitable patients, including admission details, therapeutic objectives, blood-gases, ventilator changes, drugs administered, investigations undertaken and any care events (such as physiotherapy, suctioning, turning, etc). Whilst this amount of information was not required by the advisor, it was felt that it may prove useful in identifying the causes of any decision mismatch observed.

The ventilator/patient observations and PaCO₂ goal required by the advisor were extracted from this data, and the changes advised were then compared with those made by the anaesthetist, see Appendix F. The decision differences were assessed using statistical and qualitative analysis.

In order to provide a yardstick against which the clinical performance could be measured, the statistical and qualitative analysis was also performed on the closed-loop advisor responses, see Figure 8.1. These were the ventilator changes prescribed by the advisor in response to the observations generated by the anaesthetist during their simulated maintenance of the virtual patients (this is the same data used in the correlation analysis of the advisor's closed-loop performance, see Section 7.5). The possible causes of decision mismatch using the clinical data are then discussed.

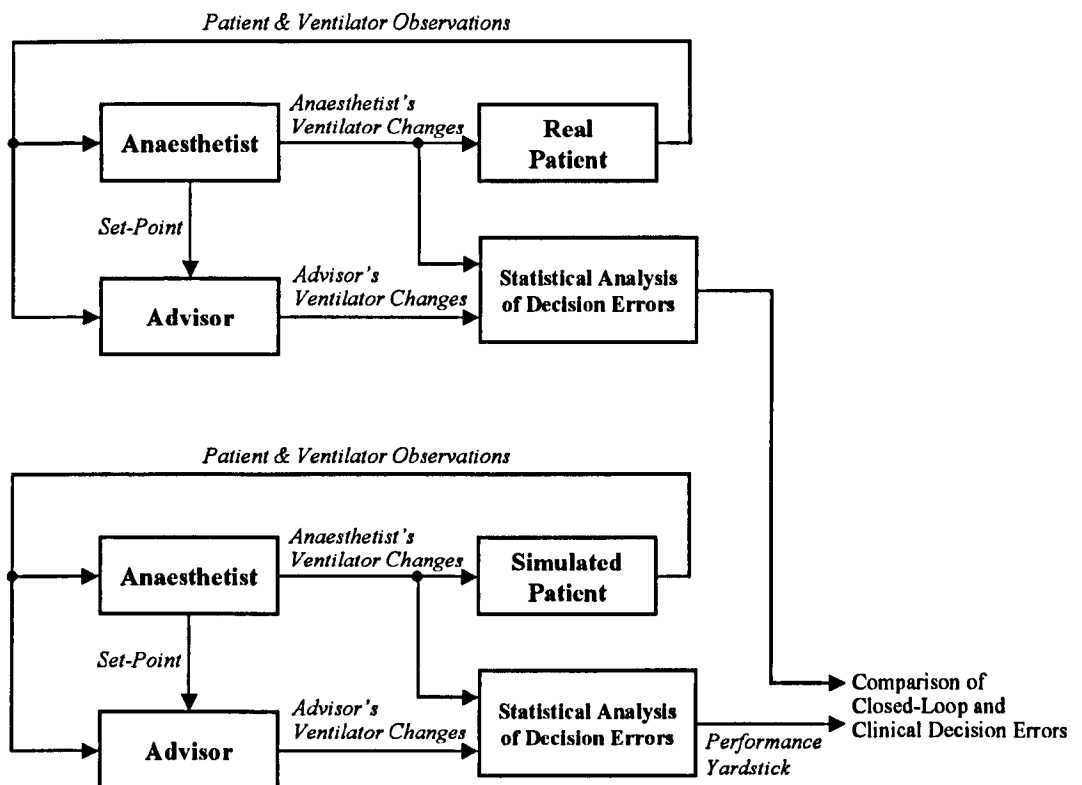


Figure 8.1: Block diagram showing the comparison made between the decision performance of the advisor based on data collected in ICU, and using the data generated by the anaesthetist when performing simulated closed-loop of the virtual patients (yardstick performance). Ideally the clinical performance should be similar to the simulated performance.

8.3 Synopsis of Collected Data

Eleven patients were recorded in total. Ten of these were during the 3-week period at HRI and the eleventh was recorded at Castle Hill Hospital ICU. A brief description of each patient follows, with an indication of the number of usable blood-gas observation and ventilator changes made.

Patient 1: A 58-year-old, male smoker with known COPD (chronic obstructive pulmonary disease) and emphysema electively ventilated following an aorto bi-femoral graft. He required warm-up and fluid support and was placed on PRVC mode of ventilation. This constituted a fairly straightforward ventilation problem with no major lung complications. However, they were haemodynamically challenged. The patient was eventually weaned from the ventilator after a brief spell on pressure support (PS) mode of ventilation. *6 sets of observation data; 6 ventilator changes (2 FIO₂, 2 MV, 2 VT)*

Patient 2: A 27-year-old male admitted to ICU following a motorcycle accident. He had sustained multiple head, chest and limb injuries and was intubated at the scene. The head had massive contusions (swelling) and the pupils were fixed. The chest was bleeding with broken ribs and a pneumothorax (for which 2 chest drains were inserted). He was placed on VC mode of ventilation. The head injury and chest damage were the primary considerations, together with oxygen management. The head injury required good ventilation in order to reduce PaCO₂ and help minimise inter-cranial pressure. However the presence of the pneumothorax complicated matters. The performance of the lung fluctuated depending upon the effectiveness of the drain and also the

amount of air that was being directed into usable lung space. The use of too much ventilation just blew the pneumothorax open. The lungs were also filling due to internal bleeding. Consequently the shunt fraction was increasing, requiring constant suctioning. After suctioning the lung function would improve allowing the FI_{O_2} to be maintained or reduced as appropriate. Data collection was stopped when the patient was transferred onto high-frequency jet ventilation (HFJV). *39 sets of observation data; 48 ventilator changes (18 FI_{O_2} , 3 PEEP, 8 MV, 2 RR, 7 VT)*

Patient 3: A 57-year-old female with COPD, admitted with ventilatory failure after a chest infection. She had also incurred a superior lateral myocardial infarction. Her blood pressure was very low and she had an elevated heart rate (120 b.p.m.). She had probably had a central vascular stroke. Both the heart and lungs were deficient. The lungs were stiff due to COPD and therefore provide a challenge in terms of PIP. She was ventilated using PRVC mode of ventilation. Treatment was eventually withdrawn and the patient died. *25 sets of observation data; 12 ventilator changes (5 FI_{O_2} , 1 PEEP, 2 MV, 2 RR, 2 VT)*

Patient 4: A 28-year-old male admitted following a pedestrian road traffic accident, with possible drugs/drink involvement. He had sustained multiple head injuries and a chest drain was inserted since there was a high risk of pneumothorax. He had no hyperventilation response, and a fixed dilated pupil response, the prognosis was poor. He was ventilated using VC mode of ventilation. Treatment was eventually withdrawn and the patient died. *13 sets of observation data; 13 ventilator changes (3 FI_{O_2} , 4 MV, 3 RR, 3 VT)*

Patient 5: A 74-year-old female with post-ventricular failure, having arrested at home. Her lung condition was good, and she was ventilated using VC mode of ventilation. The patient's progress was poor and she became acutely acidotic with SaO_2 below 95 %. The relatives agreed to withdraw treatment and the patient died. *12 sets of observation data; 13 ventilator changes (4 FI_{O_2} , 1 PEEP, 2 MV, 2 RR, 4 VT)*

Patient 6: A 71-year-old female with sepsis in the lung or abdominal region, occurring after surgery. The patient was beginning to show evidence of ARDS, with general stiffening of the lungs as exhibited by elevated PIP levels. Patient was initially ventilated using VC, which was later changed to PRVC. She made steady improvement and were weaned after 3-days. *12 sets of observation data; 14 ventilator changes (8 FI_{O_2} , 3 MV, 3 RR)*

Patient 7: A 76-year-old male with complications, following hindquarter amputation. This amputation was required, after surgery to remove an aneurysm resulted in vascular failure. The patient had become slightly septic with bilateral chest consolidation. They were ventilated using PRVC mode of ventilation. His condition became progressively worse with increased shunt and reduced PaO_2 . The patient died after 10-days of treatment. However only the first two days were recorded. *8 sets of observation data; 13 ventilator changes (4 FI_{O_2} , 2 PEEP, 2 MV, 2 RR, 1 VT)*

Patient 8: A 71-year-old female requiring ventilation after an operation to repair a perforated bowel. Only one ventilator change was usable since the patient soon began triggering breaths for themselves. The patient was eventually weaned from ventilator. *1 set of observation data; 1 ventilator change (1 FI_{O_2})*

Patient 9: A 59-year-old male being ventilated post-operatively, following a right carotid endarterectomy. Patient had a mild stroke during surgery and periods of bradycardia (< 40 b.p.m). They had a myocardial infarction 3-years ago and a history of hypertension. His lungs were healthy and he was ventilated initially using VC mode of ventilation then switched to PS (pressure support). The patient was weaned after over night observation. *3 sets of observation data; 2 ventilator changes (2 FIO₂)*

Patient 10: A 48-year-old female heavy smoker with hypertension, admitted after arrest at home. Lungs stiff requiring PRVC mode of ventilation. Cardio function was initially unstable and the patient arrested at the first attempt to wean. Patient successfully weaned after cardiac function stabilised. *5 sets of observation data; 3 ventilator changes (1 FIO₂, 1 MV, 1 VT)*

Patient 11: A previously healthy 75-year-old male admitted from theatre, following an elective aortic aneurysm repair. Initially ventilated using VC, then switched to PC (pressure control). Patient was mildly acidotic, with moderate lung stiffness. *2 sets of observation data; 4 ventilator changes (2 MV, 2 RR)*

8.4 Statistical Performance Analysis

The mean error (\bar{E}), standard error ($\sigma_{|E|}$), mean absolute error ($|\bar{E}|$), maximum error ($|\hat{E}|$) and correlation coefficient (r) between the changes made by the anaesthetist and those proposed by the advisor, were calculated for each ventilator control. The results of this analysis are shown in Table 8.1, and was repeated using the simulated closed-loop data, to provide a measure against which the clinical performance could be compared, see Table 8.2. A value for the TIN correlation coefficient using the clinical data is not given since no changes were made by the anaesthetist, causing the sum of the squared deviations to be zero and hence the result of the correlation formula to be ∞ . It should also be noted that in 25 cases the TIN was not recorded and therefore no TIN advice could be generated in these instances.

It is clear from this analysis that the advisor's ability to match the anaesthetist's decisions was measurably worse than observed using the closed-loop data. This is not unexpected since the virtual patients are well behaved and not subject to the measurement errors that occur in the real ICU setting.

The best performance was observed in the FIO₂ decisions, with a correlation of $r = 0.751$. However, $|\bar{E}|$ was almost twice that observed using the closed-loop data and $|\hat{E}|$ of 21 % was unacceptably large.

In addition to the increased absolute mean and standard deviation of the errors, there was also a bias observed in the VT and RR decisions. The advisor was tending to prescribe lower VT and higher RR than the anaesthetist did. This is confirmed if we compare the frequency distribution of the decision errors produced using the clinical and closed-loop data, see Figure 8.2. In some cases this was caused by therapeutic considerations outside of the advisor's knowledge. In others it appears to be simply a question of different treatment styles, see Section 8.6.

Control	\bar{E}	$\sigma_{\bar{E}}$	$ \bar{E} $	$ \hat{E} $	r
FI _O ₂ (%)	-0.75	6.37	4.37	21.00	0.751
PEEP (cmH ₂ O)	-0.40	1.93	1.44	7.00	0.176
MV (l/min)	-0.23	1.58	1.13	5.40	0.430
RR (rpm)	1.04	1.82	1.70	6.00	0.276
VT (ml)	-77.0	69.9	85.9	270.0	0.258
TIN (%)	4.72	4.07	4.72	15.00	-

Table 8.1: Statistical analysis of decision errors between actual ventilator changes and those proposed by the advisor using the clinical data.

Control	\bar{E}	$\sigma_{\bar{E}}$	$ \bar{E} $	$ \hat{E} $	r
FI _O ₂ (%)	0.89	3.97	2.37	10.00	0.891
PEEP (cmH ₂ O)	-0.24	0.95	0.55	4.00	0.781
MV (l/min)	-0.10	0.48	0.34	1.37	0.909
RR (rpm)	-0.43	1.07	0.80	2.50	0.860
VT (ml)	8.68	25.00	15.26	70.00	0.891
TIN (%)	-0.76	4.72	2.39	10.00	0.653

Table 8.2: Statistical analysis of decision errors between actual ventilator changes and those proposed by the advisor, using the simulated closed-loop data (see Figure 8.1 for clarification of the difference between clinical and simulated closed-loop data).

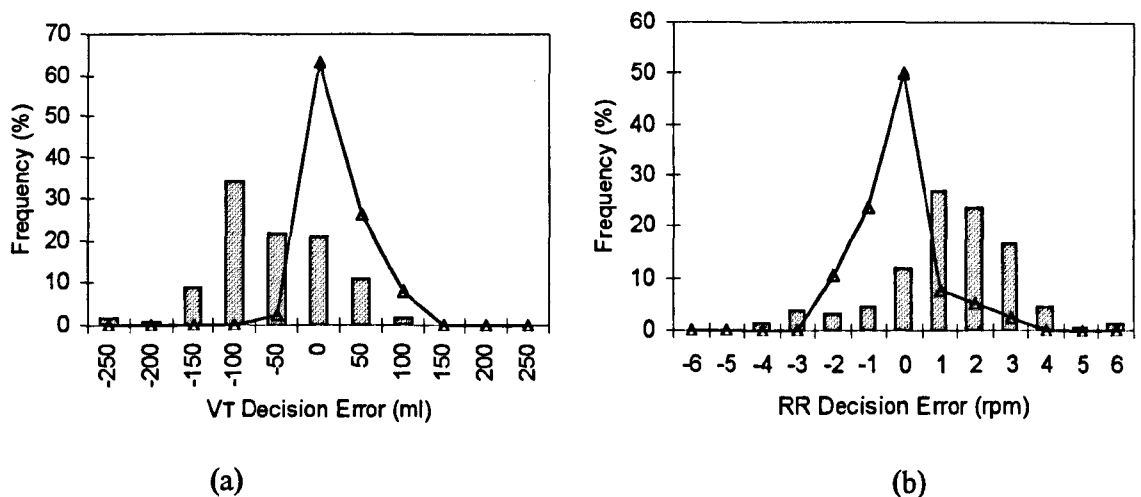


Figure 8.2: Frequency distribution of the decision errors for (a) tidal volume and (b) respiratory rate between the actual and advised changes using the clinical data (grey bars) and simulated closed-loop data (black line).

8.5 Qualitative Performance Analysis

Whilst the statistical analysis gives us a measure of the relative performance of the advisor, it does not indicate what number of the decisions match the anaesthetists exactly, how many are good approximations and how many are just not acceptable.

Calculating the frequency distribution of the errors does not identify decisions that have relatively small errors but represent ventilator changes in different directions. These are more likely to be unsafe than changes being made in the same direction. It was therefore proposed to use a qualitative scoring approach. The computed advice was classed as either *exact*, *good*, *moderate* or *poor* (X), with the classification criteria defined as follows;

- 1). *exact* – when the advised decision (x) exactly matches the anaesthetist's (y);

$$x - y = 0 \quad (8.1)$$

- 2). *good* – when the error between the advised (x) and anaesthetist decision (y) is less than or equal to some threshold (A);

$$|x - y| \leq A \quad (8.2)$$

The choice of threshold for each ventilator setting is given in Table 8.3. These were chosen to be equal to the smallest ventilator changes normally made by an anaesthetist.

- 3). *moderate* – when the decision error is less than some higher threshold (B) and the change is not in opposing directions;

$$|x - y| \leq B \text{ AND } (\text{sign}(x) = \text{sign}(y) \text{ OR no change in either } x \text{ or } y) \quad (8.3)$$

The threshold (B) for each ventilator setting was double that for A , see Table 8.3.

- 4). *poor* (X) – the decision error is greater than B , or greater than A and in the opposite direction;

$$|x - y| > B \text{ OR } (|x - y| > A \text{ AND } \text{sign}(x) = -\text{sign}(y)) \quad (8.4)$$

Ventilator Control	A	B
FiO ₂ (%)	5	10
PEEP (cmH ₂ O)	1	2
MV (l/min)	0.5	1
RR (rpm)	50	100
VT (ml)	1.5	3
TIN (%)	5	10

Table 8.3: Qualitative scoring thresholds *good* (A) and *moderate* (B), for each ventilator control.

Each decision was scored using these classification criteria and the individual results are shown in Appendix F, together with the scoring frequency for each ventilator control across the entire data set (see Table F.2).

Obviously the choice of scoring threshold will greatly affect the frequency distribution. Therefore, in order to provide a standard against which the clinical performance can be measured the above scoring algorithm was also applied to the closed-loop decisions, see Table F.3.

Figure 8.3 compares the percentage distribution of the decision scoring for the clinical and simulated data. It can be clearly seen that the clinical performance was worse than the simulated performance in every ventilator control. Considering all the decisions together, the advisor gave *exact* or *good* matching in only 48.6 % of cases, compared to 82.5 % using the closed-loop data. Of greater concern though is that 23.5 % of the advice given was a *poor* match. Such a level of mismatch is not tolerable.

8.6 Discussion

This poor level of performance is perhaps to be expected since examination of the clinical data identified several possible causes of decision mismatch. These are as follows;

Anomalous Decisions

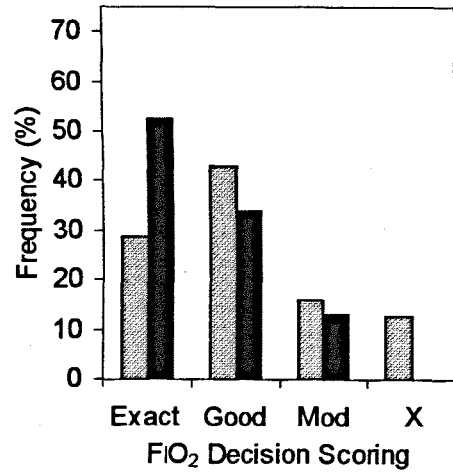
This includes changes made by the anaesthetist that seem contrary to all the clinical indications, and are often corrected at the next blood-gas sample or sooner. This occurs relatively infrequently, although similar decision errors were observed during the simulated closed-loop ventilation (see Section 7.4).

An obvious example occurred in the clinical data at observation 1 in Patient 1, when the anaesthetist increased MV from 7.5 up to 8.0 l/min despite the PaCO₂ being on the low side of normal. This was corrected one hour later, at the next blood-gas sample time.

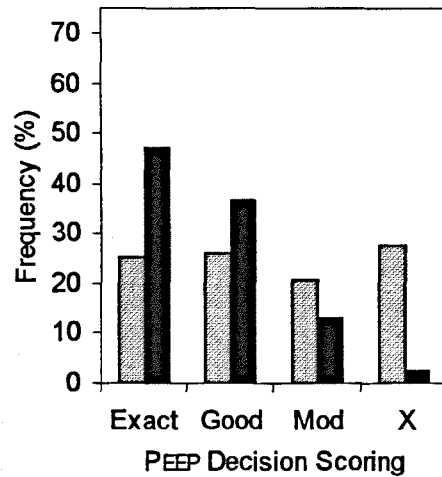
Advisor Naivety

This is when the anaesthetist's decisions are based upon information outside of the advisor's knowledge paradigm. This often includes reluctance by the anaesthetist to make ventilator changes until other treatment possibilities have been considered, even when presented with measurements that would suggest otherwise. This probably constitutes the main cause of decision mismatch and was highlighted in the motor-cycle accident patient (Patient 2), where many of the decisions were delayed or contraindicated by extenuating factors. For example;

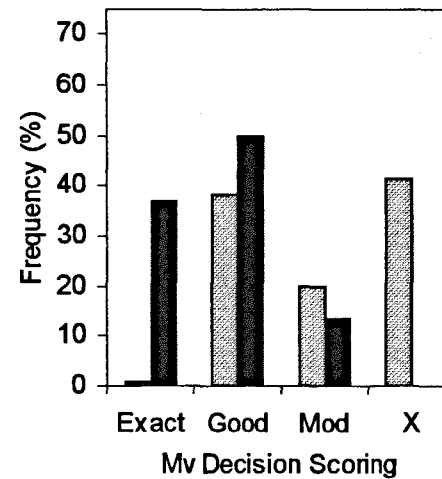
- 1). A larger VT was employed to maintain the level of ventilation necessary to keep PaCO₂ at approximately 4 kPa. This was a difficult compromise between the need for low PaCO₂ (because of head injury) and air being lost through the pneumothorax and chest drain.
- 2). FiO₂ was not increased in response to falling PaO₂ as this was caused by blood filling the lungs. This was suctioned first, with the FiO₂ only being increased if the PaO₂ did not improve.



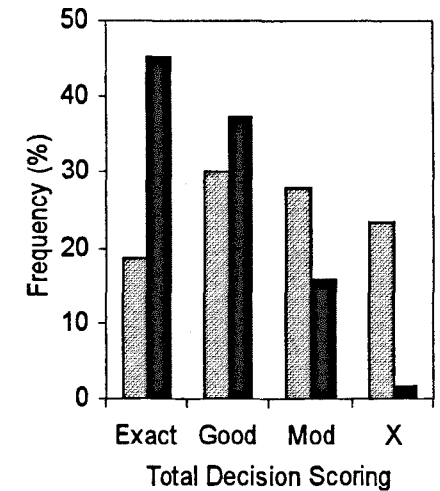
(a).



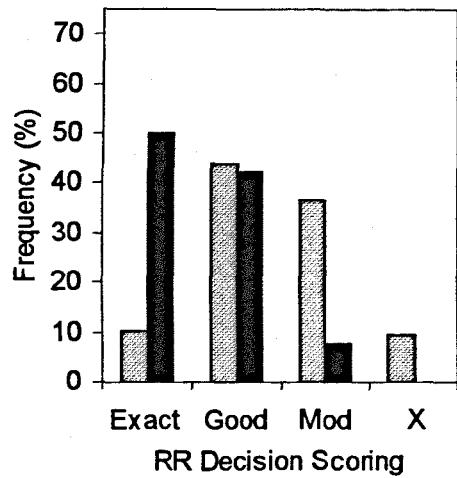
(c).



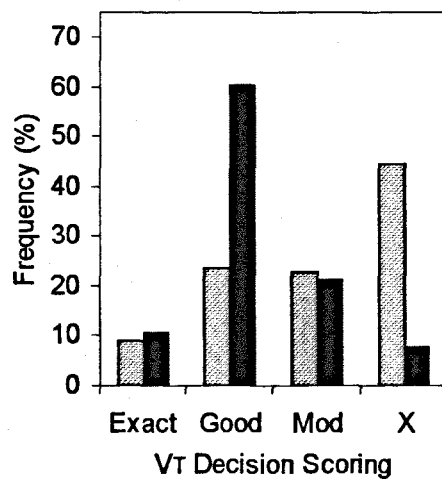
(e).



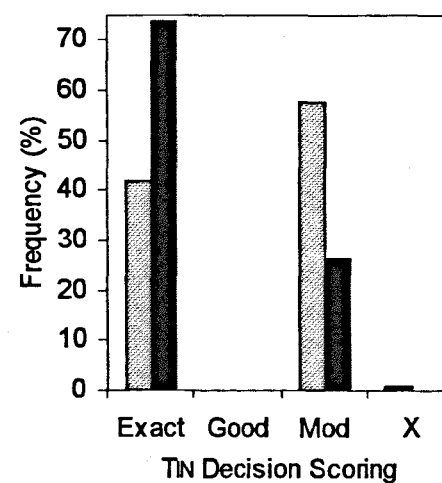
(g).



(b).



(d).



(f).

Key:
 Clinical Data
 Simulated Data

Figure 8.3: Frequency distribution (expressed as percentage of total) of the decision scoring for (a) FIO₂, (b) RR, (c) PEEP, (d) VT, (e) MV, (f) TN and (g) all decisions considered together. Scoring is compared for the clinical data and the simulated data (see key). Actual score frequency and percentages are shown in Table F.2 (see Appendix F)

Differing Therapeutic Styles

Anaesthetists do not approach patient treatment in the same way. Therefore the advisor's decisions may score less favourably against one anaesthetist than another. What is important is that the computed advice is safe, and has a variance smaller than the variability in the anaesthetists' decisions. This is an important consideration for future work (see Chapter 9).

For example the advisor always increased TIN from 25 % to 33 %. Some anaesthetists set a normal I:E ratio using a TIN of 33 %, ignoring any pause time. Others include TPAUSE (usually set at 10 %) and therefore reduce TIN to 25 % accordingly. Which one is correct? The advisor is correct using the first case, but wrong with respect to the second.

Measurement Rejection

The advisor takes the observation data at face value, whereas the anaesthetist may be suspicious of sudden changes. For example a sudden fall in PaO₂ if not met by a similar drop in SaO₂ would be rejected as a measurement error and the blood-gases reanalysed.

Anaesthetist Not Present

During the night when an anaesthetist is on-call they will only be requested to make changes to the ventilator settings if the patient condition worsens. The patient measurements are still recorded and may indicate an improvement that the advisor would respond to, but do not require intervention by an anaesthetist. Obviously the time at which an observation is made has an important bearing on any changes made. This would need including into the advisor rules and highlights the need for hierarchical control (see Chapter 9).

Set-point Ranges

The advisor uses a single set point for PaCO₂ whereas the anaesthetist will stop making changes to MV when the PaCO₂ is within an acceptable range. Consequently the advisor continues to make unnecessary refinements to the level of MV. A similar problem exists for normal RR and VT settings.

Genuine Rule Errors

Despite the above causes of decision mismatch, there will be occasions when the difference is simply a matter of an incorrect rule-consequent or the need of a new observation class / variable, to better separate the decision space. Possible examples of these and suggested modifications are given below;

- 1). In Patient 2, at the beginning of ventilation the clinician was more cautious in reducing the FIO₂ than the advisor. This seems to correspond to the margin of safety observed during the closed-loop validation. The PaO₂ is reasonable at approx. 20 kPa but not high enough to warrant the size of changes proposed by the advisor. The consequents at $PaO_2 = HI$ and $FIO_2 = EHI/MAX$ need reducing from -35 % to -10 % and at $PaO_2 = SHI$ and $FIO_2 = EHI$ from -20 % to -10 %.
- 2). The inclusion of a new PaO₂ set at 20 kPa, or the peak of HIGH changed from 25 kPa to 20 kPa, since this seems to be a common PaO₂ level giving a margin of safety in the patient's oxygenation.

- 3). In Patient 6 the clinician is allowing permissive hypocapnia to compensate for the acute acidosis and keep pH above 7.25, as defined in the therapeutic goals. This indicates the need for pH as an observation variable, as originally proposed in the prototype MV control rules. This had been removed in the modified advisor. It appears to be the set definitions that were incorrect, requiring instead a much wider set membership for normal pH.

8.7 Summary & Conclusions

The clinical performance of the advisor was disappointing, with only the FIO_2 control giving a reasonable level of decision matching. However, the validation process has highlighted areas that need to be addressed before the advisor can be considered *safe*. It is only when a certain level of safety has been achieved, that bedside clinical trial can be commenced. The following features need to be incorporated into the advisor if it is to perform safely.

- 1). The advisor must be able to detect and ignore possible measurement errors. This is a measure of its robustness.
- 2). Changes need to be negated when the patient's gases lie within a set-point range. This is more critical in patients where unnecessary modification to the ventilation can destabilise their condition. As it stands the advisor is too sensitive to input changes close to the PaCO_2 set-point goal.
- 3). The ability to wait to see if a patient's condition is making slight improvement before adopting a more aggressive ventilation regime. Again this is more critical in patients that may be destabilised by changes in their ventilation.

The best strategy to meet these shortfalls is through the use of carefully constructed patient scenarios that match some of the complex clinical behaviour observed. These will be repeatable and enable the improvements in advisor performance to be quantified.

This concludes the description of all work undertaken thus far. The final conclusions are given in the next chapter together with considerations for future work.

Chapter 9: Conclusions & Future Work

This thesis has described the development of a fuzzy-based advisor for the maintenance of patients on artificial ventilation in ICU. It has been shown that the use of a computer-model of the respiratory process provides a rapid methodology for rule-elicitation, validation and refinement. Simulated closed-loop assessment of the advisor performance, together with feedback from a clinical expert, rapidly highlighted rule errors. It also enabled the identification of non-convergent and limit-cycle behaviour in the rules, a function not possible using real clinical data. The model allowed the representation of a wide range of patient patho-physiology and unlike recorded patient data enabled quantitative evaluation of the efficacy of alternative advisor rules. This model-based approach forms a strong platform for future advisor development and testing, enabling confidence to be established in the advice generated before bedside testing is commenced.

Patient Model Development & Validation

About half of the research project involved the selection and development of a suitable patient model and its validation against clinical data. The model developed was selected for its ability to represent a variety of respiratory pathology and trauma whilst avoiding excessive complexity. The majority of its parameters are routinely monitored in a typical ICU environment, therefore minimising the number of system unknowns. By keeping these unknowns to a minimum it was possible to match the model to real patient data using a solution-searching algorithm. This model can be classed as a white-box model since it is physiologically meaningful and interpretable.

The model selected used a compartmental structure similar to that employed by Dickinson (1977) in earlier work and by Thomsen et al (1989) in recent extensive studies. It described pulmonary gas exchange in the lungs using three functional areas or compartments (Riley & Cournard, 1949); an ideal alveolus, where all gas exchange takes place, a dead space representing lung areas that are ventilated but not perfused, and a shunt that is a fraction of cardiac output, representing both anatomical shunts and lung areas that are perfused but not ventilated. The circulatory system was divided into 4 additional compartments representing the alveolar, tissue, venous and pulmonary pools. Only the transport of O₂ and CO₂ were modelled and these were linked through the inverse gas dissociation functions (Kelman 1966 and 1967). These functions were used to derive the partial gas pressures that drive diffusion across the lung membrane from gas contents, as well as generate the model outputs of arterial and venous PO₂ and PCO₂.

No attempt was made to model the respiratory control of ventilation since it was assumed that the patients were on mandatory ventilation and performing no breathing for themselves. A continuous-ventilation model of the lung was chosen over breath-by-breath models since it more than adequately described the changes in PaO₂ and PaCO₂ routinely monitored in ICU. The use of a breath-by-breath model would only have added unnecessary complexity.

Classical sensitivity analysis of the model parameters was performed, and it identified cardiac output (\dot{Q}_t), O₂ consumption (\dot{V}_{O_2}), CO₂ production (\dot{V}_{CO_2}), shunt (\dot{Q}_s/\dot{Q}_t) and dead space (VD) to be of particular importance to blood-gas outcomes. Since these parameters are not

routinely measured, clinical validation of the model was difficult. Cardiac output is subject to large measurement errors and is only monitored in patients with unstable cardiac function making them less suitable for study. The measurement of $\dot{V}O_2$ and $\dot{V}CO_2$ requires the use of a metabolic computer and it was therefore necessary to borrow one for the purposes of the study. Unfortunately it was only available for a limited period, greatly reducing the amount of clinical data that could be collected. Four patients were recorded in all, representing 9 ventilator changes.

The data collected were used to investigate the model's ability to predict arterial and venous blood-gases in response to changes in ventilator settings. This was achieved by applying the patient measurements prior to any ventilator change to the model, and then iteratively adjusting shunt, dead space and P_{50} until the simulated steady-state blood-gases matched those measured. The ventilator changes made on the real patients were then applied to the tuned model, and the simulated and actual responses compared.

The model was shown to be qualitatively correct. However, establishing whether it can give accurate quantitative blood-gas predictions is unlikely without the collection of further clinical data that is both well behaved and free from measurement error. Until regular and accurate measurement of \dot{Q}_t , $\dot{V}O_2$ and $\dot{V}CO_2$ become available and data are routinely logged on a patient data management system for easy retrieval, true clinical validation will be difficult. The correlation coefficients and standard deviation of the response errors indicated only moderate predictive performance, but these results were comparable with those obtained by Hinds et al (1983) in a similar study.

However this did not undermine the suitability of the model for advisor rule-validation, since it was possible to construct virtual patient scenarios that exhibited behaviour similar to the types of patient encountered in ICU. Five virtual patient scenarios were modelled in order to test the advisor rules. These represented routinely encountered patient types and included; a patient with healthy lungs being ventilated post-operatively, an acute asthmatic, a patient with lobar pneumonia, a patient with head injuries and a patient with acute ARDS. The scenarios were constructed to be as realistic as possible but also typical of the patient-types they represented. When an anaesthetist was asked to ventilate the virtual patients, they felt that the model responded as expected to ventilator changes and were representative of the pathologies simulated.

The model was originally developed to simulate patients on continuous mandatory ventilation (CMV); in particular volume control (VC) and pressure regulated volume control (PRVC). Obviously this only represents a sub-set of the modes currently in use. Other ventilation modes include synchronised intermittent mandatory ventilation (SIMV) where the breaths are synchronised to patient effort, and continuous positive airway pressure (CPAP) where the patient is breathing for themselves but is given support to maintain lung volume and oxygenation. If the advisor is to be valid in all possible scenarios, then the model used for simulated closed-loop validation will only be useful if it can represent these modes of ventilation and the majority of pathologies encountered in ICU. This will require better modelling of the airway dynamics and their interaction with the ventilator, as well as better models of the ventilators themselves. It may also require the inclusion of models relating to the respiratory control of ventilation, since as the patient moves from CMV (perhaps via SIMV) to

CPAP the patient begins to breath unaided. However, the inclusion of greater model complexity must be carefully balanced against its ability to be tuned to real patient data.

Other areas for possible model improvement and investigation include; the addition of alveolar compartments representing \dot{V}/\dot{Q} mismatch and the investigation of the causes of steady-state PV_{O_2} error and identification of methods to tune it to observed values. Finally, the manner in which shunt and dead space respond in different disease states or traumas may best be modelled using statistical or neuro-fuzzy sub-systems. In this way the basic model structure will remain simple, with more complex behaviour being switched in and out as required. This will create a grey-box model of a patient's patho-physiology and provide a balance between physically describable physiology and more complex variable interactions.

Advisor Development & Validation

Initial control rules were handcrafted using known physiological relationships, nomograms and via discussion with an anaesthetist. Individual rule-bases were constructed for FIO_2 , PEEP, MV and VT-RR control. This was later extended to include rules for I:E control through changes to TIN.

The prototype advisor was then connected to the virtual patients described earlier, and allowed to run in simulated closed-loop control. New advice was generated at the blood-gas sample times established by the anaesthetist during their simulated ventilation of the virtual patients. In this way direct comparison of the patient histories was possible.

The prototype advisor gave poor decision matching when compared with the ventilator changes prescribed by the anaesthetist. In some cases the patient diverged from acceptable levels. However the causes of decision error were easily identified via inspection of the rules that were contributing to the mismatch. In some instances it was simply a matter of changing the value of the rule-consequent, in others new fuzzy classes or even new rule-antecedents were required to better separate the decision space. Improvements to the advisor were implemented where possible, and its performance re-evaluated using simulated closed-loop control.

The modified advisor showed significant improvement in decision matching for the FIO_2 , MV and RR-VT sub-systems. There was no longer any divergent behaviour, and PaO_2 , $PaCO_2$ and PIP maintenance closely followed that produced by the anaesthetist, although some differences in prescribed ventilator setting still existed. In some instances the advisor suggested MV changes that avoided the $PaCO_2$ undershoot or overshoot produced by the anaesthetist. Also of note is that the ARDS patient required more cautious ventilation in terms of FIO_2 increases and RR and VT changes. These differences were clearly identified using the simulated closed-loop approach. However, encapsulating them in the rules was not possible without compromising the decisions required for normal ventilation. This decision dichotomy and others like it encountered during the evaluation are pathology specific. They require different rules depending upon the presenting condition and are best handled using a hierarchical control structure. Such an approach has been successfully implemented in the control of neuro-muscular block [Shieh et al, 1996, 1997] and anaesthesia [Linkens 1993; Shieh et al, 1998].

The closed-loop simulation only provided limited stimulation of the available control rules and it will therefore be necessary to construct additional virtual patients that fire different rules, including those at the observation extremes.

Clinical validation of the advisor against ventilator changes made in ICU resulted in a poor level of decision matching. This was disappointing, but careful examination showed that decision mismatch was caused by one of or a combination of the following; (1) an inability to reject measurement errors; (2) the use of broader ranges of acceptable gases that require no refinement of the ventilator settings; (3) decisions based on information outside of the advisor paradigm and (4) a tendency on the part of an anaesthetist to wait to see if a patient's condition improves before making ventilator changes that might destabilise certain patients. These add further weight to the need for hierarchical control.

The ability to create pseudo-realistic patient scenarios may have other advantages for knowledge elicitation. One of the biggest problems in producing an advisory system is that treatment styles vary between hospital ICUs and even between individual anaesthetists. This often reflects the ventilation strategies and accepted norms in vogue at the time they did their initial training, as well as the variability in patient types encountered. Using the patient model, a library of patient scenarios can be created that represent a wide range of pathology and trauma. These can include critical events, untenable scenarios and measurement errors. Different anaesthetists could then be asked to care for the patients as they would a real patient and the variation in treatment styles recorded. Because the scenarios are repeatable, direct comparison between anaesthetist styles would be possible. The consensus or average care profiles can then be identified and the data used to train the advisor. It should also help to isolate pathology-specific strategies that require different control rules from those required for normal control.

If the model can be successfully tuned to real patient data, then the generation of scenario libraries will be much simpler. It will also be possible to use the model on-line to predict the outcomes of advice given and therefore assess its suitability.

Initial advisor development used handcrafting of the rules. However, when there are more than 3 rule-antecedents this quickly becomes cumbersome, and is better achieved using automated techniques such as self-organising fuzzy-logic control (SOFLC). Using the patient-model and a library of virtual patients a SOFLC based advisor can quickly be trained and its performance compared directly against other advisor rule-bases.

A major restricting factor to rule testing and development was the speed at which patient simulations could be performed. The model was written using MATLAB and SIMULINK, which provides benefits in terms of rapid research and development but are slow to run. This is because they are interpretative run-time languages and are by nature much slower than compiler languages such as C. Compilers are available for MATLAB and SIMULINK but the improvement in performance experienced by other researchers was not significant. Therefore before predictive-control or self-learning fuzzy logic can be explored using the patient-model, it will require implementing in C or C++. MATLAB supports the integration of C programs and therefore advisor development can be continued using this platform.

If an advisor is to become truly useful it must form an integral part of any computerised patient data management system currently in place. It is not reasonable to expect clinicians or nursing staff to enter information into a separate stand-alone system [Standage, 1997]. Therefore any future development must consider data transfer protocols between existing management systems.

In conclusion, model-based advisor validation has demonstrated advantages over decision comparisons made using clinical data alone. It provided a method for assessing the closed-loop stability of the advisor, and successfully highlighted differences in decision behaviour from that of an anaesthetist. This enabled rapid refinement of handcrafted rules and will form a validation platform for the development of new rules for future ventilation strategies. However, the advisor is not yet in a usable finished form, and will require enhancing before bedside validation can be considered. A hierarchical control strategy will be needed, since universal control rules cannot adequately encapsulate the entire decision processes of an anaesthetist.

Appendix A

SIMULINK Block Diagrams of the Patient Model

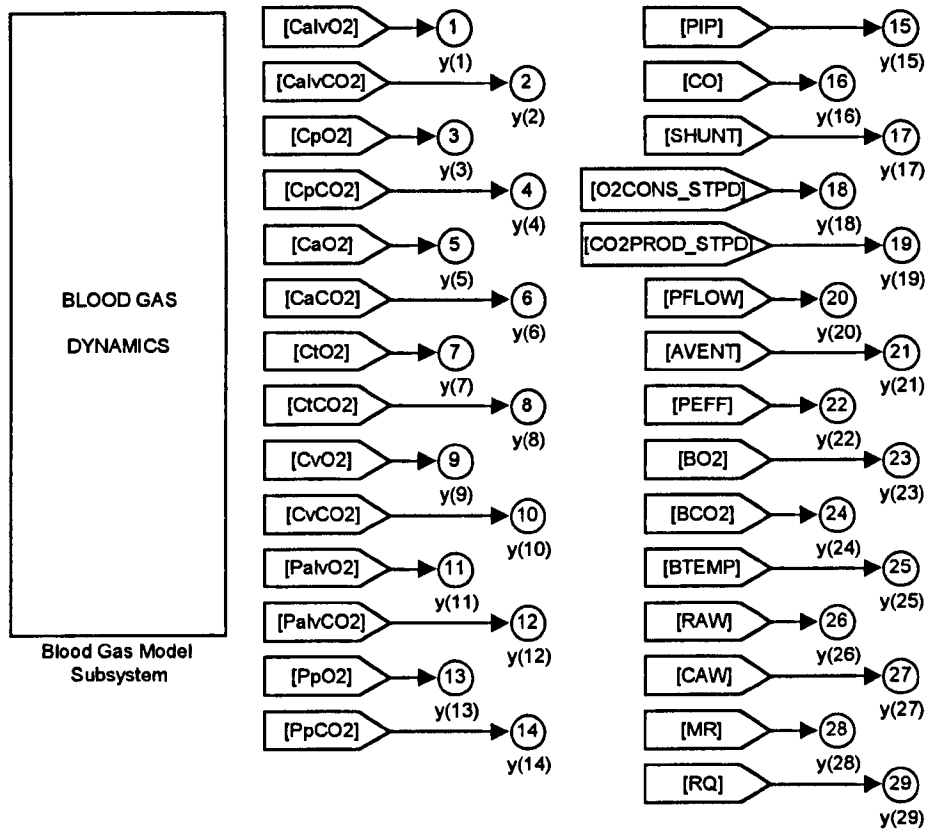


Figure A.1: Top level diagram of the SIMULINK model, with *FROM* blocks passing all of the model parameters and output variables to the MATLAB workspace for inspection and manipulation. The *Blood Gas Model Subsystem* contains the actual model representations and has a global call in its input mask to a MATLAB structure that contains all of the required input parameters.

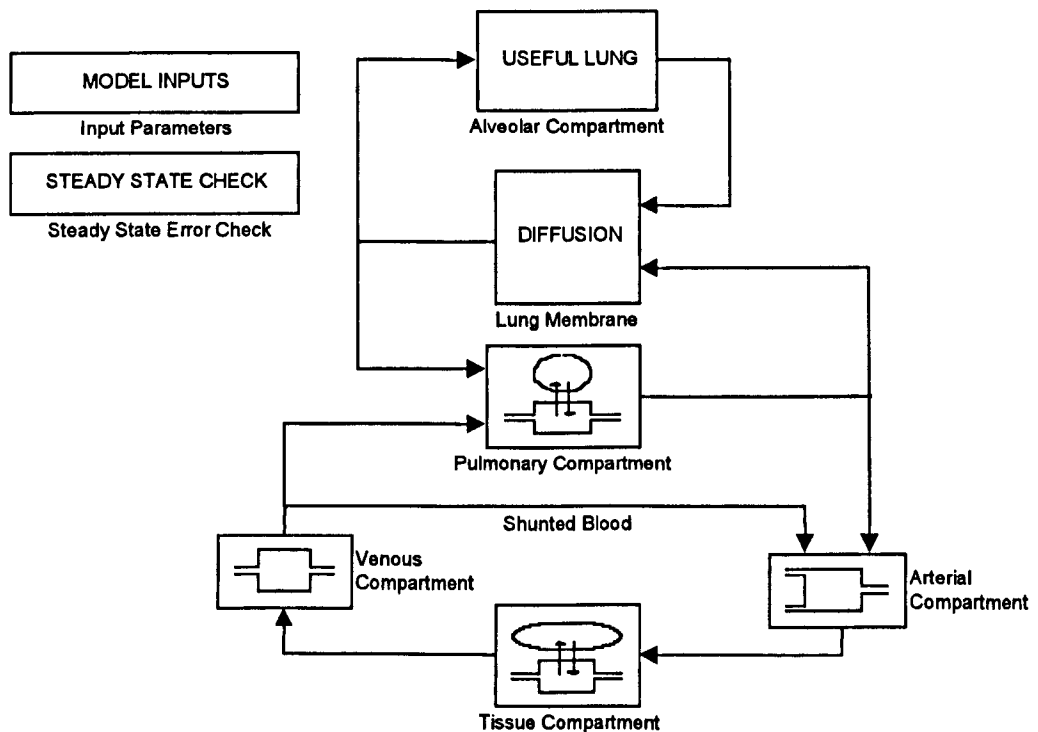


Figure A.2: *Blood Gas Model Subsystem* – showing the compartments of the patient model. The *Input Parameters* module copies the MATLAB input structure into the local parameter labels used within the compartment subsystems. The *Steady State Error Check* module, stops the simulation when the blood-gas content and pressures have reached steady-state, or the simulation stop time has been reached.

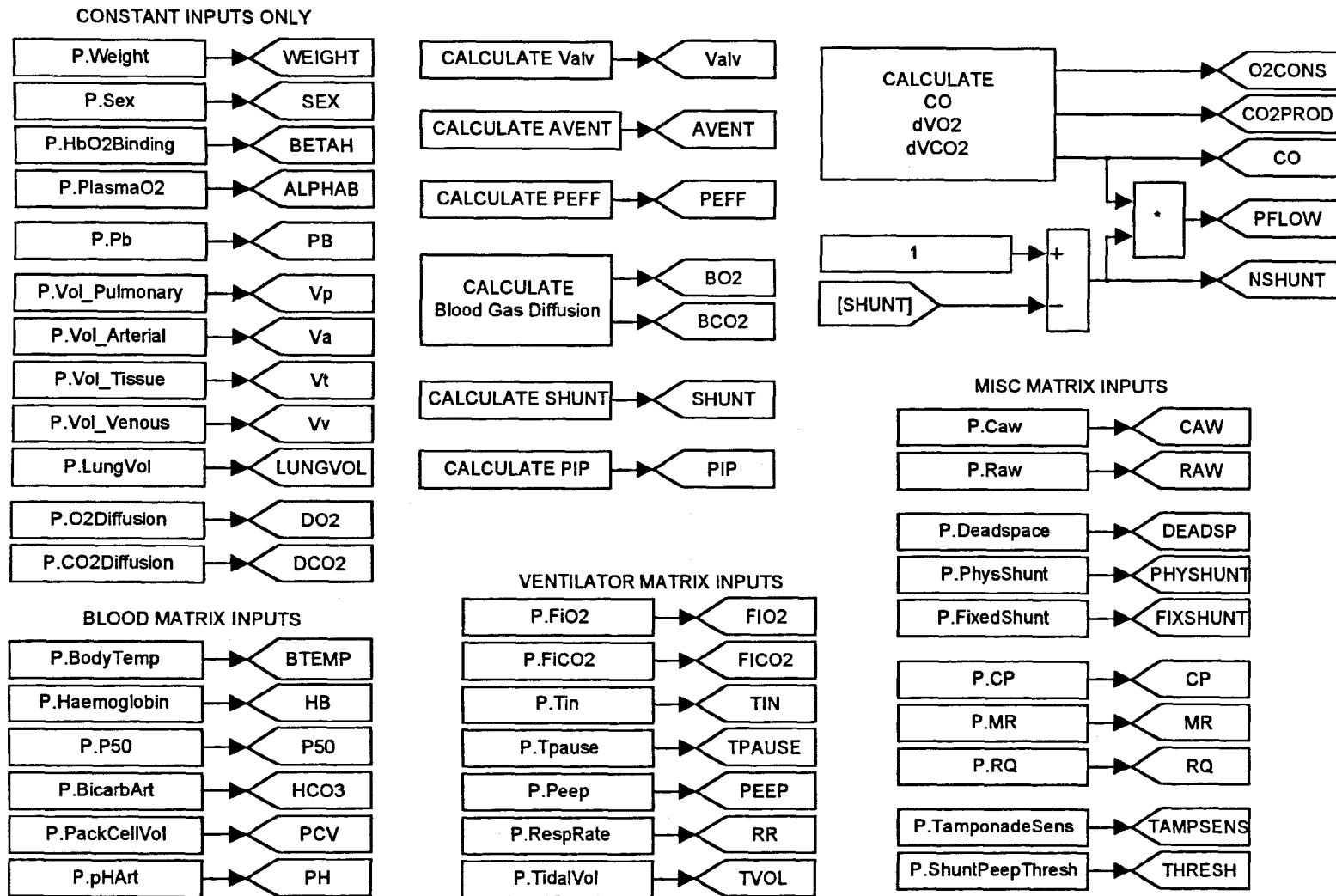


Figure A.3: *Input Parameters* – this subsystem, maps the values in the MATLAB input structure (e.g. P.FIO2) into *GOTO* blocks. These enable the parameters to be used elsewhere in the system by using a corresponding *FROM* block. This module also derives parameter values used by the model, from various input values (e.g. AVENT from TVOL (VT), RR and DEADSP (VD)).

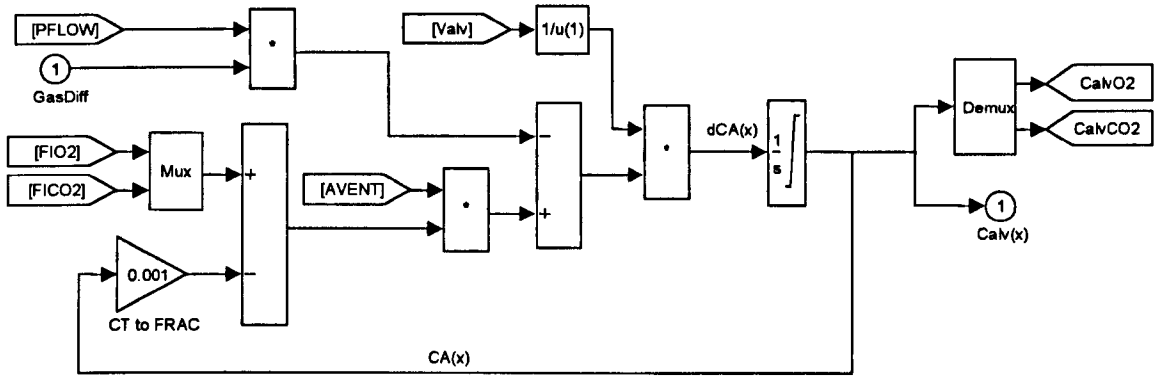


Figure A.4: *Alveolar Compartment* – representation of the mass transport equations 4.5 and 4.27.

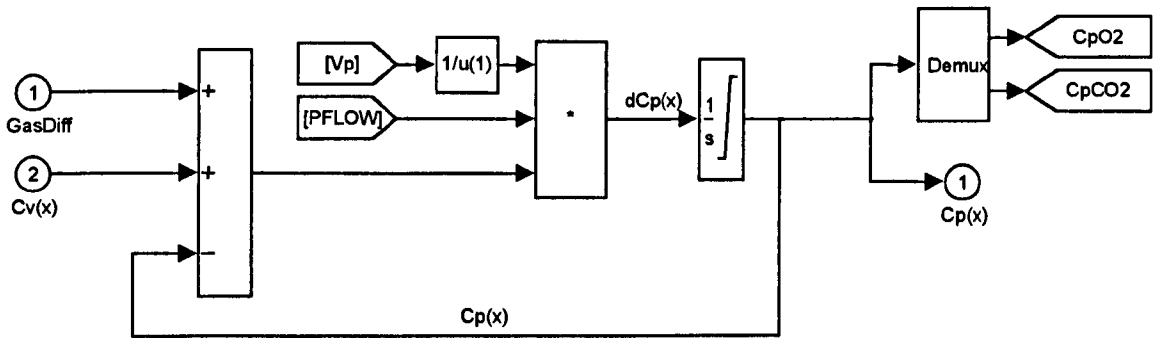


Figure A.5: *Pulmonary Compartment* – representation of the mass transport equations 4.4 and 4.26.

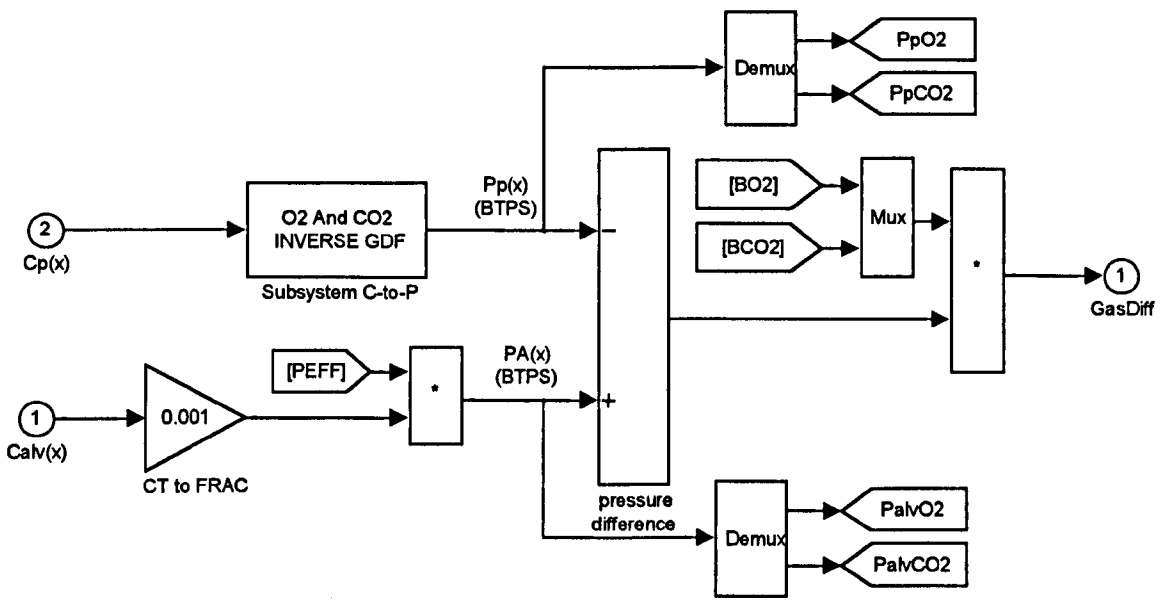


Figure A.6: *Lung Membrane* – representation of model equations 4.6 and 4.28.

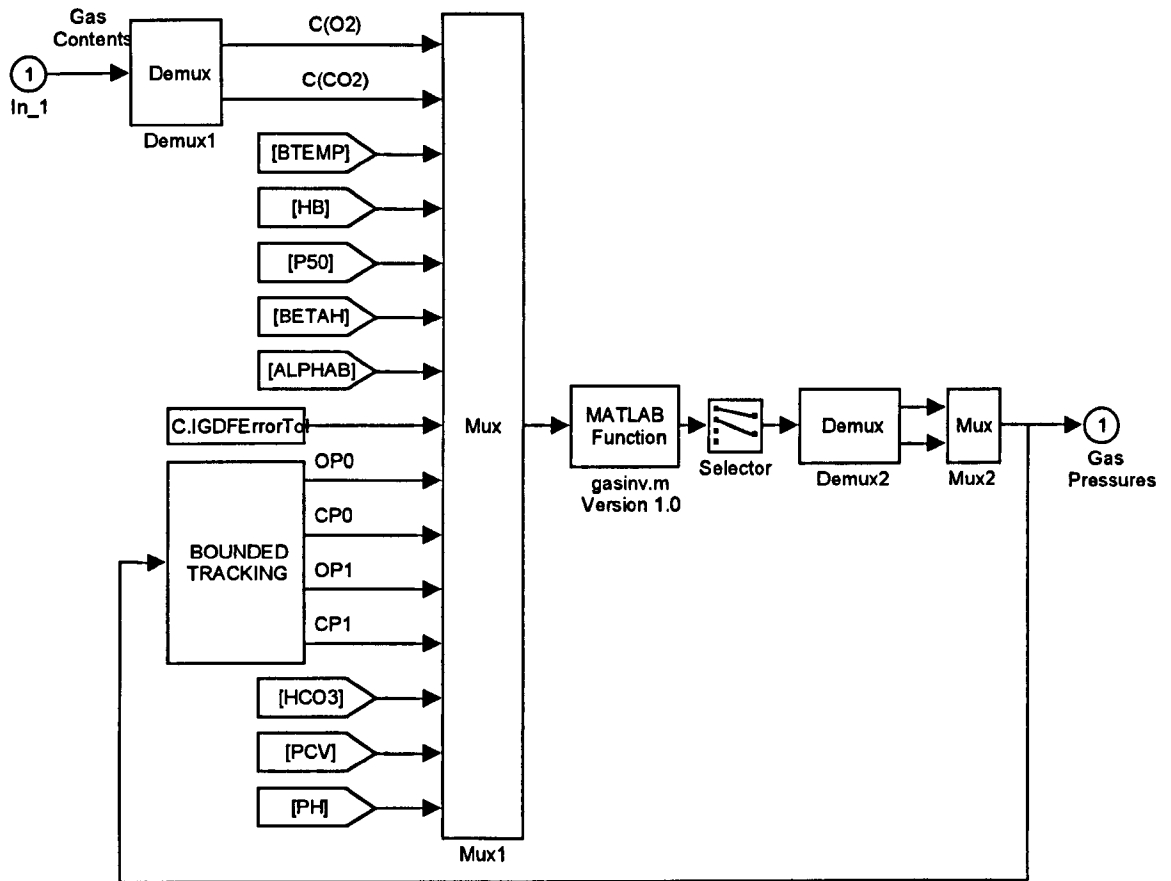


Figure A.7: *Subsystem C-to-P* – converts the pulmonary gas contents to partial pressures using the MATLAB inverse gas dissociation function *gasinv.m*.

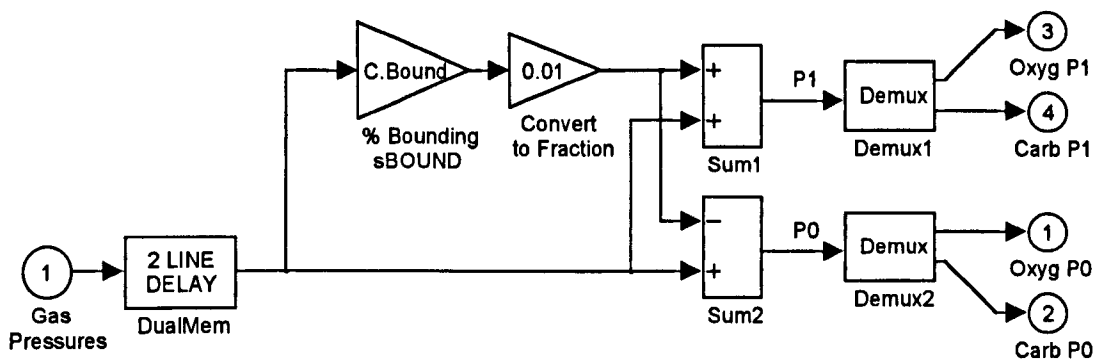


Figure A.8: *Bounded Tracking* – implements the bounded tracking algorithm of equation 4.46.

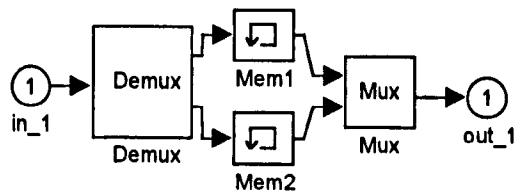


Figure A.9: *DualMem* – provides the previous gas pressures used in the bounded tracking.

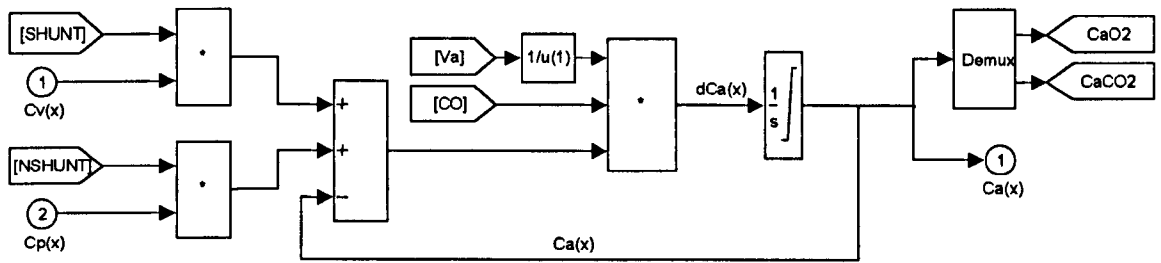


Figure A.10: *Arterial Compartment* – representation of mass transport equations 4.1 and 4.23.

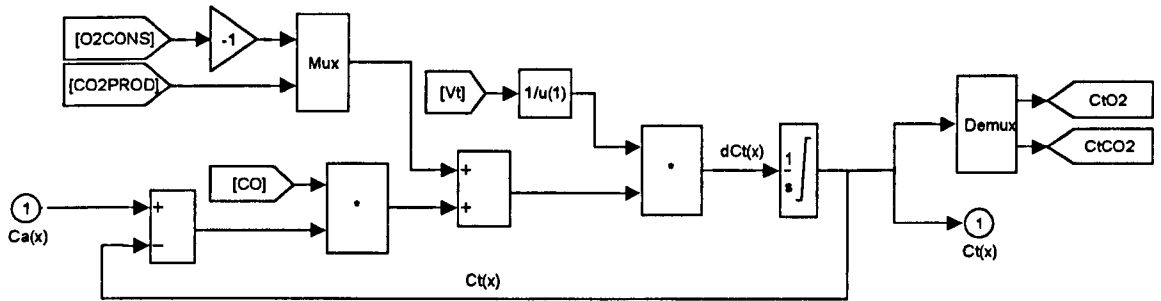


Figure A.11: *Tissue Compartment* – representation of mass transport equations 4.2 and 4.14.

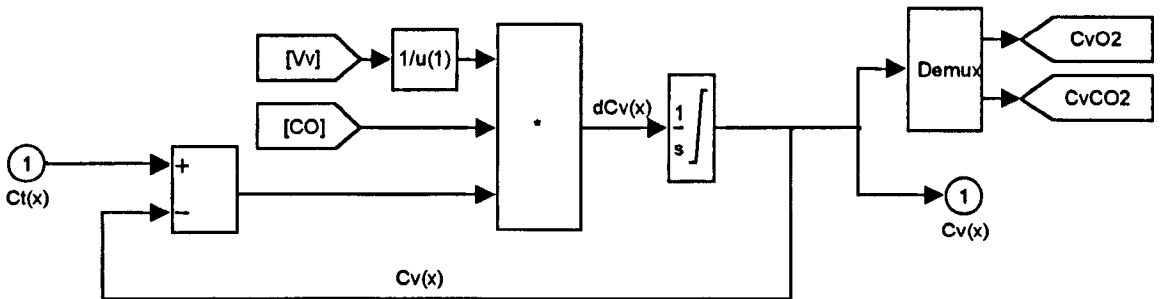


Figure A.12: *Venous Compartment* – representation of mass transport equations 4.3 and 4.25.

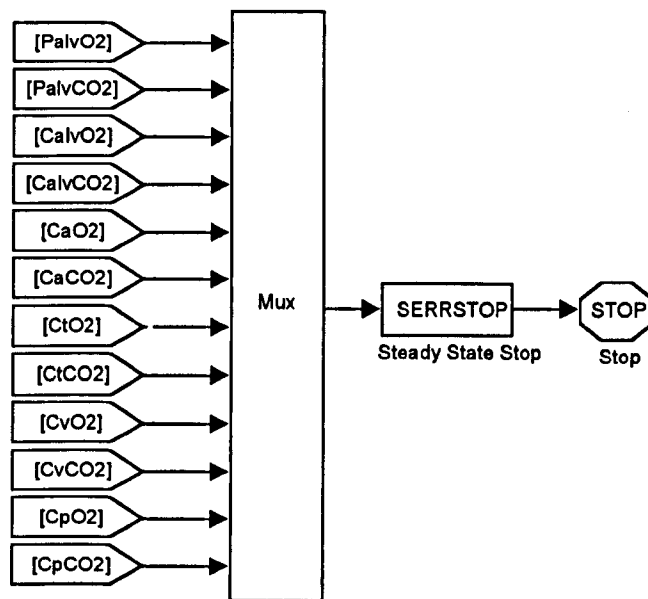


Figure A.13: *Steady State Error Check* – passes all gas content and pressures into the *serrstop.m* MATLAB function to check for steady state convergence.

Appendix B

Data Collected For Patient-Model Validation and Ethical Committee Guidelines

B.1 Patient Data

PATIENT 1 RECORD 1 (14/2/94)				
GENERAL INFORMATION				
Status: Cardiogenic shock, Sepsis, Multi-system failure.				
Drugs: Adrenaline, Flolan, Dopamine				
Support: SIMV Ventilation, Dialysis, Fluid balance, Blood infusions				
Measurements: PAC, CVC, SAC, Deltatrac II, Thermo-dilution CO Measurements				
Female, 65 years, 165 cm, 69 kg				
VENTILATOR ARRANGEMENT				
Puritan -Bennett 7200a, Disposable Tubing (2.5m insp., 2m exp.)				
Bennett Cascade Filter (gives good humidification.), SIMV mode with sloping square wave driving waveform				
METABOLIC COMPUTER (DELTATRAC II) RESULTS				
Gas Temperature (°C)	28.4			
Ambient Pressure (kPa)	102.525			
Ambient CO ₂ (% STPD)	0.05			
Non-Protein RQ	0.86			
Body Surface Area (m ²): Deltatrac2	1.76			
SAMPLE RESULTS				
TIME	14:18	14:48	15:32	16:17
VENTILATOR SETTINGS				
FiO ₂ (%)	55			
Respiratory Rate (rpm)	24	26		
Tidal Volume (ml) [set (measured)]	700 (680)			
PEEP (cmH ₂ O)	10			
I:E Ratio (I/E)	0.8	0.6		
PIP (cmH ₂ O)	30.2	36.2		
Mean Airway Pressure (cmH ₂ O)	21.0	24.5		
SYSTEMIC ARTERY BLOOD (Arterial Catheter)				
PaO ₂ (kPa)	17.2	17.9	? 15.8	18.0
PaCO ₂ (kPa)	4.30	4.30	3.90	4.00
Co-oximeter O ₂ Saturation (%)	99.0	99.0	99.0	99.0
pH	7.540	7.530	7.560	7.560
Standard Bicarbonate (mmol/l)	31.0	30.0	30.0	31.0
Base Excess (mmol/l)	+7	+6	+6	+7
Hb (g/100ml)	11.6			

PULMONARY ARTERY BLOOD (Pulmonary Artery Catheter)				
PvO ₂ (kPa)	4.4	4.6	4.1	4.3
PvCO ₂ (kPa)	5.00	4.90	4.70	4.60
Co-oximeter O ₂ Saturation (%)	69.0	71.0	65.0	68.0
Standard Bicarbonate (mmol/l)	29.0	29.0	30.0	30.0
pH	7.490	7.490	7.520	7.520
OTHER MEASUREMENTS				
Blood Temperature (°C)	36.5	36.4	36.5	36.6
O ₂ Saturation (%) Oximeter	96	97	95	98
Cardiac Output (l/min)	4.9	5.8	4.9	5.2
Cardiac Index	2.75	3.25	2.75	2.92
Heart Rate (bpm)	106	103	103	105
O ₂ Consumption (ml/min)	273.8	278.2	278.6	284.7
CO ₂ Production (ml/min)	239.1	238.9	238.2	242.8
Metabolic Rate (kcal/24hr)	1901	1923	1924	1969
Respiratory Quotient	0.878	0.860	0.855	0.854
PRESSURES				
Systolic B.P. (mmHg)	116	138	152	132
Diastolic B.P. (mmHg)	-	-	-	-
Mean Arterial B.P. (mmHg)	64	73	81	70
Central Venous B.P. (mmHg)	12	13	14	12
Mean Pulmonary B.P. (mmHg)	27	28	31	29
Wedge Pressure (mmHg)	10	11	12	11

Notes:

Measurement 3 for PaO₂ appears to be too low, probably a measurement error.

PATIENT 1 RECORD 2 (15/2/94)				
GENERAL INFORMATION				
Status: Cardiogenic shock, Sepsis, Multi-system failure.				
Drugs: Adrenaline, Flolan, Dopamine; Reduction of sedation during test but no arousal.				
Support: SIMV Ventilation, Dialysis, Fluid balance, Blood infusions				
Measurements: PAC, SAC, Deltatrac II, Thermo-dilution CO Measurements				
Female, 65 years, 165 cm, 69 kg				
VENTILATOR ARRANGEMENT				
Puritan -Bennett 7200a, Disposable Tubing (2.5m insp., 2m exp.)				
Bennett Cascade Filter (gives good humidification.)				
SIMV mode with sloping square wave driving waveform				
METABOLIC COMPUTER (DELTATRAC II) RESULTS				
Gas Temperature (°C)	28.4			
Ambient Pressure (kPa)	100.391			
Ambient CO ₂ (% STPD)	0.06			
Non-Protein RQ	0.86			
Body Surface Area (m ²): Deltatrac2	1.76			
SAMPLE RESULTS				
TIME	15:03	15:28	16:03	16:53
VENTILATOR SETTINGS				
FiO ₂ (%)	50		45	
Respiratory Rate (rpm)	20			
Tidal Volume (ml) [set (measured)]	700 (670)			
PEEP (cmH ₂ O)	5			
I:E Ratio (I/E)	1.1			
PIP (cmH ₂ O)	22.6		22.7	
Mean Airway Pressure (cmH ₂ O)	11.9		13.1	
SYSTEMIC ARTERY BLOOD (Arterial Catheter)				
PaO ₂ (kPa)	12.4	12.3	10.4	10.5
PaCO ₂ (kPa)	5.80	5.16	4.72	5.08
Co-oximeter O ₂ Saturation (%)	95.6	97.8	95.4	95.0
pH	7.452	7.493	7.507	7.495
Standard Bicarbonate (mmol/l)	30.7	30.1	28.4	29.7
Base Excess (mmol/l)	+6.7	+7.0	+5.8	+6.7
Hb (g/100ml)	10.6			

PULMONARY ARTERY BLOOD (Pulmonary Artery Catheter)				
PvO ₂ (kPa)	4.80	5.00	5.36	5.58
PvCO ₂ (kPa)	6.06	5.75	4.70	4.70
Co-oximeter O ₂ Saturation (%)	71.2	74.2	72.9	70.6
Standard Bicarbonate (mmol/l)	32.0	31.7	31.0	31.1
pH	7.450	7.469	7.490	7.474
OTHER MEASUREMENTS				
Blood Temperature (°C)	36.5	36.4	36.5	36.5
O ₂ Saturation (%) Oximeter	98	98	97	97
Cardiac Output (l/min)	7.2	8.3	8.3	8.0
Cardiac Index	4.04	4.66	4.66	4.49
Heart Rate (bpm)	97	97	98	98
O ₂ Consumption (ml/min)	279.0	293.7	286.9	292.5
CO ₂ Production (ml/min)	244.7	253.3	245.7	244.8
Metabolic Rate (kcal/24hr)	1940	2035	1985	2012
Respiratory Quotient	0.879	0.865	0.857	0.838
PRESSURES				
Systolic B.P. (mmHg)	111	146	145	127
Diastolic B.P. (mmHg)	45	64	53	45
Mean Arterial B.P. (mmHg)	66	81	77	71
Central Venous B.P. (mmHg)	14	15	14	12
Mean Pulmonary B.P. (mmHg)	29	38	31	30
Wedge Pressure (mmHg)	16	18	17	15

Notes:

Instability in PRIOR PaCO₂ measurements (11.03 % variation), also reflected in arterial pH change. Unable to say which point is incorrect therefore the average has to be used. This may lead to bad V_D estimate and hence poor response matching.

Instability in PRIOR \dot{Q}_t (15.1 % variation).

PATIENT 1 RECORD 3 (21/2/94)				
GENERAL INFORMATION				
Status: Cardiogenic shock, Sepsis, Multi-system failure.				
Drugs: Adrenaline (being reduced), Flolan, Dopamine				
Support: SIMV Ventilation, Dialysis, Fluid balance, Blood infusions				
Measurements: PAC, SAC, Deltatrac II, Cardiac output calculated.				
Female, 65 years, 165 cm, 60 kg (reduced)				
VENTILATOR ARRANGEMENT				
Puritan -Bennett 7200a, Disposable Tubing (2.5m insp., 2m exp.)				
Bennett Cascade Filter (gives good humidification.)				
SIMV mode with sloping square wave driving waveform				
METABOLIC COMPUTER (DELTATRAC II) RESULTS				
Gas Temperature (°C)	29.2			
Ambient Pressure (kPa)	100.791			
Ambient CO ₂ (% STPD)	0.04			
Non-Protein RQ	0.89			
Body Surface Area (m ²): Deltatrac2	1.65			
SAMPLE RESULTS				
TIME	11:49	12:13	12:39	13:22
VENTILATOR SETTINGS				
FiO ₂ (%)	55		60	
Respiratory Rate (rpm)	18			
Tidal Volume (ml) [set (measured)]	900 (870)			
PEEP (cmH ₂ O)	7.5			
I:E Ratio (I/E)	1.0			
PIP (cmH ₂ O)	24.0		24.0	
Mean Airway Pressure (cmH ₂ O)	13.6		13.7	
SYSTEMIC ARTERY BLOOD (Arterial Catheter)				
PaO ₂ (kPa)	8.5	8.8	9.2	9.3
PaCO ₂ (kPa)	4.87	4.72	4.69	4.78
Co-oximeter O ₂ Saturation (%)	-	-	-	-
pH	7.490	? 7.437	7.494	7.480
Standard Bicarbonate (mmol/l)	29	? 25.5	28.5	28.1
Base Excess (mmol/l)	5.3	? 1	4.7	4.2
Hb (g/100ml)	9.6	-	9.8	10.1

PULMONARY ARTERY BLOOD (Pulmonary Artery Catheter)				
PvO ₂ (kPa)	5.3	5.3	5.5	5.5
PvCO ₂ (kPa)	5.52	5.41	5.17	5.46
Co-oximeter O ₂ Saturation (%)	-	-	-	-
Standard Bicarbonate (mmol/l)	29.5	29.1	28.4	29.1
pH	7.468	7.468	7.469	7.465
OTHER MEASUREMENTS				
Blood Temperature (°C)	36.7	36.7	-	36.6
O ₂ Saturation (%) Oximeter	100	100	-	100
Cardiac Output (l/min) <i>derived</i>	13.36	13.18	13.38	13.16
Cardiac Index	-	-	-	-
Heart Rate (bpm)	100	102	-	100
O ₂ Consumption (ml/min)	289.4	282.1	279.1	284.4
CO ₂ Production (ml/min)	253.6	252.2	242.2	243.4
Metabolic Rate (kcal/24hr)	2012	1970	1934	1966
Respiratory Quotient	0.879	0.896	0.869	0.860
PRESSURES				
Systolic B.P. (mmHg)	140	134	-	114
Diastolic B.P. (mmHg)	50	49	-	44
Mean Arterial B.P. (mmHg)	80	76	-	65
Central Venous B.P. (mmHg)	13	13	-	12
Mean Pulmonary B.P. (mmHg)	32	31	-	29
Wedge Pressure (mmHg)	15	15	-	16

Notes:

Possible measurement error in arterial pH, standard bicarbonate and BE results for point 2. Drop in pH would normally be due to PaCO₂ increase over short time periods, but in this case PaCO₂ reduces.

Cardiac output derived using $\dot{Q}_t = \frac{\dot{V}_{O_2}}{C(a-v)O_2}$ with CaO₂ and CvO₂ derived from gas tensions using the gas dissociation functions. Estimates seem large, giving rise to large shunt estimates.

PATIENT 1 RECORD 4 (21/2/94)				
GENERAL INFORMATION				
Status: Cardiogenic shock, Sepsis, Multi-system failure.				
Drugs: Adrenaline (being reduced), Flolan, Dopamine				
Support: SIMV Ventilation, Dialysis, Fluid balance, Blood infusions				
Measurements: PAC, SAC, Deltatrac II				
Female, 65 years, 165 cm, 60 kg (reduced)				
VENTILATOR ARRANGEMENT				
Puritan -Bennett 7200a, Disposable Tubing (2.5m insp., 2m exp.)				
Bennett Cascade Filter (gives good humidification.)				
SIMV mode with sloping square wave driving waveform				
METABOLIC COMPUTER (DELTATRAC II) RESULTS				
Gas Temperature (°C)	29.2			
Ambient Pressure (kPa)	100.791			
Ambient CO ₂ (% STPD)	0.04			
Non-Protein RQ	0.89			
Body Surface Area (m ²): Deltatrac2	1.65			
SAMPLE RESULTS				
TIME	12:39	13:22	14:13	-
VENTILATOR SETTINGS				
FiO ₂ (%)	60		65	
Respiratory Rate (rpm)	18			
Tidal Volume (ml) [set (measured)]	900 (870)		900 (880)	
PEEP (cmH ₂ O)	7.5			
I:E Ratio (I/E)	1.0			
PIP (cmH ₂ O)	24.0		24.0	
Mean Airway Pressure (cmH ₂ O)	13.7		13.7	
SYSTEMIC ARTERY BLOOD (Arterial Catheter)				
PaO ₂ (kPa)	9.2	9.3	9.7	-
PaCO ₂ (kPa)	4.69	4.78	4.79	-
Co-oximeter O ₂ Saturation (%)	-	-	-	-
PH	7.494	7.480	7.503	-
Standard Bicarbonate (mmol/l)	28.5	28.1	29.4	-
Base Excess (mmol/l)	4.7	4.2	5.9	-
Hb (g/100ml)	9.8	10.1	10.1	-

PULMONARY ARTERY BLOOD (Pulmonary Artery Catheter)				
PvO ₂ (kPa)	5.5	5.5	5.6	-
PvCO ₂ (kPa)	5.17	5.46	5.29	-
Co-oximeter O ₂ Saturation (%)	-	-	-	-
Standard Bicarbonate (mmol/l)	28.4	29.1	29.3	-
pH	7.469	7.465	7.476	-
OTHER MEASUREMENTS				
Blood Temperature (°C)	-	36.6	36.5	-
O ₂ Saturation (%) Oximeter	-	100	100	-
Cardiac Output (l/min) <i>derived</i>	13.38	13.16	13.11	-
Cardiac Index	-	-	-	-
Heart Rate (bpm)	-	100	96	-
O ₂ Consumption (ml/min)	279.1	284.4	266.2	-
CO ₂ Production (ml/min)	242.2	243.4	235.6	-
Metabolic Rate (kcal/24hr)	1934	1966	1853	-
Respiratory Quotient	0.869	0.860	0.889	-
PRESSURES				
Systolic B.P. (mmHg)	-	114	129	-
Diastolic B.P. (mmHg)	-	44	47	-
Mean Arterial B.P. (mmHg)	-	65	72	-
Central Venous B.P. (mmHg)	-	12	12	-
Mean Pulmonary B.P. (mmHg)	-	29	31	-
Wedge Pressure (mmHg)	-	16	16	-

Notes:

Cardiac output derived using $\dot{Q}_t = \frac{\dot{V}_{O_2}}{C(a-v)O_2}$ with CaO₂ and CvO₂ derived from gas tensions using the gas dissociation functions. Estimates seem large, giving rise to large shunt estimates.

PATIENT 2 RECORD 1 (22/2/94)				
GENERAL INFORMATION				
Status: Post operative emergency with acute aortic aneurism.				
Drugs: Dopamine 200mg/50ml @ 2ml/hr. Increased to 5ml/L at 15:30				
Support: Ventilation, Blood and plasma infusions at 15:35				
Measurements: CVC, SAC, Deltatrac II.				
Male, 69 years, 180 cm, 82 kg				
VENTILATOR ARRANGEMENT				
Siemens Servo 300, Standard Non-disposable tubing + PALL Filter				
CMV mode with square wave driving waveform				
METABOLIC COMPUTER (DELTATRAC II) RESULTS				
Gas Temperature (°C)	29.1			
Ambient Pressure (kPa)	100.658			
Ambient CO ₂ (% STPD)	0.05			
Non-Protein RQ	0.82			
Body Surface Area (m ²): Deltatrac2	2.01			
SAMPLE RESULTS				
TIME	15:00	15:35	16:05	16:40
VENTILATOR SETTINGS				
FiO ₂ (%)*	40		35	
Respiratory Rate (rpm)	17		16	
Tidal Volume (ml) [set (measured)]	700		700	
PEEP (cmH ₂ O)	2		3	
I:E Ratio (I/E)	0.333			
PIP (cmH ₂ O)	36.0		32.0	
Mean Airway Pressure (cmH ₂ O)	-		-	
SYSTEMIC ARTERY BLOOD (Arterial Catheter)				
PaO ₂ (kPa)	20.5	21.3	17.1	18.5
PaCO ₂ (kPa)	5.36	5.15	4.93	4.44
Co-oximeter O ₂ Saturation (%)	-	-	-	-
pH	7.369	7.383	7.400	7.435
Standard Bicarbonate (mmol/l)	24.1	24.2	24.4	24.6
Base Excess (mmol/l)	-1.1	-0.9	-0.7	-0.5
Hb (g/100ml)	10.8	-	11.2	10.5
CENTRAL VENOUS BLOOD (Central Venous Catheter)				
PvO ₂ (kPa)	4.70	5.00	5.20	5.50

PvCO ₂ (kPa)	6.36	6.45	5.95	5.40
Co-oximeter O ₂ Saturation (%)	-	-	-	-
Standard Bicarbonate (mmol/l)	24.4	24.4	24.4	24.4
pH	7.325	7.320	7.367	7.372
OTHER MEASUREMENTS				
Blood Temperature – rectal (°C)	35.9	36.6	36.9	37.2
O ₂ Saturation (%) Oximeter	100	100	97	97
Cardiac Output (l/min) <i>derived</i>	7.70	5.91	6.85	8.07
Cardiac Index	-	-	-	-
Heart Rate (bpm)	94	96	95	97
O ₂ Consumption (ml/min)	368.5	314.2	309.7	308.4
CO ₂ Production (ml/min)	282.3	264.8	267.8	267.3
Metabolic Rate (kcal/24hr)	2499	2168	2149	2141
Respiratory Quotient	0.766	0.845	0.865	0.866
PRESSURES				
Systolic B.P. (mmHg)	115	95	110	130
Diastolic B.P. (mmHg)	60	50	60	65
Mean Arterial B.P. (mmHg)	85	65	75	90
Central Venous B.P. (mmHg)	12	9	10	12
Mean Pulmonary B.P. (mmHg)	-	-	-	-
Wedge Pressure (mmHg)	-	-	-	-

Notes:

Cardiac output derived using $\dot{Q}_t = \frac{\dot{V}_{O_2}}{C(a-v)O_2}$ with CaO₂ and CvO₂ derived from gas tensions using the gas dissociation functions. Estimates seem large, giving rise to large shunt estimates.

PATIENT 3 RECORD 1 (01/3/94)				
GENERAL INFORMATION				
Status: Paraplegic with post operative complications, septic shock, kidney failure				
Drugs: Paracetamol, Renal Dopamine				
Support: Ventilation				
Measurements: PAC, SAC, Deltatrac II, Thermodilution C.O. measurements.				
Female, 47 years, 154 cm, 50 kg				
VENTILATOR ARRANGEMENT				
Siemens Servo 900c, Standard disposable tubing (2.5m insp, 1.5m exp) + Bennett Cascade II Filter SIMV mode + pressure support (inspiratory time 67 %, pause time 10 %).				
METABOLIC COMPUTER (DELTATRAC II) RESULTS				
Gas Temperature (°C)	29.6			
Ambient Pressure (kPa)	100.658			
Ambient CO ₂ (% STPD)	0.05			
Non-Protein RQ	0.82			
Body Surface Area (m ²): Deltatrac2	1.46			
SAMPLE RESULTS				
TIME	13:01	--	13:37	--
VENTILATOR SETTINGS				
FiO ₂ (%)	65		70	
Respiratory Rate (rpm)	16			
Tidal Volume (ml) [set (measured)]	618		615	
PEEP (cmH ₂ O)	10			
I:E Ratio (I/E)	2.0			
PIP (cmH ₂ O)	35.0		33.8	
Mean Airway Pressure (cmH ₂ O)	-		20	
SYSTEMIC ARTERY BLOOD (Arterial Catheter)				
PaO ₂ (kPa)	8.1	-	7.8	-
PaCO ₂ (kPa)	5.12	-	5.31	-
Co-oximeter O ₂ Saturation (%)	95	-	90	-
PH	7.349	-	7.356	-
Standard Bicarbonate (mmol/l)	22.3	-	23.2	-
Base Excess (mmol/l)	-3.2	-	-2.1	-
Hb (g/100ml)	10.4	-	10.1	-

PULMONARY ARTERY BLOOD (Pulmonary Artery Catheter)				
PvO ₂ (kPa)	4.5	-	4.6	-
PvCO ₂ (kPa)	5.61	-	5.48	-
Co-oximeter O ₂ Saturation (%)	-	-	-	-
Standard Bicarbonate (mmol/l)	23.2	-	22.5	-
pH	7.359	-	7.351	-
OTHER MEASUREMENTS				
Blood Temperature (°C)	38.8	-	38.8	-
O ₂ Saturation (%) Oximeter	96	-	94	-
Cardiac Output (l/min)	7.5	-	7.2	-
Cardiac Index	5.1	-	4.89	-
Heart Rate (bpm)	130	-	128	-
O ₂ Consumption (ml/min)	218.6	-	202.1	-
CO ₂ Production (ml/min)	179.6	-	162.1	-
Metabolic Rate (kcal/24hr)	1491	-	1372	-
Respiratory Quotient	0.824	-	0.802	-
PRESSURES				
Systolic B.P. (mmHg)	110	-	114	-
Diastolic B.P. (mmHg)	50	-	52	-
Mean Arterial B.P. (mmHg)	72	-	70	-
Central Venous B.P. (mmHg)	8	-	14	-
Mean Pulmonary B.P. (mmHg)	20	-	24	-
Wedge Pressure (mmHg)	8	-	8	-

PATIENT 3 RECORD 2 (01/3/94)				
GENERAL INFORMATION				
Status: Paraplegic with post operative complications, septic shock, kidney failure				
Drugs: Paracetamol, Renal Dopamine				
Support: Ventilation, Plasma infusions stopped at 13:42				
Measurements: PAC, SAC, Deltatrac II, Thermodilution C.O. measurements.				
Female, 47 years, 154 cm, 50 kg				
VENTILATOR ARRANGEMENT				
Siemens Servo 900c, Standard disposable tubing (2.5m insp, 1.5m exp) + Bennett Cascade II Filter SIMV mode + pressure support (inspiratory time 67 %, pause time 10 %).				
METABOLIC COMPUTER (DELTATRAC II) RESULTS				
Gas Temperature (°C)	29.6			
Ambient Pressure (kPa)	100.658			
Ambient CO ₂ (% STPD)	0.05			
Non-Protein RQ	0.82			
Body Surface Area (m ²): Deltatrac2	1.46			
SAMPLE RESULTS				
TIME	13:37	--	14:30	--
VENTILATOR SETTINGS				
FiO ₂ (%)	70		75	
Respiratory Rate (rpm)	16			
Tidal Volume (ml) [set (measured)]	615			
PEEP (cmH ₂ O)	10			
I:E Ratio (I/E)	2.0			
PIP (cmH ₂ O)	33.8			
Mean Airway Pressure (cmH ₂ O)	20			
SYSTEMIC ARTERY BLOOD (Arterial Catheter)				
PaO ₂ (kPa)	7.8	-	10.0	-
PaCO ₂ (kPa)	5.31	-	5.28	-
Co-oximeter O ₂ Saturation (%)	90	-	93	-
PH	7.356	-	7.348	-
Standard Bicarbonate (mmol/l)	23.2	-	22.7	-
Base Excess (mmol/l)	-2.1	-	-2.7	-
Hb (g/100ml)	10.1	-	9.9	-

PULMONARY ARTERY BLOOD (Pulmonary Artery Catheter)				
PvO ₂ (kPa)	4.6	-	4.8	-
PvCO ₂ (kPa)	5.48	-	5.15	-
Co-oximeter O ₂ Saturation (%)	-	-	-	-
Standard Bicarbonate (mmol/l)	22.5	-	-	-
pH	7.351	-	7.346	-
OTHER MEASUREMENTS				
Blood Temperature (°C)	38.8	-	38.8	-
O ₂ Saturation (%) Oximeter	94	-	96	-
Cardiac Output (l/min)	7.2	-	5.9	-
Cardiac Index	4.89		4.01	
Heart Rate (bpm)	128		112	
O ₂ Consumption (ml/min)	202.1	-	210.5	-
CO ₂ Production (ml/min)	162.1	-	173.3	-
Metabolic Rate (kcal/24hr)	1372	-	1437	-
Respiratory Quotient	0.802	-	0.826	-
PRESSURES				
Systolic B.P. (mmHg)	114	-	100	-
Diastolic B.P. (mmHg)	52	-	50	-
Mean Arterial B.P. (mmHg)	70	-	66	-
Central Venous B.P. (mmHg)	14	-	16	-
Mean Pulmonary B.P. (mmHg)	24	-	26	-
Wedge Pressure (mmHg)	8	-	11	-

PATIENT 3 RECORD 3 (02/3/94)				
GENERAL INFORMATION				
Status: Paraplegic with post operative complications, septic shock, kidney failure				
Drugs: Renal Dopamine, Patient becoming more aware at last measurement.				
Support: Ventilation				
Measurements: PAC, CVC, SAC, Deltatrac II, Thermodilution C.O. measurements.				
Female, 47 years, 154 cm, 50 kg				
VENTILATOR ARRANGEMENT				
Puritan Bennett 7200A, Standard disposable tubing (2.5m insp, 1.5m exp) + Bennett Cascade II Filter				
SIMV mode (sloping square wave)				
METABOLIC COMPUTER (DELTATRAC II) RESULTS				
Gas Temperature (°C)	29.3			
Ambient Pressure (kPa)	100.658			
Ambient CO ₂ (% STPD)	0.06			
Non-Protein RQ	0.88			
Body Surface Area (m ²): Deltatrac2	1.46			
SAMPLE RESULTS				
TIME	11:13	11:45	12:54	13:28
VENTILATOR SETTINGS				
FiO ₂ (%)	75		70	
Respiratory Rate (rpm)	16			
Tidal Volume (ml) [set (measured)]	590			
PEEP (cmH ₂ O)	10.3		10.2	
I:E Ratio (I/E)	1.43			
PIP (cmH ₂ O)	39.6		38.8	
Mean Airway Pressure (cmH ₂ O)	-		-	
SYSTEMIC ARTERY BLOOD (Arterial Catheter)				
PaO ₂ (kPa)	11.6	11.8	11.3	11.7
PaCO ₂ (kPa)	5.22	5.27	5.30	5.39
Co-oximeter O ₂ Saturation (%)	-	-	-	-
pH	7.363	7.368	7.378	7.359
Standard Bicarbonate (mmol/l)	23.3	23.7	24.3	23.6
Base Excess (mmol/l)	-2	-1.5	-0.7	-1.6
Hb (g/100ml)	10.4		10.6	

CENTRAL VENOUS BLOOD (Central Venous Catheter)				
PvO ₂ (kPa)	4.5	5.0	5.0	4.8
PvCO ₂ (kPa)	5.82	5.79	5.70	5.87
Co-oximeter O ₂ Saturation (%)	-	-	-	-
Standard Bicarbonate (mmol/l)	23.8	23.2	23.6	23.8
pH	7.360	7.347	7.360	7.355
PULMONARY ARTERY BLOOD (Pulmonary Artery Catheter)				
PvO ₂ (kPa)	4.6	4.6	4.7	4.7
PvCO ₂ (kPa)	5.69	5.65	5.84	5.83
Co-oximeter O ₂ Saturation (%)	-	-	-	-
Standard Bicarbonate (mmol/l)	-	23.3	24.0	24.0
pH	7.354	7.359	7.361	7.362
OTHER MEASUREMENTS				
Blood Temperature (°C)	37.2	37.2	37.2	37.2
O ₂ Saturation (%) Oximeter	98	98	98	98
Cardiac Output (l/min)	5.6	6.0	5.8	6.6
Cardiac Index	3.80	4.08	3.94	4.48
Heart Rate (bpm)	105	108	109	112
O ₂ Consumption (ml/min)	217.6	211.8	214.6	219.0
CO ₂ Production (ml/min)	193.5	186.9	186.1	187.4
Metabolic Rate (kcal/24hr)	1511	1471	1481	1508
Respiratory Quotient	0.894	0.883	0.869	0.857
PRESSURES				
Systolic B.P. (mmHg)	145	148	140	149
Diastolic B.P. (mmHg)	65	67	65	67
Mean Arterial B.P. (mmHg)	95	100	94	100
Central Venous B.P. (mmHg)	8	8	6	9
Mean Pulmonary B.P. (mmHg)	24	23	22	23
Wedge Pressure (mmHg)	? 18	7	7	7

PATIENT 4 RECORD 1 (03/3/94)				
GENERAL INFORMATION				
Status: Septic shock, kidney problems				
Drugs: Unknown				
Support: Ventilation, Fluid balance, Plasma/Colloid infusions				
Measurements: PAC, SAC, Deltatrac II, Thermodilution C.O. measurements.				
Female, 56 years, 157 cm, 76 kg				
VENTILATOR ARRANGEMENT				
Siemens Servo 300, Standard disposable tubing (1.5m insp, 1.5m exp) + Fisher & Packel MR600 Filter				
CMV (pressure regulated volume control)				
METABOLIC COMPUTER (DELTATRAC II) RESULTS				
Gas Temperature (°C)	25.4			
Ambient Pressure (kPa)	100.395			
Ambient CO ₂ (% STPD)	0.04			
Non-Protein RQ	0.79			
Body Surface Area (m ²): Deltatrac2	1.77			
SAMPLE RESULTS				
TIME	13:53	14:26	15:07	15:43
VENTILATOR SETTINGS				
FiO ₂ (%)	50			
Respiratory Rate (rpm)	14	12		
Tidal Volume (ml) [set (measured)]	700 (693)	700 (689)		
PEEP (cmH ₂ O)	5			
I:E Ratio (I/E)	1.56	1.85		
PIP (cmH ₂ O)	31.0	35.0		
Mean Airway Pressure (cmH ₂ O)	14	15		
SYSTEMIC ARTERY BLOOD (Arterial Catheter)				
PaO ₂ (kPa)	11.9	11.1	11.5	11.9
PaCO ₂ (kPa)	3.9	3.68	4.16	4.03
Co-oximeter O ₂ Saturation (%)	96.9	96.6	96.8	97.0
pH	7.333	7.374	7.363	7.384
Standard Bicarbonate (mmol/l)	18.6	19.5	20.4	21.0
Base Excess (mmol/l)	-8.0	-9.1	-5.8	-5.1
Hb (g/100ml)	? 15.4	11.8	11.6	11.9

PULMONARY ARTERY BLOOD (Pulmonary Artery Catheter)				
PvO ₂ (kPa)	6.0	5.9	5.9	5.9
PvCO ₂ (kPa)	4.21	4.04	4.35	4.49
Co-oximeter O ₂ Saturation (%)	82.9	83.8	83.2	83.9
Standard Bicarbonate (mmol/l)	19.8	19.2	20.0	21.4
pH	7.353	7.350	7.350	7.372
OTHER MEASUREMENTS				
Blood Temperature (°C)	38.0	37.9	37.9	37.9
O ₂ Saturation (%) Oximeter	95	96	97	97
Cardiac Output (l/min)	10.5	11.8	10.1	11.1
Cardiac Index	5.76	6.48	5.54	6.09
Heart Rate (bpm)	150	146	148	148
O ₂ Consumption (ml/min)	242.5	233.3	269.0	262.2
CO ₂ Production (ml/min)	208.4	198.7	207.5	200.3
Metabolic Rate (kcal/24hr)	1674	1607	1819	1768
Respiratory Quotient	0.862	0.852	0.771	0.765
PRESSURES				
Systolic B.P. (mmHg)	100	100	101	99
Diastolic B.P. (mmHg)	50	51	52	52
Mean Arterial B.P. (mmHg)	68	70	69	69
Central Venous B.P. (mmHg)	14	18	17	17
Mean Pulmonary B.P. (mmHg)	32	34	34	35
Wedge Pressure (mmHg)	15	16	17	19

B.2 Ethical Committee Guidelines

Location of Research

To be carried out at two centres; (1) Intensive Care Unit, Hull Royal Infirmary (2) Intensive Care Unit, Castle Hill Hospital

Subjects

The clinical investigation will be based on patients who are being mechanically ventilated in the above intensive care units.

Informed Consent

At the initial stages of the work no changes will be made to patient treatment. The study will be based on accurate recording of normal therapy.

At a later stage alterations may be made to ventilator settings. These will be restricted to changes within the normal range for therapy in the specific clinical situation. Predictions from the system as to optimum therapy will be regarded as advisory only. Any change to ventilator therapy will be made on the basis of the clinical judgement of the anaesthetist in charge. However during this stage of the work, where therapy may be influenced by the trial, informed consent will be obtained from the patient where possible.

Permission of other Professionals

The consultant in overall charge of the cases will be asked for permission for their patients to be entered into the trial.

Substances to be Given

No changes to drugs, etc given will be made for the study.

Samples

Blood gases will be measured by the normal methods employed for intensive care using normal sample sizes for the equipment employed. More regular samples, up to 4 time per hour, may be taken but no more than might be required in an individual anaesthetist's normal practice during ventilation.

Risks

It is not considered that there are any special risks to the patients or staff involved in the study.

Benefits

There will be no financial benefit to subjects or staff involved.

Facilities

There will be no significant affect on nursing or laboratory workload.

Appendix C

Simulated Patient Definitions

C.1 Normal Lung Patient

NORMAL LUNGS			
Physiological Shunt (%)			
Time (min)	Value	Function	
0	8	init. value	
30	2	ramp	
300	0	ramp	
Body Temperature (°C)			
Time (min)	Value	Functions	
0	35	initial value	
120	37	ramp	

Table C.1: Event profiles for Normal Lung patient scenario.

C.2 Lobar Pneumonia Patient

LOBAR PNEUMONIA			
Physiological Shunt (%)			
Time (min)	Value	Function	
0	32	init. value	
120	30	ramp	
120	25	step	
240	23	ramp	
360	21	ramp	
360	16	step	
1440	7	ramp	
Body Temperature (°C)			
Time (min)	Value	Function	
0	35	init. value	
120	37	ramp	

Table C.2 Continued Overleaf...

LOBAR PNEUMONIA Continued...			
Metabolic Rate (%)			
Time (min)	Value	Function	
0	135	init. value	
1440	100	ramp	
Respiratory Quotient			
Time (min)	Value	Function	
0	0.75	init. value	
1440	0.8	ramp	
Airway Resistance (cmH₂O/sec)			
Time (min)	Value	Function	
0	15	init. value	
1440	10	ramp	
Lung Compliance (l/cmH₂O)			
Time (min)	Value	Function	
0	0.02	init. value	
120	0.03	step	
360	0.04	step	
720	0.05	step	
Arterial Bicarbonate (mmol/l)			
Time (min)	Value	Function	
0	16	init. value	
1440	24	ramp	

Table C.2 Continues Overleaf...

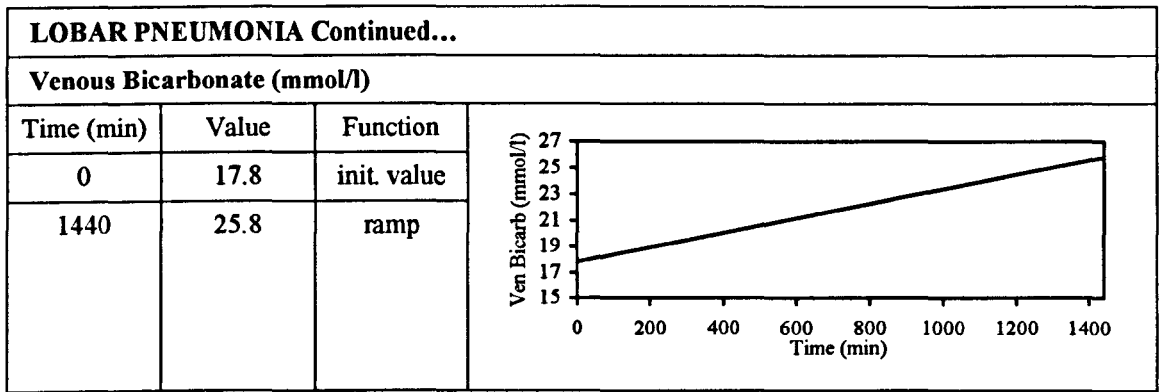


Table C.2: Event profiles for Lobar Pneumonia patient scenario.

C.3 Acute Asthmatic Patient

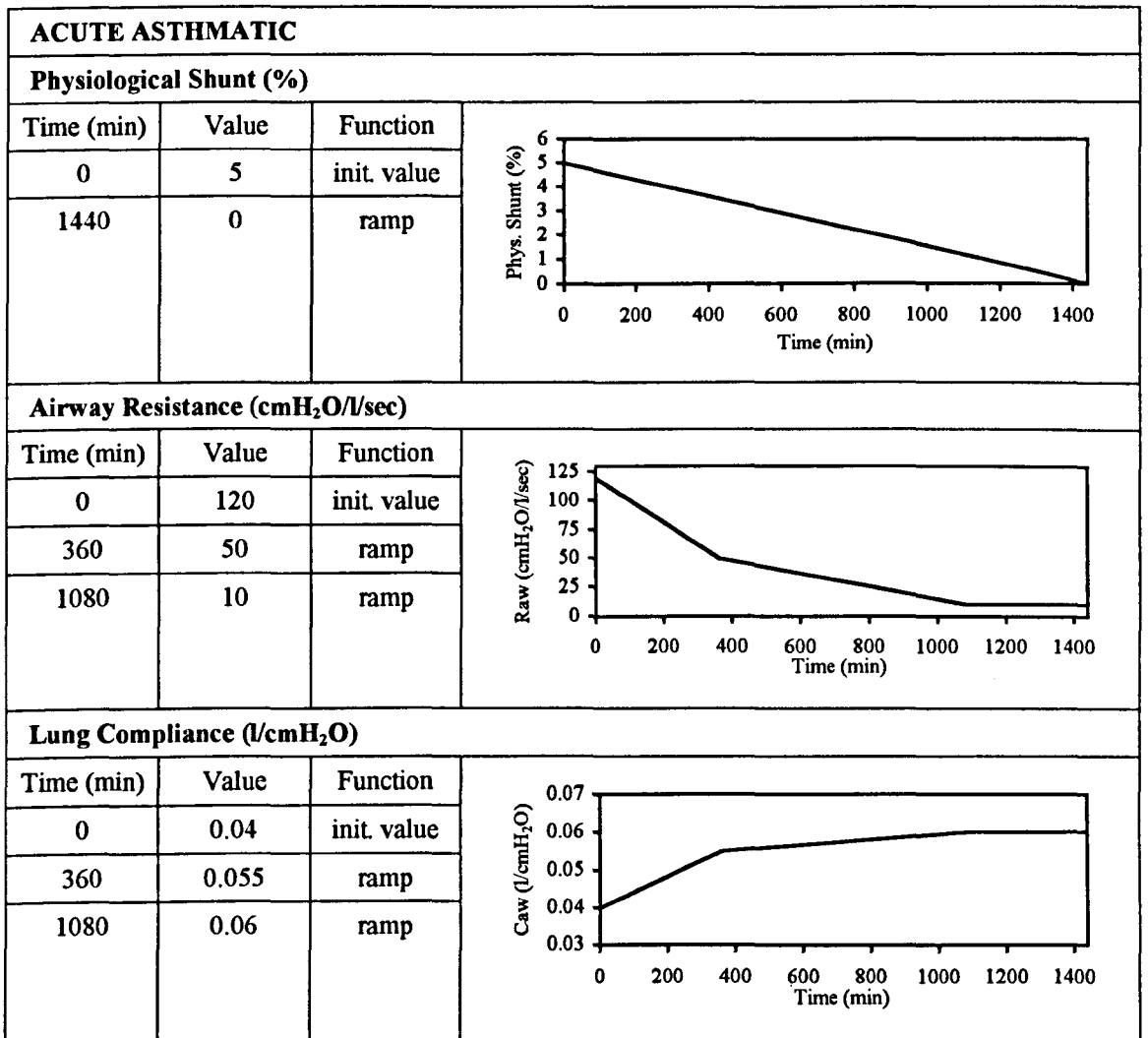
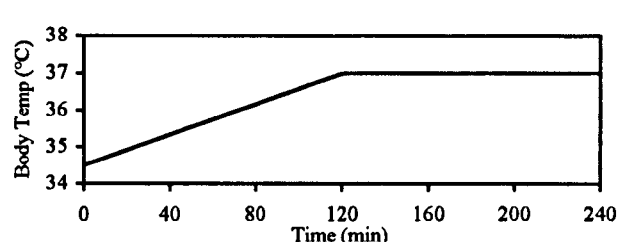


Table C.3: Event profiles for Acute Asthmatic patient scenario.

C.4 Head Injury Patient

HEAD INJURY		
Body Temperature (°C)		
Time (min)	Value	Function
0	34.5	init. value
120	37	ramp

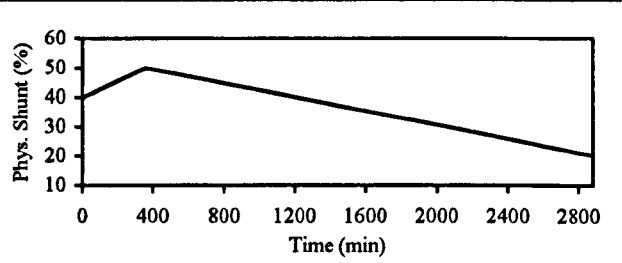


The graph plots Body Temperature (°C) on the y-axis (ranging from 34 to 38) against Time (min) on the x-axis (ranging from 0 to 240). The temperature starts at 34.5°C at 0 minutes, increases linearly to 37°C at 120 minutes, and then remains constant at 37°C until 240 minutes.

Table C.4: Event profiles for Head Injury patient scenario.

C.5 ARDS Patient

ARDS		
Physiological Shunt (%)		
Time (min)	Value	Function
0	40	init. value
360	50	ramp
2880	20	ramp



The graph plots Phys. Shunt (%) on the y-axis (ranging from 10 to 60) against Time (min) on the x-axis (ranging from 0 to 2800). The shunt starts at 40% at 0 minutes, rises to a peak of 50% at 360 minutes, and then gradually decreases to 20% at 2880 minutes.

Table C.5: Event profiles for ARDS patient scenario.

C.6 Patient Initial Conditions

	Normal Lungs	Lobar Pneumon.	Acute Asthmatic	Head Injury	ARDS
Patient Parameters					
Sex	male	female	female	male	male
Weight (kg)	75	60	60	85	75
Height (cm)	165	150	150	190	180
Age (years)	50	65	47	22	50
Body Temperature (°C)	35	38.5	37	34.5	38
Cardiac Output (l/min) †	4.82	6.15	4.65	5.35	6.90
O ₂ Consum. (ml/min: STPD) †	213.2	343.8	222.7	220.6	317.3
CO ₂ Prod. (ml/min: STPD) †	170.6	257.9	178.2	176.5	253.8
Metabolic Rate (%)	100	135	100	100	110
Respiratory Quotient	0.8	0.75	0.8	0.8	0.8
Cardiac Efficiency (%)	100	100	100	100	100
Tamponade Sensitivity (%)	100	100	100	100	100
Dead Space (ml: ATPS) †	165	132	132	187	165
Physiological Shunt (%)	8	32	5	3	40
Fixed Shunt (%)	2	3	1	2	2
PEEP Threshold (cmH ₂ O)	6	60	100	4	70
Haemoglobin (g/l)	140	116	130	140	140
Arterial Bicarbonate (mmol/l)	24	16	24	24	24
Venous Bicarbonate (mmol/l)	25.8	17.8	25.8	25.8	25.8
Packed Cell Volume (%) †	42	34.8	39	42	42
Airway Resist. (cmH ₂ O/l/sec)	7	15	120	7	10
Lung Compliance (l/cmH ₂ O)	0.08	0.02	0.04	0.07	0.015
Ventilator Settings					
FiO ₂ (%: STPD)	60	50	50	70	50
PEEP (cmH ₂ O)	4	0	0	0	0
VT (ml: ATPS)	750	600	600	700	700
RR (rpm)	12	14	12	12	12
TIN (%)	33	33	40	33	33
TPAUSE (%)	10	10	10	10	10
Atmospheric Conditions					
Barometric Pressure (kPa)	101.325	101.325	101.325	101.325	101.325
Air Temperature (°C)	25	20	20	20	20
Inspired FiCO ₂ (%: STPD)	0.05	0.05	0.05	0.05	0.05

Table C.6 continued overleaf...

Continued...	Normal Lungs	Lobar Pneumon.	Acute Asthmatic	Head Injury	ARDS
Fixed Parameters					
Hb O ₂ Binding Capacity (ml/g)	1.34	1.34	1.34	1.34	1.34
Plasma O ₂ Solubility (ml/l/kPa)	0.225	0.225	0.225	0.225	0.225
P50 (kPa)	3.5774	3.5774	3.5774	3.5774	3.5774
O ₂ Lung Diff. (ml/kPa/min)	450	450	450	450	450
CO ₂ Lung Diff. (ml/kPa/min)	1500	1500	1500	1500	1500
Reference Only					
Systolic Blood Press. (mmHg)	135	120	120	120	120

† Calculated from empirical formulae

Table C.6: Initial patient parameters and ventilator settings for the Normal Lung, Lobar Pneumonia, Asthmatic, Head Injury and ARDS virtual patient scenarios.

Appendix D

Closed Loop Decision History Data

	1	2	3	4	5	6
Time (hours)	0.0	0.5	1.0	2.5	5.5	8.5
Patient Observations						
PaO ₂ (kPa)	42.90	27.24	21.67	21.82	23.86	19.28
PaCO ₂ (kPa)	3.08	4.68	5.36	5.93	4.73	5.23
Arterial pH	7.60	7.43	7.38	7.34	7.43	7.39
PIP (cmH ₂ O)	16.6	15.5	12.7	12.7	13.2	13.0
SaO ₂ (%)	99.9	99.5	99.1	99.0	99.3	98.8
T _{BODY} (°C)	35.0	35.5	36.0	37.0	37.0	37.0
Cardiac Output (l/min)	4.82	5.06	5.46	5.95	5.95	5.95
O ₂ Consump. (ml/min)	213	226	238	263	263	263
CO ₂ Prod. (ml/min)	171	181	191	211	211	211
Effective Shunt (%)	4.7	2.7	3.2	2.7	2.0	2.0
Metab. Rate (%)	100	100	100	100	100	100
Respiratory Quotient	0.80	0.80	0.80	0.80	0.80	0.80
Raw (cmH ₂ O/l/sec)	7.0	7.0	7.0	7.0	7.0	7.0
Caw (l/cmH ₂ O)	0.08	0.08	0.08	0.08	0.08	0.08
Ventilator Settings						
FiO ₂ (%)	60	40	35	35	35	30
PEEP (cmH ₂ O)	4.0	4.0	2.0	2.0	2.0	2.0
VT (ml)	750	750	700	700	700	700
RR (rpm)	12.0	8.0	8.0	8.0	10.0	9.0
Mv (l/min)	9.00	6.00	5.60	5.60	7.00	6.30
T _{IN} (%)	33	33	33	33	33	33
Advised Ventilator Settings						
FiO ₂ (%)	40	35	35	35	30	WEAN
PEEP (cmH ₂ O)	4.0	2.0	2.0	2.0	2.0	
VT (ml)	750	700	700	700	700	
RR (rpm)	8.0	8.0	8.0	10.0	9.0	
Mv (l/min)	6.00	5.60	5.60	7.00	6.30	
T _{IN} (%)	33	33	33	33	33	

Table D.1: Anaesthetist decision history for Normal Lung patient.

	1	2	3	4	5	6
Time (hours)	0.0	0.5	1.0	2.5	5.5	8.5
Patient Observations						
PaO ₂ (kPa)	42.90	21.26	18.14	17.74	19.14	19.22
PaCO ₂ (kPa)	3.08	5.11	5.49	5.93	5.41	5.32
Arterial pH	7.60	7.39	7.37	7.34	7.38	7.38
PIP (cmH ₂ O)	16.6	11.7	11.1	10.7	11.0	11.2
SaO ₂ (%)	99.9	99.2	98.7	98.4	98.8	98.8
T _{BODY} (°C)	35.0	35.5	36.0	37.0	37.0	37.0
Cardiac Output (l/min)	4.82	5.30	5.60	6.11	6.11	6.11
O ₂ Consump. (ml/min)	213	226	239	263	263	263
CO ₂ Prod. (ml/min)	171	181	191	211	211	211
Effective Shunt (%)	4.7	3.6	3.6	3.1	2.0	2.0
Metab. Rate (%)	100	100	100	100	100	100
Respiratory Quotient	0.80	0.80	0.80	0.80	0.80	0.80
Raw (cmH ₂ O/l/sec)	7.0	7.0	7.0	7.0	7.0	7.0
Caw (l/cmH ₂ O)	0.08	0.08	0.08	0.08	0.08	0.08
Ventilator Settings						
FiO ₂ (%)	60	35	31	30	30	30
PEEP (cmH ₂ O)	4.0	1.0	0.5	0.0	0.0	0.0
VT (ml)	750	700	690	700	710	720
RR (rpm)	12.0	8.0	8.0	8.0	8.5	8.5
Mv (l/min)	9.00	5.60	5.52	5.60	6.04	6.12
T _{IN} (%)	33	33	33	33	33	33
Advised Ventilator Settings						
FiO ₂ (%)	35	31	30	30	30	30
PEEP (cmH ₂ O)	1.0	0.5	0.0	0.0	0.0	0.0
VT (ml)	700	690	700	710	720	720
RR (rpm)	8.0	8.0	8.0	8.5	8.5	8.5
Mv (l/min)	5.60	5.52	5.60	6.04	6.12	6.12
T _{IN} (%)	33	33	33	33	33	33

Table D.2: Prototype advisor decision history for Normal Lung patient.

	1	2	3	4	5	6
Time (hours)	0.0	0.5	1.0	2.5	5.5	8.5
Patient Observations						
PaO ₂ (kPa)	42.90	25.57	21.04	21.71	23.34	23.35
PaCO ₂ (kPa)	3.08	5.34	5.49	5.70	5.31	5.31
Arterial pH	7.60	7.38	7.37	7.35	7.38	7.38
PIP (cmH ₂ O)	16.6	12.8	11.1	11.2	11.3	10.8
SaO ₂ (%)	99.9	99.4	99.1	99.0	99.2	99.2
T _{BODY} (°C)	35.0	35.5	36.0	37.0	37.0	37.0
Cardiac Output (l/min)	4.82	5.22	5.60	6.07	6.07	6.11
O ₂ Consump. (ml/min)	213	226	239	263	263	263
CO ₂ Prod. (ml/min)	171	181	191	211	211	211
Effective Shunt (%)	0.0	0.0	0.0	0.0	0.0	0.0
Metab. Rate (%)	100	100	100	100	100	100
Respiratory Quotient	0.80	0.80	0.80	0.80	0.80	0.80
Raw (cmH ₂ O/l/sec)	0.7	0.7	0.7	0.7	0.7	0.7
Caw (l/cmH ₂ O)	0.82	0.82	0.82	0.82	0.82	0.82
Ventilator Settings						
FiO ₂ (%)	60	40	35	35	35	35
PEEP (cmH ₂ O)	4.0	2.0	0.5	0.5	0.5	0.0
VT (ml)	750	710	690	690	690	690
RR (rpm)	12.0	7.5	8.0	8.5	9.0	9.0
Mv (l/min)	9.00	5.33	5.52	5.87	6.21	6.21
T _{IN} (%)	33	33	33	33	33	33
Advised Ventilator Settings						
FiO ₂ (%)	40	35	35	35	35	35
PEEP (cmH ₂ O)	2.0	0.5	0.5	0.5	0.0	0.0
VT (ml)	710	690	690	690	690	700
RR (rpm)	7.5	8.0	8.5	9.0	9.0	9.0
Mv (l/min)	5.33	5.52	5.87	6.21	6.21	6.30
T _{IN} (%)	33	33	33	33	33	33

Table D.3: Refined advisor decision history for Normal Lung patient.

	1	2	3	4	5	6	7	8	9	10	11
Time (hours)	0.0	0.5	1.5	2.5	4.5	6.5	9.5	12.5	18.5	24.5	25.5
Patient Observations											
PaO ₂ (kPa)	9.54	9.79	9.91	11.11	11.65	18.05	16.80	15.25	20.22	19.70	14.93
PaCO ₂ (kPa)	8.58	6.88	6.17	5.31	4.91	4.16	4.61	4.68	4.54	4.55	5.38
Arterial pH	7.02	7.12	7.17	7.24	7.29	7.37	7.35	7.37	7.42	7.45	7.38
PIP (cmH ₂ O)	36.4	42.1	42.9	32.8	32.5	27.3	25.3	22.0	19.3	16.3	15.8
SaO ₂ (%)	80.5	86.2	88.7	93.4	94.9	98.5	98.2	97.8	98.9	99.0	97.9
T _{body} (°C)	38.5	38.5	38.4	38.3	38.2	38.1	37.9	37.7	37.3	37.0	37.0
Cardiac Output (l/min)	6.15	6.05	5.98	5.88	5.75	5.59	5.40	5.18	4.82	4.57	4.57
O ₂ Consump. (ml/min)	344	341	336	330	319	309	293	278	248	223	223
CO ₂ Prod. (ml/min)	258	256	253	249	243	236	226	216	196	178	178
Effective Shunt (%)	35.0	32.4	31.5	25.9	24.0	17.7	16.3	14.9	12.1	9.8	9.8
Metab. Rate (%)	135	134	133	131	128	126	121	117	108	100	100
Respiratory Quotient	0.75	0.75	0.75	0.76	0.76	0.76	0.77	0.78	0.79	0.80	0.80
Raw (cmH ₂ O/l/sec)	15.0	14.9	14.7	14.5	14.1	13.6	13.0	12.4	11.1	10.0	10.0
Caw (l/cmH ₂ O)	0.02	0.02	0.02	0.03	0.03	0.04	0.04	0.05	0.05	0.05	0.05
Ventilator Settings											
FiO ₂ (%)	50	70	80	80	80	80	70	60	60	50	40
PEEP (cmH ₂ O)	0.0	4.0	4.0	4.0	4.0	4.0	4.0	4.0	4.0	2.0	2.0
V _T (ml)	600	600	600	600	600	600	600	600	550	550	550
RR (rpm)	14.0	18.0	20.0	20.0	20.0	20.0	16.0	16.0	14.0	12.0	10.0
M _v (l/min)	8.40	10.80	12.00	12.00	12.00	12.00	9.60	9.60	7.70	6.60	5.50
T _{IN} (%)	33	33	33	33	33	33	33	33	33	33	33
Advised Ventilator Settings											
FiO ₂ (%)	70	80	80	80	80	70	60	60	50	40	WEAN
PEEP (cmH ₂ O)	4.0	4.0	4.0	4.0	4.0	4.0	4.0	4.0	2.0	2.0	
V _T (ml)	600	600	600	600	600	600	600	550	550	550	
RR (rpm)	18.0	20.0	20.0	20.0	20.0	16.0	16.0	14.0	12.0	10.0	
M _v (l/min)	10.80	12.00	12.00	12.00	12.00	9.60	9.60	7.70	6.60	5.50	
T _{IN} (%)	33	33	33	33	33	33	33	33	33	33	

Table D.4: Anaesthetist decision history for Lobar Pneumonia patient.

	1	2	3	4	5	6	7	8	9	10	11
Time (hours)	0.0	0.5	1.5	2.5	4.5	6.5	9.5	12.5	18.5	24.5	25.5
Patient Observations											
PaO ₂ (kPa)	9.54	9.70	10.18	12.28	12.79	20.26	13.43	13.80	15.66	15.64	13.83
PaCO ₂ (kPa)	8.58	7.00	6.44	5.45	4.83	4.15	4.13	4.20	4.03	4.20	5.00
Arterial pH	7.02	7.11	7.15	7.23	7.30	7.37	7.40	7.41	7.47	7.48	7.41
PIP (cmH ₂ O)	36.4	41.0	41.0	31.8	34.7	28.7	27.3	22.8	21.0	19.7	18.1
SaO ₂ (%)	80.5	85.5	88.9	94.7	96.0	98.8	97.3	97.6	98.4	98.5	97.7
T _{BODY} (°C)	38.5	38.5	38.4	38.3	38.2	38.1	37.9	37.7	37.3	37.0	37.0
Cardiac Output (l/min)	6.15	6.05	5.98	5.87	5.74	5.57	5.40	5.18	4.82	4.50	4.54
O ₂ Consump. (ml/min)	344	341	336	330	319	309	293	278	248	223	223
CO ₂ Prod. (ml/min)	258	256	253	249	243	236	226	216	196	178	178
Effective Shunt (%)	35.0	32.7	31.4	25.6	23.8	17.6	16.3	14.9	12.1	9.5	9.7
Metab. Rate (%)	135	134	133	131	128	126	121	117	108	100	100
Respiratory Quotient	0.75	0.75	0.75	0.76	0.76	0.76	0.77	0.78	0.79	0.80	0.80
Raw (cmH ₂ O/l/sec)	15.0	14.9	14.7	14.5	14.1	13.6	13.0	12.4	11.1	10.0	10.0
Caw (l/cmH ₂ O)	0.02	0.02	0.02	0.03	0.03	0.04	0.04	0.05	0.05	0.05	0.05
Ventilator Settings											
FiO ₂ (%)	50	67	82	90	88	84	60	56	51	42	37
PEEP (cmH ₂ O)	0.0	3.5	4.0	4.5	4.5	4.5	4.0	4.0	4.0	4.0	3.0
Vt (ml)	600	590	570	560	650	640	650	640	610	610	610
RR (rpm)	14.0	18.0	20.0	21.0	18.5	18.5	16.5	15.0	14.0	11.5	9.5
Mv (l/min)	8.40	10.62	11.40	11.76	12.03	11.84	10.73	9.60	8.54	7.02	5.80
T _{IN} (%)	33	33	33	33	33	33	33	33	33	33	33
Advised Ventilator Settings											
FiO ₂ (%)	67	82	90	88	84	60	56	51	42	37	35
PEEP (cmH ₂ O)	3.5	4.0	4.5	4.5	4.5	4.0	4.0	4.0	4.0	3.0	2.0
Vt (ml)	590	570	560	650	640	650	640	610	610	610	590
RR (rpm)	18.0	20.0	21.0	18.5	18.5	16.5	15.0	14.0	11.5	9.5	9.5
Mv (l/min)	10.62	11.40	11.76	12.03	11.84	10.73	9.60	8.54	7.02	5.80	5.61
T _{IN} (%)	33	33	33	33	33	33	33	33	33	33	33

Table D.5: Prototype advisor decision history for Lobar Pneumonia patient.

	1	2	3	4	5	6	7	8	9	10	11
Time (hours)	0.0	0.5	1.5	2.5	4.5	6.5	9.5	12.5	18.5	24.5	25.5
Patient Observations											
PaO ₂ (kPa)	9.54	9.65	9.69	10.97	11.56	17.78	15.49	15.65	20.26	21.74	16.14
PaCO ₂ (kPa)	8.58	6.91	6.06	5.21	4.91	4.43	4.73	4.78	4.55	4.46	5.36
Arterial pH	7.02	7.11	7.18	7.25	7.29	7.35	7.34	7.36	7.42	7.46	7.38
PIP (cmH ₂ O)	36.4	40.2	41.5	31.4	31.0	25.3	24.0	21.3	20.2	18.3	16.7
SaO ₂ (%)	80.5	85.5	88.2	93.3	94.8	98.3	97.8	97.9	99.0	99.2	98.3
T _{body} (°C)	38.5	38.5	38.4	38.3	38.2	38.1	37.9	37.7	37.3	37.0	37.0
Cardiac Output (l/min)	6.15	6.05	5.98	5.88	5.75	5.59	5.40	5.18	4.82	4.54	4.57
O ₂ Consump. (ml/min)	344	341	336	330	319	309	293	278	248	223	223
CO ₂ Prod. (ml/min)	258	256	253	249	243	236	226	216	196	178	178
Effective Shunt (%)	0.4	0.3	0.3	0.3	0.2	0.2	0.2	0.1	0.1	0.1	0.1
Metab. Rate (%)	135	134	133	131	128	126	121	117	108	100	100
Respiratory Quotient	0.75	0.75	0.75	0.76	0.76	0.76	0.77	0.78	0.79	0.80	0.80
Raw (cmH ₂ O/l/sec)	1.5	1.5	1.4	1.4	1.4	1.3	1.3	1.2	1.1	1.0	1.0
Caw (l/cmH ₂ O)	0.20	0.20	0.20	0.31	0.31	0.41	0.41	0.51	0.51	0.51	0.51
Ventilator Settings											
FiO ₂ (%)	50	67	76	79	79	79	66	61	60	53	43
PEEP (cmH ₂ O)	0.0	3.5	4.0	4.0	4.0	4.0	4.0	4.0	4.0	3.0	2.0
Vt (ml)	600	600	600	600	600	600	600	600	600	600	600
RR (rpm)	14.0	18.0	20.5	20.5	20.0	18.5	15.5	14.0	12.5	11.0	9.0
Mv (l/min)	8.40	10.80	12.30	12.30	12.00	11.10	9.30	8.40	7.50	6.60	5.40
T _{IN} (%)	33	40	40	40	40	40	40	33	33	33	33
Advised Ventilator Settings											
FiO ₂ (%)	67	76	79	79	79	66	61	60	53	43	36
PEEP (cmH ₂ O)	3.5	4.0	4.0	4.0	4.0	4.0	4.0	4.0	3.0	2.0	2.5
Vt (ml)	600	600	600	600	600	600	600	600	600	600	600
RR (rpm)	18.0	20.5	20.5	20.0	18.5	15.5	14.0	12.5	11.0	9.0	9.0
Mv (l/min)	10.80	12.30	12.30	12.00	11.10	9.30	8.40	7.50	6.60	5.40	5.40
T _{IN} (%)	40	40	40	40	40	40	33	33	33	33	33

Table D.6: Revised advisor decision history for Lobar Pneumonia patient.

	1	2	3	4	5
Time (hours)	0.0	0.5	2.5	8.5	10.5
Patient Observations					
PaO ₂ (kPa)	28.68	20.43	21.01	23.08	20.58
PaCO ₂ (kPa)	3.93	5.55	5.57	5.49	4.68
Arterial pH	7.51	7.37	7.36	7.37	7.44
PIP (cmH ₂ O)	51.1	31.5	25.6	14.9	15.2
SaO ₂ (%)	99.6	98.9	98.9	99.1	99.1
T _{BODY} (°C)	37.0	37.0	37.0	37.0	37.0
Cardiac Output (l/min)	4.65	4.65	4.65	4.65	4.65
O ₂ Consump. (ml/min)	223	223	223	223	223
CO ₂ Prod. (ml/min)	178	178	178	178	178
Effective Shunt (%)	6.0	5.9	5.5	4.2	3.8
Metab. Rate (%)	100	100	100	100	100
Respiratory Quotient	0.80	0.80	0.80	0.80	0.80
Raw (cmH ₂ O/l/sec)	120.3	114.2	90.8	41.8	34.7
Caw (l/cmH ₂ O)	0.04	0.04	0.05	0.06	0.06
Ventilator Settings					
FiO ₂ (%)	50	40	40	40	35
PEEP (cmH ₂ O)	0.0	0.0	0.0	0.0	0.0
V _T (ml)	600	450	400	400	450
RR (rpm)	12.0	12.0	14.0	14.0	14.0
Mv (l/min)	7.20	5.40	5.60	5.60	6.30
T _{IN} (%)	40	50	50	50	50
Advised Ventilator Settings					
FiO ₂ (%)	40	40	40	35	WEAN
PEEP (cmH ₂ O)	0.0	0.0	0.0	0.0	
V _T (ml)	450	400	400	450	
RR (rpm)	12.0	14.0	14.0	14.0	
Mv (l/min)	5.40	5.60	5.60	6.30	
T _{IN} (%)	50	50	50	50	

Table D.7: Anaesthetist decision history for Acute Asthmatic patient.

	1	2	3	4	5
Time (hours)	0.0	0.5	2.5	8.5	10.5
Patient Observations					
PaO ₂ (kPa)	28.68	14.97	15.32	16.57	17.03
PaCO ₂ (kPa)	3.93	5.25	5.22	5.06	5.09
Arterial pH	7.51	7.39	7.39	7.40	7.40
PIP (cmH ₂ O)	51.0	38.6	31.9	19.5	18.1
SaO ₂ (%)	99.6	98.0	98.1	98.4	98.5
T _{BODY} (°C)	37.0	37.0	37.0	37.0	37.0
Cardiac Output (l/min)	4.65	4.65	4.65	4.65	4.65
O ₂ Consump. (ml/min)	223	223	223	223	223
CO ₂ Prod. (ml/min)	178	178	178	178	178
Effective Shunt (%)	6.0	5.9	5.5	4.2	3.8
Metab. Rate (%)	100	100	100	100	100
Respiratory Quotient	0.80	0.80	0.80	0.80	0.80
Raw (cmH ₂ O/l/sec)	120.0	114.1	90.7	41.6	34.9
Caw (l/cmH ₂ O)	0.04	0.04	0.05	0.06	0.06
Ventilator Settings					
FI _{O₂} (%)	50	30	30	30	30
PEEP (cmH ₂ O)	0.0	0.0	0.0	0.0	0.0
V _T (ml)	600	520	520	570	590
RR (rpm)	12.0	10.5	10.5	9.5	9.0
Mv (l/min)	7.20	5.46	5.46	5.42	5.31
T _{IN} (%)	40	40	40	40	40
Advised Ventilator Settings					
FI _{O₂} (%)	30	30	30	30	30
PEEP (cmH ₂ O)	0.0	0.0	0.0	0.0	0.0
V _T (ml)	520	520	570	590	580
RR (rpm)	10.5	10.5	9.5	9.0	9.0
Mv (l/min)	5.46	5.46	5.42	5.31	5.22
T _{IN} (%)	40	40	40	40	40

Table D.8: Prototype advisor decision history for Acute Asthmatic patient.

	1	2	3	4	5
Time (hours)	0.0	0.5	2.5	8.5	10.5
Patient Observations					
PaO ₂ (kPa)	28.68	20.43	17.98	19.68	20.38
PaCO ₂ (kPa)	3.93	5.55	5.46	5.24	5.07
Arterial pH	7.51	7.37	7.37	7.39	7.40
PIP (cmH ₂ O)	51.0	31.5	26.6	16.3	17.3
SaO ₂ (%)	99.6	98.9	98.6	98.9	99.0
T _{BODY} (°C)	37.0	37.0	37.0	37.0	37.0
Cardiac Output (l/min)	4.65	4.65	4.63	4.63	4.63
O ₂ Consump. (ml/min)	223	223	223	223	223
CO ₂ Prod. (ml/min)	178	178	178	178	178
Effective Shunt (%)	0.1	0.1	0.1	0.0	0.0
Metab. Rate (%)	100	100	100	100	100
Respiratory Quotient	0.80	0.80	0.80	0.80	0.80
Raw (cmH ₂ O/l/sec)	11.8	11.2	8.9	4.1	3.4
Caw (l/cmH ₂ O)	0.41	0.42	0.47	0.57	0.58
Ventilator Settings					
FiO ₂ (%)	50	40	35	35	35
PEEP (cmH ₂ O)	0.0	0.0	0.5	0.5	0.5
V _T (ml)	600	450	440	450	490
RR (rpm)	12.0	12.0	12.5	12.5	11.5
Mv (l/min)	7.20	5.40	5.50	5.63	5.64
T _{IN} (%)	40	50	50	50	40
Advised Ventilator Settings					
FiO ₂ (%)	40	35	35	35	35
PEEP (cmH ₂ O)	0.0	0.5	0.5	0.5	0.5
V _T (ml)	450	440	450	490	500
RR (rpm)	12.0	12.5	12.5	11.5	11.0
Mv (l/min)	5.40	5.50	5.63	5.64	5.50
T _{IN} (%)	50	50	50	40	33

Table D.9: Revised advisor decision history for Acute Asthmatic patient.

	1	2	3	4	5	6
Time (hours)	0.0	0.5	2.5	3.5	5.5	11.5
Patient Observations						
PaO ₂ (kPa)	51.82	32.04	22.88	23.58	19.66	19.66
PaCO ₂ (kPa)	3.47	4.42	5.42	3.90	4.50	4.50
Arterial pH	7.55	7.45	7.38	7.51	7.45	7.45
PIP (cmH ₂ O)	13.0	12.5	12.5	13.5	13.0	13.0
SaO ₂ (%)	99.9	99.7	99.1	99.4	99.0	99.0
T _{BODY} (°C)	34.5	35.1	37.0	37.0	37.0	37.0
Cardiac Output (l/min)	5.35	5.69	6.71	6.71	6.71	6.71
O ₂ Consump. (ml/min)	221	238	289	289	289	289
CO ₂ Prod. (ml/min)	176	190	231	231	231	231
Effective Shunt (%)	5.0	5.0	5.0	5.0	5.0	5.0
Metab. Rate (%)	100	100	100	100	100	100
Respiratory Quotient	0.80	0.80	0.80	0.80	0.80	0.80
Raw (cmH ₂ O//sec)	7.0	7.0	7.0	7.0	7.0	7.0
Caw (l/cmH ₂ O)	0.07	0.07	0.07	0.07	0.07	0.07
Ventilator Settings						
FiO ₂ (%)	70	50	40	40	35	35
PEEP (cmH ₂ O)	0.0	0.0	0.0	0.0	0.0	0.0
VT (ml)	700	700	700	700	700	700
RR (rpm)	12.0	10.0	10.0	14.0	12.0	12.0
Mv (l/min)	8.40	7.00	7.00	9.80	8.40	8.40
T _{IN} (%)	33	33	33	33	33	33
Advised Ventilator Settings						
FiO ₂ (%)	50	40	40	35	35	CONTINUE UNTIL PATIENT WAKES FROM COMA
PEEP (cmH ₂ O)	0.0	0.0	0.0	0.0	0.0	
VT (ml)	700	700	700	700	700	
RR (rpm)	10.0	10.0	14.0	12.0	12.0	
Mv (l/min)	7.00	7.00	9.80	8.40	8.40	
T _{IN} (%)	33	33	33	33	33	

Table D.10: Anaesthetist decision history for Head Injury patient.

	1	2	3	4	5	6	7
Time (hours)	0.0	0.5	2.5	3.5	5.5	11.5	17.5
Patient Observations							
PaO ₂ (kPa)	51.82	23.38	16.81	16.43	16.45	16.47	16.47
PaCO ₂ (kPa)	3.47	4.73	5.70	4.76	4.69	4.63	4.63
Arterial pH	7.55	7.43	7.35	7.43	7.44	7.44	7.44
PIP (cmH ₂ O)	13.0	13.0	13.1	14.1	14.3	14.5	14.5
SaO ₂ (%)	99.9	99.4	98.3	98.5	98.5	98.5	98.5
T _{BODY} (°C)	34.5	35.1	37.0	37.0	37.0	37.0	37.0
Cardiac Output (l/min)	5.35	5.70	6.71	6.71	6.71	6.71	6.71
O ₂ Consump. (ml/min)	221	238	289	289	289	289	289
CO ₂ Prod. (ml/min)	176	190	231	231	231	231	231
Effective Shunt (%)	5.0	5.0	5.0	5.0	5.0	5.0	5.0
Metab. Rate (%)	100	100	100	100	100	100	100
Respiratory Quotient	0.80	0.80	0.80	0.80	0.80	0.80	0.80
Raw (cmH ₂ O/l/sec)	7.0	7.0	7.0	7.0	7.0	7.0	7.0
Caw (l/cmH ₂ O)	0.07	0.07	0.07	0.07	0.07	0.07	0.07
Ventilator Settings							
FiO ₂ (%)	70	40	31	30	30	30	30
PEEP (cmH ₂ O)	0.0	0.0	0.0	0.0	0.0	0.0	0.0
V _T (ml)	700	750	760	800	810	820	820
RR (rpm)	12.0	8.5	8.5	9.5	9.5	9.5	9.5
Mv (l/min)	8.40	6.38	6.46	7.60	7.70	7.79	7.79
T _{IN} (%)	33	33	33	33	33	33	33
Advised Ventilator Settings							
FiO ₂ (%)	40	31	30	30	30	30	30
PEEP (cmH ₂ O)	0.0	0.0	0.0	0.0	0.0	0.0	0.0
V _T (ml)	750	760	800	810	820	820	820
RR (rpm)	8.5	8.5	9.5	9.5	9.5	9.5	10.0
Mv (l/min)	6.38	6.46	7.60	7.70	7.79	7.79	8.20
T _{IN} (%)	33	33	33	33	33	33	33

Table D.11: Prototype advisor decision history for **Head Injury** patient.

	1	2	3	4	5	6	7
Time (hours)	0.0	0.5	2.5	3.5	5.5	11.5	17.5
Patient Observations							
PaO ₂ (kPa)	51.82	31.60	22.88	19.66	20.15	20.15	20.15
PaCO ₂ (kPa)	3.47	4.88	5.42	4.50	4.49	4.49	4.49
Arterial pH	7.55	7.41	7.38	7.45	7.45	7.45	7.45
PIP (cmH ₂ O)	13.0	12.2	12.5	13.0	13.5	13.5	13.5
SaO ₂ (%)	99.9	99.7	99.1	99.0	99.0	99.0	99.0
T _{BODY} (°C)	34.5	35.1	37.0	37.0	37.0	37.0	37.0
Cardiac Output (l/min)	5.35	5.70	6.71	6.71	6.67	6.67	6.67
O ₂ Consump. (ml/min)	221	238	289	289	289	289	289
CO ₂ Prod. (ml/min)	176	190	231	231	231	231	231
Effective Shunt (%)	0.1	0.1	0.1	0.1	0.0	0.0	0.0
Metab. Rate (%)	100	100	100	100	100	100	100
Respiratory Quotient	0.80	0.80	0.80	0.80	0.80	0.80	0.80
Raw (cmH ₂ O/l/sec)	0.7	0.7	0.7	0.7	0.7	0.7	0.7
Caw (l/cmH ₂ O)	0.71	0.71	0.71	0.71	0.71	0.71	0.71
Ventilator Settings							
FiO ₂ (%)	70	50	40	35	35	35	35
PEEP (cmH ₂ O)	0.0	0.0	0.0	0.0	0.5	0.5	0.5
VT (ml)	700	700	700	700	700	700	700
RR (rpm)	12.0	9.0	10.0	12.0	12.0	12.0	12.0
Mv (l/min)	8.40	6.30	7.00	8.40	8.40	8.40	8.40
T _{IN} (%)	33	33	33	33	33	33	33
Advised Ventilator Settings							
FiO ₂ (%)	50	40	35	35	35	35	35
PEEP (cmH ₂ O)	0.0	0.0	0.0	0.5	0.5	0.5	0.5
VT (ml)	700	700	700	700	700	700	700
RR (rpm)	9.0	10.0	12.0	12.0	12.0	12.0	12.0
Mv (l/min)	6.30	7.00	8.40	8.40	8.40	8.40	8.40
T _{IN} (%)	33	33	33	33	33	33	33

Table D.12: Revised advisor decision history for **Head Injury** patient.

	1	2	3	4	5	6	7	8	9	10	11	12	13	14	15
Time (hours)	0.0	0.5	1.5	3.5	4.5	5.5	7.5	11.5	17.5	23.5	26.5	34.5	42.5	46.5	50.5
Patient Observations															
PaO ₂ (kPa)	8.00	8.76	8.54	8.03	8.41	8.73	8.75	9.01	9.49	10.12	10.29	11.27	12.82	14.00	12.69
PaCO ₂ (kPa)	8.04	8.20	8.35	8.36	8.35	9.19	9.16	8.72	8.14	7.64	7.99	7.50	6.09	5.55	5.33
Arterial pH	7.21	7.21	7.20	7.20	7.20	7.16	7.16	7.18	7.21	7.24	7.22	7.24	7.33	7.37	7.39
PIP (cmH ₂ O)	50.9	47.9	46.8	48.1	52.9	53.5	52.3	46.3	40.0	35.8	33.8	28.4	28.0	25.8	27.6
SaO ₂ (%)	82.2	85.7	84.3	81.5	83.7	83.4	83.6	85.7	88.6	91.2	91.2	93.6	96.3	97.3	96.7
T _{BODY} (°C)	38.0	38.0	38.0	38.0	38.0	38.0	38.0	38.0	38.0	38.0	38.0	38.0	38.0	38.0	38.0
Cardiac Output (l/min)	6.90	6.84	6.84	6.85	6.78	6.79	6.78	6.76	6.73	6.70	6.69	6.70	6.67	6.71	6.71
O ₂ Consump. (ml/min)	317	317	317	317	317	317	317	317	317	317	317	317	317	317	317
CO ₂ Prod. (ml/min)	254	254	254	254	254	254	254	254	254	254	254	254	254	254	254
Effective Shunt (%)	42.0	40.5	42.1	45.2	42.7	44.1	43.9	41.5	37.8	34.1	32.3	28.3	23.2	21.3	20.3
Metab. Rate (%)	110	110	110	110	110	110	110	110	110	110	110	110	110	110	110
Respiratory Quotient	0.80	0.80	0.80	0.80	0.80	0.80	0.80	0.80	0.80	0.80	0.80	0.80	0.80	0.80	0.80
R _{aw} (cmH ₂ O/l/sec)	10.0	10.0	10.0	10.0	10.0	10.0	10.0	10.0	10.0	10.0	10.0	10.0	10.0	10.0	10.0
C _{aw} (l/cmH ₂ O)	0.02	0.01	0.01	0.01	0.01	0.01	0.01	0.01	0.02	0.02	0.02	0.02	0.03	0.03	0.03
Ventilator Settings															
FiO ₂ (%)	50	70	70	70	70	80	80	80	80	80	70	70	70	70	60
PEEP (cmH ₂ O)	0.0	4.0	4.0	4.0	10.0	10.0	10.0	10.0	10.0	10.0	10.0	8.0	8.0	6.0	6.0
V _T (ml)	700	600	550	500	450	425	425	425	425	425	425	425	475	500	550
RR (rpm)	12.0	14.0	16.0	20.0	22.0	22.0	22.0	22.0	22.0	22.0	20.0	20.0	20.0	20.0	18.0
Mv (l/min)	8.40	8.40	8.80	10.00	9.90	9.35	9.35	9.35	9.35	9.35	8.50	8.50	9.50	10.00	9.90
T _{IN} (%)	33	50	50	60	60	60	60	60	60	60	60	60	60	60	50
Advised Ventilator Settings															
FiO ₂ (%)	70	70	70	70	80	80	80	80	80	70	70	70	70	60	CONTINUE.....
PEEP (cmH ₂ O)	4.0	4.0	4.0	10.0	10.0	10.0	10.0	10.0	10.0	10.0	8.0	8.0	6.0	6.0	
V _T (ml)	600	550	500	450	425	425	425	425	425	425	425	475	500	550	
RR (rpm)	14.0	16.0	20.0	22.0	22.0	22.0	22.0	22.0	22.0	20.0	20.0	20.0	20.0	18.0	
Mv (l/min)	8.40	8.80	10.00	9.90	9.35	9.35	9.35	9.35	9.35	8.50	8.50	9.50	10.00	9.90	
T _{IN} (%)	50	50	60	60	60	60	60	60	60	60	60	60	60	50	

Table D.13: Anaesthetist decision history for ARDS patient.

	1	2	3	4	5	6	7	8	9	10	11	12	13	14	15
Time (hours)	0.0	0.5	1.5	3.5	4.5	5.5	7.5	11.5	17.5	23.5	26.5	34.5	42.5	46.5	50.5
Patient Observations															
PaO ₂ (kPa)	8.00	8.49	8.99	9.15	9.70	10.01	10.49	11.20	12.02	12.08	11.78	15.20	15.52	13.19	12.99
PaCO ₂ (kPa)	8.05	7.34	7.69	8.23	8.88	9.80	10.68	11.23	11.12	8.40	6.41	5.60	4.96	4.89	5.06
Arterial pH	7.21	7.25	7.23	7.20	7.17	7.13	7.10	7.07	7.08	7.20	7.31	7.37	7.42	7.42	7.41
PIP (cmH ₂ O)	50.9	54.6	56.4	62.1	66.1	69.1	65.9	56.9	48.2	44.7	47.2	43.4	40.9	37.7	35.0
SaO ₂ (%)	82.2	86.4	87.7	87.3	88.1	87.7	88.0	89.3	91.4	93.9	95.3	97.7	98.0	97.3	97.1
T _{BODY} (°C)	38.0	38.0	38.0	38.0	38.0	38.0	38.0	38.0	38.0	38.0	38.0	38.0	38.0	38.0	38.0
Cardiac Output (l/min)	6.90	6.84	6.83	6.80	6.76	6.75	6.74	6.72	6.69	6.66	6.65	6.60	6.61	6.68	6.72
O ₂ Consump. (ml/min)	317	317	317	317	317	317	317	317	317	317	317	317	317	317	317
CO ₂ Prod. (ml/min)	254	254	254	254	254	254	254	254	254	254	254	254	254	254	254
Effective Shunt (%)	42.0	40.5	41.5	42.6	41.4	41.7	41.1	39.2	36.3	33.1	31.3	26.5	22.5	20.9	20.4
Metab. Rate (%)	110	110	110	110	110	110	110	110	110	110	110	110	110	110	110
Respiratory Quotient	0.80	0.80	0.80	0.80	0.80	0.80	0.80	0.80	0.80	0.80	0.80	0.80	0.80	0.80	0.80
Raw (cm H ₂ O/l/sec)	10.0	10.0	10.0	10.0	10.0	10.0	10.0	10.0	10.0	10.0	10.0	10.0	10.0	10.0	10.0
Caw (l/cm H ₂ O)	0.02	0.01	0.01	0.01	0.01	0.01	0.01	0.01	0.02	0.02	0.02	0.02	0.03	0.03	0.03
Ventilator Settings															
FiO ₂ (%)	50	75	94	100	100	100	100	100	100	100	99	99	83	67	63
PEEP (cmH ₂ O)	0.0	4.0	5.0	8.0	12.0	13.5	14.0	13.5	12.5	12.0	12.0	12.0	10.0	7.0	5.5
VT (ml)	700	670	640	600	560	540	520	510	510	530	600	620	700	750	740
RR (rpm)	12.0	14.0	14.5	15.0	14.5	13.5	12.5	11.5	11.0	14.0	16.0	16.5	15.0	13.5	13.0
Mv (l/min)	8.40	9.38	9.28	9.00	8.12	7.29	6.50	5.87	5.61	7.42	9.60	10.23	10.50	10.13	9.62
T _{IN} (%)	33	33	33	33	33	33	33	33	33	33	33	33	33	33	33
Advised Ventilator Settings															
FiO ₂ (%)	75	94	100	100	100	100	100	100	100	99	99	83	67	63	60
PEEP (cmH ₂ O)	4.0	5.0	8.0	12.0	13.5	14.0	13.5	12.5	12.0	12.0	12.0	10.0	7.0	5.5	4.5
VT (ml)	670	640	600	560	540	520	510	510	530	600	620	700	750	740	750
RR (rpm)	14.0	14.5	15.0	14.5	13.5	12.5	11.5	11.0	14.0	16.0	16.5	15.0	13.5	13.0	12.5
Mv (l/min)	9.38	9.28	9.00	8.12	7.29	6.50	5.87	5.61	7.42	9.60	10.23	10.50	10.13	9.62	9.38
T _{IN} (%)	33	33	33	33	33	33	33	33	33	33	33	33	33	33	33

Table D.14: Prototype advisor decision history for ARDS patient.

	1	2	3	4	5	6	7	8	9	10	11	12	13	14	15
Time (hours)	0.0	0.5	1.5	3.5	4.5	5.5	7.5	11.5	17.5	23.5	26.5	34.5	42.5	46.5	50.5
Patient Observations															
PaO ₂ (kPa)	8.00	8.62	8.69	8.47	8.44	8.52	8.73	9.19	9.75	10.34	10.55	11.92	14.79	15.05	13.66
PaCO ₂ (kPa)	8.05	7.91	7.87	8.36	8.60	8.97	9.03	8.71	8.10	7.65	7.24	6.50	5.86	5.43	5.15
Arterial pH	7.21	7.22	7.22	7.20	7.19	7.17	7.17	7.18	7.21	7.24	7.26	7.30	7.35	7.38	7.40
PIP (cmH ₂ O)	50.9	44.7	46.0	49.3	51.6	54.5	53.1	47.1	41.3	37.0	35.4	32.2	29.5	28.9	29.5
SaO ₂ (%)	82.2	85.7	86.1	84.0	83.2	82.8	83.8	86.5	89.5	91.7	92.7	95.3	97.5	97.7	97.3
T _{BODY} (°C)	38.0	38.0	38.0	38.0	38.0	38.0	38.0	38.0	38.0	38.0	38.0	38.0	38.0	38.0	38.0
Cardiac Output (l/min)	6.90	6.84	6.83	6.82	6.81	6.80	6.79	6.76	6.72	6.69	6.69	6.66	6.67	6.70	6.72
O ₂ Consump. (ml/min)	317	317	317	317	317	317	317	317	317	317	317	317	317	317	317
CO ₂ Prod. (ml/min)	254	254	254	254	254	254	254	254	254	254	254	254	254	254	254
Effective Shunt (%)	0.4	0.4	0.4	0.4	0.4	0.5	0.4	0.4	0.4	0.3	0.3	0.3	0.2	0.2	0.2
Metab. Rate (%)	110	110	110	110	110	110	110	110	110	110	110	110	110	110	110
Respiratory Quotient	0.80	0.80	0.80	0.80	0.80	0.80	0.80	0.80	0.80	0.80	0.80	0.80	0.80	0.80	0.80
Raw (cmH ₂ O/l/sec)	1.0	1.0	1.0	1.0	1.0	1.0	1.0	1.0	1.0	1.0	1.0	1.0	1.0	1.0	1.0
Caw (l/cmH ₂ O)	0.15	0.15	0.14	0.12	0.11	0.11	0.11	0.13	0.16	0.19	0.20	0.24	0.28	0.30	0.31
Ventilator Settings															
FIO ₂ (%)	50	70	80	81	82	83	84	84	84	83	82	81	81	74	66
PEEP (cmH ₂ O)	0.0	4.0	5.0	6.0	7.0	8.5	9.5	10.5	11.0	10.5	10.0	9.5	8.0	6.5	5.5
V _T (ml)	700	550	520	490	470	450	440	430	430	430	440	460	500	560	620
RR (rpm)	12.0	16.5	18.5	20.0	21.0	21.5	21.5	21.5	21.5	21.5	21.5	21.0	19.5	17.5	16.0
Mv (l/min)	8.40	9.08	9.62	9.80	9.87	9.68	9.46	9.25	9.25	9.25	9.46	9.66	9.75	9.80	9.92
T _{IN} (%)	33	50	50	60	60	60	60	60	60	50	50	50	50	50	50
Advised Ventilator Settings															
FIO ₂ (%)	70	80	81	82	83	84	84	84	83	82	81	81	74	66	63
PEEP (cmH ₂ O)	4.0	5.0	6.0	7.0	8.5	9.5	10.5	11.0	10.5	10.0	9.5	8.0	6.5	5.5	4.5
V _T (ml)	550	520	490	470	450	440	430	430	430	440	460	500	560	620	620
RR (rpm)	16.5	18.5	20.0	21.0	21.5	21.5	21.5	21.5	21.5	21.5	21.0	19.5	17.5	16.0	15.5
Mv (l/min)	9.08	9.62	9.80	9.87	9.68	9.46	9.25	9.25	9.25	9.46	9.66	9.75	9.80	9.92	9.61
T _{IN} (%)	50	50	60	60	60	60	60	60	60	50	50	50	50	50	50

Table D.15: Refined advisor decision history for ARDS patient

Appendix E
Advisor Control Rules
and Control Space Maps

E.1 Prototype Control Rules

FI₂ Prototype Control Rules

- [1] If (PaO₂ = VHI) AND (FiO₂ = VHI-MAX) THEN [dFiO₂ = N6 (-50)]
- [2] If (PaO₂ = HI) AND (FiO₂ = VHI-MAX) THEN [dFiO₂ = N5 (-35)]
- [3] If (PaO₂ = VHI) AND (FiO₂ = HI) THEN [dFiO₂ = N4 (-30)]
- [4] If (PaO₂ = HI-VHI) AND (FiO₂ = MED) THEN [dFiO₂ = N3 (-20)]
- [5] If (PaO₂ = HI) AND (FiO₂ = HI) THEN [dFiO₂ = N3 (-20)]
- [6] If (PaO₂ = SHI) AND (FiO₂ = VHI-MAX) THEN [dFiO₂ = N3 (-20)]
- [7] If (PaO₂ = SHI) AND (FiO₂ = HI) THEN [dFiO₂ = N2 (-15)]
- [8] If (PaO₂ = SHI) AND (FiO₂ = MED) THEN [dFiO₂ = N1 (-10)]
- [9] If (PaO₂ = N) THEN [dFiO₂ = Z (0)]
- [10] If (PaO₂ = SHI-VHI) AND (FiO₂ = MIN) THEN [dFiO₂ = Z (0)]
- [11] If (PaO₂ = VLO-SLO) AND (FiO₂ = MAX) THEN [dFiO₂ = Z (0)]
- [12] If (PaO₂ = VLO-SLO) AND (FiO₂ = VHI) THEN [dFiO₂ = P1 (10)]
- [13] If (PaO₂ = SLO) AND (FiO₂ = MIN-HI) THEN [dFiO₂ = P2 (20)]
- [14] If (PaO₂ = LO) AND (FiO₂ = MED-HI) THEN [dFiO₂ = P3 (30)]
- [15] If (PaO₂ = VLO) AND (FiO₂ = HI) THEN [dFiO₂ = P3 (30)]
- [16] If (PaO₂ = LO) AND (FiO₂ = MIN) THEN [dFiO₂ = P4 (40)]
- [17] If (PaO₂ = VLO) AND (FiO₂ = MED) THEN [dFiO₂ = P5 (50)]
- [18] If (PaO₂ = VLO) AND (FiO₂ = MIN) THEN [dFiO₂ = P6 (70)]

PEEP Prototype Control Rules

- [1] If (PaO₂ = VHI) AND (FiO₂ = MIN) AND (PEEP = MAX) THEN [dPEEP = N8 (-16)]
- [2] If (PaO₂ = SHI-HI) AND (FiO₂ = MIN) AND (PEEP = MAX) THEN [dPEEP = N7 (-12)]
- [3] If (PaO₂ = VHI) AND (FiO₂ = MED-MAX) AND (PEEP = MAX) THEN [dPEEP = N7 (-12)]
- [4] If (PaO₂ = VHI) AND (PEEP = HIGH) THEN [dPEEP = N6 (-8)]
- [5] If (PaO₂ = N) AND (FiO₂ = MIN) AND (PEEP = MAX) THEN [dPEEP = N6 (-8)]
- [6] If (PaO₂ = SHI-HI) AND (FiO₂ = MED-MAX) AND (PEEP = MAX) THEN [dPEEP = N6 (-8)]
- [7] If (PaO₂ = VHI) AND (PEEP = MED) THEN [dPEEP = N5 (-6)]
- [8] If (PaO₂ = SHI-HI) AND (FiO₂ = MIN) AND (PEEP = HIGH) THEN [dPEEP = N5 (-6)]
- [9] If (PaO₂ = HI) AND (FiO₂ = MED-HI) AND (PEEP = HIGH) THEN [dPEEP = N5 (-6)]
- [10] If (PaO₂ = N) AND (FiO₂ = MED) AND (PEEP = MAX) THEN [dPEEP = N5 (-6)]
- [11] If (PaO₂ = VHI) AND (FiO₂ = MIN) AND (PEEP = LOW) THEN [dPEEP = N4 (-4)]
- [12] If (PaO₂ = N-HI) AND (FiO₂ = MIN-MED) AND (PEEP = MED) THEN [dPEEP = N4 (-4)]
- [13] If (PaO₂ = HI) AND (FiO₂ = HI-VHI) AND (PEEP = MED) THEN [dPEEP = N4 (-4)]
- [14] If (PaO₂ = N) AND (FiO₂ = MIN-HI) AND (PEEP = HIGH) THEN [dPEEP = N4 (-4)]
- [15] If (PaO₂ = SHI) AND (FiO₂ = MED-VHI) AND (PEEP = HIGH) THEN [dPEEP = N4 (-4)]
- [16] If (PaO₂ = HI) AND (FiO₂ = VHI-MAX) AND (PEEP = HIGH) THEN [dPEEP = N4 (-4)]
- [17] If (PaO₂ = LO-SLO) AND (FiO₂ = MIN-MED) AND (PEEP = MAX) THEN [dPEEP = N4 (-4)]
- [18] If (PaO₂ = N) AND (FiO₂ = HI-MAX) AND (PEEP = MAX) THEN [dPEEP = N4 (-4)]
- [19] If (PaO₂ = SHI-HI) AND (FiO₂ = MIN) AND (PEEP = LOW) THEN [dPEEP = N3 (-3)]
- [20] If (PaO₂ = VHI) AND (FiO₂ = MED-HI) AND (PEEP = LOW) THEN [dPEEP = N3 (-3)]
- [21] If (PaO₂ = N) AND (FiO₂ = MIN) AND (PEEP = LOW) THEN [dPEEP = N2 (-2)]
- [22] If (PaO₂ = HI) AND (FiO₂ = MED) AND (PEEP = LOW) THEN [dPEEP = N2 (-2)]
- [23] If (PaO₂ = VHI) AND (FiO₂ = VHI-MAX) AND (PEEP = LOW) THEN [dPEEP = N2 (-2)]
- [24] If (PaO₂ = LO-SLO) AND (FiO₂ = MIN) AND (PEEP = MED-HIGH) THEN [dPEEP = N2 (-2)]
- [25] If (PaO₂ = N-SHI) AND (FiO₂ = HI) AND (PEEP = MED) THEN [dPEEP = N2 (-2)]
- [26] If (PaO₂ = SHI) AND (FiO₂ = VHI) AND (PEEP = MED) THEN [dPEEP = N2 (-2)]
- [27] If (PaO₂ = HI) AND (FiO₂ = MAX) AND (PEEP = MED) THEN [dPEEP = N2 (-2)]
- [28] If (PaO₂ = LO-SLO) AND (FiO₂ = MED) AND (PEEP = HIGH) THEN [dPEEP = N2 (-2)]

- [29] If (PaO2 = N) AND (FiO2 = VHI) AND (PEEP = HIGH) THEN [dPEEP = N2 (-2)]
- [30] If (PaO2 = SHI) AND (FiO2 = MAX) AND (PEEP = HIGH) THEN [dPEEP = N2 (-2)]
- [31] If (PaO2 = VLO) AND (FiO2 = MIN) AND (PEEP = MAX) THEN [dPEEP = N2 (-2)]
- [32] If (PaO2 = HI) AND (FiO2 = HI) AND (PEEP = LOW) THEN [dPEEP = N1 (-1)]
- [33] If (PaO2 = SLO-VHI) AND (FiO2 = MIN) AND (PEEP = OFF) THEN [dPEEP = Z (0)]
- [34] If (PaO2 = N-SHI) AND (FiO2 = MED-HI) AND (PEEP = OFF-LOW) THEN [dPEEP = Z (0)]
- [35] If (PaO2 = HI-VHI) AND (FiO2 = MED-MAX) AND (PEEP = OFF) THEN [dPEEP = Z (0)]
- [36] If (PaO2 = SHI) AND (FiO2 = VHI-MAX) AND (PEEP = OFF-LOW) THEN [dPEEP = Z (0)]
- [37] If (PaO2 = LO-SLO) AND (FiO2 = MIN) AND (PEEP = LOW) THEN [dPEEP = Z (0)]
- [38] If (PaO2 = SLO) AND (FiO2 = MED-HI) AND (PEEP = LOW-MED) THEN [dPEEP = Z (0)]
- [39] If (PaO2 = N) AND (FiO2 = VHI-MAX) AND (PEEP = LOW) THEN [dPEEP = Z (0)]
- [40] If (PaO2 = HI) AND (FiO2 = VHI-MAX) AND (PEEP = LOW) THEN [dPEEP = Z (0)]
- [41] If (PaO2 = VLO) AND (FiO2 = MIN) AND (PEEP = MED-HIGH) THEN [dPEEP = Z (0)]
- [42] If (PaO2 = LO) AND (FiO2 = MED-HI) AND (PEEP = MED) THEN [dPEEP = Z (0)]
- [43] If (PaO2 = N) AND (FiO2 = VHI) AND (PEEP = MED) THEN [dPEEP = Z (0)]
- [44] If (PaO2 = VLO) AND (FiO2 = MED) AND (PEEP = HIGH-MAX) THEN [dPEEP = Z (0)]
- [45] If (PaO2 = LO-SLO) AND (FiO2 = HI-VHI) AND (PEEP = HIGH-MAX) THEN [dPEEP = Z (0)]
- [46] If (PaO2 = N) AND (FiO2 = MAX) AND (PEEP = HIGH) THEN [dPEEP = Z (0)]
- [47] If (PaO2 = VLO) AND (FiO2 = HI-MAX) AND (PEEP = MAX) THEN [dPEEP = Z (0)]
- [48] If (PaO2 = LO-SLO) AND (FiO2 = MAX) AND (PEEP = MAX) THEN [dPEEP = Z (0)]
- [49] If (PaO2 = VLO) AND (FiO2 = MIN-MED) AND (PEEP = LOW) THEN [dPEEP = P1 (2)]
- [50] If (PaO2 = LO) AND (FiO2 = MED-HI) AND (PEEP = LOW) THEN [dPEEP = P1 (2)]
- [51] If (PaO2 = SLO) AND (FiO2 = VHI) AND (PEEP = LOW-MED) THEN [dPEEP = P1 (2)]
- [52] If (PaO2 = VLO) AND (FiO2 = MED-HI) AND (PEEP = MED) THEN [dPEEP = P1 (2)]
- [53] If (PaO2 = LO) AND (FiO2 = VHI) AND (PEEP = MED) THEN [dPEEP = P1 (2)]
- [54] If (PaO2 = N-SHI) AND (FiO2 = MAX) AND (PEEP = MED) THEN [dPEEP = P1 (2)]
- [55] If (PaO2 = VLO) AND (FiO2 = HI-VHI) AND (PEEP = HIGH) THEN [dPEEP = P1 (2)]
- [56] If (PaO2 = LO-SLO) AND (FiO2 = MAX) AND (PEEP = HIGH) THEN [dPEEP = P1 (2)]
- [57] If (PaO2 = VLO-LO) AND (FiO2 = MIN-HI) AND (PEEP = OFF) THEN [dPEEP = P2 (4)]
- [58] If (PaO2 = SLO) AND (FiO2 = MED-MAX) AND (PEEP = OFF) THEN [dPEEP = P2 (4)]
- [59] If (PaO2 = LO) AND (FiO2 = VHI) AND (PEEP = OFF-LOW) THEN [dPEEP = P2 (4)]
- [60] If (PaO2 = N) AND (FiO2 = VHI-MAX) AND (PEEP = OFF) THEN [dPEEP = P2 (4)]
- [61] If (PaO2 = VLO) AND (FiO2 = HI-MAX) AND (PEEP = LOW) THEN [dPEEP = P2 (4)]
- [62] If (PaO2 = LO-SLO) AND (FiO2 = MAX) AND (PEEP = LOW-MED) THEN [dPEEP = P2 (4)]
- [63] If (PaO2 = VLO) AND (FiO2 = VHI-MAX) AND (PEEP = MED) THEN [dPEEP = P2 (4)]
- [64] If (PaO2 = VLO) AND (FiO2 = MAX) AND (PEEP = HIGH) THEN [dPEEP = P2 (4)]
- [65] If (PaO2 = VLO) AND (FiO2 = VHI-MAX) AND (PEEP = OFF) THEN [dPEEP = P3 (8)]
- [66] If (PaO2 = LO) AND (FiO2 = MAX) AND (PEEP = OFF) THEN [dPEEP = P3 (8)]

MV Prototype Control Rules

- [1] If (ePaCO2 = NB) AND (ePh = VALK) THEN [dMv = N6 (-60)]
- [2] If (ePaCO2 = NB) AND (ePh = ALK) THEN [dMv = N5 (-45)]
- [3] If (ePaCO2 = NB) AND (ePh = NORM) THEN [dMv = N4 (-30)]
- [4] If (ePaCO2 = NS) AND (ePh = ALK-VALK) THEN [dMv = N4 (-30)]
- [5] If (ePaCO2 = NS) AND (ePh = NORM) THEN [dMv = N3 (-15)]
- [6] If (ePaCO2 = Z) AND (ePh = VALK) THEN [dMv = N3 (-15)]
- [7] If (ePaCO2 = NB-Z) AND (ePh = VACID-ACID) AND (ePip = VHIGH) THEN [dMv = N3 (-15)]
- [8] If (ePaCO2 = Z) AND (ePh = NORM-ALK) AND (ePip = VHIGH) THEN [dMv = N3 (-15)]
- [9] If (ePaCO2 = PS-PB) AND (ePh = ALK-VALK) AND (ePip = VHIGH) THEN [dMv = N3 (-15)]
- [10] If (ePaCO2 = NB-Z) AND (ePh = VACID-ACID) AND (ePip = HIGH) THEN [dMv = N2 (-10)]
- [11] If (ePaCO2 = Z) AND (ePh = NORM-ALK) AND (ePip = HIGH) THEN [dMv = N2 (-10)]
- [12] If (ePaCO2 = PS-PB) AND (ePh = ALK-VALK) AND (ePip = HIGH) THEN [dMv = N2 (-10)]
- [13] If (ePaCO2 = PS-PB) AND (ePh = VACID-NORM) AND (ePip = VHIGH) THEN [dMv = N2 (-10)]
- [14] If (ePaCO2 = Z) AND (ePh = ALK) AND (ePip = OKAY-ALARM) THEN [dMv = N1 (-5)]

- [15] If (ePaCO2 = NB-NS) AND (ePh = VACID-ACID) AND (ePip = OK-ALARM) THEN [dMv = Z (0)]
- [16] If (ePaCO2 = Z) AND (ePh = ACID-NORM) AND (ePip = OKAY-ALARM) THEN [dMv = Z (0)]
- [17] If (ePaCO2 = PS-PB) AND (ePh = ALK-VALK) AND (ePip = OK-ALARM) THEN [dMv = Z (0)]
- [18] If (ePaCO2 = Z) AND (ePh = VACID) AND (ePip = ALARM) THEN [dMv = Z (0)]
- [19] If (ePaCO2 = PS) AND (ePh = NORM) AND (ePip = ALARM-HIGH) THEN [dMv = Z (0)]
- [20] If (ePaCO2 = PS-PB) AND (ePh = VACID-ACID) AND (ePip = HIGH) THEN [dMv = Z (0)]
- [21] If (ePaCO2 = PB) AND (ePh = NORM) AND (ePip = HIGH) THEN [dMv = Z (0)]
- [22] If (ePaCO2 = Z) AND (ePh = VACID) AND (ePip = OKAY-NRALARM) THEN [dMv = P1 (15)]
- [23] If (ePaCO2 = PS) AND (ePh = VACID-ACID) AND (ePip = ALARM) THEN [dMv = P1 (15)]
- [24] If (ePaCO2 = PB) AND (ePh = ACID-NORM) AND (ePip = ALARM) THEN [dMv = P1 (15)]
- [25] If (ePaCO2 = PS) AND (ePh = NORM) AND (ePip = OKAY-NRALARM) THEN [dMv = P2 (25)]
- [26] If (ePaCO2 = PS) AND (ePh = VACID-ACID) AND (ePip = NRALARM) THEN [dMv = P2 (25)]
- [27] If (ePaCO2 = PB) AND (ePh = ACID-NORM) AND (ePip = NRALARM) THEN [dMv = P2 (25)]
- [28] If (ePaCO2 = PB) AND (ePh = VACID) AND (ePip = ALARM) THEN [dMv = P2 (25)]
- [29] If (ePaCO2 = PS) AND (ePh = VACID-ACID) AND (ePip = OKAY) THEN [dMv = P3 (50)]
- [30] If (ePaCO2 = PB) AND (ePh = NORM) AND (ePip = OKAY) THEN [dMv = P3 (50)]
- [31] If (ePaCO2 = PB) AND (ePh = VACID) AND (ePip = NRALARM) THEN [dMv = P3 (50)]
- [32] If (ePaCO2 = PB) AND (ePh = ACID) AND (ePip = OKAY) THEN [dMv = P4 (75)]
- [33] If (ePaCO2 = PB) AND (ePh = VACID) AND (ePip = OKAY) THEN [dMv = P5 (100)]

VT-RR Prototype Control Rules

- [1] If (RR = MIN-LOW) AND (eVTnorm = PB) THEN [dVt = N7 (-35)]
- [2] If (RR = MIN) AND (eVTnorm = PS) THEN [dVt = N6 (-30)]
- [3] If (RR = MED) AND (eVTnorm = PB) THEN [dVt = N5 (-25)]
- [4] If (RR = VLOW-LOW) AND (eVTnorm = PS) THEN [dVt = N4 (-20)]
- [5] If (RR = MIN) AND (eVTnorm = Z) THEN [dVt = N3 (-15)]
- [6] If (RR = MED) AND (eVTnorm = PS) THEN [dVt = N3 (-15)]
- [7] If (RR = HIGH) AND (eVTnorm = PB) THEN [dVt = N3 (-15)]
- [8] If (RR = VLOW-VHIGH) AND (eVTnorm = Z) AND (ePip = VHIGH) THEN [dVt = N3 (-15)]
- [9] If (RR = VLOW) AND (eVTnorm = Z) AND (ePip = ALARM-HIGH) THEN [dVt = N2 (-10)]
- [10] If (RR = LOW-MED) AND (eVTnorm = Z) AND (ePip = HIGH) THEN [dVt = N2 (-10)]
- [11] If (RR = MIN-VHIGH) AND (eVTnorm = NS) AND (ePip = VHIGH) THEN [dVt = N2 (-10)]
- [12] If (RR = HIGH-MAX) AND (eVTnorm = PS) AND (ePip = VHIGH) THEN [dVt = N2 (-10)]
- [13] If (RR = VHIGH-MAX) AND (eVTnorm = PB) AND (ePip = VHIGH) THEN [dVt = N2 (-10)]
- [14] If (RR = MIN) AND (eVTnorm = NS) AND (ePip = OKAY-HIGH) THEN [dVt = N1 (-5)]
- [15] If (RR = VLOW) AND (eVTnorm = Z) AND (ePip = OKAY-NRALARM) THEN [dVt = N1 (-5)]
- [16] If (RR = HIGH) AND (eVTnorm = PS) AND (ePip = OKAY-HIGH) THEN [dVt = N1 (-5)]
- [17] If (RR = VHIGH-MAX) AND (eVTnorm = PB) AND (ePip = OKAY-HIGH) THEN [dVt = N1 (-5)]
- [18] If (RR = VLOW-LOW) AND (eVTnorm = NS) AND (ePip = ALARM-HIGH) THEN [dVt = N1 (-5)]
- [19] If (RR = LOW-HIGH) AND (eVTnorm = Z) AND (ePip = ALARM) THEN [dVt = N1 (-5)]
- [20] If (RR = VHIGH) AND (eVTnorm = PS) AND (ePip = ALARM-HIGH) THEN [dVt = N1 (-5)]
- [21] If (RR = MED-VHIGH) AND (eVTnorm = NS) AND (ePip = HIGH) THEN [dVt = N1 (-5)]
- [22] If (RR = HIGH-VHIGH) AND (eVTnorm = Z) AND (ePip = HIGH) THEN [dVt = N1 (-5)]
- [23] If (RR = MAX) AND (eVTnorm = PS) AND (ePip = HIGH) THEN [dVt = N1 (-5)]
- [24] If (RR = LOW-MED) AND (eVTnorm = Z) AND (ePip = OKAY-NRALARM) THEN [dVt = Z (0)]
- [25] If (RR = VLOW) AND (eVTnorm = NS) AND (ePip = NRALARM) THEN [dVt = Z (0)]
- [26] If (RR = HIGH) AND (eVTnorm = Z) AND (ePip = NRALARM) THEN [dVt = Z (0)]
- [27] If (RR = VHIGH) AND (eVTnorm = PS) AND (ePip = NRALARM) THEN [dVt = Z (0)]
- [28] If (eVTnorm = NB) AND (ePip = ALARM-VHIGH) THEN [dVt = Z (0)]
- [29] If (RR = MED-MAX) AND (eVTnorm = NS) AND (ePip = ALARM) THEN [dVt = Z (0)]
- [30] If (RR = VHIGH-MAX) AND (eVTnorm = Z) AND (ePip = ALARM) THEN [dVt = Z (0)]
- [31] If (RR = MAX) AND (eVTnorm = PS) AND (ePip = ALARM) THEN [dVt = Z (0)]
- [32] If (RR = MAX) AND (eVTnorm = NS-Z) AND (ePip = HIGH-VHIGH) THEN [dVt = Z (0)]

- [33] If (RR = VLOW) AND (eVTnorm = NS) AND (ePip = OKAY) THEN [dVt = P1 (2)]
- [34] If (RR = VHIGH) AND (eVTnorm = PS) AND (ePip = OKAY) THEN [dVt = P1 (2)]
- [35] If (RR = MIN) AND (eVTnorm = NB) AND (ePip = OKAY-NRALARM) THEN [dVt = P2 (5)]
- [36] If (RR = HIGH) AND (eVTnorm = Z) AND (ePip = OKAY) THEN [dVt = P2 (5)]
- [37] If (RR = LOW) AND (eVTnorm = NS) AND (ePip = NRALARM) THEN [dVt = P2 (5)]
- [38] If (RR = MAX) AND (eVTnorm = PS) AND (ePip = NRALARM) THEN [dVt = P2 (5)]
- [39] If (RR = LOW) AND (eVTnorm = NS) AND (ePip = OKAY) THEN [dVt = P3 (10)]
- [40] If (RR = MAX) AND (eVTnorm = PS) AND (ePip = OKAY) THEN [dVt = P3 (10)]
- [41] If (RR = VLOW-MAX) AND (eVTnorm = NB) AND (ePip = NRALARM) THEN [dVt = P3 (10)]
- [42] If (RR = MED-MAX) AND (eVTnorm = NS) AND (ePip = NRALARM) THEN [dVt = P3 (10)]
- [43] If (RR = VHIGH-MAX) AND (eVTnorm = Z) AND (ePip = NRALARM) THEN [dVt = P3 (10)]
- [44] If (RR = VLOW) AND (eVTnorm = NB) AND (ePip = OKAY) THEN [dVt = P4 (15)]
- [45] If (RR = MED-HIGH) AND (eVTnorm = NS) AND (ePip = OKAY) THEN [dVt = P4 (15)]
- [46] If (RR = VHIGH) AND (eVTnorm = Z) AND (ePip = OKAY) THEN [dVt = P4 (15)]
- [47] If (RR = LOW) AND (eVTnorm = NB) AND (ePip = OKAY) THEN [dVt = P5 (25)]
- [48] If (RR = VHIGH) AND (eVTnorm = NS) AND (ePip = OKAY) THEN [dVt = P5 (25)]
- [49] If (RR = MAX) AND (eVTnorm = Z) AND (ePip = OKAY) THEN [dVt = P5 (25)]
- [50] If (RR = MAX) AND (eVTnorm = NS) AND (ePip = OKAY) THEN [dVt = P6 (35)]
- [51] If (RR = MED-VHIGH) AND (eVTnorm = NB) AND (ePip = OKAY) THEN [dVt = P7 (40)]
- [52] If (RR = MAX) AND (eVTnorm = NB) AND (ePip = OKAY) THEN [dVt = P8 (50)]

E.2 Refined Control Rules

FIO2 Refined Control Rules

- [1] If (PaO2 = VHI) AND (FiO2 = MAX) THEN [dFiO2 = N9 (-50)]
- [2] If (PaO2 = VHI) AND (FiO2 = EHI) THEN [dFiO2 = N8 (-40)]
- [3] If (PaO2 = HI) AND (FiO2 = EHI-MAX) THEN [dFiO2 = N7 (-35)]
- [4] If (PaO2 = VHI) AND (FiO2 = VHI) THEN [dFiO2 = N6 (-30)]
- [5] If (PaO2 = HI) AND (FiO2 = VHI) THEN [dFiO2 = N5 (-25)]
- [6] If (PaO2 = VHI) AND (FiO2 = MED_HI-HI) THEN [dFiO2 = N4 (-20)]
- [7] If (PaO2 = HI) AND (FiO2 = HI) THEN [dFiO2 = N4 (-20)]
- [8] If (PaO2 = SHI) AND (FiO2 = MAX) THEN [dFiO2 = N4 (-20)]
- [9] If (PaO2 = HI) AND (FiO2 = MED_HI) THEN [dFiO2 = N3 (-15)]
- [10] If (PaO2 = SHI-VHI) AND (FiO2 = MED) THEN [dFiO2 = N2 (-10)]
- [11] If (PaO2 = SHI) AND (FiO2 = HI-EHI) THEN [dFiO2 = N2 (-10)]
- [12] If (PaO2 = VHI) AND (FiO2 = VLOW-LOW) THEN [dFiO2 = N1 (-5)]
- [13] If (PaO2 = SHI-HI) AND (FiO2 = LOW) THEN [dFiO2 = N1 (-5)]
- [14] If (PaO2 = N) AND (FiO2 = EHI-MAX) THEN [dFiO2 = N1 (-5)]
- [15] If (PaO2 = N) AND (FiO2 = MIN-VHI) THEN [dFiO2 = Z (0)]
- [16] If (PaO2 = SHI-HI) AND (FiO2 = MIN-VLOW) THEN [dFiO2 = Z (0)]
- [17] If (PaO2 = VHI) AND (FiO2 = MIN) THEN [dFiO2 = Z (0)]
- [18] If (PaO2 = SHI) AND (FiO2 = MED_HI) THEN [dFiO2 = Z (0)]
- [19] If (PaO2 = SLO) AND (FiO2 = VHI-MAX) THEN [dFiO2 = Z (0)]
- [20] If (PaO2 = LO) AND (FiO2 = EHI-MAX) THEN [dFiO2 = Z (0)]
- [21] If (PaO2 = VLO) AND (FiO2 = MAX) THEN [dFiO2 = Z (0)]
- [22] If (PaO2 = LO) AND (FiO2 = VHI) THEN [dFiO2 = P1 (5)]
- [23] If (PaO2 = LO-SLO) AND (FiO2 = HI) THEN [dFiO2 = P2 (10)]
- [24] If (PaO2 = VLO) AND (FiO2 = VHI-EHI) THEN [dFiO2 = P2 (10)]
- [25] If (PaO2 = SLO) AND (FiO2 = MED_HI) THEN [dFiO2 = P3 (15)]
- [26] If (PaO2 = SLO) AND (FiO2 = MIN-MED) THEN [dFiO2 = P4 (20)]
- [27] If (PaO2 = LO) AND (FiO2 = LOW-MED_HI) THEN [dFiO2 = P4 (20)]
- [28] If (PaO2 = VLO) AND (FiO2 = HI) THEN [dFiO2 = P5 (30)]
- [29] If (PaO2 = LO) AND (FiO2 = VLOW) THEN [dFiO2 = P6 (35)]

- [30] If (PaO2 = LO) AND (FiO2 = MIN) THEN [dFiO2 = P7 (40)]
- [31] If (PaO2 = VLO) AND (FiO2 = MED_HI) THEN [dFiO2 = P7 (40)]
- [32] If (PaO2 = VLO) AND (FiO2 = LOW-MED) THEN [dFiO2 = P8 (50)]
- [33] If (PaO2 = VLO) AND (FiO2 = VLOW) THEN [dFiO2 = P9 (65)]
- [34] If (PaO2 = VLO) AND (FiO2 = MIN) THEN [dFiO2 = P10 (70)]

PEEP Refined Control Rules

- [1] If (PaO2 = VHI) AND (FiO2 = MIN) AND (PEEP = MAX) THEN [dPEEP = N6 (-16)]
- [2] If (PaO2 = SHI-HI) AND (FiO2 = MIN) AND (PEEP = MAX) THEN [dPEEP = N5 (-12)]
- [3] If (PaO2 = VHI) AND (FiO2 = MED-MAX) AND (PEEP = MAX) THEN [dPEEP = N5 (-12)]
- [4] If (PaO2 = VHI) AND (PEEP = HIGH) THEN [dPEEP = N4 (-8)]
- [5] If (PaO2 = N) AND (FiO2 = MIN) AND (PEEP = MAX) THEN [dPEEP = N4 (-8)]
- [6] If (PaO2 = SHI-HI) AND (FiO2 = MED-MAX) AND (PEEP = MAX) THEN [dPEEP = N4 (-8)]
- [7] If (PaO2 = VHI) AND (PEEP = MED) THEN [dPEEP = N3 (-6)]
- [8] If (PaO2 = SHI-HI) AND (FiO2 = MIN) AND (PEEP = HIGH) THEN [dPEEP = N3 (-6)]
- [9] If (PaO2 = HI) AND (FiO2 = MED-HI) AND (PEEP = HIGH) THEN [dPEEP = N3 (-6)]
- [10] If (PaO2 = N) AND (FiO2 = MED) AND (PEEP = MAX) THEN [dPEEP = N3 (-6)]
- [11] If (PaO2 = HI-VHI) AND (FiO2 = MIN) AND (PEEP = LOW) THEN [dPEEP = N2 (-4)]
- [12] If (PaO2 = N-HI) AND (FiO2 = MIN-MED) AND (PEEP = MED) THEN [dPEEP = N2 (-4)]
- [13] If (PaO2 = HI) AND (FiO2 = HI-VHI) AND (PEEP = MED) THEN [dPEEP = N2 (-4)]
- [14] If (PaO2 = N) AND (FiO2 = MIN-HI) AND (PEEP = HIGH) THEN [dPEEP = N2 (-4)]
- [15] If (PaO2 = SHI) AND (FiO2 = MED-VHI) AND (PEEP = HIGH) THEN [dPEEP = N2 (-4)]
- [16] If (PaO2 = HI) AND (FiO2 = VHI-MAX) AND (PEEP = HIGH) THEN [dPEEP = N2 (-4)]
- [17] If (PaO2 = LO-SLO) AND (FiO2 = MIN-MED) AND (PEEP = MAX) THEN [dPEEP = N2 (-4)]
- [18] If (PaO2 = N) AND (FiO2 = HI-MAX) AND (PEEP = MAX) THEN [dPEEP = N2 (-4)]
- [19] If (PaO2 = N-SHI) AND (FiO2 = MIN) AND (PEEP = LOW) THEN [dPEEP = N1 (-2)]
- [20] If (PaO2 = HI-VHI) AND (FiO2 = MED-HI) AND (PEEP = LOW) THEN [dPEEP = N1 (-2)]
- [21] If (PaO2 = LO-SLO) AND (FiO2 = MIN) AND (PEEP = MED-HIGH) THEN [dPEEP = N1 (-2)]
- [22] If (PaO2 = N-SHI) AND (FiO2 = HI) AND (PEEP = MED) THEN [dPEEP = N1 (-2)]
- [23] If (PaO2 = SHI) AND (FiO2 = VHI) AND (PEEP = MED) THEN [dPEEP = N1 (-2)]
- [24] If (PaO2 = HI) AND (FiO2 = MAX) AND (PEEP = MED) THEN [dPEEP = N1 (-2)]
- [25] If (PaO2 = LO-SLO) AND (FiO2 = MED) AND (PEEP = HIGH) THEN [dPEEP = N1 (-2)]
- [26] If (PaO2 = N) AND (FiO2 = VHI) AND (PEEP = HIGH) THEN [dPEEP = N1 (-2)]
- [27] If (PaO2 = SHI) AND (FiO2 = MAX) AND (PEEP = HIGH) THEN [dPEEP = N1 (-2)]
- [28] If (PaO2 = VLO) AND (FiO2 = MIN) AND (PEEP = MAX) THEN [dPEEP = N1 (-2)]
- [29] If (PaO2 = SLO-VHI) AND (FiO2 = MIN) AND (PEEP = OFF) THEN [dPEEP = Z (0)]
- [30] If (PaO2 = HI-VHI) AND (FiO2 = MED-MAX) AND (PEEP = OFF) THEN [dPEEP = Z (0)]
- [31] If (PaO2 = N-SHI) AND (FiO2 = HI) AND (PEEP = OFF-LOW) THEN [dPEEP = Z (0)]
- [32] If (PaO2 = SHI) AND (FiO2 = VHI-MAX) AND (PEEP = OFF-LOW) THEN [dPEEP = Z (0)]
- [33] If (PaO2 = LO-SLO) AND (FiO2 = MIN) AND (PEEP = LOW) THEN [dPEEP = Z (0)]
- [34] If (PaO2 = SLO) AND (FiO2 = MED-HI) AND (PEEP = LOW-MED) THEN [dPEEP = Z (0)]
- [35] If (PaO2 = N-SHI) AND (FiO2 = MED) AND (PEEP = LOW) THEN [dPEEP = Z (0)]
- [36] If (PaO2 = SLO-N) AND (FiO2 = VHI) AND (PEEP = LOW) THEN [dPEEP = Z (0)]
- [37] If (PaO2 = HI-VHI) AND (FiO2 = VHI-MAX) AND (PEEP = LOW) THEN [dPEEP = Z (0)]
- [38] If (PaO2 = N) AND (FiO2 = MAX) AND (PEEP = LOW) THEN [dPEEP = Z (0)]
- [39] If (PaO2 = VLO) AND (FiO2 = MIN) AND (PEEP = MED-HIGH) THEN [dPEEP = Z (0)]
- [40] If (PaO2 = LO) AND (FiO2 = MED-HI) AND (PEEP = MED) THEN [dPEEP = Z (0)]
- [41] If (PaO2 = N) AND (FiO2 = VHI) AND (PEEP = MED) THEN [dPEEP = Z (0)]
- [42] If (PaO2 = VLO) AND (FiO2 = MED) AND (PEEP = HIGH-MAX) THEN [dPEEP = Z (0)]
- [43] If (PaO2 = LO-SLO) AND (FiO2 = HI-VHI) AND (PEEP = HIGH-MAX) THEN [dPEEP = Z (0)]
- [44] If (PaO2 = N) AND (FiO2 = MAX) AND (PEEP = HIGH) THEN [dPEEP = Z (0)]
- [45] If (PaO2 = VLO) AND (FiO2 = HI-MAX) AND (PEEP = MAX) THEN [dPEEP = Z (0)]
- [46] If (PaO2 = LO-SLO) AND (FiO2 = MAX) AND (PEEP = MAX) THEN [dPEEP = Z (0)]

- [47] If (PaO2 = N-SHI) AND (FiO2 = MED) AND (PEEP = OFF) THEN [dPEEP = P1 (2)]
- [48] If (PaO2 = VLO) AND (FiO2 = MIN-MED) AND (PEEP = LOW) THEN [dPEEP = P1 (2)]
- [49] If (PaO2 = LO) AND (FiO2 = MED) AND (PEEP = LOW) THEN [dPEEP = P1 (2)]
- [50] If (PaO2 = VLO) AND (FiO2 = MED-HI) AND (PEEP = MED) THEN [dPEEP = P1 (2)]
- [51] If (PaO2 = LO-SLO) AND (FiO2 = VHI) AND (PEEP = MED) THEN [dPEEP = P1 (2)]
- [52] If (PaO2 = N-SHI) AND (FiO2 = MAX) AND (PEEP = MED) THEN [dPEEP = P1 (2)]
- [53] If (PaO2 = VLO) AND (FiO2 = HI-VHI) AND (PEEP = HIGH) THEN [dPEEP = P1 (2)]
- [54] If (PaO2 = LO-SLO) AND (FiO2 = MAX) AND (PEEP = HIGH) THEN [dPEEP = P1 (2)]
- [55] If (PaO2 = VLO-LO) AND (FiO2 = MIN-HI) AND (PEEP = OFF) THEN [dPEEP = P2 (4)]
- [56] If (PaO2 = SLO) AND (FiO2 = MED-MAX) AND (PEEP = OFF) THEN [dPEEP = P2 (4)]
- [57] If (PaO2 = LO) AND (FiO2 = VHI) AND (PEEP = OFF) THEN [dPEEP = P2 (4)]
- [58] If (PaO2 = N) AND (FiO2 = VHI-MAX) AND (PEEP = OFF) THEN [dPEEP = P2 (4)]
- [59] If (PaO2 = LO) AND (FiO2 = HI) AND (PEEP = LOW) THEN [dPEEP = P2 (4)]
- [60] If (PaO2 = SLO) AND (FiO2 = MAX) AND (PEEP = LOW-MED) THEN [dPEEP = P2 (4)]
- [61] If (PaO2 = VLO) AND (FiO2 = VHI-MAX) AND (PEEP = MED) THEN [dPEEP = P2 (4)]
- [62] If (PaO2 = LO) AND (FiO2 = MAX) AND (PEEP = MED) THEN [dPEEP = P2 (4)]
- [63] If (PaO2 = VLO) AND (FiO2 = MAX) AND (PEEP = HIGH) THEN [dPEEP = P2 (4)]
- [64] If (PaO2 = VLO) AND (FiO2 = HI-MAX) AND (PEEP = LOW) THEN [dPEEP = P3 (6)]
- [65] If (PaO2 = LO) AND (FiO2 = VHI-MAX) AND (PEEP = LOW) THEN [dPEEP = P3 (6)]
- [66] If (PaO2 = VLO) AND (FiO2 = VHI-MAX) AND (PEEP = OFF) THEN [dPEEP = P4 (8)]
- [67] If (PaO2 = LO) AND (FiO2 = MAX) AND (PEEP = OFF) THEN [dPEEP = P4 (8)]

MV Refined Control Rules

- [1] If (ePaCO2 = NB) AND (Pip = VHIGHIGH) THEN [dMv = N6 (-60)]
- [2] If (ePaCO2 = NB) AND (Pip = LOW-HIGH) THEN [dMv = N5 (-55)]
- [3] If (ePaCO2 = NM) THEN [dMv = N4 (-30)]
- [4] If (ePaCO2 = NS) THEN [dMv = N3 (-15)]
- [5] If (ePaCO2 = Z-PM) AND (Pip = EHIGHIGH) THEN [dMv = N3 (-15)]
- [6] If (ePaCO2 = PB) AND (Pip = EHIGHIGH) THEN [dMv = N2 (-10)]
- [7] If (ePaCO2 = Z) AND (Pip = VHIGHIGH) THEN [dMv = N1 (-5)]
- [8] If (ePaCO2 = Z) AND (Pip = LOW-HIGH) THEN [dMv = Z (0)]
- [9] If (ePaCO2 = PS-PM) AND (Pip = MED-VHIGHIGH) AND (eVTnorm = NB) THEN [dMv = Z (0)]
- [10] If (ePaCO2 = PB-PVB) AND (Pip = HIGH-VHIGHIGH) AND (eVTnorm = NB) THEN [dMv = Z (0)]
- [11] If (ePaCO2 = PVB) AND (Pip = EHIGHIGH) AND (eVTnorm = NB) THEN [dMv = Z (0)]
- [12] If (ePaCO2 = PS) AND (Pip = HIGH-VHIGHIGH) AND (eVTnorm = OK) THEN [dMv = Z (0)]
- [13] If (ePaCO2 = PS) AND (Pip = MED) AND (eVTnorm = OK) THEN [dMv = P1 (5)]
- [14] If (ePaCO2 = PM) AND (Pip = VHIGHIGH) AND (eVTnorm = OK) THEN [dMv = P1 (5)]
- [15] If (ePaCO2 = PVB) AND (Pip = EHIGHIGH) AND (eVTnorm = OK) THEN [dMv = P1 (5)]
- [16] If (ePaCO2 = PB) AND (Pip = MED) AND (eVTnorm = NB) THEN [dMv = P2 (10)]
- [17] If (ePaCO2 = PB-PVB) AND (Pip = VHIGHIGH) AND (eVTnorm = OK) THEN [dMv = P2 (10)]
- [18] If (ePaCO2 = PS) AND (Pip = LOW) THEN [dMv = P3 (15)]
- [19] If (ePaCO2 = PM) AND (Pip = MED-HIGH) AND (eVTnorm = OK) THEN [dMv = P3 (15)]
- [20] If (ePaCO2 = PVB) AND (Pip = MED) AND (eVTnorm = NB) THEN [dMv = P4 (20)]
- [21] If (ePaCO2 = PB-PVB) AND (Pip = HIGH) AND (eVTnorm = OK) THEN [dMv = P5 (25)]
- [22] If (ePaCO2 = PM) AND (Pip = LOW) THEN [dMv = P6 (30)]
- [23] If (ePaCO2 = PB-PVB) AND (Pip = MED) AND (eVTnorm = OK) THEN [dMv = P6 (30)]
- [24] If (ePaCO2 = PB) AND (Pip = LOW) THEN [dMv = P7 (60)]
- [25] If (ePaCO2 = PVB) AND (Pip = LOW) THEN [dMv = P8 (90)]

VT-RR Refined Control Rules

- [1] If (RR = MIN-LOW) AND (eVTnorm = PM) AND (Pip = EHIGH) THEN [dVt = N7 (-35)]
- [2] If (RR = MIN) AND (eVTnorm = PM) AND (Pip = LOW-VHIGH) THEN [dVt = N6 (-30)]
- [3] If (RR = MIN-MED) AND (eVTnorm = Z-PS) AND (Pip = VHIGH-EHIGH) THEN [dVt = N5 (-25)]
- [4] If (RR = HIGH) AND (eVTnorm = PS-PM) AND (Pip = VHIGH-EHIGH) THEN [dVt = N5 (-25)]
- [5] If (RR = VLOW-MED) AND (eVTnorm = PM) AND (Pip = VHIGH) THEN [dVt = N5 (-25)]
- [6] If (RR = HIGH) AND (eVTnorm = Z) AND (Pip = EHIGH) THEN [dVt = N5 (-25)]
- [7] If (RR = MED) AND (eVTnorm = PM) AND (Pip = EHIGH) THEN [dVt = N5 (-25)]
- [8] If (RR = MIN) AND (eVTnorm = PS) AND (Pip = LOW-HIGH) THEN [dVt = N4 (-20)]
- [9] If (RR = VLOW-LOW) AND (eVTnorm = PM) AND (Pip = LOW-HIGH) THEN [dVt = N4 (-20)]
- [10] If (RR = MIN-HIGH) AND (eVTnorm = NM-NS) AND (Pip = EHIGH) THEN [dVt = N4 (-20)]
- [11] If (RR = MIN) AND (eVTnorm = Z) AND (Pip = LOW-HIGH) THEN [dVt = N3 (-15)]
- [12] If (RR = MED) AND (eVTnorm = PM) AND (Pip = LOW-HIGH) THEN [dVt = N3 (-15)]
- [13] If (RR = MIN-HIGH) AND (eVTnorm = NS) AND (Pip = VHIGH) THEN [dVt = N3 (-15)]
- [14] If (RR = VHIGH) AND (eVTnorm = Z-PS) AND (Pip = EHIGH) THEN [dVt = N3 (-15)]
- [15] If (RR = VLOW-LOW) AND (eVTnorm = PS) AND (Pip = LOW-HIGH) THEN [dVt = N2 (-10)]
- [16] If (RR = MED) AND (eVTnorm = PS) AND (Pip = MED) THEN [dVt = N2 (-10)]
- [17] If (RR = MIN-VLOW) AND (eVTnorm = NM-NS) AND (Pip = HIGH) THEN [dVt = N2 (-10)]
- [18] If (RR = LOW-MED) AND (eVTnorm = NS) AND (Pip = HIGH) THEN [dVt = N2 (-10)]
- [19] If (RR = VLOW-LOW) AND (eVTnorm = Z) AND (Pip = HIGH) THEN [dVt = N2 (-10)]
- [20] If (RR = MIN-HIGH) AND (eVTnorm = NM) AND (Pip = VHIGH) THEN [dVt = N2 (-10)]
- [21] If (RR = VHIGH) AND (eVTnorm = NM-NS) AND (Pip = EHIGH) THEN [dVt = N2 (-10)]
- [22] If (RR = MAX) AND (eVTnorm = PS-PM) AND (Pip = EHIGH) THEN [dVt = N2 (-10)]
- [23] If (RR = VHIGH) AND (eVTnorm = PM) AND (Pip = EHIGH) THEN [dVt = N2 (-10)]
- [24] If (RR = MIN) AND (eVTnorm = NS) AND (Pip = LOW-MED) THEN [dVt = N1 (-5)]
- [25] If (RR = MED) AND (eVTnorm = PS) AND (Pip = LOW) THEN [dVt = N1 (-5)]
- [26] If (RR = HIGH) AND (eVTnorm = PM) AND (Pip = LOW-HIGH) THEN [dVt = N1 (-5)]
- [27] If (RR = VLOW-LOW) AND (eVTnorm = NS-Z) AND (Pip = MED) THEN [dVt = N1 (-5)]
- [28] If (RR = MED) AND (eVTnorm = NS) AND (Pip = MED) THEN [dVt = N1 (-5)]
- [29] If (RR = LOW-MED) AND (eVTnorm = NM) AND (Pip = HIGH) THEN [dVt = N1 (-5)]
- [30] If (RR = MED) AND (eVTnorm = PS) AND (Pip = HIGH) THEN [dVt = N1 (-5)]
- [31] If (RR = VHIGH) AND (eVTnorm = PM) AND (Pip = HIGH-VHIGH) THEN [dVt = N1 (-5)]
- [32] If (RR = VHIGH) AND (eVTnorm = NM-NS) AND (Pip = VHIGH) THEN [dVt = N1 (-5)]
- [33] If (RR = VHIGH-MAX) AND (eVTnorm = PS) AND (Pip = VHIGH) THEN [dVt = N1 (-5)]
- [34] If (RR = MAX) AND (eVTnorm = PM) AND (Pip = VHIGH) THEN [dVt = N1 (-5)]
- [35] If (RR = MIN) AND (eVTnorm = NB) THEN [dVt = Z (0)]
- [36] If (RR = MIN-VLOW) AND (eVTnorm = NM) AND (Pip = LOW-MED) THEN [dVt = Z (0)]
- [37] If (RR = VLOW-MED) AND (eVTnorm = NS-Z) AND (Pip = LOW) THEN [dVt = Z (0)]
- [38] If (RR = HIGH-VHIGH) AND (eVTnorm = PS) AND (Pip = LOW-HIGH) THEN [dVt = Z (0)]
- [39] If (RR = LOW-MED) AND (eVTnorm = NM) AND (Pip = MED) THEN [dVt = Z (0)]
- [40] If (RR = MED-VHIGH) AND (eVTnorm = Z) AND (Pip = MED-HIGH) THEN [dVt = Z (0)]
- [41] If (RR = VHIGH) AND (eVTnorm = PM) AND (Pip = MED) THEN [dVt = Z (0)]
- [42] If (RR = VLOW-MAX) AND (eVTnorm = NB) AND (Pip = HIGH-EHIGH) THEN [dVt = Z (0)]
- [43] If (RR = HIGH-MAX) AND (eVTnorm = NM-NS) AND (Pip = HIGH) THEN [dVt = Z (0)]
- [44] If (RR = MAX) AND (eVTnorm = Z-PM) AND (Pip = HIGH) THEN [dVt = Z (0)]
- [45] If (RR = MAX) AND (eVTnorm = NM-Z) AND (Pip = VHIGH-EHIGH) THEN [dVt = Z (0)]
- [46] If (RR = HIGH-VHIGH) AND (eVTnorm = Z) AND (Pip = VHIGH) THEN [dVt = Z (0)]
- [47] If (RR = VHIGH) AND (eVTnorm = PM) AND (Pip = LOW) THEN [dVt = P1 (2)]
- [48] If (RR = LOW) AND (eVTnorm = NM) AND (Pip = LOW) THEN [dVt = P2 (5)]
- [49] If (RR = HIGH) AND (eVTnorm = Z) AND (Pip = LOW) THEN [dVt = P2 (5)]
- [50] If (RR = HIGH-VHIGH) AND (eVTnorm = NS) AND (Pip = MED) THEN [dVt = P2 (5)]
- [51] If (RR = MAX) AND (eVTnorm = PS-PM) AND (Pip = MED) THEN [dVt = P2 (5)]
- [52] If (RR = MAX) AND (eVTnorm = PM) AND (Pip = LOW) THEN [dVt = P3 (10)]

[53] If (RR = VLOW-MAX) AND (eVTnorm = NB) AND (Pip = MED) THEN [dVt = P3 (10)]
 [54] If (RR = HIGH-MAX) AND (eVTnorm = NM) AND (Pip = MED) THEN [dVt = P3 (10)]
 [55] If (RR = MAX) AND (eVTnorm = NS-Z) AND (Pip = MED) THEN [dVt = P3 (10)]
 [56] If (RR = VLOW) AND (eVTnorm = NB) AND (Pip = LOW) THEN [dVt = P4 (15)]
 [57] If (RR = HIGH) AND (eVTnorm = NS) AND (Pip = LOW) THEN [dVt = P4 (15)]
 [58] If (RR = VHIGH) AND (eVTnorm = Z) AND (Pip = LOW) THEN [dVt = P4 (15)]
 [59] If (RR = MAX) AND (eVTnorm = PS) AND (Pip = LOW) THEN [dVt = P4 (15)]
 [60] If (RR = MED) AND (eVTnorm = NM) AND (Pip = LOW) THEN [dVt = P5 (20)]
 [61] If (RR = LOW) AND (eVTnorm = NB) AND (Pip = LOW) THEN [dVt = P6 (25)]
 [62] If (RR = VHIGH) AND (eVTnorm = NS) AND (Pip = LOW) THEN [dVt = P6 (25)]
 [63] If (RR = MAX) AND (eVTnorm = Z) AND (Pip = LOW) THEN [dVt = P6 (25)]
 [64] If (RR = MAX) AND (eVTnorm = NS) AND (Pip = LOW) THEN [dVt = P7 (35)]
 [65] If (RR = MED) AND (eVTnorm = NB) AND (Pip = LOW) THEN [dVt = P8 (40)]
 [66] If (RR = HIGH-VHIGH) AND (eVTnorm = NM) AND (Pip = LOW) THEN [dVt = P8 (40)]
 [67] If (RR = HIGH) AND (eVTnorm = NB) AND (Pip = LOW) THEN [dVt = P9 (50)]
 [68] If (RR = MAX) AND (eVTnorm = NM) AND (Pip = LOW) THEN [dVt = P9 (50)]
 [69] If (RR = VHIGH-MAX) AND (eVTnorm = NB) AND (Pip = LOW) THEN [dVt = P10 (60)]

TIN New Control Rules

[1] If (Pip = OKAY) AND (Tin = MAX) THEN [dTin = N2 (-20)]
 [2] If (Pip = OKAY) AND (Tin = MED-HI) THEN [dTin = N1 (-10)]
 [3] If (Pip = MED-HI) AND (Tin = MAX) THEN [dTin = N1 (-10)]
 [4] If (Pip = OKAY-MED) AND (Tin = NORM) THEN [dTin = Z (0)]
 [5] If (Pip = MED-HI) AND (Tin = MED-HI) THEN [dTin = Z (0)]
 [6] If (Pip = VHI) AND (Tin = MAX) THEN [dTin = Z (0)]
 [7] If (Pip = HI) AND (Tin = NORM) THEN [dTin = P1 (10)]
 [8] If (Pip = VHI) AND (Tin = MED-HI) THEN [dTin = P1 (10)]
 [9] If (Pip = VHI) AND (Tin = NORM) THEN [dTin = P2 (20)]

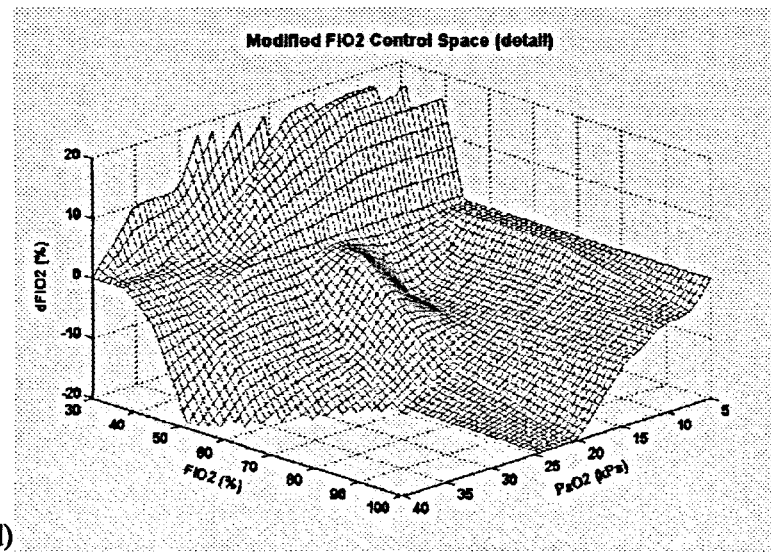
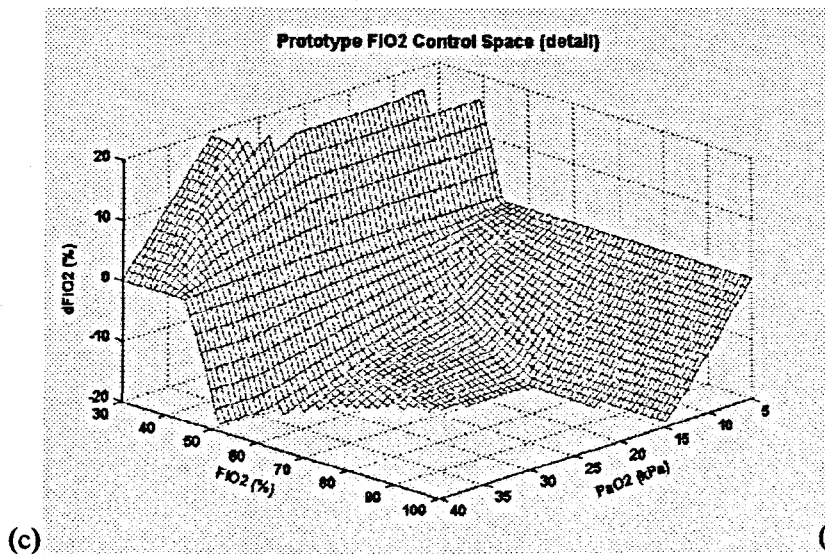
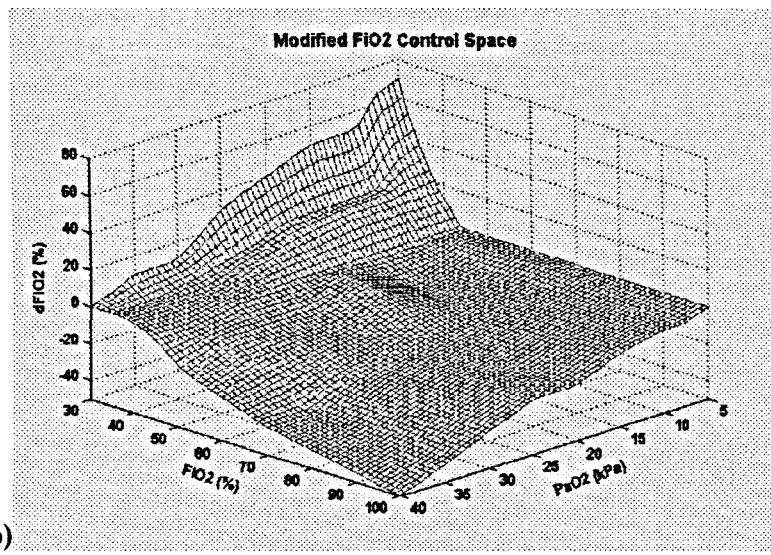
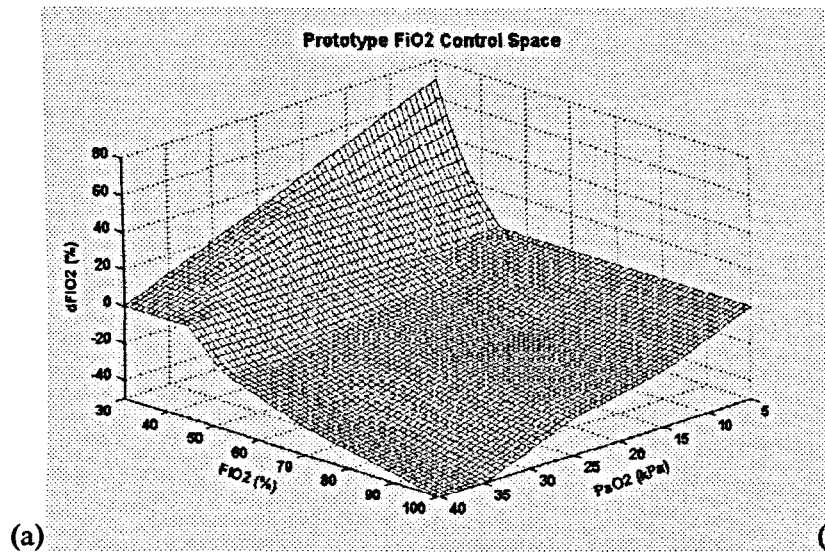


Figure E.1: The output behaviour of (a) the prototype and (b) the modified FiO₂ advisor, for all possible combinations of PaO₂ and FiO₂ input. The region of output between $\pm 20\%$ has been expanded in figures (c) and (d) to give a clearer picture of the controller behaviour due to the variability of scale in the advice given.

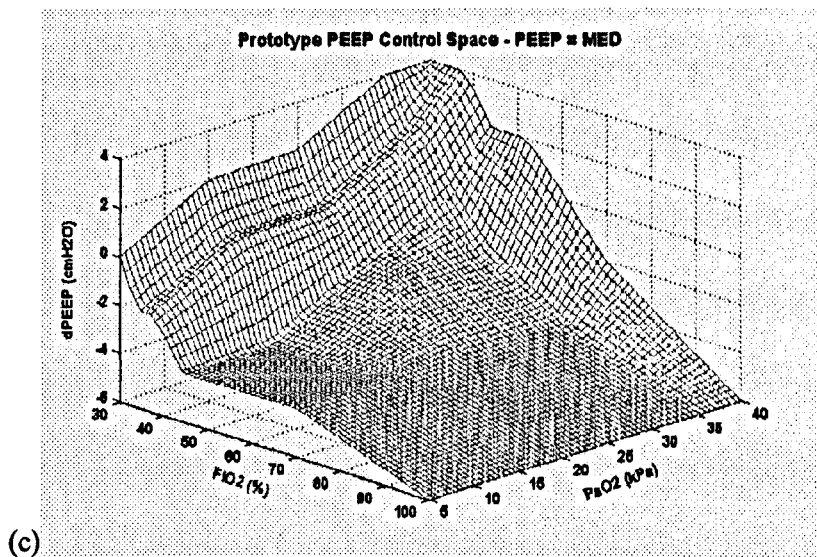
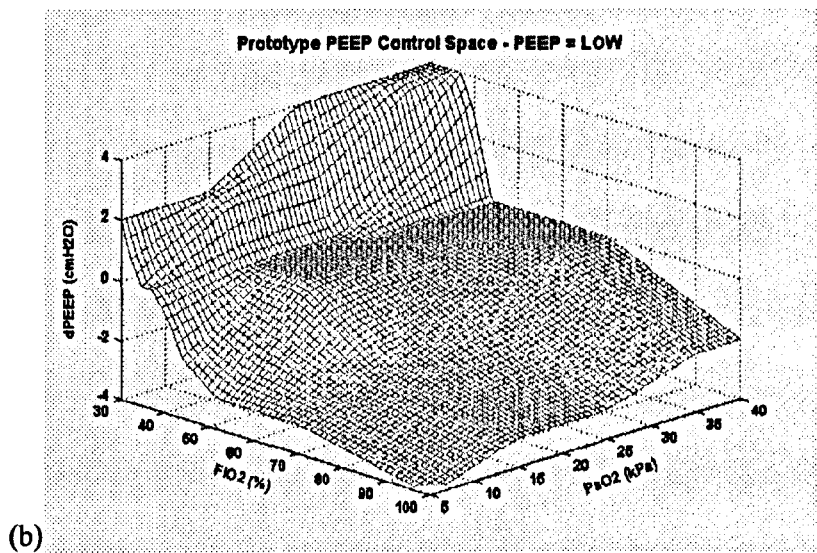
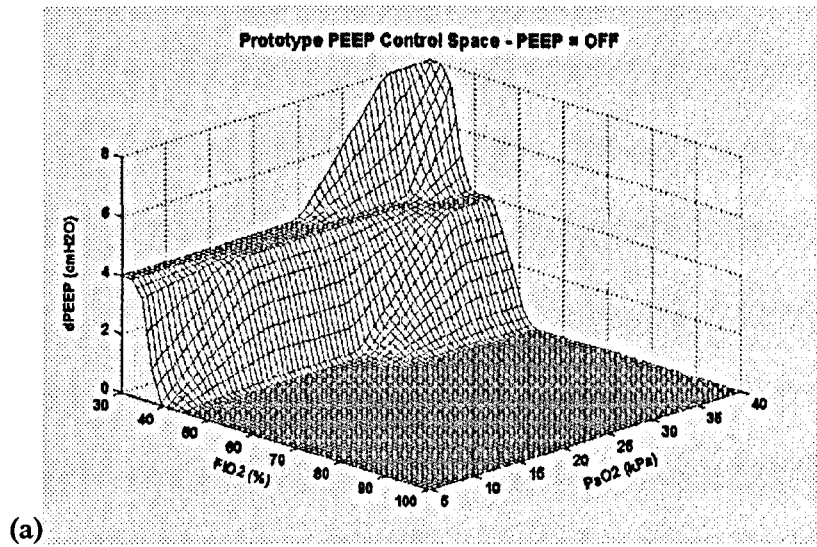


Figure continued overleaf...

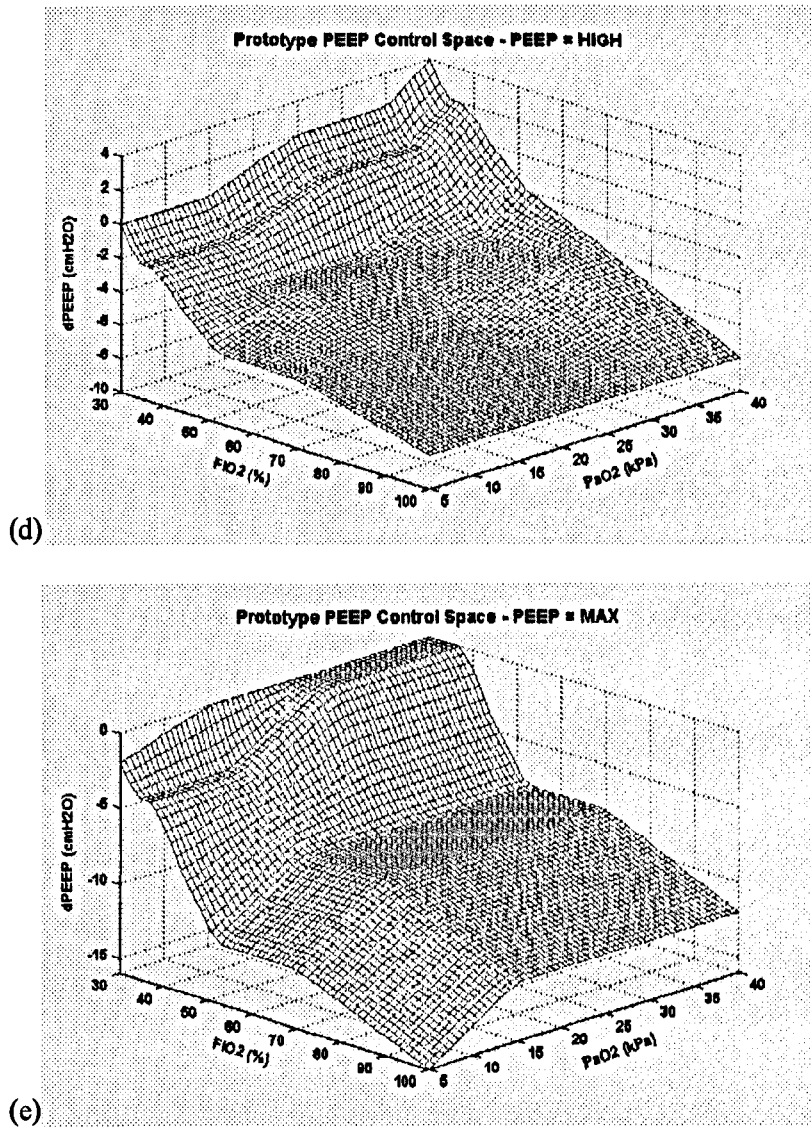


Figure E.2: The output behaviour of the **prototype PEEP advisor**, for all possible combinations of PaO_2 and FIO_2 input. Control space plots are shown for each PEEP fuzzy linguistic class; (a) OFF (0 cmH_2O), (b) LOW (4 cmH_2O), (c) MEDIUM (8 cmH_2O), (d) HIGH (12 cmH_2O) and (e) MAX (16 cmH_2O).

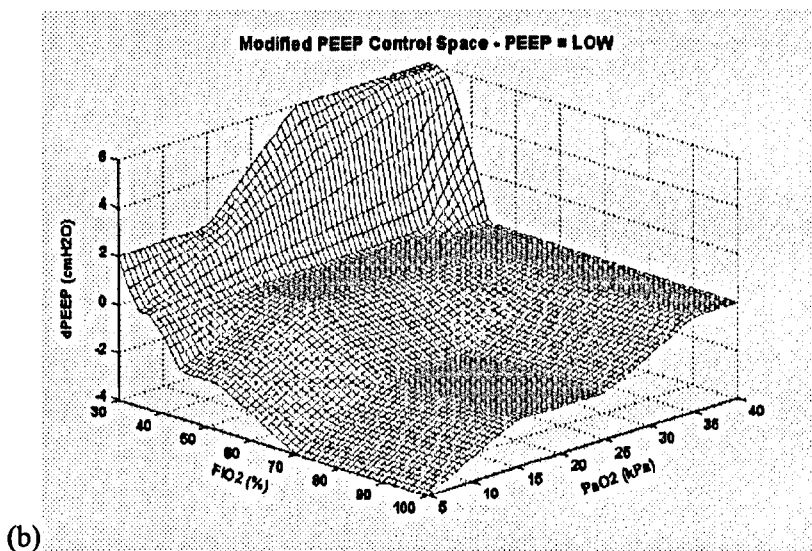
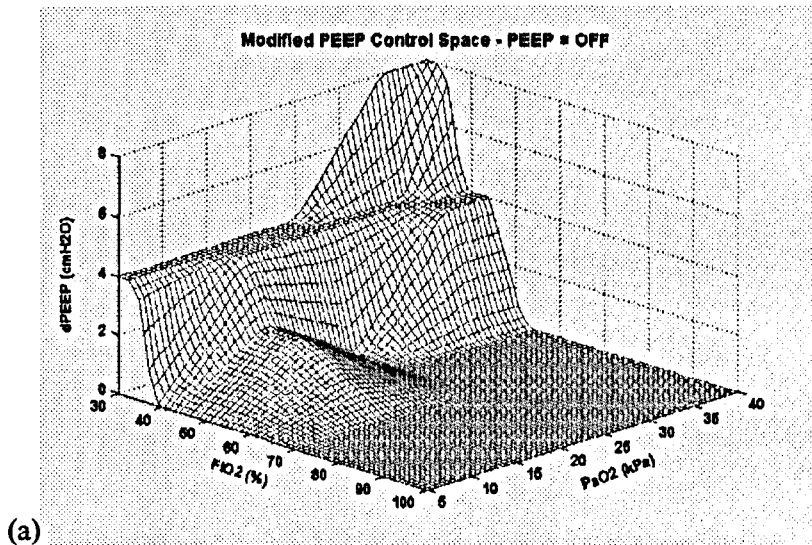


Figure E.3: The output behaviour of the **modified** PEEP advisor, for all possible combinations of PaO_2 and FIO_2 input. Control space plots are shown for the PEEP fuzzy linguistic classes; (a) OFF (0 cmH_2O) and (b) LOW (4 cmH_2O). The plots for MEDIUM, HIGH, and MAX are not shown since they are identical to those of Figure E.2 (c) to (e).

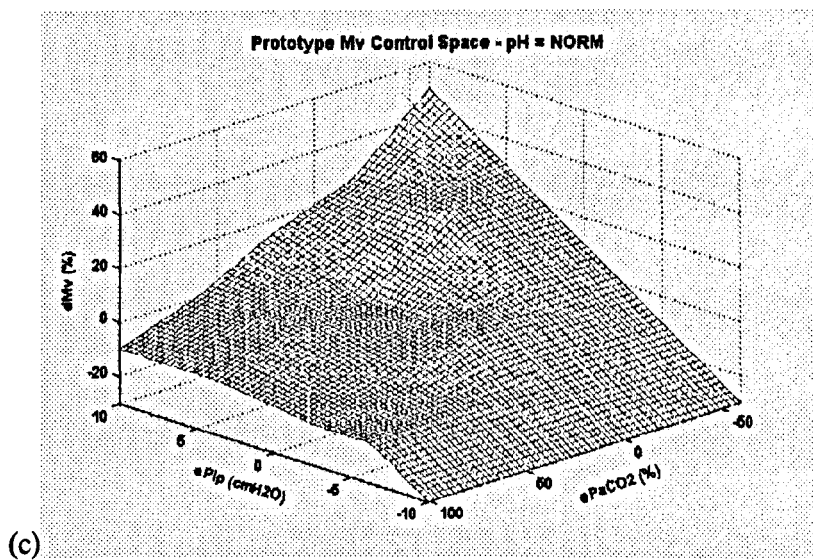
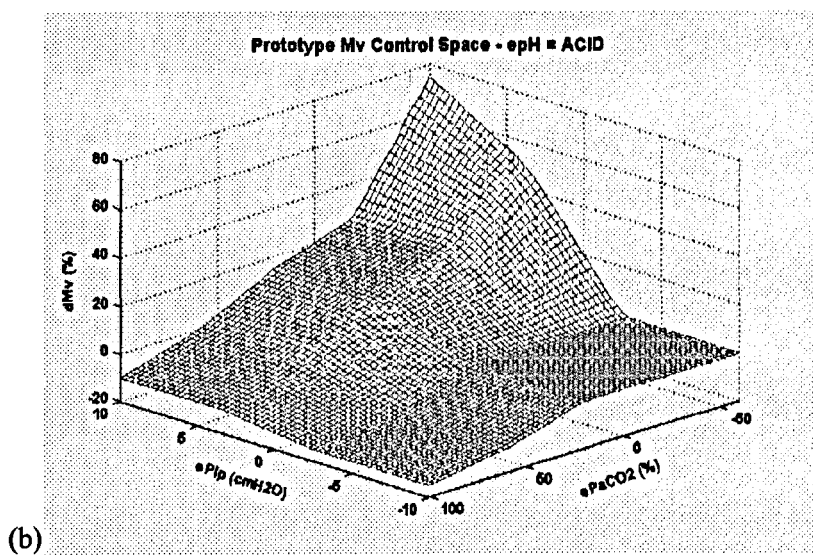
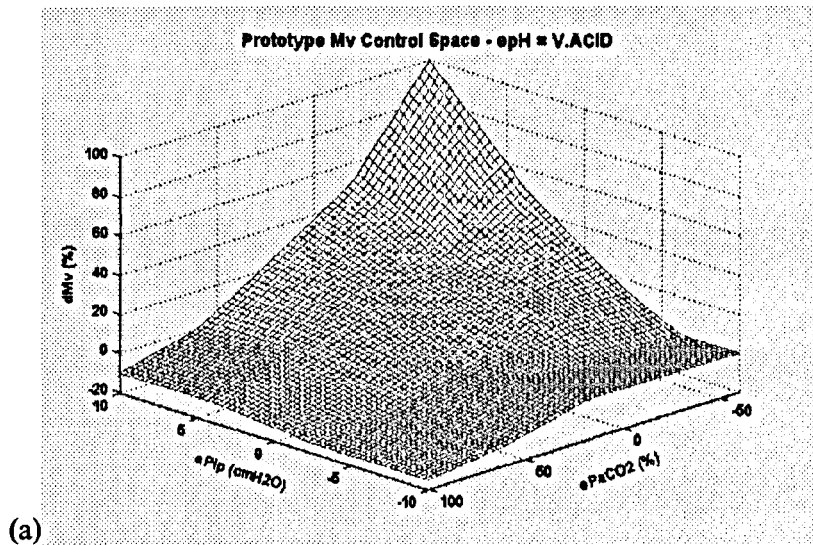


Figure continued overleaf...

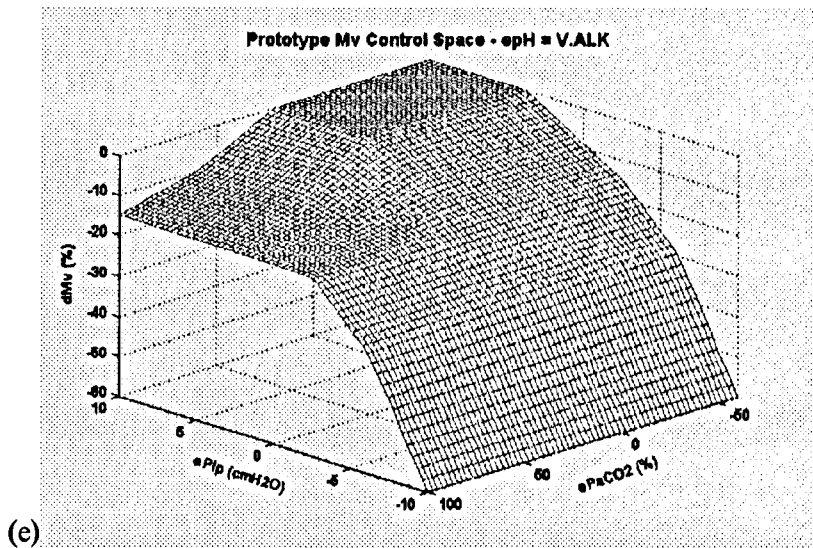
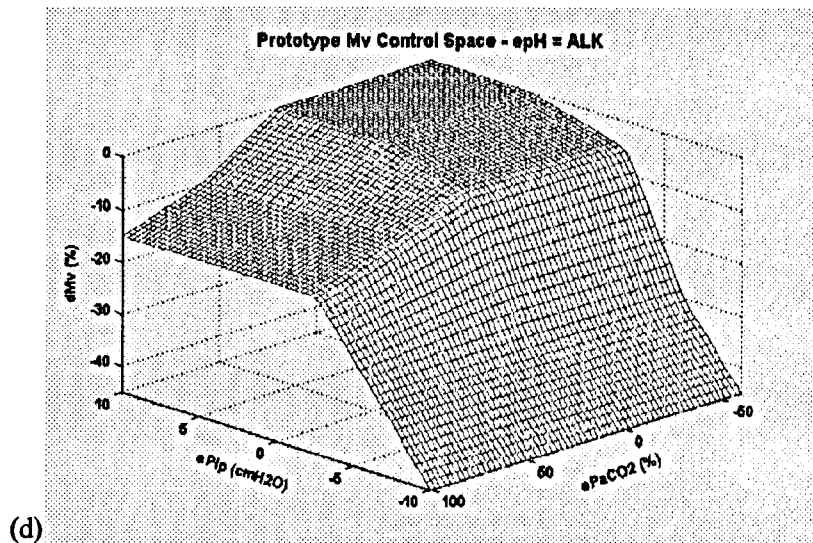
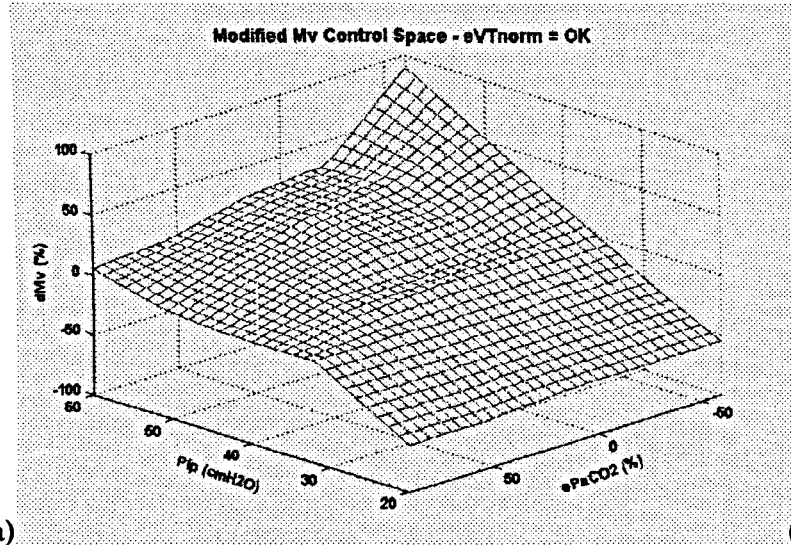
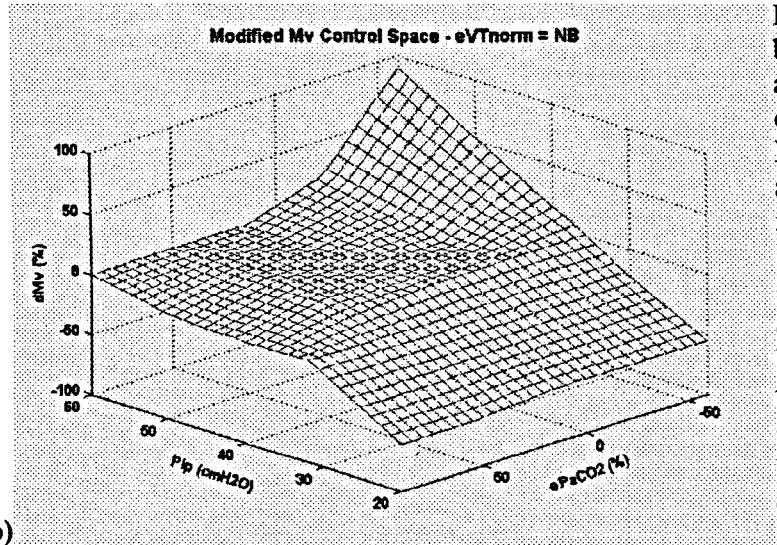


Figure E.4: The output behaviour of the **prototype Mv** advisor, for all possible combinations of $ePaCO_2$ and $ePIP$ input. Control space plots are shown for the epH fuzzy linguistic classes; (a) V.ACID (-0.29), (b) ACID (-0.17), (c) NORMAL (0), (d) ALK (+0.15) and (e) V.ALK (+0.38).

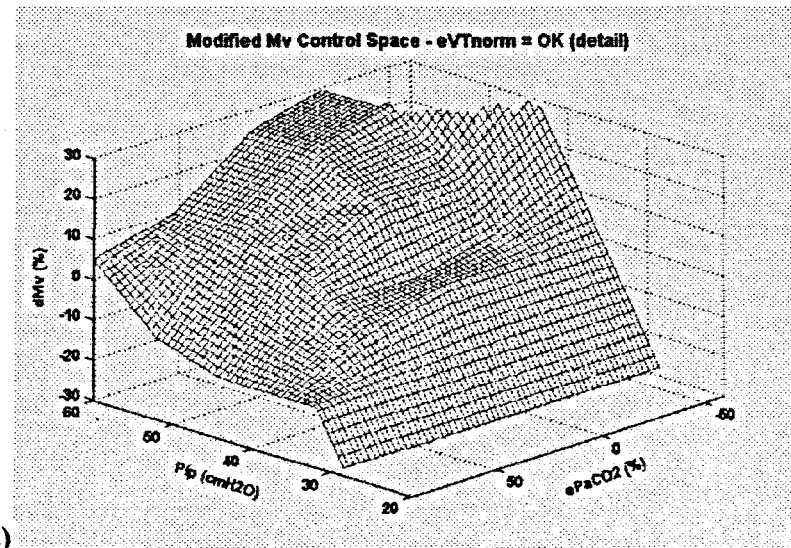


(a)

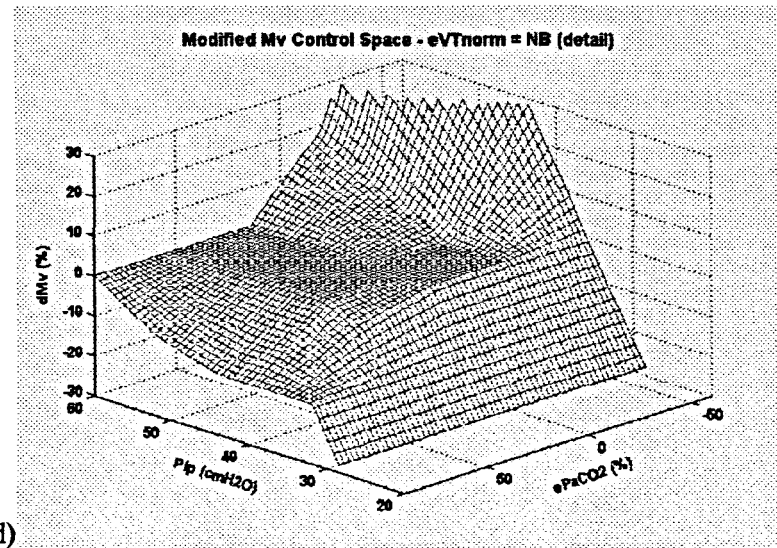


(b)

Figure E.5: The output behaviour of the modified MV advisor, for all possible combinations of $ePaCO_2$ and PIP input. Control space plots are shown for each eVT_{NORM} fuzzy linguistic class; (a) OK (-15 %) and (b) NB (-35 %). The region of output between ± 30 % has been expanded in (c) and (d) to give a clearer picture of the controller behaviour due to the variability of scale in the advice given.



(c)



(d)

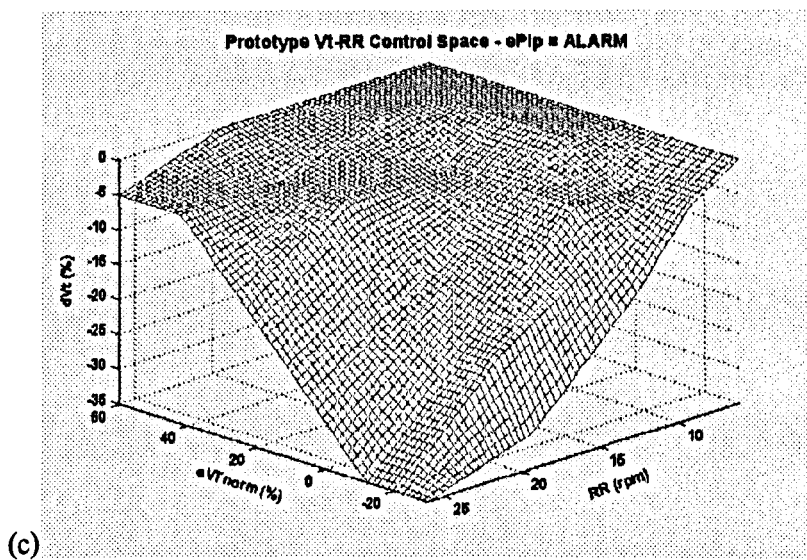
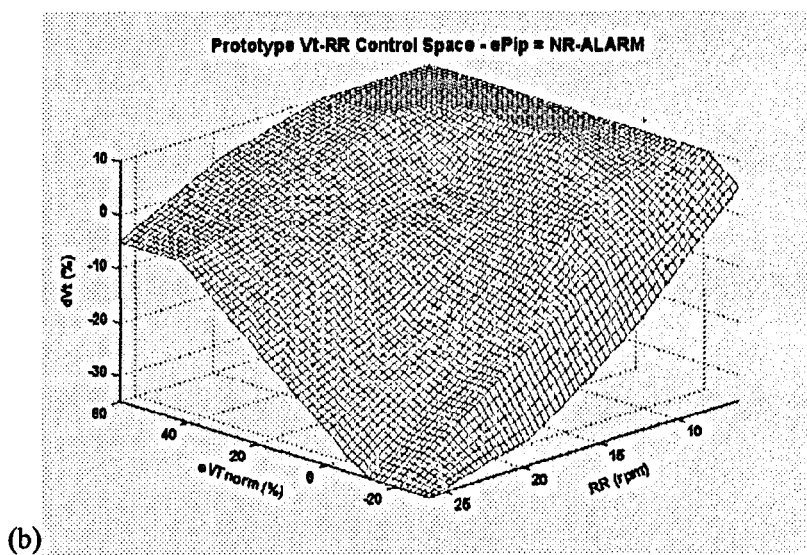
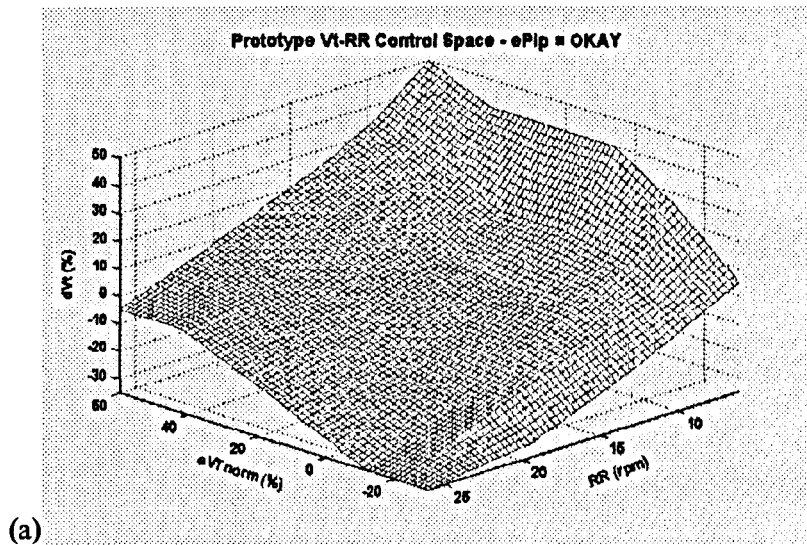


Figure continued overleaf...

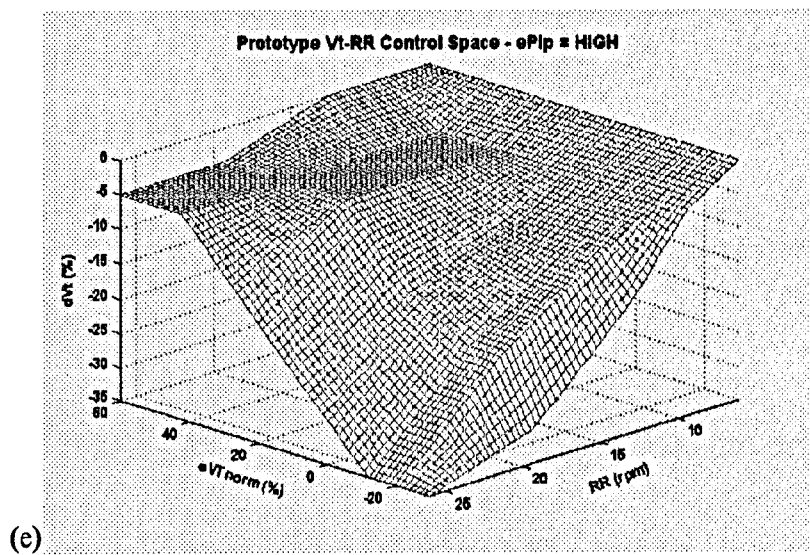
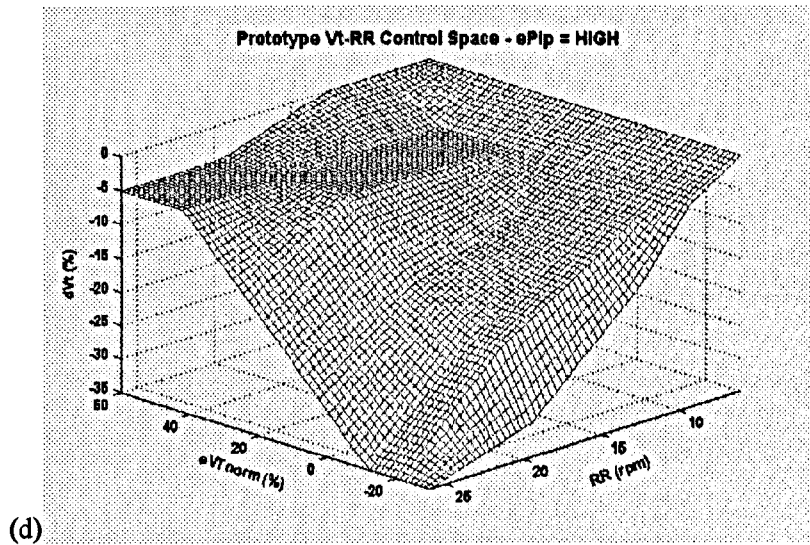


Figure E.6: The output behaviour of the prototype VT-RR advisor, for all possible combinations of eVT_{NORM} and RR input. Control space plots are shown for the ePIP fuzzy linguistic classes; (a) OKAY (-10 cmH₂O), (b) NEAR ALARM (-5 cmH₂O), (c) ALARM (0 cmH₂O), (d) HIGH (+5 cmH₂O) and (e) V.HIGH (+10 cmH₂O).

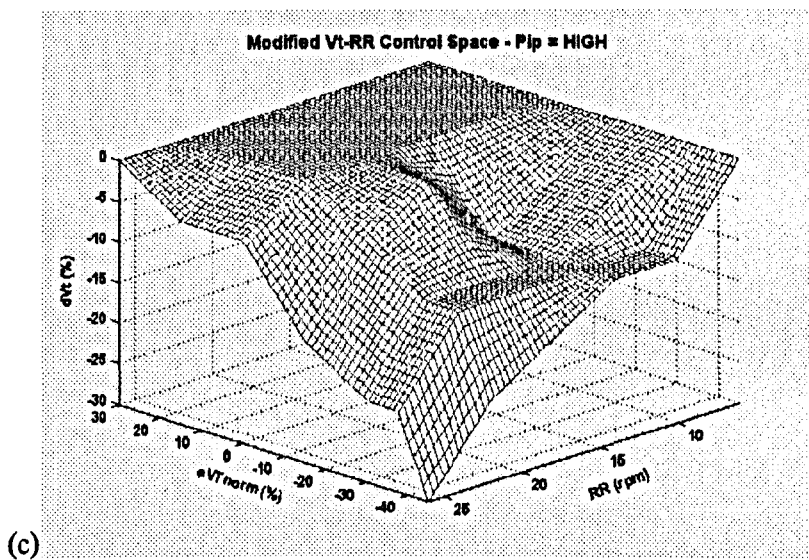
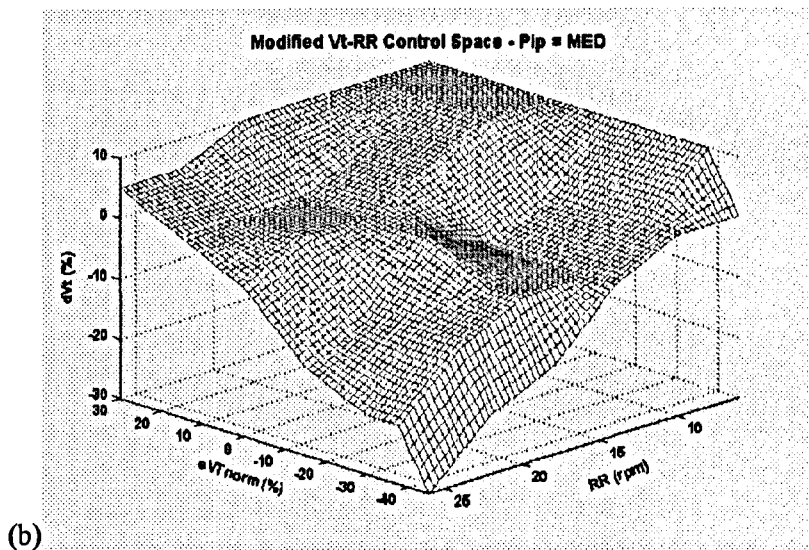
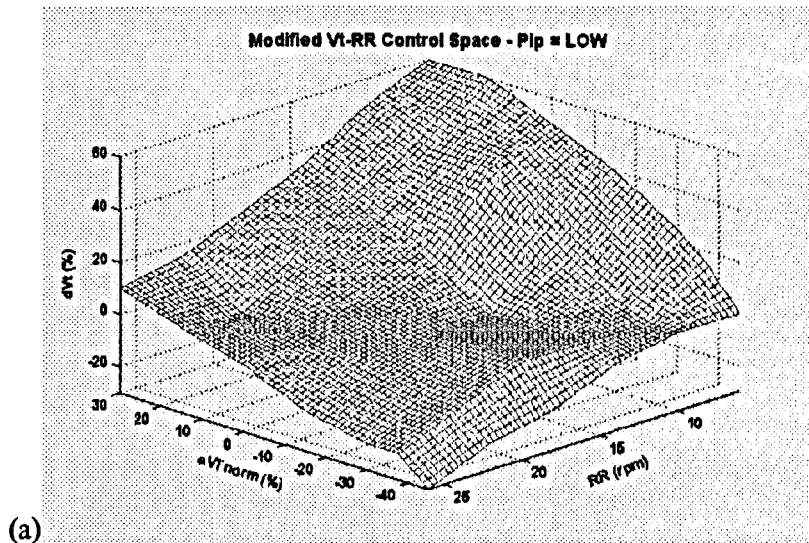


Figure continued overleaf...

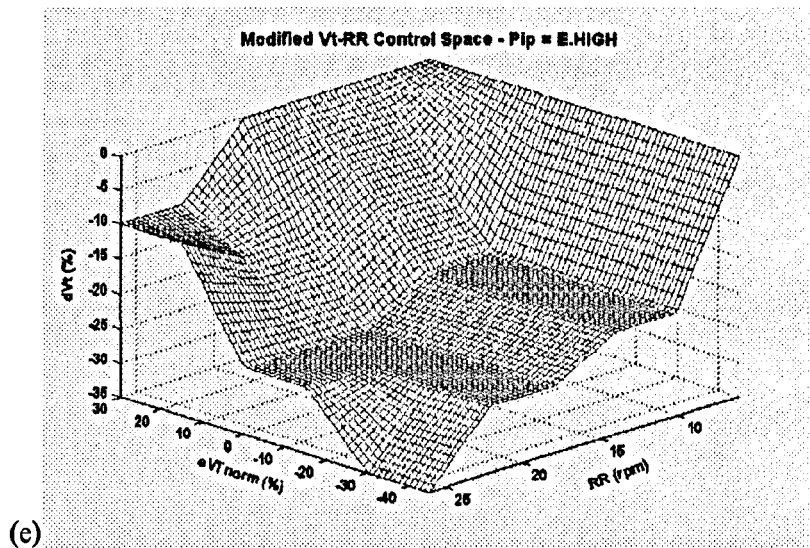
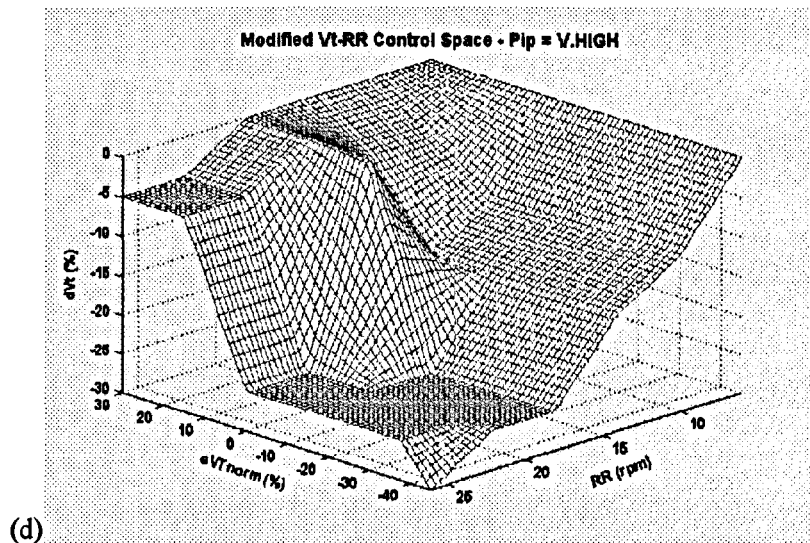


Figure E.7: The output behaviour of the modified VT-RR advisor, for all possible combinations of eVT_{NORM} and RR input. Control space plots are shown for the PIP fuzzy linguistic classes; (a) LOW (20 cmH₂O), (b) MEDIUM (30 cmH₂O), (c) HIGH (40 cmH₂O), (d) V.HIGH (50 cmH₂O) and (e) E.HIGH (60 cmH₂O).

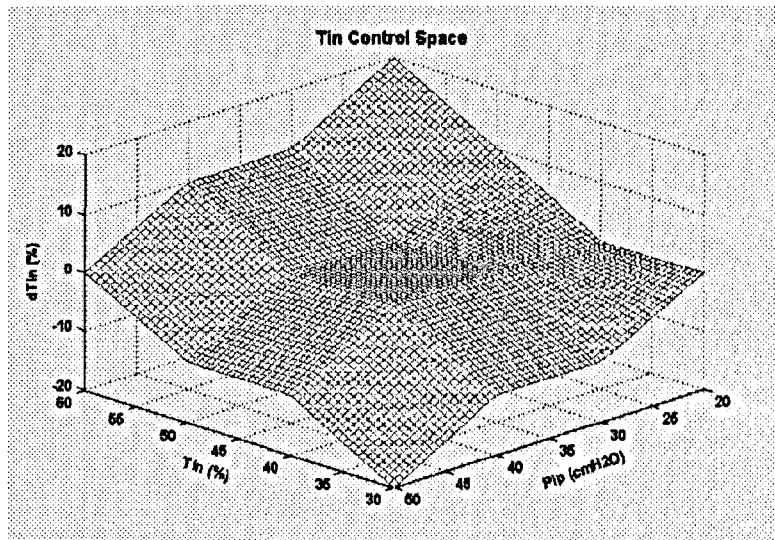


Figure E.8: The output behaviour of the **modified TIN** advisor, for all possible combinations of TIN and PIP input. This advisor subsystem was not present in the prototype advisor.

Appendix F

Advisor Responses to Clinical Data
and Decision Scoring

	15	16	17	18	19	20	21	22	23	24	25	26	27	28	29	30	31	32	33	34	
Observations																					
PaO ₂ (kPa)	21.4	10.3	13.1	10.3	18.0	10.9	19.7	12.5	14.3	10.6	11.7	11.1	11.1	10.1	10.1	14.1	14.1	13.8	10.7	9.8	
PaCO ₂ (kPa)	3.70	3.54	3.40	3.50	3.82	3.70	4.18	3.83	4.17	4.00	4.10	4.00	4.00	4.35	4.35	4.90	4.67	4.84	4.86	4.93	
pH	7.57	7.57	7.60	7.58	7.54	7.57	7.56	7.54	7.53	7.51	7.49	7.51	7.51	7.50	7.50	7.43	7.44	7.45	7.43	7.42	
PIP (cmH ₂ O)	27.0	28.0	27.0	27.0	29.0	25.0	24.0	25.0	29.0	29.0	29.0	29.0	29.0	29.0	29.0	28.0	29.0	38.0	29.0	35.0	
Weight (kg)	65.0	65.0	65.0	65.0	65.0	65.0	65.0	65.0	65.0	65.0	65.0	65.0	65.0	65.0	65.0	65.0	65.0	65.0	65.0	65.0	
FiO ₂ (%)	40	35	35	35	40	40	45	45	45	45	45	50	55	50	55	80	75	70	70	70	
Peep (cmH ₂ O)	7.5	7.5	7.5	0	0	0	0	0	0	0	0	0	0	0	0	0	0	0	0	0	
Mv (l/min)	14.54	15.01	15.01	15.01	15.01	15.01	15.01	15.01	15.01	15.01	15.01	15.01	15.01	15.01	15.01	15.01	15.01	16.50	16.50	16.50	
RR (rpm)	16	16	16	16	16	16	16	16	16	16	16	16	16	16	16	16	16	16	16	16	
Vt (ml)	938	938	938	938	938	938	938	938	938	938	938	938	938	938	938	938	938	1031	1031	1031	
Tin (%)	33	33	33	33	33	33	33	33	33	33	33	33	33	33	33	33	33	33	33	33	
Target PaCO ₂ (kPa)	3.8	3.8	3.8	3.8	3.8	3.8	3.8	3.8	3.8	3.8	3.8	3.8	3.8	3.8	3.8	3.8	3.8	3.8	3.8	3.8	
Anaesthetist's New Settings																					
FiO ₂ (%)	35	35	35	40	40	45	45	45	45	45	50	55	50	55	80	75	70	70	70	70	
Peep (cmH ₂ O)	7.5	7.5	0.0	0.0	0.0	0.0	0.0	0.0	0.0	0.0	0.0	0.0	0.0	0.0	0.0	0.0	0.0	0.0	0.0	0.0	
Mv (l/min)	15.01	15.01	15.01	15.01	15.01	15.01	15.01	15.01	15.01	15.01	15.01	15.01	15.01	15.01	15.01	15.01	16.50	16.50	16.50	20.00	
RR (rpm)	16.0	16.0	16.0	16.0	16.0	16.0	16.0	16.0	16.0	16.0	16.0	16.0	16.0	16.0	16.0	16.0	16.0	16.0	16.0	16.0	
Vt (ml)	938	938	938	938	938	938	938	938	938	938	938	938	938	938	938	938	1031	1031	1031	1250	
Tin (%)	33	33	33	33	33	33	33	33	33	33	33	33	33	33	33	33	33	33	33	33	
Advisor New Settings																					
FiO ₂ (%)	35	46	35	46	35	47	37	44	41	54	47	56	60	63	66	75	70	65	74	77	
PEEP (cmH ₂ O)	3.5	5.0	4.0	1.0	1.0	1.5	1.0	1.5	1.5	2.0	1.5	2.5	2.0	3.5	3.0	1.0	0.5	0.0	1.5	3.0	
MV (l/min)	14.63	13.96	13.43	13.81	15.04	14.63	16.01	15.12	15.96	15.34	15.49	15.34	15.34	15.88	15.88	17.60	16.75	18.59	18.99	18.90	
RR (rpm)	17.5	17.0	17.0	17.0	18.0	17.5	18.5	18.0	18.5	18.0	18.0	18.0	18.0	18.5	18.5	19.5	19.0	19.0	19.5	19.5	
Vt (ml)	830	820	800	810	840	830	870	850	870	850	860	850	850	870	870	900	890	980	980	980	
Tin (%)	33	33	33	33	33	33	33	33	33	33	33	33	33	33	33	33	33	40	33	40	
Decision Difference																					
FiO ₂ (%)	0	11	0	6	-5	2	-8	-1	-4	9	-3	1	10	8	-14	0	0	-5	4	7	
Peep (cmH ₂ O)	-4.0	-2.5	4.0	1.0	1.0	1.5	1.0	1.5	1.5	2.0	1.5	2.5	2.0	3.5	3.0	1.0	0.5	0.0	1.5	3.0	
Mv (l/min)	-0.38	-1.05	-1.58	-1.20	0.03	-0.38	1.00	0.11	0.95	0.33	0.48	0.33	0.33	0.87	0.87	2.59	0.25	2.09	2.49	-1.10	
RR (rpm)	1.5	1.0	1.0	1.0	2.0	1.5	2.5	2.0	2.5	2.0	2.0	2.0	2.0	2.5	2.5	3.5	3.0	3.0	3.5	3.5	
Vt (ml)	-108	-118	-138	-128	-98	-108	-68	-88	-68	-88	-78	-88	-88	-68	-68	-38	-141	-51	-51	-270	
Tin (%)	0	0	0	0	0	0	0	0	0	0	0	0	0	0	0	0	0	7	0	7	
Scoring																					
FiO ₂ score	exact	X	exact	mod	good	good	mod	good	good	mod	good	good	X	mod	X	exact	exact	good	good	mod	
Peep score	X	X	X	good	good	mod	good	mod	mod	mod	mod	X	mod	X	X	good	good	exact	mod	X	
Mv score	good	X	X	X	good	good	X	good	mod	good	good	good	good	mod	mod	X	good	X	X	X	
RR score	good	good	good	good	mod	good	mod	mod	mod	mod	mod	mod	mod	mod	mod	X	mod	mod	X	X	
Vt score	X	X	X	X	mod	X	mod	mod	mod	mod	mod	mod	mod	mod	mod	good	X	mod	mod	X	
Tin score	exact	exact	exact	exact	exact	exact	exact	exact	exact	exact	exact	exact	exact	exact	exact	exact	exact	exact	mod	exact	mod

				Patient 5:												Patient 6:					
	11	12	13	1	2	3	4	5	6	7	8	9	10	11	12	1	2	3	4	5	
Observations																					
PaO ₂ (kPa)	18.3	24.2	14.3	78.5	26.4	24.6	13.6	9.9	9.2	10.2	10.6	10.5	11.8	12	11.8	14.7	14.6	15.1	11.8	11.2	
PaCO ₂ (kPa)	3.33	3.50	4.04	2.74	3.39	2.88	3.80	4.19	4.72	4.00	3.92	4.00	3.93	3.98	4.06	4.17	3.71	3.64	3.47	3.43	
pH	7.58	7.56	7.50	7.54	7.45	7.41	7.34	7.30	7.27	7.33	7.32	7.28	7.26	7.24	7.18	7.18	7.22	7.24	7.27	7.37	
PiP (cmH ₂ O)	36.00	34.00	32.00	33.0	25.0	24.0	21.0	24.0	23.0	26.0	26.0	26.0	26.0	26.0	27.0	44.0	31.0	32.0	31.0	29.0	
Weight (kg)	70.0	70.0	70.0	78.3	78.3	78.3	78.3	78.3	78.3	78.3	78.3	78.3	78.3	78.3	78.3	54.0	54.0	54.0	54.0	54.0	
FiO ₂ (%)	40	40	40	80	50	50	45	45	45	60	70	70	70	70	70	95	95	80	70	60	
Peep (cmH ₂ O)	0	0	0	0	0	0	0	0	0	0	0	0	5	5	5	4	4	4	4	4	
Mv (l/min)	16.50	16.50	16.50	12.50	9.00	9.00	7.99	7.99	7.99	8.00	9.49	9.49	9.49	9.49	9.49	10.50	11.20	10.50	10.50	10.50	
RR (rpm)	22	22	22	17	12	12	12	12	12	13	13	13	13	13	13	15	16	15	15	15	
Vt (ml)	750	750	750	735	750	750	666	666	666	615	730	730	730	730	730	700	700	700	700	700	
Tin (%)	-	-	-	25	25	25	25	25	25	25	25	25	25	25	25	25	25	25	25	25	
Target PaCO ₂ (kPa)	4.00	4.00	4.00	4.00	4.00	4.00	4.00	4.00	4.00	4.00	4.00	4.00	4.00	4.00	4.00	5.3	5.3	5.3	5.3	5.3	
Anaesthetist's New Settings																					
FiO ₂ (%)	40	40	40	50	50	45	45	45	60	70	70	70	70	70	70	95	80	70	60	50	
Peep (cmH ₂ O)	0	0	0	0.0	0.0	0.0	0.0	0.0	0.0	0.0	0.0	5.0	5.0	5.0	5.0	4.0	4.0	4.0	4.0	4.0	
Mv (l/min)	16.50	16.50	16.50	9.00	9.00	7.99	7.99	7.99	8.00	9.49	9.49	9.49	9.49	9.49	9.49	11.20	10.50	10.50	10.50	7.00	
RR (rpm)	22	22	22	12.0	12.0	12.0	12.0	12.0	13.0	13.0	13.0	13.0	13.0	13.0	13.0	16.0	15.0	15.0	15.0	10.0	
Vt (ml)	750	750	750	750	750	666	666	666	615	730	730	730	730	730	730	700	700	700	700	700	
Tin (%)	-	-	-	25	25	25	25	25	25	25	25	25	25	25	25	25	25	25	25	25	
Advisor New Settings																					
FiO ₂ (%)	35	35	37	50	40	40	42	59	64	69	75	75	71	70	71	83	84	72	71	64	
PEEP (cmH ₂ O)	0.5	0.0	1.0	0.0	0.0	0.0	1.5	2.5	3.0	3.0	2.0	2.0	4.5	4.5	4.5	4.0	4.0	4.0	4.0	4.0	
MV (l/min)	13.78	14.44	16.54	8.59	7.65	6.48	7.59	8.29	9.17	8.00	9.30	9.49	9.35	9.44	9.57	8.24	7.84	7.22	6.96	6.87	
RR (rpm)	18.5	19.5	22.0	12.5	10.5	9.0	11.5	12.5	14.0	13.0	13.0	13.0	13.0	13.0	13.5	14.5	14.0	13.0	12.5	12.5	
Vt (ml)	750	750	750	700	730	740	660	650	660	610	720	720	720	720	720	560	570	560	560	560	
Tin (%)	40	40	33	33	33	33	33	33	33	33	33	33	33	33	33	40	33	33	33	33	
Decision Difference																					
FiO ₂ (%)	-5	-5	-3	0	-10	-5	-3	14	4	-1	5	5	1	0	1	-12	4	2	11	14	
Peep (cmH ₂ O)	0.5	0.0	1.0	0.0	0.0	0.0	1.5	2.5	3.0	3.0	2.0	-3.0	-0.5	-0.5	-0.5	0.0	0.0	0.0	0.0	0.0	
Mv (l/min)	-2.72	-2.06	0.04	-0.41	-1.35	-1.51	-0.40	0.29	1.17	-1.50	-0.19	0.00	-0.14	-0.05	0.08	-2.96	-2.66	-3.28	-3.54	-0.13	
RR (rpm)	-3.5	-2.5	0.0	0.5	-1.5	-3.0	-0.5	0.5	1.0	0.0	0.0	0.0	0.0	0.0	0.5	-1.5	-1.0	-2.0	-2.5	2.5	
Vt (ml)	0	0	0	-50	-20	74	-6	-16	45	-120	-10	-10	-10	-10	-10	-140	-130	-140	-140	-140	
Tin (%)	-	-	-	8	8	8	8	8	8	8	8	8	8	8	8	15	8	8	8	8	
Scoring																					
FiO ₂ score	good	good	good	exact	mod	good	good	X	good	good	good	good	good	good	exact	good	X	good	good	X	X
Peep score	good	exact	good	exact	exact	exact	mod	X	X	X	mod	X	good	good	good	exact	exact	exact	exact	exact	
Mv score	X	X	good	good	X	X	good	good	X	X	good	exact	good	good	good	X	X	X	X	good	
RR score	X	mod	exact	good	good	mod	good	good	good	exact	exact	exact	exact	exact	good	good	mod	mod	mod	mod	
Vt score	exact	exact	exact	good	good	mod	good	good	good	X	good	good	good	good	good	X	X	X	X	X	
Tin score	n/a	n/a	n/a	mod	mod	mod	mod	mod	mod	mod	mod	mod	mod	mod	mod	X	mod	mod	mod	mod	

								Patient 7:								Pat 8:	Patient 9:		
	6	7	8	9	10	11	12	1	2	3	4	5	6	7	8	1	1	2	3
Observations																			
PaO ₂ (kPa)	11.2	13.9	20.2	15.7	18.6	19	15.6	7.8	11.4	9.3	11.6	9.2	7.3	7.9	8.4	22.5	19.7	13.4	9.8
PaCO ₂ (kPa)	4.50	4.62	4.39	4.60	4.58	4.82	4.63	5.54	5.70	6.00	5.68	6.50	6.11	5.94	5.15	5.60	4.81	4.88	4.70
pH	7.30	7.32	7.21	7.36	7.30	7.28	7.29	7.38	7.36	7.31	7.35	7.31	7.38	7.38	7.43	7.47	7.42	7.42	7.40
PIP (cmH ₂ O)	25.0	25.0	23.0	23.0	22.0	23.0	23.0	21.0	21.0	21.0	22.0	21.0	23.0	23.0	25.0	29.0	19.0	19.0	18.0
Weight (kg)	54.0	54.0	54.0	54.0	54.0	54.0	54.0	80.0	80.0	80.0	80.0	80.0	80.0	80.0	80.0	55.0	97.9	97.9	97.9
FiO ₂ (%)	50	60	60	55	55	55	50	60	70	70	70	65	70	80	80	55	45	40	40
Peep (cmH ₂ O)	4	4	5	4	4	4	4	5	5	7	7	7	7	7	7	5	0	0	0
Mv (l/min)	7.00	7.00	7.00	7.00	7.00	7.00	7.00	9.80	9.80	9.80	9.80	9.80	10.50	10.50	12.00	6.00	9.00	9.00	9.00
RR (rpm)	10	10	10	10	10	10	10	14	14	14	14	14	15	15	15	10	12	12	12
Vt (ml)	700	700	700	700	700	700	700	700	700	700	700	700	700	700	800	600	750	750	750
Tin (%)	25	25	25	25	25	25	25	25	25	25	25	25	25	25	25	-	-	-	-
Target PaCO ₂ (kPa)	5.3	5.3	5.3	5.3	5.3	5.3	5.3	5.50	5.50	5.50	5.50	5.50	5.50	5.50	5.50	4.60	4.60	4.60	4.60
Anaesthetist's New Settings																			
FiO ₂ (%)	60	60	55	55	55	50	45	70	70	70	65	70	80	80	80	45	40	40	45
Peep (cmH ₂ O)	4.0	4.0	4.0	4.0	4.0	4.0	4.0	5.0	7.0	7.0	7.0	7.0	7.0	7.0	15.0	5.0	0.0	0.0	0.0
Mv (l/min)	7.00	7.00	7.00	7.00	7.00	7.00	7.00	9.80	9.80	9.80	9.80	10.50	10.50	12.00	12.00	6.00	9.00	9.00	9.00
RR (rpm)	10.0	10.0	10.0	10.0	10.0	10.0	10.0	14.0	14.0	14.0	14.0	15.0	15.0	15.0	15.0	10.0	12.0	12.0	12.0
Vt (ml)	700	700	700	700	700	700	700	700	700	700	700	700	700	800	800	600	750	750	750
Tin (%)	25	25	25	25	25	25	25	25	25	25	25	25	25	25	25	-	-	-	-
Advisor New Settings																			
FiO ₂ (%)	55	60	53	50	48	48	41	78	72	79	71	77	80	83	81	45	37	38	55
PEEP (cmH ₂ O)	4.0	4.0	3.5	4.0	3.5	3.5	4.0	6.5	4.5	7.0	5.5	7.0	8.0	8.5	8.0	3.0	1.0	1.0	1.5
MV (l/min)	5.95	6.09	5.81	6.09	6.06	6.37	6.13	9.85	10.12	10.62	10.10	11.46	11.42	11.17	11.22	6.63	9.41	9.54	9.18
RR (rpm)	10.5	11.0	10.5	11.0	11.0	11.5	11.0	14.0	14.5	15.0	14.5	15.5	15.5	15.5	14.5	12.0	12.5	12.5	12.0
Vt (ml)	560	560	560	560	560	560	560	700	710	720	700	740	730	720	770	560	750	750	750
Tin (%)	33	33	33	33	33	33	33	33	33	33	33	33	33	33	33	33	33	33	33
Decision Difference																			
FiO ₂ (%)	-5	0	-2	-5	-7	-2	-4	8	2	9	6	7	0	3	1	0	-3	-2	10
Peep (cmH ₂ O)	0.0	0.0	-0.5	0.0	-0.5	-0.5	0.0	1.5	-2.5	0.0	-1.5	0.0	1.0	1.5	-7.0	-2.0	1.0	1.0	1.5
Mv (l/min)	-1.05	-0.91	-1.19	-0.91	-0.95	-0.63	-0.88	0.05	0.32	0.82	0.30	0.96	0.92	-0.83	-0.78	0.63	0.40	0.54	0.18
RR (rpm)	0.5	1.0	0.5	1.0	1.0	1.5	1.0	0.0	0.5	1.0	0.5	0.5	0.5	0.5	-0.5	2.0	0.5	0.5	0.0
Vt (ml)	-140	-140	-140	-140	-140	-140	-140	0	10	20	0	40	30	-80	-30	-40	0	0	0
Tin (%)	8	8	8	8	8	8	8	8	8	8	8	8	8	8	8	-	-	-	-
Scoring																			
FiO ₂ score	good	exact	good	good	mod	good	good	mod	good	mod	X	mod	exact	good	good	exact	good	good	mod
Peep score	exact	exact	good	exact	good	good	exact	mod	X	exact	mod	exact	good	mod	X	mod	good	good	mod
Mv score	X	mod	X	mod	mod	mod	mod	good	good	mod	good	mod	mod	mod	mod	mod	good	mod	good
RR score	good	good	good	good	good	good	good	exact	good	good	good	good	good	good	good	good	good	good	exact
Vt score	X	X	X	X	X	X	X	exact	good	good	exact	good	good	good	good	good	exact	exact	exact
Tin score	mod	mod	mod	mod	mod	mod	mod	mod	mod	mod	mod	mod	mod	mod	mod	n/a	n/a	n/a	n/a

	Patient 10:					Patient 11:	
	1	2	3	4	5	1	2
Observations							
PaO ₂ (kPa)	12.9	19.6	17.3	14.1	13.2	11.9	12.3
PaCO ₂ (kPa)	4.87	4.09	4.38	4.50	4.73	6.55	5.81
pH	7.43	7.50	7.51	7.52	7.50	7.12	7.18
PIP (cmH ₂ O)	37.0	37.0	38.0	35.0	36.0	28.0	31.0
Weight (kg)	54.2	54.2	54.2	54.2	54.2	76.0	76.0
FiO ₂ (%)	75	75	75	65	65	40	40
Peep (cmH ₂ O)	9	9	9	9	9	4	4
Mv (l/min)	9.60	9.60	9.60	9.00	9.00	5.72	7.80
RR (rpm)	12	12	12	12	12	11	15
Vt (ml)	800	800	800	750	750	520	520
Tin (%)	50	50	50	50	50	-	-
Target PaCO ₂ (kPa)	4.60	4.60	4.60	4.60	4.60	4.80	4.80
Anaesthetist's New Settings							
FiO ₂ (%)	75	75	65	65	55	40	40
Peep (cmH ₂ O)	9.0	9.0	9.0	9.0	9.0	4.0	4.0
Mv (l/min)	9.60	9.60	9.00	9.00	9.00	7.80	9.36
RR (rpm)	12.0	12.0	12.0	12.0	12.0	15.0	18.0
Vt (ml)	800	800	750	750	750	520	520
Tin (%)	50	50	50	50	50	-	-
Advisor New Settings							
FiO ₂ (%)	73	60	63	62	63	41	40
PEEP (cmH ₂ O)	7.0	5.5	6.0	6.0	6.0	3.0	3.0
MV (l/min)	9.66	8.54	9.12	8.82	9.04	6.40	7.95
RR (rpm)	14.5	13.0	14.0	14.0	14.5	12.0	15.0
Vt (ml)	660	650	650	620	620	540	530
Tin (%)	50	50	50	50	50	33	33
Decision Difference							
FiO ₂ (%)	-2	-15	-2	-3	8	1	0
Peep (cmH ₂ O)	-2.0	-3.5	-3.0	-3.0	-3.0	-1.0	-1.0
Mv (l/min)	0.06	-1.06	0.12	-0.18	0.04	-1.40	-1.41
RR (rpm)	2.5	1.0	2.0	2.0	2.5	-3.0	-3.0
Vt (ml)	-140	-150	-100	-130	-130	20	10
Tin (%)	0	0	0	0	0	-	-
Scoring							
FiO ₂ score	good	X	good	good	mod	good	exact
Peep score	mod	X	X	X	X	good	good
Mv score	good	X	good	good	good	X	X
RR score	mod	good	mod	mod	mod	mod	mod
Vt score	X	X	mod	X	X	good	good
Tin score	exact	exact	exact	exact	exact	n/a	n/a

Table F.1: The observation data required by the modified advisor extracted from the clinical records collected (see Section 8.2 for a brief synopsis of the patients recorded). All records were from patients on VC or PRVC modes of ventilation. The changes to the ventilator settings made by the attending anaesthetist are compared against those proposed by the advisor. The decision difference is shown together with the results of the qualitative scoring, see Section 8.4.

Frequency				
	Exact	Good	Moderate	Poor
FIO₂	36	54	20	16
PEEP	32	33	26	35
MV	1	48	25	52
RR	13	55	46	12
VT	11	30	29	56
TIN	42	0	58	1
Total	135	220	204	172
Percentage of Total				
	Exact	Good	Moderate	Poor
FIO₂	28.6	42.9	15.9	12.6
PEEP	25.4	26.2	20.6	27.8
MV	0.9	38.1	19.8	41.2
RR	10.3	43.7	36.5	9.5
VT	8.8	23.8	23.0	44.4
TIN	41.6	0.0	57.4	1.0
Total	18.5	30.1	27.9	23.5

Table F.2: The qualitative scoring frequency distribution of the decision matching achieved by the advisor in response to the **clinical data**.

Frequency				
	Exact	Good	Moderate	Poor
FIO₂	20	13	5	0
PEEP	18	14	5	1
MV	14	19	5	0
RR	19	16	3	0
VT	4	23	8	3
TIN	28	0	10	0
Total	103	85	36	4
Percentage of Total				
	Exact	Good	Moderate	Poor
FIO₂	52.6	34.2	13.2	0.0
PEEP	47.4	36.8	13.2	2.6
MV	36.8	50.0	13.2	0.0
RR	50.0	42.1	7.9	0.0
VT	10.5	60.5	21.1	7.9
TIN	73.7	0.0	26.3	0.0
Total	45.2	37.3	15.8	1.7

Table F.3: The qualitative scoring frequency distribution of the decision matching achieved by the advisor in response to the **simulated closed-loop data**.

Nomenclature

α_b	oxygen carrying capacity of the blood plasma
β_h	oxygen combining capacity of haemoglobin
2,3-DPG	organic phosphate 2,3-diphosphoglycerate
ARDS	adult respiratory distress syndrome
ATPS	atmospheric temperature pressure saturated
BCO_2	diffusion capacity of the lung for carbon dioxide (per litre of blood flowing in pulmonary capillaries)
BO_2	diffusion capacity of the lung for oxygen (per litre of blood flowing in pulmonary capillaries)
BPDIAS	diastolic blood pressure
BPSYS	systolic blood pressure
BROPUS	block diagram representations of patient under simulation
BTPS	body temperature pressure saturated
C.O.	cardiac output (same as \dot{Q}_t)
$CaCO_2$	concentration of carbon dioxide in arterial blood
$CACO_2$	concentration of carbon dioxide in alveolar gas
CaO_2	concentration of oxygen in arterial blood
CAO_2	concentration of oxygen in alveolar gas
C_{AW}	airway compliance
$CCO_2 / C(CO_2)$	concentration of carbon dioxide
$C_{et}CO_2$	end-tidal concentration of carbon dioxide
CMV	continuous mandatory ventilation
$CO_2 / C(O_2)$	concentration of oxygen
CoG	centre-of-gravity
CoLA	centre-of-largest area
COPD	chronic obstructive pulmonary disease
CoS	centre-of-sums
CP	percentage of normal cardiac output
CPAP	continuous positive airway pressure
$CpCO_2$	concentration of carbon dioxide in pulmonary blood
CpO_2	concentration of oxygen in pulmonary blood
CRI	compositional rule of inference
$CtCO_2$	concentration of carbon dioxide in tissue blood
CtO_2	concentration of oxygen in tissue blood
CVC	central venous catheter
$CvCO_2$	concentration of carbon dioxide in venous blood
CvO_2	concentration of oxygen in venous blood
DCO_2	diffusion capacity of the lung for carbon dioxide
DO_2	diffusion capacity of the lung for oxygen

ePaCO ₂	error from PaCO ₂ set-point
epH	error from normal pH
ePIP	error from PIP set-point
eV _T _{NORM}	error from normal tidal volume
FAC	femoral artery catheter
FAVeM	fuzzy-logic based advisor for ventilation management
FICO ₂	fractional concentration of inspired carbon dioxide
FIO ₂	fractional concentration of oxygen in inspired breath
FISMAT	fuzzy logic public domain toolbox for MATLAB
FKBC	fuzzy knowledge based controller
FoM	first of maxima
FRC	functional residual capacity
GDF	gas dissociation function
GUI	graphical user interface
[H ⁺]	concentration of hydrogen ions
Hb	haemoglobin concentration
HCO ₃ ⁻	bicarbonate
HR	heart rate
I:E	inspiratory-expiratory time ratio
ICU	intensive care unit
IGDF	inverse gas dissociation function
IPPV	intermittent positive pressure ventilation
IRI	individual rule of inference
LoM	last of maxima
LVF	left ventricular failure
MATLAB	Matrix Laboratory – proprietary software for mathematical development
MIDoM	middle of maxima
MoM	mean of maxima
MR	percentage of normal metabolic rate
MV	minute volume
MV _{NORM}	normal minute volume (based on weight)
ODC	oxygen dissociation curve
OPM	observation processing module
P ₅₀	50 % saturation normal operating point of the oxygen dissociation curve
PAC	pulmonary artery catheter
PaCO ₂	partial pressure of carbon dioxide in arterial blood
PACO ₂	partial pressure of carbon dioxide in alveolar gas
PaO ₂	partial pressure of oxygen in arterial blood
PAO ₂	partial pressure of oxygen in alveolar gas
PB	atmospheric pressure

PbCO ₂	partial pressure of carbon dioxide in brain tissue
PbO ₂	partial pressure of oxygen in brain tissue
PCO ₂	partial pressure of carbon dioxide
PCV	packed cell volume or haematocrit
PEEP	positive end expiratory pressure
PH ₂ O	partial pressure of water
PIP	peak inspiratory pressure
pK	logarithm of the inverse of the apparent first dissociation constant
PMEAN	mean alveolar or airway pressure
PO ₂	partial pressure of oxygen
PpCO ₂	partial pressure of carbon dioxide in pulmonary blood
PpO ₂	partial pressure of oxygen in pulmonary blood
PRVC	pressure regulated volume control
PSS	parameter sensitivity score
PvCO ₂	partial pressure of carbon dioxide in venous blood
P \bar{v} CO ₂	partial pressure of carbon dioxide in mixed venous blood
PvO ₂	partial pressure of oxygen in venous blood
\dot{Q}_s/\dot{Q}_t	shunt fraction (same as X)
\dot{Q}_s	shunt blood flow
\dot{Q}_t	cardiac output (same as C.O.)
RAC	radial artery catheter
R _{AW}	airway resistance
RH	relative humidity
RQ	respiratory gas exchange ratio or respiratory quotient
RR	respiratory rate
RTA	road traffic accident
SA	sensitivity analysis
SHBODC	standard human blood oxygen dissociation curve
SIMULINK	proprietary software for block diagram model development and simulation
SIMV	synchronised intermittent mandatory ventilation
SO ₂	percent saturation of haemoglobin with oxygen
SOPAVent	simulation of patient under artificial ventilation
STPD	standard temperature pressure dry
TLC	total lung capacity
t _E	expiratory time
t _I	inspiratory time
TIN	inspiratory time as percentage of whole breath
TPAUSE	pause time after inspiration as percentage of whole breath
UoD	universe of discourse

\dot{V}	volume of ventilation per minute
V_a	arterial blood volume
V_A	alveolar gas volume
\dot{V}_A	alveolar ventilation per minute
VC	volume control
\dot{V}_{CO_2}	rate of carbon dioxide production per minute
VD	dead space volume
\dot{V}_D	dead space ventilation per minute
\dot{V}_{O_2}	rate of oxygen consumption per minute
V_p	pulmonary blood volume
VT	tidal volume
V_t	tissue blood volume
$V_{T_{NORM}}$	normal tidal volume (based upon patient weight)
V_v	venous blood volume
V_{WB}	whole blood volume
\dot{V}/\dot{Q}	ventilation-perfusion ratio
WT	weight
X	shunt fraction (same as \dot{Q}_s/\dot{Q}_t)

Bibliography

- [1] ABBOD MF, LINKENS DA, [1998]. "Anaesthesia monitoring and control using fuzzy logic fusion", *Biomedical Engineering - Applications, Basis & Communications*, **10**(4), pp. 225-235.
- [2] ADAIR GS, [1925]. "The haemoglobin system. VI. The oxygen dissociation curve of haemoglobin", *Journal of Biology & Chemistry*, **63**, pp. 529-545.
- [3] ALWAN M, [1992]. "The estimation of the physiological parameters of the respiratory system", M.Sc. *Thesis*, University of Bradford, UK.
- [4] ANDERSEN JB, [1988]. "Choice of ventilator strategy", Siemens Servo Ventilator Systems.
- [5] ARKAD K, GILL H, LUDWIGS U, SHAHSAVAR N, GAO XM, WIGERTZ O, [1991]. "Medical logic module (MLM) representation of knowledge in a ventilator treatment advisory system", *International Journal of Clinical Monitoring & Computing*, **8**(1), pp. 43-48.
- [6] ATKINSON LV, HARLEY PJ, HUDSON JD, [1989]. "Numerical methods with Fortran 77 - A practical introduction", Publ. Addison-Wesley.
- [7] BARBINI P, CEVENINI G, LUTCHEN K R, URSINO M, [1994]. "Estimating respiratory mechanical parameters of ventilated patients: a critical study in the routine intensive-care unit", *Medical & Biological Engineering & Computing*, **32**, pp. 153-160.
- [8] BECKER K, THULL B, KASMACHER-LEIDINGER H, STEMMER J, RAU G, KALFF G, ZIMMERMANN HJ, [1997]. "Design and validation of an intelligent patient monitoring and alarm system based on a fuzzy logic process model", *Artificial Intelligence in Medicine*, **11**(1), pp. 33-53.
- [9] BELLAZZI R, SIVIERO C, BELLAZZI R, [1994]. "Mathematical-modelling of erythropoietin therapy in uremic anemia - Does it improve cost-effectiveness", *Haematologica*, **79**(2), pp. 154-164.
- [10] BEN-HAIM SA, DINNAR U, SAIDEL GM, [1988]. "Optimal design of mechanical ventilator waveform using a mathematical model of the ventilatory system", *Medical & Biological Engineering & Computing*, **26**, pp. 419-424.
- [11] BENATAR SR, HEWLETT AM, NUNN JF, [1973]. "The use of iso-shunt lines for control of oxygen therapy", *British Journal of Anaesthesia*, **45**, pp. 711-718.
- [12] BOVERIE S, *et al.*, [1991]. "Fuzzy logic control compared with other automated control approaches", *Proceedings: 13th IEEE-CDC Conf. Decision And Control*, Brighton UK, December 11-13.
- [13] CAPEK JM, ROY RJ, [1988]. "Non-invasive measurement of cardiac output using partial CO₂ re-breathing", *IEEE Transactions on Biomedical Engineering*, **35**(9), pp. 653-661.
- [14] CAROLLO A, TOBAR A, HERNANDEZ C, [1993]. "A rule-based post-operative pain controller", *International Journal of Biomedical Computing*, **33**, pp. 267-276.
- [15] COLEMAN TG, RANDAL JE, [1983]. "HUMAN: A Comprehensive Physiological Model", **26**(1), pp.15-21.
- [16] CURATOLO M, DERIGHETTI M, PETERSEN-FELIX S, FEIGENWINTER P, FISCHER M, ZBINDEN AM, [1996]. "Fuzzy logic control of inspired isoflurane and oxygen concentrations using minimal flow anaesthesia", *British Journal of Anaesthesia*, **76**(2), pp. 245-50.
- [17] DEFARES JG, [1964]. "Principles of feedback control and their application to the respiratory control system", *Handbook of Physiology*, Publ. American Physiological Society, Washington D.C., pp. 649-680.
- [18] DEFARES JG, DERKSEN HE, DUYFF JW, [1960]. "Cerebral blood flow in the regulation of respiration", *Acta. Physiol. Pharmacol. Neerl.*, **9**, pp. 327-360.
- [19] DELOG RH, EGER EI (II), [1975]. "MAC expanded: AD₅₀ and AD₀₅ values of common inhalational anesthetics in man", *Anesthesiology*, **42**, pp. 384-389.

- [20] DICKINSON CJ, [1977]. *A Computer Model of Human Respiration*, Publ. MTP Press, Lancaster, England.
- [21] DOJAT M, HARF A, TOUCHARD D, LAFOREST M, LEMAIRE F, BROCHARD L, [1996]. "Evaluation of a knowledge-based system providing ventilatory management and decision for extubation", *American Journal of Respiratory & Critical Care Medicine*, **153**(3), pp. 997-1004.
- [22] DOJAT M, PACHET F, GUESSOUM Z, TOUCHARD D, HARF A, BROCHARD L, [1997]. "NeoGanesh: a working system for the automated control of assisted ventilation in ICUs", *Artificial Intelligence in Medicine*, **11**(2), pp. 97-117.
- [23] DORKIN HL, LUTCHEN KR, JACKSON AC, [1988]. "Human respiratory input impedance from 4-200 Hz: physiological and modelling considerations", *Journal of Applied Physiology*, **64**, pp. 2.
- [24] DRIANKOV D, HELLENDORRN H, REINFRANK M, [1993]. "An introduction to fuzzy control", Publ. Springer-Verlag.
- [25] FAGAN LM, [1980]. "VM: Representing time-dependent relations in a medical setting", Ph.D. Thesis, Stanford University, USA
- [26] FARHI LE, RAHN H, [1955]. "A theoretical analysis of the alveolar-arterial O₂ difference with special reference to the distribution effect", *Journal of Applied Physiology*, **7**, pp. 699.
- [27] FARR BR, FAGAN LM, [1989]. "Decision-theoretic evaluation of therapy plans", *Proceedings: 13th Ann. Symp. on Computer Applications in Medical Care*, pp. 188-192.
- [28] FARRELL EJ, SIEGEL JH, [1973]. "Investigation of cardiorespiratory abnormalities through computersimulation.", *Computers and Biomedical Research*, **5**, pp. 161-186.
- [29] FERNANDO TL, PACKER JS, CADE JF, [1995]. "A closed-loop system for controlling blood-oxygen and carbon-dioxide levels in mechanically ventilated patients", *Control Engineering Practice*, **3**(10), pp. 1433-1440.
- [30] GEDEON A, FORSLUND L, HEDENSTIERNA G, ROMANO E, [1980]. "A new method for non-invasive bedside determination of pulmonary blood flow", *Medical & Biological Engineering & Computing*, **18**(July), pp. 411-418.
- [31] GOSLING P, [1995]. "How to Guides: Blood gas analysis", *Care of the Critically Ill*, **11**, pp. 1.
- [32] GREGORY IC, [1974]. "The oxygen and carbon monoxide capacities of foetal and adult blood", *Journal of Physiology*, **236**, pp. 625.
- [33] GRODINS FS, GRAY JS, SCHROEDER KR, NORINS AL, JONES RW, [1954]. "Respiratory responses to CO₂ inhalation. A theoretical study of a non-linear biological regulator", *Journal of Applied Physiology*, **7**, pp. 283-308.
- [34] GRODINS FS, BUELL J, BART AJ, [1967]. "Mathematical analysis and digital simulation of the respiratory control system", *Journal of Applied Physiology*, **22**, pp. 260-276.
- [35] HERNANDEZSANDE C, MORETBONILLO V, ALONSOBETANZOS A, [1989]. "ESTER - An expert system for management of respiratory weaning therapy", *IEEE Transactions on Biomedical Engineering*, **36**(5), pp. 559-564.
- [36] HILL EP, POWER GG, LONGO LD, [1973]. "Mathematical simulation of pulmonary O₂ and CO₂ exchange", *American Journal of Physiology*, **224**, pp. 904-917.
- [37] HINDS CJ, INGRAM D, ADAMS L, COLE PV, DICKINSON CJ, KAY J, KRAPEZ JR, WILLIAMS J, [1980]. "An evaluation of the clinical potential of a comprehensive model of human respiration in artificially ventilated patients", *Clinical Science*, **58**, pp. 83-91.
- [38] HINDS CJ, ROBERTS MJ, INGRAM D, DICKINSON CJ, [1984]. "Computer-simulation to predict patient responses to alterations in the ventilation regime", *Intensive Care Medicine*, **10**(1), pp. 13-22.

- [39] HINDS CJ, INGRAM D, DICKINSON CJ, [1982]. "Self-instruction and assessment in techniques of intensive-care using a computer-model of the respiratory system", *Intensive Care Medicine*, 8(3), pp. 115-123.
- [40] JACKSON AC, LUTCHEN KR, [1987]. "Modelling of respiratory system impedance in dogs", *Journal of Applied Physiology*, 62, pp. 414-420.
- [41] JANG JR, [1993]. "ANFIS: Adaptive-network based fuzzy inference system", *IEEE Transactions on Systems, Man & Cybernetics*, 23(3), pp. 665-685.
- [42] KAUFMAN A, [1975]. "Introduction to theory of fuzzy subsets", Publ. Academic Press, New York.
- [43] KELMAN GR, [1966]. "Digital computer subroutine for the conversion of oxygen tension into saturation", *Journal of Applied Physiology*, 21, pp. 1375-1376.
- [44] KELMAN GR, [1967]. "Digital computer procedure for the conversion of pCO₂ into blood CO₂ content", *Respiration Physiology*, 3, pp. 111-115.
- [45] KELMAN GR, [1968]. "Computer programs for the production of O₂-CO₂ diagrams", *Respiration Physiology*, 4, pp. 260.
- [46] KELMAN GR, [1970]. "A new lung model: An investigation with the aid of a digital computer", *Computers & Biomedical Research*, 3, pp. 241-248.
- [47] KWOK HF, LINKENS DA, MAHFOUF M, MILLS GH, SIMPSON CL, GOODE KM, [2000]. "Fuzzy logic knowledge elicitation for model-based ventilator management in ICU", Draft Paper, Dept. Automatic Control and Systems Eng., Univ. of Sheffield, UK.
- [48] LAUBSCHER TP, HEINRICHS W, WEILER N, HARTMANN G, BRUNNER JX, [1994]. "An adaptive lung ventilation controller", *IEEE Transactions on Biomedical Engineering*, 41, pp. 51-59.
- [49] LEANING MS, [1980]. "*The validity and validation of mathematical models*", PhD Thesis, London: City University.
- [50] LEANING MS, PULLEN HE, CARSON ER, AL-DAHAN M, RAJKUMAR N, FINKELSTEIN L, [1983]. "Modelling a complex biological system: the human cardiovascular system – 2. Model validation, reduction and development", *Trans. Institute of Measurement & Control*, 5, pp. 87-98.
- [51] LINKENS DA, ABBOD MF, [1993]. "Anaesthesia simulators for the design of supervisory rule-based control in the operating theatre", *Computing & Control Engineering Journal*, 4(2), pp. 55-62.
- [52] LINKENS DA, ABBOD MF, BACKORY JK, [1996]. "Fuzzy logic control of depth of anaesthesia using auditory evoked responses", *IEEE Colloquium on Fuzzy Logic Control in Practice*, IEEE Savoy Place, London: 15 Nov, 4, pp. 1-6.
- [53] LINKENS DA, MAHFOUF M, [1988]. "Fuzzy logic knowledge based control for muscle relaxant anaesthesia", *IFAC Modelling and Control in Medicine*, Venice, Italy, pp. 185-190.
- [54] LLOYD BB, CUNNINGHAM DJC, [1963]. "A quantitative approach to the regulation of human respiration", In: *The Regulation of Human Respiration*, Publ. Blackwell, Oxford, pp. 331-349.
- [55] LONGOBARDO GS, CHERNIACK NS, GOTHE B, [1989]. "Factors affecting respiratory system stability", *Annals of Biomedical Engineering*, 17, pp. 377-396.
- [56] LUTCHEN KR, COSTA KD, [1990]. "Physiological interpretations based on lumped element models fitted to respiratory impedance data", *IEEE Transactions on Biomedical Engineering*, BME-37, pp. 1076-1086.
- [57] MAHUTTE CK, JAFFE MB, SASSOON CSH, WONG DH, [1991]. "Cardiac output from carbon dioxide production and arterial and venous oximetry", *Critical Care Medicine*, 19(10), pp. 1270-1277.
- [58] MAMDANI EH, GAINES BR, [1981]. *Fuzzy Reasoning and its Applications*, Publ. London: Academic

- [59] MARTINI F, [1992]. *Fundamentals of Anatomy and Physiology, 2nd Edition*, Publ. Prentice Hall
- [60] MASON DG, EDWARDS ND, LINKENS DA, REILLY CS, [1996]. "Performance assessment of a fuzzy controller for atracurium-induced neuromuscular block", *British Journal of Anaesthesia*, **76**(3), pp. 396-400.
- [61] MASON DG, LINKENS DA, ABBOD MF, EDWARDS ND, REILLY CS, [1994]. "Automated delivery of muscle-relaxants using fuzzy-logic control", *IEEE Engineering in Medicine & Biology Magazine*, **13**(5), pp. 678-686.
- [62] MASON DG, ROSS JJ, EDWARDS ND, LINKENS DA, REILLY CS, [1997]. "Self-learning fuzzy control of atracurium-induced neuromuscular block during surgery", *Medical & Biological Engineering & Computing*, **35**(5), pp. 498-503.
- [63] MEAD J, [1961]. "Mechanical properties of lungs", *Physiol. Rev.*, **41**, pp. 281.
- [64] MEAD J, [1969]. "Contribution of compliance of airways to frequency dependent behaviour in lungs", *Ibid.*, **26**, pp. 670-673.
- [65] MEAD J, AGOSTONI E, [1964]. "Dynamics of breathing", *Handbook of Physiology*, Sect. 3 (1), pp. 1.
- [66] MEIER R, NIEUWLAND J, ZBINDEN AM, HACISALIHZADE SS, [1992]. "Fuzzy logic control of blood pressure during anesthesia", *IEEE Control Systems Magazine*, **12**, pp. 12-17.
- [67] MIKSCH S, HORN W, POPOW C, PAKY, F, [1993]. "VIE-VENT: Knowledge-based monitoring and therapy planning of the artificial ventilation of newborn infants", *Artificial Intelligence in Medicine*, Publ. IOS Press, pp. 218-229.
- [68] MILHORN HT, BENTON R, ROSS R, GUYTON AC. [1965]. "A mathematical model of the human respiratory control system", *Biophysical Journal*, **5**, pp. 27-46.
- [69] MILHORN HT, BROWN DR, [1971]. "Steady-state simulation of the human respiratory control system", *Computers & Biomedical Research*, **3**, pp. 604-619.
- [70] MILHORN HT, REYNOLDS WJ, [1973]. "Digital simulation of the chemical control of ventilation", *Regulation & Control in Physiological Systems*, Publ. Instrument Society of America, Pittsburgh, pp. 256-261.
- [71] MILLER PL, [1985]. "Goal-directed critiquing by computer: Ventilator management", *Computers & Biomedical Research*, **18**, pp. 422-438.
- [72] MODELL HI, FARHI LE, OLSZOWSKA AJ, [1974]. "Physiology teaching through computer simulations - Problems and promises", *Physiol. Teach.*, **3**, pp. 14-16.
- [73] MUSHIN WW, RENDELL-BAKER L, THOMPSON PW, MAPLESON WW, [1980]. "Automatic ventilation of the lungs: 3rd edition", Publ. Blackwell Scientific Publications.
- [74] NEMOTO T, HATZAKIS E, THORPE CW, OLIVENSTEIN R, DIAL S, BATES JH, [1999]. "Automatic control of pressure support mechanical ventilation using fuzzy logic", *American Journal of Respiratory & Critical Care Medicine*, **160**, pp. 550-556.
- [75] NOSHIRO M, MATSUNAMI T, TAKAKUDA K, RYUMAE S, KAGAWA T, SHIMIZU M, FUJINO T, [1994]. "Fuzzy and conventional control of high-frequency ventilation", *Medical & Biological Engineering & Computing*, **32**(4), pp. 377-383.
- [76] NUNN JF, [1993]. *Applied Respiratory Physiology*, Publ. Butterworth-Heinemann Ltd.
- [77] PETROS AJ, DORE CJ, NUNN JF, [1993]. "Modification of the iso-shunt lines for low inspired oxygen concentration", *Br J. Anaesth.*, **71**.
- [78] PIIPER J, SCHEID P, [1981]. "Model for capillary-alveolar equilibration with special reference to O₂ uptake in hypoxia", *Respiration Physiology*, **46**, pp. 193-208.
- [79] REVOW M, ENGLAND SJ, O'BEIRNE H, BRYAN AC, [1989]. "A model of the maturation of respiratory control in the newborn infant", *IEEE Transactions on Biomedical Engineering*, **36**(4), pp. 414-423.

- [80] RILEY RL, COURNARD A, [1949]. "Ideal alveolar air and the analysis of ventilation-perfusion relationships in the lungs", *Journal of Applied Physiology*, **1**, pp. 825-847.
- [81] ROIZEN MF, HERRIGAN RW, FRAZER BM, [1981]. "Anesthetic doses blocking adrenergic (stress) and cardiovascular responses to incision MAC-BAR", *Anesthesiology*, **54**, pp. 390-398.
- [82] ROSE KA, [1987]. "Sensitivity analysis in ecological simulation models", In *Systems & Control Encyclopaedia*, pp. 4230-4235.
- [83] ROUGHTON FJ, [1964]. "Transport of oxygen and carbon dioxide", In *Handbook of Physiology*, Sect III, 1, Publ. American Physiology Society, Washington DC, pp. 767-825.
- [84] ROUGHTON FJ, SEVERINGHAUS JW, [1973]. "Accurate determination of O₂ dissociation curve of human blood above 98.7 % saturation with data on O₂ solubility in unmodified human blood from 0 °C to 37 °C", *Journal of Applied Physiology*, **35**, pp. 861-869.
- [85] RUDOWSKI R, FROSTELL C, GILL H, [1989]. "A knowledge-based support system for mechanical ventilation of the lungs. The KISIVAR concept prototype", *Computer Methods & Programs in Biomedicine*, **30**, pp. 59-70.
- [86] RUDOWSKI R, LUDWIGS UG, MATUSZEWSKI A, BAEHRENDTZ S, MATELL G, [1991]. "Statistical models for prediction of arterial oxygen and carbon dioxide tensions during mechanical ventilation", *Computer Methods & Programs in Biomedicine*, **34**, pp. 191-199.
- [87] RUIZ R, BORCHES D, GONZALEZ A, CORRAL J, [1993]. "A new sodium-nitroprusside-infusion controller for the regulation of arterial blood pressure", *Biomedical Instrumentation & Technology*, **27**(3), pp. 244-251.
- [88] RUTLEDGE, GW, [1994]. "VentSim: A simulation model of cardiopulmonary physiology", *Proceedings: 18th Ann. Symp. on Computer Applications in Medical Care*, (SCAMC-94) Washington D.C., Publ. McGraw-Hill, New York, pp. 878-883.
- [89] RUTLEDGE GW, [1995]. *Dynamic Selection of Models*, Ph.d. Thesis, Section of Medical Informatics, Stanford University, USA.
- [90] SARHAN NAS, [1983]. "Modelling and simulation of breathing, its pattern and control in man", Ph.D. Thesis, Dept. Systems Science, City University, London, UK.
- [91] SAUNDERS KB, BALI HN, CARSON ER, [1980]. "A breathing model of the respiratory system: the controlled system", *Journal of Theoretical Biology*, **84**, pp. 135-161.
- [92] SCHAUBLIN J, DERIGHETTI M, FEIGENWINTER P, PETERSENFELIX S, ZBINDEN AM, [1996]. "Fuzzy-logic control of mechanical ventilation during anaesthesia", *British Journal of Anaesthesia*, **77**(5), pp. 636-641.
- [93] SCHWID HA, [1987]. "A flight simulator for general anesthesia training", *Computers & Biomedical Research*, **20**, pp. 64-75.
- [94] SCHWID HA, O'DONNELL D, [1992]. "Anesthesiologists' management of simulated critical incidents", *The Journal of Anesthesiology*, **76**(4), pp. 495-501.
- [95] SELVAKUMAR S, SHARAN M, SINGH MP, [1992]. "Mathematical-model for the exchange of gases in the lungs with special reference to carbon-monoxide", *Medical & Biological Engineering & Computing*, **30**(5), pp. 525-532.
- [96] SEVERINGHAUS JW, [1966]. "Blood gas calculator", *Journal of Applied Physiology*, **21**, pp. 1108-1116.
- [97] SEVERINGHAUS JW, [1979]. "Simple, accurate equations for human blood O₂ dissociation computations", *Journal of Applied Physiology*, **46**, pp. 599-602.
- [98] SHAHSAVAR N, FROSTELL C, GILL H, LUDWIGS U, MATELL G, WIGERTZ O, [1989]. "Knowledge base design for decision support in respirator therapy", *International Journal of Clinical Monitoring & Computing*, **6**, pp. 223-231.

- [99] SHAHSAVAR N, GILL H, WIGERTZ O, FROSTELL C, MATELL G, LUDWIGS U, [1991]. "KAVE - A tool for knowledge acquisition to support artificial- ventilation", *Computer Methods & Programs in Biomedicine*, **34**(03-Feb), pp. 115-123.
- [100] SHARANM, SINGH MP, AMINATAEI A, [1989]. "A mathematical model for the computation of the oxygen dissociation curve in human blood", *Biosystems*, **22**, pp. 249-260.
- [101] SHIEH J, CHANG L, FAN S, LIU C, HUANG H, [1998]. "Automatic control of anaesthesia using hierarchical structure", *Biomedical Engineering - Applications, Basis & Communications*, **10**, pp. 195-201.
- [102] SHIEH J, CHANG L, FAN S, LIU C, [1996]. "Hierarchical monitoring and fuzzy control of muscle relaxation", *Biomedical Engineering - Applications, Basis & Communications*, **8**, pp. 392-402.
- [103] SHIEH J, CHANG L, FAN S, LIU C, [1997]. "Hierarchical monitoring and fuzzy logic control of neuromuscular block with mivacurium", *Biomedical Engineering - Applications, Basis & Communications*, **9**, pp. 261-267.
- [104] SINGER RB, HASTINGS AB, [1948]. "An improved clinical method for the estimation of disturbances of the acid-base balance of human blood", *Medicine*, **27**, pp. 223-242.
- [105] SINGH RNP, ROTH BD, [1988]. "EVP: An expert patient-ventilator manager for chemical warfare casualties", *Publ. ACM New York USA*, pp. 1024-1032.
- [106] SITTIG DF, [1988]. "COMPAS: A computerised patient advice system to direct ventilatory care", Ph.d. Thesis, Department of Medical Informatics, University of Utah, UT, USA
- [107] SKINNER JB, KNOWLES G, ARMSTRONG RF, INGRAM D, [1983]. "The use of computerised learning in intensive care: An evaluation of a new teaching program", *Medical Education*, **17**, pp. 49-53.
- [108] SLAVIN G, NUNN JF, CROW J, DORE CJ, [1982]. "Bronchiolectasis - a complication of artificial ventilation", *Brit. Med. J.*, **285**, pp. 931.
- [109] SNOWDEN S, BROWNLEE KG, DEAR, PR, [1997]. "An expert system to assist neonatal intensive care", *Journal of Medical Engineering & Technology*, **21**, 2, pp. 67-73.
- [110] STANDAGE T, [1997]. "Is there a computer in the house", *The Daily Telegraph*, 14 Oct, pp.4-5.
- [111] SUGENO M (ed.) [1988]. *Industrial Application of Fuzzy Control*, Publ. Amsterdam, North Holland, pp. 125-138.
- [112] SUGIURA T, MIZUSHINA S, KIMURA M, FUKUI Y, HARADA Y, [1991]. "A fuzzy approach to the rate control in an artificial cardiac- pacemaker regulated by respiratory rate and temperature - a preliminary-report", *Journal of Medical Engineering & Technology*, **15**(3), pp. 107-110.
- [113] SUMMERS R, CARSON ER, ANDREASSEN S, [1992]. "Causal probabilistic modelling for clinical decision support in the high dependency environment", *Proceedings: 14th Annual Int. Conf. of the IEEE Engineering in Medicine & Biology Society*, Publ. IEEE, pp. 869-870.
- [114] SUMMERS R, CARSON ER, CRAMP DG, LEANING MS, [1988]. "AIRS - An artificial intelligent respirator system", *Modelling & Control in Biomedical Systems. Selected Papers from the IFAC Symposium*, Publ. Pergamon, Oxford, UK, **1**, pp. 583-587.
- [115] SUMMERS R, CARSON ER, [1991]. "Evaluation of intelligent decision aids for application in critical care medicine", *Proceedings: Ann. Int. Conf. of the IEEE Engineering in Medicine & Biology Society*, **13**, Parts 1-5, pp. 1310-1311.
- [116] SUMMERS R, LEANING MS, CRAMP DG, CARSON ER, [1987]. "A knowledge-based approach to ventilator management", *Proceedings: 9th Ann. Conf. of the IEEE Engineering in Medicine & Biology Society*, **1-4**, pp. 379-381.

- [117] SUN Y, KOHANE I, STARK AR, [1994]. "Fuzzy-logic assisted control of inspired oxygen in ventilated newborn-infants", *Journal of the American Medical Informatics Association*, **SS**, pp. 756-761.
- [118] TAYLOR AE, REHDER K, HYATT RE, PARKER JC, [1989]. *Clinical Respiratory Physiology: A Saunders Monograph in Physiology*, Publ. W. B. Saunders Company.
- [119] THOMSEN G, SHEINER L, [1989]. "SIMV: An application of mathematical modelling in ventilator management", *Proceedings: 13th Ann. Symp. on Computer Applications in Medical Care*, Publ. IEEE Comput. Soc. Press, pp. 320-324.
- [120] TOMOVIC R, [1963]. "Sensitivity analysis of dynamic systems", In *Systems & Control Encyclopaedia*, Publ. McGraw-Hill, New York.
- [121] TONG RM [1997]. "A control engineering review of fuzzy control", *Automatica*, **13**, pp. 559-569.
- [122] TSUTSUI T, ARITA S, [1994]. "Fuzzy-logic control of blood-pressure through enflurane anesthesia", *Journal of Clinical Monitoring*, **10**(2), pp. 110-117.
- [123] VASIL'EVA OI, IONOV IP, KANTOR PS, UL'YANOV SV, [1989]. "Dual control of the artificial ventilation process with use of a fuzzy controller in the feedback circuit", *Biomedical Engineering*, **23**(1), pp. 7-17.
- [124] VIDAL MELO MF, ABREU MG, GIANNELLA-NETO A, [1992]. "Non-invasive cardiac output estimates during quiet respiration through partial CO₂ re-breathing", pp. 689-690.
- [125] WALD A, JASON D, MURPHY TW, MAZZIA VDB, [1969]. "A computer system for respiratory parameters", *Computers & Biomedical Research*, **2**, pp. 411.
- [126] WEILER N, HEINRICHS W, KESSLER W, [1994]. "The ALV-mode: a safe closed loop algorithm for ventilation during total intravenous anaesthesia", *International Journal of Clinical Monitoring & Computing*, **11**, pp. 85-88.
- [127] WEST JB, [1979]. *Respiratory Physiology - the essentials, 2nd Edition*, Publ. Blackwell Scientific Publications.
- [128] WEST J, [1969]. "Ventilation-perfusion inequality and overall gas exchange in computer models of the lung", *Respiration Physiology*, **7**, pp. 88-110.
- [129] YAMAMOTO WS, RAUB WF, [1967]. "Models of the regulation of external respiration in mammals. Problems and promises", *Computers & Biomedical Research*, **1**, pp. 65-104.
- [130] YAN J, RYAN M, POWER J, [1994]. *Using fuzzy logic: Towards intelligent systems*, Publ. Prentice Hall.
- [131] YING H, SHEPPARD LC, TUCKER DM, [1988]. "Expert-system-based fuzzy control of mean arterial pressure by drug infusion", *Med. Prog. Technol.*, **13**, pp. 202-215.
- [132] YING H, McEACHERN M, EDDLEMAN DW, SHEPPARD LC, [1992]. "Fuzzy control of mean arterial-pressure in postsurgical patients with sodium-nitroprusside infusion", *IEEE Transactions on Biomedical Engineering*, **39**(10), pp. 1060-1070.
- [133] YOUNG JD, MCQUILLAN P, [1993]. "Comparison of thoracic electrical bioimpedance and thermodilution for the measurement of cardiac index in patients with severe sepsis", *British Journal of Anaesthesia*, **70**(1), pp. 58-62.
- [134] ZADEH LA, [1965]. "Fuzzy Sets", *Information & Control*, **8**, pp. 28-44.
- [135] ZAMEL N, JONES JG, BACH SM, NEWBERG L, [1974]. "Analog computation of alveolar pressure and airway resistance during maximum expiratory flow", *Journal of Applied Physiology*, **36**, pp. 240.
- [136] ZBINDEN AM, FEIGENWINTER P, PETERSEN-FELIX S, HACISALIHZADE S, [1995]. "Arterial pressure control with isoflurane using fuzzy logic", *British Journal of Anaesthesia*, **74**(1), pp. 66-72.